

UC Santa Barbara

UC Santa Barbara Electronic Theses and Dissertations

Title

Updating the Rulebook: Sustainable Methods for the Construction and Functionalization of Small Molecules Utilizing Micellar Catalysis

Permalink

<https://escholarship.org/uc/item/3xj7f0z8>

Author

Gabriel, Christopher Michael

Publication Date

2017

Peer reviewed|Thesis/dissertation

UNIVERSITY OF CALIFORNIA

Santa Barbara

Updating the Rulebook: Sustainable Methods for the Construction and Functionalization of
Small Molecules Utilizing Micellar Catalysis

A dissertation submitted in partial satisfaction of the
requirements for the degree Doctor of Philosophy
in Chemistry

by

Christopher Michael Gabriel

Committee in charge:

Professor Bruce H. Lipshutz

Professor Donald H. Aue, Chair

Professor Javier Read de Alaniz

Professor Trevor Hayton

June 2017

The dissertation of Christopher Michael Gabriel is approved.

Bruce H. Lipshutz

Donald H. Aue, Committee Chair

Javier Read de Alaniz

Trevor Hayton

May 2017

Updating the Rulebook: Sustainable Methods for the Construction and Functionalization of
Small Molecules Utilizing Micellar Catalysis

Copyright © 2017

by

Christopher Michael Gabriel

ACKNOWLEDGEMENTS

I would like to start by mentioning how grateful that I am to have had the opportunity to work for and with Professor Bruce H. Lipshutz. My first interaction with him where he painted this extravagant picture of how a Nigishi cross-coupling could take place in water was my first indication that he would ask me to step outside of my comfort zone. And he did. Often during and after conversations with Bruce, I would be scratching my head thinking, "He wants me to do what?" I think that the mentality of constantly pushing the envelope is what makes him so successful and you really see this in all of his students as well. One particular thing that has always stood out to me about him is his willingness to help the students in his group and also in his classes. This is certainly true in our relationship, where Bruce has helped me on many fronts including: establishing an internship at Novartis in Basel, sending me to Boston to train associates at AstraZeneca on cross-coupling in under micellar catalysis conditions, nominating me for the Ralph M. Parsons Foundation Graduate Fellowship (which I received) as well the ACS Division of Organic Chemistry's Graduate Research Symposium (and I went), and getting me an interview with Tom Colacot at Johnson Matthey. Chances are that Bruce is the only person who will ever read this (other than my wife) and so I will say Thank You for all you have given me. My hope is that someday a first year graduate student will read this so that I can grandfather an important piece of information about Bruce to which I attribute my success in completing the difficult path to becoming a PhD which is this: Bruce is a person, he puts his pants on one leg at a time (so I assume), talk to him about what's going on; I feel that this

message extends past our group but it is important not to fear your PI but rather work with them such that everyone can benefit from the research whether results are good or bad.

I would also like to thank my committee including: Donald Aue, Javier Read de Alaniz, and Trevor Hayton. I chose Dr. Aue simply based on the fact that he had actually advised my research. He has always been willing to sit down and hash out some of the less trivial questions that I had which are reflected in this dissertation in a) understanding possible mechanistic pathways of Pd nanoparticle-catalyzed reductions (Chapters II and V), as well as b) considering structural modifications to decrease the activation energy required for hydrazone hydrolysis (Chapter VI). Dr. Read de Alaniz is my favorite professor of all time which is actually saying more than it sounds like since I have been in college for 12 years. At UCSD I took a graduate course in advanced synthesis with Dr. Theorakis, and when taking the same course as part of my graduate requirements with Javier, I felt that there was no comparison: UCSB is just better at chemistry. Never again will I be able to see the words “*in situ*” without hearing Javier’s voice. While I have not interacted with Dr. Hayton as much as I could have, he was chosen on the basis of his impressive career as an inorganic chemist which parallels much of our research as we highly focus on transition metal catalysis. His comments on my research during my 2nd year exam led me to focus on other aspects of my methodology for Pd nanoparticle-catalyzed reductions which were certainly appreciated both in terms of developing further technologies as well as preparing me for future discussions.

If the fate of my PhD was not dependent on the above mentioned men, I would thank my wife, Katherine, in the first page even before the title. I owe this all too her. She has had my back through all of this and I mean ALL. I met Katherine after receiving my Associate’s degree in my year off before starting at UCSD to accomplish my Bachelor’s degree. How many times have I told her I would be done in five minutes only to show up an hour later?

Throughout the course of my studies she has always understood, and like the teacher that she is, she knows that I pursue this accomplishment not for the money, but for my selfish passion for chemistry. Over the course of my graduate studies, she has given me two beautiful children, Stella and Gregory, who she selflessly devotes her life to while I pursue my lifelong goal of becoming a doctor of chemistry. I love her more than words can say, and with every hour that I spend in lab, I am pushing to give her the life she deserves.

A look at my publication history will reveal that I have been informally co-advised by Fabrice Gallou. Fabrice was my mentor during my six month internship at Novartis in Basel, Switzerland. I would like to start by saying thanks for the opportunity, which I owe to Bruce as well. I had never been outside of North America prior to this experience which really allowed my family and I the chance to explore a world that we had never seen before. In terms of research, Fabrice welcomes my input with an open mind and aids to guide my ideas in the direction of accomplishing the highest scientific impact from the perspective of an accomplished process chemist. Walking with Fabrice through Novartis Headquarters you instantly recognize that he is a celebrity, yet he is the kind of guy who will call you on his vacation to talk about a cool new project idea. I am truly grateful to have Fabrice in my circle of close contacts and I look forward to working with him in the future.

Of course I have to give thanks to those incredibly important men and women who I have worked with over the course of my college career. To start, the members of the Hermann lab at UCSD, specifically Kevin Rynearson, my mentor, who prepared me for my role as an organic researcher by teaching me important fundamentals and techniques, many of which I still use to this day. My mentor at Ardea Biosciences, Samedy Ouk who taught me how to work quickly and gave me two pieces of advice that I still carry with me: a) the NMR never lies, and b) share your success. My original lab mate at UCSB, Matt Hageman

whose organization and diligence I truly admire in addition to being a great friend. Eric Slack for his contributions on the *Z*-selective semi-reduction of alkynes project. Megan Keener, who was my undergrad while contributing to the peptide and amide bond formation project. My current labmate and good friend, Evan Landstrom, who I bounce ideas off of constantly and has made me laugh more times than I would ever admit. Many of the current and past Lipshutz group members with impeccable scientific intuition such as Nick Isely who did early work on the hydrazone cross coupling project, Sachin Handa, Roscoe Lindstadt, Dan Lippincot, James Fennewald, Carl Peterson, Margery Cortes, as well as Nick Lee, Florence Bigorne, and Piyatida Klumphu who contributed on the co-solvent project. Many of the workers at Novartis in Basel, especially Michael Parmentier who worked through the Fe/ppm Pd-catalyzed nitro group reduction scale-up protocol with me, as well as Christian Riegert, Marian Lanz, and Vincent Bordas.

I need to thank my mom, Marcie Stanislaw, and dad, Richard Gabriel, for everything. I knew that when I grew up I could be anything, and they gave me every opportunity to do so. My brother, Greg Gabriel, and sister, Amanda Gabriel have always been a strong support system and my best friends. Also, my uncle Jim Sparing, for teaching me algebra and showing me that being a nerd was actually pretty cool. Last but not least, Jesus Christ our loving God through whom all things are possible.

VITA OF CHRISTOPHER MICHAEL GABRIEL
May 2017

Education

- Sep 2012 – May 2017 University of California, Santa Barbara
Ph.D. in Organic Chemistry
- Sep 2009 – June 2012 University of California, San Diego
B.S. in Chemistry
- Jan 2005 – Aug 2008 Fullerton College
A.A. in Chemistry

Research Experience

- Aug 2008 - June 2009 Ferro Electronic Material Systems,
R&D Technician II, Applied Technologies
Research Area: *Aluminum and silver conductor
pastes for solar cell applications.*
- Nov 2010 - June 2012 University of California, San Diego
Undergraduate Student Researcher
Supervisor: Professor Thomas Hermann
Research Areas: *Synthesis of translational
inhibitors for the Internal Ribosomal Entry Site
(IRES) Hepatitis C RNA Genome.*
- June 2011 - Aug 2012 Ardea Biosciences
Drug Metabolism/Medicinal Chemistry Intern
Research Areas: *Metabolite ID for URATI
inhibitors; Synthesis of novel URATI
inhibitors.*
- Sep 2012 - May 2017 University of California, Santa Barbara
Graduate Student Researcher
Supervisor: Professor Bruce H. Lipshutz
Research Areas: *Micellar Catalysis, Transition
Metal Catalysis, Peptide Coupling,
Heterocyclic Transformations.*
- Jul 2015 - Dec 2015 Novartis AG
Process Chemistry Intern
Supervisor: Fabrice Gallou inhibitors; Research
Areas: *Process development, incorporation of
surfactant technology for the synthesis of API's
for research and development projects.*

Teaching Experience

- Sep 2012 - June 2016 University of California, Santa Barbara
9 positions as teaching assistant held in 3
different chemistry courses.
- Sep 2013 – Oct 2013 University of California, Santa Barbara
Volunteer for SciTrek, introducing 3rd graders
to chemistry.

Awards

- 2015 Ralph M. Parsons Foundation Graduate Fellowship
2014 Outstanding Service to the Department Award -UCSB Chemistry Department
2012-2013 Member of Phi Lambda Upsilon
2009-2011 SMART Grant Recipient
2008 Future Educators and Teachers of America Scholarship
2007-2008 Joel Hail Scholarship in Natural Science

Publications

- 2017 *Sustainable and Scalable Fe/ppm Pd nanoparticle Nitro Group Reductions in Water at Room Temperature*
Gabriel, C. M.; Parmentier, M.; Riegert, C.; Lanz, M.; Handa, S.; Lipshutz, B. H.; Gallou, F.
Org. Process Res. Dev. **2017**, *21*, 247.
- 2017 *Effects of Co-solvents on Reactions Run under Micellar Catalysis Conditions*
Gabriel, C. M.; Lee, N. R.; Bigorne, F.; Klumphu, P.; Parmentier, M.; Gallou, F.; Lipshutz, B. H.
Org. Lett., **2017**, *19*, 194.
- 2015 *Amide and Peptide Bond Formation in Water at Room Temperature*
Gabriel, C. M.; Keener, M.; Gallou, F.; Lipshutz, B. H.
Org. Lett., **2015**, *17*, 3968.
- 2014 *A Palladium Nanoparticle–Nanomicelle Combination for the Stereoselective Semihydrogenation of Alkynes in Water at Room Temperature*
Slack, E.; **Gabriel, C. M.**; Lipshutz, B. H.
Angew. Chem., Int. Ed. **2014**, *53*, 14051.
- 2014 *2-Aminobenzoxazole Ligands of the Hepatitis C Virus Internal Ribosome Entry Site*
Rynearson, K. D.; Charrette, B.; **Gabriel, C.**; Moreno, J.; Boerneke, M. A.; Dibrov, S. M.; Hermann, T.
Bioorg. Med. Chem. Lett. **2014**, *24*, 3521.

ABSTRACT

Updating the Rulebook: Sustainable Methods for the Construction and Functionalization of Small Molecules Utilizing Micellar Catalysis

by

Christopher Michael Gabriel

Over the past two centuries, the field of organic chemistry has expanded to facilitate transformations for the synthesis of complex molecular scaffolds of increasing variability. With these advancements, however, the dependence on organic solvents as reaction medium remains. This research describes a general alternative to organic solvents by employing the designer surfactant, TPGS-750-M, under aqueous conditions, which spontaneously assembles to form micellar aggregates (nanoreactors) providing conditions under which organic transformations favorably take place. Key features of this technology include: low reaction temperatures, the ability to recycle the reaction medium (and often the catalyst), as well as low production of organic waste as quantified by Sheldon's E Factors.

Under micellar catalysis conditions it was discovered that nanoparticle-catalyzed reactions are especially well suited to take place including the *Z*-selective semi-reductions of alkynes as well as nitro-group reductions that take place at room temperature with exceptional yields and selectivity. Both systems undergo reduction by the use of borohydride salts as the hydride source allowing these procedures to take place under ambient conditions.

An environmentally responsible method for amide and peptide bond synthesis is also described, not only replacing egregious organic solvents such as DCM and DMF, but also

eliminating the need for explosive HOBt by incorporation of an oxime activator, Oxyma, in the form of uronium coupling reagent COMU.

Furthermore, as an ultimate goal of this chemistry is to minimize potential waste on scale, procedural modifications are described by the incorporation of minimal co-solvents for a survey of reaction types. These modifications investigated impact on reaction yield, rate, and physical aspects of a reaction mixture such that technology developed in lab can reach its highest potential when considered on an industrial scale.

I. Going Green

1.1 Micellar Catalysis

“Going Green” has become such a common idea in the past few decades that it is now somewhat of a cliché. Global warming is now appreciated and accepted in the scientific community as it graduates from its status as a theory into the role of unstoppable force. The more that we understand about climate change the more we humans begin to recognize our impact. It is no hidden fact that current atmospheric levels of CO₂ are astronomically higher than levels prior to the industrial revolution. The impact of CFC’s on the ozone layer is yet another instance of how efficiently humans are destroying the environment. Government intervention on our ability to pollute and produce waste is surprisingly minimal as many of those in seats of high power still refuse to submit to the overwhelming amount of data that suggests that a major change is needed to take place in order for the earth to continue as a beautiful and habitable planet. It is then up to us, the citizens of the world to make the change.

One area specifically which requires change is that of molecular synthesis. In the 21st century, western medicine is trusted, proven, and expected often in the form of prescription or over-the-counter pharmaceuticals. The major feedstock of the hydrocarbon based or “organic” active pharmaceutical ingredients (API) is crude oil. The past two centuries have led to discoveries and developments for the purification of chemical species from crude oil from which biologically important molecular scaffolds can be constructed. It is not simply the chemical entity which is generally constructed from this non-renewable feedstock, but also the organic solvents which are usually required for their synthesis. After one use of an

organic solvent in a chemical process, the waste is incinerated, further depleting our resources and generating pollution in the atmosphere. The alarming dependence of western culture on crude oil seems impossible to overcome, however by recognizing outlets for hampering the use of the diminishing resources, we can prolong the lifetime of the Earth's supply while slowing the rate at which waste is produced.

Several advances have been made in the area of sustainable or "Green Chemistry," such as the use of biomass derived feedstocks often by the conversion of carbohydrates into higher value fine chemicals.¹ This is a significant step in the right direction, however minimal effort has been made to replace organic solvents with a renewable or even recyclable feedstock. While the use of "green solvents" such as ethanol, isopropanol, acetic acid, ethyl acetate, and 2-methyltetrahydrofuran serve as valuable alternatives to traditional organic solvents,² their virtues are more greatly attributed to the associated cost, handling, and disposal; yet rarely are these solvents recycled. Water as a solvent for organic transformations is commonly disregarded due to its highly polar nature and inability to dissolve reaction components, yet is frequently employed as a means to enrich products upon reaction completion by the removal of polar reagents or by-products. In terms of feedstock, water is a renewable resource which is available in amounts larger than what would ever be required. It literally falls from the sky. Water is also clearly safer from the user's perspective in comparison to even the safest organic solvents such as ethanol in that it is non-flammable and completely non-toxic.

Until recently, the use of water as a solvent has generally been utilized either as a biphasic mixture with organic solvent or in the presence of a phase transfer catalyst with very few methods using water alone for "on-water" reactions.³ Surfactants provide a non-canonical approach to utilize water as a solvent by solubilizing reaction components by

means of micellar aggregates. This technology has been used widely for solubilizing organic material in water for thousands of years and is most easily recognized in our daily lives in the form of soap, however is sparingly used in the arena of organic chemistry.⁴

In 2008, the use of nonionic tocopherol based surfactant PTS-600⁵ was exploited for the first time for the use in olefin-cross metathesis in water (Figure 1).⁶ This methodology was the seminal publication from our group for synthesis by means of micellar catalysis by the use of a benign-by-design surfactant yielding exceptional results for neutral organic reactants in the absence of organic solvent at room temperature. Since the initial disclosure of this work, the scope of aqueous micellar catalysis utilizing PTS-600 has expanded to a large array of transformations including: ring-closing-metathesis, transition metal cross-couplings (ie. Heck,⁶ Suzuki-Miyaura,⁷ Miyuara Borylations,⁹ Sonogashira,¹⁰ Buchwald-Hartwig,¹¹ Negishi,¹² and C-H activation.¹³ These works later gave rise to surfactants as a catalyst support within the lipophilic region of ubiquinol based designer surfactant PQS effecting Ru-catalyzed cross/ring-closing-metatheses,¹⁴ Rh-catalyzed asymmetric 1,4-additions,¹⁵ as well as organocatalysis.¹⁶ Modifications to PTS-600 were later made by shortening the diester chain, extending the PEG portion, and capping the PEG chain with a methyl group leading to the development of the next generation surfactant TPGS-750-M.¹⁷ This surfactant was found to outperform PTS-600 for a variety of transformations on the basis of product yield which is proposed to be the consequence of the increased particle size of the micelle (PTS-600 = 24 nm; TPGS-750-M = 53 nm). Since the advent of TPGS-750-M, our group has utilized this surfactant as a staple for developing sustainable methods under micellar catalysis conditions, expanding the scope of transformations to include reductions,¹⁸ oxidations,¹⁹ nucleophilic aromatic substitutions,²⁰ and nanoparticle catalyzed processes.^{18c,g,h,21,22} Additionally, our library of benign surfactants has been extended to

include newly developed “Nok” based on a β -sitosterol core, paralleling the applications of TPGS-750-M, but from a more renewable feedstock.²³

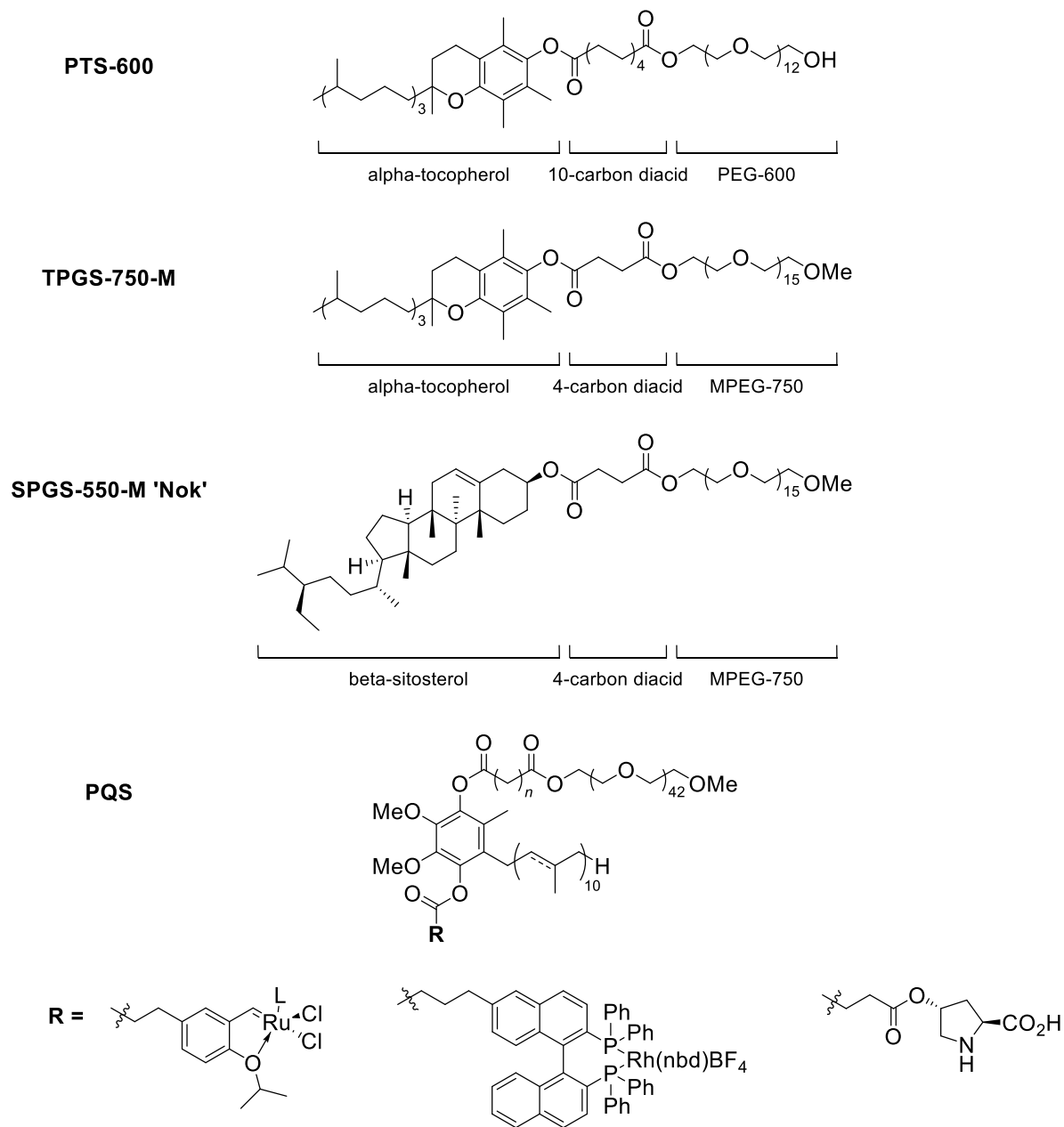


Figure 1. Lipshutz Group designer surfactants.

The use of aqueous micellar catalysis for the synthesis and functionalization of organic scaffolds is the focus of the work presented within this dissertation. The use of this technology extends past the ability to utilize water as the gross reaction medium, by considering the amount of waste generated by these methods measuring Sheldon's E Factor²⁴ in comparison to traditional methods in organic solvent, as well as leveraging the aqueous nature of the reaction mixture for in-flask work-ups and recycling capabilities. My work specifically has been focused on "updating" traditional methods, some older than a century, where classical procedures have unmet environmental concerns especially on the basis of solvent usage, waste generated, recyclability, and safety. Some of the methods include: the Z-selective semi-reduction of alkynes (Chapter II), amide and peptide bond formation (Chapter III), reduction of nitroarenes (Chapter V) and the Fisher indole Ssynthesis (Chapter VI), all taking place under aqueous micellar catalysis conditions. While it may be convenient to view these methods as a simple solvent switch, many additional parameters must be considered in an aqueous environment and experience in these techniques has led to significant advancements in the field by considering the influence of salts,^{18a,c} pH,²⁵ and miscibility^{18h,26} on reaction yields and selectivity; all concepts which are presented within this work (vide infra).

Furthermore, it should be noted that while my efforts in the field of organic synthesis have been highly focused on developing methods in aqueous media, the theme of constructing methodologies that have minimal environmental impact as the highest priority has impacted my outlook on organic synthesis as a whole beyond the scope of transformations in water. Much of what is done in our labs which may be termed "Green Chemistry" translates in industrial processes as good process chemistry. What is meant by this is that these are considerations which need to be commonplace in organic synthesis by

looking closely at safety, reagent availability, ease of preparation and purification, waste generation, and cost; many of parameters highlighted as the “12 Principles of Green Chemistry.” These themes are presented herein for projects that I have either led^{18h,25,26} or collaborated on.^{18c}

1.2 References

1. Donate, P.M. *Chem. Biol. Technol. Agric.* **2014**, *1*, 4.
2. MacMillan, D. S.; Murray, J.; Sneddon, H. F.; Jamieson, C.; Watson, A. J. B. *Green Chem.* **2013**, *15*, 596.
3. a) S. Narayan, J. Muldoon, M. G. Finn, V. V. Fokin, H. C. Kolb, K. B. Sharpless, *Angew. Chem., Int. Ed.* **2005**, *44*, 3275. b) Duplais, C.; Krasovskiy, A.; Wattenberg, A.; Lipshutz, B. H. *Chem. Comm.* **2010**, 46, 562.
4. La Sorella, G.; Strukul, G.; Scarso, A. *Green Chem.* **2015**, *17*, 644.
5. a) Borowy-Borowski, H.; Sikorska-Walker, M.; Walker, P. R. *Water-Soluble Compositions of Bioactive Lipophilic Compounds*. U.S. Patent 6,045,826, Apr 4, **2000**. (b) Borowy-Borowski, H.; Sikorska-Walker, M.; Walker, P. R. *Water-Soluble Compositions of Bioactive Lipophilic Compounds*. U.S. Patent 6,191,172, Feb 20, **2001**. (c) Borowy-Borowski, H.; Sikorska-Walker, M.; Walker, P. R. *Water-Soluble Compositions of Bioactive Lipophilic Compounds*. U.S. Patent 6,632,443, Oct 14, **2003**. PTS referenced from *Org. Lett.* **2008**, *10*, 1325
6. Lipshutz, B. H.; Aguinaldo, G. T.; Ghorai, S.; Voigtritter, K. *Org. Lett.* **2008**, *10*, 1325.
7. Lipshutz, B. H.; Taft B. R. *Org. Lett.* **2008** *10*, 1329.
8. a) Lipshutz, B. H.; Petersen, T. B.; Abela, A. *Org. Lett.* **2008**, *10*, 1333. b) Lipshutz, B. H.; Abela, A. R. *Org. Lett.* **2008**, *10*, 5329.
9. Lipshutz, B. H.; Moser, R.; Voigtritter, K. R. *Isr. J. Chem.* **2010**, *50*, 691.
10. Lipshutz, B. H.; Chung, D. W.; Rich, B. *Org. Lett.* **2008**, *10*, 3793.
11. Lipshutz, B. H.; Chung, D. W.; Rich, B. *Adv. Syn. Catal.* **2009**, *351*, 1717.
12. a) Krasovskiy, A.; Duplais, C.; Lipshutz, B. H. *J. Am. Chem. Soc.* **2009**, *131*, 15592. b) A. Krasovskiy, A.; Duplais, C.; Lipshutz, B. H. *Org. Lett.* **2010**, *12*, 4742.

13. Nishikata, T.; Lipshutz, B. H. *Org. Lett.* **2010**, *12*, 1972.
14. a) Lipshutz, B. H.; Ghorai, S. *Org. Lett.* **2009**, *11*, 705. b) Lipshutz, B. H.; Ghorai, S. *Tetrahedron* **2010**, *66*, 1057.
15. Lipshutz, B. H.; Isley, N.; Moser, R.; Leuser, H.; Taft, B. R. *Adv. Syn. Catal.* **2012**, *354*, 3175.
16. Lipshutz, B. H.; Ghorai, S. *Org. Lett.* **2012**, *14*, 422.
17. Lipshutz, B. H.; Ghorai, S.; Abela, A. R.; Moser, R.; Nishikata, T.; Duplais, C.; Krasovskiy, A. *J. Org. Chem.* **2011**, *76*, 4379.
18. a) Huang, S.; Voigtritter, K.; Unger, J. B.; Lipshutz, B. H. *Synlett* **2010**, *13*, 2041. b) Kelly, S. M.; Lipshutz, B. H. *Org. Lett.* **2014**, *16*, 98. c) Slack, E. D.; Gabriel, C. M.; Lipshutz, B. H. *Angew. Chem., Int. Ed.* **2014**, *53*, 14051. d) Isley, N. A.; Hageman, M. S.; Lipshutz, B. H. *Green Chem.* **2015**, *17*, 893. e) Bhattacharjya, A.; Klumphu, P.; Lipshutz, B. H. *Org. Lett.* **2015**, *17*, 1122. f) Fennewald, J. C.; Landstrom, E. B.; Lipshutz, B. H. *Tetrahedron Lett.* **2015**, *56*, 3608. g) Feng, J.; Handa, S.; Gallou, F.; Lipshutz, B. H. *Angew. Chem., Int. Ed.* **2016**, *55*, 8979. h) Gabriel, C. M.; Parmentier, M.; Riegert, C.; Lanz, M.; Handa, S.; Lipshutz, B. H.; Gallou, F. *Org. Process Res. Dev.* **2017**, *21*, 247.
19. a) Lipshutz, B. H.; Hageman, M.; Fennewald, J. C.; Linstadt, R.; Slack, E.; Voigtritter, K. *Chem. Comm.* **2014**, *50*, 11378. b) Handa, S.; Fennewald, J. C.; Lipshutz, B. H. *Angew. Chem., Int. Ed.* **2014**, *53*, 3432.
20. a) Isley, N. A.; Linstadt, R. T. H.; Kelly, S. M.; Gallou, F.; Lipshutz, B. H. *Org. Lett.* **2015**, *17*, 4734. b) Lee, N. R.; Gallou, F.; Lipshutz, B. H. *Org. Process Res. Dev.* **2017**, *21*, 218.
21. Handa, S.; Wang, Ye; Gallou, F.; Lipshutz, B. H. *Science* **2015**, *349*, 1087.
22. Handa, S.; Slack, E. D.; Lipshutz, B. H. *Angew. Chem., Int. Ed.* **2015**, *54*, 11994.
23. Klumphu, P.; Lipshutz, B. H. *J. Org. Chem.* **2014**, *79*, 888.
24. a) Sheldon, R. A. *Chem. Ind.* **1992**, 903. b) Lipshutz, B. H.; Ghorai, S. *Green Chem.* **2014**, *16*, 3660. c) Lipshutz, B. H.; Isley, N. A.; Fennewald, J. C.; Slack, E. D. *Angew. Chem., Int. Ed.* **2013**, *52*, 10911.
25. C. M.; Keener, M.; Gallou, F.; Lipshutz, B. H. *Org. Lett.* **2015**, *17*, 3968.
26. Gabriel, C. M.; Lee, N. R.; Bigorne, F.; Klumphu, P.; Parmentier, M.; Gallou, F.; Lipshutz, B. H. *Org. Lett.* **2017**, *19*, 194.

II. Stereoselective Semi-Reduction of Alkynes in Water at Room Temperature

2.1 Introduction

Stereo-defined alkenes represent a functionality found ubiquitously in synthesis both in terms of target molecules such as drugs and natural products (Figure 1) as well as versatile intermediates in organic synthesis. The geometry of an alkene not only influences the properties of a molecule but can also greatly influence molecular geometry in further transformations.¹ Access to stereo-defined alkenes has long been an area of intense research and while many methods exist for the synthesis of *E*-alkenes, the less thermodynamically favorable *Z*-alkene remains a challenge to this day.^{2,3} In addition to the relative thermodynamic stability of *E*-alkenes over *Z*-alkenes, challenges for this transformation are met on the basis of generality, harsh reaction conditions, chemo-selectivity, and waste generation.

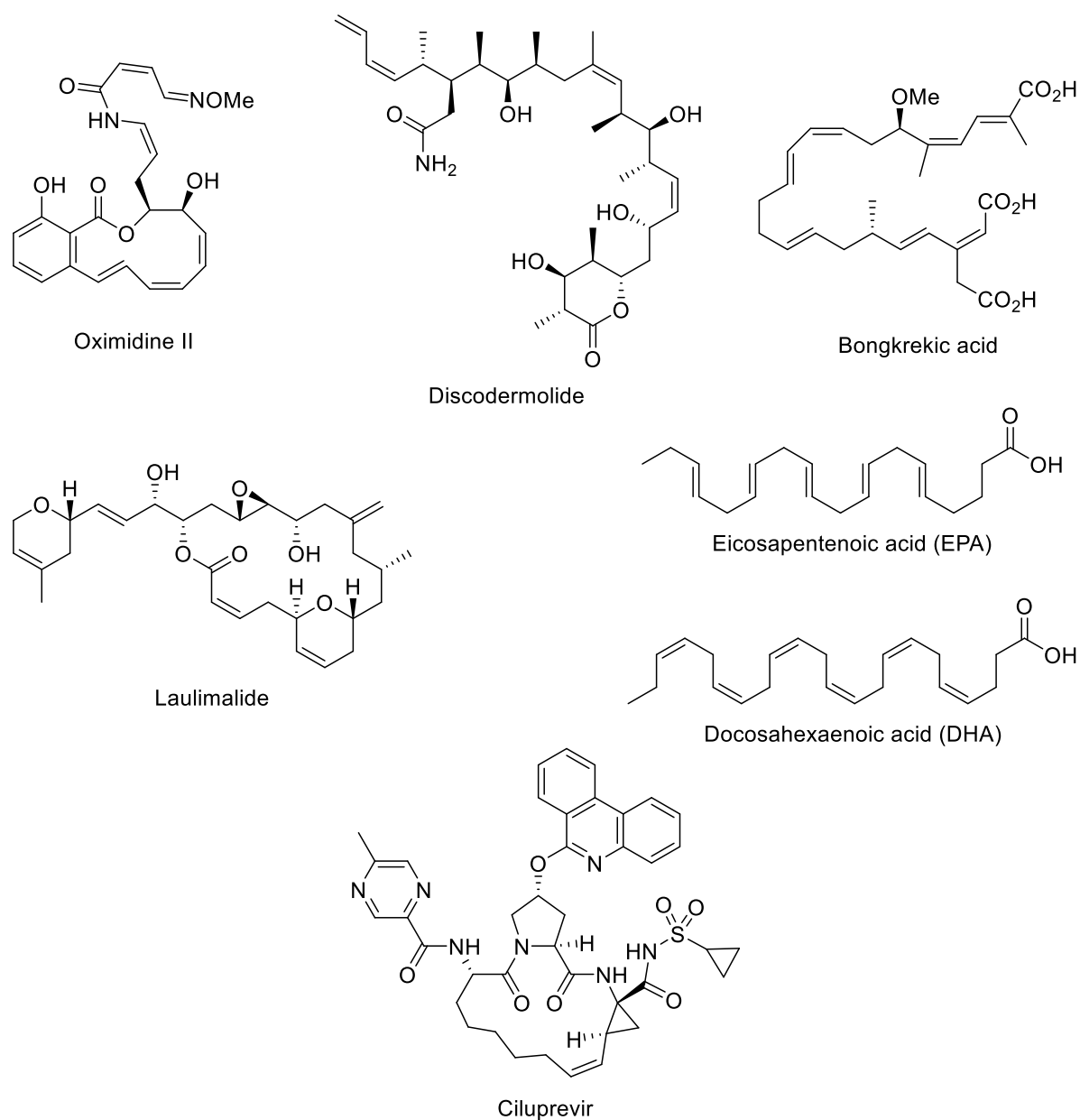
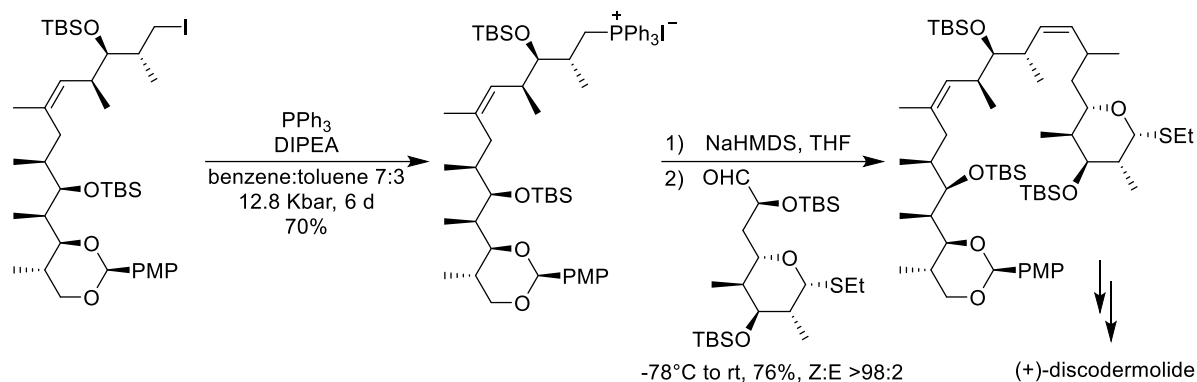


Figure 1. Representative examples of important drugs and natural products containing stereo-defined alkenes.

Z-Alkenes can be accessed by a number of ways with the most common strategies including: 1) Wittig olefination,⁴ 2) olefin metathesis,⁵ 3) cross coupling,⁶ and 4) semi-reduction of alkynes.^{2,7-15} This chapter focuses on the development of methodology for the

semi-reduction of alkynes, but it is certainly well placed to note other important milestones for this synthesis of this important moiety.

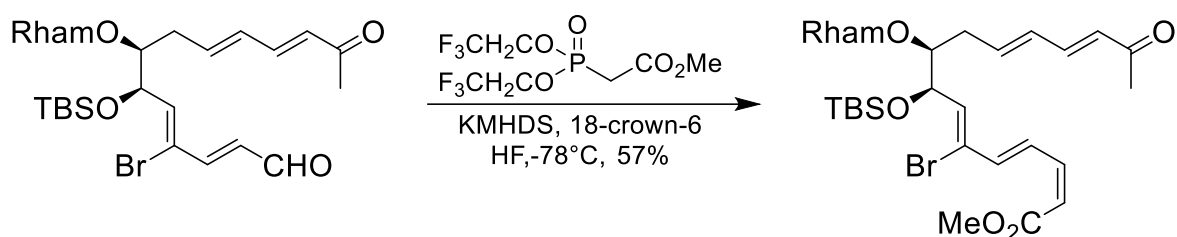
First reported in 1954,⁴ the Wittig olefination is still used as a powerful method for accessing *Z*-olefins. The installation of the olefin goes by means of substitution of a phosphine ylide onto an aldehyde often affording high selectivity for the *Z*-geometry as the result of the steric bulk of the phosphine group. The phosphine ylide is often generated from the corresponding triaryl- or trialkylphosphine and an alkyl halide with subsequent deprotonation under basic conditions. This transformation is highly regarded by the synthetic community with Georg Wittig receiving the Nobel Prize for his work in 1979. Furthermore, the Wittig olefination has been used extensively for the synthesis of natural products including Petrosiol E,¹⁶ Cermizine D,¹⁷ (-)-Maoecrystal V,¹⁸ and Palhinine A & D.¹⁹ An excellent example of how this transformation has been leveraged is represented by the synthesis of (+)-discodermolide by Smith and coworkers (Scheme 1).²⁰



Scheme 1. Wittig reaction *en route* to (+)-discodermolide.

Mechanistically similar to the Wittig olefination is the Horner Wadsworth Emmons olefination (HWE) which generally affords the *E*-geometry from aldehydes.²¹ In comparison

to the Wittig olefination, electron deficient alkyl phosphonate esters are used in place of the triaryl- or trialkylphosphonium ylides, selectively favoring the thermodynamic *E*-olefin. Still and Gennari modified this procedure by the use of bis(trifluoroalkyl)phosphonoesters and trifluoroethanol favoring the *Z*-olefin with high selectivity.²² The Still-Gennari modification of the HWE olefination gives rise to α,β -unsaturated ketones, esters, and cyanides, and has been used in the total synthesis of spinosyn A by Roush and coworkers. (Scheme 2).²³



Scheme 2. Use of the Still-Gennari modification of the HWE olefination *en route* to spinosyn A.

Tremendous synthetic advancements have been made for *Z*-selective olefin metathesis as well. This transformation is not generally sought after as products from cross-metathesis often lead to the *E*-isomer and the *Z*-geometry usually only occurs for ring closing metathesis (RCM) because the *E*-olefinic product would cause too much strain for small sized rings. One of the first reports of *Z*-alkenes via olefin metathesis was exemplified by means of ring opening cross-metathesis (ROCM) from a cyclobutene substrate, showing only moderate selectivity as the result of minimizing steric interaction between the substrate and the ligands of Grubbs' first generation catalyst.²⁴ Another report with much higher selectivities utilized Hoveyda-Grubbs second generation catalyst and a related pyridine coordinated analogue offered selectivities up to $Z:E = 96:4$ when cross methathesis was carried out on enyne substrates.²⁵ This example was particularly interesting, showing orthogonality to alkyne substrates which would be reduced under semi-reduction conditions.

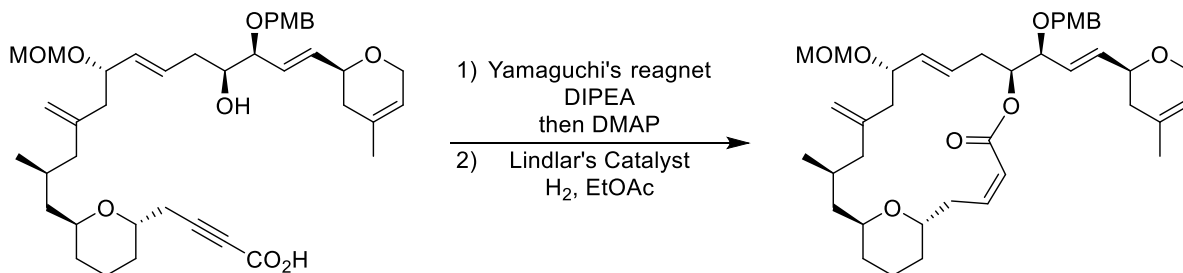
Mo and W have also been proven to offer selective access to *Z*-alkenes.^{26,27} An early example was reported by Crowe and coworkers for Mo-catalyzed cross metathesis of acrylonitriles with Shrock catalyst, however selectivities were moderate with in the best case achieving *Z:E* = 9:1.^{26a} Much better selectivities (*Z:E* > 98:2) have been reported with Mo-MAP for ROCM where the catalyst possesses a highly bulky biaryl framework which was proposed to effect stereo-retention of cyclic alkenes to *Z*-defined styrenes.^{26b} This same catalyst has been shown to deliver exceptional *Z*-selectivity for the cross-metathesis of vinyl ethers and was used as a key step in the synthesis of plasmalogen C16:0.^{26c} A similar example was reported for the highly *Z*-selective (*Z:E* > 98:2) ring-opening metathesis polymerization (ROMP) to afford polymers bearing a *cis*-syndiotactic configuration from substituted bicyclo[2.2.1]hepta-2,5-dienes which was catalyzed by a Mo complex containing the bulky hexaisopropyltriphenoxide (HIPTO) ligand.^{26d} Catalysts of W bearing many similarities to their Mo counterparts have also been shown to afford *Z*-alkenes selectively, where W-MAP catalyzed cross-metathesis yields the homo-coupled product with *Z:E* > 98:2.^{27a} W catalysts bearing the HIPTO ligand have also shown success producing *Z*-alkenes by cross metathesis with vinylic alcohols and sulfonamides to afford homo-coupled products with reasonable selectivities (*Z:E* = 91:9).^{27b}

Cross-coupling offers the advantage of retaining stereochemistry from the partner undergoing the coupling event, however *Z*-selectivity of a prior functionalization step is required. An excellent example of the utility of this reaction is the total synthesis of oximidine II by Molander and coworkers.²⁸ In this report, Pd-catalyzed Suzuki-Miyaura (SM) cross coupling was used as the ring closing step from an *E*-configured alkene bearing BF₃K, which was coupled with a *Z*-alkene with a terminal bromide. This example shows the applicability of this reaction to both alkene configurations maintaining stereo-chemistry. A

more recent report by the Trost group described the total synthesis of Leustroducsin B where a Hiyama cross coupling event was used to access a *Z,Z*-diene.²⁹ In 2012, our group investigated SM couplings from various vinyl halides, unveiling a direct correlation between stereo-retention and catalyst structure.³⁰ It was found that Pd(*t*Bu₃)₂ and PdCl₂(AmPhos)₂ led to significant, and in some cases near complete, isomerization to afford the undesired *E*-styrene product while catalysts such as Pd(P(*o*-Tol)₃)₂ and PdCl₂(PPh₃)₂ afforded *Z*-styrenyl products with high stereo-retention up to *Z:E* = 99:1 in many cases.

One of the most common methods for accessing *Z*-alkenes is by the semi-reduction of alkynes.² A widely utilized system for the partial hydrogenation of alkynes is the Lindlar reduction. First introduced in the early 1950's, the Lindlar reduction remains as the fundamental approach presented in organic chemistry textbooks for this transformation.³¹ Though Lindlar's catalyst comes in many forms, this type of heterogeneous catalysis stems from the use of supported Pd(0), typically on BaSO₄ or CaCO₃ with variable amounts of other additives such as Pb(OAc)₂. Quinoline is often used to "poison" the catalyst in order to achieve higher *Z*-olefin selectivities and suppress over-reduction. In addition, a sacrificial oxidant such as cyclohexene may be used and may be reduced in place of the desired alkene product to further suppress over-reduction.³² The use of such "deactivators", "poisons", and "sacrificial oxidants" is crucial for this catalyst as alkene isomerization to the more thermodynamically more stable *E*-olefin may readily occur, along with reduction of either configuration of the product olefin to the corresponding alkane. Furthermore, additive stoichiometry optimization is commonplace depending on the nature of the alkyne and careful reaction progress monitoring (by either H₂ consumption or reaction conversion) are critical for a high yielding and selective transformation. An impressive example of how the Lindlar reduction can be exploited is represented by the total synthesis of (-)-Laulimalide by

Ghosh and coworkers where the semi-hydrogenation was employed late-stage following a Yamaguchi macrolactonization (Scheme 3).³³ Due to the many challenges that may arise when optimizing conditions to a specific substrate, the Lindlar reduction lacks generality, both in terms of alkyne type and functional tolerance, and reaction monitoring is operationally tedious.

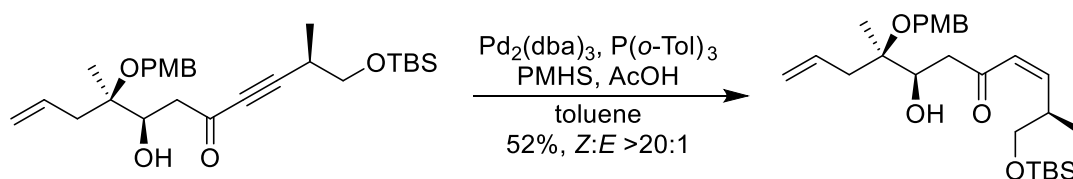


Scheme 3. Use of the Lindlar reduction *en route* to (-)-Laulimalide.

Another system which is similar in nature to the developed method to be presented in this chapter is use of P2-Ni (Brown's Catalyst), developed during World War II.³⁴ The heterogenous nickel-boride catalyst synthesized from Ni(OAc)₂·4H₂O and NaBH₄ in EtOH. The catalyst has been used as an alternative to Lindlar's catalyst as net semi-reduction occurs via a hydrogenation pathway. Selectivity improves by the use of ethylenediamine (eda) as an additive.³⁵ This system benefits from its functional group compatibility, tolerating alkenes, amides, acetals, oxazoles, benzyl ethers, silyl ethers, and free hydroxyl groups.² While this classical system shows many advantages even over some of the more recent communications, drawbacks include the requirement for H₂ as reductant and instability of the catalyst (very sensitive to oxygen), requiring synthesis of P2-Ni immediately before alkyne reduction.

To circumvent many of the associated drawbacks with semi-hydrogenation either by Lindlar's catalyst and related platanoid supported catalyst systems under hydrogenation conditions, much focus has been geared toward effecting the partial reduction via hydride transfer.² This approach takes advantage of stoichiometric control by solid or liquid hydride sources as opposed to H₂. In addition, highly pressurized systems are not required for this approach in most cases often lending these procedures as safer and operationally simpler alternatives. While many examples of alkyne semi-reduction to *Z*-alkenes exist in the literature, this section will focus mainly on examples that relate to the scope of this chapter.

The first known report of homogeneous catalytic hydride transfer for the reduction of alkynes was reported in 1989 by Trost and coworkers.³⁶ The conditions employed Pd₂(dba)₃·CHCl₃ and P(*o*-Tol)₃ with acetic acid and TMHDS as the cooperative hydride source. While only poor selectivity was achieved, with the best reported selectivity being *Z*:*E* = 2.6:1 this work set the stage for an entire field of chemistry. Notable features of these conditions are the relatively short reaction times (1 to 20 minutes) and compatibility with substrates bearing alkenes, nitro groups, and esters. This method was later used by the same group for the total synthesis of (-)-Ushikulide A, where good selectivity of the *Z*-enone was achieved (*Z*:*E* >20:1) from the corresponding ynone in the presence of an alkene, silyl ether, and a PMB ether (Scheme 4).³⁷ This same reduction was attempted under Lindlar's conditions however, the spectator alkene was completely reduced.



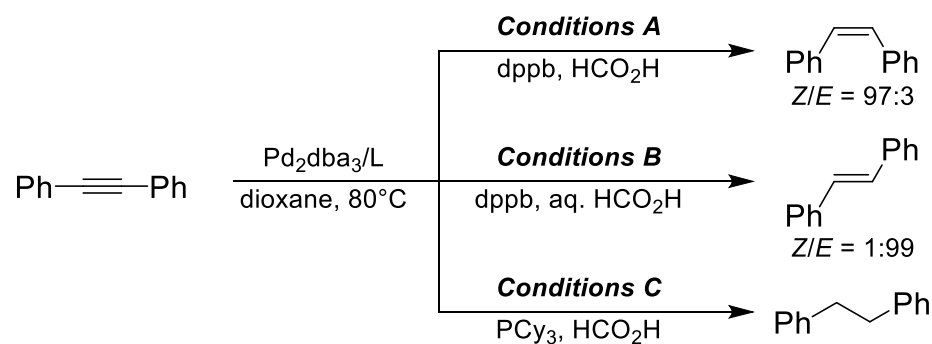
Scheme 4. Trost's selective Pd-catalyzed hydride transfer *en route* to (-)-Ushikulide A.

In a later communication by Sato and coworkers, milder conditions were employed for the highly *Z*-selective Pd-catalyzed semi reduction of alkenes via hydride transfer from HCO₂H-Et₃N.³⁸ In this report, the more bulk and electron rich ligand P(tBu)₃ was used with Pd₂dba₃·CHCl₃ to afford selectivities as high as *Z*:*E* = 98:2 for several examples. Functional compatibility was shown for substrates bearing esters, free alcohols, silyl ethers, and PMB ethers, however extended reaction times favor isomerization to the undesired *E*-alkene.

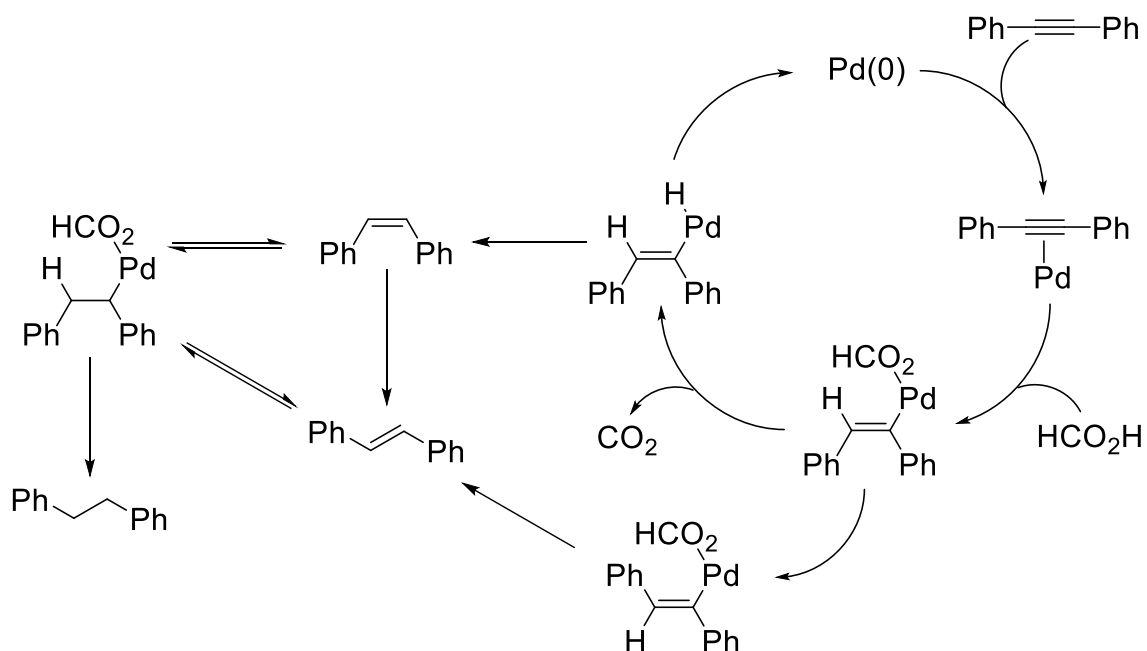
Another important example of hydride transfer via Pd(0) catalysis was reported by Elsevier and coworkers which showed an intriguing correlation between solvent and selectivity.³⁹ The catalyst for this system relies on Pd(IMes)(MA) which is generated *in situ* from Pd(tBuDAB)(MA), 1,3-bis(mesityl)imidazolium chloride, and potassium *t*-butoxide. Excellent selectivity for the *Z*-alkene as achieved in many cases (up to *Z*:*E* = 98:2) when the reaction was conducted in MeCN, however a complete selectivity switch was observed for some aliphatic alkynes when THF was used as solvent. Mechanistic studies showed that coordination of MeCN to the active Pd catalyst liberates the *Z*-alkene, preventing isomerization and over reduction for many electron rich systems. This method is limited by the poor functional group compatibility, although ketones and esters survive these conditions. Interestingly, Wu and coworkers noticed a pronounced decrease in selectivity when MeOH was used in place of THF for the reduction of various phenylacetylene derivatives under conditions employing Pd(OAc)₂ and NaOMe.⁴⁰

One of the more impressive systems for this transformation was the work reported by Shen *et. al* which describes a hydride transfer system which could be tuned to effect high selectivity for both *Z* and *E* isomers as well as the fully saturated alkane product (Scheme 5).⁴¹ The scope of this methodology seemed to be limited to the synthesis of various styrene analogues, however several functional groups were tolerated including boronic esters,

pyridine, esters, aryl halides, nitroarenes, and benzyl ethers. The key to selectivity in this case was the use of Pd₂dba₃/dppb with formic acid either under anhydrous conditions to afford the *Z*-alkene or in the presence of water to selectively afford the *E*-isomer, while the fully saturated product was acquired from a ligand switch to PCy₃. The change in selectivity was proposed to be due to isomerization of the alkenylpalladium species prior to decarboxylation and subsequent reductive elimination, however the role of water was not mentioned (Scheme 6). The increased reducing abilities of the system incorporating PCy₃ as ligand was explained on the basis of this catalysts poor ability to facilitate β-hydride elimination, thus allowing further a decarboxylation/hydride insertion sequence to take place readily prior to reductive elimination. This work was an excellent example of the capabilities of heterogeneous Pd catalysis for hydride transfer, yet some notable drawbacks of this system are the requirement of high temperatures in 1,4-dioxane which is a highly toxic solvent.⁴²



Scheme 5. Effects of water and ligand on reduction selectivity.



Scheme 6. Mechanism described by Shen *et al.*

With the impressive developments made in this field it seems that selectivity is so highly regarded as an important objective, that the use of high temperatures and egregious solvents is not taken into consideration. While selectivity is of utmost importance for developing suitable conditions for the synthesis of *Z*-alkenes, other parameters are certainly worth exploring especially on the basis of sustainability. One of the premier factors that would constitute a method as environmentally responsible is the amount and nature of waste generated for a given process. So the question is, how green are these methods? It is no question that waste generation by the use of stoichiometric reagents would generate at least stoichiometric waste as is the case with olefination via the Wittig and HWE reactions. In fact, the waste generated by these reactions is comparable to some of the catalytic methods, due to the lack of recyclability of the organic solvents and the catalysts being employed. As mentioned previously, many of these transformations require some of the more dangerous

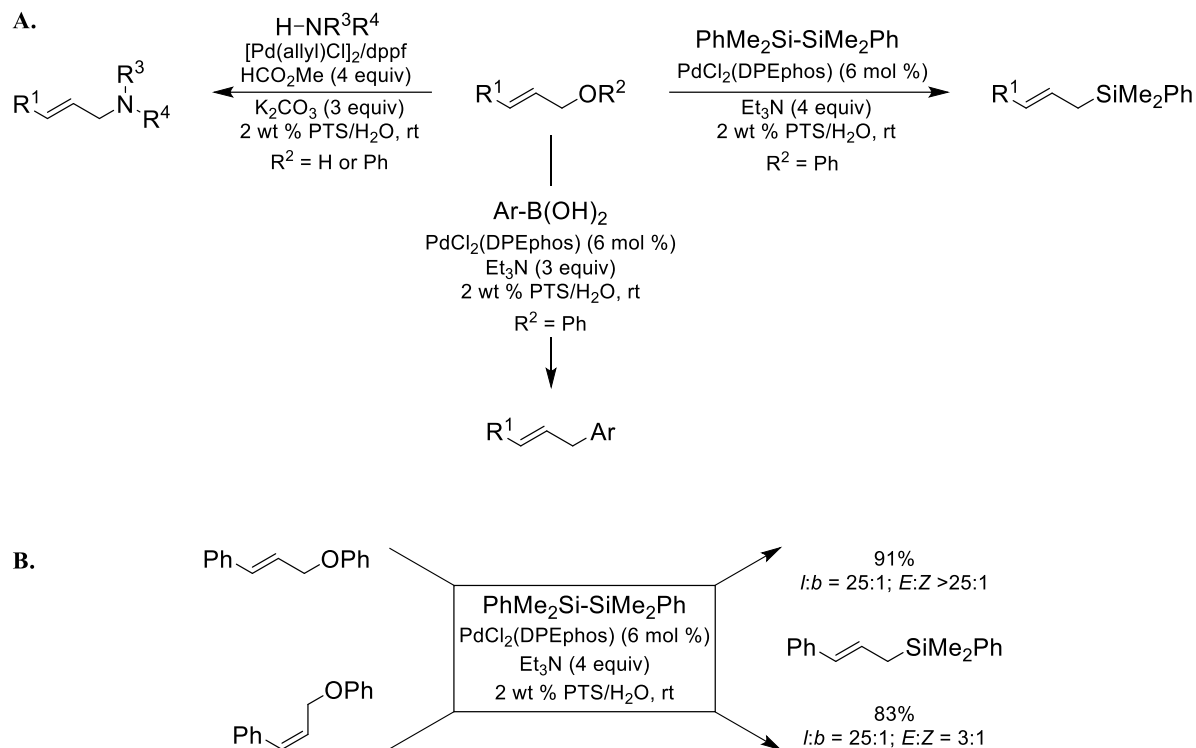
solvents such as MeCN and 1,4-dioxane. Not only are these solvents toxic,⁴² but their high miscibility in water requires more complicated work up procedures for the isolation of products. Also, many of these procedures require temperatures well outside of room temperature which requires additional energy, where HWE reactions require cooling, many of the hydride transfer chemistries require high temperatures. Furthermore, hydrogenation in many cases requires high pressures of flammable H₂ which is certainly a concern in terms of safety and operational simplicity. It seems then, that in order to meet many of the criteria which defines a sustainable process, many of these tremendous advancements have fundamental limitations.

From the perspective of green chemistry, these drawbacks can be addressed by first installing parameters for the method followed by the development of the chemistry itself. That is, the reaction should take place using benign solvents, offer the potential for recyclability, reduce waste, minimize energy (in the form of heating and cooling), and with operational simplicity and safety.⁴³

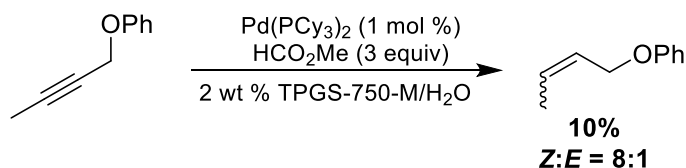
2.2 Previous Work

In order to address many of the environmental concerns associated with current alkyne semi-reduction methods, the parameters were set in place that a general and highly selective procedure would utilize aqueous micellar catalysis at room temperature. Our efforts towards the goal of developing such a method came serendipitously, however, with the initial focus on delivering a tandem process for an unrelated transformation. In fact, the early work on semi-reductions in the Lipshutz group was to selectively access the *E*-allylic phenyl ethers and alcohols from their corresponding propargyl precursors. The strategy was intended to supplement earlier work from our group, where allylic ethers and alcohols were found as

excellent electrophiles for Pd(0) cross coupling with boronic acids, amines, and disilanes (Scheme 7A).⁴⁴ From this precedent, it was well understood that highest selectivity to the linear-brached product resulted from pure *trans*-disubstituted alkenes (Scheme 7B). Furthermore, it was found that methyl formate greatly increased the reaction rate for these transformations. Initial experiments towards a one-pot procedure from propargylic materials to allylic substitution products came by means of a modified procedure from Shen *et. al* under aqueous micellar conditions, where methyl formate was used in place of formic acid.⁴¹ Based on these prior findings, we believed that it was feasible that high selectivity could be achieved for the *E*-alkene product based on the aqueous environment. Furthermore, both the reduction and substitution methods utilize the same catalyst, so it was perceived that this approach was certainly possible. Initial attempts at the semi-reduction gave low conversion, yet interestingly, when Pd(PCy₃)₂ was screened enrichment of the *Z*-isomer was observed (Scheme 8). In stark contrast with the method that this reduction was based on,⁴¹ the project shifted focus to further increasing the *Z*-selectivity of the semi-reduced product as very few methods exist for the *Z*-selective semi-reduction of alkynes under aqueous conditions.



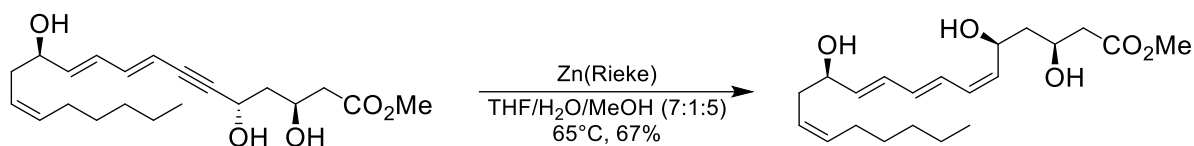
Scheme 7. A. Allylic alcohol/phenylether cross coupling in micellar catalysis conditions;
 B. Cross coupling selectivity from stereo-defined allylic phenylethers



Scheme 8. Initial discovery of Z-selective semi-reduction of alkynes.

To date, very few methods for the Z-selective semi-reduction of alkynes under aqueous conditions exist, the most common of which is the use of activated zinc.⁴⁵ Many preparations of activated zinc have been reported and these reductions are generally run in a mixture of MeOH and water. The use of this method is highlighted by its ability to reduce conjugated polyenes. An example of its use is represented by the synthesis of 3-hydroxyleukotriene B₄, where a conjugated alkyne underwent semi-reduction in the

presence of both *cis* and *trans*-disubstituted alkenes (Scheme 9).⁴⁶ Some of the drawbacks of this method include the use of super-stoichiometric Zn as well as isomerization, over reduction, and polymerization with extended reaction times. In addition, use of activated Zn for semi-reduction is not generally compatible with substrates bearing esters, ketones, nitriles, alkyl halides.^{2,45}



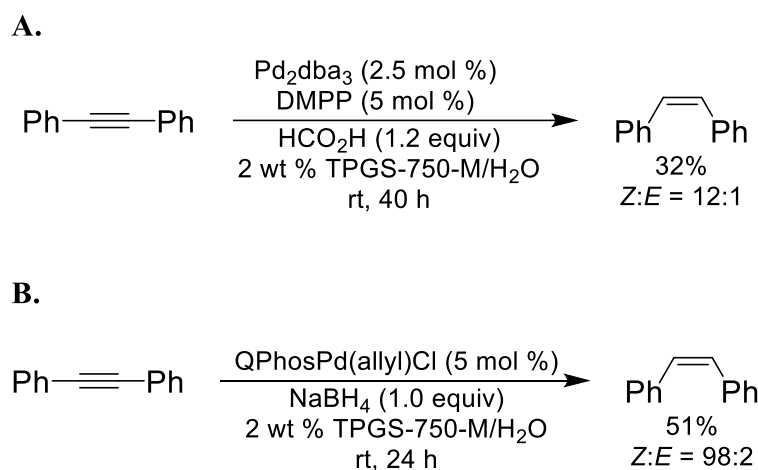
Scheme 9. Active Zn-mediated Z-selective semi-reduction *en route* to 3-hydroxyleukotriene B4.

Furthermore, the opportunity for catalyst and solvent recycling is a rare occurrence for this transformation. In 2013, Mitsudome *et. al* reported a Pd nanocomposite catalyst that offered good selectivity for the reduction phenylacetylenes and simple aliphatic alkynes and showed that the catalyst could be recovered and reused for a subsequent reduction.⁴⁷ While this was a step in the right direction, the only report to our knowledge where both the catalyst and solvent were recycled was a communication by Chandrasekhar and coworkers. Chandrasekhar's work showed that PEG-400 could be used for Lindlar reductions allowing for catalyst and solvent reuse by extraction of the product alkene with diethyl ether. This work parallels some of the capabilities of the method which will soon be described (*vide infra*). As previously described, drawbacks of this method include limitations in terms of generality and the use of H₂ as the stoichiometric reductant.

2.3 Results and Discussion

Initial screening consisted of an exhaustive survey of Pd sources and ligand with 1.2 equivalents of formic acid. From these experiments it was realized that while formic

acid/Pd(0) system did result in enrichment of the *Z*-alkene, selectivity was moderate and conversion was poor even with extended reaction times and increased reductant loading. The best of these systems came from the use of ligands such as DMPP with Pd₂dba₃ at 5 mol % loading which afforded the product in only 32% conversion with *Z*:*E* = 12:1 over 40 hours (Scheme 10A). Further screening efforts found that NaBH₄ gave much higher conversion and selectivity, delivering 51% conversion and *Z*:*E* = 98:2 for a system catalyzed by QPhosPd(allyl)Cl (5%) after 24h (Scheme 10B).

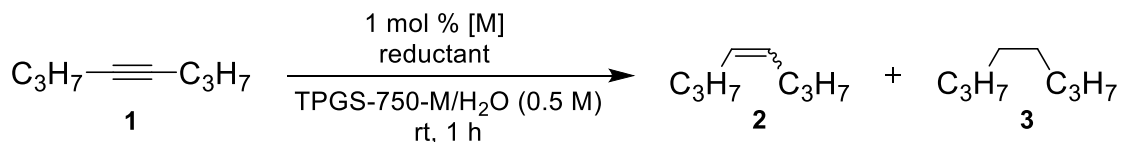


Scheme 10. Initial optimization of *Z*-selective semi-reduction of phenylacetylene under homogeneous Pd-H transfer conditions.

Over the course of further catalyst evaluation, the method was plagued once again by low conversion. While screening conditions, an observation was made that some of the more successful systems appeared to generate small amounts of Pd aggregates suggesting that this system may be catalyzed by Pd nanoparticles. To investigate this possibility, intentional generation of Pd nanoparticles from various palladium sources with NaBH₄ in the absence of a ligand was carried out, not unlike the synthesis of Brown's catalyst. The conditions screened included **A**: metal salt/complex under H₂ atmosphere; **B**: hydrogenation in the presence of nanoparticles synthesized with five equivalents NaBH₄ relative to metal; and **C**:

use of NaBH₄ as the stoichiometric reductant after first generating the nanoparticles in situ (procedures represented in the Experimental Section of this chapter).

Under these conditions, quantitative conversion could be achieved for the reduction of 4-octyne showing nearly perfect selectivity when Pd(OAc)₂ and PdI₂ were employed with NaBH₄ as reductant (Table 1, entries 10 & 13), yet interestingly over-reduction to the corresponding alkane was observed for PdCl₂ under all conditions. Other group 10 metal salts or complexes (e.g., NiCl₂, Ni(OAc)₂, Pd₂(dba)₃) were either inactive or led to mixtures of *E*- and *Z*-alkenes. Alternatively, a similar outcome can be realized using a balloon of hydrogen gas in place after prior reduction of Pd(OAc)₂ with NaBH₄ (entry 9), however activation of the catalyst (nanoparticle synthesis) was appear to be necessary for optimal conversion and selectivity.



entry	[M]	condition	1	2-(Z)	2-(E)	3
1	NiCl ₂	A	100%	0%	0%	0%
2	NiCl ₂	B	90%	9%	1%	0%
3	Ni(OAc) ₂	A	100%	0%	0%	0%
4	Pd ₂ dba ₃	A	0%	25%	25%	50%
5	PdCl ₂	A	0%	0%	0%	100%
6	PdCl ₂	B	0%	0%	0%	100%
7	PdCl ₂	C	0%	0%	0%	100%
8	Pd(OAc) ₂	A	100%	0%	0%	0%
9	Pd(OAc) ₂	B	0%	25%	<1%	75%
10	Pd(OAc) ₂	C	100%	99%	<1%	0%
11	PdI ₂	A	100%	0%	0%	0%
12	PdI ₂	B	50%	49%	<1%	0%
13	PdI ₂	C	100%	99%	<1%	0%

^aPercentages determined by GC/MS

Table 1. Metal salt/complex screening for heterogeneous semi-reduction of **1**.

The use of NaBH₄ with the nanoparticles generated from Pd(OAc)₂ then became the optimal system for investigation on an expanded substrate scope. This system was decided upon as suitable conditions to meet some of the environmental concerns associated with preexisting methods. Environmental and safety drawbacks associated with hydrogenation conditions are met by the use of sub-stoichiometric NaBH₄ which provides access to a system in which the equivalence of H₂ can easily be controlled and directed towards the alkyne substrate alleviating the need for excess reagent and high pressures. The catalyst is easily prepared by use of relatively inexpensive and readily available Pd(OAc)₂ (1 mol %) admixed with NaBH₄ (0.05 equiv) via sonication, followed by the addition of water containing 2 wt % TPGS-750-M. Upon stirring at ambient temperature, a black suspension (“black water”) is obtained (Figure 2A). It should be noted that this catalyst suspension can be generated in situ or as a bulk suspension for the use over several reactions. Prepared as a bulk suspension, the black water shows no loss in catalytic activity over several weeks, however the mixture should be stirred under an atmosphere of Ar. A cryo-TEM image of nanoparticles generated from Pd(OAc)₂ shows an interesting phenomenon, where micelles aggregate around the particles using the PEG chain of the surfactant as a ligand⁴⁸ to bring the catalyst close to the reaction site and allow for uniform dispersion of the mixture. (Figure 2B).

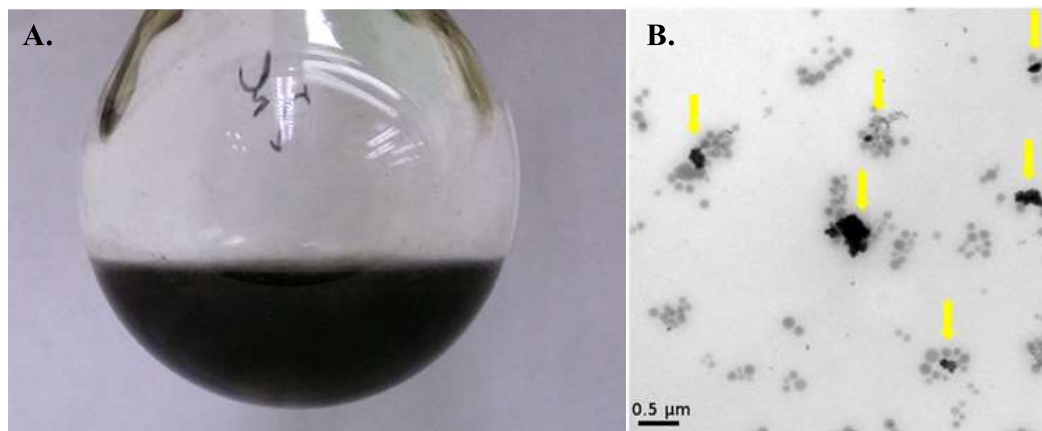
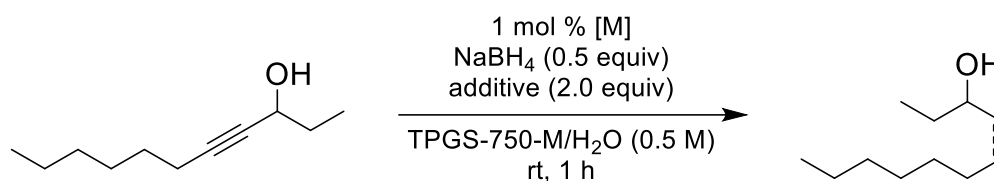


Figure 2. A. Bulk catalyst suspension in 2 wt % TPGS-750-M/H₂O “Black Water”;
B. Cryo-TEM image of nanoparticle-nanomicelle interaction.

Upon investigation of the scope this method, it was soon realized that functionalized alkynes such as propargylic alcohols, had diminished selectivities and in fact over reduction of the alkyne was observed once again. It was hypothesized that the polar functionality could coordinate to the Pd and its close proximity to the reduced *Z*-alkene would facilitate further modifications to the product such as isomerization and reduction to the alkane. To address this, several salt additives were considered and it was discovered that incorporation of LiCl (2 equiv) led to high *Z*-selectivity and conversions once more (Table 2). Other lithium salts such as LiBr and LiOH did show some improvement over the control, while interestingly Li₂CO₃ was found to further diminish selectivity. NaCl had no effect on the outcome of the reaction. Since the development of this method, a similar system was developed by our group utilizing Pd(OAc)₂ doped Fe nanoparticles to catalyze nitro group reductions in aqueous TPGS-750-M solution with NaBH₄.⁴⁹ Based on the findings presented by Table 2, several salts were screened concluding that KCl (1.0 equiv) improves the rate and overall conversion of nitro group reduction, and in fact KBH₄ could be used to arrive at the same results (Chapter V).⁵⁰ The similar findings for orthogonal transformations suggests that the

reactivity of NaBH₄ may in fact be hampered by the use of the added LiCl leading to a system less prone to over-reduction. Furthermore, Guella and coworkers investigated the catalytic hydrolysis of NaBH₄ by Pd/C, a similar system to these optimized conditions, which suggested Pd-BH₃⁻ species as a key intermediate in the generation of the active palladium hydride.⁵¹ Adapting this model to our systems, it is possible that the Li⁺ counterion may be playing a significant role in effecting the hydrolysis of the palladium boride.

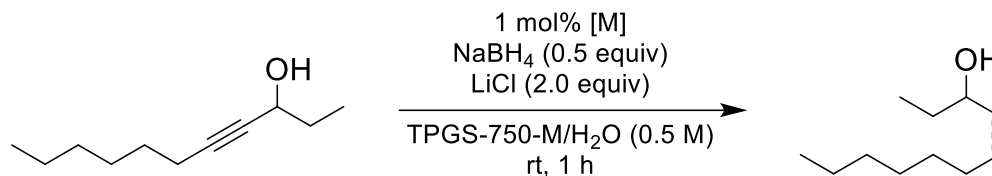


entry	additive	Conv. (%)	Z	E	Alkane
1	none	100	33	33	33
2	NaCl	100	33	33	33
3	LiOH	74	93	7	0
4	LiBr	80	15	5	0
5	LiCl	100	96	4	0
6	Li ₂ CO ₃	100	28	41	29

Table 2. Additive screening on Black Water reduction.

Attention was then brought to the effect of solvent. As our goal was to provide a system incorporating water as the gross reaction medium, several surfactants were screened under the newly optimized conditions (Table 3). It was found that the choice of TPGS-750-M as surfactant was critical (entries 7 & 9), while the corresponding hydrogenation “on water”⁵² (i.e., in the absence of the surfactant) afforded mostly the over-reduced, saturated product (entry 1). In fact, replacement of TPGS-750-M with other commercially available surfactants led to decreased selectivity and varying amounts of over reduction were apparent in all cases. When our conditions were carried out in organic solvent, poor conversion resulted, yet

selectivity was retained, and in fact improved by the use of MeCN (entry 13). While organic solvents screened may not be useful under these conditions, the selectivity observed may explain the superior performance of TPGS-750-M. When compared to SPGS-550-M (“Nok”),⁵³ TPGS-750-M is very structurally similar, with both surfactants bearing a methylated PEG chain linked by succinate diester to a polycyclic lipophilic scaffold, however the tocopherol core of TPGS-750-M contains a benzopyran (Chapter I). It is believed that the oxygen of this benzopyran may play a role in coordination to the catalyst, similar to the results reported by Elsevier and coworkers where coordination of MeCN was shown to greatly influence *Z*-selectivity.³⁹



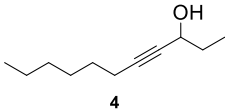
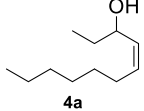
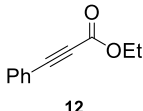
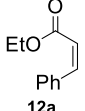
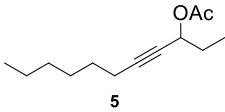
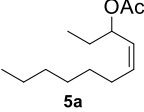
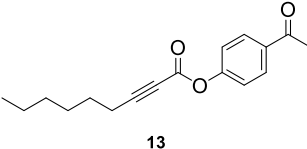
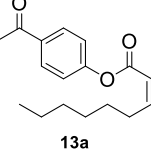
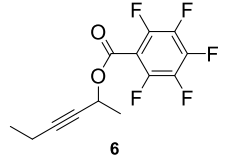
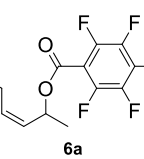
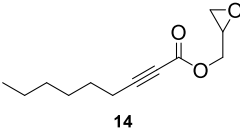
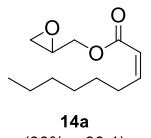
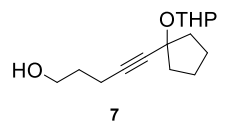
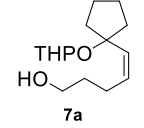
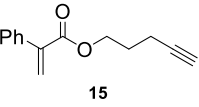
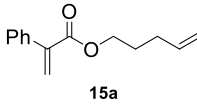
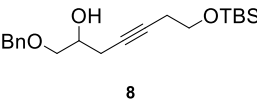
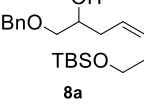
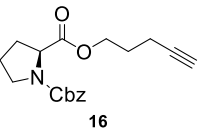
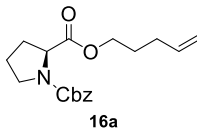
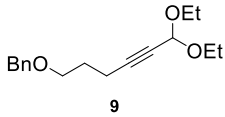
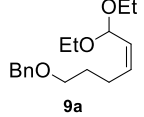
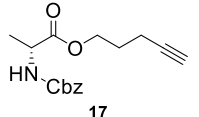
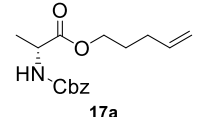
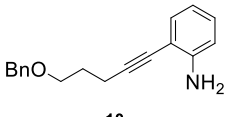
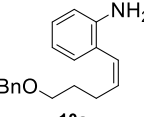
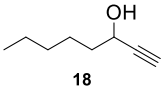
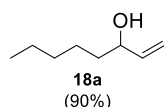
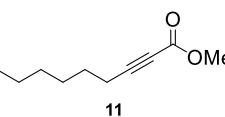
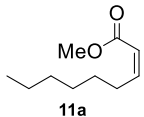
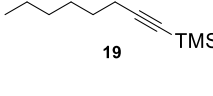
Entry	Solvent	Pd ^a	Conversion ^b	Z	E	alkane
1	water	Pd(OAc) ₂	100	25	25	50
2	Cremophor ^c	Pd(OAc) ₂	100	25	25	50
3	Brij 30 ^c	Pd(OAc) ₂	100	0	0	100
4	Triton X ^c	Pd(OAc) ₂	100	50	25	25
5	SDS ^c	Pd(OAc) ₂	100	14	14	72
6	SPGS ^c	Pd(OAc) ₂	100	14	28	58
7	TPGS^c	Pd(OAc)₂	100	95	5	<1
8	TPGS ^c	PdCl ₂	100	0	0	100
9	TPGS ^c	PdI ₂	100	95	5	<1
10	TPGS ^d	Pd(OAc) ₂	100	90	5	5
11	none	Pd(OAc) ₂	100	30	40	30
12	DME	Pd(OAc) ₂	58	86	12	2
13	MeCN	Pd(OAc) ₂	8	96	4	<1
14	THF	Pd(OAc) ₂	9	89	8	3

All reactions were run at 0.5 M of substrate to solvent; ratios were determined by GC-MS; ^a1 mol% Pd; ^bDetermined by GC-MS; ^c2 wt% solution; ^d5 wt% solution

Table 3. Surfactant and organic solvent screening for the semi-reduction of **4**.

With the optimized conditions in hand, the scope of this transformation was examined for various alkynes including unsymmetrically disubstituted, terminal, and conjugated systems (Figure 4). Additional examples of propargylic and homopropargylic alcohols and their ester derivatives led to excellent *Z*-selectivity under the general conditions (entries 1-5), as did the corresponding acetal (entry 6). A conjugated aryl alkyl alkyne (entry 7) afforded the corresponding styrenyl array with *Z*:*E* = 95:5 showing applicability to substrates bearing anilines. As expected, free hydroxyl groups (entries 1, 4, 5, & 15) afforded quantitative

conversion in most cases, with exceptional selectivity. A major highlight of these conditions is the ability to obtain *Z*- α,β -unsaturated esters, a major limitation of many semi-reduction methods.² Interestingly, a ketone (entry 10) and an epoxide (entry 11) survived the conditions, affording high conversions without effecting these sensitive functionalities. However, the ketone was reduced in the absence of Pd. Terminal cases (entries 12-15) reacted to afford the targeted mono-substituted alkenes without over reduction, yet some reduction of the olefin in an acrylate was observed leading to the drop in yield (entry 12). Even under these basic conditions stereo-defined α -amino acids such as proline and alanine derivatives (entries 13, 14) showed no epimerization. Benzyl ethers and N-Cbz groups remained fully intact, which are generally not suitable under standard Pd(0) catalyzed hydrogenation conditions such as Pd/C.⁵⁴ A representative TMS-acetylene showed absolutely no conversion under these conditions which could be used as a protection strategy for terminal alkynes in the presence of an alkyne undergoing semi-reduction (entry 16). In all cases, reductions were complete within 45 minutes.

entry	alkyne	product [yield(%) ^a , Z:E ratio]	entry	alkyne	product [yield(%) ^a , Z:E ratio]
1		 4a (90%; 96:4)	9 ^c		 12a (90%; 95:5)
2		 5a (99%; >99:1)	10 ^d		 13a (95%; >99:1)
3		 6a (96%; >99:1)	11		 14a (90%; >99:1)
4		 7a (98%; >99:1)	12 ^c		 15a (82%)
5		 8a (91%; >99:1)	13 ^e		 16a (98%)
6		 9a (98%; >99:1)	14 ^e		 17a (97%)
7		 10a (90%; 95:5)	15 ^e		 18a (90%)
8		 11a (85%; >99:1)	16 ^e		no reaction

All reactions were run at a substrate concentration of 0.5 M, with 2 equiv LiCl, 0.5 equiv NaBH₄, using a stock catalyst mixture from Pd(OAc)₂ and NaBH₄ at a 1:5 ratio in degassed 2 wt % TPGS-750-M/H₂O. ^ayield of isolated products are reported. ^bNo deprotection of protected alcohols or amines was detected. ^cRun with 1 equiv LiCl. ^dReduction of ketone was observed if no palladium was present. ^eNo LiCl.

Figure 4. Representative example of Z-selective semi-reduction in Black Water.

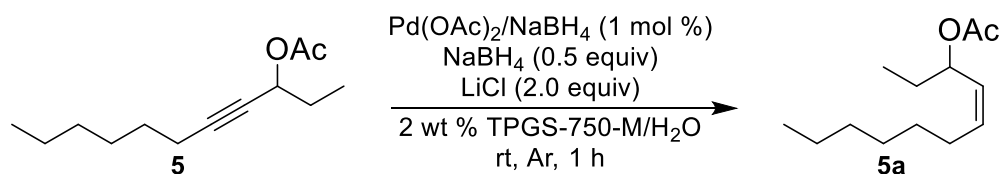
As mentioned previously, one parameter of the system that was sought after when developing this method was the potential for recycling the catalyst and aqueous solvent. Upon reaction completion, an in-flask extraction may be used for isolation of the alkene product. The choices of extraction solvent are those of low polarity such as hydrocarbons (e.g., hexanes) or ethereal solvents (Et₂O or MTBE). The use of these solvents is preferred over EtOAc, as leaching of the Pd into the organic phase is observed, thus removing recyclable catalyst from the reaction mixture and complicating subsequent purification. The partition between MTBE and the active catalyst mixture is shown in Figure 5. TPGS-750-M is essentially insoluble in all extraction solvents described, including EtOAc.



Figure 5. Extraction of product with MTBE from Black Water.

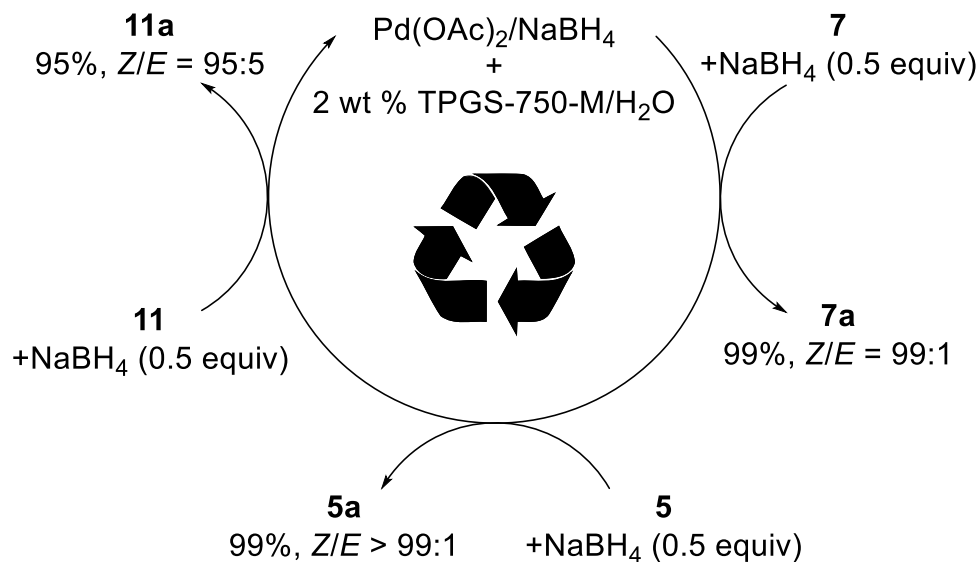
After isolation of the crude product via extraction, the remaining water, surfactant, LiCl, and palladium catalyst can be reused for subsequent reactions with the addition of fresh NaBH₄ (0.5 equiv) and substrate. The catalyst was found to be sensitive to air, and thus the extraction/recycle process is conducted under an inert atmosphere of Ar. This is easily

achieved by the use of cylindrical reaction vessels fitted with a septum, such as a microwave vial, with extracts being removed via syringe. Using this process, it was observed that the mixture could be recycled up to five times without effecting yield or stereo-chemical outcome (Table 3). In terms of organic waste, the minimal amount of solvent required for isolation results in an especially low E Factor⁵⁵ of 3.4, about five times lower than typical values of 25-100 associated with pharmaceutical processes. The flexibility of our recycling efforts can be further exploited by using the reaction mixture for various starting materials affording the expected results of high conversion and selectivity (Scheme 11).



entry	reaction	SM mass	theoretical yield	isolated yield	percent yield
1	A	500 mg	505 mg	458 mg	91%
2	B	500 mg	505 mg	478 mg	95%
3	C	500 mg	505 mg	464 mg	92%
4	D	500 mg	505 mg	494 mg	98%
5	E	500 mg	505 mg	468 mg	93%
6	F	500 mg	505 mg	480 mg	95%

Table 3. Recycle of surfactant, H₂O, LiCl, and Pd catalyst for the semi-reduction of **5** over six reactions.



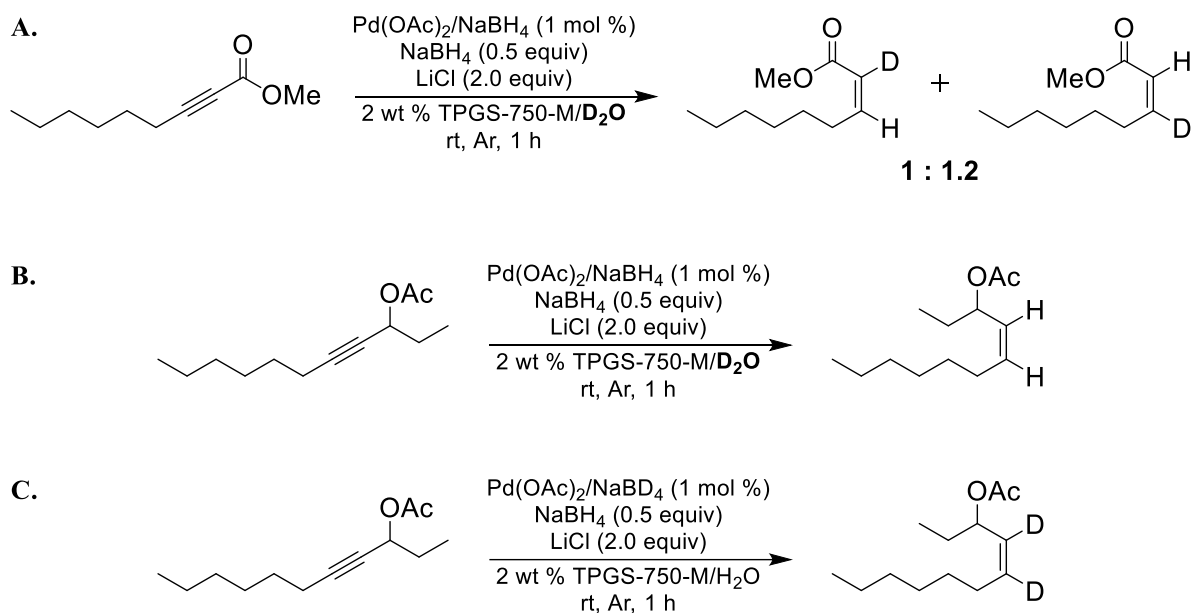
Scheme 11. Recycling Black Water with varying substrates.

Mechanistically, heterogeneous catalysis is often regarded as a “black box” as much is yet to be understood about the composition, structure, and pathway by which substrates are reduced. Initially, we had considered that the semi-reduction goes by means of a hydrogenation pathway, where the catalytic hydrolysis of NaBH₄ generates H₂ in situ which seeks preferential dissolution into the micellar core. This hypothesis was considered on the basis that the dissolution of gases, including H₂, is far greater in hydrocarbon solvent than in water (Table 4).⁵⁶ In addition, it is possible that H₂ is absorbed onto the surface of the catalyst. This hypothesis was further supported by deuterium studies on substrate **11**. Under otherwise standard conditions D₂O was used in place of H₂O showing only moderate site selectivity for hydride incorporation, with essentially a 1:2 ratio of enoate products containing one alkenyl deuterium (Scheme 12A). Electronically the β-carbon of the enoate would be preferred under a Pd-H mechanism, and the lack of site preference supports the scrambling of H-D on the surface of the catalyst followed by a *cis*-mode of addition. These

results were intriguing, as the reduction procedure is conducted under flow of argon, which should purge the system of any residual H₂. Furthermore, it should be noted that during catalyst activation rapid evolution of gas is observed, while no effervescence is observed upon addition of the NaBH₄ to the reaction in the presence of the alkyne starting material. This reduction pathway is further complicated by additional deuterium studies on the non-conjugated alkyne **4** under the same conditions. Interestingly, no deuterium incorporation was observed (Scheme 12B), suggesting that both hydrides were delivered from NaBH₄ without participation by water, supporting a Pd-H mechanism. Under conditions where NaBD₄ was employed with H₂O, complete deuterium incorporation was observed (Scheme 12C). Thus, it is likely that two pathways for this semi-reduction may be possible, which is remarkable considering the exceptional *Z*-selectivity found for both substrates.

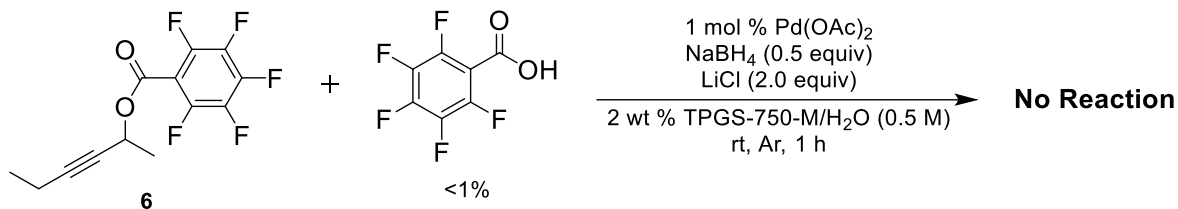
	H ₂		O ₂	
	Solubility (M)	M _{org} /M _{aq}	Solubility (M)	M _{org} /M _{aq}
H ₂ O	7.83 x 10 ⁻⁴	-	1.28 x 10 ⁻³	-
<i>n</i> -Hexane	8.27 x 10 ⁻³	10.6	2.38 x 10 ⁻²	18.6
<i>n</i> -Octane	5.92 x 10 ⁻³	7.6	1.86 x 10 ⁻²	14.5
<i>n</i> -Decane	4.73 x 10 ⁻³	6.0	1.53 x 10 ⁻³	12.0
Toluene	3.42 x 10 ⁻³	4.4	1.00 x 10 ⁻³	7.9

Table 4. Solubility of H₂ and O₂ in water and organic solvents.



Scheme 12. A. Semi-reduction of **11** in D_2O ; B. Semi-reduction of **5** in D_2O ; C. Semi-reduction of **5** with $NaBD_4$.

The developed method addresses many of the safety and environmental concerns associated with hydrogenation by considering parameters such as benign solvents, relatively inexpensive and readily available catalyst materials, recycling capabilities of the majority of the reaction components, and operational simplicity while delivering exceptional *Z*-selectivity in excellent yields within short reaction times at room temperature. The advances made by this newly developed method are highly general, yet limitations have been observed. For example, carboxylic acids have been shown to completely shut down reactivity of the catalyst. In one case, it was observed that a trace acid impurity present in a starting material (**6**) led to no conversion whatsoever, while the pure material yielded the *Z*-alkene nearly quantitatively (Scheme 13). Poor chemoselectivity was also noted for ynones as well as substrates bearing nitroarenes which give a complex mixture of products under these conditions.



Scheme 13. Acid sensitivity of Black Water semi-reductions.

2.4 Summary and Conclusions

In conclusion, a heterogeneous catalyst has been developed from Pd(OAc)₂ and NaBH₄ for the highly selective and general semi-reduction of alkynes under aqueous micellar catalysis conditions.⁵⁷ To our knowledge, this is the first report of a semi-reduction in the absence of organic solvent, and is a great improvement over some of the most widely used egregious solvents associated with this transformation (e.g., 1,4-dioxane, DMF).² The interactions between metal and micellar nanoparticles in water has been used to synthetic advantage, enabling development of new technology that provides a broadly applicable solution to the problem of alkyne semi-reductions, including disubstituted, terminal, and conjugated systems. Major consideration is taken on the basis of environmental sustainability which is exemplified by the recyclability of the water, surfactant, catalyst, and LiCl additive. Furthermore, organic waste resulting from isolation of the product olefin is minimized as proven by the low E Factor of 3.4.

This work represents the first example of heterogeneous catalysis under aqueous micellar conditions in our group and has since led to an expanding portfolio of projects. Since the communication of this work in *Angewante Chemie* (International Edition) in 2014, several other methods have been published based on heterogeneous systems including nitro-group reductions^{49,50} and Suzuki-Miyaura cross-couplings.⁵⁸ Forthcoming work from the Lipshutz

group includes aza-click chemistry catalyzed by Cu/Fe nanoparticles as well as several other heterogeneous systems for reduction chemistry.

2.5 Experimental Procedures

General Information

A solution of 2 wt % TPGS-750-M/H₂O solution was prepared by dissolving TPGS-750-M in degassed HPLC grade water and was stored under argon. TPGS-750-M was made as previously described⁵⁹ and is available from Sigma-Aldrich (catalog #733857). All commercially available reagents were used without further purification. Thin layer chromatography (TLC) was done using Silica Gel 60 F₂₅₄ plates (Merck, 0.25 mm thick). Flash chromatography was done in glass columns using Silica Gel 60 (EMD, 40-63 μm). GC-MS data was recorded on a 5975C Mass Selective Detector coupled with a 7890A Gas Chromatograph (Agilent Technologies). A capillary column (HP-5MS cross-linked 5% phenylmethyl-polysiloxanediphenyl, 30 m x 0.250 mm, 0.25 micron, Agilent Technologies) was employed. Helium was used as the carrier gas at a constant flow of 1 mL/min. ¹H and ¹³C NMR were recorded at 22 °C on a Varian UNITY INOVA at 500 MHz. Chemical shifts in ¹H NMR spectra are reported in parts per million (ppm) on the δ scale from an internal standard of residual CDCl₃ (7.27 ppm) or the central peak of DMSO-*d*₆ (2.50 ppm). Data are reported as follows: chemical shift, multiplicity (s = singlet, d = doublet, t = triplet, q = quartet, quin = quintet), integration, and coupling constant in Hertz (Hz). Chemical shifts in ¹³C chemical spectra are reported in ppm on the δ scale from the central peak of residual CDCl₃ (77.00 ppm) or the central peak of DMSO-*d*₆ (39.51 ppm). IR data were collected on a Perkin Elmer Spectrum Two UATR FT-IR Spectrometer and peaks were described according to relative intensity and resolution as follows: s = strong, m = medium, w = weak,

br = broad. Chiral HPLC data were collected using a Shimadzu LC-20AT Prominence liquid chromatograph coupled with Shimadzu SPD-M20A Prominence diode array detector. HPLC method ran at 1 mL/min using 10% v/v isopropanol/hexanes through a ChiralPAK[®] AD-H column.

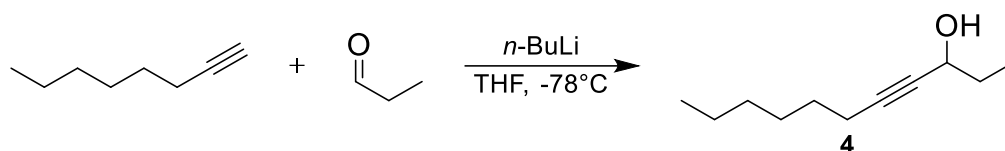
Metal Salt/Complex Screening Conditions

Condition A: To a H₂ purged microwave vial with Teflon coated stir bar, metal salt (1.0 mol %) was transferred followed by 2 wt % TPGS-750-M/H₂O (1.0 mL, 0.5 M) and 4-octyne (0.5 mmol). The vial was sealed and allowed to stir for ca. 1 h at 23 °C under a balloon of H₂.

Condition B: To an Ar purged microwave vial with Teflon coated stir bar, metal salt (1.0 mol %) was transferred followed by NaBH₄ (0.5 mol %) and the dry mixture was allowed to sonicate for 5 min prior to the addition of 2 wt % TPGS-750-M/H₂O (0.5 M) and 4-octyne (0.5 mmol). The vial was sealed and allowed to stir for ca. 1 h at 23 °C under a balloon of H₂.

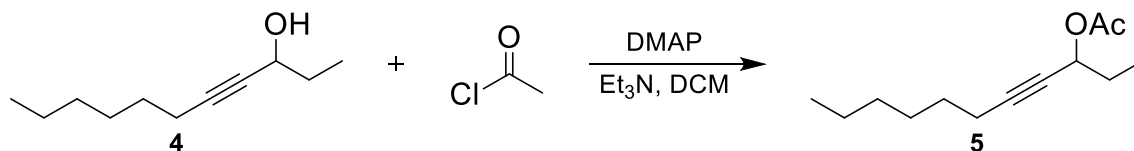
Condition C: To an Ar purged microwave vial with Teflon coated stir bar, metal salt (1.0 mol %) was transferred followed by NaBH₄ (0.5 mol %) and the dry mixture was allowed to sonicate for 5 mins prior to the addition of 2 wt % TPGS-750-M/H₂O (0.5 M) and 4-octyne (0.5 mmol). After stirring for ca. 10 min, the reaction was charged with NaBH₄ (1.0 equiv) and allowed to stir for ca. 1 h at 23 °C under Ar atmosphere.

Preparation of Substrates



Scheme 14. Preparation of undec-4-yn-3-ol, **4**.

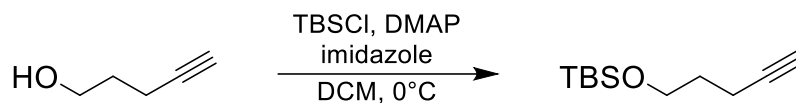
Undec-4-yn-3-ol (4). To an argon-purged oven-dried 250 mL round bottom flask with Teflon coated stir bar, 1-octyne (3.0 mL, 20.0 mmol) and dry THF (50 mL) were transferred. The mixture was stirred and maintained at -78°C as n -butyllithium (2.41 M in hexanes, 8.3 mL, 20.0 mmol) was added drop-wise. After stirring for 1 h, propionaldehyde (1.5 mL, 20.0 mmol) was added drop-wise and the reaction was allowed to come to rt. The aqueous phase was discarded and the organic phase was washed with NH_4Cl saturated water solution (2 x 50 mL), H_2O (50 mL), dried over anhydrous NaSO_4 , filtered, and evaporated under reduced pressure. Impurities were removed by distillation (50°C , 5 torr) to yield undec-4-yn-3-ol (2.61 g, 15.5 mmol) as a colorless oil (78%).



Scheme 15. Preparation of undec-4-yn-3-yl acetate, **5**.

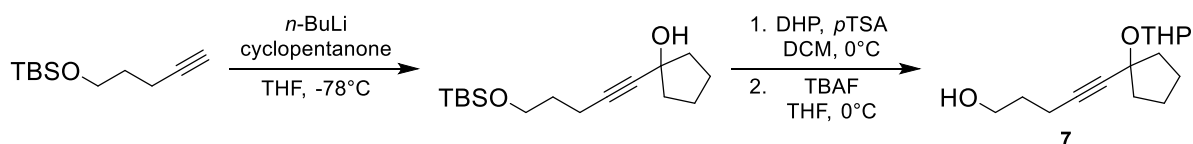
Undec-4-yn-3-yl acetate (5). To an argon-purged oven-dried 100 mL round bottom flask with Teflon coated stir bar, undec-4-yn-3-ol (0.82 g, 4.9 mmol), dry DCM (20 mL), DMAP (30.0 mg, 0.2 mmol), and triethylamine (1.4 mL, 9.8 mmol) were transferred. The

mixture was stirred and maintained at 0 °C under an argon atmosphere as acetyl chloride (0.5 mL, 7.3 mmol) was added drop-wise. The reaction continued to stir at 0 °C for 10 min and then at 23 °C for 30 min. The reaction was transferred to a separatory funnel and was washed with H₂O (3 x 50 mL), dried over anhydrous Na₂SO₄, filtered and condensed under reduced pressure. The crude product was purified by flash chromatography (1:19 EtOAc/hexanes) to yield undec-4-yn-3-yl acetate (0.77 g, 3.7 mmol) as a colorless oil (75%).



Scheme 16. *O*-TBS protection of 4-pentyn-1-ol.

5-(1-((Tetrahydro-2H-pyran-2-yl)oxy)cyclopentyl)pent-4-yn-1-ol. To an argon-purged oven-dried 100 mL round bottom flask with Teflon coated stir bar, 4-pentyn-1-ol (1.19 g, 17 mmol) and DCM (50 mL) was syringed to the flask. The cap was removed and to the flask DMAP (207 mg, 1.7 mmol) and imidazole (1.39 g, 20.4 mmol) were added. The cap and argon were then replaced and this was then cooled to 0 °C. The cap was removed and TBSCl (3.07 g, 20.37 mmol) was added to the flask as a solid and the cap and argon were replaced. Within 30 min the solution went to a hazy white. This was then allowed to warm to rt for 2 h. The crude material was then passed over Celite into a flask and the solvent was evaporated *in vacuo* until insoluble material appeared. This was then transferred to a separatory funnel and washed with NH₄Cl saturated water solution, extracted with hexanes, washed with brine, dried over anhydrous MgSO₄, and filtered. The filtrate was then concentrated under reduced pressure and purified by a silica plug eluting with hexanes to yield *t*-butyldimethyl(pent-4-yn-1-yloxy)silane (2.81 g, 18.36 mmol) of the desired protected alcohol as a colorless oil (90%).



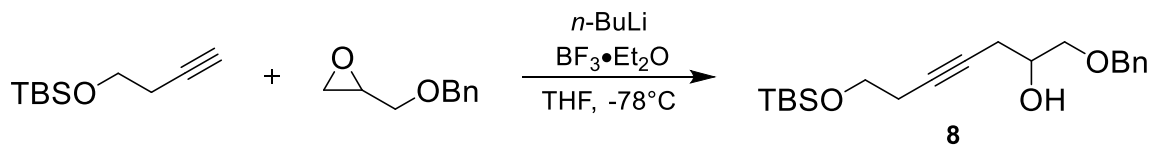
Scheme 17. Preparation of alkyne **7**.

5-(1-((Tetrahydro-2H-pyran-2-yl)oxy)cyclopentyl)pent-4-yn-1-ol (7). To an argon-purged oven-dried 100 mL round bottom flask with Teflon coated stir bar, *t*-butyldimethyl(pent-4-yn-1-yloxy)silane (2.5 g, 13.59 mmol) was syringed, followed by THF (35 mL). This was cooled to $-78\text{ }^{\circ}\text{C}$ and *n*-butyllithium (5.27 mL, 12.91 mmol, 2.45 M, 0.95 equiv) was syringed into the flask drop-wise over 10 min. The mixture was stirred at $-78\text{ }^{\circ}\text{C}$ for 1 h. Cyclopentanone (1.41 g, 12.91 mmol) was then syringed into the flask quickly. The solution went to a light yellow. This was allowed to warm to rt overnight, and then worked up with NH_4Cl saturated water solution, extracted with Et_2O , washed with brine, dried of anhydrous MgSO_4 and filtered. The filtrate was concentrated under reduced pressure and the crude material purified by column chromatography with (1:9 EtOAc/hexanes) to yield 1-(benzyloxy)-7-((*t*-butyldimethylsilyl)oxy)hept-4-yn-2-ol with sufficient purity for the following reaction.

To an argon-purged oven-dried 100 mL round bottom flask with Teflon coated stir bar, impure 1-(benzyloxy)-7-((*t*-butyldimethylsilyl)oxy)hept-4-yn-2-ol was transferred followed by DCM (27 mL). *p*-Toluenesulfonic acid (26 mg, 0.136 mmol) was then added to this and the mixture was cooled to $0\text{ }^{\circ}\text{C}$. Dihydropyran (2.28 g, 27.16 mmol) was then syringed in as one portion and left for 30 min to warm to rt. This was then quenched by a saturated solution of NaHCO_3 , extracted with Et_2O , washed with brine, dried over anhydrous MgSO_4 , filtered, and concentrated under reduced pressure. The isolated *t*-butyldimethyl((5-(1-((tetrahydro-

2H-pyran-2-yl)oxy)cyclopentyl)pent-4-yn-1-yl)oxy)silane as a crude oil was used as is for the next step.

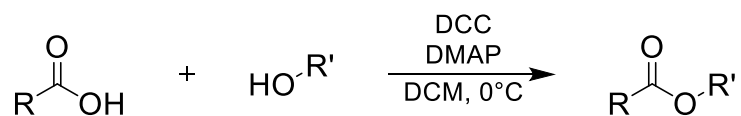
To an argon-purged oven-dried 100 mL round bottom flask with Teflon coated stir bar containing *t*-butyldimethyl((5-(1-((tetrahydro-2H-pyran-2-yl)oxy)cyclopentyl)pent-4-yn-1-yl)oxy)silane, THF (25 mL) was transferred followed by TBAF (4.26 g, 16.31 mmol, 1.2 equiv). The reaction was stirred for 30 min and then cooled to 0 °C before quenching with a few drops of 2 M HCl. This material was then extracted with Et₂O, washed with brine, dried over anhydrous MgSO₄, and filtered. The filtrate was concentrated under reduced pressure and then purified by column chromatography (1:4 EtOAc/hexanes) to yield pure 5-(1-((tetrahydro-2H-pyran-2-yl)oxy)cyclopentyl)pent-4-yn-1-ol (2.0 g, 7.94 mmol) as a colorless oil (62% over 3 steps).



Scheme 18. Preparation of alkyne **8**.

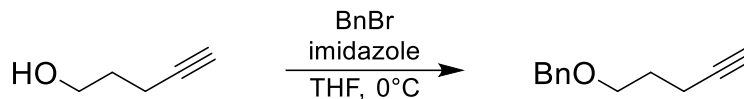
1-(Benzyloxy)-7-((*t*-butyldimethylsilyl)oxy)hept-4-yn-2-ol (8). To an oven-dried 25 mL round bottom flask with Teflon coated stir bar, purged with argon, (but-3-yn-1-yloxy)(*t*-butyl)dimethylsilane (1.68 g, 9.14 mmol) and THF (5 mL) were transferred. The reaction was then cooled to -78 °C and *n*-butyllithium (2.86 mL, 6.86 mmol, 2.4 M) was added followed by 2-((benzyloxy)methyl)oxirane (0.75 g, 4.57 mmol), and then BF₃·Et₂O (0.644 g, 4.57 mmol), after which a bright orange color was observed. The reaction continued to stir at -78 °C for 1 h and was then allowed to slowly warm to 0 °C and left at 0 °C for 1 h. This was then quenched at 0 °C with saturated NH₄Cl, extracted with ether, washed by brine,

dried over anhydrous MgSO_4 , and filtered. The filtrate was concentrated under reduced pressure and the crude material then purified by flash chromatography (15:85 Et_2O /hexanes) to yield 1-(benzyloxy)-7-((*t*-butyldimethylsilyl)oxy)hept-4-yn-2-ol (1.05 g, 2.87 mmol) as a colorless oil (63%).



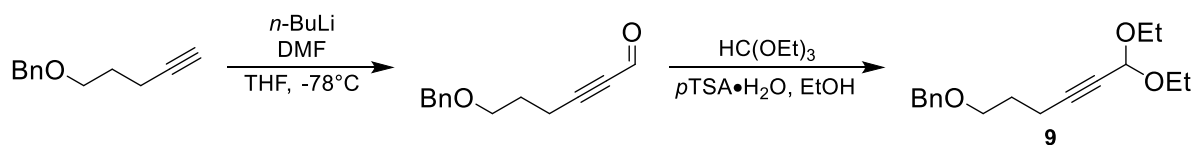
Scheme 19. General DCC coupling conditions for preparation of substrates **6**, **13**, **14**, **15**, **16**, and **17**.

General procedure for DCC coupling products.⁶⁰ To an argon-purged oven-dried 25 mL round bottom flask with Teflon coated stir bar, carboxylic acid (5.0 mmol), dry DCM (5.0 mL), alcohol (7.5 mmol), and DMAP (30.5 mg, 0.25 mmol) were transferred. The mixture was stirred and maintained at 0 °C as DCC (1.3 g, 6.5 mmol) was added all at once. The reaction continued to stir at 0 °C for 5 min and then at 23 °C for 3 h. The contents were vacuum filtered and the filtrate was concentrated under reduced pressure. The crude was dissolved in DCM (30 mL) and washed with 1 M HCl solution in water (2 x 25 mL), NaHCO_3 saturated water solution (2 x 30 mL), dried over anhydrous Na_2SO_4 , filtered, and concentrated under reduced pressure. The crude product was purified by flash chromatography on silica gel with a gradient eluent of hexanes and EtOAc.



Scheme 20. *O*-benzyl protection of 4-pentyn-1-ol.

((Pent-4-yn-1-yloxy)methyl)benzene. To an argon-purged, oven-dried 100 mL round bottom flask with Teflon coated stir bar, pent-4-yn-1-ol (1.69 g, 20.1 mmol), dry THF (20.0 mL), and imidazole (2.7 mg, 0.04 mmol) were transferred. The mixture was stirred and maintained at 0 °C as NaH (66% dispersion in mineral oil, 2.2 g, 60.4 mmol) was added all at once. After stirring for 10 min, benzyl bromide (4.13 g, 24.2 mmol) was added drop-wise. The reaction was allowed to come to rt overnight. The reaction was then transferred to a separatory funnel, washed with H₂O (2 x 50 mL), NH₄Cl saturated water solution (2 x 50 mL), and brine (50 mL), dried over anhydrous NaSO₄, filtered, and evaporated under reduced pressure. The crude product was purified by flash chromatography (1:99 EtOAc/hexanes) to yield ((pent-4-yn-1-yloxy)methyl)benzene (3.50 g, 20.1 mmol) as a colorless oil (99%).

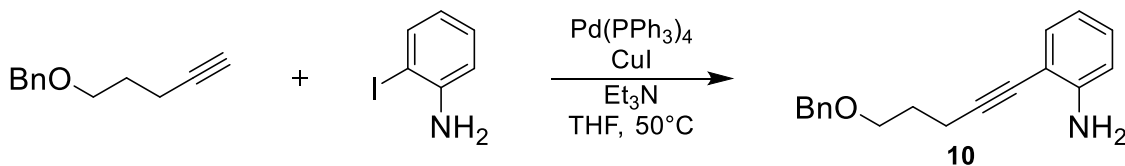


Scheme 21. Synthesis of **9** from ((pent-4-yn-1-yloxy)methyl)benzene.

((6,6-Diethoxyhex-4-yn-1-yl)oxy)methyl)benzene. To an argon purged oven-dried 250 mL round bottom flask with Teflon coated stir bar, ((pent-4-yn-1-yloxy)methyl)benzene (1.69 g, 9.7 mmol) and dry THF (25 mL) were transferred. The mixture was stirred and maintained at -78 °C as *n*-butyllithium (2.04 M in hexanes, 5.2 mL, 10.7 mmol) was added

drop-wise. After stirring for 1 h, DMF (1.5 mL, 19.4 mmol) was added all at once. The reaction was allowed to come to rt overnight. The solution was cannulated into a vigorously stirring biphasic solution prepared from KH_2PO_4 (52.5 mL, 38.9 mmol), and MTBE (38.9 mL) at 0 °C. The aqueous phase was removed and the organic phase was dried over anhydrous NaSO_4 , filtered, and evaporated under reduced pressure.⁶¹ The crude product was purified by flash chromatography (1:9 EtOAc/hexanes) to yield 6-(benzyloxy)hex-2-ynal (1.48 g, 7.3 mmol) as a colorless oil (75%).

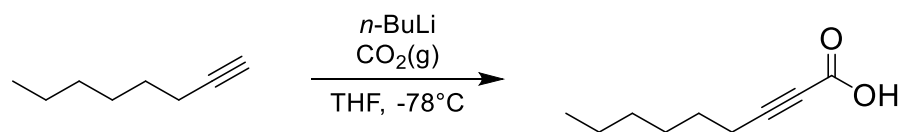
To an argon-purged oven-dried 100 mL round bottom flask with Teflon coated stir bar, 6-(benzyloxy)hex-2-ynal (1.06 g, 5.2 mmol), ethanol (52.0 mL), triethylorthoformate (1.0 mL, 6.3 mmol) and *p*-toluenesulfonic acid monohydrate (0.70 g, 3.7 mmol) were transferred. The reaction stirred at 23 °C for 1 h before quenching with 500 mg solid Na_2CO_3 . The mixture was then diluted in diethyl ether (50 mL) and washed with H_2O (50 mL), Na_2CO_3 saturated water solution (2 x 50 mL), and brine (50 mL), dried over anhydrous NaSO_4 , filtered, and evaporated under reduced pressure. The crude product was purified by flash chromatography (1:99 EtOAc/hexanes) to yield (((6,6-diethoxyhex-4-yn-1-yl)oxy)methyl)benzene (1.18 g, 4.3 mmol) as a colorless oil (83%).



Scheme 22. Synthesis of **10** by Sonogashira cross coupling.

2-(5-(Benzyloxy)pent-1-yn-1-yl)aniline. To an argon-purged oven-dried 25 mL round bottom flask with Teflon coated stir bar, 2-iodoaniline (0.52 g, 2.4 mmol), dry THF (4.8 mL), ((pent-4-yn-1-yl)oxy)methyl)benzene (0.46 g, 2.6 mmol), and triethylamine (1.5 mL,

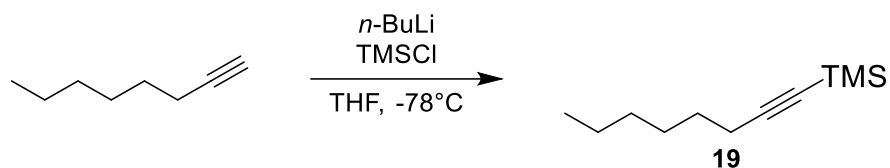
23.9 mmol) were transferred. An oven-dried water-jacketed reflux condenser was then affixed to the flask and the system was purged with argon several times. Pd(PPh₃)₄ (55.3 mg, 0.05 mmol) and CuI (4.6 mg, 0.02 mmol) were added and the reaction was allowed to stir at 50 °C overnight under an argon atmosphere. The mixture was then diluted with Et₂O (20 mL), washed with H₂O (2 x 25 mL) and NaHCO₃ saturated water solution (2 x 25 mL), dried over anhydrous Na₂SO₄, filtered, and evaporated under reduced pressure. The crude product was purified by flash chromatography (1:9 EtOAc/hexanes) to yield 2-(5-(benzyloxy)pent-1-yn-1-yl)aniline (0.49 g, 1.8 mmol) as a red oil (78%).



Scheme 23. ynoic acid synthesis.

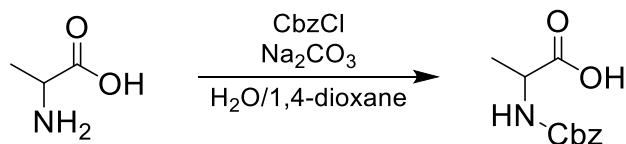
Non-2-ynoic acid.⁶² To an argon-purged oven-dried 250 mL round bottom flask with Teflon coated stir bar, 1-octyne (2.9 mL, 19.8 mol), and dry THF (50 mL) were transferred. The mixture was stirred and maintained at -78 °C as *n*-butyllithium (2.41 M in hexanes, 9.1 mL, 21.8 mmol) was added drop-wise. After stirring for 1 h, the temperature was increased to 0 °C. CO₂ was then bubbled through the reaction for 30 min as the flask was slowly brought to rt. The reaction was quenched with 1 M HCl solution in water (10 mL) at 0 °C and brought to rt. The aqueous phase was discarded and the product was extracted with 1 M NaOH solution in water (3 x 50 mL). The aqueous fractions were collected, acidified with conc HCl and then extracted with Et₂O (3 x 50 mL). The combined organic phase was dried over anhydrous NaSO₄, filtered, and evaporated under reduced pressure. The crude product

was distilled (170 °C, 2 torr) to yield undec-4-yn-3-ol (2.80 g, 18.2 mmol) as a colorless oil (92%).



Scheme 24. Synthesis of **19**.

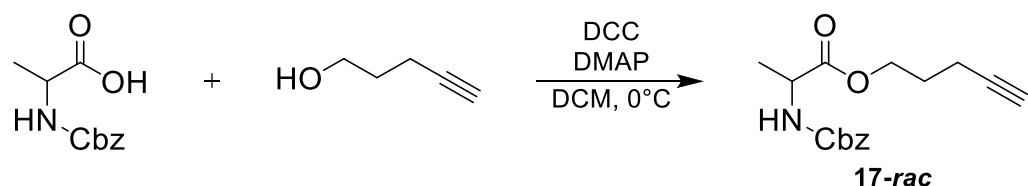
Trimethyl(oct-1-yn-1-yl)silane (19). To an argon-purged oven-dried 100 mL round bottom flask with Teflon coated stir bar, oct-1-yne (1.2 g, 10.9 mmol) and dry THF (27.2 mL) were transferred. The mixture stirred and maintained at -78 °C as *n*-butyllithium (2.4 M in hexanes, 5.0 mL, 12.0 mmol) was added dropwise. After stirring for 1 h, chlorotrimethylsilane (1.7 mL, 13.1 mmol) was added drop-wise and allowed to come to rt overnight. The reaction was quenched with NH₄Cl saturated water solution (10 mL) at 0 °C and brought to rt. The aqueous phase was discarded and the organic phase was washed with NH₄Cl saturated water solution (2 x 50 mL), dried over anhydrous Na₂SO₄, filtered, and evaporated under reduced pressure. The crude product was purified by flash chromatography (hexanes) to yield trimethyl(oct-1-yn-1-yl)silane (1.64 g, 9.0 mmol) as a yellow oil (83%).



Scheme 25. Cbz-protection of *DL*-alanine.

Pent-4-yn-1-yl ((benzyloxy)carbonyl)-*DL*-alaninate.⁶³ To an argon-purged oven-dried 50 mL round bottom flask with Teflon coated stir bar, *DL*-alanine (448.3 mg, 7.5 mmol),

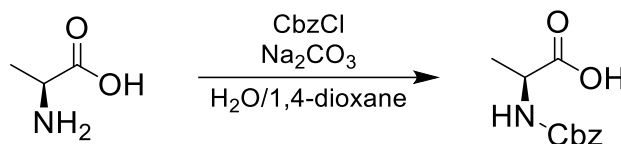
H₂O (16.8 mL), and Na₂CO₃ (1.6 g, 15.1 mmol) were transferred. The solution was stirred at 0 °C as benzyl chloroformate (1.0 g, 6.0 mmol) in 1,4-dioxane (4.8 mL) was transferred drop-wise over 30 min. The reaction continued to stir at 0 °C for 1 h and at 23 °C for 3 h. The contents were then diluted with diethyl ether (50 mL) and washed with 1 M HCl solution in H₂O (50 mL). The organic phase was collected and the aqueous solution was extracted with Et₂O (2 x 50 mL). The organic fractions were combined and were dried over anhydrous Na₂SO₄, filtered, and concentrated under reduced pressure to afford crude ((benzyloxy)carbonyl)-DL-alanine as white crystals with sufficient purity for the following reaction.



Scheme 26. Synthesis of **17-rac** HPLC standard for epimerization study.

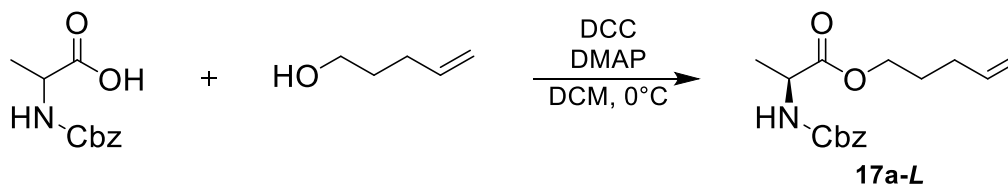
Pent-4-en-1-yl ((benzyloxy)carbonyl)-DL-alaninate (17-rac). To an oven-dried 25 mL round bottom flask with Teflon coated stir bar, argon was purged and pent-4-en-1-ol (635 mg, 7.5 mmol), dry DCM (5.0 mL), ((benzyloxy)carbonyl)-DL-alanine (1.1 g, 5.0 mmol), and DMAP (122.17 mg, 0.3 mmol) were transferred. The mixture was stirred and maintained at 0 °C as DCC (1.3 g, 6.5 mmol) was added all at once. The reaction was continued with stirring at 0 °C for 5 min and then at 23 °C for 3 h. The contents were then vacuum filtered and the filtrate was concentrated under reduced pressure. The crude was dissolved in DCM (25 mL) and washed with 1 M HCl solution in water (2 x 30 mL), NaHCO₃ saturated water solution (2 x 30 mL), dried over anhydrous Na₂SO₄, filtered and concentrated under reduced pressure. The crude product was purified by flash

chromatography (1:3 EtOAc/hexanes) to yield pent-4-en-1-yl ((benzyloxy)carbonyl)-DL-alaninate (1.06 g, 3.7 mmol) as a colorless oil (73%).



Scheme 27. Cbz-protection of *L*-alanine.

Pent-4-en-1-yl ((benzyloxy)carbonyl)-L-alaninate. To an argon-purged oven-dried 50 mL round bottom flask with Teflon coated stir bar, *L*-alanine (671.4 mg, 7.5 mmol), H₂O (25.1 mL), and Na₂CO₃ (2.4 g, 22.6 mmol) were transferred. The solution was stirred at 0 °C as benzyl chloroformate (1.4 g, 8.3 mmol) in 1,4-dioxane (6.6 mL) was transferred dropwise over 30 min. The reaction continued to stir at 0 °C for 1 h and at 23 °C for 3 h. The contents were then diluted with Et₂O (50 mL) and 1 M HCl solution in water (50 mL). The organic phase was collected and the aqueous solution was extracted with Et₂O (2 x 50 mL). The organic fractions were dried over anhydrous Na₂SO₄, filtered, and concentrated under reduced pressure to afford crude ((benzyloxy)carbonyl)-*L*-alanine as white crystals with sufficient purity for the following reaction.

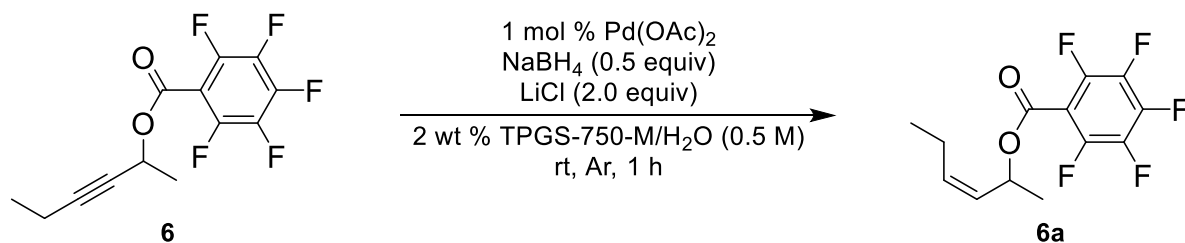


Scheme 28. Synthesis of **17a-L** HPLC standard for epimerization study.

Pent-4-en-1-yl ((benzyloxy)carbonyl)-L-alaninate (17a-L). To an argon-purged oven-dried 50 mL round bottom flask with Teflon coated stir bar, pent-4-en-1-ol (0.6 mL, 5.7

mmol), dry DCM, ((benzyloxy)carbonyl)-L-alanine (0.85 g, 3.8 mmol), and DMAP (23.3 mg, 0.2 mmol) were transferred. The mixture was stirred and maintained at 0 °C as DCC (1.02 g, 5.0 mmol) was added all at once. The reaction was continued with stirring at 0 °C for 5 min and then 23 °C for 3 h. The contents were then vacuum filtered and the filtrate was concentrated under reduced pressure. The crude was dissolved in DCM (50 mL) and washed with 1 M HCl solution in water (2 x 30 mL), NaHCO₃ saturated water solution (2 x 30 mL), dried over anhydrous Na₂SO₄, filtered, and concentrated under reduced pressure. The crude product was purified by flash chromatography (1:3 EtOAc/hexanes) to yield pent-4-en-1-yl ((benzyloxy)carbonyl)-L-alaninate (0.78 g, 2.7 mmol) as a colorless oil (71%).

Semi-Reduction Procedures



Scheme 29. General Semi-Reduction Conditions.

Optimized Reduction Procedure: To an oven-dried 20 x 70 mm microwave vial with Teflon coated stir bar, purged with argon, was transferred Pd(OAc)₂ (1.0 mg, 0.005 mmol) and NaBH₄ (0.9 mg, 0.025 mmol). The dry mixture was allowed to stir for 20 min after which fine black particles were observed. TPGS-750-M (2 wt %) solution in degassed HPLC grade water (0.9 mL) was then transferred drop-wise causing gas to evolve from the mixture. The mixture was vigorously stirred for an additional 20 min and then centrifuged resulting in a black suspension. The vial was then charged with hex-3-yn-2-yl 2,3,4,5,6-pentafluorobenzoate acetate (133.2 mg, 0.456 mmol) and vigorously stirred for 20 min

before the addition of LiCl (42.5 mg, 1.0 mmol) and NaBH₄ (9.5 mg, 0.25 mmol). A vent needle was then inserted into the septum allowing for argon to circulate over the reaction. After stirring 1 h at 23 °C, the reaction was worked up by extraction with EtOAc (3 x 2 mL), filtration through a plug of silica, and was concentrated under reduced pressure. The crude product was purified by flash chromatography (1:19 EtOAc/hexanes) to yield (Z)-hex-3-en-2-yl 2,3,4,5,6-pentafluorobenzoate (112.3 mg, 0.436 mmol) as a colorless oil (97%).

Note: Best results were obtained when using NaBH₄ of very fine particle size, such as that obtained from Alfa Aesar (catalog #13432).

Preparation of Bulk Catalyst Suspension

To an oven-dried 25 mL round bottom flask with Teflon coated stir bar, purged with argon, was transferred Pd(OAc)₂ (12.8 mg, 0.057 mmol) followed by NaBH₄ (10.8 mg, 0.29 mmol). The dry mixture was sonicated under a balloon of argon for 60 min and fine black particles were observed. 2 wt % TPGS-750-M solution in degassed HPLC grade water (6.0 mL) was then transferred drop-wise causing gas to evolve from the mixture. Sonication continued for 30 min and then the remaining volume of 2 wt % TPGS-750-M solution (5.4 mL) was added. After 15 min, the mixture was removed from the sonication bath and allowed to stir vigorously. The mixture is observed as a black suspension. The catalyst suspension remains active for several weeks and should be kept under an inert atmosphere while vigorously stirring to retain good mixing.

Aqueous Surfactant Recycling Procedures

Reaction A. An Ar-purged, microwave vial with Teflon coated stir bar was charged with a premade catalyst suspension (as described previously), undec-4-yn-3-yl acetate **5** (0.5 g, 2.38 mmol) and LiCl (24 mg, 0.57 mmol). After stirring for 5 min under argon, NaBH₄ (46 mg, 1.19 mmol) was charged to the system and a vent needle was inserted into the septum

allowing for argon to circulate over the reaction. After stirring for ca. 1 h, the vent needle was removed and the product alkene (*Z*)-undec-4-en-3-yl acetate (**5a**) was extracted under Ar with 3 x 1.0 mL MTBE, passed through a plug of anhydrous Na₂SO₄, concentrated under reduced pressure, and purified via flash chromatography to yield 458 mg (91%).

Reaction B (1st Recycle). The remaining aqueous mixture was then charged with additional undec-4-yn-3-yl acetate **5** (0.5 g, 2.38 mmol) and LiCl (24 mg, 0.57 mmol). After stirring for 5 min under argon, NaBH₄ (46 mg, 1.19 mmol) was charged to the system and a vent needle was inserted into the septum allowing for argon to circulate over the reaction. After stirring for ca. 1 h, the vent needle was removed and the product alkene (*Z*)-undec-4-en-3-yl acetate (**5a**) was extracted under Ar with 3 x 1.0 mL MTBE, passed through a plug of anhydrous Na₂SO₄, concentrated under reduced pressure, and purified via flash chromatography to yield 478 mg (95%).

Reaction C (2nd Recycle). The remaining aqueous mixture was then charged with additional undec-4-yn-3-yl acetate **5** (0.5 g, 2.38 mmol) and LiCl (24 mg, 0.57 mmol). After stirring for 5 min under argon, NaBH₄ (46 mg, 1.19 mmol) was charged to the system and a vent needle was inserted into the septum allowing for argon to circulate over the reaction. After stirring for ca. 1 h, the vent needle was removed and the product alkene (*Z*)-undec-4-en-3-yl acetate (**5a**) was extracted under Ar with 3 x 1.0 mL MTBE, passed through a plug of anhydrous Na₂SO₄, concentrated under reduced pressure, and purified via flash chromatography to yield 464 mg (92%).

Reaction D (3rd Recycle). The remaining aqueous mixture was then charged with additional undec-4-yn-3-yl acetate **5** (0.5 g, 2.38 mmol) and LiCl (24 mg, 0.57 mmol). After stirring for 5 min under argon, NaBH₄ (46 mg, 1.19 mmol) was charged to the system and a vent needle was inserted into the septum allowing for argon to circulate over the reaction.

After stirring for ca. 1 h, the vent needle was removed and the product alkene (*Z*)-undec-4-en-3-yl acetate (**5a**) was extracted under Ar with 3 x 1.0 mL MTBE, passed through a plug of anhydrous Na₂SO₄, concentrated under reduced pressure, and purified via flash chromatography to yield 494 mg (98%).

Reaction E (4th Recycle). The remaining aqueous mixture was then charged with additional undec-4-yn-3-yl acetate **5** (0.5 g, 2.38 mmol) and LiCl (24 mg, 0.57 mmol). After stirring for 5 min under argon, NaBH₄ (46 mg, 1.19 mmol) was charged to the system and a vent needle was inserted into the septum allowing for argon to circulate over the reaction. After stirring for ca. 1 h, the vent needle was removed and the product alkene (*Z*)-undec-4-en-3-yl acetate (**5a**) was extracted under Ar with 3 x 1.0 mL MTBE, passed through a plug of anhydrous Na₂SO₄, concentrated under reduced pressure, and purified via flash chromatography to yield 468 mg (93%).

Reaction F (4th Recycle). The remaining aqueous mixture was then charged with additional undec-4-yn-3-yl acetate **5** (0.5 g, 2.38 mmol) and LiCl (24 mg, 0.57 mmol). After stirring for 5 min under argon, NaBH₄ (46 mg, 1.19 mmol) was charged to the system and a vent needle was inserted into the septum allowing for argon to circulate over the reaction. After stirring for ca. 1 hour, the vent needle was removed and the product alkene (*Z*)-undec-4-en-3-yl acetate (**5a**) was extracted under Ar with 3 x 1.0 mL MTBE, passed through a plug of anhydrous Na₂SO₄, concentrated under reduced pressure, and purified via flash chromatography to yield 480 mg, (95%).

E Factor Determination Procedure

An oven-dried, Ar-purged, 10 mL round bottom flask with Teflon coated stir bar was charged with Pd(OAc)₂ (5.3 mg, 0.024 mmol) and NaBH₄ (4 mg, 0.11 mmol). The flask was sealed with a septum and a balloon of argon was attached. The dry mixture was stirred for 5

min until all of the solids appeared as black aggregates. Degassed 2 wt % TPGS-750-M/H₂O (3.0 mL) was then charged to the solids and the mixture was allowed to stir for ca. 30 min at which point all bubbling had subsided. The remaining 2 wt % TPGS-750-M/H₂O (1.76 mL) was then added into the flask, washing down the sides of the vial into the black suspension mixture. Undec-4-yn-3-yl acetate (500 mg, 2.38 mmol) and LiCl (24 mg, 0.574 mmol) were then charged. After stirring for 5 min under argon, NaBH₄ (32 mg, 0.86 mmol) was charged to the system. The reaction stirred for ca. 1 h and the suspension turned from black to light gray. The product alkene (*Z*)-undec-4-en-3-yl acetate (**5a**) was then extracted with 3 x 0.68 mL MTBE, passed through a plug of anhydrous Na₂SO₄, concentrated under reduced pressure, and purified via flash chromatography to yield 446 mg, (89%).

E Factor Calculations (without water)

$$\text{E Factor} = (\text{Mass of Organic Waste}) / (\text{Mass of Product})$$

$$\text{Mass of Organic Waste} = (2.0 \text{ mL MTBE}) (0.740 \text{ g/mL}) = 1509.6 \text{ mg}$$

$$\text{Mass of Product} = 446 \text{ mg}$$

$$\text{E Factor} = (1509.6 \text{ mg}) / (446 \text{ mg}) = \mathbf{3.4}$$

E Factor Calculations (with water)

$$\text{E Factor} = (\text{Mass of Organic Waste} + \text{Aqueous Waste}) / (\text{Mass of Product})$$

$$\text{Mass of Water} = (4.76 \text{ mL}) (1.0 \text{ g/mL}) = 4760 \text{ mg}$$

$$\text{E Factor} = (1509.6 \text{ mg} + 4760 \text{ mg}) / (446 \text{ mg}) = \mathbf{14.1}$$

Deuterium Procedures

A 2 wt % solution of TPGS-750-M was made with D₂O in place of HPLC grade water. The catalyst solution was prepared according to the general “black water” procedure. To an oven-dried microwave vial with a Teflon coated stir bar, Pd(OAc)₂ (1.2 mg, 0.006 mmol) and NaBH₄ (2 mg, 0.053 mmol) were added. The mixture was then capped and an argon

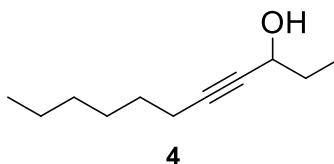
balloon was attached. The solids were then stirred for 30 min until the mixture went black. To this was added a 2 wt % solution of TPGS-750-M in D₂O. This was left for 2 h to stir leading to a black homogeneous-looking mixture. The cap was then removed and LiCl (48 mg, 1.19 mmol) was added. The vial was then capped and the argon flow returned. Then, methyl 2-octynoate, **11**, (100 mg, 0.595 mmol) was syringed into the flask. This was left for 5 min to allow the oil to homogenize. The vial was then opened again and NaBH₄ (11 mg, 0.29 mmol) was added in one portion. The vial was then capped and under argon, the reaction was maintained for 1 h. The crude material was then extracted by Et₂O and passed over anhydrous NaSO₄ and the solvent removed under vacuum. This resulted in incomplete conversion of the starting material to the product. Comparison of the alkene protons to the methyl ester showed a 1:1.2:3 ratio of the alkene protons and the methyl ester.

To an oven-dried microwave vial with Teflon coated stir bar, Pd(OAc)₂ (1.2 mg, 0.006 mmol) and NaBH₄ (2 mg, 0.053 mmol) were added. The vessel was then capped and an argon balloon was attached. The solids were then stirred for 30 min until the mixture went black. To this was added a 2 wt % solution of TPGS-750-M in D₂O. This was left for 2 h to stir leading to a black homogeneous-looking mixture. The cap was then removed and LiCl (48 mg, 1.19 mmol) was added to the solution. The vial was then capped and the argon flow returned. Then, methyl 2-octynoate (100 mg, 0.595 mmol) was syringed into the flask. This was left for 5 min to allow the oil to homogenize. Then the vial was opened again and NaBH₄ (11 mg, 0.29 mmol) was added as one portion. The vial was then capped and under argon the reaction was maintained for 1 h. The crude material was then extracted with Et₂O and passed over anhydrous NaSO₄ and the solvent removed under vacuum. This resulted in incomplete conversion of the starting material to the product. Comparison of the alkene

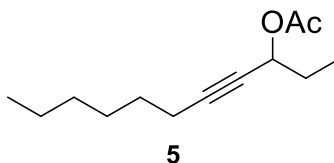
protons to the acyl methyl showed a 1:1:3 ratio of the alkene protons and the acyl methyl protons.

2.6 Compound Data

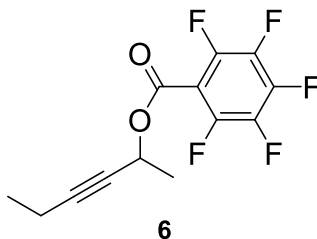
Characterization of Alkynes



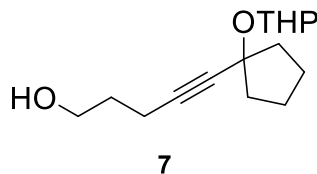
Undec-4-yn-3-ol (4). R_f 0.29 (1:3 Et₂O/hexanes); colorless oil, 2.61 g (78%). ¹H NMR (500 MHz, CDCl₃) δ 4.25 (m, 1H), 2.37 (s, 1H), 2.16 (td, 2H), 1.64 (m, 2H), 1.46 (quin, 2H), 1.37-1.30 (m, 2H), 1.30-1.21 (m, 4H), 0.95 (t, 3H), 0.85 (t, 3H); ¹³C NMR (125 MHz, CDCl₃) δ 85.28, 81.04, 63.72, 31.20, 31.06, 28.56, 28.39, 22.41, 18.53, 13.87, 9.32. IR (neat): 3342 (m, br), 2959 (m), 2930 (m), 2873 (m), 2859 (m), 2244 (w) cm⁻¹.



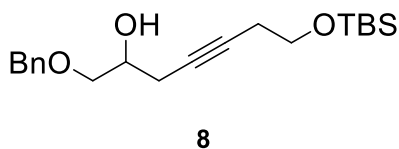
Undec-4-yn-3-yl acetate (5). R_f 0.20 (1:19 Et₂O/hexanes); colorless oil, 0.77 g (75%). ¹H NMR (500 MHz, CDCl₃) δ 5.31 (td, 1H), 2.21 (td, 2H), 2.08 (s, 3H), 1.75 (m, 2H), 1.50 (m, 2H), 1.41-1.23 (m, 6H), 1.00 (t, 3H), 0.89 (t, 3H); ¹³C NMR (125 MHz, CDCl₃) δ 169.97, 86.19, 77.33, 65.63, 31.20, 28.40, 28.38, 28.29, 22.44, 21.00, 18.60, 13.91, 9.27; IR (neat): 2931 (m), 2859 (m), 2251 (m), 1740 (s) cm⁻¹. HRMS (ESI, [C₁₃H₂₂O₂ + Na]⁺) calcd 233.1517, found m/z 233.1523.



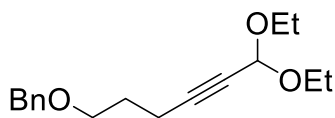
Hex-3-yn-2-yl 2,3,4,5,6-pentafluorobenzoate (6). R_f 0.29 (1:19 diethyl ether/hexanes); colorless oil, 1.02 g (78%). ^1H NMR (500 MHz, CDCl_3) δ 5.71 (qt, 1H, $J = 6.49, 2.08$ Hz), 2.24 (qd, 2H, $J = 7.53, 2.08$ Hz), 1.60 (d, 3H), 1.15 (t, 3H); ^{13}C NMR (125 MHz, CDCl_3) δ 158.07, 146.36, 144.30, 142.13, 138.67, 136.64, 88.29, 76.64, 63.78, 21.64, 13.45, 12.34. IR (neat): 2985 (m), 2941 (m), 2853 (m) 2249 (m), 1739 (s) cm^{-1} . HRMS (EI, $[\text{C}_{13}\text{H}_9\text{F}_5\text{O}_2]$) calcd 292.0523, found m/z 292.0531.



5-(1-((Tetrahydro-2H-pyran-2-yl)oxy)cyclopentyl)pent-4-yn-1-ol (7). R_f 0.20 (1:3 EtOAc/hexanes); colorless oil, 2.0 g (62%). ^1H NMR (500 MHz, CDCl_3) δ 5.04 (m, 1H), 3.93 (m, 1H), 3.75 (t, 2H, $J = 12.20, 5.97$) 3.51 (m, 1H) 2.34 (m, 2H), 2.00-1.64 (m, 13H), 1.52 (m, 3H); ^{13}C NMR (125 MHz, CDCl_3) δ . 96.21, 84.07, 82.59, 80.85, 63.25, 61.79, 41.24, 40.37, 32.01, 31.29, 25.44, 23.29, 22.86, 20.22 IR (neat): 3445 (b), 3065 (w) 2928 (s) 2856 (s) 1471 (s) cm^{-1} . HRMS (ESI, $[\text{C}_{15}\text{O}_3\text{H}_{24} + \text{Na}]^+$) calcd 275.1620, found m/z 275.1623.

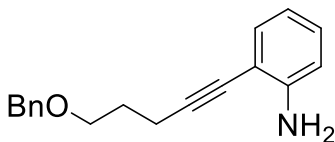


1-(Benzyloxy)-7-((*t*-butyldimethylsilyl)oxy)hept-4-yn-2-ol (8). R_f 0.10 (1:9 EtOAc/hexanes); colorless oil, 1.05 g (63%). $^1\text{H NMR}$ (500 MHz, CDCl_3) δ 7.34 (m, 5H), 4.57 (s, 2H), 3.92 (m, 1H), 3.681 (t, 2H), 3.60 (dd, 1H, $J = 13.43, 9.52, 3.91$ Hz), 3.490 (dd, 1H, $J = 16.12, 9.52, 6.59$), 2.42 (m, 2H), 2.37 (m, 2H), 0.90 (s, 9H), 0.07 (s, 6H); IR (neat): 3460 (br), 3032 (w), 2958 (s), 2927 (s), 2856 (s), 1471 (m), 1255 (s) cm^{-1} . HRMS (ESI, $[\text{C}_{20}\text{H}_{32}\text{O}_2\text{Si} + \text{Na}]^+$) calcd 371.2018, found m/z 371.2023.



9

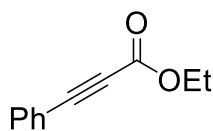
(((6,6-Diethoxyhex-4-yn-1-yl)oxy)methyl)benzene. R_f 0.40 (1:3 Et_2O /hexanes); colorless oil, 1.18 g (83%). $^1\text{H NMR}$ (500 MHz, CDCl_3) δ 7.37-7.32 (m, 4H), 7.30-7.26 (m, 1H), 5.25 (t, 1H, $J = 1.56$ Hz), 4.51 (s, 2H), 3.77-3.70 (m, 2H), 3.60-3.54 (m, 4H), 2.39 (td, 2H, $J = 7.27, 1.56$ Hz), 1.85 (m, 2H), 1.23 (t, 3H); $^{13}\text{C NMR}$ (125 MHz, CDCl_3) δ 138.32, 128.24, 127.46, 127.43, 91.34, 85.62, 75.93, 72.84, 68.65, 60.48, 28.44, 15.42, 15.00. IR (neat): 3030 (m), 2975 (m), 2928 (m), 2880 (m), 2238 (m), 17.12 (m), 1148 (s), 1102 (s), 1077 (s), 1049 (s), 1004 (s) cm^{-1} . HRMS (ESI, $[\text{C}_{17}\text{H}_{24}\text{O}_3 + \text{Na}]^+$) calcd 299.3658, found m/z 299.1626.



10

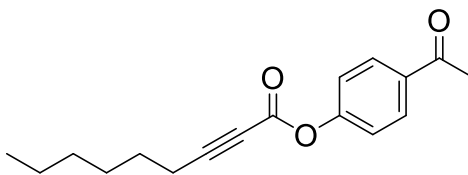
2-(5-(Benzyloxy)pent-1-yn-1-yl)aniline (10). R_f 0.49 (1:3 EtOAc/hexanes); red oil, 487.4 mg (78%). $^1\text{H NMR}$ (500 MHz, DMSO-d_6) δ 7.37-7.31 (m, 4H), 7.30-7.26 (m, 1H), 7.06 (dd, 1H), 7.00 (m, 1H), 6.66 (dd, 1H), 6.47 (dt, 1H), 5.19 (s, 2H), 4.49 (s, 2H), 3.56 (t,

2H), 2.53 (t, 2H), 1.83 (quin, 2H); ^{13}C NMR (125 MHz, DMSO- d_6) δ 149.26, 138.56, 131.42, 128.77, 128.21, 127.38, 127.32, 115.65, 113.54, 106.70, 94.49, 77.63, 71.84, 68.37, 28.61, 15.99. IR (neat): 3468 (m), 3372 (m), 3062 (m), 3029 (m), 2926 (m), 2857 (m) cm^{-1} . HRMS (EI, $[\text{C}_{18}\text{H}_{19}\text{NO}]^+$) calcd 265.1467, found m/z 265.1466.



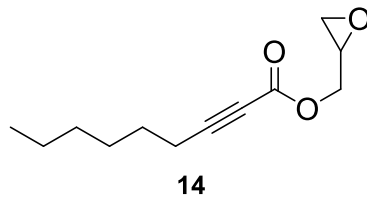
12

Ethyl 3-phenylpropiolate (12). R_f 0.31 (1:9 Et₂O/hexanes); colorless oil, 732.3 mg (95%). ^1H NMR (500 MHz, CDCl₃) δ 7.60-7.57 (m, 2H), 7.46-7.42 (m, 1H), 7.39-7.35 (m, 2H), 4.30 (q, 2H), 1.36 (t, 3H); ^{13}C NMR (125 MHz, CDCl₃) δ 154.03, 132.94, 130.58, 128.54, 119.64, 86.01, 80.71, 62.06, 14.07. IR (neat): 3060 (w), 2983 (m), 2938 (w), 2906 (w), 2235 (m), 2209 (m), 1703 (s) cm^{-1} .

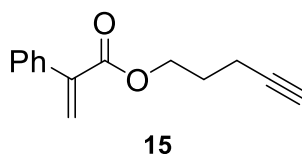


13

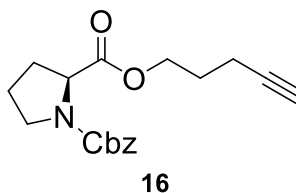
4-Acetylphenyl non-2-ynoate (13). R_f 0.19 (1:3 Et₂O/hexanes); colorless oil, 0.54 g (81%). ^1H NMR (500 MHz, CDCl₃) δ 8.00 (m, 2H), 7.24 (m, 2H), 2.59 (s, 3H), 2.40 (t, 2H), 1.62 (quin, 2H), 1.47-1.39 (m, 2H), 1.36-1.27 (m, 4H), 0.9 (t, 3H); ^{13}C NMR (125 MHz, CDCl₃) δ 196.64, 153.64, 151.19, 135.00, 129.94, 121.59, 93.10, 72.39, 31.12, 28.47, 27.31, 26.53, 22.39, 18.78, 13.95. IR (neat): 2954 (m), 2929 (m), 2859 (m), 1730 (s), 1686 (s) cm^{-1} . HRMS (ESI, $[\text{C}_{17}\text{H}_{20}\text{O}_3 + \text{Na}]^+$) calcd 295.1310, found m/z 295.1308.



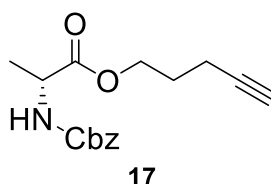
Oxiran-2-ylmethyl non-2-ynoate (14). R_f 0.16 (1:9 EtOAc/hexanes); colorless oil, 0.34 g (60%). ^1H NMR (500 MHz, CDCl_3) δ 4.44 (dd, 1H, 12.20, 3.37 Hz), 4.04 (dd, 1H, 12.20, 6.23 Hz), 3.25 (m, 1H), 2.87 (dd, 1H), 2.67 (dd, 1H, $J = 4.93, 2.60$ Hz), 2.35 (t, 2H), 1.62-1.56 (m, 2H), 1.44-1.38 (m, 2H), 1.36-1.25 (m, 4H), 0.90 (t, 3H); ^{13}C NMR (125 MHz, CDCl_3) δ 153.42, 90.90, 72.57, 66.05, 48.93, 44.74, 31.18, 28.50, 27.43, 22.44, 18.71, 13.99. IR (neat): $\nu = 2958$ (m), 2930 (m), 2860 (m), 2235 (m), 1712 (s), 1244 (s) cm^{-1} . HRMS (ESI, $[\text{C}_{12}\text{H}_{18}\text{O}_3 + \text{Na}]^+$) calcd 233.1154, found m/z 233.1165.



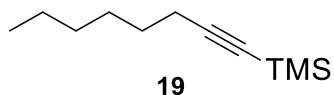
Pent-4-yn-1-yl 2-phenylacrylate (15). R_f 0.16 (1:9 Et_2O /hexanes); colorless oil, 671.0 mg (63%). ^1H NMR (500 MHz, CDCl_3) δ 7.46-7.43 (m, 2H), 7.40-7.33 (m, 3H), 6.38 (d, 1H, $J = 1.30$ Hz), 5.92 (d, 1H, $J = 1.30$ Hz), 4.36 (t, 2H), 2.32 (dt, 2H), 2.01 (t, 1H), 1.94 (quin, 2H); ^{13}C NMR (125 MHz, CDCl_3) δ 166.42, 141.20, 136.51, 128.10, 127.99, 127.91, 126.57, 82.75, 69.04, 63.41, 27.32, 15.11. IR (neat): 3290 (m), 3061 (w), 2960 (m), 2118 (w), 1731 (s), 1690 (m) cm^{-1} . HRMS (ESI, $[\text{C}_{14}\text{H}_{14}\text{O}_2]^+$) calcd 214.0994, found m/z 214.0988.



1-Benzyl 2-(pent-4-yn-1-yl) (S)-pyrrolidine-1,2-dicarboxylate (16). R_f 0.26 (1:3 EtOAc/hexanes); colorless oil, 1.20 g (76%). ^1H NMR (500 MHz, CDCl_3) δ 7.40-7.27 (m, 5H), 5.23-5.01 (m, 2H), 4.37 (ddd, 1H), 4.25 (m, 1H), 4.11 (m, 1H), 3.67-3.58 (m, 1H), 3.57-3.46 (m, 1H), 2.31-2.19 (m, 2H), 2.17 (dt, 1H), 2.05-1.94 (m, 2H), 1.94-1.84 (m, 2H), 1.72 (m, 1H); ^{13}C NMR (125 MHz, CDCl_3) δ 172.70, 172.52, 154.81, 154.24, 136.70, 136.55, 128.42, 128.38, 127.93, 127.86, 127.85, 82.95, 82.71, 69.11, 68.99, 66.97, 63.54, 63.46, 59.25, 58.88, 46.91, 46.39, 30.94, 29.92, 27.48, 27.30, 24.29, 23.50, 15.07, 14.98. IR (neat): 3289 (m), 3033 (w), 2956 (m), 2882 (m), 2118 (w), 1773 (s), 1700 (s) cm^{-1} . HRMS (ESI, $[\text{C}_{18}\text{H}_{21}\text{NO}_4 + \text{Na}]^+$) calcd 338.1368, found m/z 338.1380.

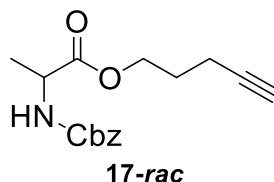


Pent-4-yn-1-yl ((benzyloxy)carbonyl)-D-alaninate (17). R_f 0.06 (1: 9 EtOAc/hexanes); colorless oil, 0.85 g (69%). ^1H NMR (500 MHz, DMSO-d_6) δ 7.76 (d, 1H), 7.44-7.27 (m, 5H), 5.03 (s, 2H), 4.14-4.03 (m, 3H), 2.82 (m, 1H), 2.20 (dt, 2H), 1.74 (quin, 2H), 1.27 (d, 3H); ^{13}C NMR (125 MHz, CDCl_3) δ 172.72, 155.45, 136.09, 128.22, 127.84, 127.82, 82.55, 69.08, 66.55, 63.62, 49.41, 27.10, 18.17, 14.81. IR (neat): 3295 (m, br), 3033 (m) 2938 (m), 2118 (m), 1709 (s) cm^{-1} . HRMS (ESI, $[\text{C}_{16}\text{H}_{21}\text{NO}_4 + \text{Na}]^+$) calcd 312.1212, found m/z 312.1205.



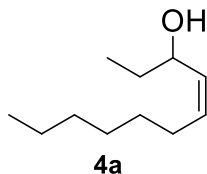
Trimethyl(oct-1-yn-1-yl)silane (19). R_f 0.51 (hexanes); yellow oil, 1.64 g (83%). ^1H NMR (500 MHz, CDCl_3) δ 2.22 (t, 2H), 1.52 (quin, 2H), 1.42-1.35 (m, 2H), 1.35-1.25 (m,

4H), 0.9 (t, 3H), 0.15 (s, 9H); ^{13}C NMR (125 MHz, CDCl_3) δ 107.78, 84.21, 31.27, 28.59, 28.45, 22.50, 19.85, 14.01, 0.17. IR (neat): 2958 (m), 2931 (m), 2860 (m), 2175 (m) cm^{-1} .

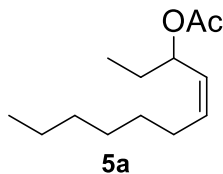


Pent-4-yn-1-yl ((benzyloxy)carbonyl)-DL-alaninate (17-rac). R_f 0.06 (1: 9 EtOAc/hexanes); colorless oil, 1.06 g (73%). ^1H NMR (500 MHz, CDCl_3) δ 7.38-7.30 (m, 5H), 5.39 (s, 1H) 5.11 (s, 2H), 4.39 (quin, 1H), 4.25 (t, 2H), 2.29 (m, 2H), 1.98 (t, 1H), 1.87 (quin, 2H), 1.42 (d, 2H); ^{13}C NMR (125 MHz, CDCl_3) δ 172.86, 155.53, 136.23, 128.46, 128.10, 128.04, 82.67, 69.17, 66.83, 63.88, 49.60, 27.29, 18.62, 15.04. IR (neat): 3296 (m, br), 3034 (w) 2941 (m), 2118 (w), 1714 (s) cm^{-1} .

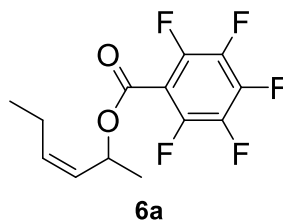
Characterization of Alkenes



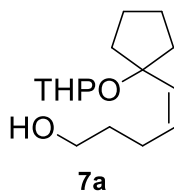
(Z)-Undec-4-en-3-ol (4a). R_f 0.22 (1:3 diethyl ether/hexanes); colorless oil, 86.9 mg (90%). ^1H NMR (500 MHz, CDCl_3) δ 5.50 (dtd, 1H, $J = 10.90, 0.78$ Hz), 5.35 (ddt, $J = 10.90, 8.82$ Hz), 4.35 (dtd, 1H, $J = 8.82, 0.78$ Hz), 2.08 (m, 2H), 1.62 (m, 1H), 1.46 (m, 1H), 1.39-1.23 (m, 9H), 0.92-0.87 (m, 6H); ^{13}C NMR (125 MHz, CDCl_3) δ 132.54, 132.22, 69.03, 31.66, 30.33, 29.66, 28.92, 27.70, 22.57, 14.03, 9.66. IR (neat): 3344 (m, br), 3006 (w), 2958 (m), 2924 (m), 2873 (m), 2855 (m), 1656 (w) cm^{-1} .



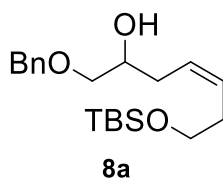
(Z)-Undec-4-en-3-yl acetate (5a). R_f 0.11 (1:19 Et₂O/hexanes); colorless oil, 105.3 mg (99%). ¹H NMR (500 MHz, CDCl₃) δ 5.5 (dtd, 1H, $J = 10.90, 0.78$ Hz), 5.47 (dtd, 1H, $J = 9.08, 0.78$ Hz), 5.28 (ddt, 1H, $J = 10.90, 9.08$ Hz), 2.20-2.06 (m, 2H), 2.02 (s, 3H), 1.67 (m, 1H), 1.53 (m, 1H), 1.39-1.23 (m, 8H), 0.88 (t, 6H); ¹³C NMR (125 MHz, CDCl₃) δ 170.33, 134.33, 127.71, 71.63, 31.67, 29.48, 28.92, 27.89, 27.76, 22.58, 21.27, 14.02, 9.40. IR (neat): 3013 (m), 2959 (m), 2926 (m), 2925 (m), 2873.2 (m), 1737 (s), 1652 (w) cm⁻¹. HRMS (EI, [C₁₃H₂₄O₂]) calcd 212.1776, found m/z 212.1785.



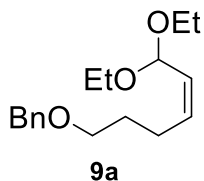
(Z)-Hex-3-en-2-yl 2,3,4,5,6-pentafluorobenzoate (6a). R_f 0.53 (1:19 Et₂O/hexanes); colorless oil, 112.3 mg (97%). ¹H NMR (500 MHz, CDCl₃) δ 5.94 (dq, 1H, $J=9.08, 6.49, 0.78$ Hz), 5.60 (dtd, 1H, $J = 10.90, 7.40, 0.78$ Hz), 5.42 (ddt, $J = 10.90, 9.08, 1.56$), 2.30-2.13 (m, 2H), 1.43 (d, 3H), 1.02 (t, 3H); ¹³C NMR (125 MHz, CDCl₃) δ 158.25, 146.16, 144.08, 141.91, 136.57, 136.17, 127.38, 70.21, 21.17, 20.75, 13.99. IR (neat): 2971 (m), 2936 (m), 2879 (m) 1736 (s), 1652 (w) cm⁻¹. HRMS (EI, [C₁₃H₁₁F₅O₂]) calcd 294.0679, found m/z 294.0686.



(Z)-5-(1-((Tetrahydro-2H-pyran-2-yl)oxy)cyclopentyl)pent-4-en-1-ol (7a). R_f 0.20 (1:3 EtOAc/hexanes); colorless oil, 98.0 mg (98%). ^1H NMR (500 MHz, CDCl_3) δ 5.74 (t, 1H, $J = 11.68, 3.37, 1.82$ Hz), 5.46 (dq, 1H, $J = 11.42, 8.04, 6.23$ Hz), 4.68 (m, 1H), 3.930 (m, 1H), 3.65 (t, 2H), 3.45 (m, 1H), 2.45-1.49 (m, 21H); ^{13}C NMR (125 MHz, CDCl_3) δ 133.76, 133.45, 95.92, 86.99, 63.72, 62.12, 39.76, 39.02, 32.55, 32.55, 34.39, 25.40, 25.18, 23.22, 22.94, 20.71. IR (neat): 3476 (br), 3016 (w), 2940 (s), 2867 (s), 1726 (w), 1440 (m), 1352 (m) cm^{-1} . HRMS (ESI, $[\text{C}_{15}\text{O}_3\text{H}_{26} + \text{Na}]^+$) calcd 277.1779, found m/z 277.1772.

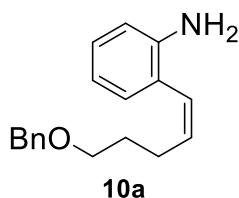


(Z)-1-(Benzyloxy)-7-((t-butyltrimethylsilyloxy)hept-4-en-2-ol (8a). R_f 0.12 (1:9 EtOAc/hexanes); colorless oil, 92.0 mg (91%). ^1H NMR (500 MHz, CDCl_3) δ 7.34 (m, 1H), 5.22 (m, 2H), 3.85 (m, 1H), 3.62 (t, 2H, $J = 14.88, 7.44$ Hz), 3.51 (dd, 1H, $J = 12.98, 9.34, 3.63$ Hz), 3.67 (dd, 1H, $J = 15.62, 10.04, 6.69$ Hz), 2.45 (d, 1H), 2.29 (m, 5H), 0.89 (s, 9H), 0.05 (s, 6H); ^{13}C NMR (125 MHz, CDCl_3) δ 138.03, 129.11, 128.43, 127.74, 126.51, 73.93, 73.39, 70.18, 62.74, 31.51, 31.08, 25.97, 18.41. IR (neat): 3460 (br), 3032 (w), 2958 (s), 2927 (s), 2856 (s), 1471 (m), 1255 (s) cm^{-1} . HRMS (ESI, $[\text{C}_{20}\text{H}_{34}\text{O}_2\text{Si} + \text{Na}]^+$) calcd 373.2157, found m/z 373.2175.

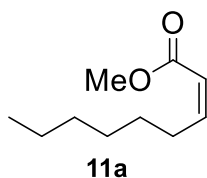


(Z)-(((6,6-Diethoxyhex-4-en-1-yl)oxy)methyl)benzene. R_f 0.33 (1:3 Et₂O/hexanes); colorless oil, 145.0 mg (99%). ^1H NMR (500 MHz, CDCl_3) δ 7.37-7.33 (m, 4H), 7.31-7.27

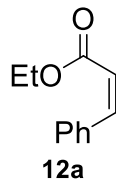
(m, 1H), 5.64 (dtd, 1H, $J = 11.16, 7.53, 1.04$ Hz), 5.51 (dtd, 1H, $J = 11.16, 6.75, 1.04$), 5.22 (dd, 1H, $J = 6.75, 1.04$ Hz), 4.51 (s, 2H), 3.65 (m, 2H), 3.51 (m, 4H), 2.27 (qd, 2H, $J = 7.53, 1.30$ Hz), 1.73 (quin, 2H), 1.22 (t, 6H); ^{13}C NMR (125 MHz, CDCl_3) δ 138.51, 133.85, 128.29, 127.86, 127.52, 127.45, 97.58, 72.84, 69.54, 60.48, 29.40, 24.64, 15.27. IR (neat): $\nu = 3029$ (m), 2974 (m), 2928 (m), 2865 (m), 1682 (w), 1100 (s), 1051 (s) cm^{-1} . HRMS (ESI, $[\text{C}_{17}\text{H}_{26}\text{O}_3 + \text{Na}]^+$) calcd 301.1780, found m/z 301.1772.



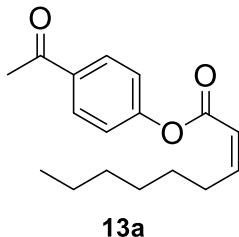
(Z)-2-(5-(Benzyloxy)pent-1-en-1-yl)aniline (10a). R_f 0.47 (1:3 EtOAc/hexanes); red oil, 104.0 mg (93%), ^1H NMR (500 MHz, DMSO-d_6) δ 7.35-7.24 (m, 5H), 6.96-6.92 (m, 2H), 6.65-6.62 (m, 1H), 6.49 (td, 1H), 6.29 (dt, 1H), 5.64 (dt, 1H, $J = 11.42$ Hz); ^{13}C NMR (125 MHz, DMSO-d_6) δ 145.99, 138.61, 131.61, 129.04, 128.14, 127.62, 127.37, 127.24, 125.80, 121.02, 115.49, 114.51, 111.03, 71.77, 69.07, 29.39, 24.96. IR (neat): 3465 (m), 3370 (m), 3061 (w), 3028 (m), 3002 (m), 2925 (m), 2854 (m), 1689 (m) cm^{-1} . HRMS (EI, $[\text{C}_{18}\text{H}_{21}\text{NO}]$) calcd 267.1623, found m/z 267.1616.



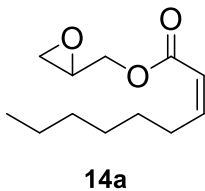
Methyl (Z)-non-2-enoate (11a). R_f 0.15 (3:97 EtOAc/hexanes); colorless oil, 91.0 mg (90%). ^1H NMR (500 MHz, CDCl_3) δ 6.22 (dt, 1H, $J = 14.90, 11.48, 7.57$ Hz), 5.76 (dt, 1H, $J = 11.48, 3.42, 1.71$ Hz), 3.70 (s, 3H), 2.64 (dq, 2H), 1.43 (m, 2H), 1.29 (m, 7H), 0.87 (t, 3H).



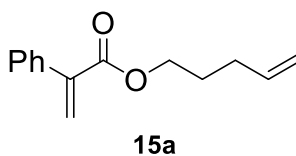
Ethyl (Z)-3-phenylacrylate (12a). R_f 0.33 (1:9 Et₂O/hexanes); colorless oil, 75.7 mg (82%), ¹H NMR (500 MHz, CDCl₃) δ 7.62-7.57 (m, 2H), 7.39-7.19 (m, 3H), 6.96 (d, 1H, J = 12.46 Hz), 5.96 (dd, 1H, J = 12.46, 0.78), 4.19 (qd, 2H), 1.26 (t, 3H); ¹³C NMR (125 MHz, CDCl₃) δ 166.20, 142.94, 134.87, 129.65, 128.94, 127.96, 119.88, 60.27, 14.07. IR (neat): 2977 (m), 2927 (m), 2855 (m), 1712 (s), 1631 (m) cm⁻¹.



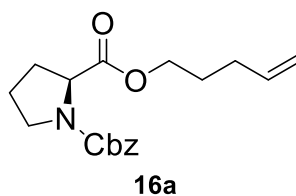
4-Acetylphenyl (Z)-non-2-enoate (13a). R_f 0.17 (1:3 Et₂O/hexanes); colorless oil, 117.3 mg (95%). ¹H NMR (500 MHz, CDCl₃) δ 8.03-8.00 (m, 2H), 7.25-7.22 (m, 2H), 6.49 (dt, 1H, J = 11.42, 7.53 Hz), 6.01 (dt, 1H, J = 11.42, 1.69 Hz), 2.72 (qd, 2H), 2.61 (s, 1H), 1.49 (quin, 2H), 1.39-1.26 (m, 6H), 0.89 (t, 3H); ¹³C NMR (125 MHz, CDCl₃) δ 196.89, 163.88, 154.61, 154.34, 134.56, 129.88, 121.87, 118.23, 31.58, 29.34, 28.98, 28.83, 26.60, 22.56, 14.05. IR (neat): 2958 (m), 2924 (m), 2853 (m), 1743 (m), 1687 (m), 1599 (m) cm⁻¹. HRMS (ESI, [C₁₇H₂₂O₃ + Na]⁺) calcd 297.1467, found m/z 297.1472.



Oxiran-2-ylmethyl (Z)-non-2-enoate (14a). R_f 0.41 (1:3 Et₂O/hexanes); colorless oil, yield 101.6 mg (95%). ¹H NMR (500 MHz, CDCl₃): δ 6.28 (dt, 1H, $J = 11.68, 7.53$ Hz), 5.80 (dt, 1H, $J = 11.68, 1.82$ Hz), 4.43 (dd, 1H, $J = 12.46, 3.11$ Hz), 3.98 (dd, 1H, $J = 12.46, 6.23$ Hz), 3.25-3.22 (m, 1H), 2.85 (dd, 1H, $J = 4.67, 4.15$ Hz), 2.68-2.63 (m, 3H), 1.47-1.41 (m, 2H), 1.37-1.25 (m, 6H), 0.88 (t, 3H); ¹³C NMR (125 MHz, CDCl₃) δ 165.89, 151.99, 118.73, 64.31, 49.42, 44.71, 31.59, 29.09, 28.93, 28.90, 22.53, 14.0. IR (neat): 2956 (m), 2926 (m), 2856 (m), 1721 (s), 1642 (m), 1242 (s) cm⁻¹. HRMS (ESI, [C₁₂H₂₀O₃ + Na]⁺) calcd 235.1310, found m/z 235.1319.

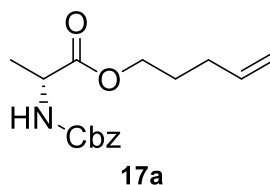


Pent-4-en-1-yl 2-phenylacrylate (15a). R_f 0.38 (1:9 Et₂O/hexanes); colorless oil, 97.3 mg (82%). ¹H NMR (500 MHz, CDCl₃) δ 7.45-7.42 (m, 2H), 7.39-7.32 (m, 3H), 6.37 (d, 1H, $J = 1.30$ Hz), 5.90 (d, 1H, $J = 1.30$ Hz), 5.83 (tq, 1H, $J = 17.13, 10.38, 6.75$ Hz), 5.06 (dq, $J = 17.13$ Hz), 5.01 (m, 1H, $J = 10.38$ Hz), 4.26 (t, 2H), 2.17 (m, 2H), 1.82 (quin, 2H); ¹³C NMR (125 MHz, CDCl₃) δ 166.76, 141.52, 137.39, 136.74, 128.27, 128.10, 128.04, 126.53, 115.33, 64.48, 30.10, 27.78. IR (neat): 3079 (m), 3026 (m), 2935 (m), 2851 (m), 1717 (s), 1641 (m), 1614 (m) cm⁻¹. HRMS (ESI, [C₁₄H₁₆O₂ + Na]⁺) calcd 239.1048, found m/z 239.1042.

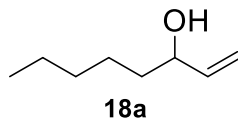


1-Benzyl 2-(pent-4-en-1-yl) (S)-pyrrolidine-1,2-dicarboxylate (16a). R_f 0.35 (1:3 EtOAc/hexanes); colorless oil, 155.3 mg (98%). ¹H NMR (500 MHz, CDCl₃) δ 7.38-7.26

(m, 5H), 5.76 (m, 1H), 5.20-5.06 (m, 2H), 5.06-4.95 (m, 2H), 4.36 (ddd, 1H), 4.15 (m, 1H), 4.00 (m, 1H), 3.66-3.58 (m, 1H), 3.56-3.45 (m, 1H), 2.28-2.16 (m, 1H), 2.12 (q, 1H), 2.05-1.84 (m, 5H), 1.74 (quin, 1H), 1.61 (quin, 1H); ^{13}C NMR (125 MHz, CDCl_3) δ 172.67, 172.49, 154.70, 154.17, 137.27, 137.11, 136.64, 136.48, 128.31, 128.25, 127.80, 127.78, 127.72, 127.67, 115.24, 115.23, 66.83, 66.82, 59.20, 58.84, 30.84, 29.83, 29.81, 29.74, 27.65, 27.53, 24.17, 23.38. IR (neat): 3066 (w), 3033 (w), 2954 (m), 2933 (m), 2890 (m), 2851 (m), 1743 (s), 1703 (s), 1641 (m) cm^{-1} . HRMS (ESI, $[\text{C}_{18}\text{H}_{23}\text{NO}_4 + \text{Na}]^+$) calcd 340.1525, found m/z 340.1525.

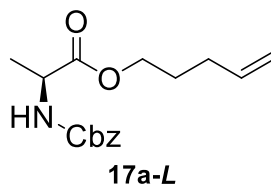


Pent-4-en-1-yl ((benzyloxy)carbonyl)-D-alaninate (17a). R_f 0.10 (1: 9 EtOAc/hexanes); colorless oil, 145.5 mg (96%). ^1H NMR (500 MHz, CDCl_3) δ 7.39-7.31 (m, 5H), 5.80 (m, 1H), 5.33 (d, 1H), 5.12 (s, 2H), 5.08-4.99 (m, 2H), 4.39 (quin, 1H), 4.16 (t, 2H), 2.13 (q, 2H), 1.76 (quin, 2H), 1.43 (d, 3H); ^{13}C NMR (125 MHz, CDCl_3) δ 172.96, 155.54, 137.15, 136.25, 128.48, 128.12, 128.06, 115.46, 66.85, 64.80, 49.64, 29.86, 27.62, 18.74. IR (neat): 3342 (m, br), 3066 (m), 3034 (m) 2939 (m), 1721 (s), 1641 (w) cm^{-1} . HRMS (ESI, $[\text{C}_{16}\text{H}_{21}\text{NO}_4 + \text{Na}]^+$) calcd 314.1368, found m/z 314.1373.



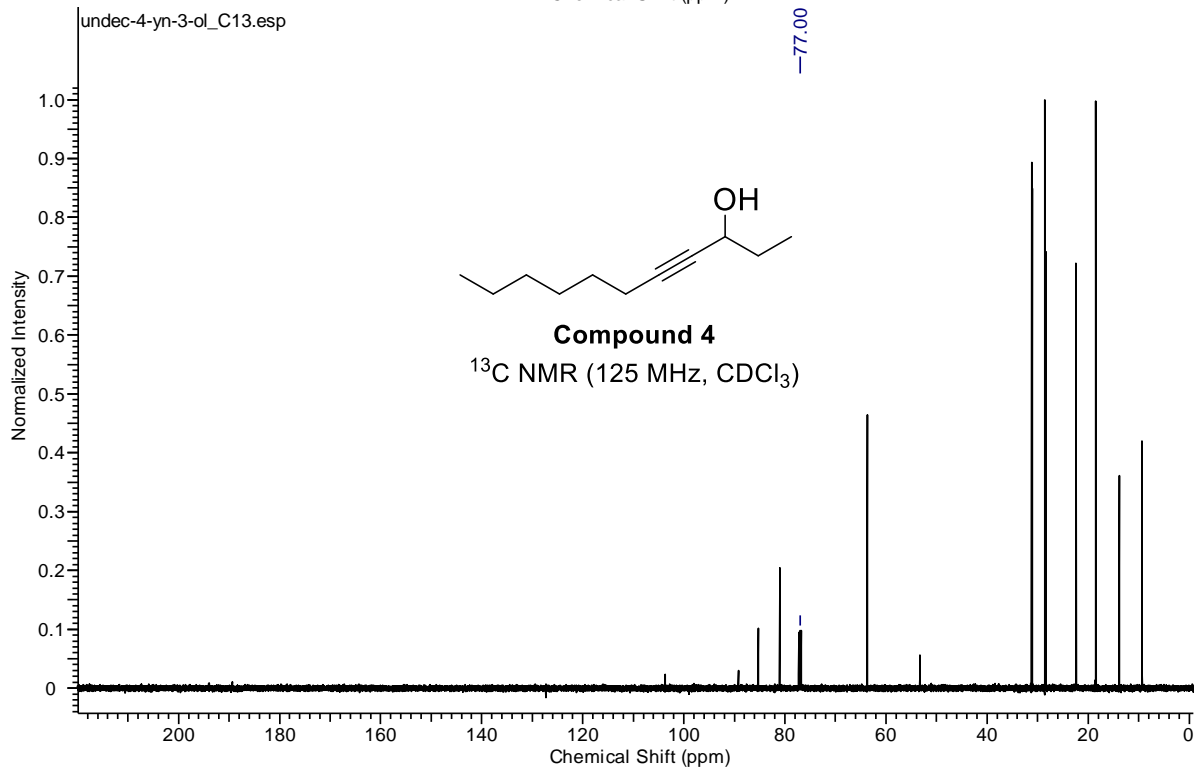
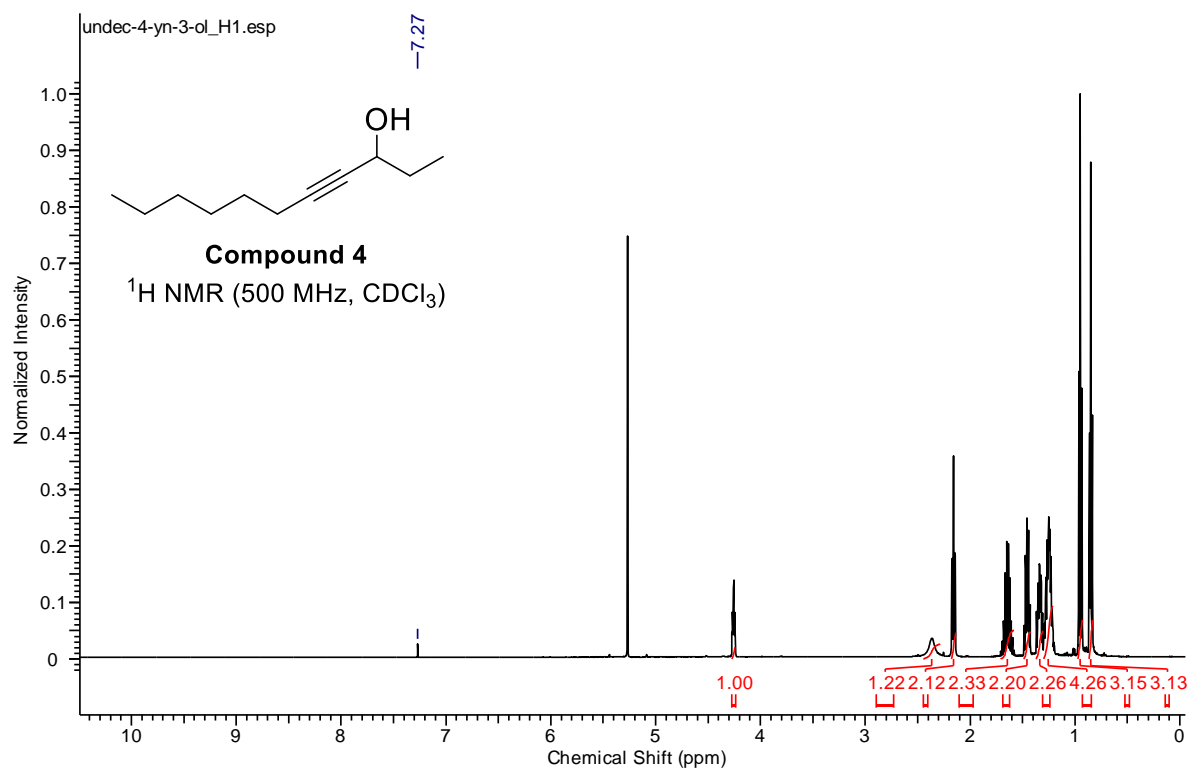
Oct-1-en-3-ol (18a). R_f 0.20 (5:95 Et_2O /hexanes); colorless oil, 91.0 mg (90%). ^1H NMR (500 MHz, CDCl_3) δ 5.857 (m, 1H), 5.21 (d, $J = 16.00$ 1H), 5.09 (d, 2H, $J = 10.43$),

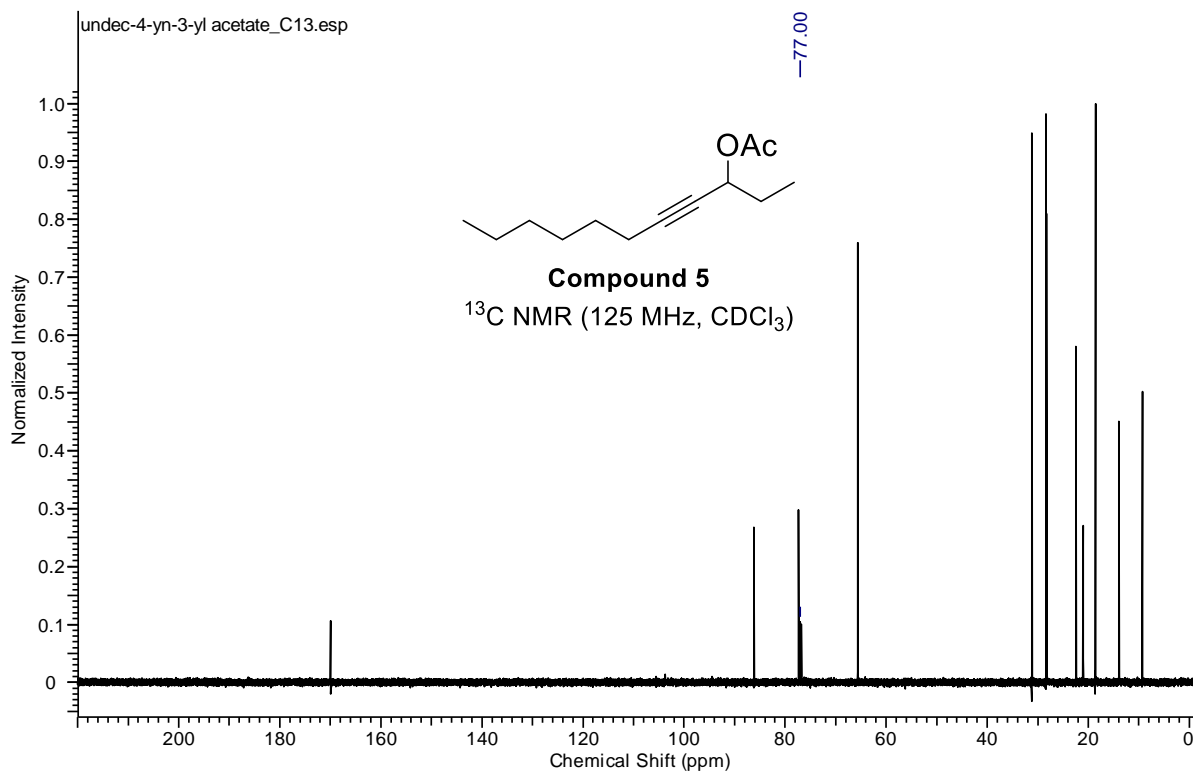
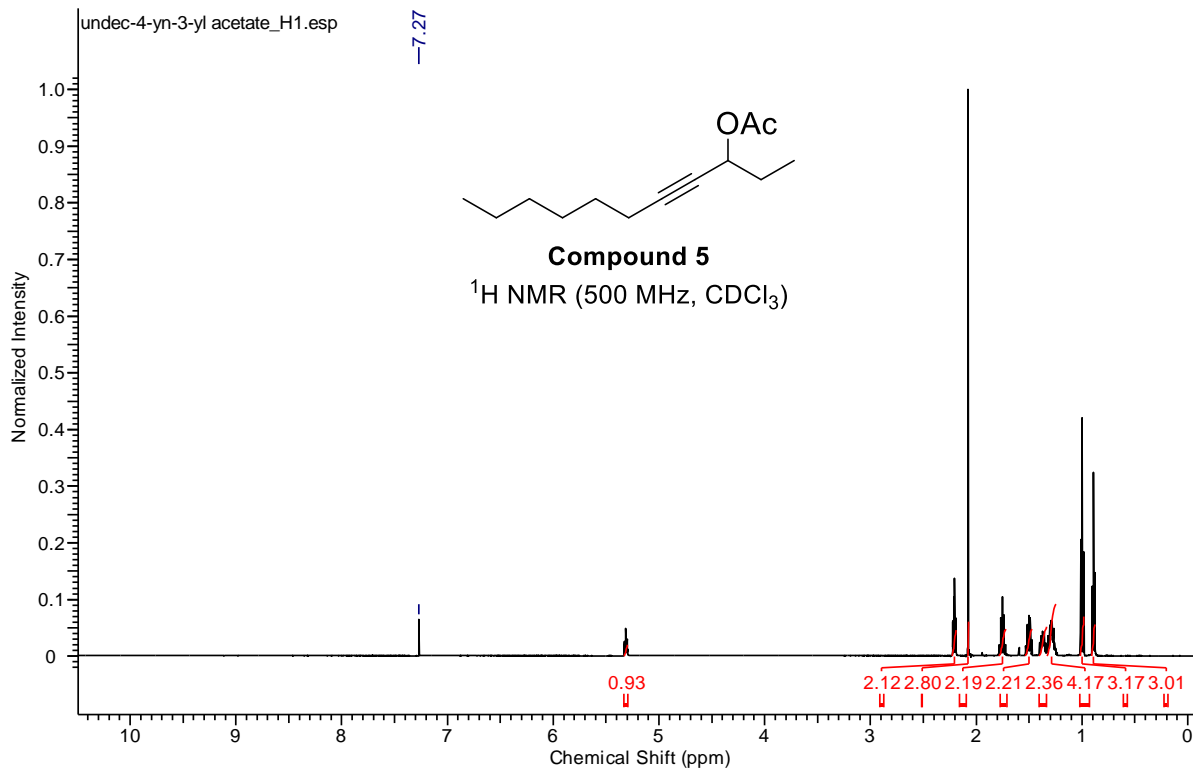
1.43 (quin, 1H $J = 23.30, 17.04, 11.48, 5.91$), 1.59-1.25 (m, 10H), 0.88 (t, $J = 13.91, 6.96$ 3H).

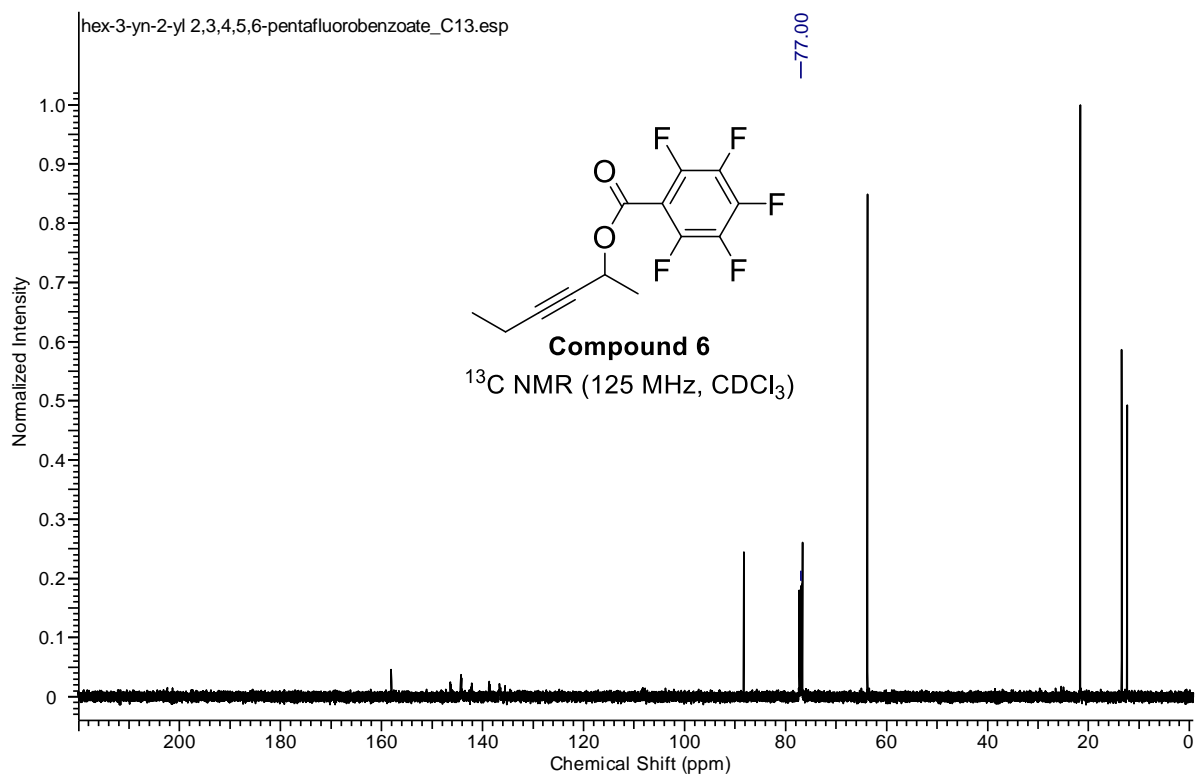
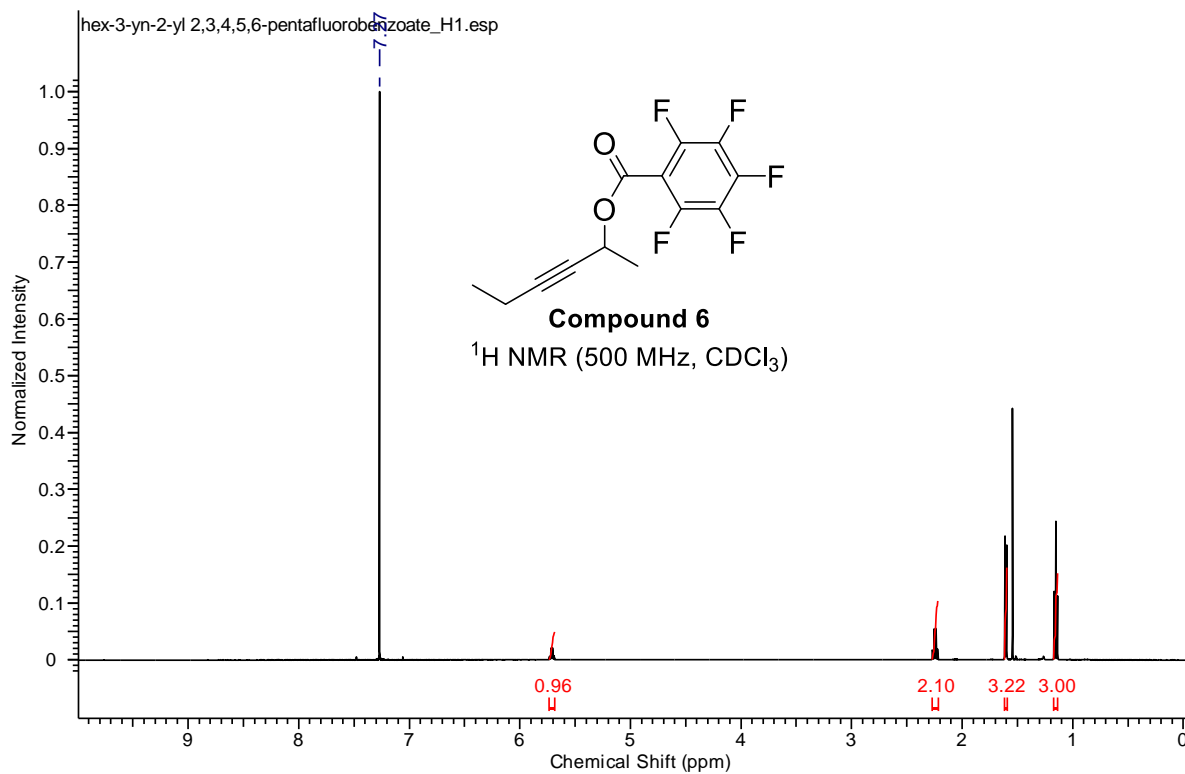


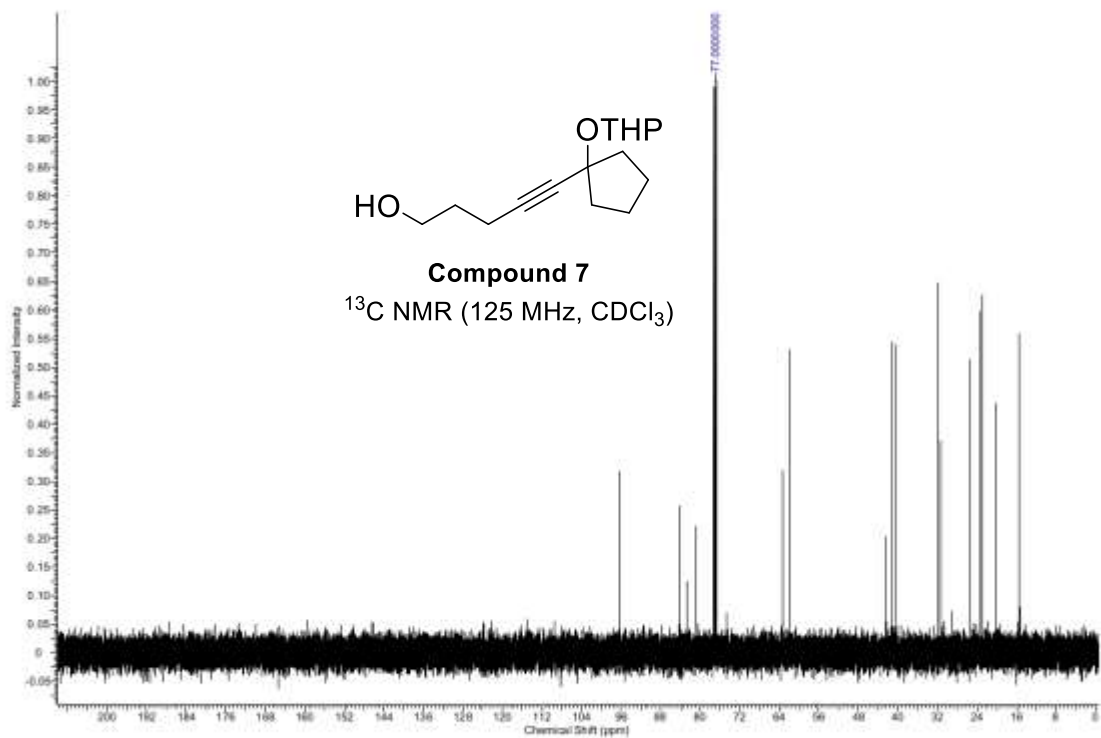
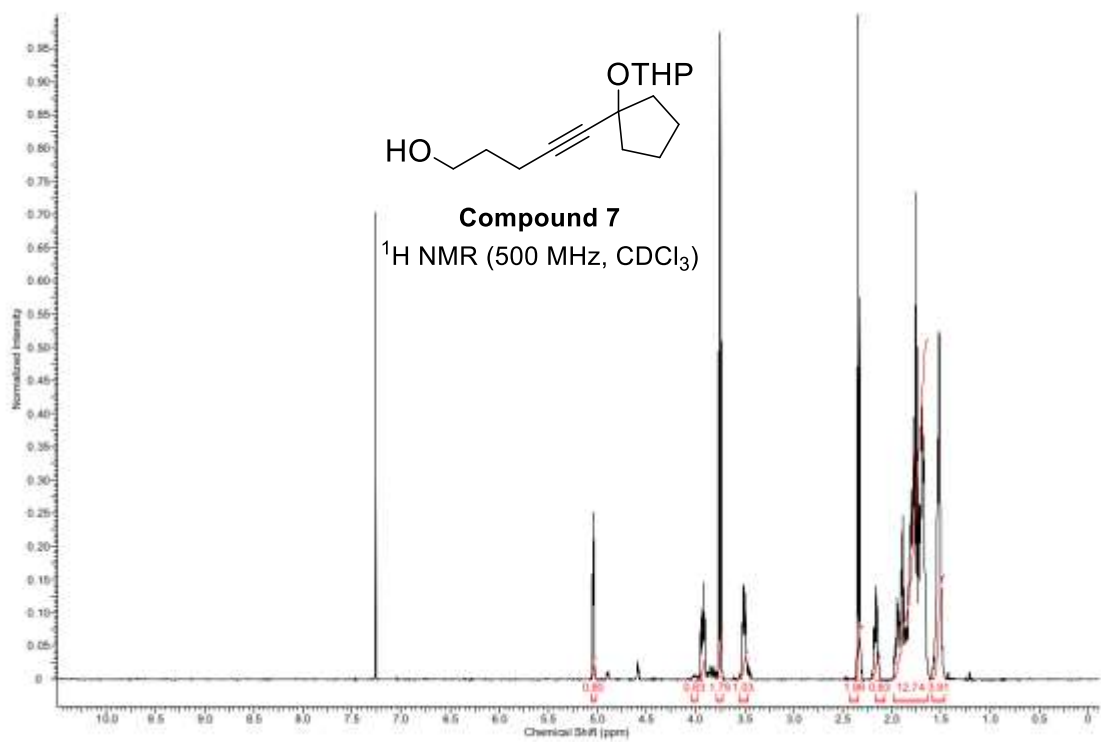
Pent-4-en-1-yl ((benzyloxy)carbonyl)-L-alaninate (17a-L). R_f 0.10 (1: 9 EtOAc/hexanes); colorless oil, 0.78 g (71%). ^1H NMR (500 MHz, CDCl_3) δ 7.38-7.29 (m, 5H), 5.79 (m, 1H), 5.44 (s, 1H), 5.11 (s, 2H), 5.07-4.99 (m, 2H), 4.39 (quin, 1H), 4.16 (t, 2H), 2.12 (q, 2H), 1.75 (quin, 2H), 1.42 (d, 3H); ^{13}C NMR (125 MHz, CDCl_3) δ 172.92, 155.52, 137.10, 136.22, 128.41, 128.04, 127.99, 115.39, 66.76, 64.71, 49.58, 29.80, 27.56, 18.60. IR (neat): 3341 (br m), 3066 (m), 3034 (m) 2923 (m), 1713 (s), 1641 (w) cm^{-1} . HRMS (ESI, $[\text{C}_{16}\text{H}_{21}\text{NO}_4 + \text{Na}]^+$) calcd 314.1368, found m/z 314.1371.

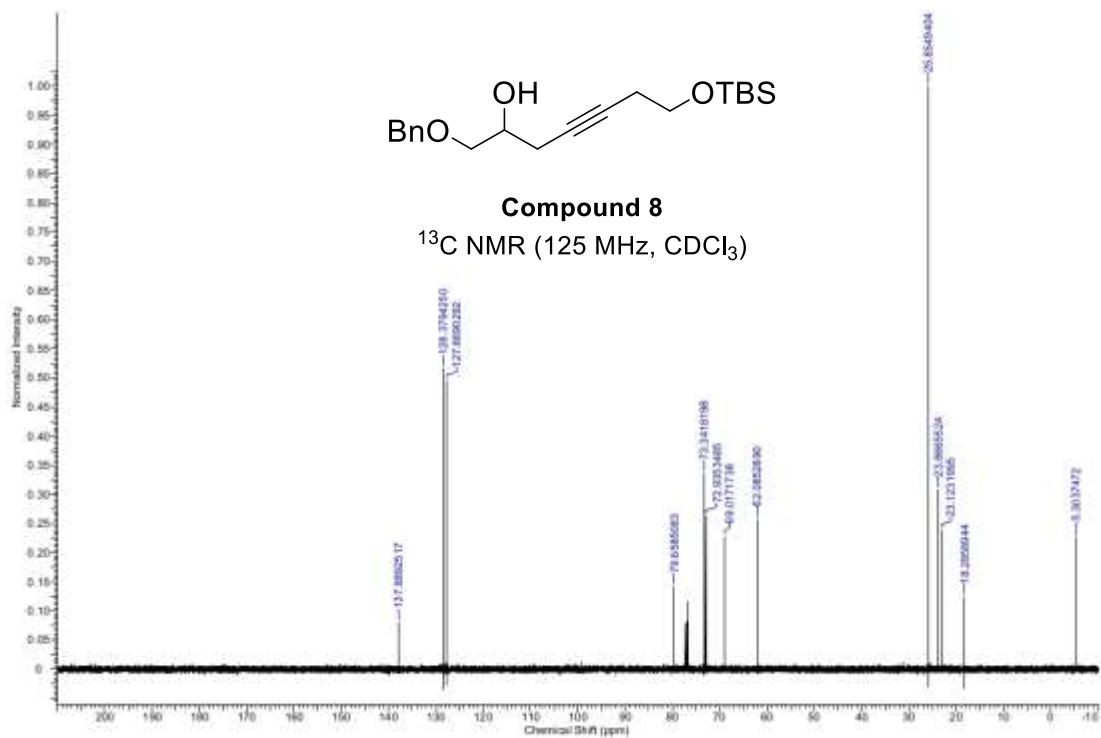
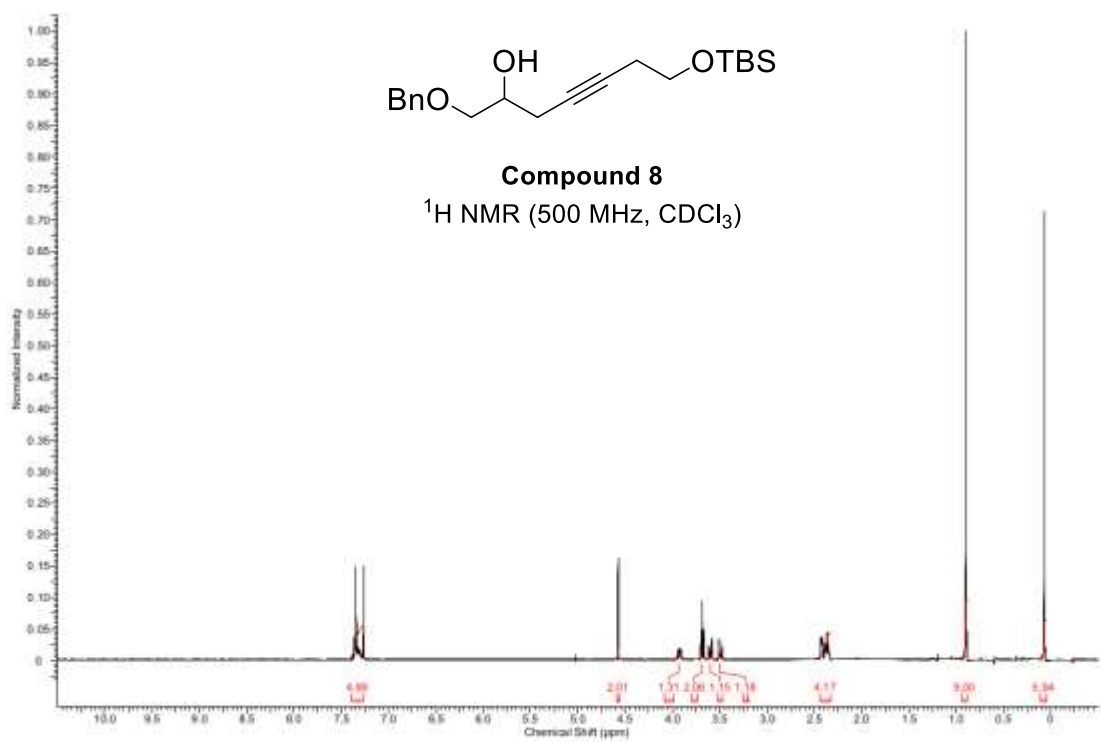
2.7 NMR Spectra

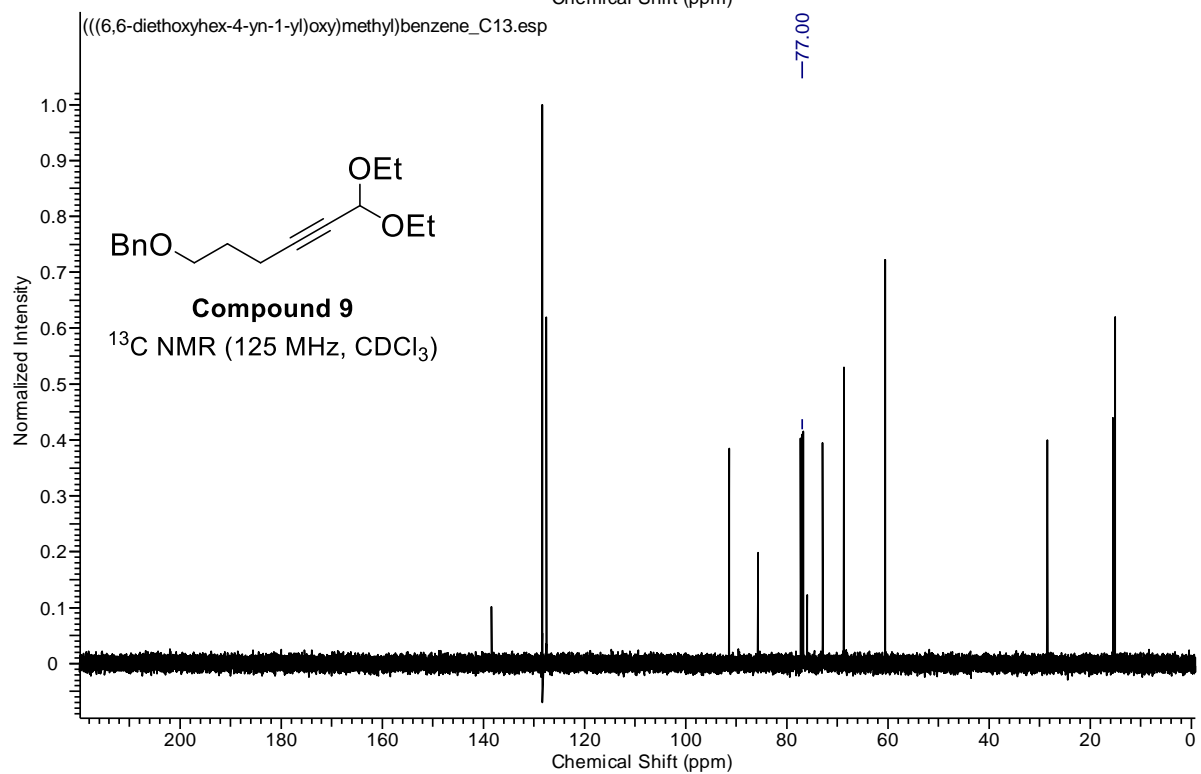
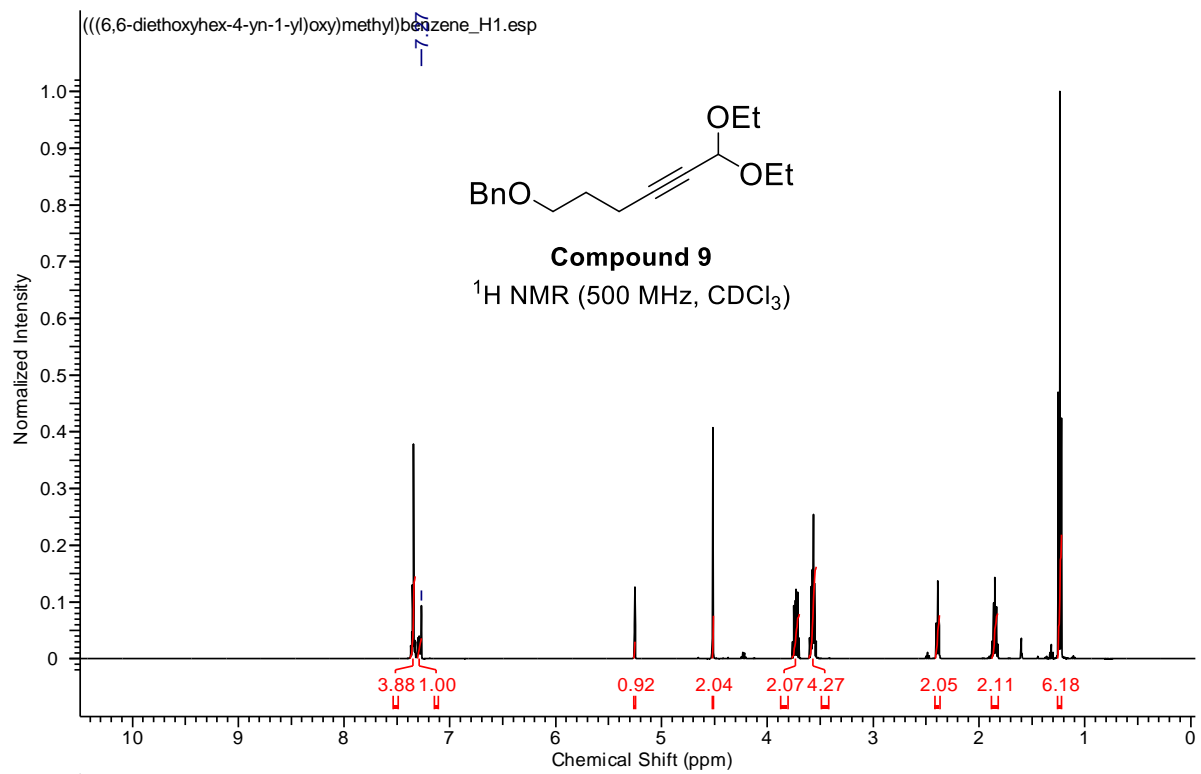


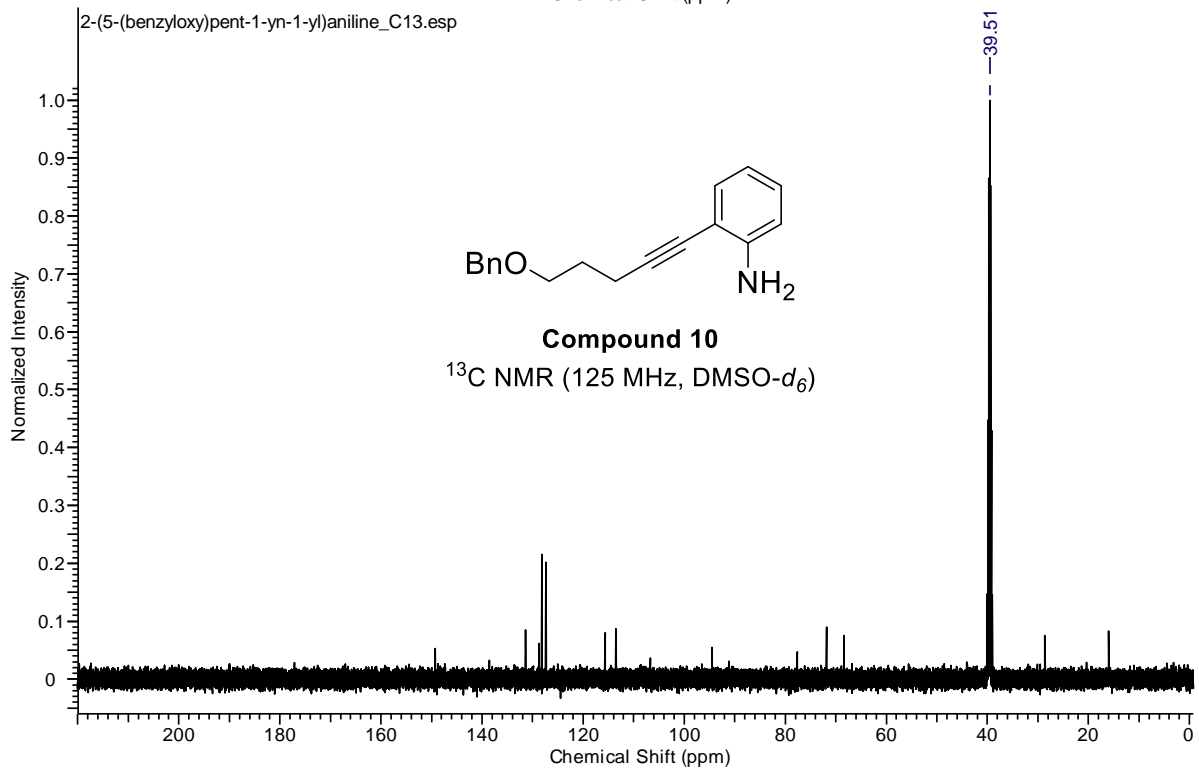
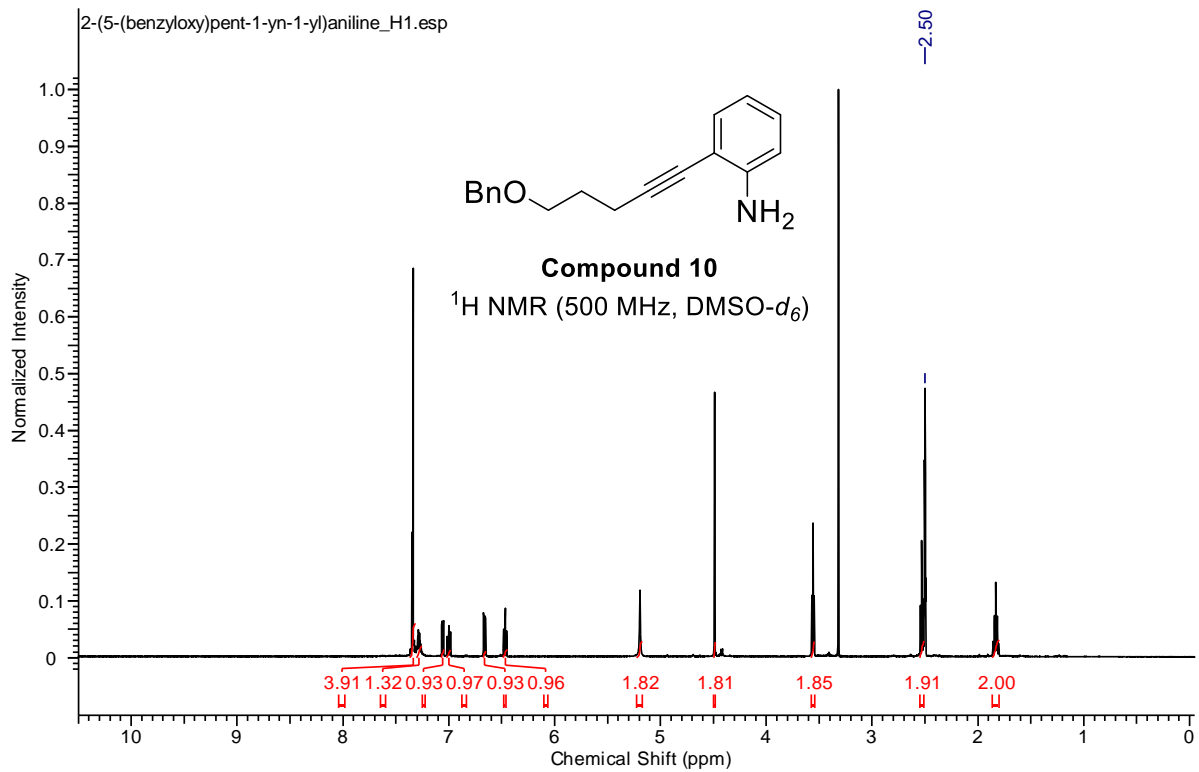


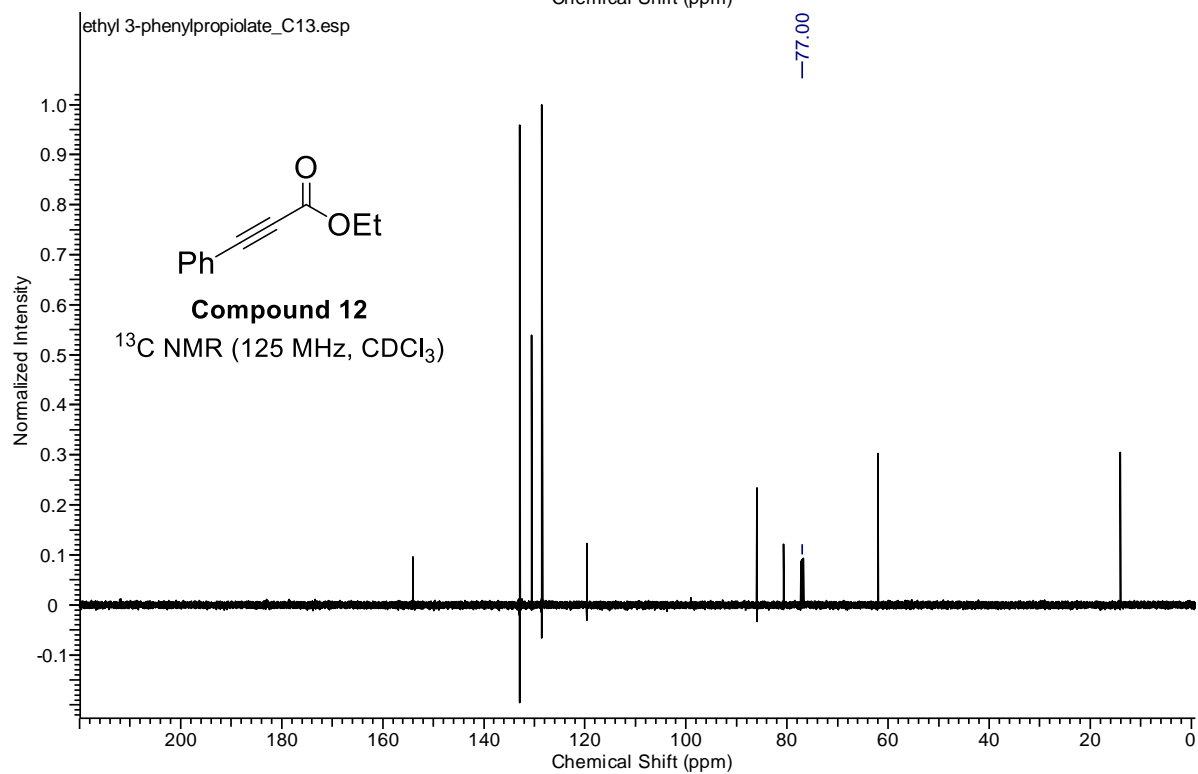
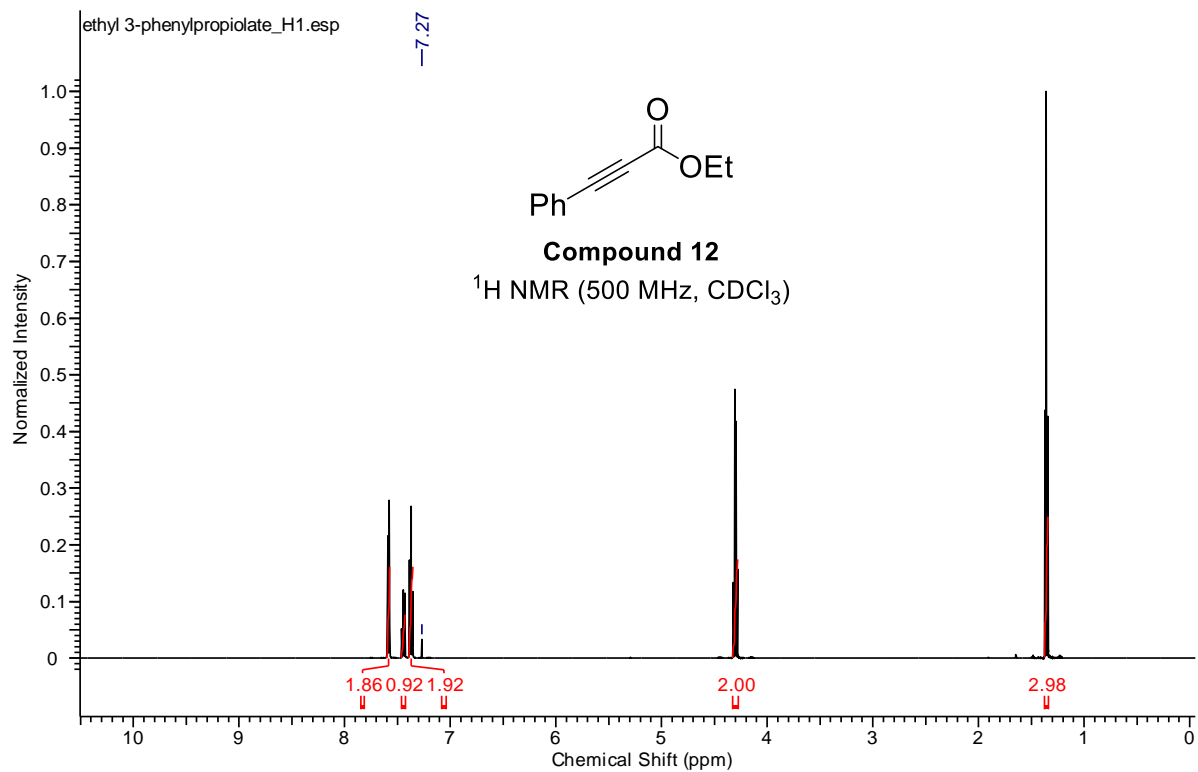


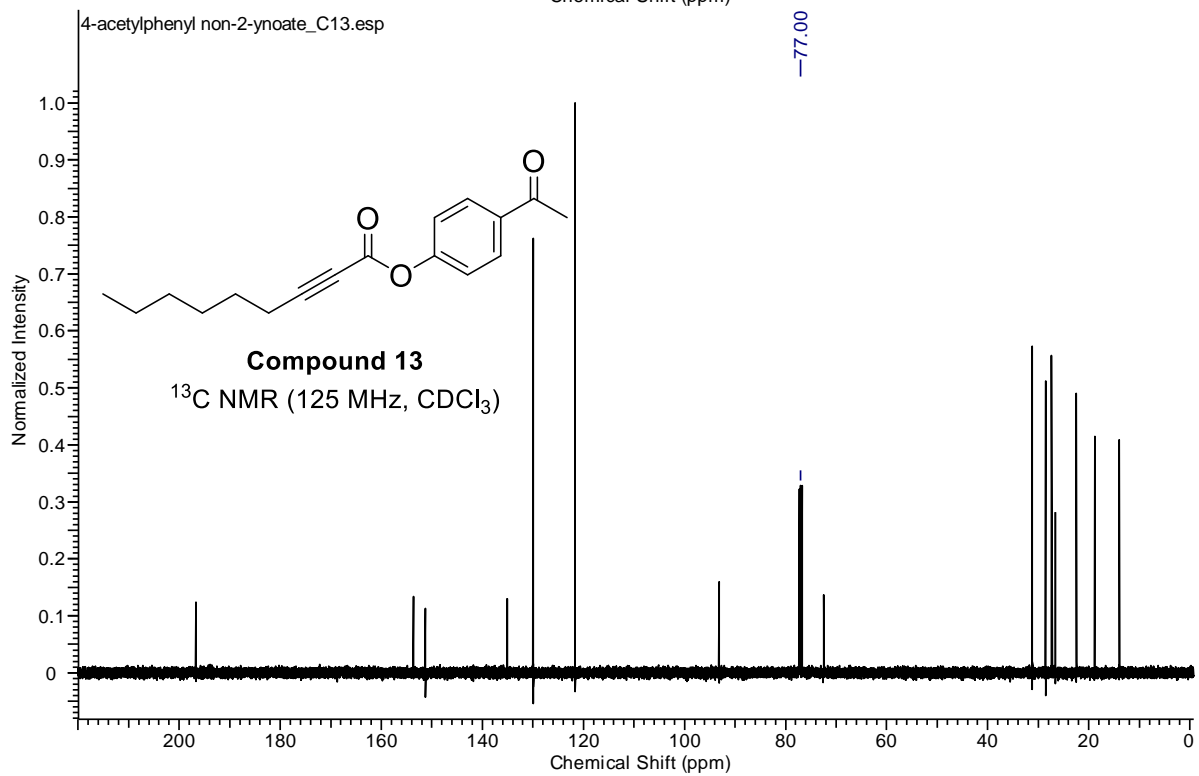
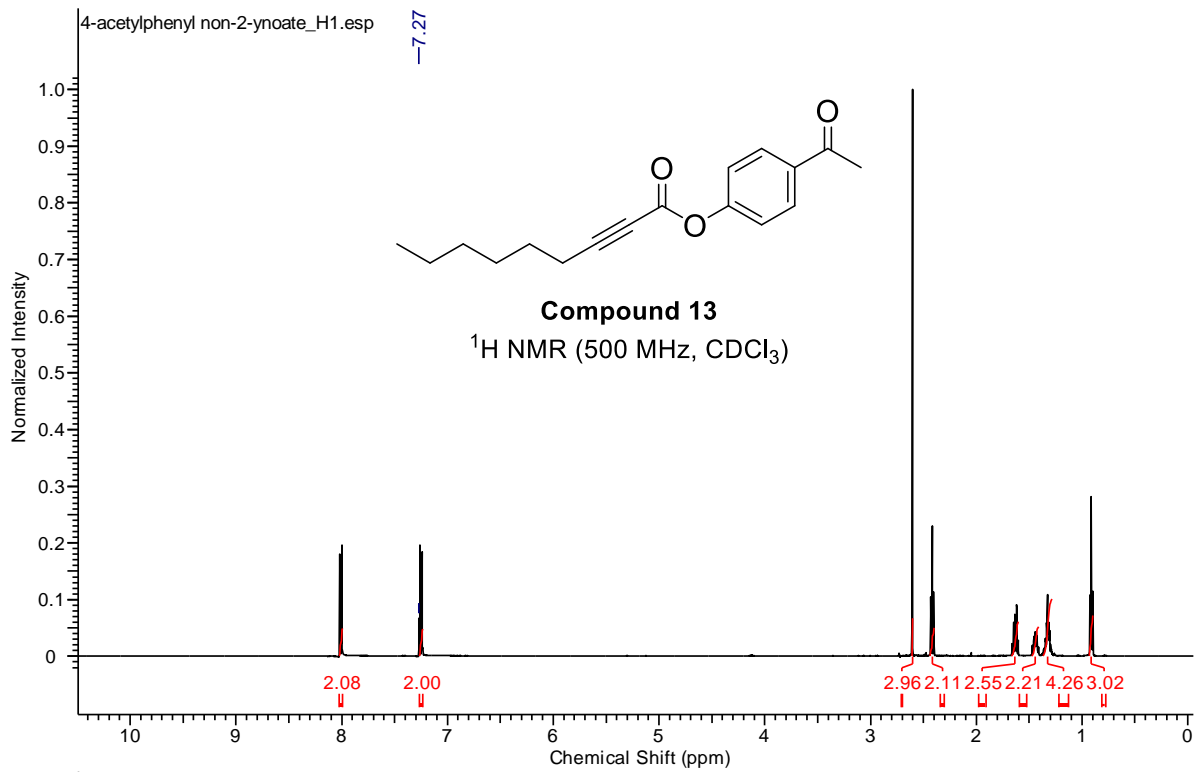


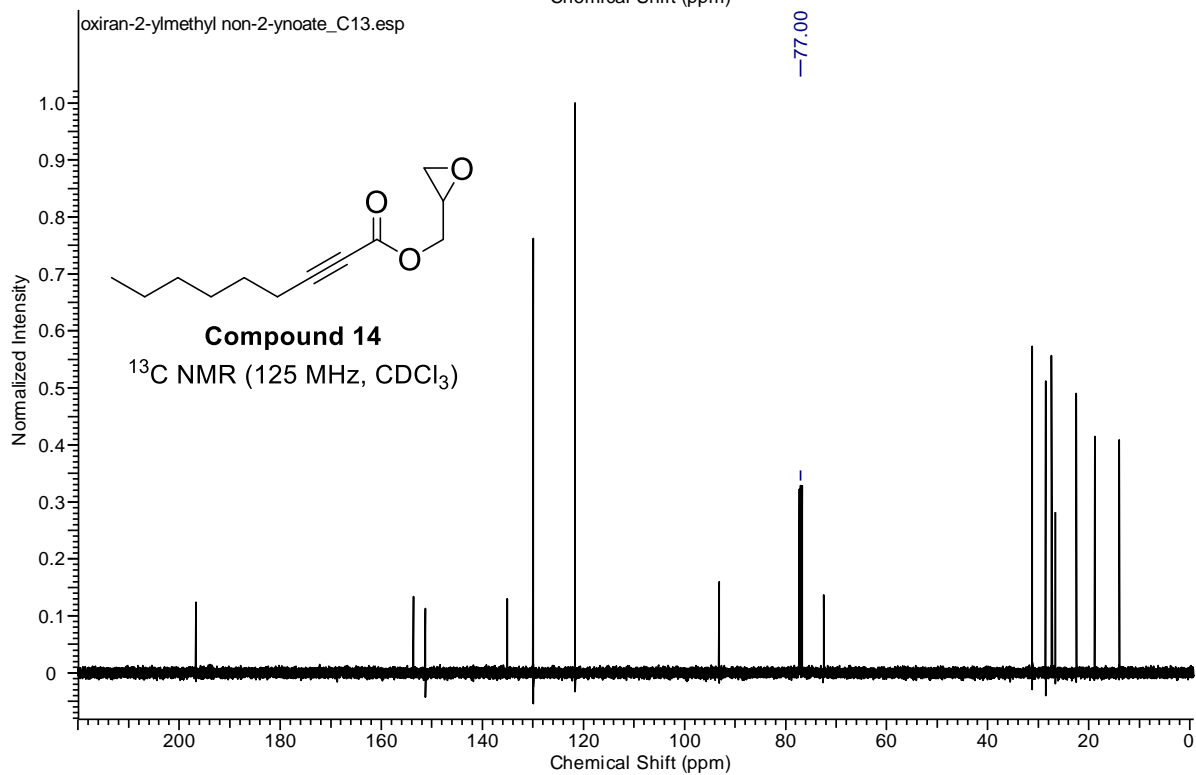
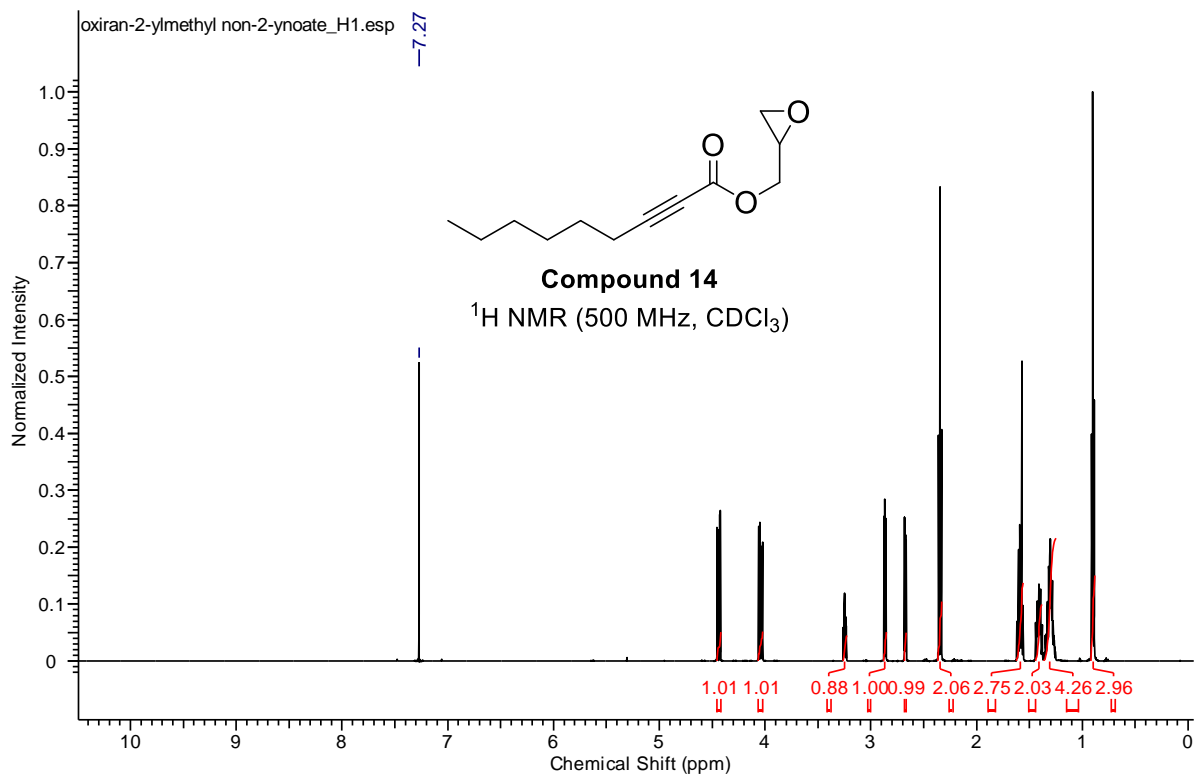


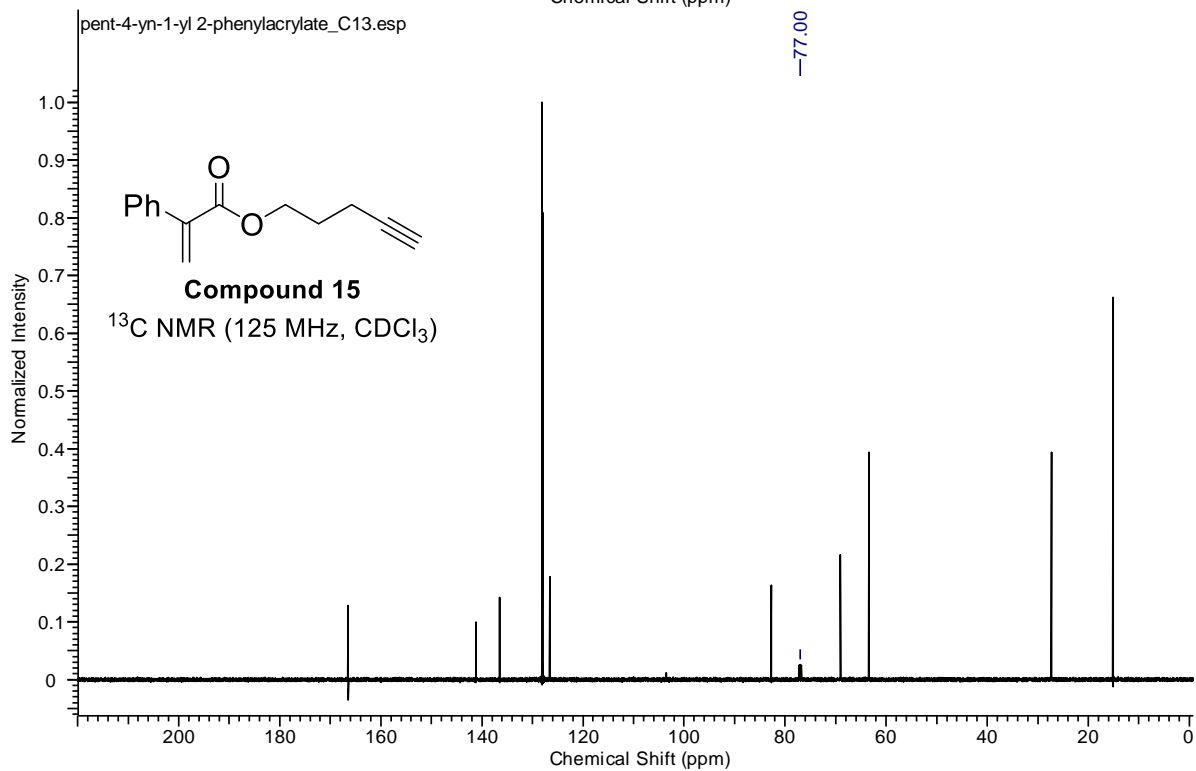
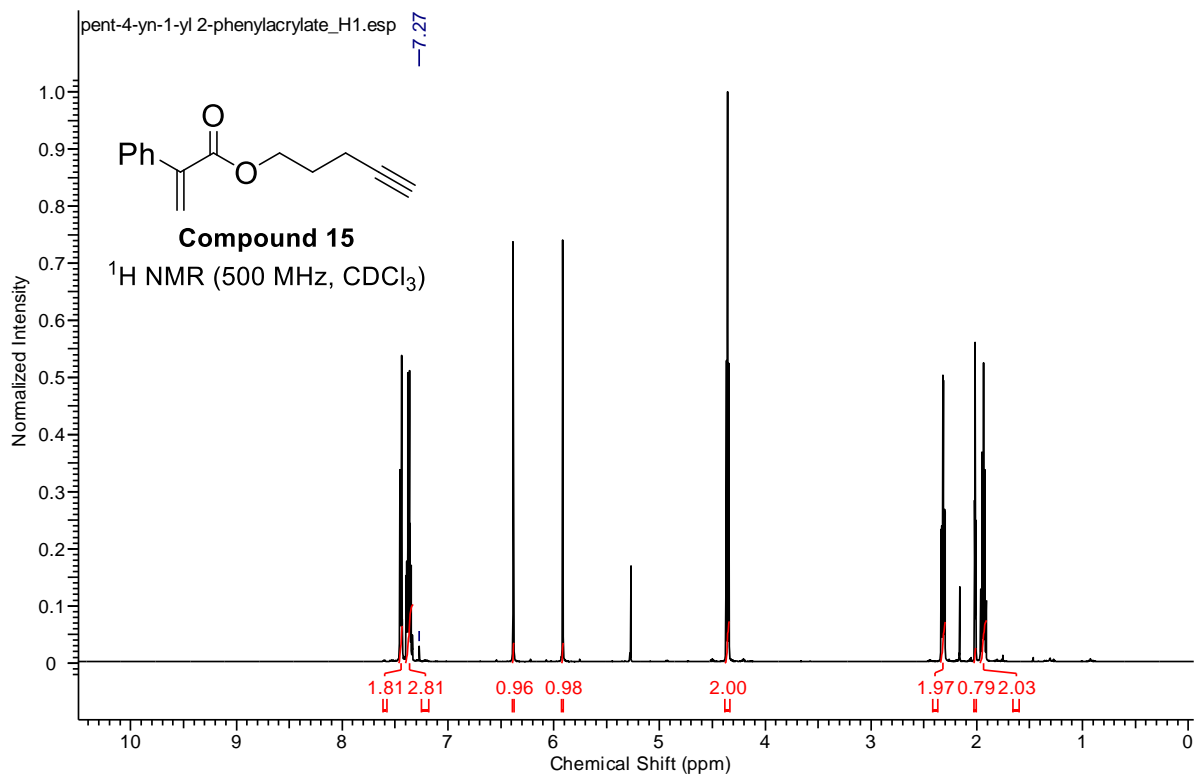


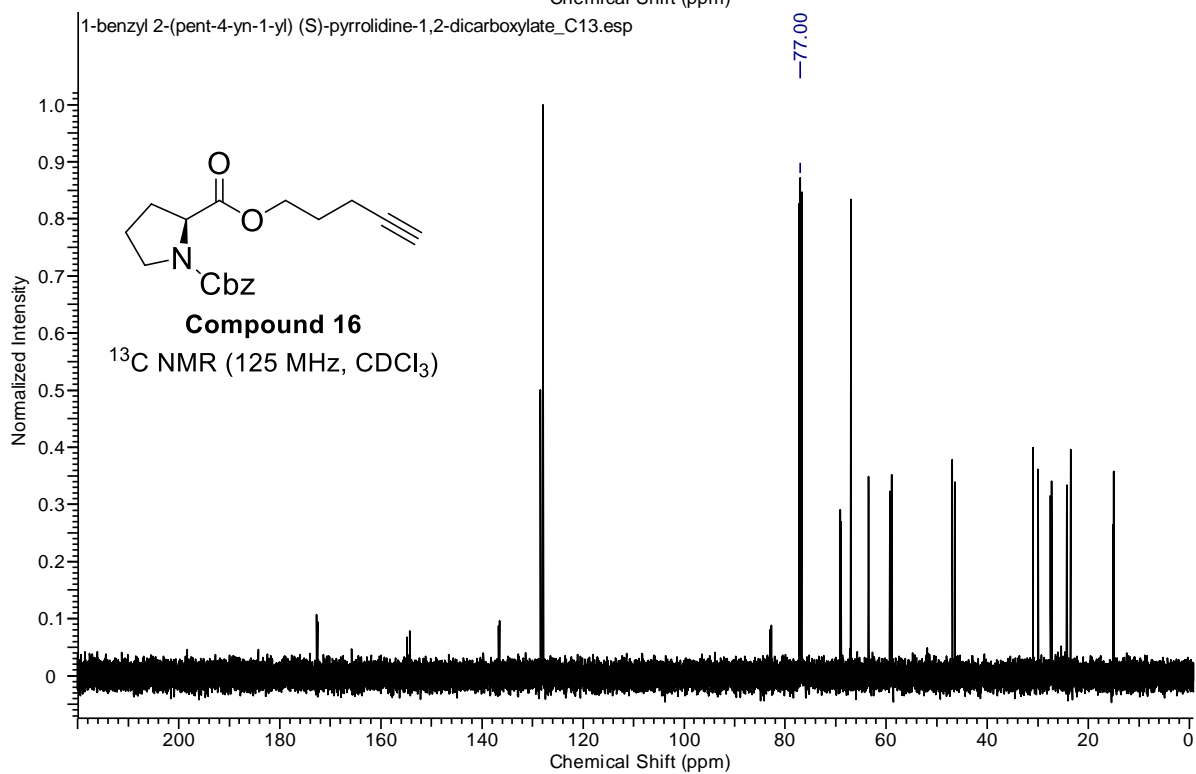
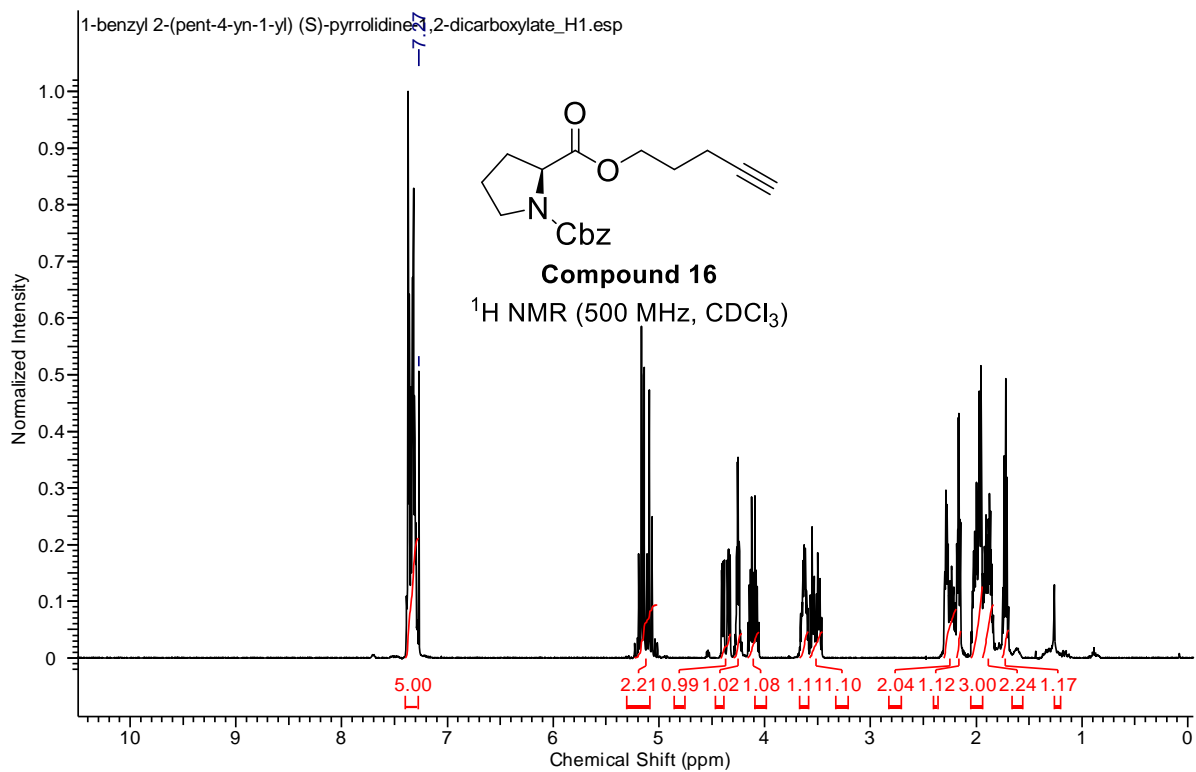


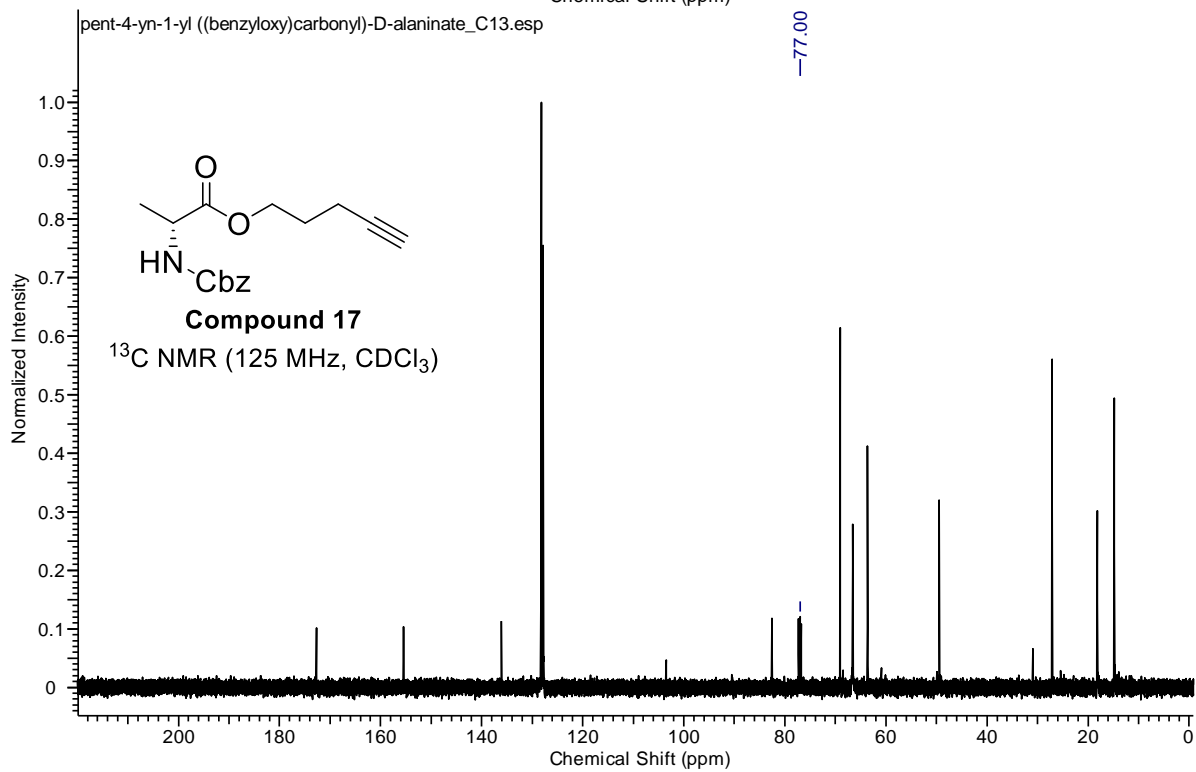
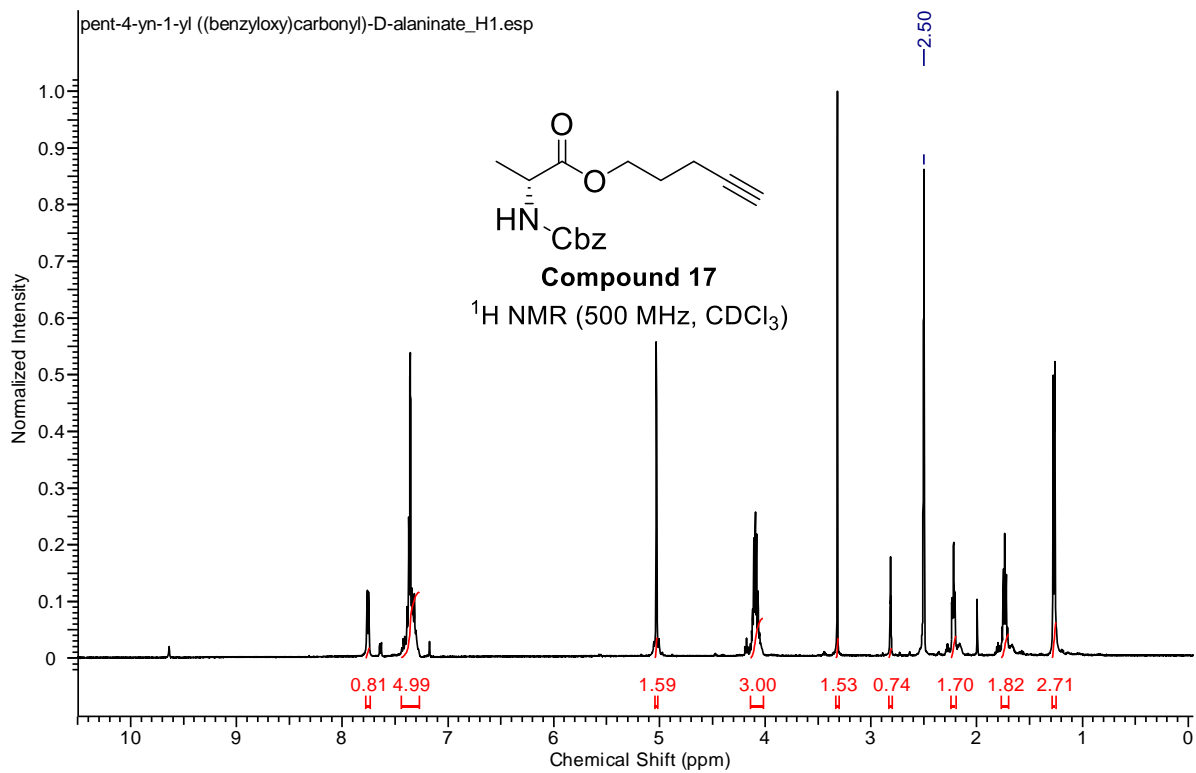


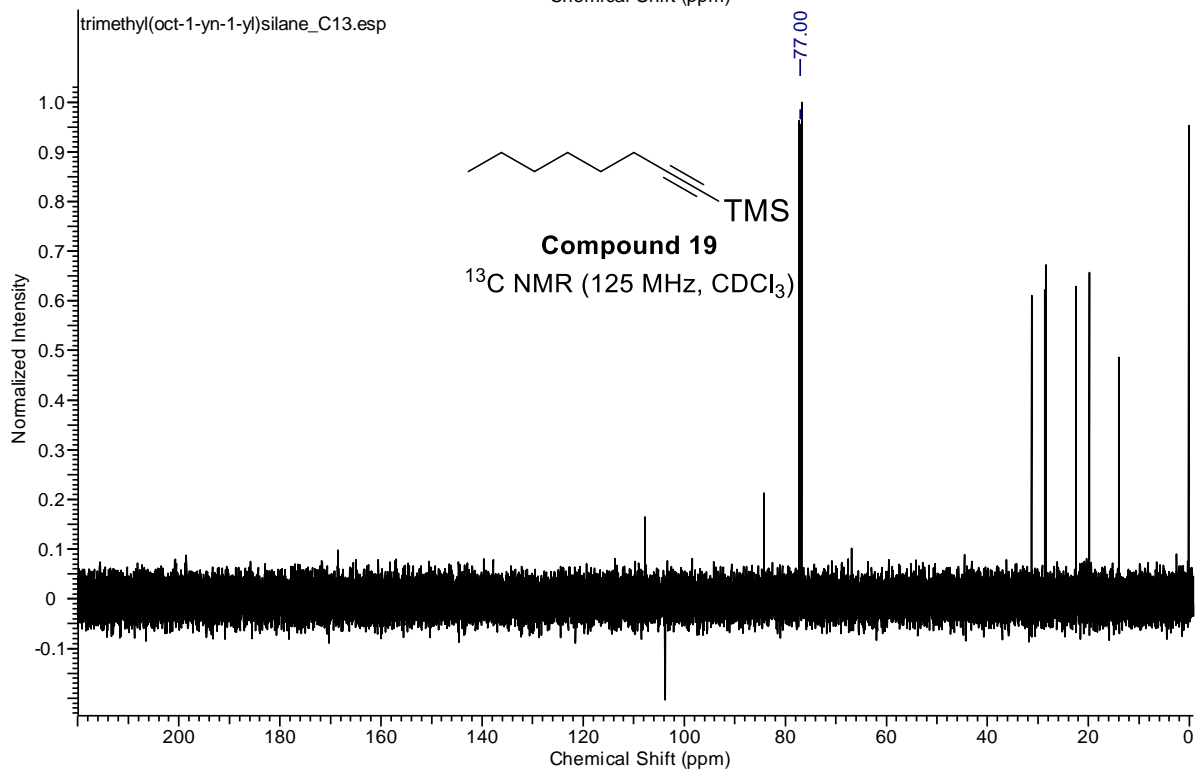
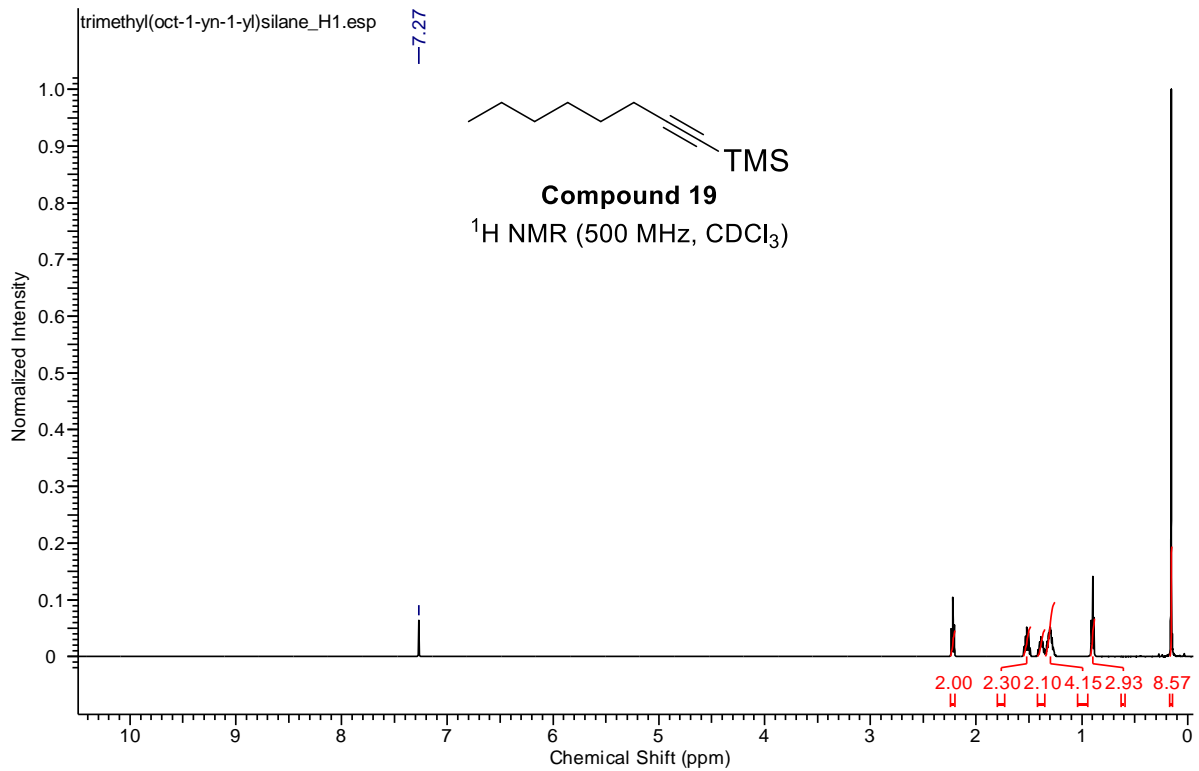


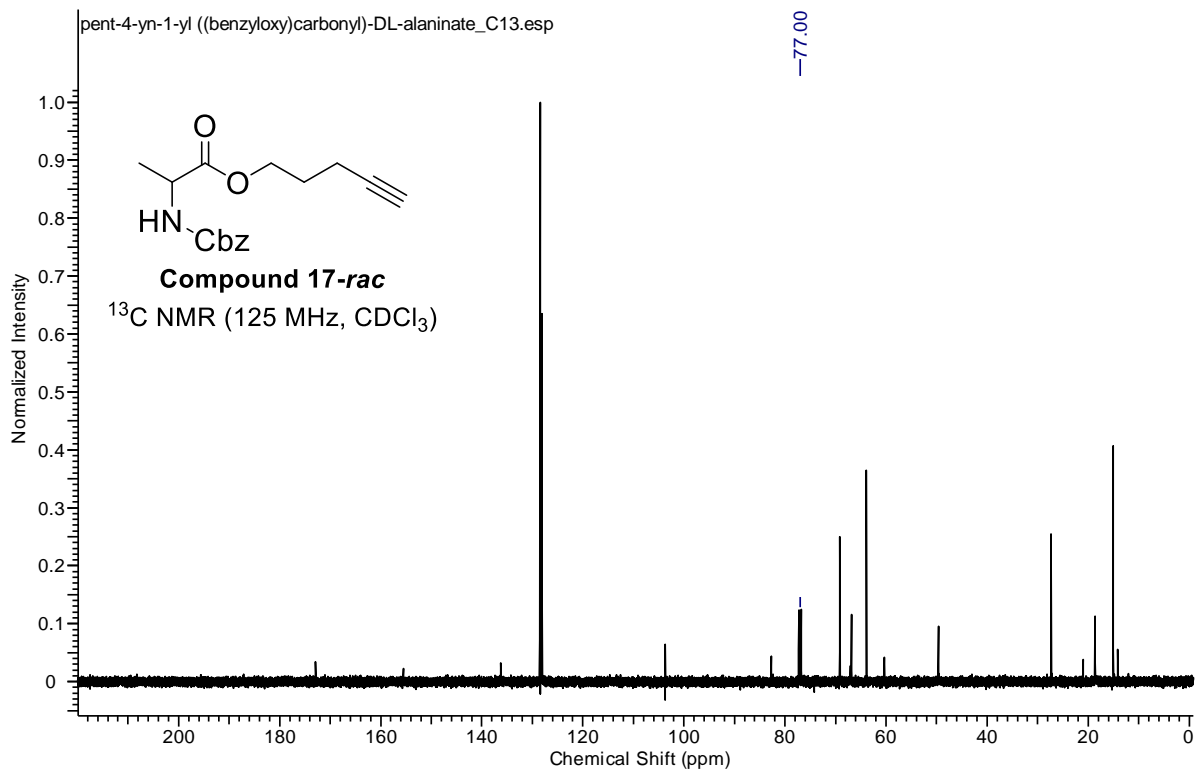
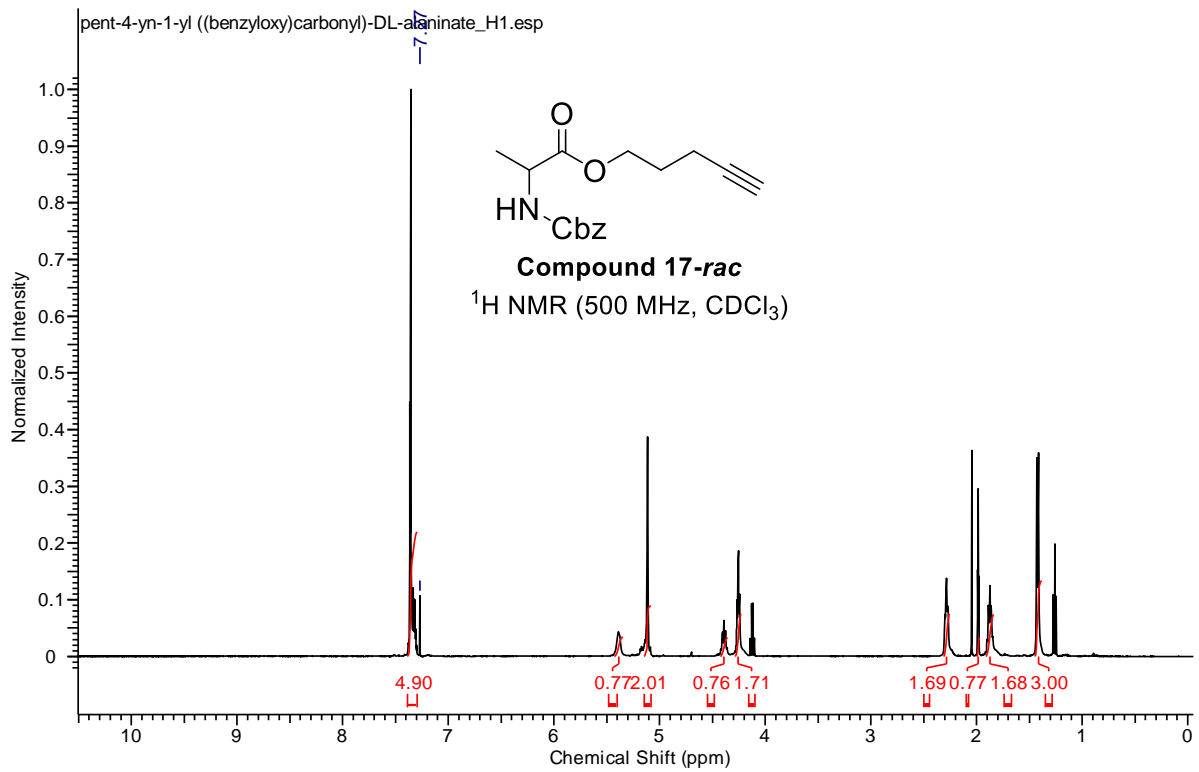


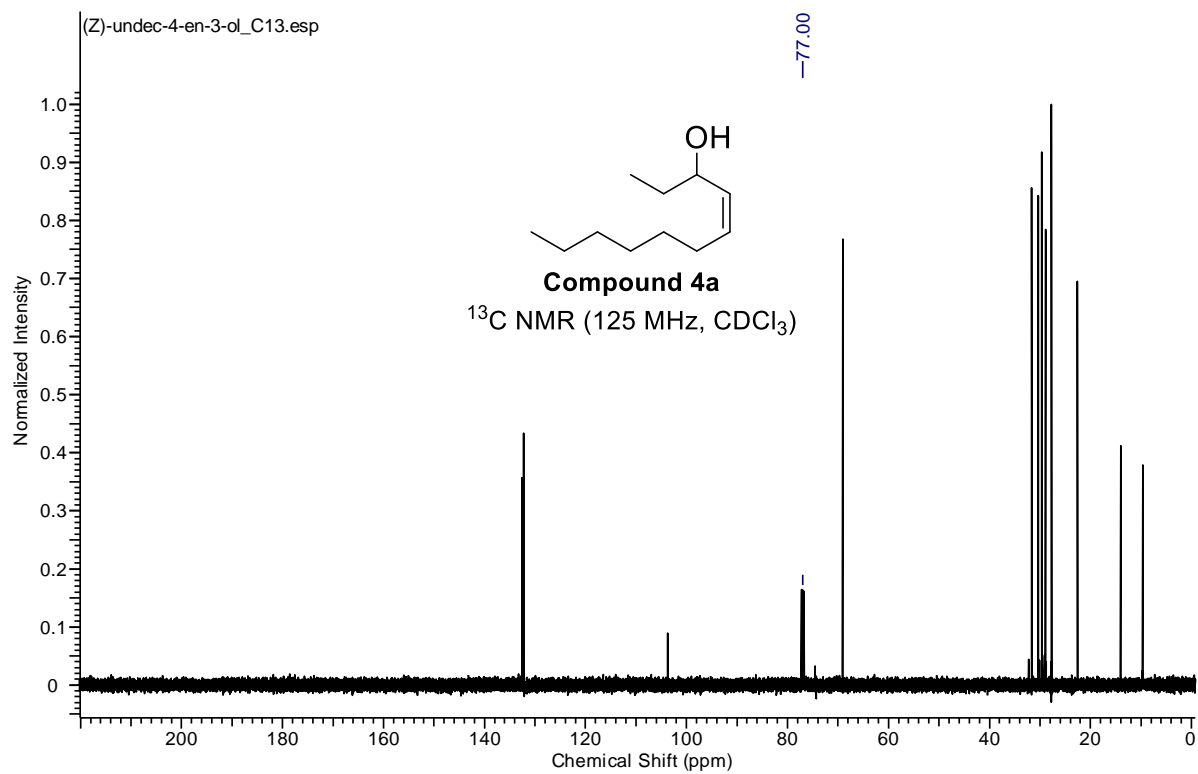
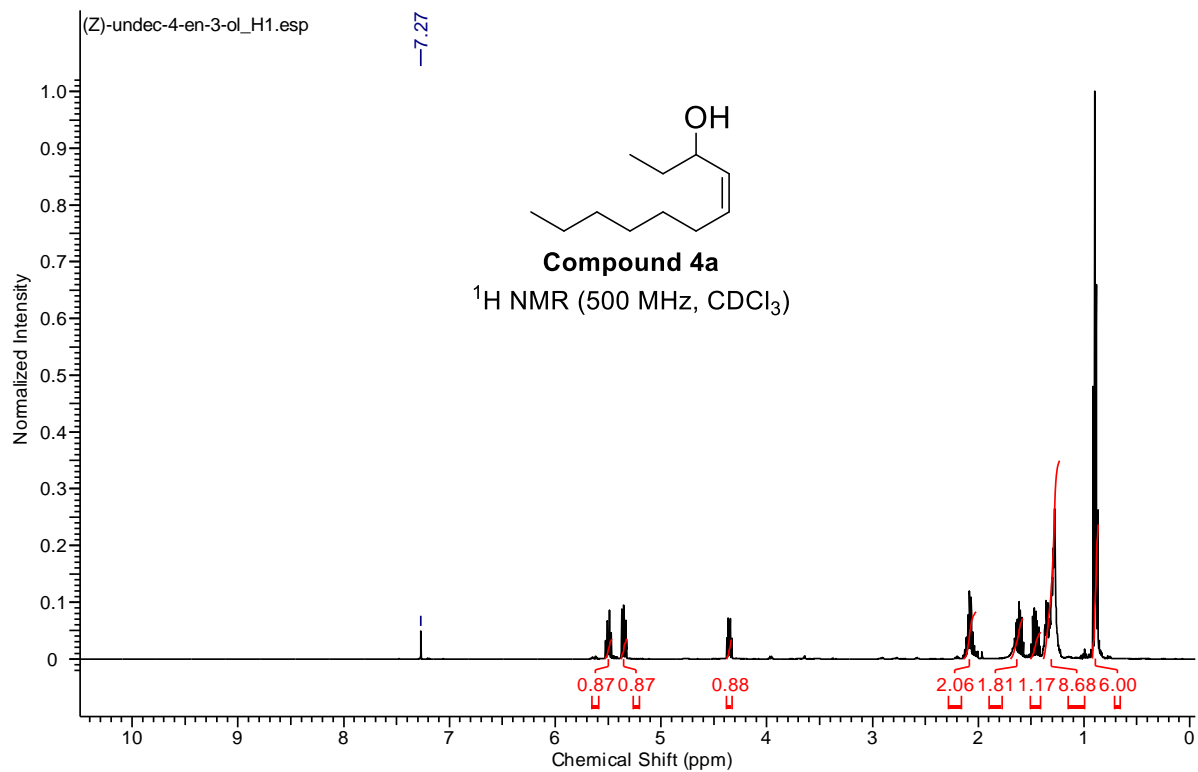


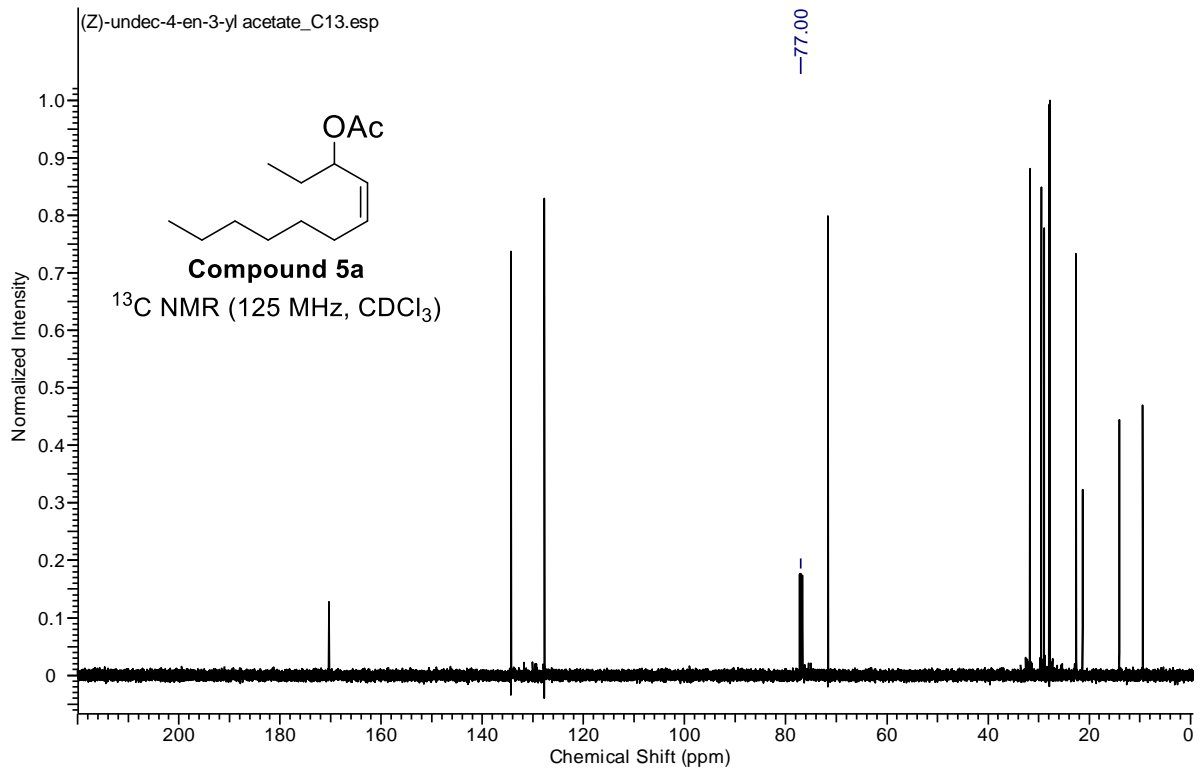
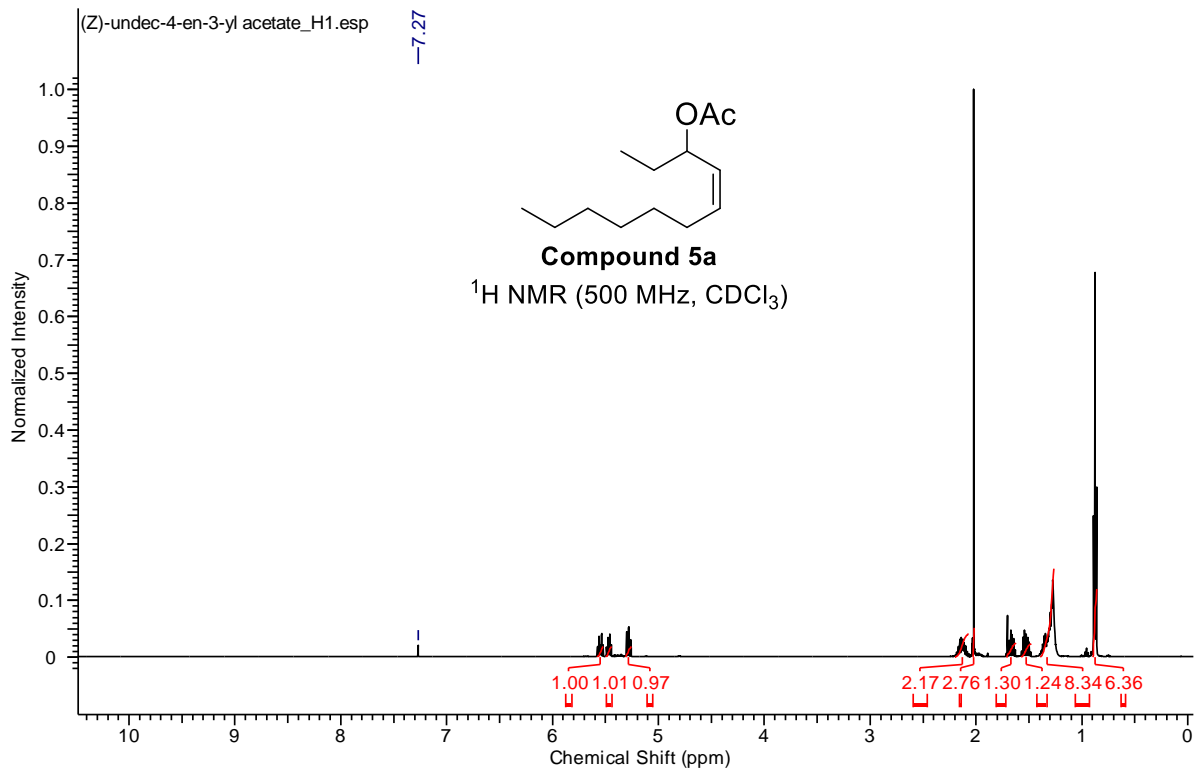


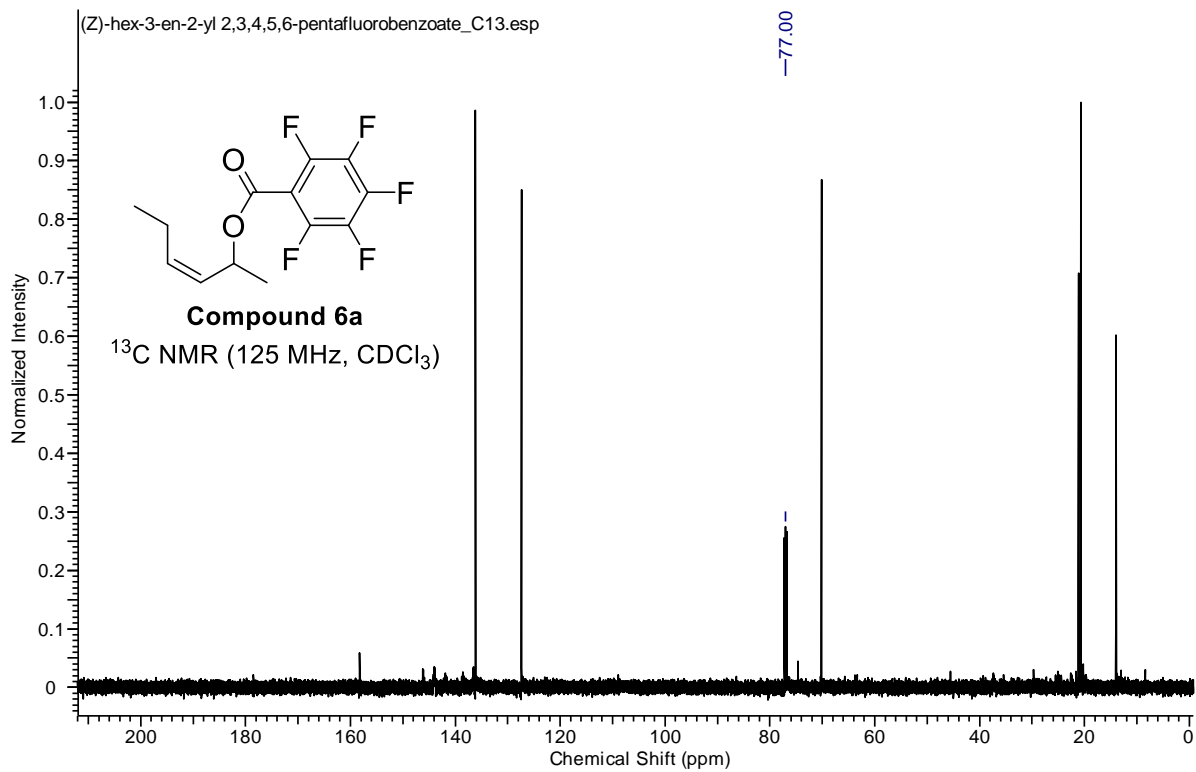
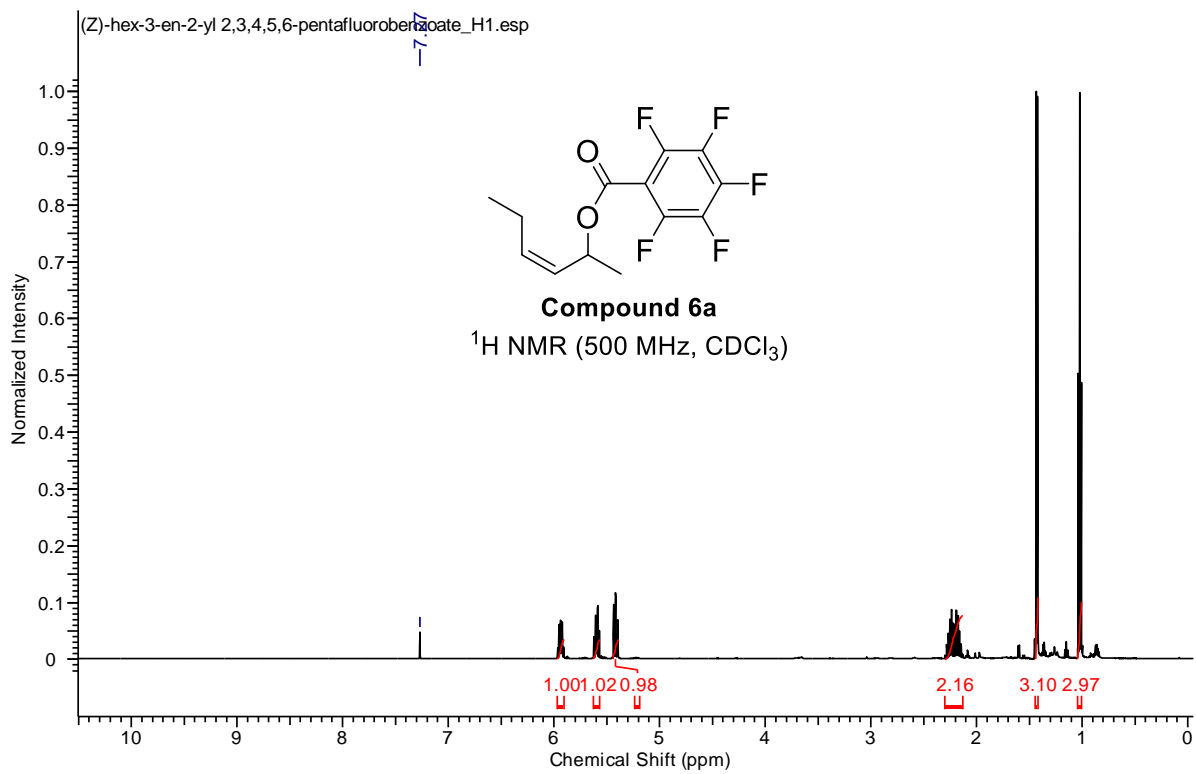


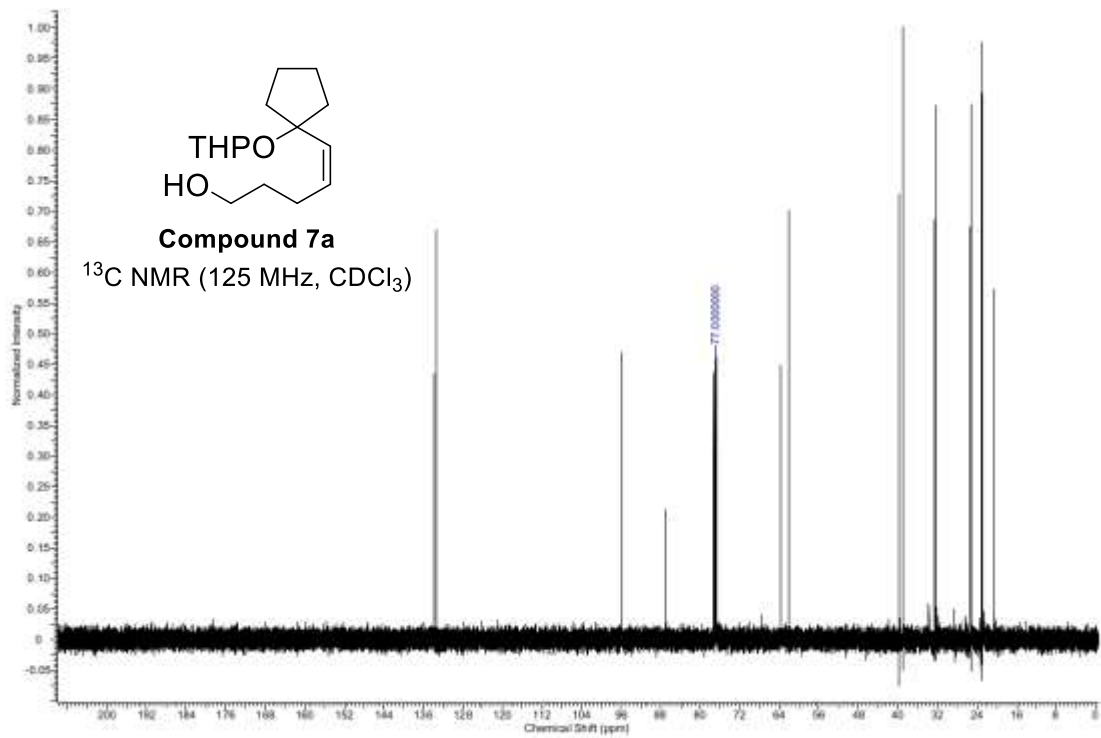
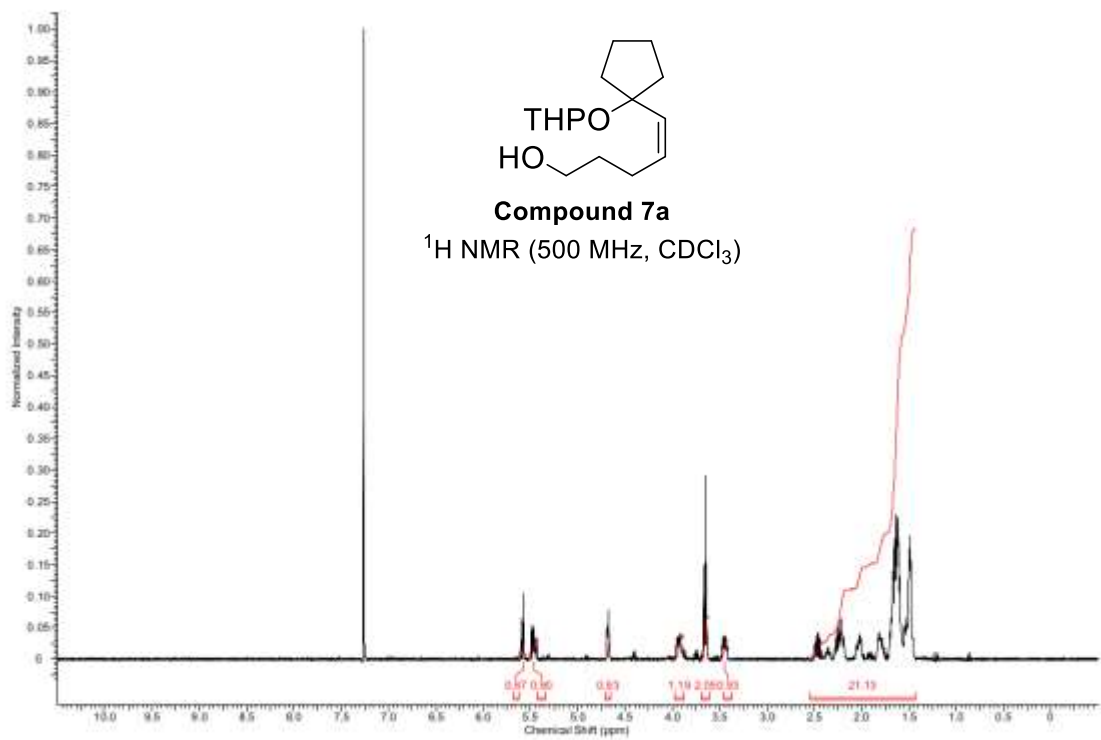


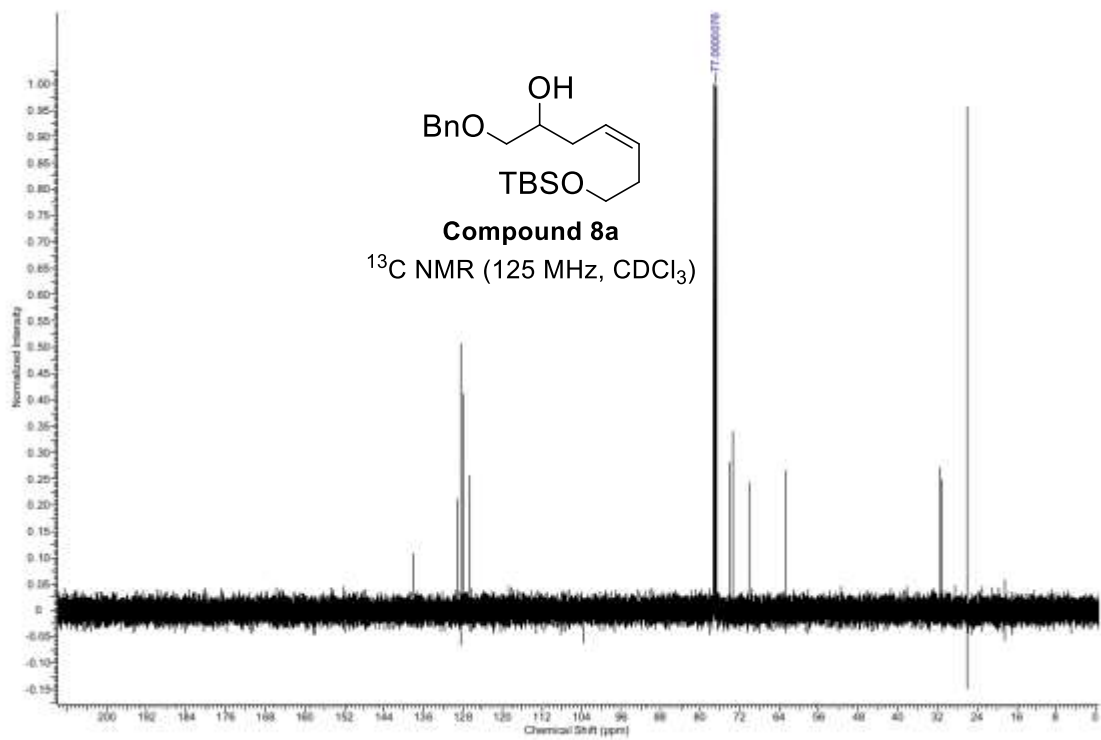
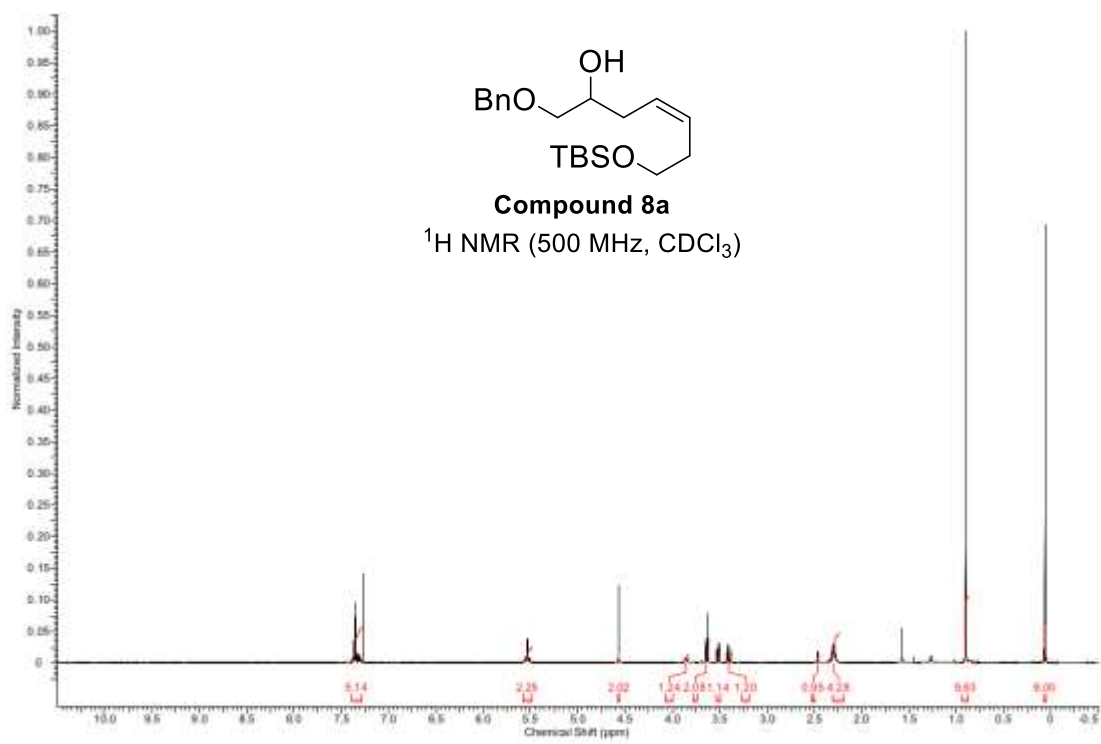


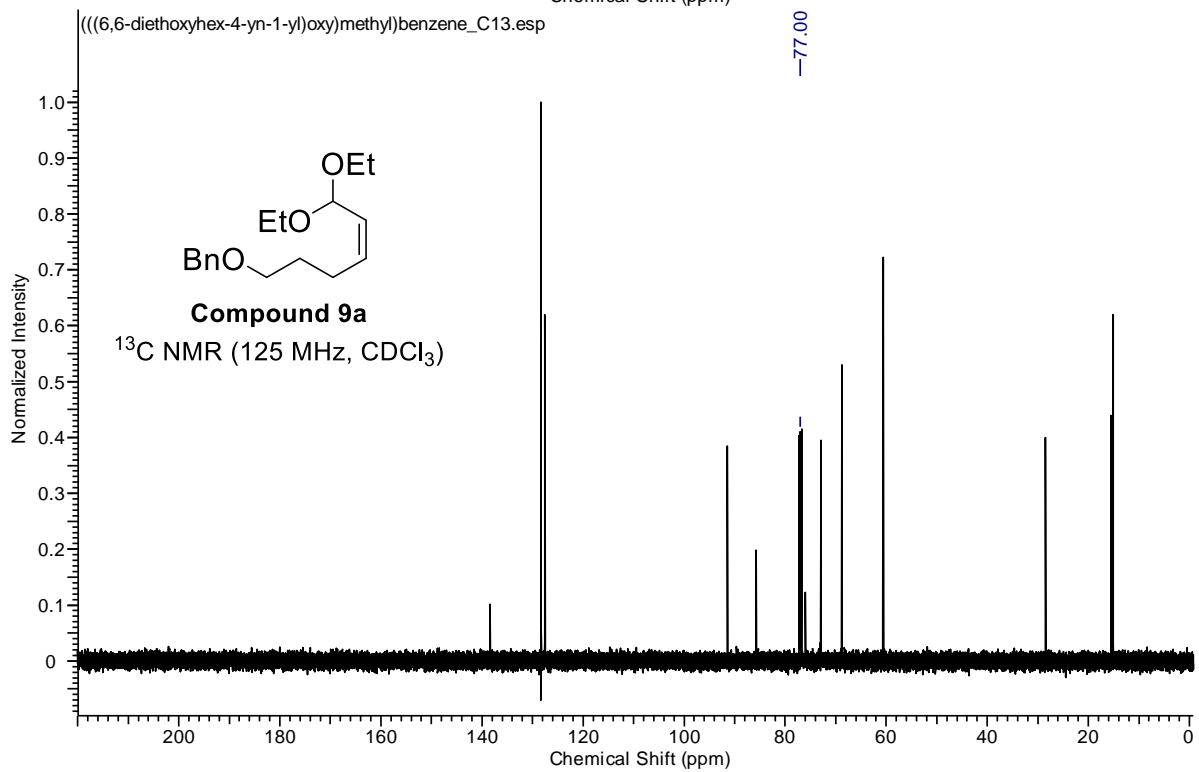
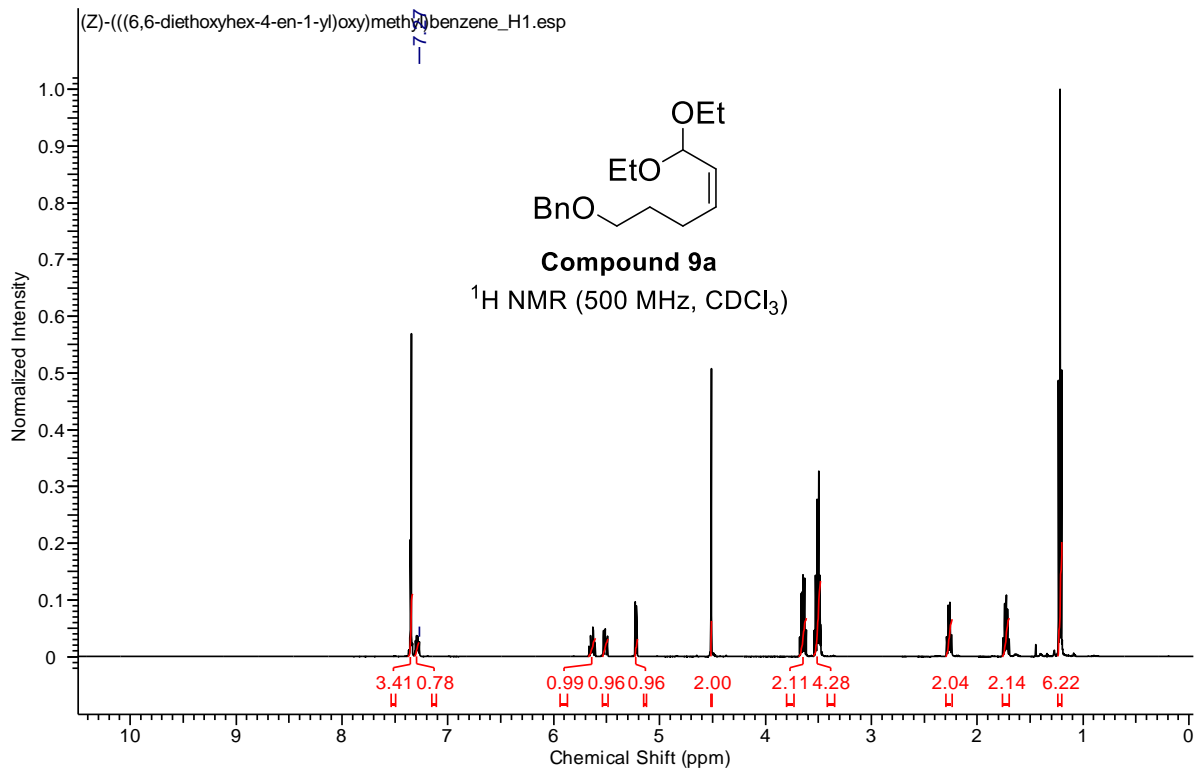


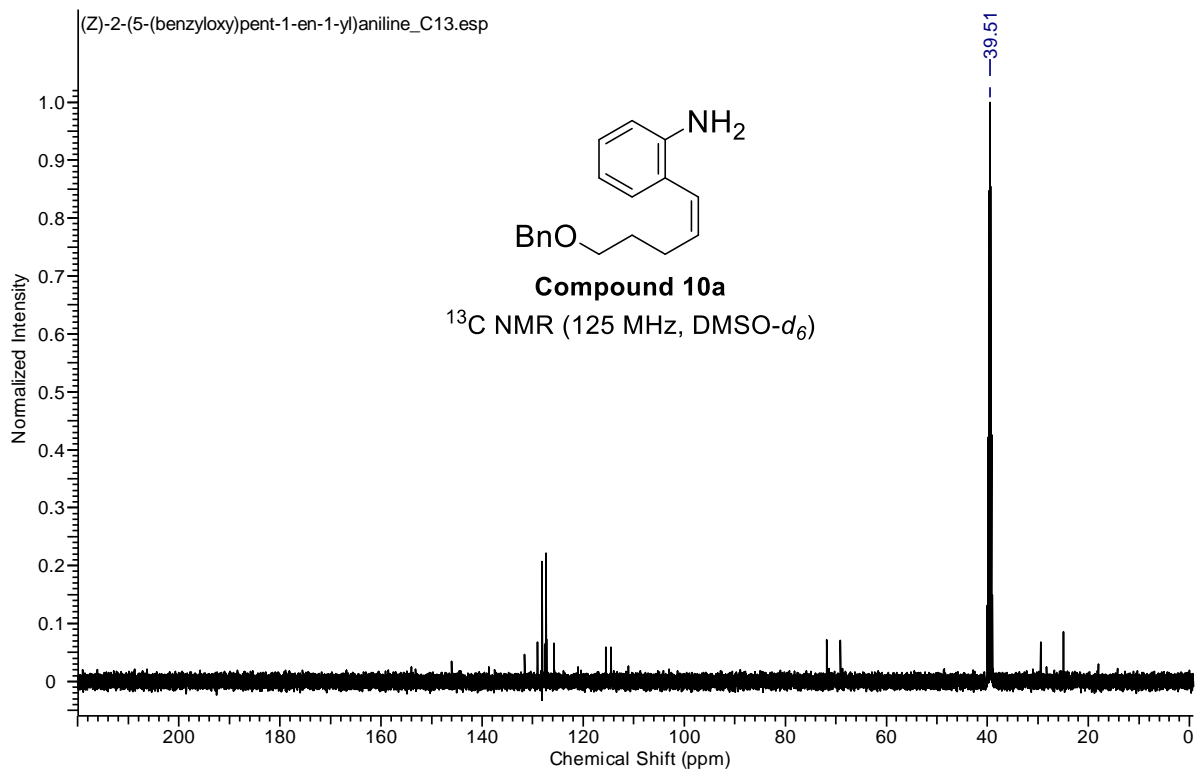
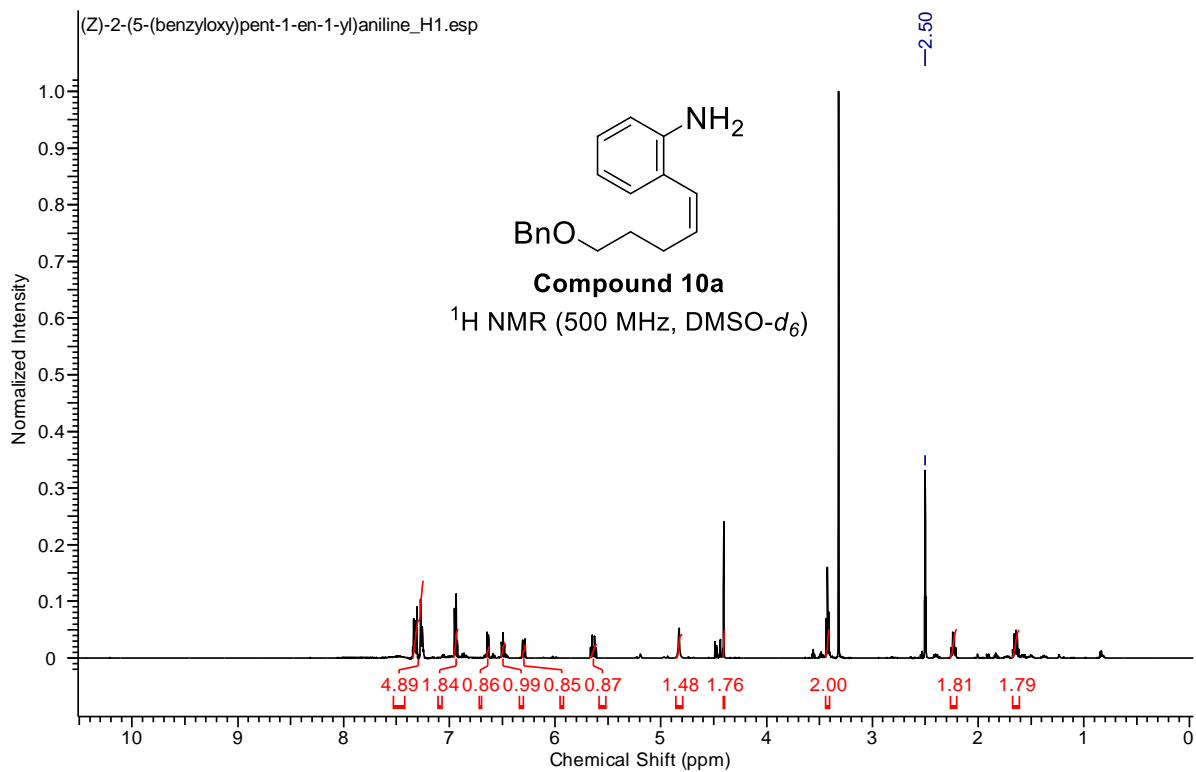


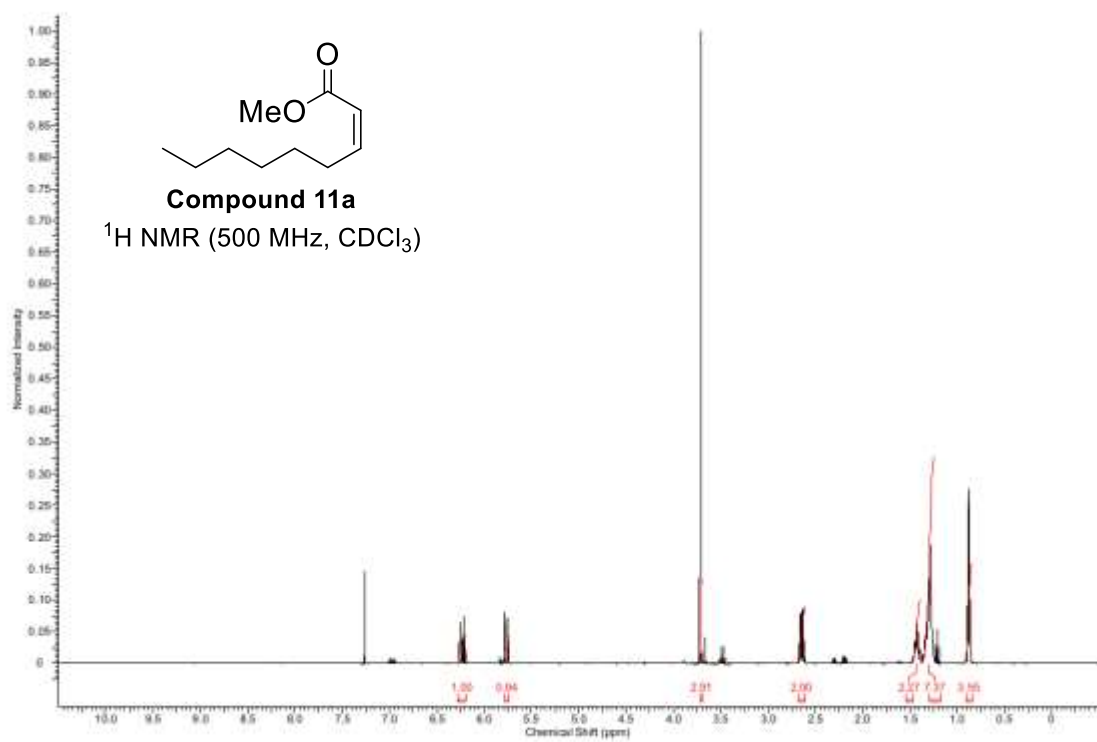


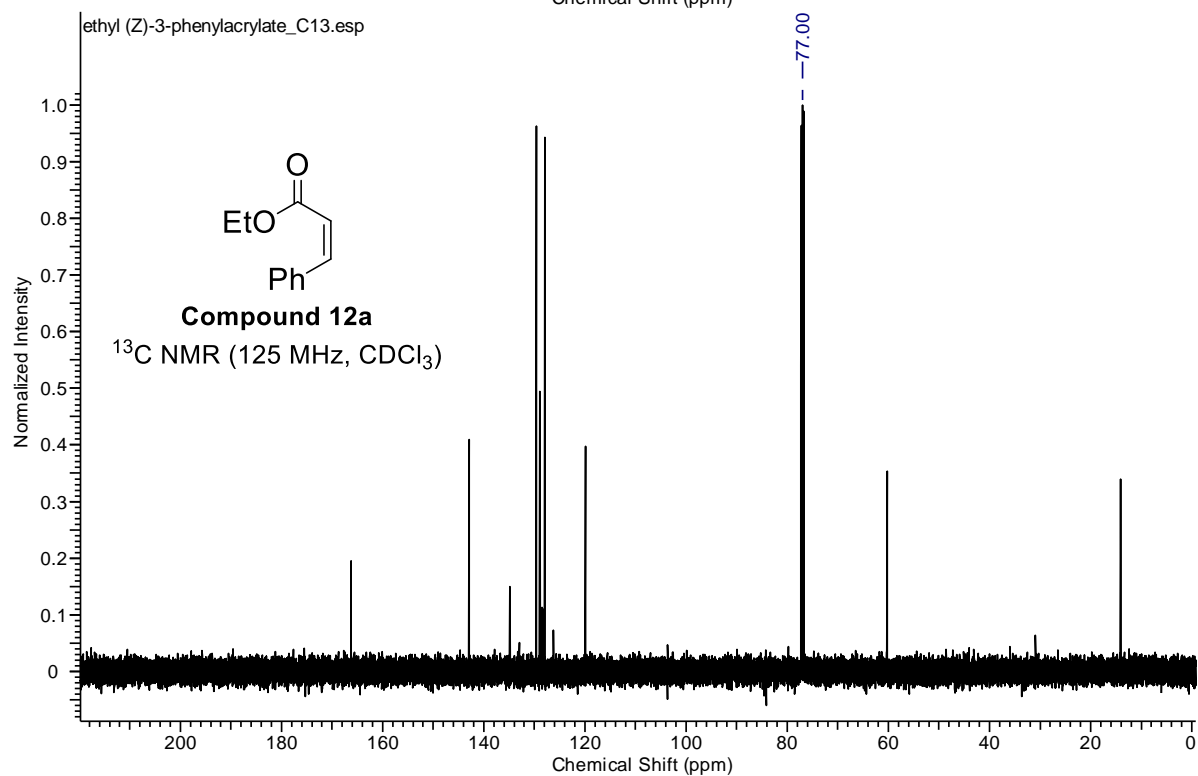
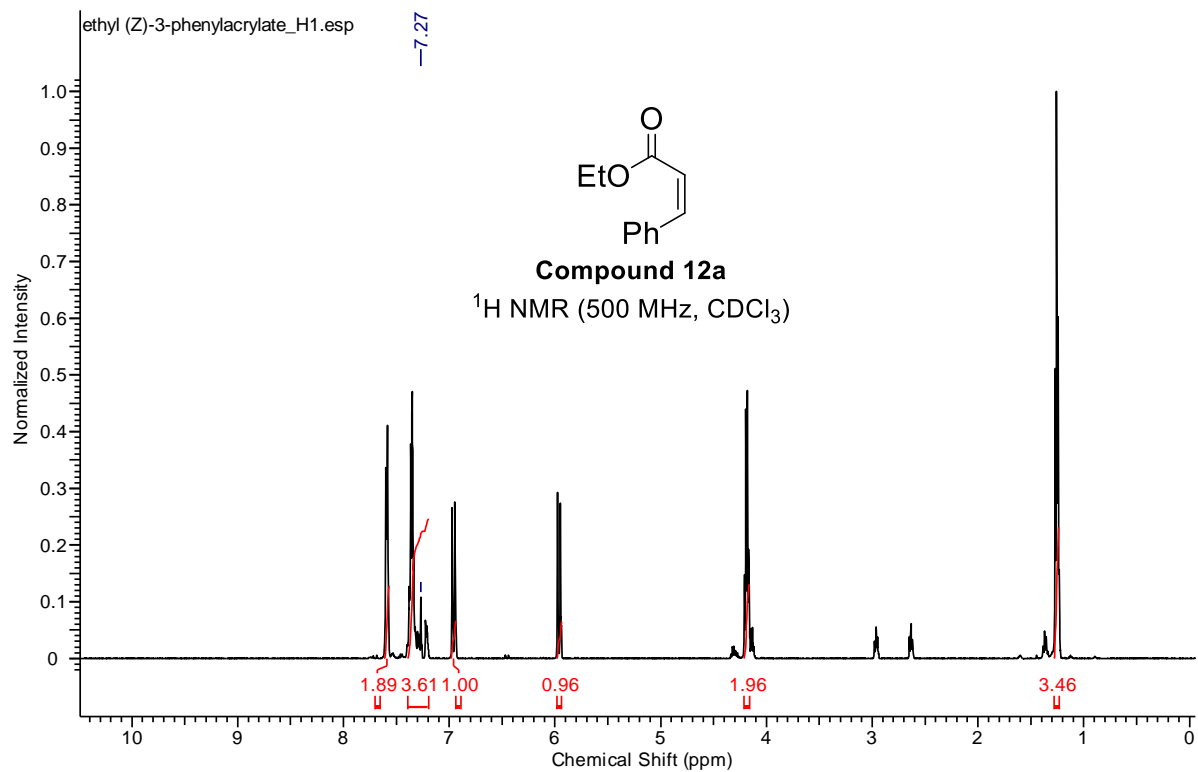


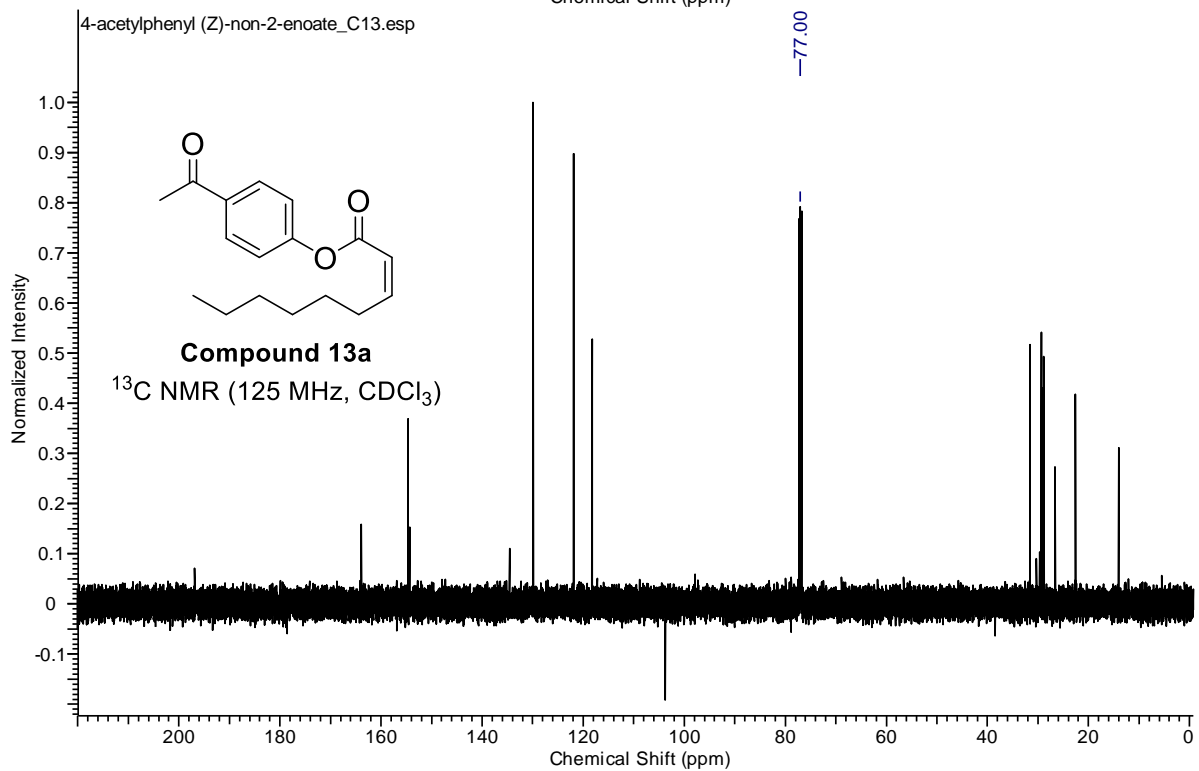
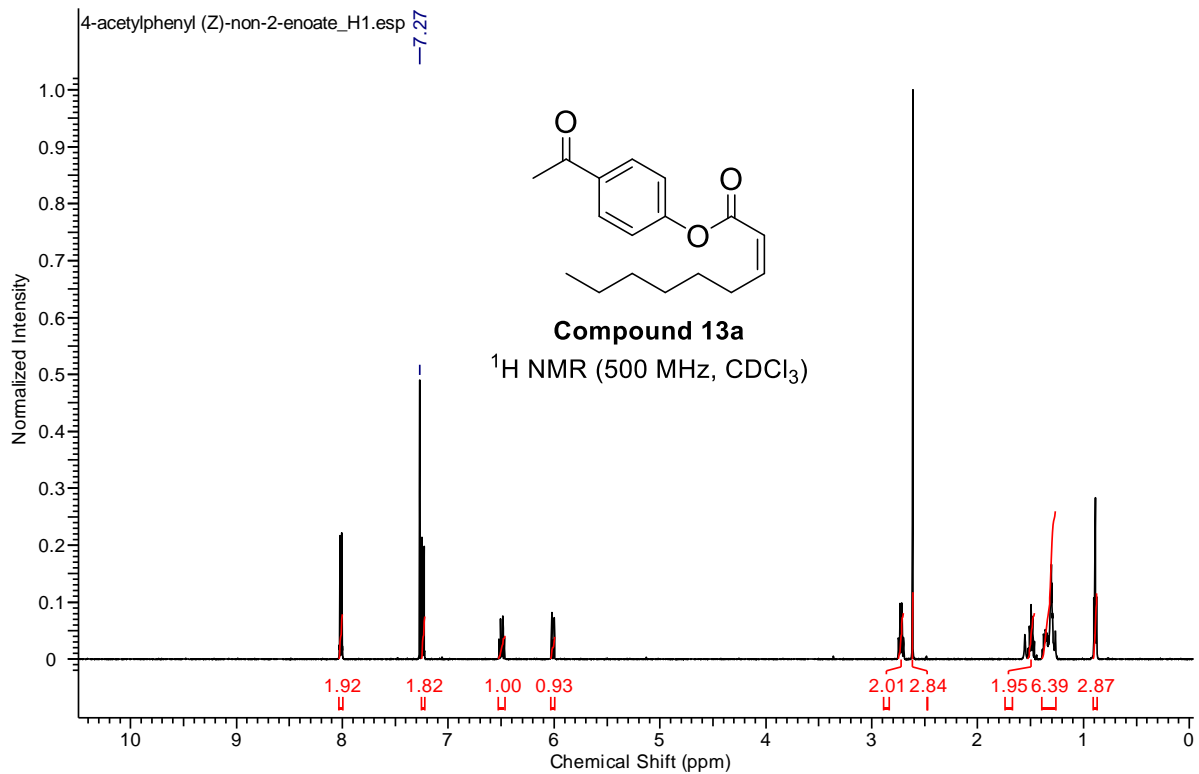


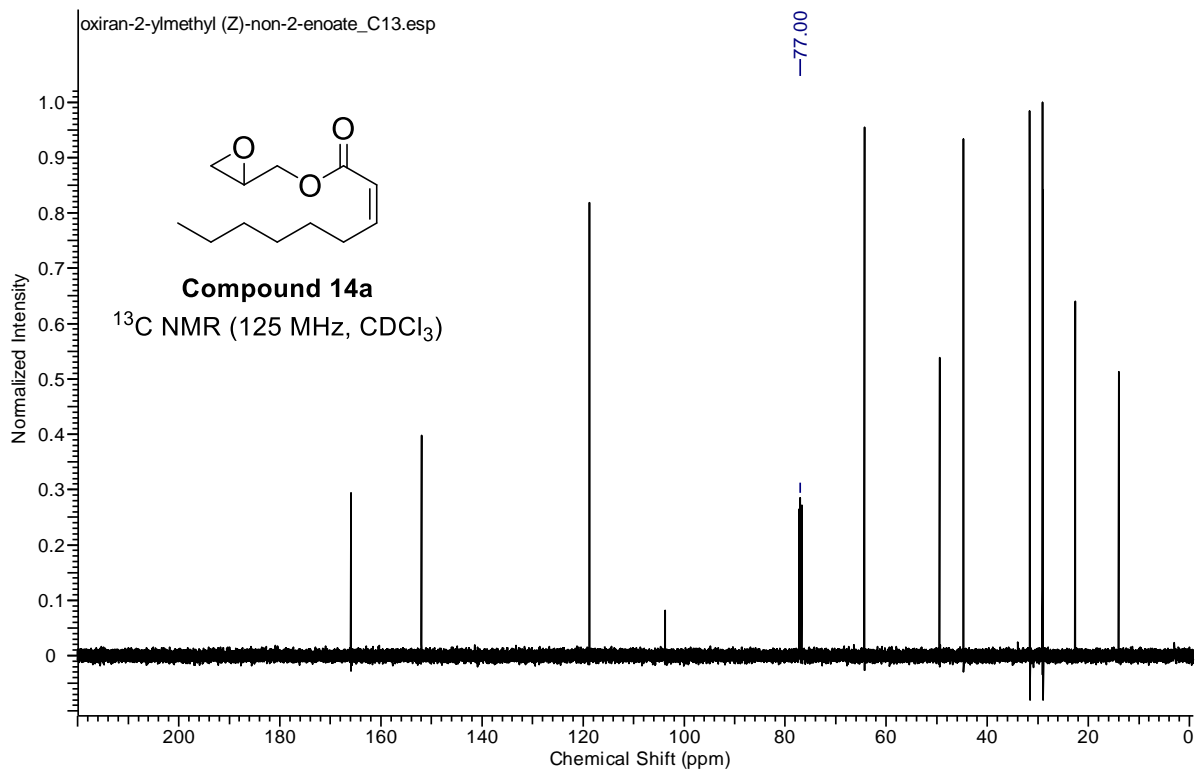
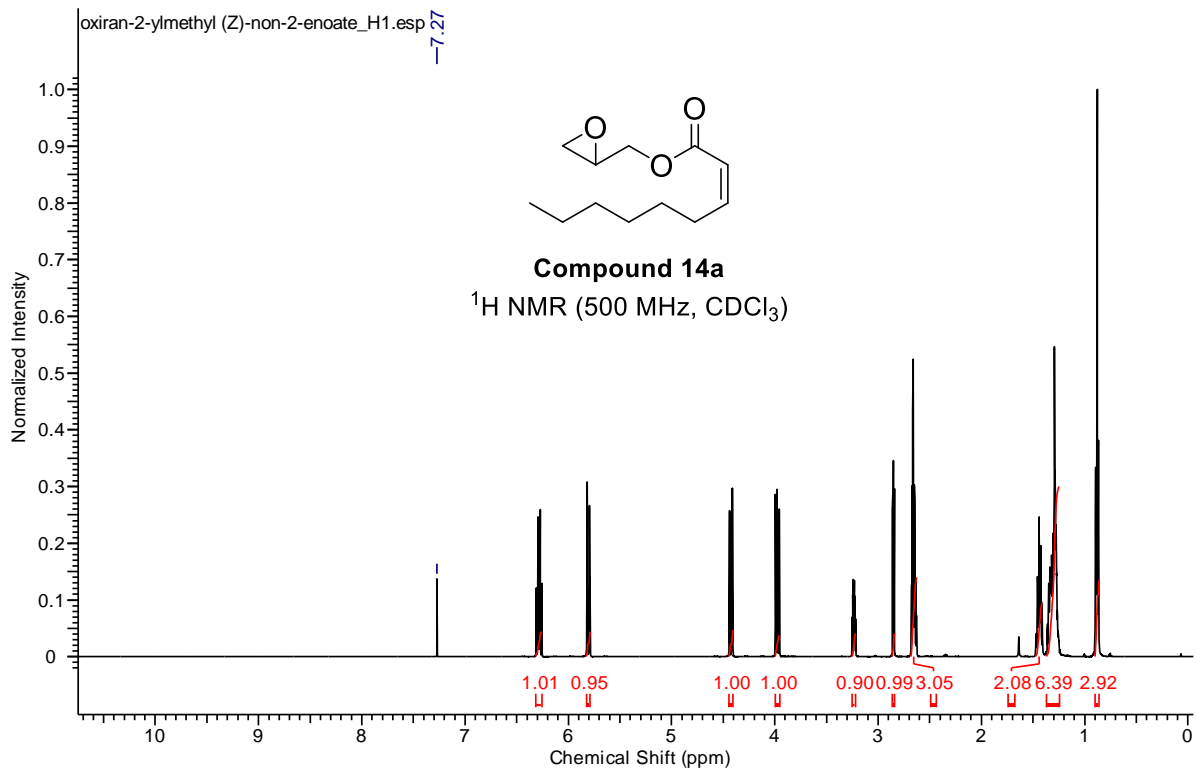


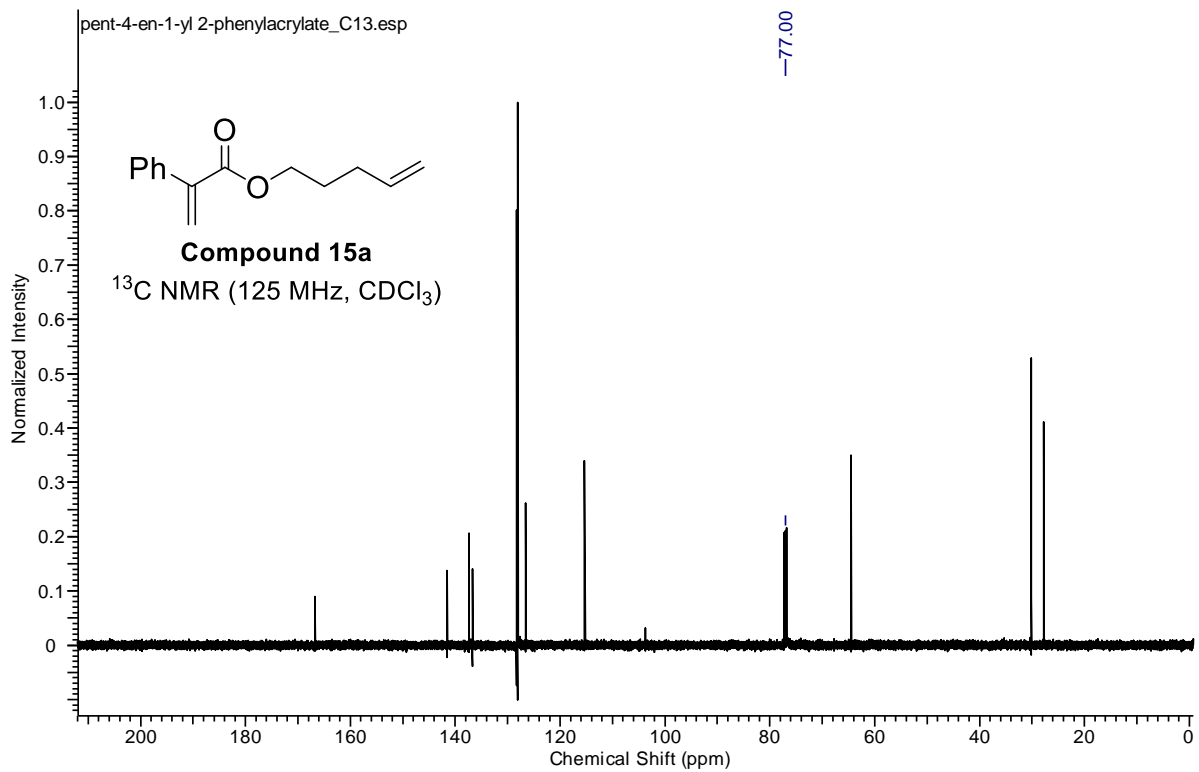
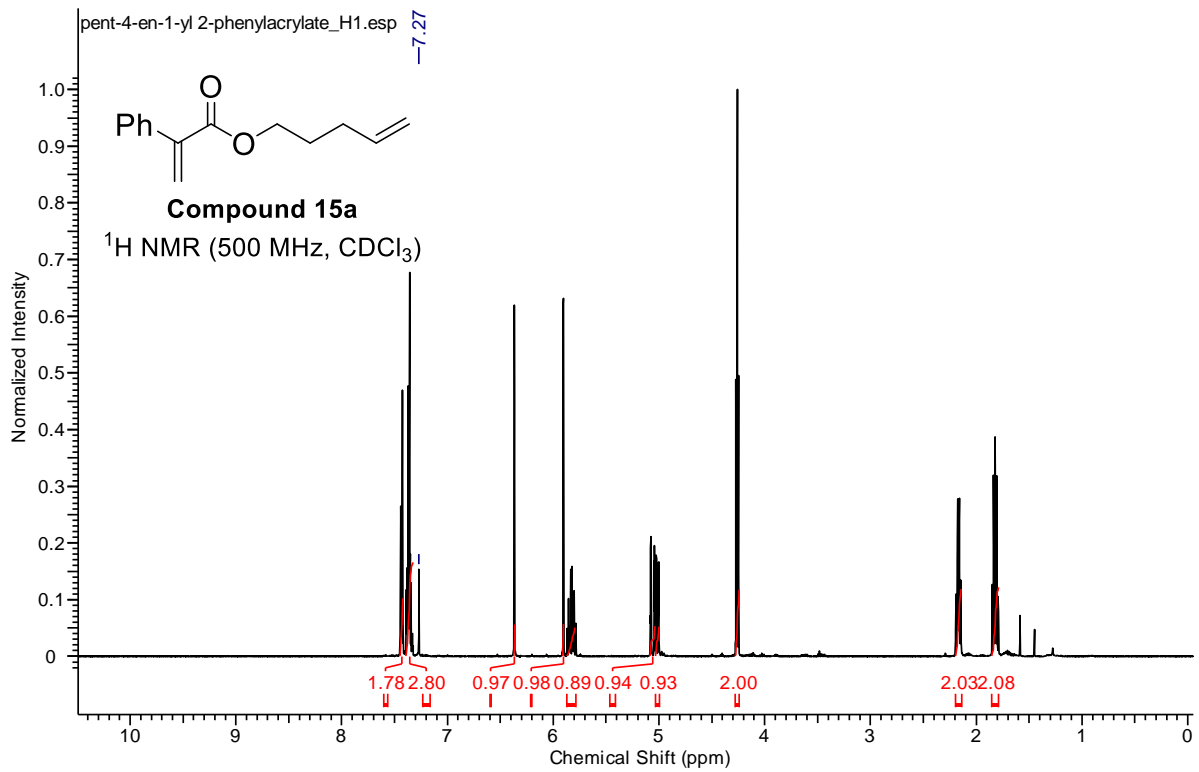


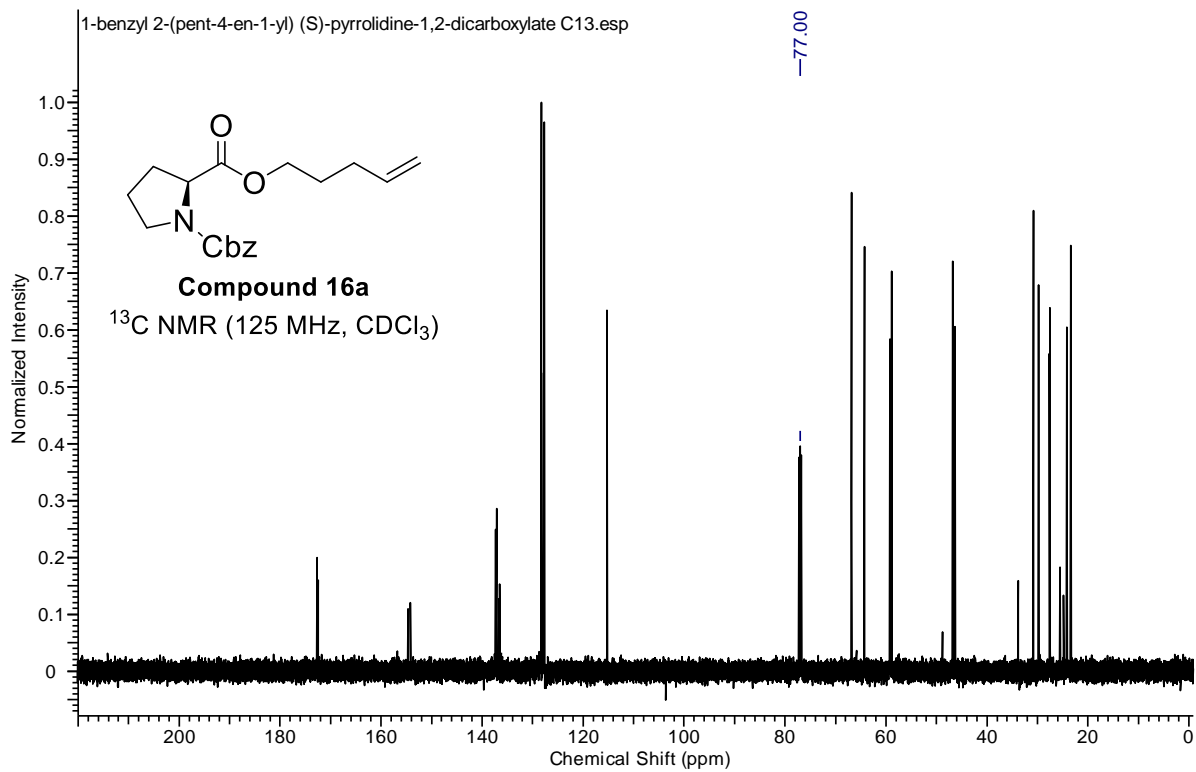
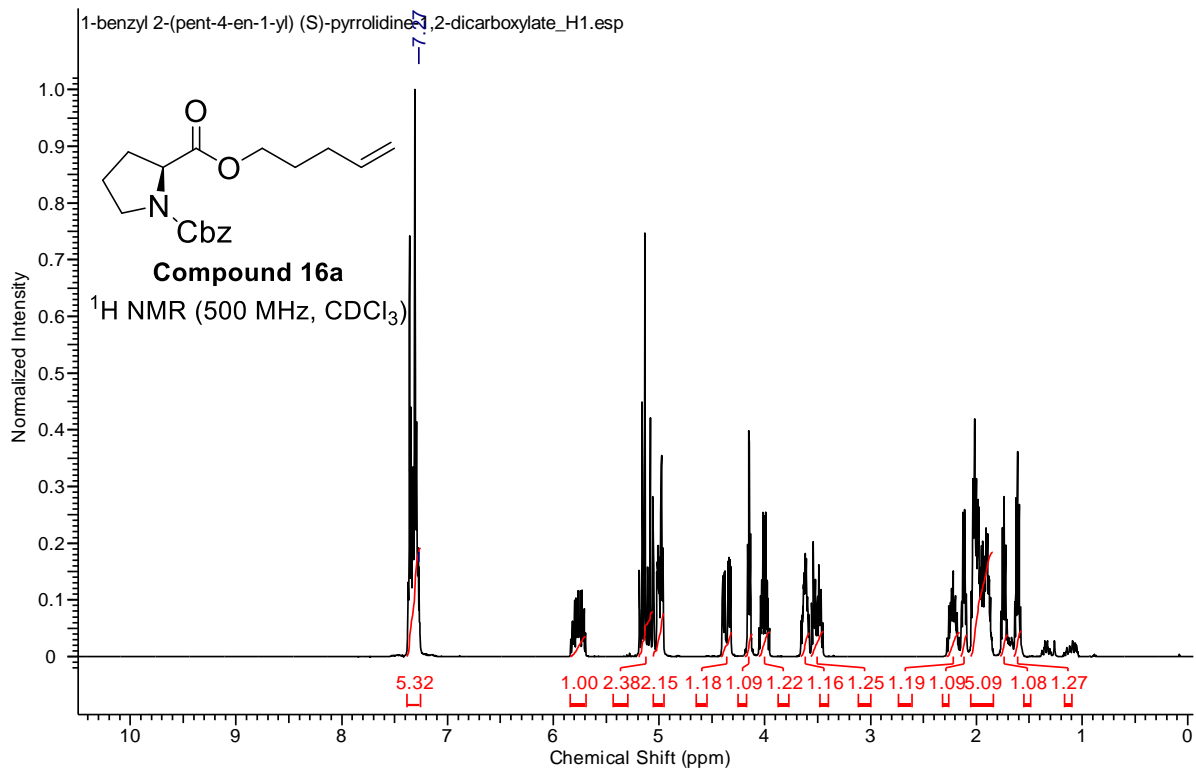


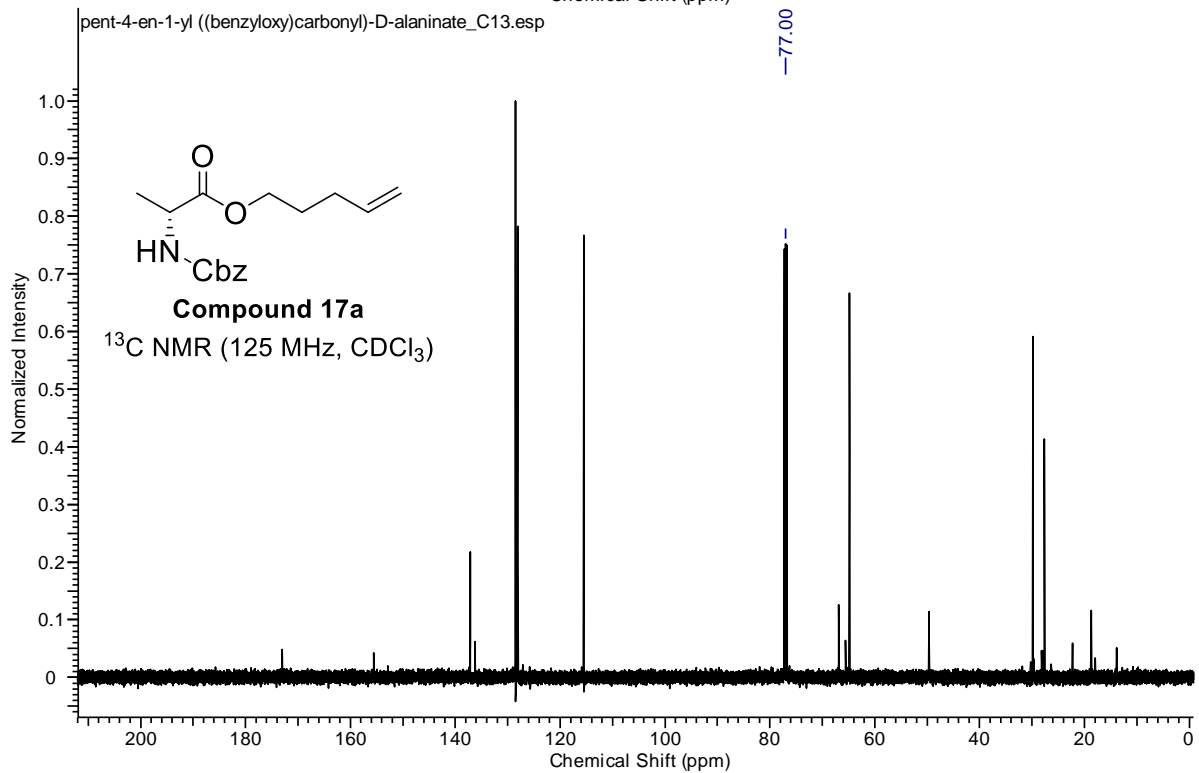
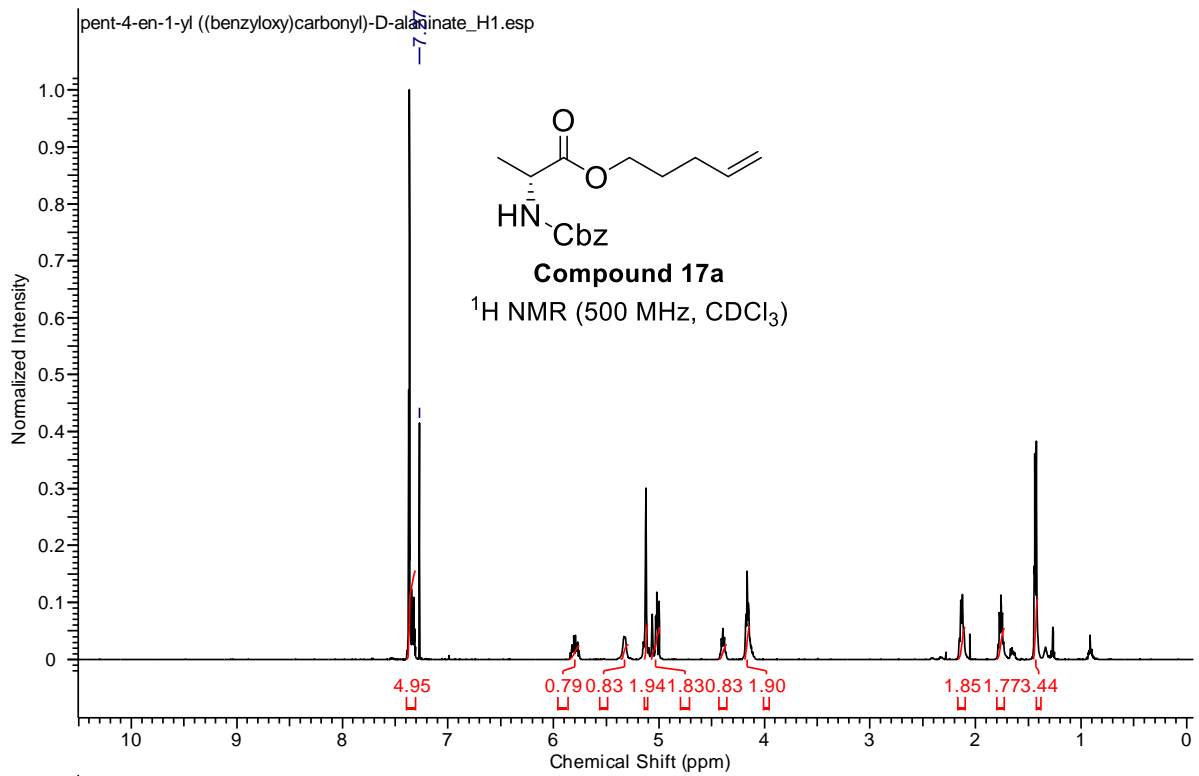


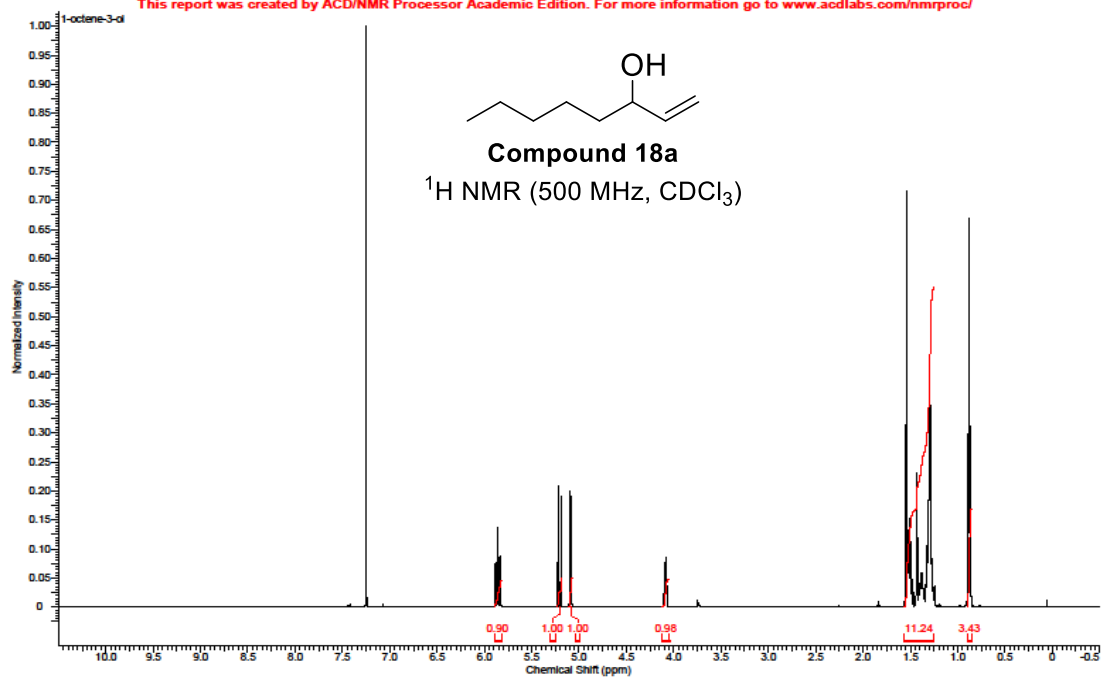






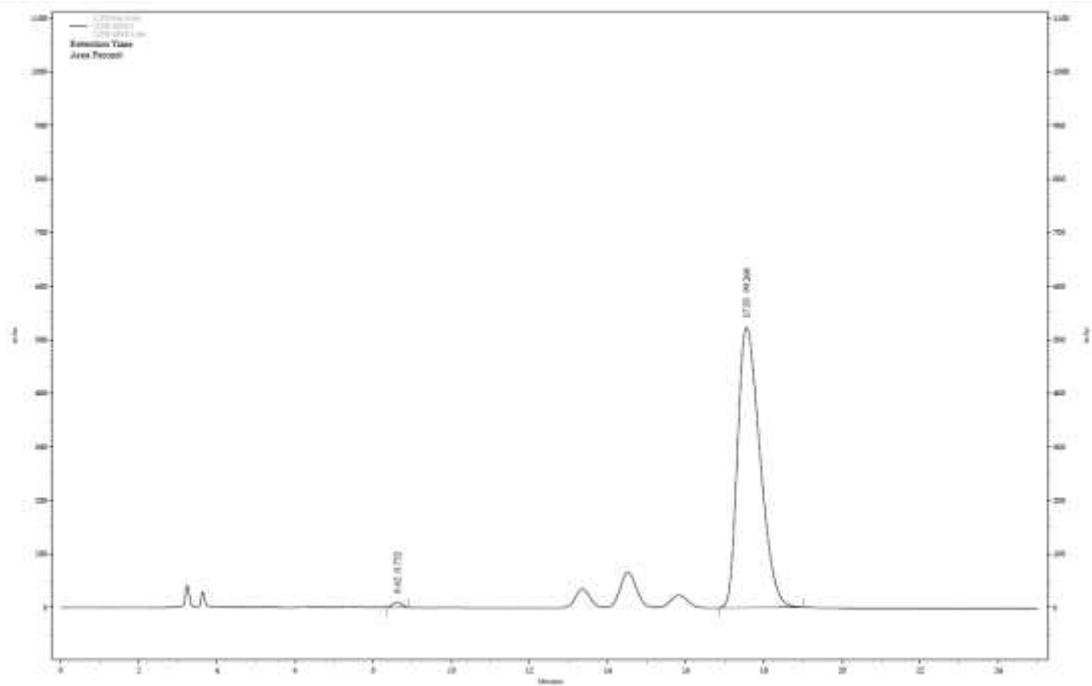






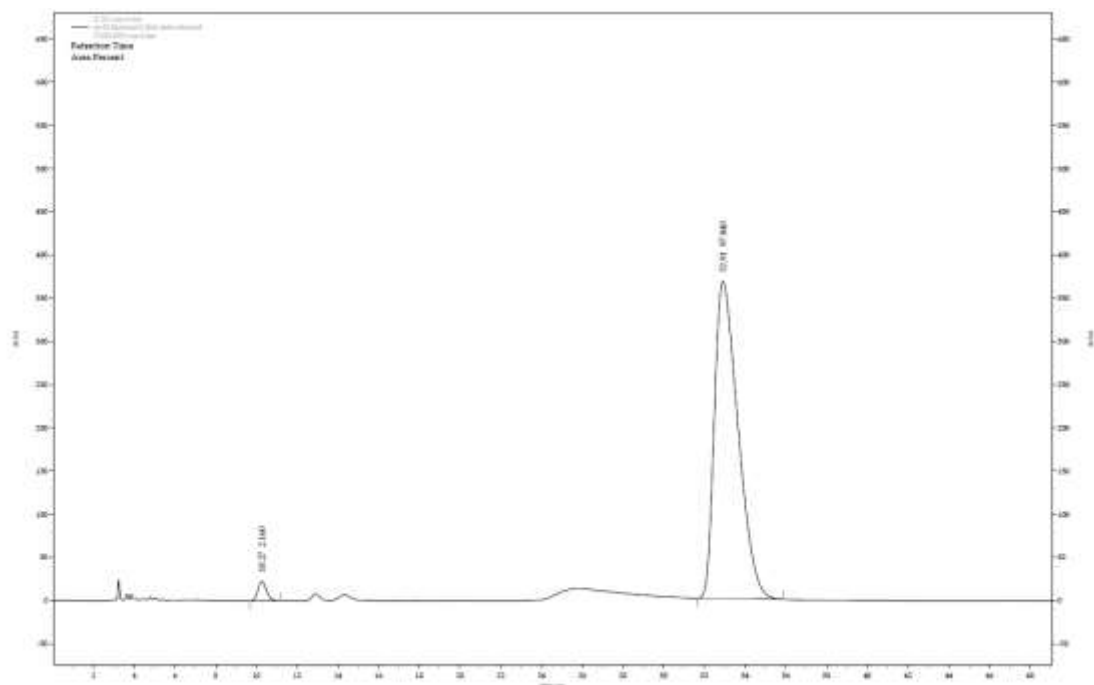
2.8 HPLC Chromatograms

Chiral Purity Analysis of Product **17a**



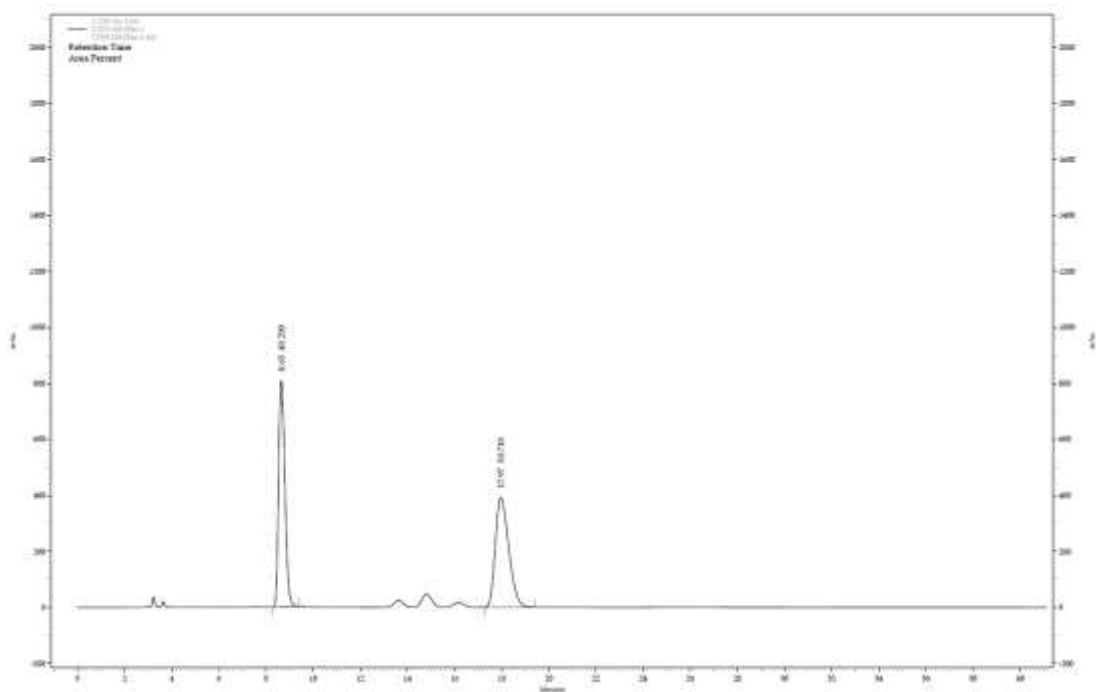
Peak	Compound	Retention Time (min)	Area [%]
1	17a-L	8.82	0.736
2	17a	17.55	99.268

Chiral Purity Analysis of Alkyne **17**

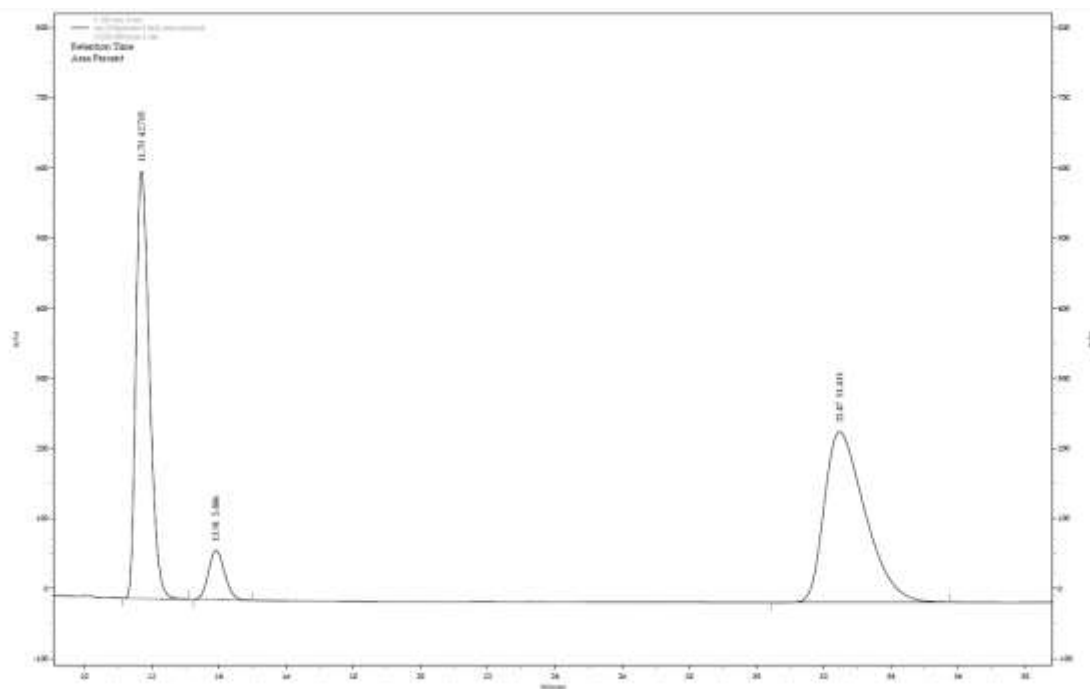


Peak	Compound	Retention Time (min)	Area [%]
1	17-L	10.27	2.160
2	17	32.91	97.840

Racemic Standard for Product 17a



Racemic Standard for Alkyne 17a



Peak	Compound	Retention Time (min)	Area [%]
1	17-L	11.70	42.703
3	17	32.47	51.411

2.9 References

1. *Stereoselective Alkene Synthesis*, Wang, J., Ed.; Springer: Heidelberg, **2012**.
2. C. Oger, L. Balas, T. Durand, J. Galano, *Chem. Rev.* **2013**, *113*, 1313
3. Arai, T.; Takahashi, O. *J. Chem. Soc., Chem. Commun.* **1995**, 1837.
4. Wittig, G.; Schöllkopf, U. *Chem. Ber.* **1954**, *87*, 1318.
5. *Olefin Metathesis: Theory and Practice*, Grela, K., Ed.; Wiley: Hoboken, NJ, **2014**.
6. *New Trends in Cross-Coupling: Theory and Applications*, Colacot, T., Ed.; RSC: Cambridge, UK, **2015**.
7. With Cu: a) A. M. Whittaker, G. Lalic, *Org. Lett.* **2013**, *15*, 1112. K. Semba, T. Fujihara, T. Xu, J. Terao, Y. Tsuji, *Adv. Synth. Catal.* **2012**, *354*, 1542; b) T. Fujihara, K. Semba, J. Terao, Y. Tsuji, *Cat. Sci. Tech.* **2014**, *4*, 1699.
8. With Au: M. Yan, T. Jin, Y. Ishikawa, T. Minato, T. Fujita, L. -Y Chen, M. Bao, N. Asao, M. -W. Chen, Y. Yamamoto, *J. Am. Chem. Soc.* **2012**, *134*, 17536.
9. With Ru: a) C. Belger, N. M. Neisius, B. Plietker, *Chem. -Eur. J.* **2010**, *16*, 12214; b) R. Hua, J. Li, *Chem. -Eur. J.* **2011**, *17*, 8462; c) M. Niu, Y. Wang, W. Li, J. Jiang, Z. Jin, *Cat. Comm.* **2013**, *38*, 77; d) A. J. Lough, R. H. Morris, L. Ricciuto, T. Schleis, *Inorg. Chim. Acta*, **1998**, *270*, 238; e) K. Radkowski, B. Sundararaju, A. Fürstner *Angew. Chem., Int. Ed.* **2012**, *51*, 355.
10. With Rh: R. R. Schrock, J. A. Osborn, *J. Am. Chem. Soc.* **1976**, *98*, 2143.
11. With Pt: A. J. Wain, *Faraday Discuss.* **2013**, *162*, 57.
12. With Ni: a) F. Alonso, I. Osante, M. Yus, *Adv. Synth. Catal.* **2006**, *348*, 305; b) A. Reyes-Sanchez, F. Canavera-Buelvas, R. Barrios-Francisco, O. L. Cifuentes-Vaca, M. Flores-Alamo, J. J. Garcia, *Organometallics*, **2011**, *30*, 3340; c) T. Chen, J. Xiao, Y. Zhou, S. Yin, L. J. Han, *J. Organomet. Chem.* **2014**, *749*, 51
13. With Cr: H. Yoshida, M. Kato, T. Ogata, *J. Org. Chem.* **1985**, *50*, 1147.
14. With V: H. S. La Pierre, J. Arnold, F. D. Toste, *Angew. Chem., Int. Ed.* **2011**, *50*, 3900.
15. With Fe: a) T. N. Gieshoff, A. Welther, M. T. Kessler, M. H. G. Prechtel, A. J. von Wangelin, *Chem. Commun.* **2014**, 2261; b) D. Srimani, Y. Diskin-Posner, Y. Ben-David, D. Milstein, *Angew. Chem., Int. Ed.* **2013**, *52*, 14131.

16. Gangadhar, P.; Reddy, A. S.; Srihari, P. *Tetrahedron* **2016**, *72*, 5807.
17. Veerasamy, N.; Carlson, E. C.; Carter, R. G. *Org. Lett.* **2012**, *14*, 1595.
18. Lu, P.; Mailyan, A.; Gu, Z.; Guptill, D. M.; Wang, H.; Davies, H. M. L.; Zakarian, A. *J. Am. Chem. Soc.* **2014**, *136*, 17738.
19. Wang, F. -X.; Du, J. -Y.; Wang, H. -B.; Zhang, P. -L.; Zhang, G. -B.; Yu, K. -Y.; Zhang, X. -Z.; An, X. -T.; Cao, Y. -X.; Fan, C. -A. *J. Am. Chem. Soc.* **2017**, *139*, 4282.
20. Smith, A. B. III; Beauchamp, T. J.; LaMarche, M.J.; Kaufman, M. D.; Qiu, Y.; Arimoto, H.; Jones, D. R.; Kobayashi, K. *J. Am. Chem. Soc.* **2000**, *122*, 8654.
21. Leopold Horner; Hoffmann, H. M. R.; Wippel, H. G. *Chem. Ber.* **1958**, *91*, 61. b) Horner, L.; Hoffmann, H. M. R.; Wippel, H. G.; Klahre, G. *Chem. Ber.* **1959**, *92*, 2499. c) Wadsworth, W. S., Jr.; Emmons, W. D. *J. Am. Chem. Soc.* **1961**, *83*, 1733. d) Wadsworth, W. S., Jr.; Emmons, W. D. *Organic Syntheses*, Coll. Vol. 5, 1973, pp. 547. e) Wadsworth, W. *Org. React.* **1977**, *25*, 73.
22. Still, W. C.; Gennari, C. *Tetrahedron Lett.* **1983**, *24*, 4405.
23. Mergott, D. J.; Frank, S. A.; Roush, W. R. *Org Lett.* **2002**, *4*, 3157.
24. Randall, M. L.; Tallarico, J. A.; Snapper, M. L. *J. Am. Chem. Soc.* **1995**, *117*, 9610.
25. a) Kang, B.; Kim, D. -H.; Do, Y.; Chang, S. *Org. Lett.* **2003**, *5*, 3041. b) Hansen, E. C.; Lee, D. *Org. Lett.* **2004**, *6*, 2035. c) Kang, B.; Lee, J. M.; Kwak, J.; Lee, Y. S.; Chang, S. *J. Org. Chem.* **2004**, *69*, 7661.
26. a) Crowe, W. E.; Goldberg, D. R. *J. Am. Chem. Soc.* **1995**, *117*, 5162. b) Ibrahim, I.; Yu, M.; Schrock, R. R.; Hoveyda, A. H. *J. Am. Chem. Soc.* **2009**, *131*, 3844. c) Meek, S. J.; O'Brien, R. V.; Llaveria, J.; Schrock, R. R.; Hoveyda, A. H. *Nature* **2011**, 471. d) Marinescu, S. C.; Schrock, R. R.; Muller, P.; Takase, M. K.; Hoveyda, A. H. *Organometallics* **2011**, *30*, 1780.
27. a) Marinescu, S. C.; Schrock, R. R.; Muller, P.; Takase, M. K.; Hoveyda, A. H. *Organometallics* **2011**, *30*, 1780. b) Jiang, A. J.; Zhao, Y.; Schrock, R. R.; Hoveyda, A. H. *J. Am. Chem. Soc.* **2009**, *131*, 16630.
28. Molander, G. A.; Dehmel, F. *J. Am. Chem. Soc.* **2004**, *126*, 10313.
29. Trost, B. M.; Biannic, B.; Brindle, C.; O'Keefe, B. M.; Hunter, T.; Ngai, M. -Y. *J. Am. Chem. Soc.* **2015**, *137*, 11594.

30. Lu, G. -P.; Voigtritter, K. R.; Cai, C.; Lipshutz, B. H. *J. Org. Chem.* **2012**, *77*, 3700.
31. H. Lindlar, *Helv. Chim. Acta* **1952**, *35*, 446.
32. Nakanishi, A.; Mori, K. *Biosci., Biotechnol., Biochem.* **2005**, *69*, 1007.
33. Ghosh, A. K.; Wang, Y.; Kim, J. T. *J. Org. Chem.* **2001**, *66*, 8973.
34. Brown, C. A.; Brown, H. C. *J. Am. Chem. Soc.* **1963**, *85*, 1003.
35. Brown, C. A. *J. Org. Chem.* **1970**, *35*, 1900.
36. Trost, B. M.; Braslau, R. *Tetrahedron Lett.* **1989**, *30*, 4657.
37. Trost, B. M.; O'Boyle B. M.; Hund D. *J. Am. Chem. Soc.* **2009**, *131*, 15061.
38. Tani, K.; Ono, N.; Okamoto, S.; Sato, F. *J. Chem. Soc., Chem. Commun.* **1993**, 386.
39. a) P. Hauwert, G. Maestri, J. W. Sprengers, M. Catellani, C. J. Elsevier, *Angew. Chem., Int. Ed.* **2008**, *47*, 3223. b) Hauwert, P.; Boerleider, R.; Warsink, S.; Weigand, J. J.; Elsevier, C. J. *J. Am. Chem. Soc.* **2010**, *132*, 16900.
40. Wei, L. L.; Wei, L. M.; Pan, W. B.; Leou, S. P.; Wu, M. J. *Tetrahedron Lett.* **2003**, *44*, 1979.
41. R. Shen, T. Chen, Y. Zhao, R. Qiu, Y. Zhou, S. Yin, X. Wang, M. Goto, L. B. Han, *J. Am. Chem. Soc.* **2011**, *133*, 17037
42. a) US Environmental Protection Agency: *1,4-Dioxane*. www.epa.gov. b) US Environmental Protection Agency: *Acetonitrile*. www.epa.gov.
43. P. T. Anastas, J. C. Warne, *Green Chemistry: Theory and Practice*; Oxford University Press: New York, **2000**.
44. a) Nishikata, T.; Lipshutz, B. H. *J. Am. Chem. Soc.* **2009**, *131*, 12103. b) Nishikata, T.; Lipshutz, B. H. *Org. Lett.* **2009**, *11*, 11. c) Nishikata, T.; Lipshutz, B. H. *Chem. Commun.* **2009**, 6472. d) Moser, R.; Nishikata, T.; and Lipshutz, B. H. *Org. Lett.* **2010**, *12*, 1.
45. a) *Handbook of reagents for organic synthesis: Oxidizing and reducing agents*; Burke, S. D., Danheiser, R. L., Eds.; John Willey: **2000**. b) Mohamed, Y. M. A.; Hansen, T. V. *Tetrahedron* **2013**, *69*, 3872.
46. Chauhan, K.; Bhatt, R. K.; Falck, J. R.; Capdevila J. H. *Tetrahedron Lett.* **1994**, *35*, 1825.

47. a) Mitsudome, T.; Takahashi, Y.; Ichikawa, S.; Mizugaki, T.; Jitsukawa, K.; Kaneda, K. *Angew. Chem., Int. Ed.* **2013**, *52*, 1481. b) Takahashi, Y.; Hashimoto, N.; Hara, T.; Shimazu, S.; T. Mitsudome, T. Mizugaki, K. Jitsukawa, K. Kaneda, *Chem. Lett.* **2011**, *40*, 405.
48. a) Z. Hou, N. Theyssen, A. Brinkmann, W. Leitner, *W. Angew. Chem., Int. Ed.* **2005**, *44*, 1346; b) B. Feng, Z. Hou, H. Yang, X. Wang, Y. Hu, H. Li, Y. Qiao, X. Zhao, Q. Huang, *Langmuir* **2010**, *26*, 2505.
49. Feng, J.; Handa, S.; Gallou, F.; Lipshutz, B. H. *Angew. Chem., Int. Ed.* **2016**, *55*, 8979.
50. Gabriel, C. M.; Parmentier, M.; Riegert, C.; Lanz, M.; Handa, S.; Lipshutz, B. H.; Gallou, F. *Org. Process Res. Dev.* **2017**, *21*, 247.
51. G. Guella, C. Zanchetta, B. Patton, A. Miotello *J. Phys. Chem. B* **2006**, *110*, 17024-17033.
52. S. Narayan, J. Muldoon, M. G. Finn, V. V. Fokin, H. C. Kolb, K. B. Sharpless, *Angew. Chem., Int. Ed.* **2005**, *44*, 3275.
53. Klumphu, P.; Lipshutz, B. H. *J. Org. Chem.* **2014**, *79*, 888.
54. Wuts, P. G. M.; *Greene, T. W. Greene's Protective Groups in Organic Synthesis*; Wiley: Hoboken, NJ, **2014**.
55. a) R. A. Sheldon, *Green Chem.* **2007**, *9*, 1273. b) B. H. Lipshutz, N. A. Isley, J. C. Fennewald, E. D. Slack, *Angew. Chem., Int. Ed.* **2013**, *52*, 10952.
56. a) C. L. Young, *Ed. IUPAC Solubility Data Series, Vol. 5/6*, Hydrogen and Deuterium, Pergamon Press: Oxford, England, **1981**; b) E. Brunner, *J. Chem. Eng. Data*, **1985**, *30*, 269. (c) R. Battino, T. R. Rettich, T. Tominaga, *J. Phys. Chem. Ref. Data*, **1983**, *12*, 163.
57. Slack, E.; Gabriel, C. M.; Lipshutz, B. H. *Angew. Chem., Int. Ed.* **2014**, *53*, 14051.
58. Handa, S.; Wang, Ye; Gallou, F.; Lipshutz, B. H. *Science* **2015**, *349*, 1087.
59. a) B. H. Lipshutz, S. Ghorai, A. R. Abela, R. Moser, T. Nishikata, C. Duplais, A. Krasovskiy, *J. Org. Chem.* **2011**, *76*, 4379; b) B. H. Lipshutz, S. Ghorai, S. *Aldrichimica Acta* **2008**, *41*, 59.
60. B. Neises, W. Steglich, *Angew. Chem., Int. Ed. Engl.* **1978**, *17*, 522.
61. M. Journet, D. Cai, L. M. DiMichele, D. Larsen, *Tetrahedron Lett.* **1998**, *39*, 6427.

62. R. T. H. Linstadt, C. Peterson, D. J. Lippincott, C. I. Jette, B. H. Lipshutz, *Angew. Chem., Int. Ed.* **2014**, *53*, 1.
63. M. Y. H. Lai, M. A. Brimble, D. J. Callis, P. W. R. Harris, M. S. Levi, F. Sieg, F. *Biorg. Med. Chem.* **2005**, *13*, 533.

III. Amide and Peptide Bond Formation in Water at Room Temperature

3.1 Introduction

The amide bond is a functionality found extensively throughout many classes of molecules. This important linkage is the key feature for the construction and stability of proteins within living systems, many of which have led to the widespread development of peptide-based drugs.¹ Furthermore, it is because of the stability and low toxicological liability that the amide/peptide linkage is so ubiquitously found across many industries, being highly prevalent throughout many of the top selling drugs including isentris, incivek, zoladex, and diovan. Amides are also found among many important agrochemicals such as boscolid, cyclaniliprole, and oxathiapiprolin. Excellent examples of how the stability of this bond can be used as functional materials are products such as Kevlar and nylon. In addition, compounds containing amides are found extensively in organocatalysis,² are prevalent in ligand scaffolds for transition metal catalysis,³ and is often the linkage of choice for directing groups in C-H activation.⁴

Amides are generally well tolerated over a wide range of reaction types due to the high activation energy required for hydrolysis⁵ as the result of delocalization of electrons across the functional group as well as their relatively high pKa of about 17-26⁶ (depending on substituents) generally making this disconnection one which can be made early or late within a synthetic route. As a synthetic handle, however dehydration of an amide to the corresponding iminium salt can be achieved with a variety of reagents to arrive at the corresponding nitrile⁷ (from 1° amides) or an electrophilic synthon for the construction of

ketones, imine derivatives,⁸ and enamines,⁹ or cyclic imines via the Bischler-Napieralski Reaction.¹⁰ Furthermore, Weinreb amides and amido-morpholines have been used extensively as stable precursors to ketones which are constructed under metalation conditions.¹¹ Amides can be reduced to the corresponding amine with LiAlH_4 ¹² while Weinreb amides can be reduced with LiAlH_4 or DIBALH to arrive at the corresponding aldehyde.¹³ Transition metal-catalyzed reduction of amides is also an intense field of study with recent advances being made with systems using Fe,^{14a,b} Ru,^{14c} Zn,^{14d} Cu,^{14e} Pt,^{14f} Mo,^{14g} Rh,^{14h} and Ni.¹⁴ⁱ Amides may also be reduced catalytically via transition metal catalysis. In the presence of Br_2 and a strong base, the Hofmann Rearrangement, can be performed on primary amides to deliver primary amines,^{15a,b} carbamates,^{15c} and ureas^{15d} with the loss of the carbonyl carbon.

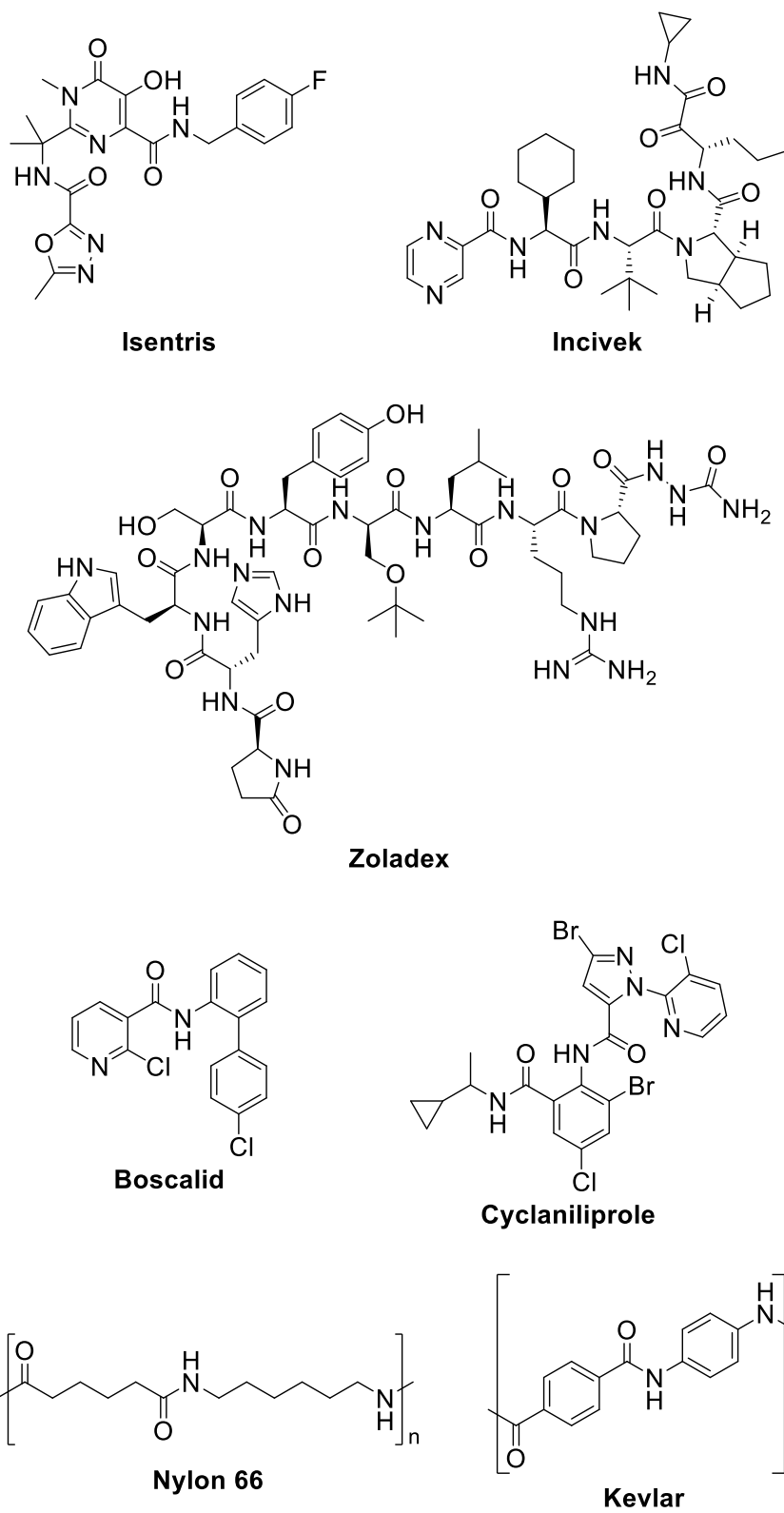
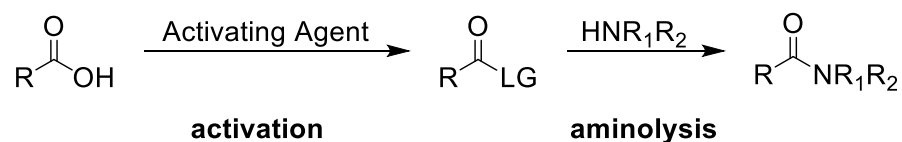


Figure 1. Representative examples of industrially important compounds containing amides.

3.2 Background

Many routes to amides exist to date and a complete overview of all synthetic procedures is not appropriate here. This section will focus on the construction of amides from carboxylic and amine starting materials as this is by far the most widely utilized disconnection for the synthesis of peptides and industrial relevant amides. Used directly, the direct condensation of a carboxylic acid with an amine is possible, however in combination, the two coupling partners form a salt and consequently require high reaction temperatures of 160-180°C which is energy intensive and generally incompatible with advanced intermediates due to the lability of sensitive functional groups and protected amino acids derivatives.^{5,16} As an alternate strategy, the acid may be activated by the displacement/direct conversion of the hydroxyl group of the carboxylic acid to a good leaving group (activation), allowing for displacement by the amine (aminolysis).¹⁷



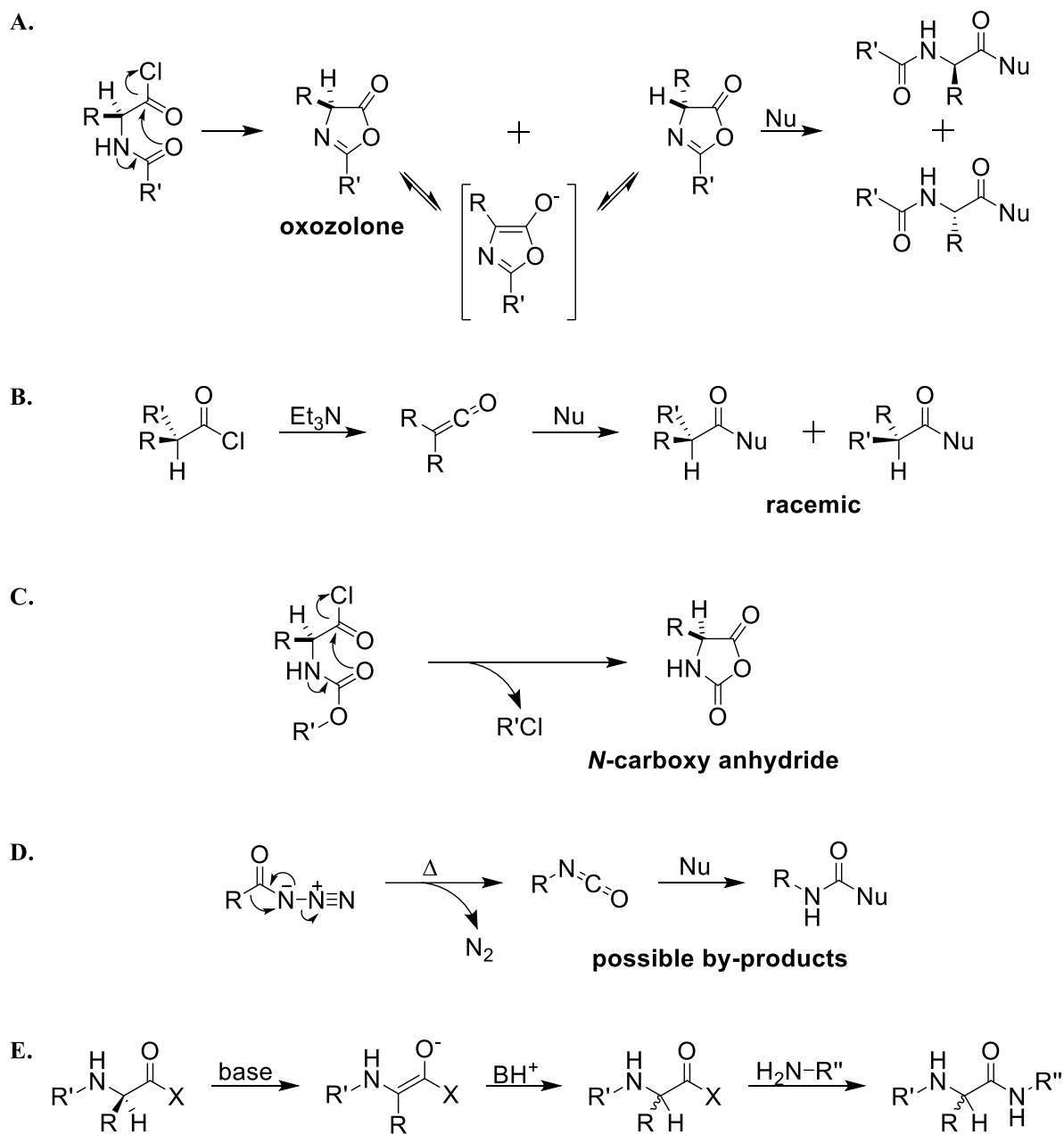
Scheme 1. Activation/aminolysis pathway for amide bond formation.

Amidation by acid activation is done using one of three approaches, where a) the reactive activated acylating species is generated prior to the amidation reaction in a separate step; b) the activated species is generated, isolated, and purified prior to amidation; or c) activation of the acylating partner is generated in situ as a one-pot procedure, reacting the active species upon its formation in the presence of an amine.¹⁷ Classically, this approach has been demonstrated in many ways, including activation as acyl halides,¹⁸ acyl azides,¹⁹ acylimidazoles,²⁰ mixed anhydrides,²¹ as well as electron deficient “activated esters”. Each

activated species has its own merits, where acyl chlorides are conveniently prepared from a variety of reagents inexpensive reagents such as thionyl chloride²² and oxalyl chloride²³ which furnish the active intermediates cleanly within short reaction times as the reaction is driven by the generation of gaseous by-products, SO₂ and CO/CO₂ respectively. Other reagents for the generation of acyl chlorides include phosphorous trichloride,^{24a} phosphorous oxychloride,^{24b} phosphorous pentachloride,^{24c,d} and cyanuric chloride.^{24e} Acyl chlorides can be stored in some cases, but hydrolysis can be problematic. While the use of acyl chlorides is a convenient procedure for amide bond formation, this approach is not necessarily appropriate for the synthesis of peptides. In addition to the liberation of quantitative HCl as a by-product which is not amenable to Boc-protected peptides,⁰ the formation of oxazolone intermediates may be encountered leading to racemization of the α -stereocenter under mildly basic conditions (Scheme 2A).¹⁷ Chiral integrity of peptides may also be compromised using acid chlorides under basic conditions as the result of ketene formation by deprotonation of the chiral α -carbon (Scheme 2B).²⁶ Other by-products that may arise from the use of acyl chlorides as well including *N*-carboxy anhydride formation (Scheme 2C).²⁷ The issue of racemization via base-promoted oxazolone formation is one that extends to several other activated acyl derivatives across a broad range of highly electrophilic activated intermediates.¹⁷

Acyl azides have been used extensively for peptide coupling showing minimal racemization in comparison to acyl chlorides, however the synthesis of such compounds requires the use of hazardous reagents such as hydrazine^{28a} and DPPA,^{28b} both of which are highly toxic and explosive.²⁹ Amidation by this method is limited by the competing Curtius rearrangement which leads to side products in the form of isocyanates which can be

hydrolyzed to the corresponding amine, and thus compete with the desired amine nucleophile (Scheme 2D).³⁰



Scheme 2. A. oxazolone formation from acyl chlorides; B. Ketene formation from acyl chloride activation; C. N-carboxy anhydride formation from acyl chloride containing amino acid derivatives; D. Curtis rearrangement of acyl azides; E. Direct enolization of amino acid derivatives.

Acyl imidazoles deliver amides in good yields with minimal racemization, however their method of preparation is reliant on the use of carbonyl diimidazole (CDI) which decomposes in the presence of water.³¹ Similar to the previous cases presented, the formation of acyl imidazoles occurs in the reaction prior to addition of the amine to the reaction mixture, and isolation of the activated amide is generally not possible due to its rapid decomposition.¹⁷

Mixed anhydrides remain as an important route to amide bonds, however their construction predominately utilizes coupling with a bulky acyl chloride,^{32a} expensive reagents such as 2-ethoxy-1-ethoxycarbonyl-1,2-dihydroquinoline (EDDQ)^{32b} again having the limitations of requiring anhydrous conditions and often low temperatures to arrive at active intermediates. Aside from the use of pivalic or carbonic anhydrides, selectivity can be an issue leading to lower overall yields and difficulties in removing by-products. Symmetrical anhydrides are simple to prepare and offer a cleaner reaction profile than their mixed counterparts, however the obvious drawback of this intermediate is the generation of one equivalent of waste from the carboxylic acid starting material.^{32c}

As it stands, the major issue facing peptide coupling comes in the form of racemization which may go through two major pathways, namely: oxazolone formation (Scheme 2A) or direct enolization (Scheme 2E). The factors which influence oxazolone formation include a.) the electrophilicity of the activated species, b.) the nature of the α -amine (oxazolone formation is less favorable for amines protected as carbamates), and substitution of the α -carbon (Figure 2).³³

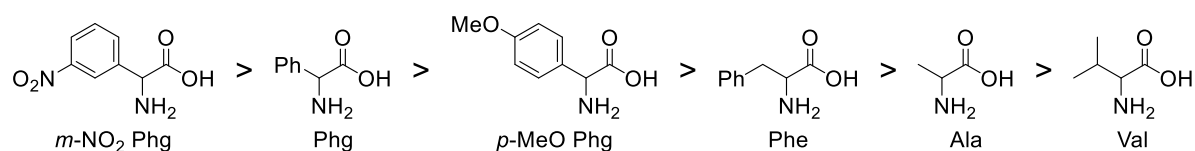
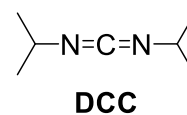
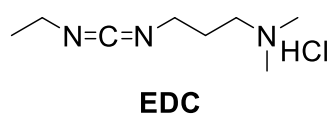
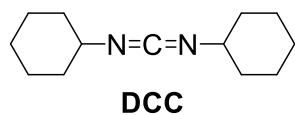


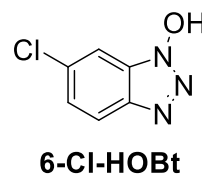
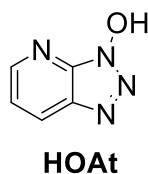
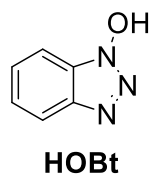
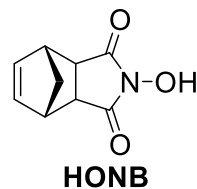
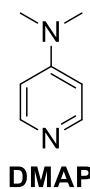
Figure 2. α -proton acidity trend for various amino acids.

Development of reagents and conditions for activating the carbonyl center with control of racemization has thus been an intense area of research for nearly a half a century. Most commonly, carbodiimide reagents are employed such as EDC,^{34a} DCC,^{34b} and DIC^{34c} to serve this purpose. The use of such reagents in combination with activators such as those derived from benzotriazoles (HOBt, HOAt, 6-Cl-HOBt) have been found as excellent additives to increase reaction rates, and suppress racemization beyond the selectivities of earlier developed activators such as DMAP, HOSu, and HONB (Figure 3).¹⁷ As a result of the dual nature of the carbodiimide/benzotriazole activation conditions, several advanced reagents have been developed that incorporate both compounds onto one scaffold as an uronium salt, such as TBTU, TATU, and TCTU or as a guanidinium salt such as HATU.¹⁷ Alternate dual activation reagents for peptide coupling are phosphonium salts that work via a similar mechanism. These advanced coupling reagents have had a profound effect on peptide coupling today both in the solution and solid phase, and have been incorporated in the synthesis of many drugs including velcade³⁵ and incivek,³⁶ and victrelis.³⁶

Carbodiimides



Activators



Advanced Coupling Reagents

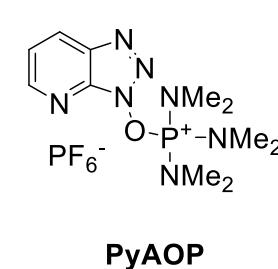
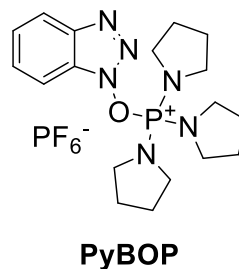
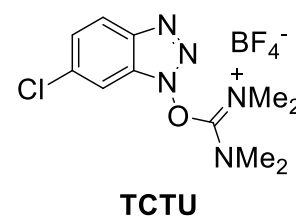
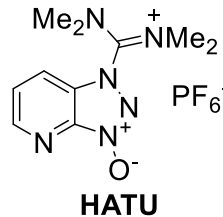
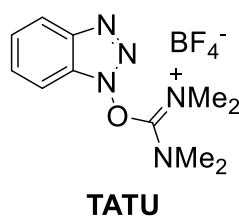
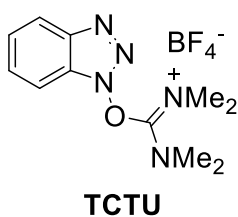


Figure 3. Common coupling reagents and activators for peptide coupling.

In an attempt to further increase the safety of these reagents, a new class of oxime-derived activators has since emerged with the goal of replacing the benzotriazole scaffold which is known to undergo autocatalytic decomposition.³⁷ That is, benzotriazoles are

explosive. Oximes were explored due to the similar pKa to benzotriazoles, and from the screening of various electron deficient oximes, an old reagent with a new application arrived as Oxyma (**1**, Figure 4).³⁸ Oxyma was found to offer excellent retention of stereochemistry with lower racemization than its benzotriazole counterparts, and can couple highly sterically hindered amino acids/peptides in high yields in short reaction times. The emerging success of this activator led to the development of a new coupling reagent, COMU (**2**), as a safer alternative to the existing state-of-the-art reagents.³⁹

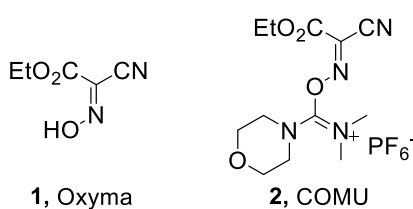


Figure 4. Structures of Oxyma and COMU.

Recently, much effort has been made towards forming amide bonds by boronic acid catalysis (BAC).⁴⁰ While this transformation shows considerable promise in the field of peptide coupling, major limitations such as the requirement of a large excess of molecular sieves, expensive catalysts, narrow substrate scope, and irreproducibility suggests that the technology has yet to mature to the point where these conditions can compete with the current technology. Similarly, impressive progress has been made in the Ni-catalyzed catalytic amide bond formation from phenyl ethers,⁴¹ however high reaction temperatures, air-sensitive reaction conditions, high loading of the expensive catalyst, and narrow substrate scope renders this method inappropriate for peptide coupling as well. Another important contribution to the field is the Ru-catalyzed amide synthesis from amines and carboxylic acids activated *in situ* with acetylenes.⁴² This method requires high reaction temperatures as

well and uses another egregious solvent: 1,4-dioxane to afford highly variable yields for peptide and amide products (18-99%). The evolution of this transformation has a long history with remarkable advancements, yet one parameter in particular seemingly overlooked is solvent usage. Standard reaction conditions for peptide coupling rely heavily on the use of DCM and DMF,¹⁷ two of the most egregious solvents in synthesis. It is quite puzzling that less effort has been made to overcome the use of these solvents especially considering their general avoidance for other transformations on scale and the correlation between racemization and the use of DMF.⁴³ While it is well understood that the use of these polar aprotic solvents effectively solvate a broad spectrum of substrates, it is quite evident that a direct replacement exists to solubilize charged species: water. Interestingly, a communication was released for the suggestion of various alternative solvents including 2-Me-THF, EtOAc, and IPA, yet water was excluded as a viable solvent for amide bond formation.⁰ It would seem that the call for a safer protocol has been answered by replacing benzotriazole activators; however, a method can hardly be considered “green” when reactions require genotoxic DMF as the reaction solvent.

The absence of a general peptide coupling in water without the use of benzotriazole activators spurred interest in our group and inspired us to develop a protocol which would utilize a safer reagent such as COMU under aqueous reaction conditions and offer a method that not only replaces DMF and DCM, but also allows for recycling of the reaction medium.⁴⁵

3.3 Early Work

Prior to our investigations on developing a sustainable method for peptide coupling, very few examples existed in the literature utilizing water as the reaction solvent. The use of

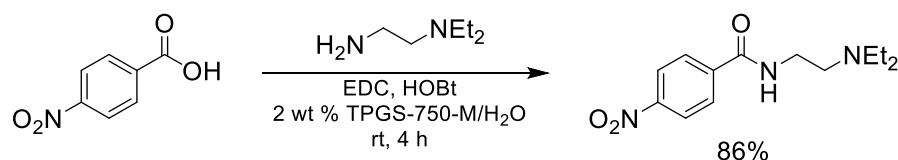
water dispersible nanoparticles for solid phase synthesis is one such example, utilizing Maryfield-type coupling under ball milling conditions.⁴⁶ This method was used to synthesize the pentapeptide natural product Leu-enkephalin and is a great development in peptide synthesis as water is generally disregarded as a solvent for solid phase peptide synthesis due to its less than optimal ability to swell peptide support resins.⁴⁷ In these reports, material solubility is overcome mechanically with zirconium beads at high shear rates and thus may not be feasible in a conventional laboratory. In addition, the limitations of this method are clear, in that many non-peptide amide bond disconnections may not contain a handle for solid phase synthesis.

PEG has been proven as an effective support for solid phase synthesis of peptides as well, where De Marco and co-workers described a method under aqueous conditions.⁴⁸ Their procedure benefits from Leuch's anhydrides,²⁷ thus alleviating the necessity for amino acid protecting groups. In addition to the limitation of being amenable solely to the synthesis of peptides, the use of neat triphosgene under microwave irradiation (for synthesis of Leuch's anhydrides) poses concerns in terms of safety,⁴⁹ and the use of basic reaction conditions (pH = 10.4) may lead to racemized products.

In the solution phase, Kurosu and co-workers developed a method in water utilizing EDC and an Oxyma derivative containing a ketal functionality for access to several short peptides under mild conditions.⁵⁰ The ketal functionality was designed to improve water solubility of the oxime and enhanced reaction rate and *de* when used in the presence of NaHCO₃. This method in particular is one that stands out among literature reports in terms of addressing safety, ease, and environmental responsibility. Limitations of this method are the lack of generality for amino acid coupling partners, in that more lipophilic amino acids require the use of a phase transfer catalyst (OTAB) or the use of DMF as a cosolvent.

On the contrary, use of DMT-Cl has been shown to work quite well under aqueous conditions for amidation of fatty acids.⁵¹ The unusual rate enhancement was attributed to incorporation of fatty acid salts in the micellar structure allowing reactions to take place at the micelle/H₂O interface. The presented substrate scope is limited to only fatty acids and aliphatic amines.

Seminal work on amidation in our studies began from a single example presented within a communication for the reduction of nitroarenes with Zn/NH₄Cl under micellar catalysis conditions.⁵² The work describes the use of EDC and HOBt with Et₃N as suitable conditions for the synthesis of a Procainamide precursor (Scheme 3). Based on these results, we set out to expand the scope and limitations of these conditions. The envisioned method would be general for amide bond formation in solution phase and would be amendable for both simple amide bonds as well as peptides under micellar catalysis conditions offering opportunity for solvent recycling.

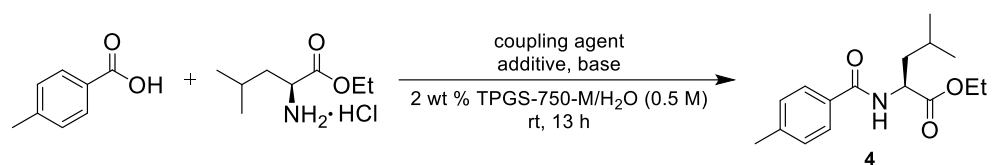


Scheme 3. Initial report of amide bond formation using TPGS-750-M/H₂O.

3.4 Results and Discussion

Looking towards developing a sustainable method for amide and peptide bond formation in water method development began by assessing the use of EDC-based activators utilizing micellar conditions as a starting point (Table 1). Rather than optimizing from a simple primary amine, the screening was carried out with Leu-OEt HCl with hopes that the optimized conditions would readily be translated to a peptide bond forming event. *p*-Toluic

acid was chosen such that the products would be easily identified (by TLC and NMR) and purified by column chromatography. From this screening, it was found that modifying the equivalents of base showed a pronounced effect, where 2.0 equivalents of Et₃N gave quantitative conversion to amide **4**, either increasing to 3.0 equivalents or dropping to 1.0 equivalent resulted in a lower isolated yield (entries 4 and 2, respectively). An explanation for this is that lower base loading leads to conditions that do not favor the nucleophilic attack of the amine onto the activated ester **5**, rationalized by the buildup of activated intermediate in the isolated product, and under base-free conditions (entry 1). Excessively basic conditions favors nucleophilic attack of the amine onto the carboxydiimide center, irreversibly forming the corresponding guanidine species evident by the complete consumption of the amine and low overall yield (Scheme 4). Although excellent conversion was achieved for EDC/HOBt system, a major focus of this work was to use a non-benzotriazole activator, such as Oxyma. In combination with EDC, only mediocre yields resulted while interestingly only 5% yield was achieved from the use of COMU (entry 8).



entry	coupling agent	additive	base	yield 4 (%) ^a	yield 5 (%)
1	EDCI (1.3 equiv)	none	none	11	33
2	EDCI (1.3 equiv)	HOBt (1.3 equiv)	Et ₃ N (1.0 equiv)	68	14
3	EDCI (1.3 equiv)	HOBt (1.3 equiv)	Et₃N (2.0 equiv)	>99	0
4	EDCI (1.3 equiv)	HOBt (1.3 equiv)	Et ₃ N (3.0 equiv)	49	0
5	EDCI (1.3 equiv)	DMAP (0.05 equiv)	Et ₃ N (2.0 equiv)	33	-
6	EDCI (1.3 equiv)	Oxyma (1.3 equiv)	Et ₃ N (2.0 equiv)	49	-
7	EDCI (1.3 equiv)	Oxyma (1.3 equiv)	Et ₃ N (3.0 equiv)	57	-
8	COMU (1.0 equiv)	none	Et ₃ N (3.0 equiv)	5	-

^aYields of isolated products.

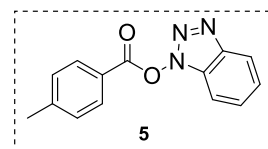
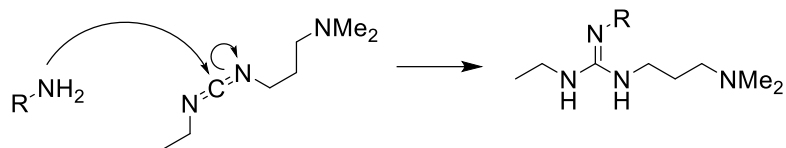
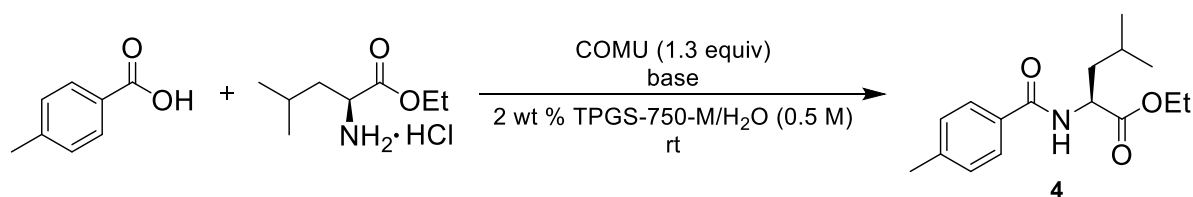


Table 1. Initial screening of coupling reagents and activators.



Scheme 4. Guanidine by-product formation with EDC.

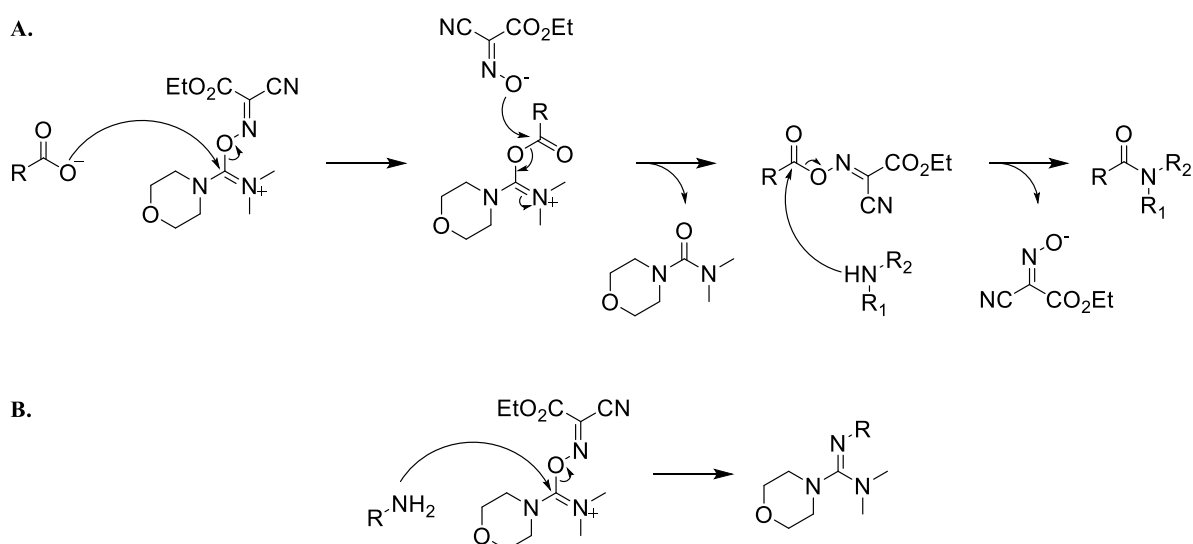
These findings suggest that amide coupling in water is highly sensitive to base and prompted the screening of several other amine bases (Table 2). An interesting correlation was found where increasing the pK_b led to higher overall yield of **4** where the weakest base in the series, N-methyl morpholine (NMM) yielded 93%, while the strongest base, 2,2,4,4-tetramethylpiperidine (TMP), yielded only 4% product. This observation is in line with the prior observation of how increased base loading diminishes product yield, increased basicity favors direct attack of the amine on COMU to generate the guanidine by-product (Scheme 5B).



entry	base ^a	time (h)	yield of 4 (%) ^a
1	Et ₃ N (2.0 equiv)	19	60
2	DIPEA (2.0 equiv)	19	65
3	DIPEA (3.0 equiv)	19	33
4	TMP (2.0 equiv)	17	4
5	NMM (2.0 equiv)	15	70
6	NMM (3.0 equiv)	13	93
7	1,4-dimethyl piperazine (3.0 equiv)	17	38
8	DBU (3.0 equiv)	17	0
9	DABCO (3.0 equiv)	17	0

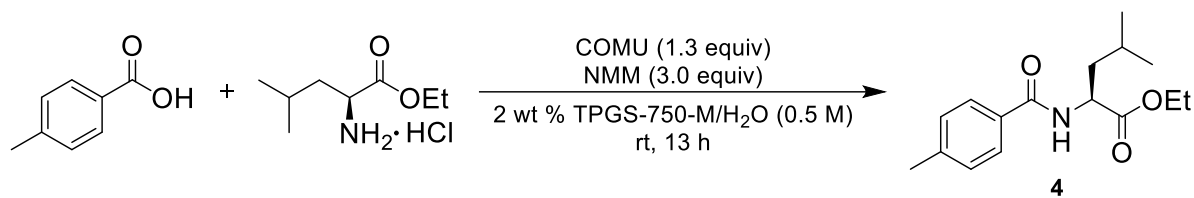
^aYields of isolated products.

Table 2. Initial base screening with COMU in aqueous micellar catalysis conditions.



Scheme 5. A. Mechanism for COMU-mediated amide bond formation. B. Guanidine by-product pathway from amine attack on COMU.

Further investigation of the reaction medium was undertaken, investigating the surfactant and its concentration, as well as the global concentration of reagents (Table 3). It is well understood for chemistry developed under micellar conditions, that certain functional groups respond with greater difficulty to emulsion formation with aqueous surfactants, including amides and nitroarenes, which may require tuning for optimal stirring. The neutral nature of the initial reaction mixture solvates reaction components well, however as the reaction proceeds, precipitation of the highly crystalline product **4** may halt stirring and effect a lower yield. It was found for the model reaction that when the TPGS-750-M concentration was increased to 4 wt %, a higher isolated yield of 97% was realized in comparison to the 93% yield obtained with 2 wt % simply on the basis of stirring. TPGS-750-M was also found to outperform the 3rd generation designer surfactant SPGS-550-M⁵³ as well as the system in the absence of surfactant.

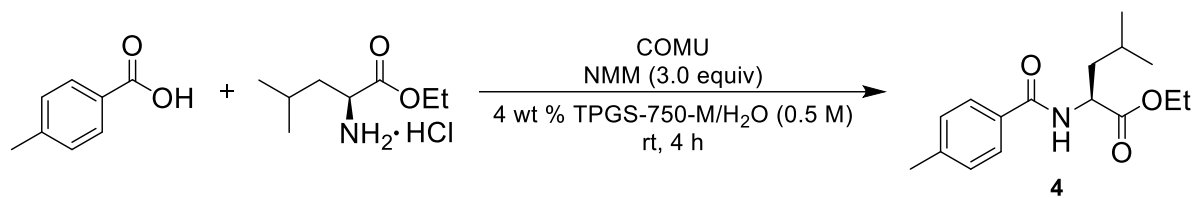


entry	solvent	conc. (M)	yield of 4 (%) ^a
1	2% TPGS-750-M/H ₂ O	0.5	93
2	2% TPGS-750-M/H ₂ O	0.25	80
3	3% TPGS-750-M/H ₂ O	0.5	89
4	4% TPGS-750-M/H₂O	0.5	97
5	2% SPGS-550-M/H ₂ O	0.5	86
6	3% SPGS-550-M/H ₂ O	0.5	82
7	H ₂ O	0.5	78

^aYields of isolated products.

Table 3. Surfactant screening for COMU-mediated amide bond formation.

At this point, it was understood that side reactions involving our coupling reagent, COMU could lead to lower conversion to the desired product. It was determined that 1.1 equivalents worked best for the synthesis of **4** showing the highest isolated yields, in comparison to 1.3 equivalents as recommended by the seminal report on COMU as a coupling reagent (Table 4). In fact, the optimized conditions established by our screening efforts afforded the product in higher yield than the system run under literature conditions in DMF (entries 2 & 5).³⁹

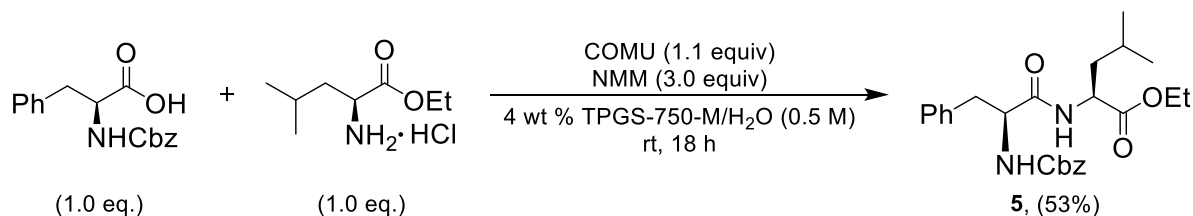


entry	COMU (equiv)	yield of 4 (%) ^a
1	1.0	77
2	1.1	86
3	1.2	83
4	1.3	53
5 ^b	1.3	74

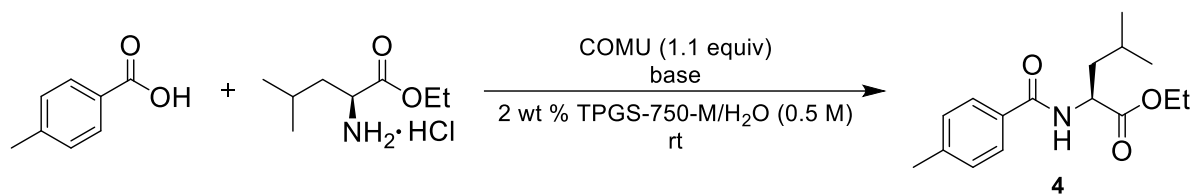
^aYields of isolated products. ^bDMF as solvent

Table 4. COMU equivalence optimization and literature comparison.

At this stage, it was perceived that the optimal conditions had been found for amide bond formation under aqueous micellar conditions, and the conditions were attempted for peptide bond formation. Unfortunately, the coupling of Z-Phe-OH with Leu-OEt·HCl afforded only a 53% isolated yield for **5** at 18 h (Scheme 6). This led to additional screening of several additional bases including many in the pyridyl series (Table 5). These bases were chosen due to their relatively high pK_b 's, allowing for neutral reaction conditions (pH = 6-7). From this screening, it was found that 2,6-lutidine not only afforded product **4** in quantitative yield, but also increased reaction rate significantly, reaching completion in only 15 minutes.



Scheme 6. Initial attempt at peptide bond formation under optimized conditions.

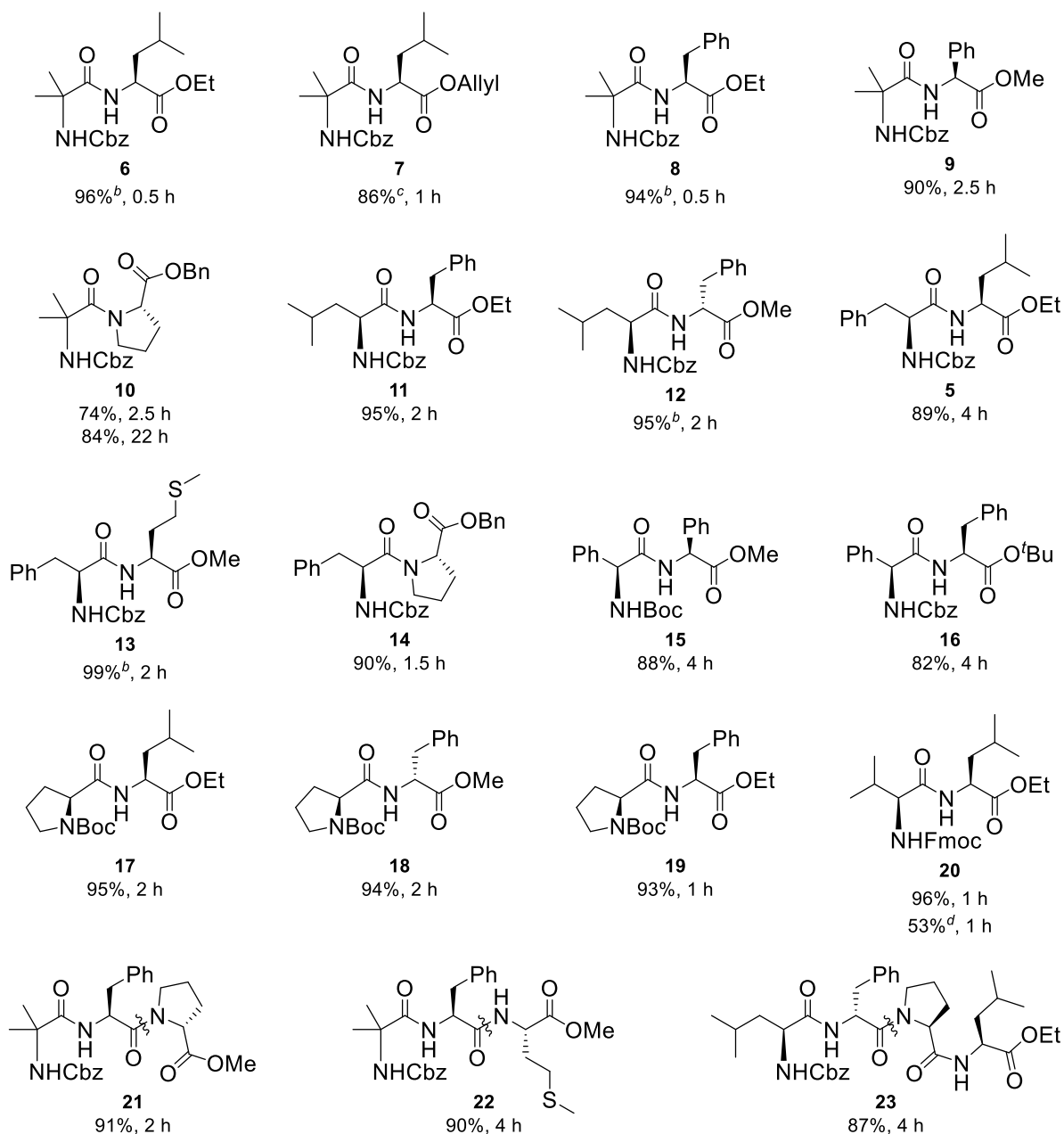


entry	base	time (h)	yield of 4 (%) ^a
1	2,6-lutidine (3.0 equiv)	0.25	>99
2	2,4,6-collidine (3.0 equiv)	4	>99
3	Quinaldine	4	92
4	2,6-di- <i>tert</i> -butyl-4-methylpyridine	4	80
5	NMI	4	80
6	NaHCO ₃ (3.0 equiv)	16	82

^aYields of isolated products.

Table 5. Weak base screening for peptide optimization.

The success of changing the base to 2,6-lutidine from NMM for the model system was then applied once again to the formation of peptide bonds, which translated quite well, requiring only 2 wt % TPGS-750-M while maintaining a global concentration of 0.5 M to deliver excellent yields in short reaction times (Figure 5). Without modification to the general method, a variety of aliphatic amino acids were coupled including sterically hindered Z-Aib-OH (products **6-10**), Boc-Phg-OH and Z-Phg-OH (**15** & **16**), and Fmoc-Val-OH (**20**) coupling nicely to hindered and secondary amines such as Phg-OMe (**9** & **15**) and prolines (**10**, **14**, **21**, & **23**). These conditions show no limitations for common amino acid protecting groups including Cbz, Boc, and Fmoc *N*-terminus protected amino acids as well as C-terminus alkyl, allyl, *tert*-butyl, and benzyl esters. The retention of Fmoc is an interesting feature of this chemistry as deprotection of this protecting group typically employs basic conditions.⁰



Conditions (by order of addition): carboxylic acid (1.1 equiv), 2 wt % TPGS-750-M/H₂O (0.5 M), 2,6-lutidine (3.1 equiv), amine HCl (1.0 equiv), COMU (1.1 equiv). ^aYields of isolated products are reported. ^b5.0 mmol scale. ^cFrom tosylate salt of Leu-OAllyl. ^dIsolated yield in the absence of TPGS-750-M.

Figure 5. Representative example of COMU peptide coupling with 2,6-lutidine and 2 wt % TPGS-750-M/H₂O.

In addition to the versatility of this method for the construction of dipeptides, several important oligopeptides were also prepared including Chlamydocin precursor **21**,⁵⁴ and

Streptocidin C precursor **23** (Figure 6).⁵⁵ The literature describing other syntheses of Chlamydocin precursor **24** highlights the utility of the newly optimized protocol in water, where yields in organic solvent were much lower (79% for both reports compared to 93%), and required low temperatures with longer reaction times (Figure 7).⁵⁶

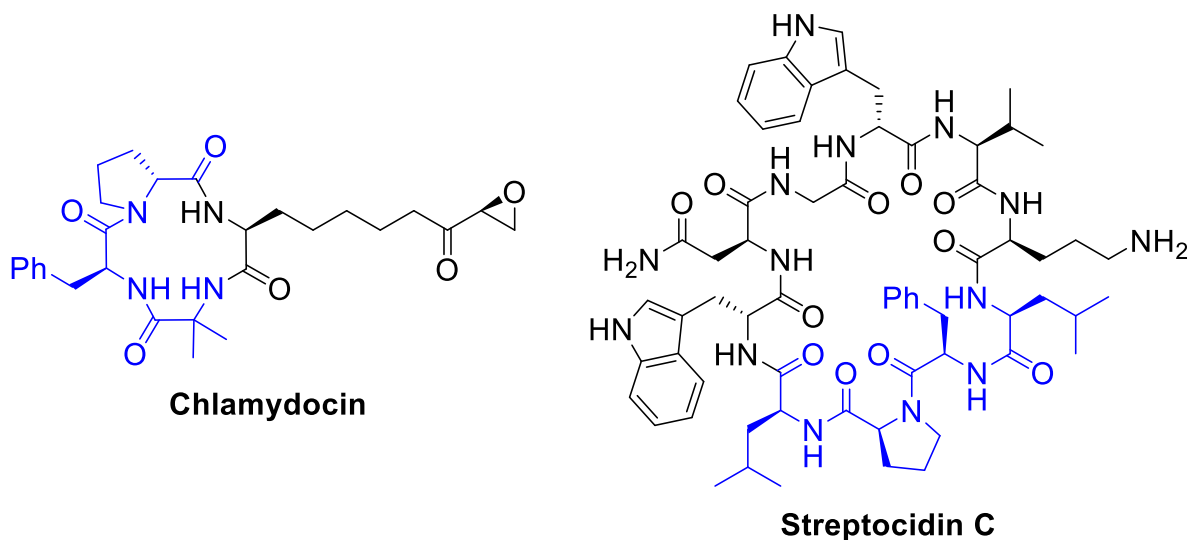
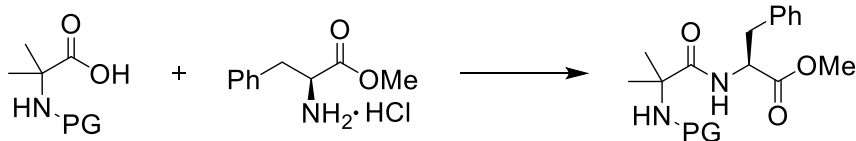


Figure 6. Structures of natural products Chlamydocin and Streptocidin C.



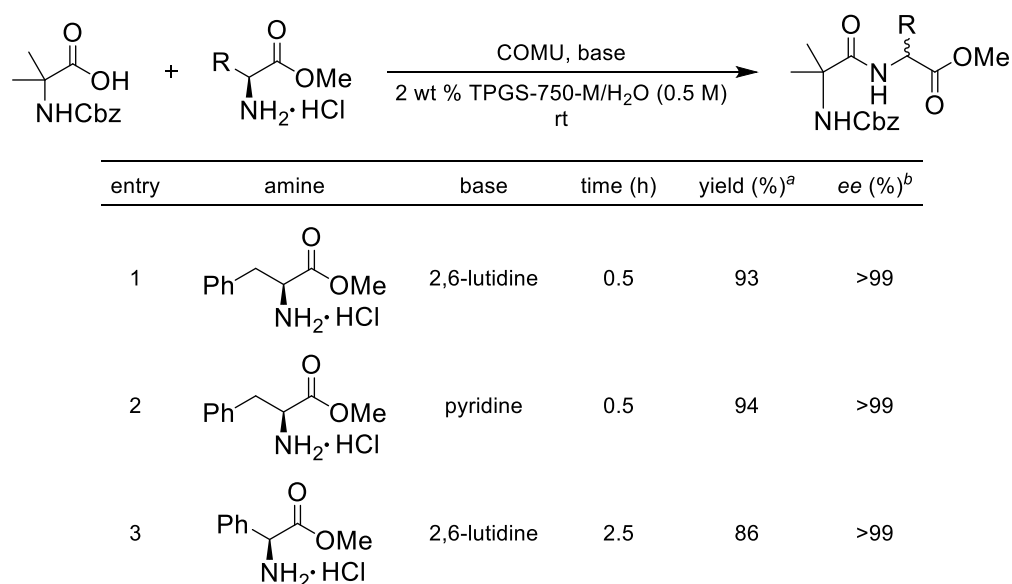
entry	coupling reagent	base	protecting group	T (°C)	time (h)	yield (%)
1	COMU	2,6-lutidine (3.1 equiv)	-Cbz	23°C	0.5	93
2 ^a	MMTM	NMM (2.0 equiv)	-Cbz	0°C to 20°C	3.0	79
3 ^b	ClCO ₂ ^t Bu	NMM (2.05 equiv)	-Boc	-20°C to 20°C	overnight	79

^aJ. Am. Chem. Soc. **2005**, 127, 16912.

^bEur. J. Org. Chem. **2009**, 371.

Figure 7. Literature comparison for initial coupling step in route to Chlamydocin.

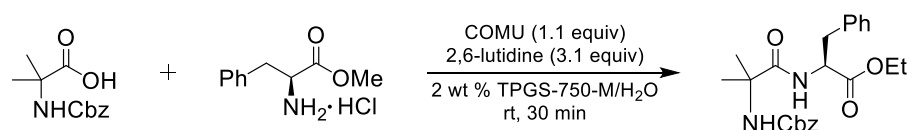
Use of 2,6-lutidine was originally pursued for its known ability as an effective base for amide couplings, while reducing the extent of epimerization/racemization due to steric bulk surrounding its basic site.⁵⁷ Under our standard conditions leading to products Z-Aib-Phg-OMe (**9**) and Z-Aib-Phe-OMe (**24**), no epimerization was observed (Table 5). Chiral integrity of these materials was maintained for the synthesis of **24** even when pyridine was used in place of 2,6-lutidine. The mildly acidic to neutral conditions (pH = 6–7) involved explains the low occurrence of epimerization which is insufficient for deprotonation of the α -proton of phenylglycine (Figure 8).⁶ Not only do the neutral conditions protect from epimerization but, in fact, effect overall conversion as well. As stated earlier, strongly basic conditions such as reactions with DBU or DABCO, resulted in a more alkaline reaction mixture (pH = 9), and no detectable coupling product was observed due to the formation of the guanidine species from the reaction of the free amine with the uronium carbon center of COMU (Scheme 5B).



^aYields of isolated products. ^bDetermined by HPLC analysis.

Figure 8. Epimerization study with 2,-6-lutidine and pyridine.

Consistent with the base effects from the initial screening in Table 1, pH of the reaction is directly related to product yield. It was found that either increasing or decreasing the pH of a reaction outside of the 6-7 window leads to lower overall yields even when 2,6-lutidine as the base (Figure 9). It is believed that in addition to diminishing the occurrence of guanidine by-products, correlation between pH and reaction yield may be due to amino acid solubility. Most coupling partners will dissolve readily into the aqueous surfactant solution containing 2,6-lutidine, which may solubilize each component as its corresponding carboxylate or ammonium salt. The increased solubility allows reactions to take place within short reaction times while slightly retarding the nucleophilicity of the amine component. Upon formation of the water insoluble amide, the surfactant plays its major role by sequestering the product within the micellar core.



Acidic		Neutral				Basic	
Component	pH	Component	pH	Component	pH	Component	pH
Carboxylic Acid	N/A	Carboxylic Acid	N/A	TPGS/H ₂ O	6-7	Carboxylic Acid	N/A
+ TPGS/0.5M HCl		+ TPGS/H ₂ O		+ 2,6-lutidine	8-9	+ TPGS/H ₂ O	
+ 2,6-lutidine	5	+ 2,6-lutidine	6	+ Carboxylic Acid	7	+ 2,6-lutidine	6
				+ Amine	6	+ Amine	6
+ Amine	5	+ Amine	6	+ Amine	6-7	+ 50% NaOH	12
+ COMU (<1 min)	5	+ COMU (<1 min)	6	+ COMU (<1 min)	6-7	+ COMU (<1 min)	8
+ COMU (30 min)	4-5	+ COMU (30 min)	6	+ COMU (30 min)	6	+ COMU (30 min)	8
Yield:	75%		94%		95%		73%

Figure 9. Peptide coupling with COMU/2,6-lutidine under standard neutral, acidic, and basic conditions.

Support for this hypothesis is that fact that these reactions do occur to varying extents in the absence of surfactant (i.e., on water), however yields may vary depending on the nature of the coupling partners and products (Figure 10). For example, significantly lower yield is

obtain for the synthesis of **20** on water (53%) compared to the reaction in aqueous TPGS-750-M (96%). In some cases, it was found that dissolution of amino acids was troublesome even with TPGS-750-M, resulting in notably reduced yields. This issue was addressed by the use of the new surfactant LB-1000-M that offered increased solubility due to the presence of a sulfone group within the aliphatic region of the surfactant, designed to mimic the solvation properties of DMSO. The results of changing surfactant were substantial, offering on average a 40% increase in yield (Figure 11).

$$\text{R-COOH} + \text{H}_2\text{N-R}' \xrightarrow[\text{2 wt \% TPGS-750-M/H}_2\text{O or H}_2\text{O}]{\text{COMU (1.1 equiv), 2,6-lutidine (3.1 equiv)}} \text{R-CO-NH-R}'$$

product	time (h)	isolated yield (%)	
		2 wt % TPGS-750-M/H ₂ O	H ₂ O
 11	0.5	94%	94%
 7	1.0	86%	75%
 20	1.0	96%	53%
 25	1.0	67%	84%

Figure 10. Representative examples for the comparison of optimized conditions to on water conditions.

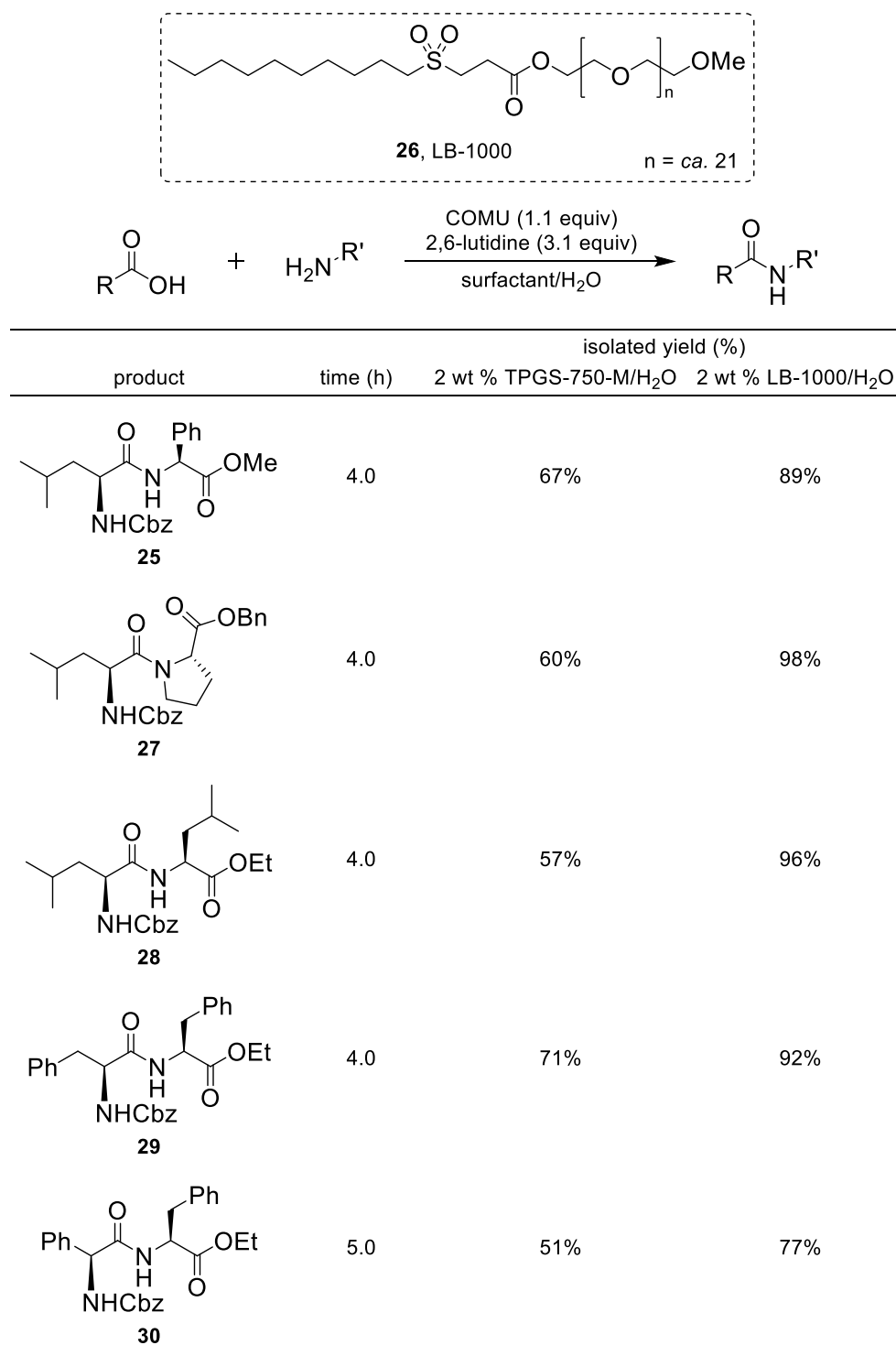


Figure 11. Comparison of optimized conditions with 2 wt % TPGS-750-M to sulfone surfactant LB-1000.

The generality of the method optimized in TPGS-750-M was further explored for products resulting from amide bond formation as illustrated in Figure 12. Without modification to the existing procedure several products were generated including simple alkanolic acid-alkylamine-derived amides (products **31–33**) and secondary amines such as piperazine in **34**. A variety of conjugated carboxylic acids produce amides as well under standard conditions including propargyl amide (**35**), as well as substituted benzamides (**36–39**). Reaction of *p*-chlorobenzoic acid with L-Trp-OMe·HCl afforded Benzotript⁵⁸ methyl ester **37** in high yield (92%) after only 2 h, while the unprotected indole nitrogen of tryptophan showed no influence on the coupling. Racemic **38** was unexpectedly challenging, affording the product in only 36% after 16 h, with the Oxyma-activated ester of 4-*n*-butoxybenzoic acid was isolated in 57% yield. Heating the reaction to 45°C circumvented the reduced electrophilicity of this activated ester to afford a 90% yield with only trace amounts of the activated intermediate remaining within only 2 h. In addition, adduct **39** was isolated in 85% yield after only 1 h from the condensation of *m*-bromobenzoic acid and the *N,O*-dimethylhydroxylamine hydrochloride, this being the first reported synthesis of a Weinreb amide¹¹ in the absence of organic solvent.

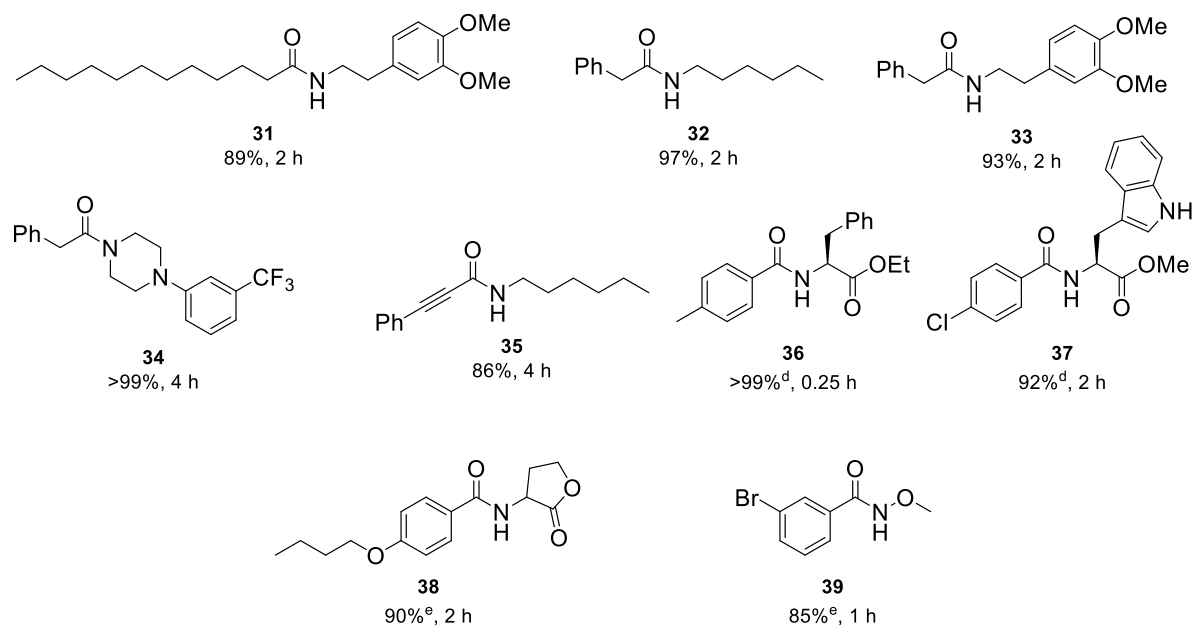


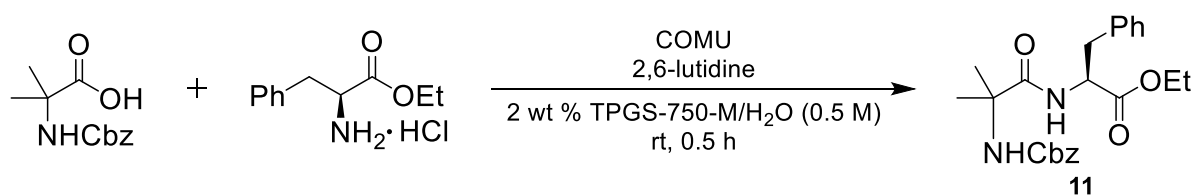
Figure 12. Representative examples of amide bond formation in water at room temperature.

Isolation of the amide or peptide is simplified based on the nature of the starting materials and by-products of COMU in water. Extraction directly from the reaction mixture with minimal amounts of organic solvent such as MTBE or *i*PrOAc is effective to remove the coupling product from the reaction mixture (Figure 13), offering an exceptionally low E Factor⁰ of 2.8 (E Factor = 7.8 when water is included in the calculation). Enrichment of the organic extracts from unreacted amine and carboxylic starting materials as well as Oxyma and the urea by-product of COMU are easily removed by washes with saturated Na₂CO₃ followed by 1 M HCl. Once enriched, the organic extracts are passed through a plug of silica which is sufficient for the isolation of pure product. In some cases column chromatography is necessary, such as the presence of unreacted activated esters, for example. It should be noted that less polar extraction solvents such as MTBE or *i*PrOAc lower the partition of Oxyma during extractions requiring less Na₂CO₃ washes during work up. Alternately, a mixture of EtOAc and hexanes suffices to afford a similar effect. Furthermore, the remaining

aqueous reaction mixture can be recycled at least four additional times without decreasing yields (Figure 14). In fact, yields were shown to increase most likely due to the increased loading of Oxyma with every subsequent reaction.



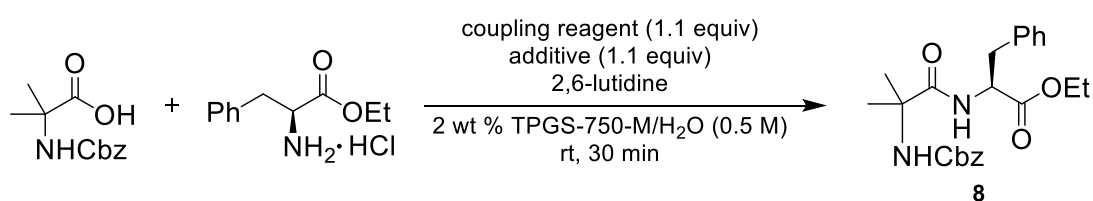
Figure 13. Extraction with MTBE directly from reaction mixture.



entry	reaction	SM mass	theoretical yield	isolated yield	percent yield
1	A	229.9 mg	412.8 mg	379.5 mg	91.9%
2	B	229.0 mg	411.2 mg	392.3 mg	95.4%
3	C	228.7 mg	410.7 mg	410.0 mg	99.8%
4	D	230.3 mg	413.6 mg	396.6 mg	95.9%
5	E	229.0 mg	411.2mg	410.6 mg	99.8%

Figure 14. Recycle capabilities of COMU-mediated peptide bond formation in water.

In order to explore the versatility of the developed conditions, many of the most commonly utilized coupling reagents were explored under our conditions (Figure 15). While this list was not intended to be exhaustive, the goal was to prove the applicability of these coupling reagents in water at room temperature. As previously described, base loading has a tremendous effect on the success of amide bond formation under micellar catalysis conditions, and it is our belief that any of the reagents described in Figure 15 could be optimized for success under aqueous conditions.



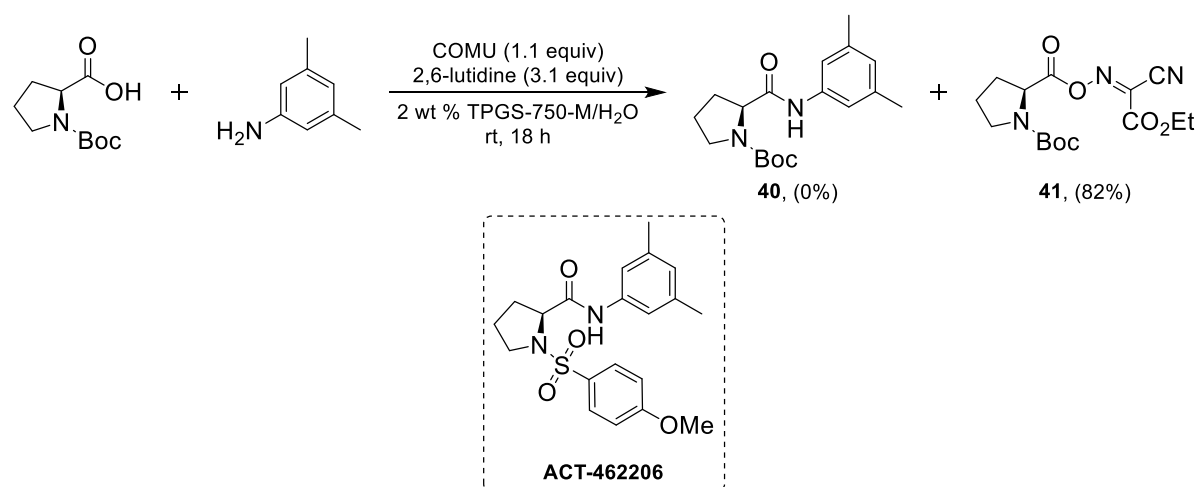
entry	coupling agent	additive	base (equiv)	yield 7 (%) ^a
1	COMU	-	3.1	94
2	EDC	HOBt	3.1	89
3	EDC	Oxyma	3.1	75
4	TBTU	-	3.1	20
5	HATU	-	3.1	46
6	PyBOP	-	3.1	27
7	PYAOP	-	3.1	28
8	MMTM	-	3.1	44
9	MMTM	-	2.1	52

^aYields of isolated products.

Figure 15. Survey of coupling reagents under optimized conditions.

Over the course of this study, one limitation of this methodology was recognized in that amide bond formation from anilines halted the reaction at the activated ester due to their poor nucleophilicity. This was observed upon attempting the coupling of Boc-Pro-OH with 3,5-xylidine for the synthesis of **40**, an important intermediate for the synthesis of ACT-

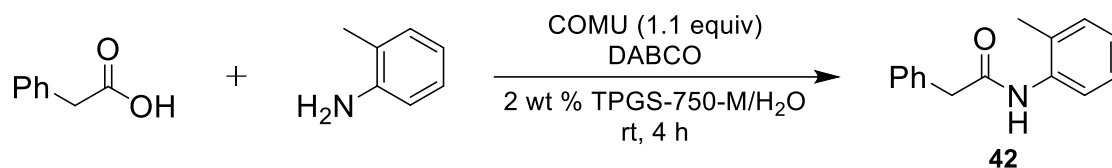
462206, Actelion's potent dual orexin receptor antagonist candidate for the treatment of insomnia (Scheme 7).⁶⁰ Several modifications were made to the existing protocol including: increased COMU loading, portion-wise COMU loading, increased global concentration to (1M), heating (to 40 °C), screening other bases (NMM and DMAP), and extended reaction times. In all cases, only the activated oxime ester of Boc-Pro-OH (**41**) was isolated. At the time of this study it was accepted as a limitation that anilines were inappropriate nucleophiles for this method and the communication was submitted absent of this product type. This limitation was one that was particularly important to overcome, as many important compounds contain this scaffold.



Scheme 7. Attempt at amide bond formation from an aniline nucleophile en route to ACT-462206.

A recent report by Parmentier and co-workers at Novartis showed that amide bonds from anilines could be effected in aqueous TPGS-750-M, utilizing EDC, HOBt, and NMM with the use of PEG-200 as co-solvent.⁶¹ This communication certainly proved that this disconnection could be possible with the use of HOBt surrogates such as COMU or Oxyma. Looking back at initial screening data from our method, it was considered that the risk of forming guanidine by-products may be less favorable even under highly basic conditions due

to the decreased nucleophilicity of anilines in comparison to aliphatic amines. Revisiting this method for the coupling of phenylacetic acid and *o*-toluidine, it was found that the amide product **42** could be effectively produced within 4 h to achieve 89% conversion (Figure 16, entry 1). Further optimization is now underway to improve conversion and expand the scope for *N*-aryl amides.



entry	DABCO (equiv)	conv. of to 42 (%) ^a
1	1.0	89%
2	2.0	77%
3	3.0	35%

^aDetermined by GC/MS.

Figure 16. COMU-mediated amide bond formation from *o*-toluidine with DABCO.

3.5 Summary and Conclusions

In summary, a mild, efficient, and general method has been developed for the synthesis of peptide and amide bonds in water at room temperature. The use of commercially available COMU alleviates the need for hazardous benzotriazole activators which pose issues in terms of safety. Furthermore, reactions take place under neutral conditions protecting valuable peptide products from racemization. These reactions take place in the absence of organic solvent, having major safety and environmental improvements over current state-of-the-art technology which generally requires egregious solvents such as DCM and DMF. Isolation and purification of the peptide/amide products is routinely simple, taking advantage of the aqueous nature of by-products to arrive at pure material after acid/base washes and filtration

through a short plug of silica. The sustainability of this method can be quantified by the low E Factor of 2.8 and the ability to recycle the aqueous reaction solvent without effecting reaction rates or yields. Further investigation into scope expansion to include aniline nucleophiles is now underway.

3.6 List of Acronyms and Abbreviations

2-Me-THF	2-methyltetrahydrofuran
6-Cl-HOBt	6-chloro-1-hydroxybenzotriazole
Aib	amino isobutyric acid
Ala	L-alanine
BAC	boronic acid catalysis
Boc	tert-butoxy carbamate
Cbz, Z	benzyloxycarbonyl
CDI	carbonyl diimidazole
COMU	1-[(1-(cyano-2-ethoxy-2-oxoethylideneaminoxy)-dimethylamino morpholinomethylene)] methanaminium hexafluorophosphate
DABCO	1,4-diazabicyclo[2.2.2]octane
DBU	1,8-diazabicyclo[5.4.0]undec-7-ene
DCC	<i>N,N'</i> -dicyclohexylcarbodiimide
DCM	dichloromethane
DiBALH	diisobutylaluminium hydride
DIC	<i>N, N'</i> -Diisopropylcarbodiimide
DIPEA	<i>N,N</i> -Diisopropylethylamine
DMAP	4-Dimethylaminopyridine
DMF	<i>N,N</i> -dimethylformamide
DMSO	Dimethyl sulfoxide
DMT-Cl	4,4'-Dimethoxytrityl chloride
DPPA	Diphenylphosphoryl azide

EDC	1-Ethyl-3-(3-dimethylaminopropyl)carbodiimide
EDDQ	2-ethoxy-1-ethoxycarbonyl-1,2-dihydroquinoline
Et ₃ N	triethylamine
EtOAc	ethyl acetate
Fmoc	9-fluorenylmethyloxycarbonyl
GC/MS	gas chromatography–mass spectrometry
HATU	<i>N</i> -[(dimethylamino)-1 <i>H</i> -1,2,3-triazolo-[4,5- <i>b</i>]pyridin-1-ylmethylene]- <i>N</i> -methylmethanaminium hexafluorophosphate <i>N</i> -oxide
HOAt	1-hydroxy-7-azabenzotriazole
HOBt	hydroxybenzotriazole
HONB	<i>N</i> -hydroxy-5-norbornene-2,3-dicarboxylimide
HOSu	<i>N</i> -hydroxysuccinimide
HPLC	high performance liquid chromatography
IPA	isopropyl alcohol
iPrOAc	isopropyl acetate
Leu	L-leucine
MMTM	4-(4,6-dimethoxy-1,3,5-triazin-2-yl)-4-methylmorpholinium tetrafluoroborate
MTBE	methyl tert-butyl ether
NMM	<i>N</i> -methyl morpholine
NMR	nuclear magnetic resonance
OTAB	octyltrimethylammonium bromide
PEG	polyethylene glycol
Phe	L-phenylalanine

Phg	L-phenylglycine
Pro	L-proline
PyAOP	[(7-azabenzotriazol-1-yl)oxy]tris(pyrrolidino) phosphonium hexafluorophosphate
PyBOP	benzotriazol-1-yloxytri(pyrrolidino) phosphonium hexafluorophosphate
SM	starting material
SPGS-550-M	β -sitosterol methoxypolyethyleneglycol succinate
TATU	<i>O</i> -(7-azabenzotriazol-1-yl)-1,1,3,3-tetramethyluronium tetrafluoroborate
TBTU	<i>N,N,N',N'</i> -Tetramethyl- <i>O</i> -(benzotriazol-1-yl)uronium tetrafluoroborate
TCTU	<i>O</i> -(6-Chlorobenzotriazol-1-yl)- <i>N,N,N',N'</i> -tetramethyluronium tetrafluoroborate
TLC	thin layer chromatography
TMP	2,2,4,4-tetramethylpiperidine
TPGS-750-M	DL- α -Tocopherol methoxypolyethylene glycol succinate
Trp	L-tryptophan
Val	L-Valine

3.7 Experimental Procedures

General Information

A solution of 2 wt % TPGS-750-M/H₂O solution was prepared by dissolving TPGS-750-M in degassed HPLC grade water and was stored under argon. TPGS-750-M was made as previously described⁶² and is available from Sigma-Aldrich (catalog #733857). All commercially available reagents were used without further purification. Thin layer chromatography (TLC) was done using Silica Gel 60 F₂₅₄ plates (Merck, 0.25 mm thick). Flash chromatography was done in glass columns using Silica Gel 60 (EMD, 40-63 μm). ¹H and ¹³C NMR were recorded at 22 °C on a Varian UNITY INOVA at 500 MHz. Chemical shifts in ¹H NMR spectra are reported in parts per million (ppm) on the δ scale from an internal standard of residual CDCl₃ (7.27 ppm) or the central peak of DMSO-d₆ (2.50 ppm). Data are reported as follows: chemical shift, multiplicity (s = singlet, d = doublet, t = triplet, q = quartet, quin = quintet), and integration. Chemical shifts in ¹³C chemical spectra are reported in ppm on the δ scale from the central peak of residual CDCl₃ (77.00 ppm) or the central peak of DMSO-d₆ (39.51 ppm). IR data were collected on a Perkin Elmer Spectrum Two UATR FT-IR Spectrometer and peaks were described according to relative intensity and resolution as follows: s = strong, m = medium, w = weak, br = broad. Chiral HPLC data were collected using a Shimadzu LC-20AT Prominence liquid chromatograph coupled with Shimadzu SPD-M20A Prominence diode array detector. HPLC method ran at 1 mL/min using 10% v/v isopropanol/hexanes through a CHIRALCEL[®] OD-H column.

General Procedure for Amide Bond Formation in Water

To a clean microwave vial with Teflon coated stir bar, carboxylic acid is transferred (1.1 equiv) followed by 2 wt % TPGS-750-M/H₂O (0.5 M) and 2,6-lutidine (3.1 equiv). After stirring ~5 min, the amine is transferred (1.0 equiv) followed by COMU (1.1 equiv). Within

1 min a successful reaction will become yellow in color which indicates the free-base form of the oxime activating agent. The reaction is monitored by TLC utilizing bromocresol green and ninhydrin or KMnO_4 to indicate disappearance of carboxylic acid and amine starting materials, respectively.

Work-up Procedure

The aqueous reaction mixture is extracted with 3 x 2 mL MTBE, EtOAc, *i*-PrOAc, or 3:1 EtOAc:hexanes. The organic extracts are then washed with 2 x 6 mL 1 M HCl and 3 x 6 mL Na_2CO_3 saturated solution in water. The organic phase is then passed through a plug of silica and evaporated to dryness.

Note: Less polar extraction solvents such as MTBE (methyl *t*-butyl ether) or *i*-PrOAc (isopropyl acetate) are generally used in order to minimize the partition of the oxime into the organic phase during basic extractions. Additional basic extractions may be required if EtOAc is used as extraction solvent. Most peptide coupling products can be isolated without additional purification; however, column chromatography can be utilized in order to purify any of the products in this work.

Coupling Reagent Screening Procedure

To a microwave vial with stir bar was transferred carboxylic acid (0.55 mmol), 2 wt % TPGS-750-M/ H_2O (1.0 mL), 2,6-lutidine, amine (0.5 mmol), and coupling reagent (+ additive). Reaction was stirred in an open vial for 30 min before extracting with 3 x 2 mL MTBE. Organic fractions were combined and washed with 2 x 6 mL 1 M HCl, 3 x 6 mL saturated Na_2CO_3 solution in water, and then filtered through a plug of silica and condensed under reduced pressure.

Aqueous Surfactant Recycling Procedures

To a clean microwave vial with Teflon coated stirbar, Z-Aib-OH (1.1 mmol) was transferred followed by 2 wt % TPGS-750-M/H₂O (2.0 mL) and 2,6-lutidine (0.36 mL). After stirring ca. 5 min, Phe-OEt-HCl (1.0 mmol) was transferred followed by COMU (1.1 mmol). After ca. 30 min, 3 x 1 mL extractions with MTBE were done followed by 2 x 1 mL 1 M HCl, and 4 x 1 mL saturated aqueous Na₂CO₃ washes and filtration through silica plug with subsequent rinse with 2 mL MTBE to obtain pure Z-Aib-Phe-OEt. To the surfactant solution remaining in the reaction flask appropriate amounts of each reagent were then added: Z-Aib-OH (1.1 mmol), 2,6-lutidine (0.36 mL), Phe-OEt-HCl (1.0 mmol), and COMU (1.1 mmol). The reaction was again allowed to stir for 30 min before work-up. This procedure was continued until the surfactant solution had been recycled five times.

E Factor Determination Procedure

To a clean microwave vial with Teflon coated stirbar, Z-Aib-OH (261.0 mg, 1.1 mmol) was transferred followed by 2 wt % TPGS-750-M/H₂O (2.0 mL) and 2,6-lutidine (0.36 mL, 3.1 mmol). After stirring ca. 5 min, Phe-OEt-HCl (230.2 mg, 1.0 mmol) was transferred followed by COMU (471.1 mg, 1.1 mmol). After ca. 30 min, the product was extracted with 1 x 0.5 mL (435.0 mg) and 1 x 0.75 mL (652.5 mg) *i*-PrOAc followed by 2 x 1 mL 1 M HCl, and 4 x 1 mL saturated aqueous Na₂CO₃ washes and filtration through silica plug to obtain pure Z-Aib-Phe-OEt (394.9 mg, 96%).

E Factor Calculations (without water)

$$\text{E Factor} = (\text{Mass of Organic Waste}) / (\text{Mass of Product})$$

$$\begin{aligned}\text{Mass of Organic Waste} &= (0.5 + 0.75) \text{ mL } i\text{PrOAc} = 1.25 \text{ mL } i\text{PrOAc} (0.870 \text{ g/mL}) \\ &= 1087.5 \text{ mg}\end{aligned}$$

$$\text{Mass of Product} = 394.9 \text{ mg}$$

$$\text{E Factor} = (1087.9 \text{ mg}) / (394.9 \text{ mg}) = 2.75$$

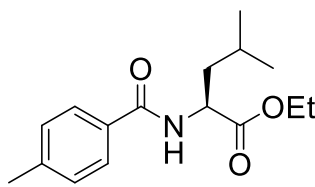
E Factor Calculations (with water)

$$\text{E Factor} = (\text{Mass of Organic Waste} + \text{Aqueous waste}) / (\text{Mass of Product})$$

$$\text{Mass of Water} = (2.0 \text{ mL}) (1.0 \text{ g/mL}) = 2000 \text{ mg}$$

$$\text{E Factor} = (1087.5 \text{ mg} + 2000 \text{ mg}) / (394.9 \text{ mg}) = 7.8$$

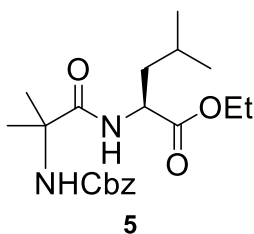
3.8 Compound Data



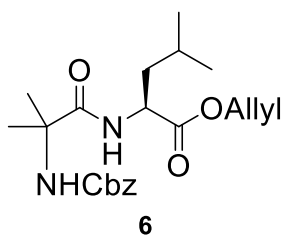
4

Ethyl (4-methylbenzoyl)-L-leucinate (4). R_f 0.28 (1:3 EtOAc/hexanes); white solid, mp: 90-91 °C, 137.8 mg (99%). ^1H NMR (500 MHz, CDCl_3) δ 7.70 (dt, 2H), 7.22 (dt, 2H), 6.58 (d, 1H), 4.84 (m, 1H), 4.22 (q, 2H), 2.39 (s, 3H), 1.79-1.71 (m, 2H), 1.71-1.61 (m, 1H), 1.30 (t, 3H), 0.99 (d, 3H), 0.97 (d, 3H). ^{13}C NMR (125 MHz, CDCl_3) δ 173.31, 166.94, 142.05, 131.12, 129.14, 127.00, 61.35, 51.09, 41.95, 24.95, 22.81, 22.09, 21.41, 14.13. IR (neat): ν = 3356 (m, br), 3076 (w), 3031 (w), 2956 (m), 2933 (m), 2872 (m), 1744 (s), 1637

(s), 1522 (s), 1501 (s). HRMS (ESI⁺, [C₁₆H₂₃NO₃ + Na]⁺) calcd 300.1576, found *m/z* 300.1573.

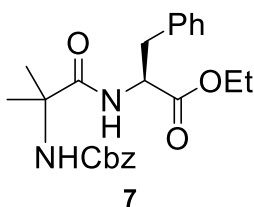


Z-Aib-Leu-OEt (6). *R_f* 0.52 (1:1 EtOAc/hexanes); white solid, mp: 63-65 °C, 181.1 mg (96%). ¹H NMR (500 MHz, DMSO-*d*₆) δ 7.38 (d, 1H), 7.38-7.27 (m, 5H), 7.22 (s, 1H), 4.98 (q, 2H), 4.22 (m, 1H), 4.05 (m, 2H), 1.66-1.54 (m, 2H), 1.47-1.40 (m, 1H), 1.35 (s, 6H), 1.16 (t, 3H), 0.85 (d, 3H), 0.81 (d, 3H); ¹³C NMR (125 MHz, DMSO-*d*₆) δ 174.16, 172.41, 154.55, 137.01, 128.27, 127.68, 127.62, 65.01, 60.27, 55.84, 50.45, 39.46, 25.41, 24.54, 24.08, 22.88, 21.11, 14.01. IR (neat): ν = 3324 (m), 3037 (w), 2982 (m), 2957 (m), 2931 (m), 2869 (m), 1748 (s), 1738 (s), 1692 (s), 1656 (s). HRMS (ESI, [C₂₃H₂₈N₂O₅ + Na]⁺) calcd 401.2052, found *m/z* 401.2036.

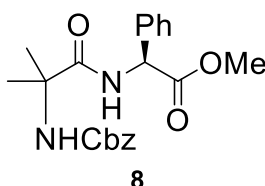


Z-Aib-Leu-OAllyl (7). *R_f* 0.30 (1:3 EtOAc/hexanes); white solid, mp: 78-80 °C, 152.7 mg (80%). ¹H NMR (500 MHz, DMSO-*d*₆) δ 7.80 (d, 1H), 7.43-7.26 (m, 5H), 7.22 (s, 1H), 5.88 (m, 1H), 5.30 (dd, 1H), 5.20 (dd, 1H), 4.99 (q, 2H), 4.55 (m, 2H), 4.30 (m, 1H), 1.70-1.56 (m, 2H), 1.52-1.43 (m, 1H), 1.36 (s, 6H), 0.85 (d, 3H), 0.81 (d, 3H); ¹³C NMR (125 MHz, DMSO-*d*₆) δ 174.25, 172.14, 154.56, 137.01, 132.41, 128.25, 127.67, 127.61, 117.61, 65.04, 64.66, 55.86, 50.50, 39.47, 25.43, 24.51, 22.87, 21.07. IR (neat): ν = 3318 (s), 3092

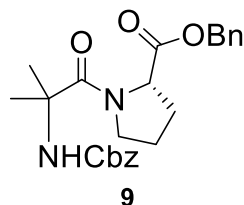
(w), 3069 (w), 3032 (w), 2960 (m), 2872 (m), 1750 (s), 1737 (s), 1670 (s), 1692 (s), 1652 (s), 1519 (s). HRMS (ESI, [C₂₁H₃₀N₂O₅ + Na]⁺) calcd 413.2052, found *m/z* 413.2048.



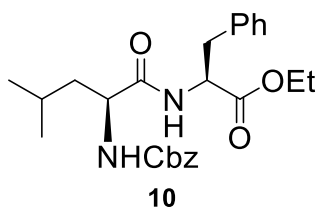
Z-Aib-Phe-OEt (8). *R_f* 0.49 (1:1 EtOAc/hexanes); white solid, mp: 94-95 °C, 206.5 mg (>99%). ¹H NMR (500 MHz, DMSO-*d*₆) δ 7.73 (d, 1H), 7.43-7.15 (m, 11H), 4.97 (s, 2H), 4.45 (dt, 1H), 4.04 (q, 2H), 3.00 (m, 2H), 1.29 (s, 6H), 1.13 (t, 3H); ¹³C NMR (125 MHz, DMSO-*d*₆) δ 174.02, 171.35, 154.52, 137.24, 136.93, 129.16, 128.28, 128.09, 127.72, 127.65, 126.41, 65.09, 60.48, 55.83, 53.56, 36.51, 25.12, 24.78, 13.92. IR (neat): ν = 3318 (m, br), 3063 (m), 3031 (m), 2983 (m), 2938 (m), 1723 (s), 1662 (s). HRMS (ESI, [C₂₃H₂₈N₂O₅ + Na]⁺) calcd 435.1896, found *m/z* 435.1879.



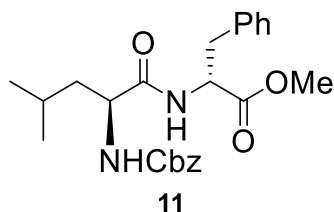
Z-Aib-Phg-OMe (9). *R_f* 0.45 (1:1 EtOAc/hexanes); white solid, mp: 125-126 °C, 179.7 mg (90%). ¹H NMR (500 MHz, DMSO-*d*₆) δ 8.13 (d, 1H), 7.40-7.28 (m, 11H), 5.40 (d, 1H), 5.00 (m, 2H), 3.63 (s, 3H), 1.38 (s, 3H), 1.36 (s, 3H); ¹³C NMR (125 MHz, DMSO-*d*₆) δ 174.02, 171.85, 154.79, 136.93, 136.56, 128.44, 128.27, 127.97, 127.69, 127.58, 127.49, 65.14, 56.24, 55.98, 52.26, 25.14, 24.73. IR (neat): ν = 3323 (m, br), 3065 (m), 2925 (m), 2854 (m), 1744 (s), 1688 (s), 1674 (s), 1660 (s). HRMS (EI⁺, [C₂₁H₂₄N₂O₅]⁺) calcd 384.1685, found *m/z* 384.1671.



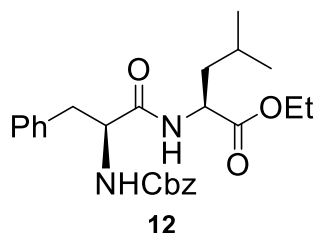
Z-Aib-Pro-OBn (10). R_f 0.14 (1:2 EtOAc/hexanes); sticky white solid, mp: 92 °C, 151.1 mg (74%, 2.5 h), 174.5 mg (84%, 22 h). ^1H NMR (500 MHz, DMSO-*d*₆) δ 7.75 (s, 1H), 7.40-7.26 (m, 10H), 5.13-5.13 (m, 4H), 4.30 (dd, 1H), 3.61 (m, 1H), 3.27 (m, 1H), 1.95 (m, 1H), 1.87-1.64 (m, 3H), 1.34 (s, 3H), 1.23 (s, 3H); ^{13}C NMR (125 MHz, DMSO-*d*₆) δ 171.93, 171.59, 154.24, 137.02, 136.06, 128.32, 128.27, 128.03, 127.92, 127.85, 127.72, 65.54, 65.16, 60.24, 55.66, 47.22, 27.30, 25.54, 25.30, 24.28. IR (neat): ν = 3307 (s), 3088 (w), 3034 (m), 2997 (m), 2970 (m), 2947 (m), 2877 (m), 1737 (s), 1718 (s), 1610 (s), 1536 (s).



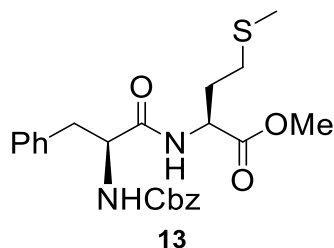
Z-Leu-Phe-OEt (11). R_f 0.18 (1:3 EtOAc/hexanes); white solid, mp: 91-92 °C, 210.5 mg (95%). ^1H NMR (500 MHz, CDCl₃) δ 7.40-7.07 (m, 10H), 6.44 (d, 1H), 5.11 (m, 3H), 4.83 (q, 1H), 4.17 (m, 3H), 3.12 (m, 2H), 1.74-1.57 (m, 2H), 1.47 (m, 1H), 1.24 (t, 3H), 0.92 (d, 6H). ^{13}C NMR (125 MHz, CDCl₃) δ 171.61, 171.15, 156.02, 136.16, 135.70, 129.31, 128.50, 128.46, 128.16, 127.99, 127.05, 67.03, 61.50, 53.45, 53.16, 41.36, 37.88, 24.60, 22.82, 21.96, 14.04. IR (neat): ν = 3315 (m), 3278 (m), 3066 (w), 3034 (w), 2956 (m), 2935 (m), 2871 (m), 1734 (s), 1682 (s), 1665 (s). HRMS (ESI⁺, [C₂₅H₃₂N₂O₅ + Na]⁺) calcd 463.2209, found m/z 463.2190.



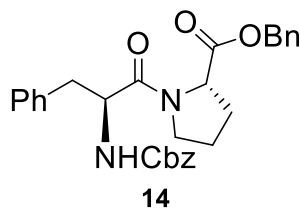
Z-Leu-D-Phe-OMe (11). R_f 0.56 (1:1 EtOAc/hexanes); white solid, mp: 114 °C, 2199.8 mg (95%). ^1H NMR (500 MHz, DMSO- d_6) δ 8.75 (d, 1H), 7.44-7.28 (m, 11H), 5.43 (d, 1H), 5.03 (s, 2H), 4.23 (dt, 1H), 3.63 (s, 3H), 1.58 (m, 1H), 1.50-1.41 (m, 1H), 1.39-1.31 (m, 1H), 0.84 (d, 3H), 0.83 (d, 3H); ^{13}C NMR (125 MHz, DMSO- d_6) δ 172.40, 170.87, 155.82, 137.06, 136.37, 128.65, 128.31, 128.20, 127.74, 127.58, 127.56, 65.34, 56.02, 52.82, 52.26, 40.85, 24.17, 22.98, 21.33. IR (neat): ν = 3298 (m), 3064 (w), 2958 (m), 2932(m), 1732 (s), 1687 (s), 1647 (s). HRMS (ESI, $[\text{C}_{24}\text{H}_{30}\text{N}_2\text{O}_5 + \text{Na}]^+$) calcd 449.2052, found m/z 449.2032.



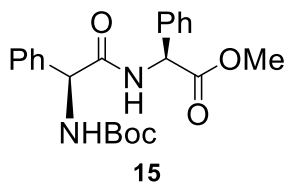
Z-Phe-Leu-OEt (6). R_f 0.66 (1:1 EtOAc/hexanes); white solid, mp: 118 °C, 189.3 mg (90%). ^1H NMR (500 MHz, DMSO- d_6) δ 8.37 (d, 1H), 7.48 (d, 1H), 7.37-7.15 (m, 10H), 4.93 (s, 2H), 4.29 (m, 2H), 4.08 (m, 2H), 3.00 (dd, 1H), 2.73 (dd, 1H), 1.71-1.46 (m, 3H), 1.17 (t, 3H), 0.91 (d, 3H), 0.86 (d, 3H). ^{13}C NMR (125 MHz, DMSO- d_6) δ 172.31, 171.83, 155.78, 138.06, 137.01, 129.17, 128.24, 127.99, 127.64, 127.40, 37.35, 24.19, 22.74, 21.33, 14.02. IR (neat): ν = 3309 (m), 3065 (m), 3034 (m), 2952 (m), 2928 (m), 2866 (m), 1727 (s), 1691 (s), 1651 (s), 1525 (s). HRMS (ES $^+$, $[\text{C}_{25}\text{H}_{32}\text{N}_2\text{O}_5 + \text{Na}]^+$) calcd 463.2209, found m/z 463.2196.



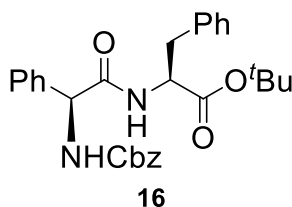
Boc-Phe-Met-OMe (13). R_f 0.44 (1:1 EtOAc/hexanes); white solid, mp: 75-77 °C, 202.4 mg (99%). ^1H NMR (500 MHz, CDCl_3) δ 7.28-7.23 (m, 2H), 7.22-7.15 (m, 3H), 6.73 (d, 1H), 5.14 (d, 1H), 4.62 (q, 1H), 4.37 (m, 1H), 3.68 (s, 3H), 3.04 (d, 2H), 2.39 (m, 2H), 2.09 (m, 1H), 2.03 (s, 3H), 1.91 (m, 1H), 1.38 (s, 9H). ^{13}C NMR (125 MHz, CDCl_3) δ 171.67, 171.09, 155.26, 136.39, 129.18, 128.45, 126.76, 80.02, 55.56, 52.29, 51.39, 37.94, 31.41, 29.58, 28.11, 15.19. IR (neat): ν = 3308 (m), 3063 (w), 2974 (m), 2919 (m), 1743 (s), 1682 (s), 1651 (s), 1520 (s). ^1H & ^{13}C NMR was in agreement with previously reported data on this compound.⁶³



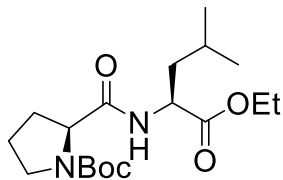
Z-Phe-Pro-OBn (14). R_f 0.23 (1:2 EtOAc/hexanes); colorless oil, 211.7 mg (90%). ^1H NMR (500 MHz, 80.0 °C, $\text{DMSO}-d_6$) δ 7.41-7.16 (m, 17H), 5.14 (m, 2H), 4.96 (m, 2H), 4.47 (m, 2H), 3.44 (m, 1H), 2.92 (dd, 1H), 2.80 (dd, 1H), 2.22-1.70 (m, 4H). ^{13}C NMR (125 MHz, 80.0 °C, $\text{DMSO}-d_6$) δ 171.05, 169.72, 153.95, 137.21, 136.61, 135.68, 128.78, 127.93, 127.80, 127.65, 127.51, 127.27, 127.23, 127.02, 125.87, 65.46, 65.10, 58.46, 53.80, 46.06, 39.51, 36.49, 28.10, 24.15. IR (neat): ν = 3302 (m), 3035 (w), 2955 (m), 1734 (s), 1689 (s), 1660 (s). HRMS (ESI⁺, $[\text{C}_{29}\text{H}_{30}\text{N}_2\text{O}_5 + \text{Na}]^+$) calcd 509.2052, found m/z 509.2029.



Boc-Phg-Phg-OMe (15). R_f 0.36 (1:2 EtOAc/hexanes); white solid, mp: 64 °C, 84.5 mg (88%). ^1H NMR (500 MHz, DMSO- d_6) δ 9.02 (d, 1H), 7.44-7.20 (m, 11H), 5.40 (m, 2H), 3.63 (s, 3H), 1.38 (s, 9H). ^{13}C NMR (125 MHz, DMSO- d_6) δ . 170.79, 170.10, 159.18, 135.82, 135.12, 128.61, 128.28, 128.17, 127.53, 127.50, 127.08, 79.91, 57.23, 56.15, 52.32, 28.13. ^1H & ^{13}C NMR was in agreement with previously reported data on this compound.⁶⁴

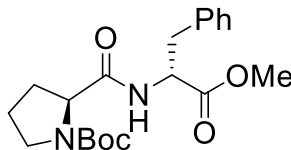


Z-Phg-Phe-O'Bu (16). R_f 0.36 (3:7 EtOAc/hexanes); white solid, mp: 124-125 °C, 2188.0 mg (82%). ^1H NMR (500 MHz, CDCl_3) δ 7.41-7.23 (m, 13H), 7.15 (d, 2H), 6.55 (d, 1H), 6.24 (d, 1H), 5.33 (d, 1H), 5.10 (m, 2H), 4.72 (q, 1H), 3.10 (m, 2H), 1.33 (s, 9H). ^{13}C NMR (125 MHz, CDCl_3) δ 169.63, 169.14, 155.55, 137.57, 136.12, 135.81, 129.37, 128.83, 128.32, 128.25, 127.94, 127.89, 127.05, 126.85, 82.25, 66.88, 58.67, 53.90, 37.77, 27.69. IR (neat): ν = 3331 (m), 3062 (m), 3031 (m), 2978 (m), 1731 (s), 1694 (s), 1652 (s). ^1H & ^{13}C NMR was in agreement with previously reported data on this compound.⁵⁰



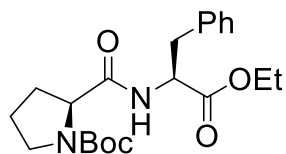
17

Boc-Pro-Leu-OEt (17). R_f 0.47 (1:1 EtOAc/hexanes); white solid, mp: 90-92 °C, 337.4 mg (95%). ^1H NMR (500 MHz, DMSO- d_6) δ 8.21-8.10 (2xd, 1H), 4.24 (m, 1H), 4.12 (m, 1H), 4.07 (m, 2H), 3.36 (m, 1H), 3.25 (m, 1H), 2.17-1.98 (m, 1H), 1.85-1.71 (m, 3H), 1.71-1.62 (m, 1H), 1.62-1.53 (m, 1H), 1.51-1.43 (m, 1H), 1.42-1.28 (2xs, 9H), 1.17 (t, 3H), 0.89 (d, 3H), 0.85 (d, 3H). ^{13}C NMR (125 MHz, DMSO- d_6) δ 172.62, 172.39, 153.25, 78.24, 60.33, 59.13, 50.15, 46.42, 30.85, 28.07, 27.88, 24.07, 22.85, 20.98, 13.99. IR (neat): ν = 3279 (m), 3083 (w), 2959 (m), 2873 (m), 1733 (s), 1690 (s), 1661 (s), 1547 (s). HRMS (ES $^+$, [C $_{18}$ H $_{32}$ N $_2$ O $_5$ + Na] $^+$) calcd 379.2209, found m/z 379.2194.



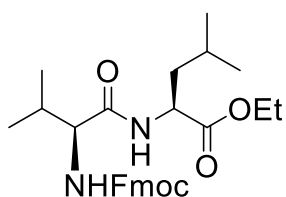
18

Boc-Pro-D-Phe-OMe (18). R_f 0.37 (1:1 EtOAc/hexanes); white solid, mp: 103-104 °C, 886.7 mg (94%). ^1H NMR (500 MHz, 80.0 °C, DMSO- d_6) δ 7.92 (d, 1H), 7.29-7.24 (m, 2H), 7.23-7.17 (m, 3H), 4.62 (m, 1H), 4.11 (m, 1H), 3.62 (s, 3H), 3.28 (m, 2H), 3.08 (m, 1H), 2.95 (m, 1H), 1.96 (m, 1H), 1.67 (m, 2H), 1.57 (s, 1H), 1.35 (s, 9H). ^{13}C NMR (125 MHz, 80.0 °C, DMSO- d_6) δ 171.67, 171.25, 153.15, 136.77, 128.59, 127.66, 125.97, 78.12, 59.16, 52.57, 51.18, 46.06, 36.73, 27.65, 22.66. IR (neat): ν = 3299 (m), 3064 (w), 3026 (w), 2974 (m), 1745 (s), 1684 (s), 1669 (s), 1545 (s). HRMS (ESI, [C $_{20}$ H $_{28}$ N $_2$ O $_5$ + Na] $^+$) calcd 399.1896, found m/z 399.1876.



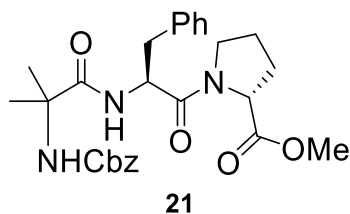
19

Boc-Pro-Phe-OEt (19). R_f 0.22 (1:2 EtOAc/hexanes); yellow oil, 183.1 mg (93%). ^1H NMR (500 MHz, 80.0 °C, DMSO- d_6) δ 7.84 (d, 1H), 7.30-7.25 (m, 2H), 7.24-7.18 (m, 3H), 4.53 (m, 1H), 4.12 (m, 1H), 4.07 (m, 1H), 3.31 (m, 2H), 3.06 (dd, 1H), 2.98 (dd, 1H), 2.04 (m, 1H), 1.79-1.67 (m, 3H), 1.32 (s, 9H), 1.14 (t, 3H). ^{13}C NMR (125 MHz, 80.0 °C, DMSO- d_6) δ 171.83, 170.80, 153.23, 136.82, 128.56, 127.70, 125.98, 78.19, 60.01, 59.16, 53.03, 46.13, 36.51, 27.64, 22.78, 13.43. IR (neat): ν = 3314 (m), 3063 (w), 3030 (w), 2977 (m), 2932 (m), 2878 (m), 1739 (s), 1673 (s), 1520 (s). ^1H & ^{13}C NMR was in agreement with previously reported data on this compound.⁶⁵

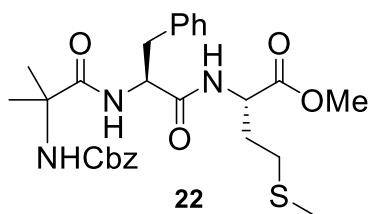


20

Fmoc-Val-Leu-OEt (20). R_f 0.25 (1:3 EtOAc/hexanes); white solid, mp: 161-162 °C, 236.3 mg (96%). ^1H NMR (500 MHz, DMSO- d_6) δ 8.23 (d, 1H), 7.88 (d, 2H), 7.74 (t, 2H), 7.41 (t, 2H), 7.38 (d, 1H), 7.31 (t, 2H), 4.32-4.18 (m, 4H), 4.06 (m, 2H), 3.92 (t, 1H), 1.99 (m, 1H), 1.70-1.44 (m, 3H), 1.15 (t, 3H), 0.90 (d, 3H), 0.88 (d, 6H), 0.82 (d, 3H); ^{13}C NMR (125 MHz, DMSO- d_6) δ 172.25, 171.37, 156.03, 143.89, 143.74, 140.69, 127.60, 127.01, 125.35, 125.33, 120.05, 65.67, 60.35, 59.87, 50.32, 46.68, 39.63, 30.44, 24.15, 22.69, 21.27, 19.12, 18.25, 13.98. IR (neat): ν = 3294 (m, br), 3065 (m), 3958 (m), 2871 (m), 1728 (s), 1692 (s), 1646 (s). HRMS (ESI⁺, [C₂₈H₃₆N₂O₅ + Na]⁺) calcd 503.2522, found m/z 503.2501.

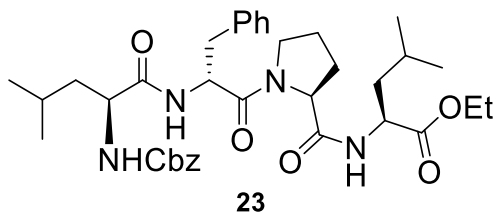


Z-Aib-Phe-D-Pro-OMe (21). R_f 0.23 (1:1 EtOAc/hexanes); white solid, mp: 96-98 °C, 226.1 mg (91%). ^1H NMR (500 MHz, 80.0 °C, DMSO- d_6) δ 7.44-7.01 (m, 12H), 5.07-4.91 (m, 2H), 4.89-4.77 (m, 1H), 4.25 (m, 1H), 3.58 (s, 3H), 3.25-3.08 (m, 2H), 2.91 (m, 2H), 2.21-1.67 (m, 4H), 1.40-1.27 (m, 6H). ^{13}C NMR (125 MHz, 80.0 °C, DMSO- d_6) δ 173.16, 171.52, 168.83, 154.33, 136.75, 136.68, 128.91, 127.84, 127.64, 127.22, 125.96, 125.55, 64.99, 58.31, 58.25, 55.82, 51.45, 51.38, 51.10, 45.98, 45.74, 39.51, 37.42, 28.14, 24.83, 24.47, 23.82. IR (neat): ν = 3313 (m, br), 3062 (w), 3030 (w), 2881 (m), 2952 (m), 2881 (w), 1721 (s), 1633 (s), 1497 (s). ^1H & ^{13}C NMR was in agreement with previously reported data on this compound.⁶⁶

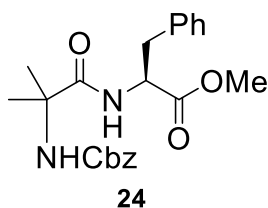


Z-Aib-Phe-Met-OMe (22). R_f 0.32 (1:1 EtOAc/hexanes); white solid, 218.9 mg (90%). ^1H NMR (500 MHz, DMSO- d_6) δ 7.99 (d, 1H), 7.80 (d, 1H), 7.56 (s, 1H), 7.40-7.13 (m, 10H), 5.00 (dd, 2H), 4.53 (m, 2H), 3.64 (s, 3H), 3.18 (dd, 1H), 2.94 (dd, 1H), 2.62-2.45 (m, 2H), 2.03 (s, 3H), 2.02-1.90 (m, 2H), 1.20 (s, 3H), 1.15 (s, 3H). ^{13}C NMR (125 MHz, DMSO- d_6) δ 173.67, 171.92, 171.19, 155.35, 138.15, 136.66, 129.14, 128.32, 127.90, 127.81, 127.71, 126.08, 65.44, 56.01, 53.72, 51.90, 51.06, 36.17, 30.53, 29.45, 25.25, 24.81, 14.51. IR (neat): ν = 3564 (m), 3458 (m), 3300 (m), 3061 (w), 3031 (w), 2951 (m), 2920

(m), 2854 (w), 1743 (m), 1695 (s), 1657 (s), 1532 (s). HRMS (ESI⁺, [C₂₇H₃₅N₃O₆S + Na]⁺) calcd 552.2144, found *m/z* 552.2135.

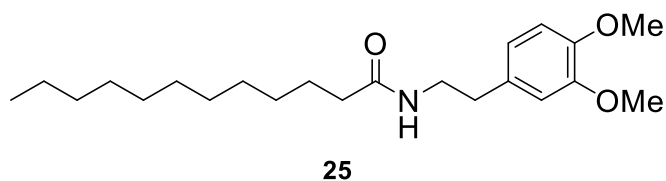


Z-Leu-D-Phe-Pro-Leu-OEt (23). *R_f* 0.17 (1:1 EtOAc/hexanes); light yellow solid, mp: 42-43 °C, 218.9 mg (87%). ¹H NMR (500 MHz, CDCl₃) δ 7.38-7.13 (m, 11H), 6.97 (d, 1H), 5.88 (d, 1H), 5.10 (q, 2H), 4.75 (q, 1H), 4.55 (m, 1H), 4.44 (m, 1H), 4.26 (q, 1H), 4.06 (m, 2H), 3.62 (m, 1H), 3.05 (m, 1H), 2.95 (dd, 1H), 2.68 (q, 1H), 2.08 (m, 1H), 1.73 (m, 2H), 1.68-1.53 (m, 6H), 1.45 (m, 1H), 1.16 (t, 3H), 0.90 (2xd, 12H). ¹³C NMR (125 MHz, CDCl₃) δ 173.30, 172.63, 170.80, 170.48, 156.56, 136.24, 135.95, 129.31, 128.46, 128.43, 128.39, 127.99, 127.81, 127.06, 66.90, 61.21, 60.47, 53.02, 51.05, 50.43, 46.71, 41.25, 40.94, 40.85, 37.79, 28.74, 24.90, 24.56, 24.03, 22.93, 22.76, 22.11, 22.00, 21.80, 13.93. IR (neat): ν = 3300 (m, br), 3062 (w), 3034 (w), 2956 (m), 2932 (m), 2871 (m), 1723 (s), 1634 (s), 1525 (s). HRMS (EI⁺, [C₃₆H₅₀N₄O₇]⁺) calcd 650.3679, found *m/z* 650.3667.

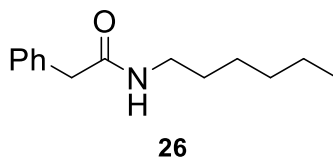


Z-Aib-Phe-OMe (24). *R_f* 0.45 (1:1 EtOAc/hexanes); white solid, mp: 84-85 °C, 185.1 mg (93%). ¹H NMR (500 MHz, DMSO-*d*₆) δ 7.75 (d, 1H), 7.42-7.14 (m, 11H), 4.97 (s, 2H), 4.48 (dt, 1H), 3.60 (s, 3H), 3.00 (m, 2H), 1.28 (s, 6H); ¹³C NMR (125 MHz, DMSO-*d*₆) δ 174.04, 171.88, 154.52, 137.24, 136.93, 129.13, 128.28, 128.10, 127.70, 127.66, 126.42, 65.10, 55.83, 53.51, 51.80, 36.46, 25.06, 24.79. IR (neat): ν = 3315 (m, br), 3065 (w), 3030

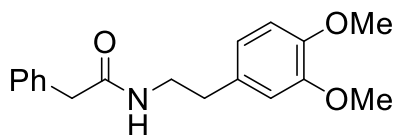
(m), 2981 (m), 2948 (m), 2927(m), 2859 (w), 1748 (s), 1688 (s), 1658 (s). ^1H & ^{13}C NMR was in agreement with previously reported data on this compound.⁶⁷



N-(3,4-dimethoxyphenethyl)dodecanamide (31). R_f 0.28 (1:1 EtOAc/hexanes); white solid, mp: 85-86 °C, 176.3 mg (89%). ^1H NMR (500 MHz, CDCl_3) δ 6.82 (d, 1H), 6.73 (m, 2H), 5.45 (s, 1H), 3.87 (2xs, 6H), 3.50 (q, 2H), 2.76 (t, 2H), 2.12 (t, 2H), 1.59 (m, 2H), 1.34-1.21 (m, 16H), 0.88 (t, 3H). ^{13}C NMR (125 MHz, CDCl_3) δ 173.08, 149.05, 147.69, 131.43, 120.61, 111.35, 103.72, 55.91, 55.85, 40.57, 36.87, 35.30, 31.88, 29.59, 29.58, 29.46, 29.34, 29.30, 29.28, 25.76, 22.65, 14.08. IR (neat): ν = 3310 (m), 2999 (w), 2954 (m), 2919 (s), 2871 (m), 2850 (m), 1637 (s), 1518 (s). ^1H & ^{13}C NMR was in agreement with previously reported data on this compound.⁶⁸

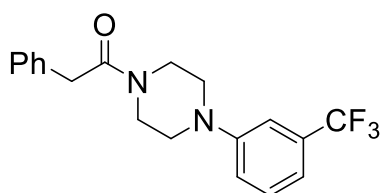


N-hexyl-2-phenylacetamide (32). R_f 0.38 (1:1 EtOAc/hexanes); white solid, mp: 54-55 °C, 118.3 mg (97%). ^1H NMR (500 MHz, CDCl_3) δ 7.39-7.24 (m, 5H), 5.34 (s, 1H), 3.58 (s, 2H), 3.20 (m, 2H), 1.57 (m, 2H), 1.41 (m, 2H), 1.31-1.18 (6H, m), 0.86 (m, 3H). ^{13}C NMR (125 MHz, CDCl_3) δ 170.79, 135.07, 129.45, 129.00, 127.31, 43.93, 39.66, 31.36, 29.38, 26.40, 22.48, 13.93. IR (neat): ν = 3252 (m), 3065 (m), 3032 (w), 2957 (m), 2935 (m), 2915 (m), 2873 (m), 2860 (m), 1655 (m), 1626 (s), 1551 (s). ^1H & ^{13}C NMR was in agreement with previously reported data on this compound.



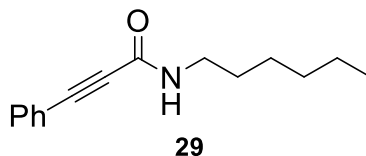
27

N-(3,4-dimethoxyphenethyl)-2-phenylacetamide (33). R_f 0.50 (EtOAc); white solid, mp: 108-109 °C, 136.7 mg (93%). ^1H NMR (500 MHz, CDCl_3) δ 7.34-7.14 (m, 5H), 6.73 (m, 1H), 6.61 (m, 1H), 6.56 (m, 1H), 5.36 (s, 1H), 3.86 (s, 3H), 3.83 (s, 3H), 3.54 (s, 2H), 3.45 (m, 2H), 2.68 (t, 3H). ^{13}C NMR (125 MHz, CDCl_3) δ 170.82, 149.01, 147.63, 134.78, 131.11, 129.39, 128.95, 127.27, 120.55, 111.77, 111.32, 55.92, 55.81, 43.89, 40.73, 35.02. IR (neat): ν = 3286 (m), 3063 (w), 3029 (w), 3001 (w), 2934 (m), 2834 (w), 1644 (s), 1514 (s). ^1H & ^{13}C NMR was in agreement with previously reported data on this compound.⁷⁰

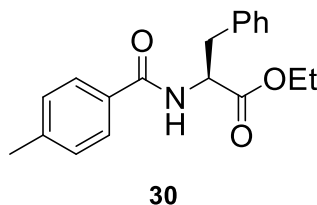


28

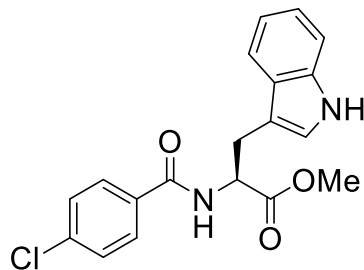
2-phenyl-1-(4-(3-(trifluoromethyl)phenyl)piperazin-1-yl)ethan-1-one (34). R_f 0.32 (1:2 EtOAc/hexanes); light yellow oil, 173.8 mg (>99%). ^1H NMR (500 MHz, CDCl_3) δ 7.39-7.32 (m, 3H), 7.30-7.24 (m, 3H), 7.12 (1H, dt), 7.07 (t, 1H), 7.03 (dd, 1H), 3.83 (t, 2H), 3.80 (s, 2H), 3.62 (t, 2H), 3.20 (t, 2H), 3.03 (t, 2H). ^{13}C NMR (125 MHz, CDCl_3) δ 169.51, 150.87, 145.37, 134.79, 131.67, 131.42, 129.67, 128.83, 128.50, 126.94, 119.24, 116.67, 112.71, 112.68, 48.95, 48.75, 45.74, 41.44, 41.08. IR (neat): ν = 3465 (w), 3063 (w), 3029 (w), 2916 (m), 2829 (m), 1731 (s), 1640 (s), 1448 (m). ^1H & ^{13}C NMR was in agreement with previously reported data on this compound.⁶⁹



N-hexyl-3-phenylpropiolamide (35). R_f 0.26 (1:2 EtOAc/hexanes); colorless oil, 100.0 mg (86%). ^1H NMR (500 MHz, CDCl_3) δ 7.58-7.51 (m, 2H), 7.45-7.33 (m, 3H), 5.97 (s, 1H), 3.35 (m, 2H), 1.63-1.52 (m, 2H), 1.41-1.27 (m, 6H), 0.90 (t, 3H). ^{13}C NMR (125 MHz, CDCl_3) δ 153.36, 132.44, 129.94, 128.47, 120.30, 84.36, 83.16, 40.00, 31.41, 29.32, 26.53, 22.52, 13.98. IR (neat): ν = 3260 (m, br), 3060 (m), 2955 (m), 2928 (m), 2857 (m), 2216 (m), 1724 (w), 1626 (s), 1538 (s). HRMS (ESI⁺, [$\text{C}_{15}\text{H}_{19}\text{NO} + \text{Na}$]⁺) calcd 252.1364, found m/z 252.1369.

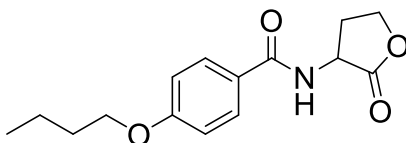


ethyl (4-methylbenzoyl)-L-phenylalaninate (36). R_f 0.35 (1:3 EtOAc/hexanes); white solid, mp: 133 °C, 153.2 mg (>99%). ^1H NMR (500 MHz, CDCl_3) δ 7.64 (dt, 2H), 7.31-7.21 (m, 5H), 7.16 (m, 2H), 6.59 (d, 1H), 5.07 (dt, 1H), 4.22 (q, 2H), 3.26 (m, 2H), 2.40 (s, 3H), 1.28 (t, 3H). ^{13}C NMR (125 MHz, CDCl_3) δ 171.64, 166.66, 142.15, 135.95, 131.11, 129.39, 129.21, 128.48, 127.06, 126.97, 61.55, 53.47, 37.97, 21.42, 14.11. IR (neat): ν = 3360 (m, br), 3031 (w), 3004 (w), 2983 (m), 2963 (m), 1750 (s), 1637 (s), 1526 (s), 1504 (s). HRMS (ESI⁺, [$\text{C}_{16}\text{H}_{23}\text{NO}_3 + \text{Na}$]⁺) calcd 334.1419, found m/z 334.1417.



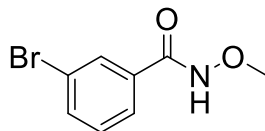
31

methyl (4-chlorobenzoyl)-L-tryptophanate (37). R_f 0.44 (1:1 EtOAc/hexanes); white solid, 163.5 mg (92%). ^1H NMR (500 MHz, CDCl_3) δ 8.42 (s, 1H), 7.59 (dt, 2H), 7.54 (d, 1H), 7.34 (d, 1H), 7.32 (dt, 2H), 7.19 (t, 1H), 7.09 (t, 1H), 6.97 (d, 1H), 6.70 (d, 1H), 5.14 (dt, 1H), 3.73 (s, 3H), 3.45 (m, 2H). ^{13}C NMR (125 MHz, CDCl_3) δ 172.25, 165.91, 137.91, 136.11, 132.09, 128.70, 128.46, 127.58, 122.81, 122.26, 119.68, 118.45, 111.36, 109.74, 53.58, 52.44, 27.49. IR (neat): ν = 3404 (m, br), 3312 (m, br), 3058 (m), 2952 (m), 2925 (m), 2853 (w), 1734 (s), 1643 (s). ^1H & ^{13}C NMR was in agreement with previously reported data on this compound.⁵⁸



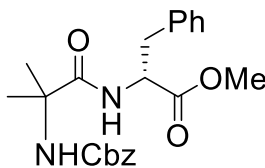
32

4-butoxy-N-(2-oxotetrahydrofuran-3-yl)benzamide (37). R_f 0.37 (3:1 EtOAc/hexanes); white solid, mp: 108-109 °C, 126.9 mg (90%). ^1H NMR (500 MHz, CDCl_3) δ 7.75 (dt, 2H), 6.93 (d, 1H), 6.87 (dt, 2H), 4.76 (ddd, 1H), 4.50 (dt, 1H), 4.32 (ddd, 1H), 3.98 (t, 2H), 2.87 (m, 1H), 2.28 (m, 1H), 1.77 (m, 2H), 1.50 (m, 2H), 0.92 (t, 3H). ^{13}C NMR (125 MHz, CDCl_3) δ 175.98, 167.27, 162.23, 128.99, 124.90, 114.24, 67.86, 66.22, 49.56, 31.11, 30.32, 19.15, 13.77. IR (neat): ν = 3707 (m), 3681 (m), 3287 (m), 2956 (m), 2935 (m), 2872 (m), 2845 (m), 1771 (s), 1641 (s), 1607 (s). HRMS (ESI⁺, $[\text{C}_{15}\text{H}_{19}\text{NO}_4 + \text{Na}]^+$) calcd 300.1212, found m/z 300.1209.



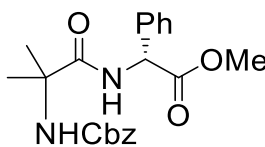
33

3-bromo-N-methoxy-N-methylbenzamide (39). R_f 0.23 (1:3 EtOAc/hexanes); colorless oil, 102.5 mg (84%). ^1H NMR (500 MHz, DMSO- d_6) δ 7.81 (t, 1H), 7.59 (dt, 1H), 7.56 (ddd, 1H), 7.26 (t, 1H), 3.53 (s, 3H), 3.33 (s, 3H). ^{13}C NMR (125 MHz, CDCl_3) δ 168.11, 135.89, 133.48, 131.15, 129.54, 126.72, 121.93, 61.12, 33.47. IR (neat): ν = 3065 (w), 2967 (m), 2934 (m), 2818 (w), 1640 (s), 1561 (m).



43

Z-Aib-D-Phe-OMe (43). R_f 0.45 (1:1 EtOAc/hexanes); white solid, mp: 84-85 °C, 182.2 mg (91%). ^1H NMR (500 MHz, DMSO- d_6) δ 7.75 (d, 1H), 7.40-7.15 (m, 11H), 4.97 (s, 2H), 4.47 (dt, 1H), 3.60 (s, 3H), 3.00 (m, 2H), 1.27 (s, 6H); ^{13}C NMR (125 MHz, DMSO- d_6) δ 174.05, 171.85, 154.52, 137.22, 136.93, 129.11, 128.26, 128.09, 127.69, 127.62, 126.41, 65.10, 55.83, 53.49, 51.77, 36.48, 25.05, 24.77. IR (neat): ν = 3315 (m, br), 3066 (w), 3030 (m), 2982 (m), 2948 (m), 2927(m), 2855 (w), 1748 (s), 1688 (s), 1658 (s). HRMS (EI $^+$, $[\text{C}_{22}\text{H}_{26}\text{N}_2\text{O}_5]^+$) calcd 398.1842, found m/z 398.1837.

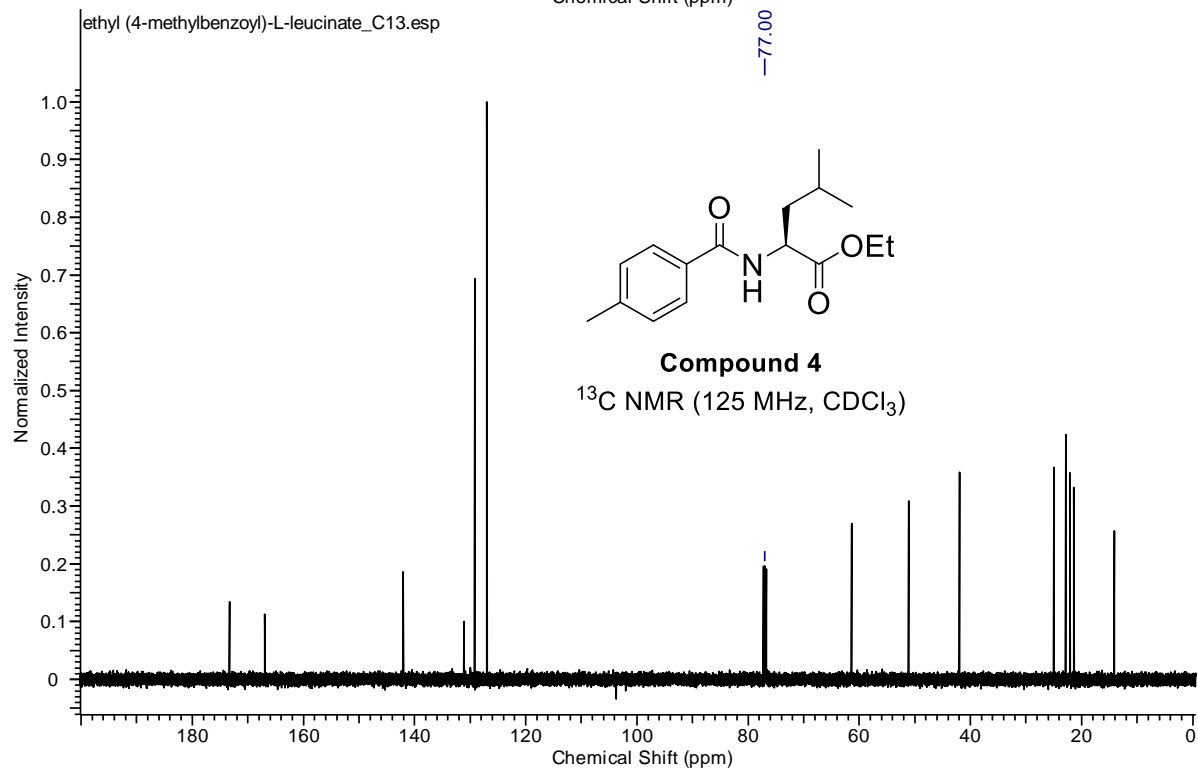
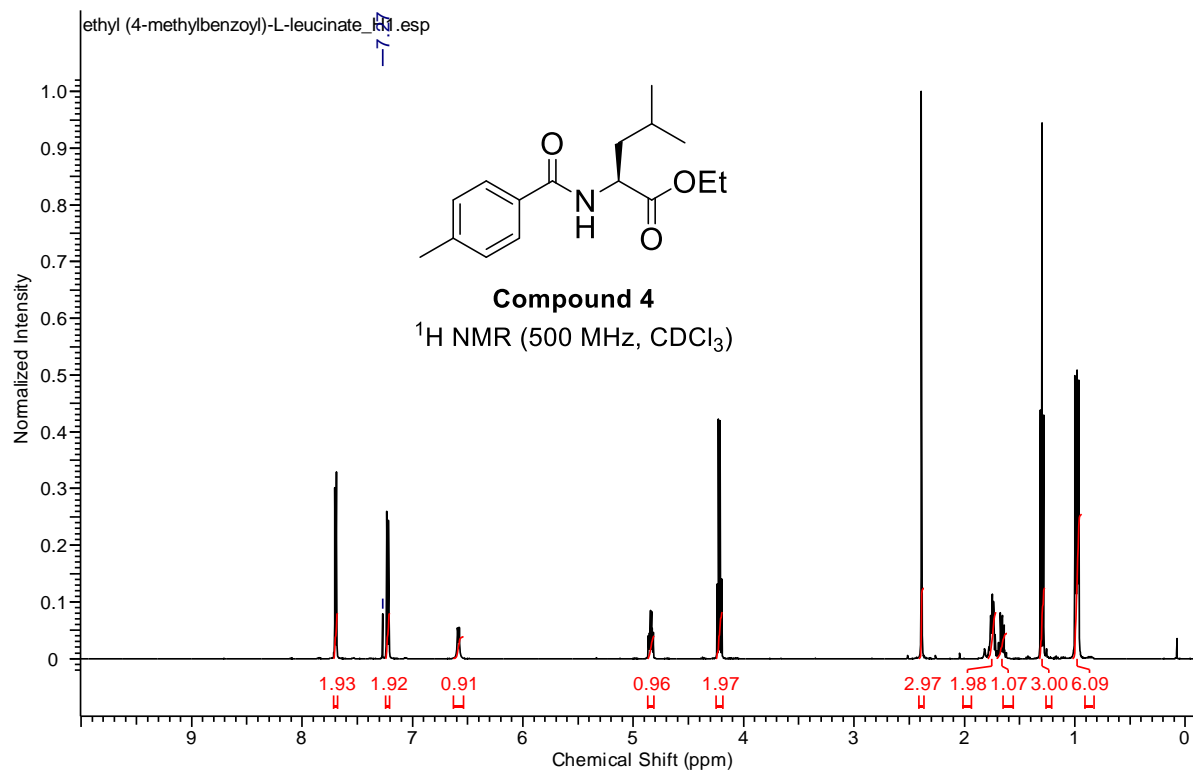


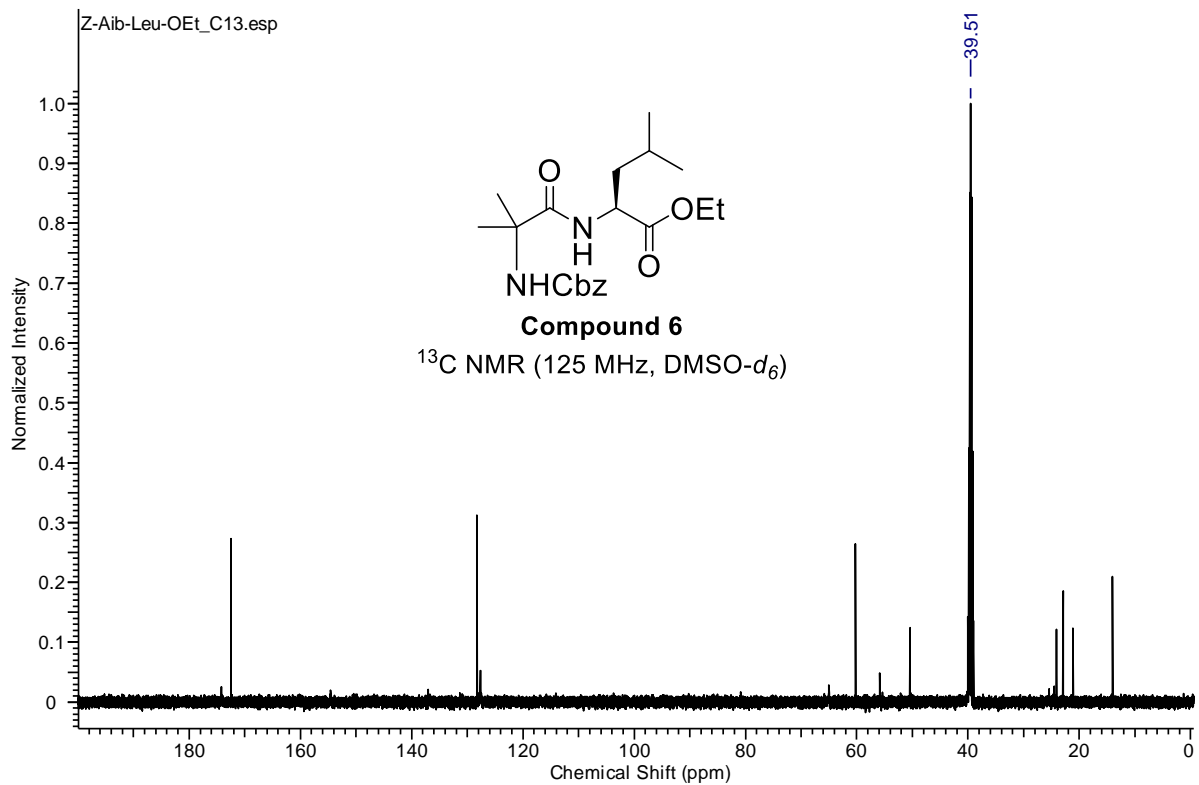
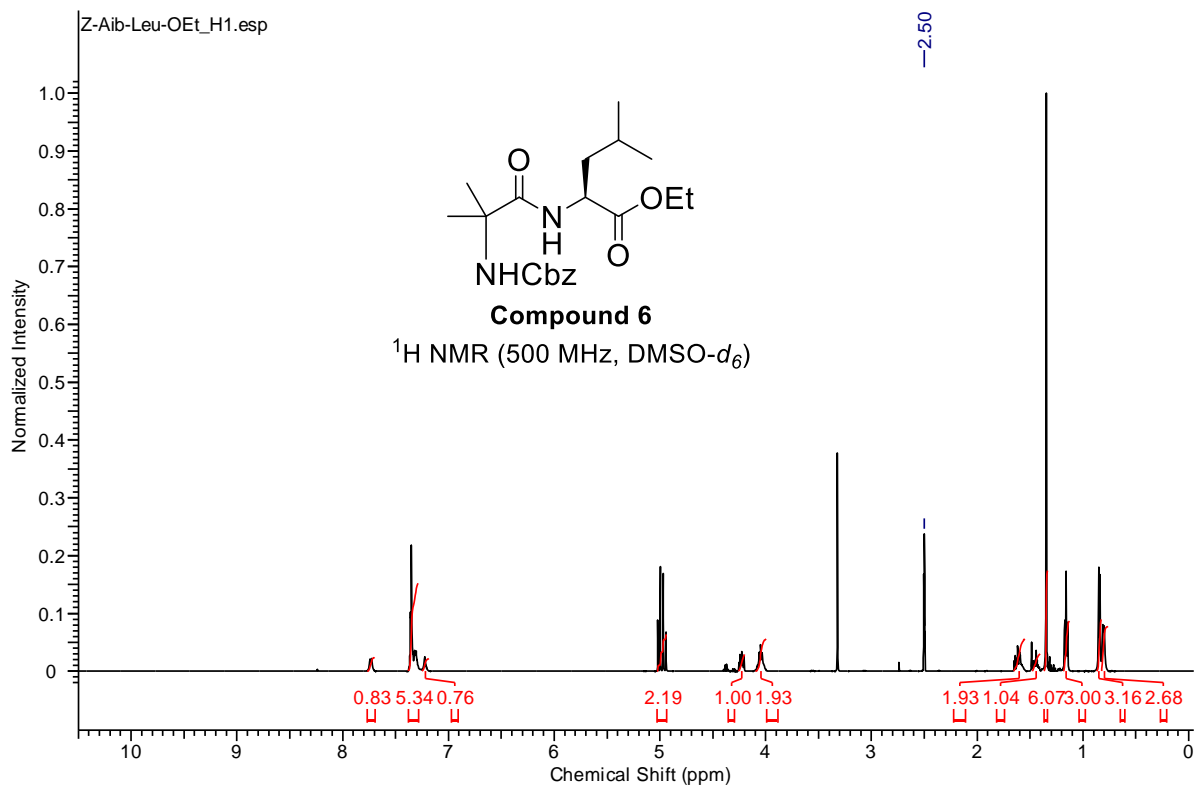
44

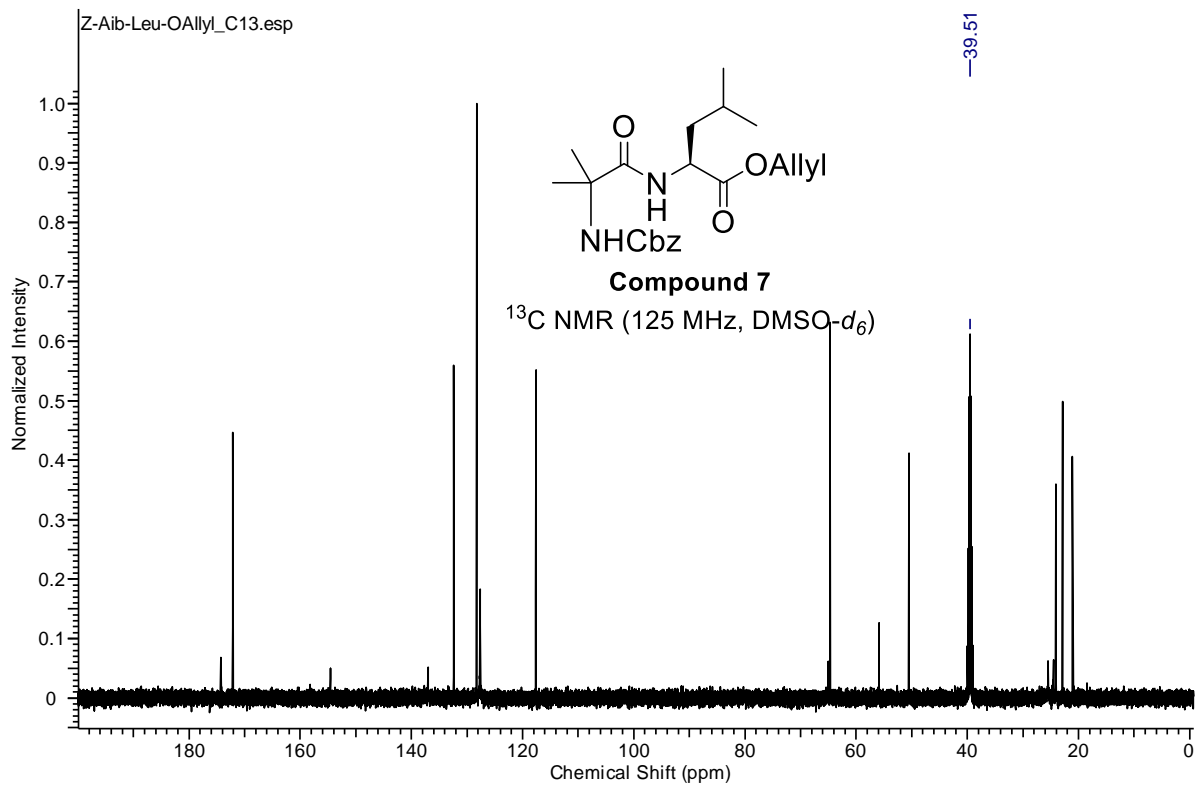
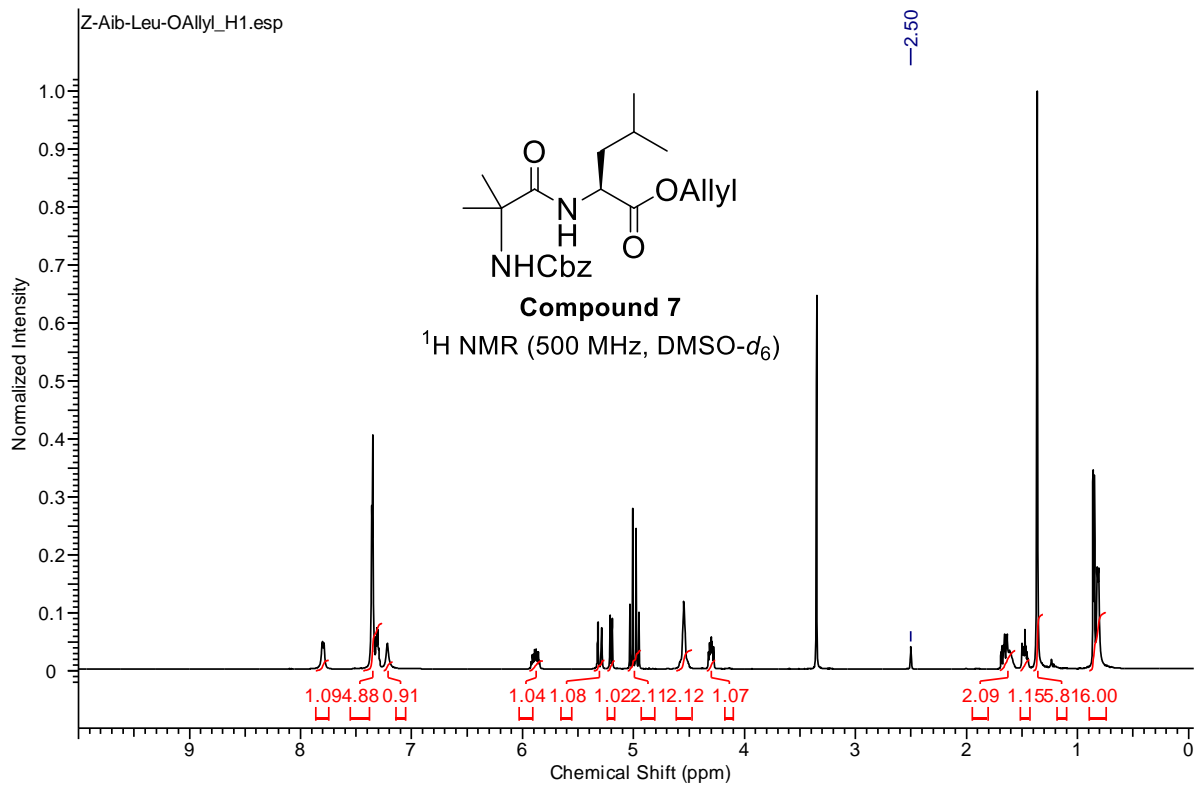
Z-Aib-D-Phg-OMe (44). R_f 0.45 (1:1 EtOAc/hexanes); white solid, mp: 125-126 °C, 173.2 mg (84%). ^1H NMR (500 MHz, DMSO- d_6) δ 8.13 (d, 1H), 7.40-7.28 (m, 11H), 5.40

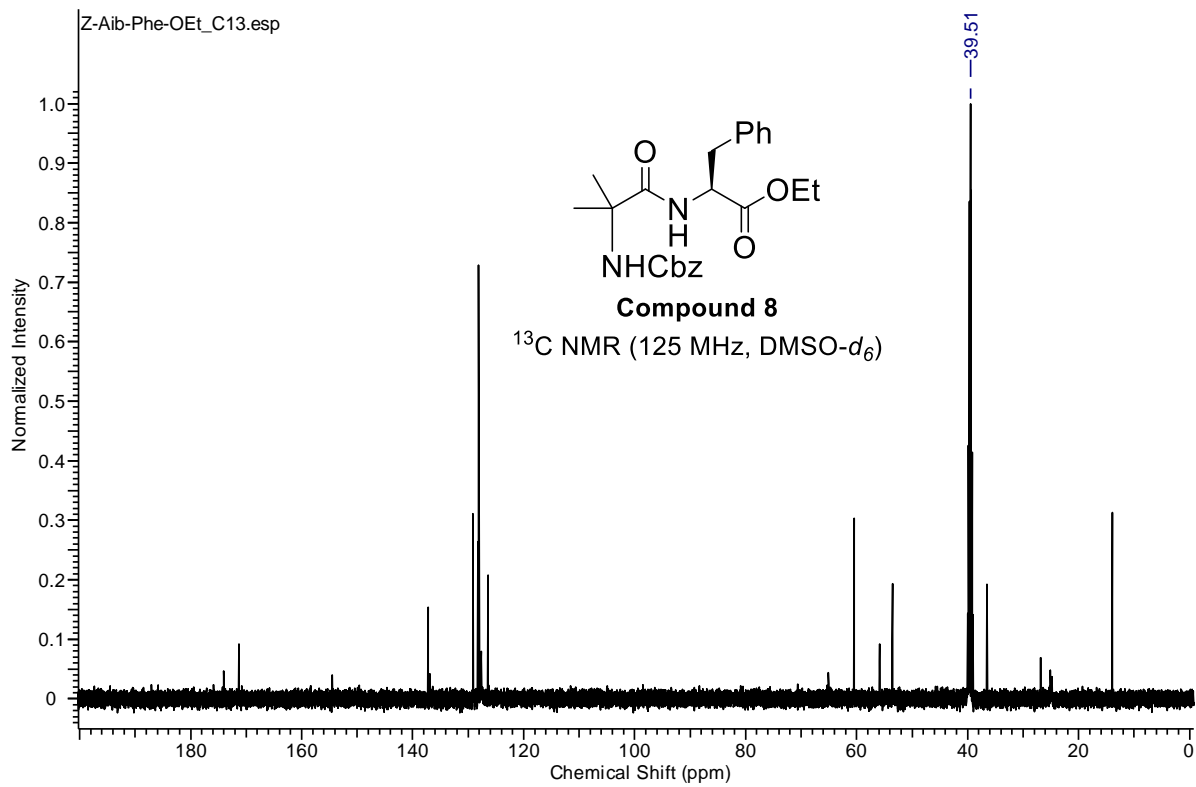
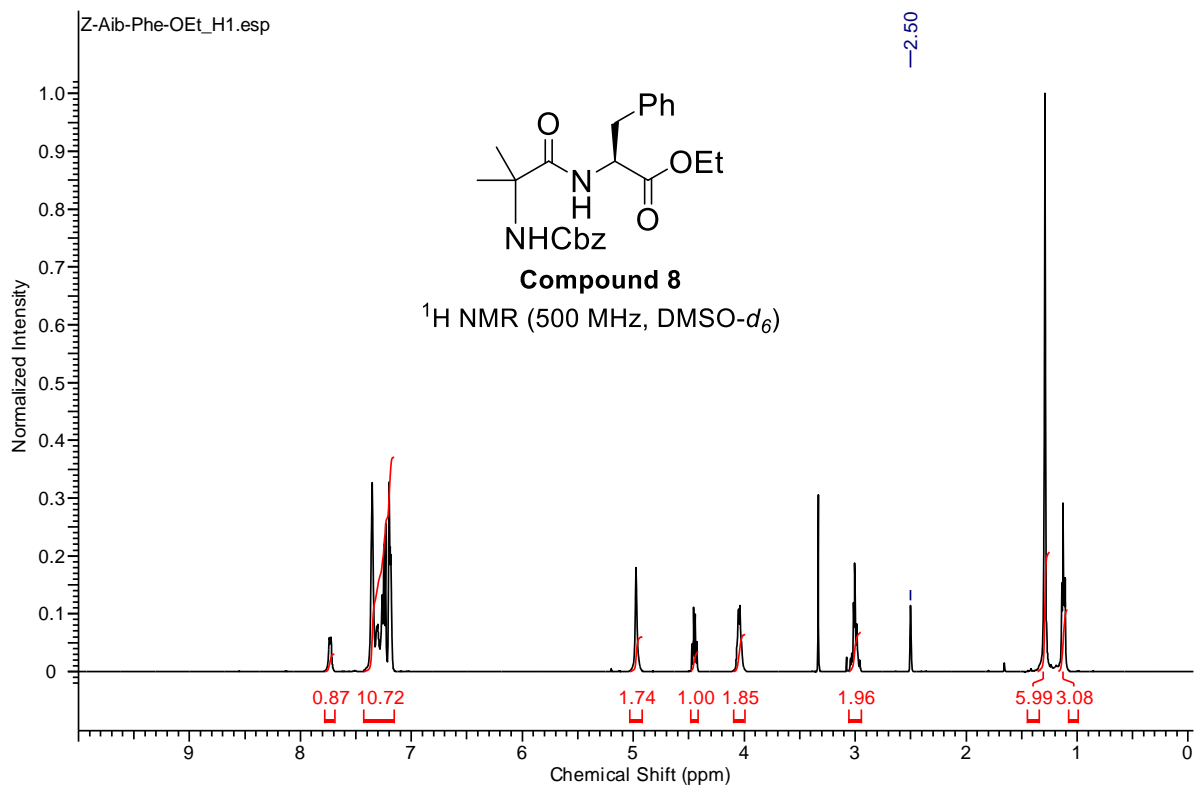
(d, 1H), 5.00 (m, 2H), 3.63 (s, 3H), 1.38 (s, 3H), 1.36 (s, 3H); ^{13}C NMR (125 MHz, DMSO-*d*₆) δ 174.03, 170.85, 154.79, 136.93, 136.56, 128.44, 128.27, 127.97, 127.69, 127.57, 127.49, 65.14, 56.24, 55.98, 52.26, 25.16, 24.75. IR (neat): ν = 3323 (m, br), 3063 (m), 2974 (m), 2948 (m), 1744 (s), 1687 (s), 1674 (s), 1660 (s). HRMS (EI⁺, [C₂₁H₂₄N₂O₅]⁺) calcd 384.1685, found *m/z* 384.1673.

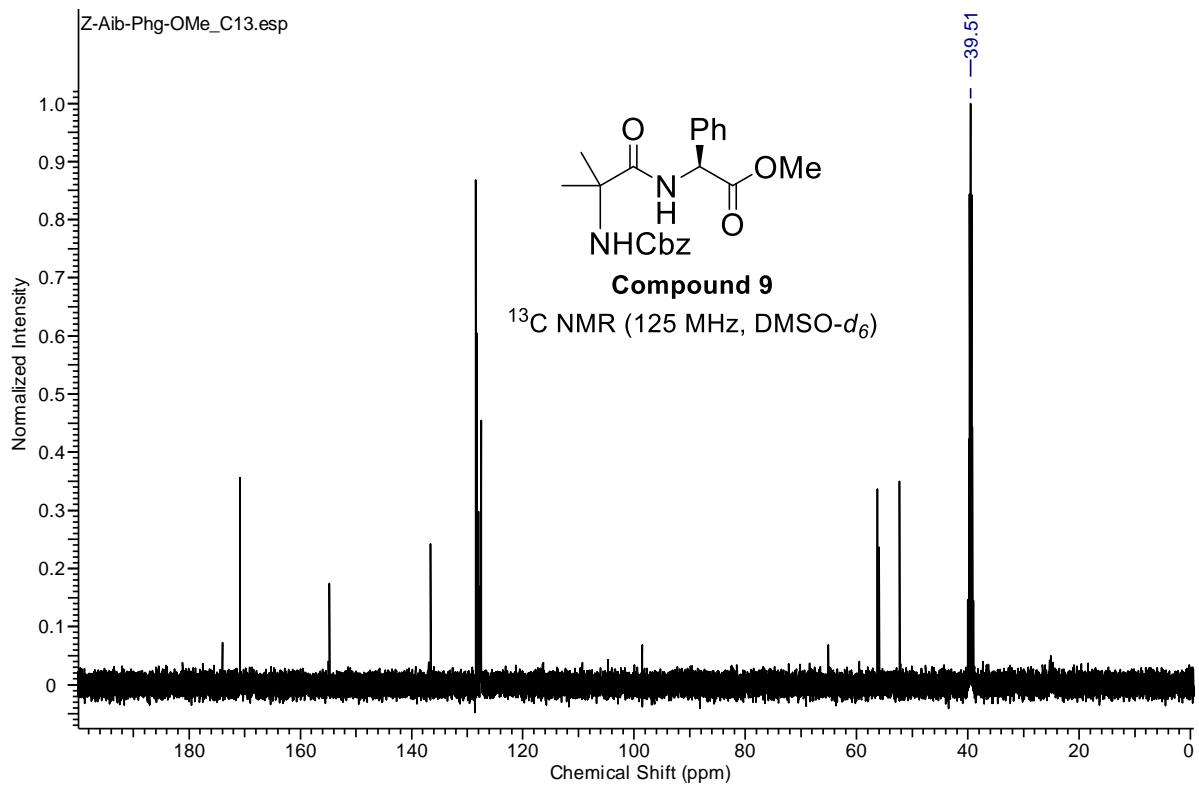
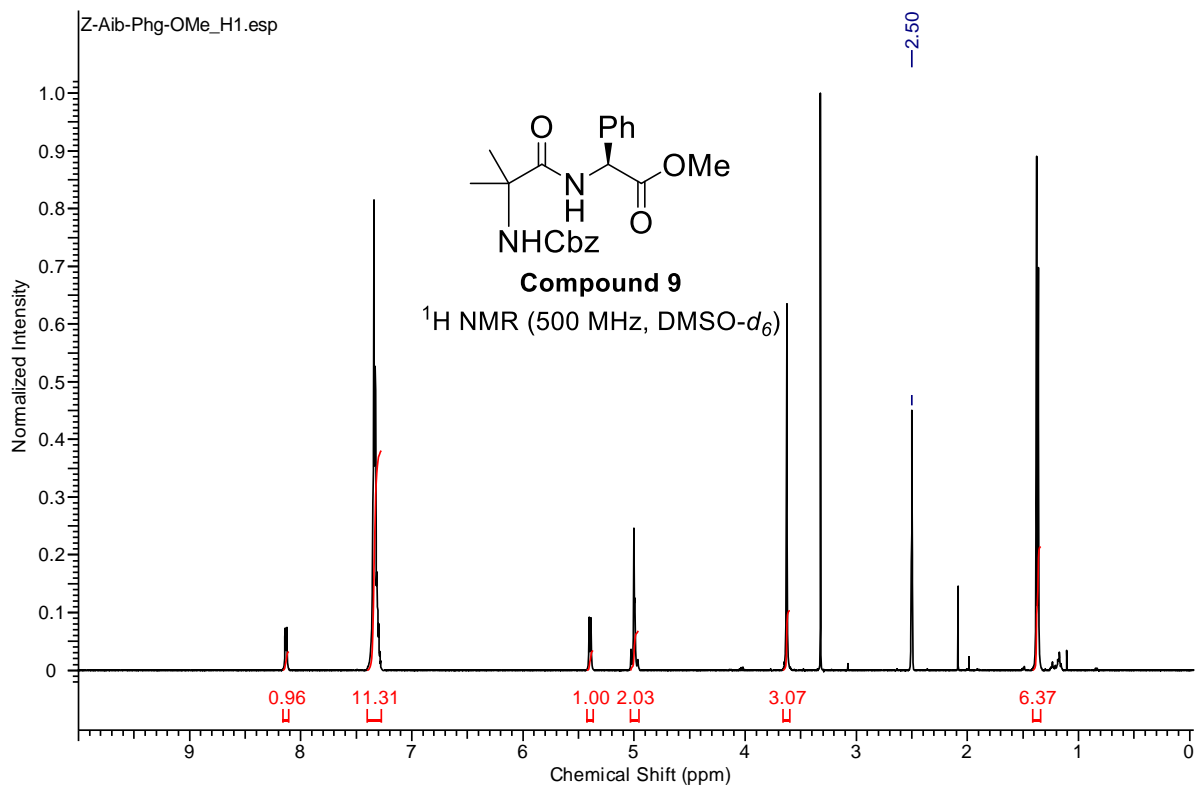
3.9 NMR Spectra

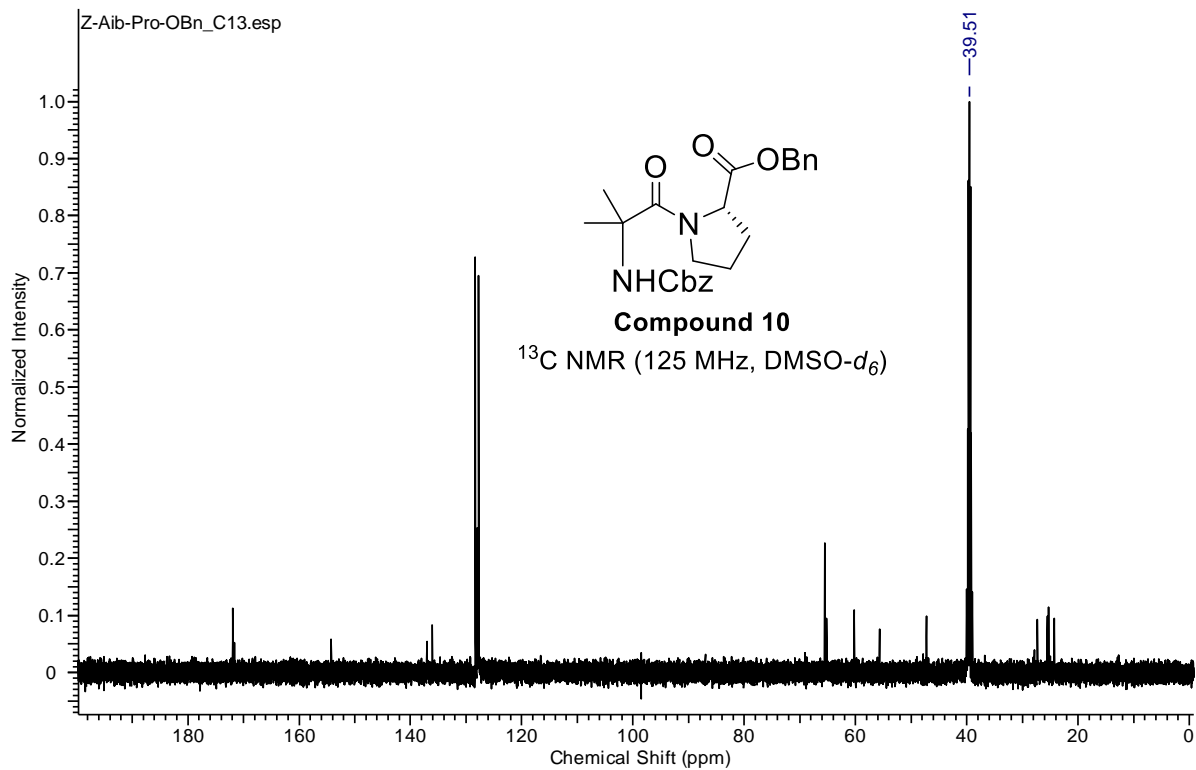
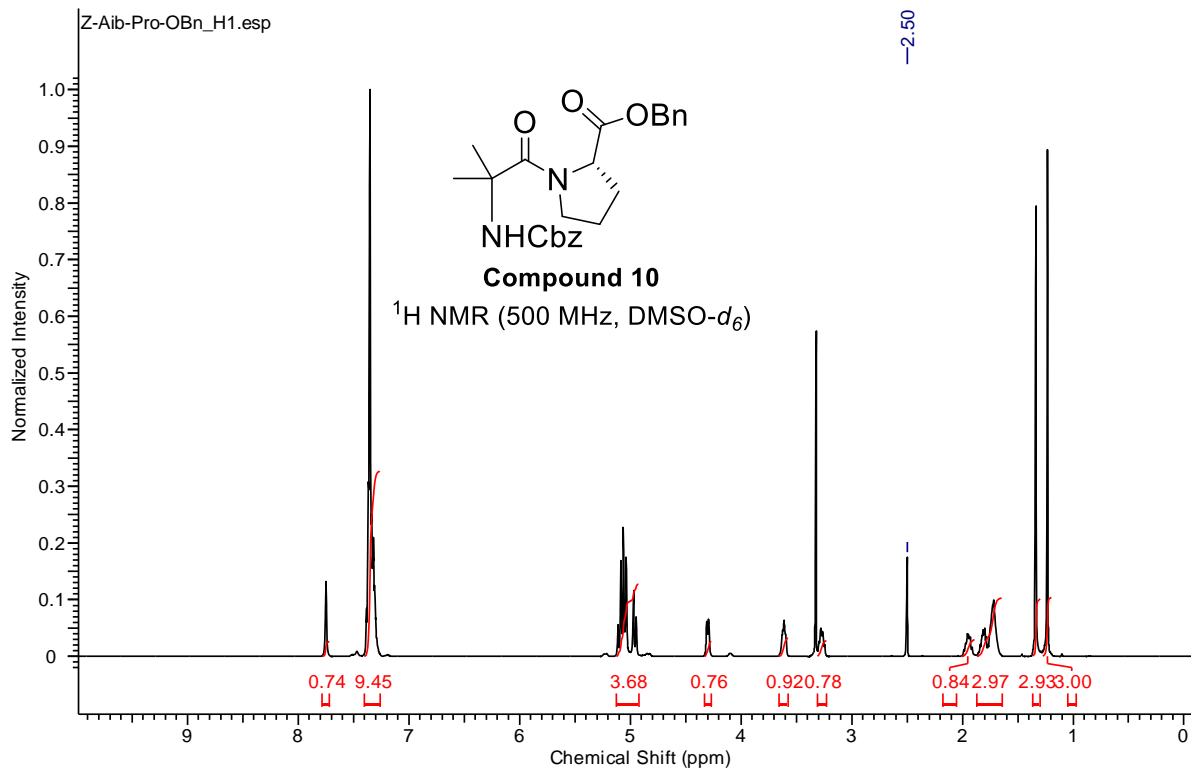


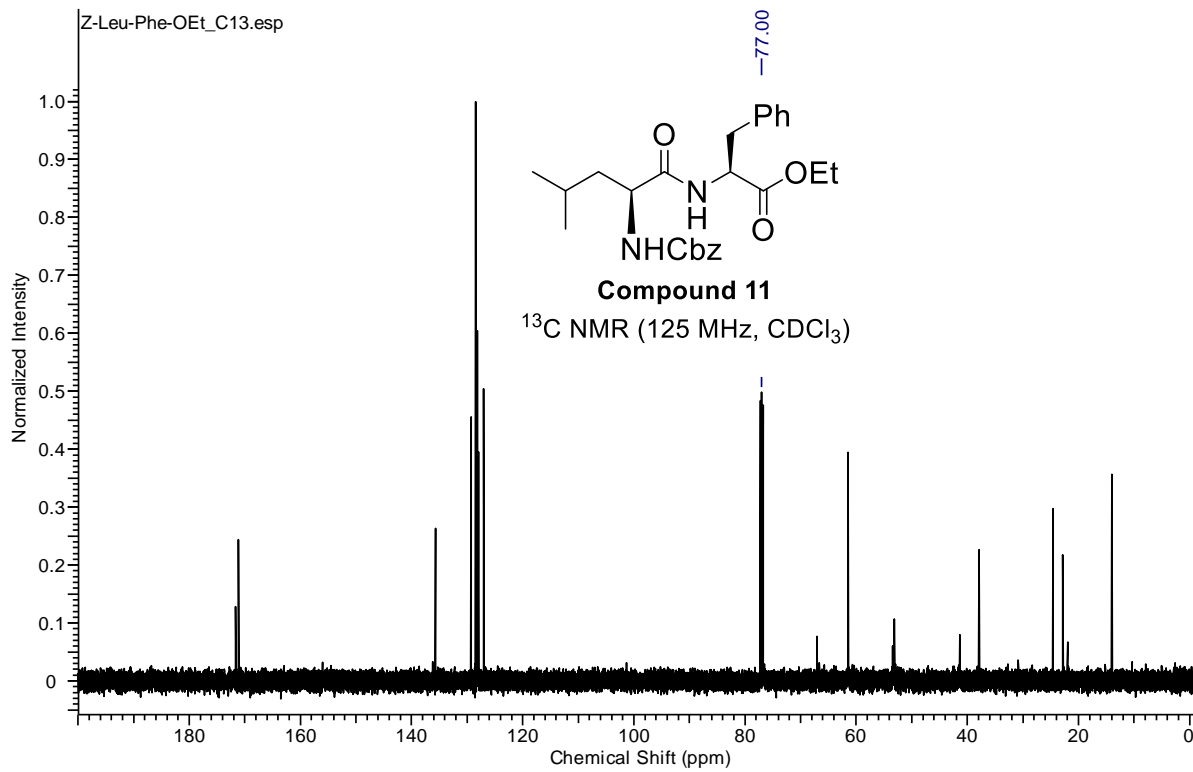
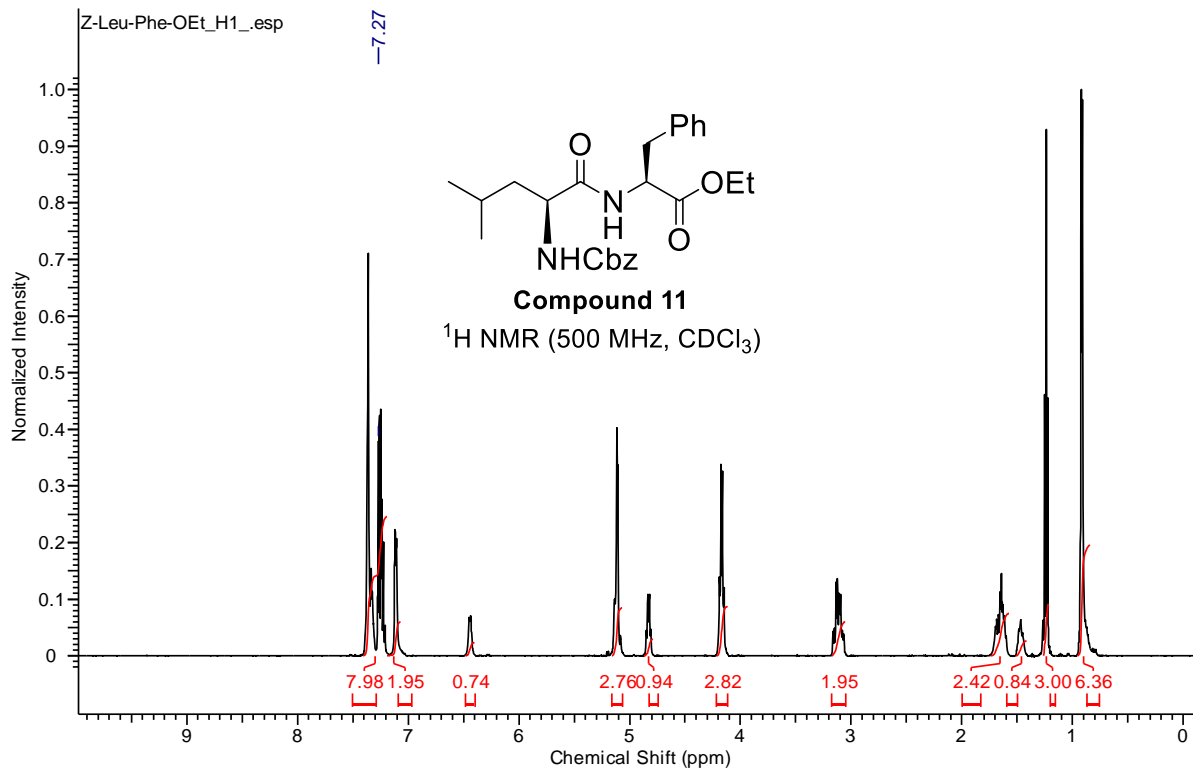


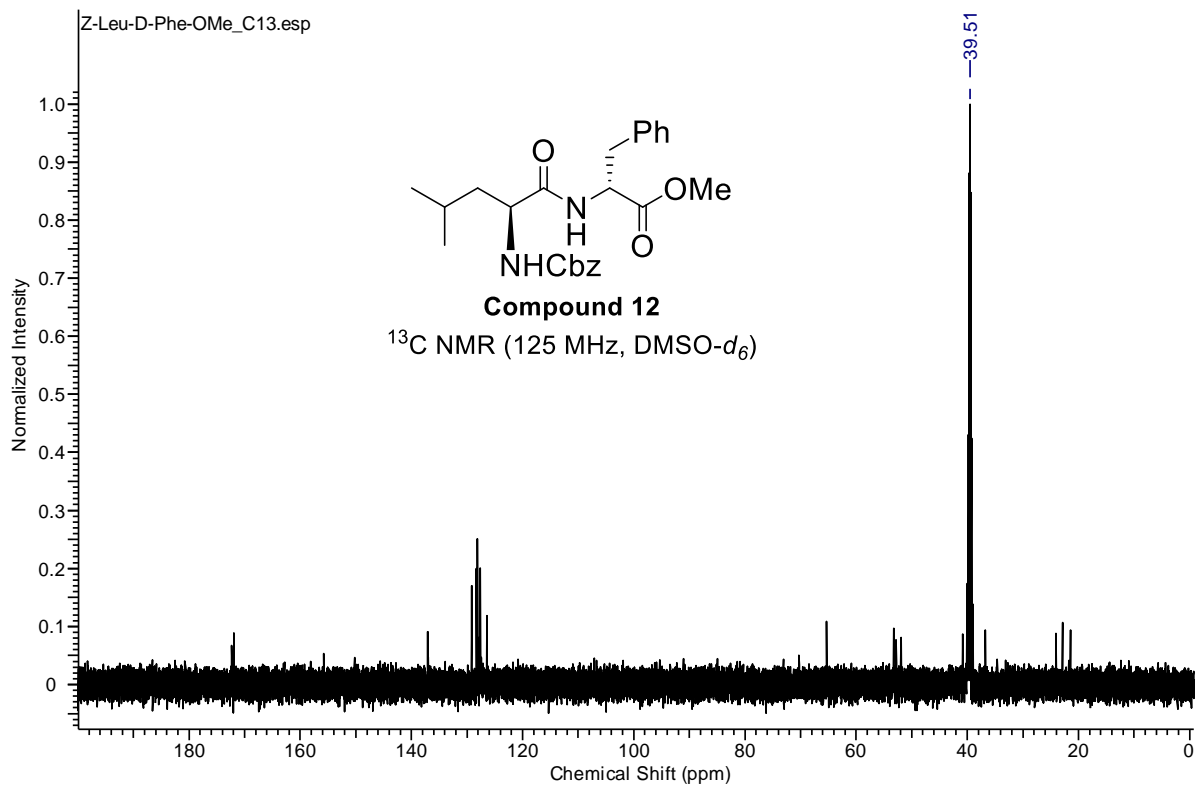
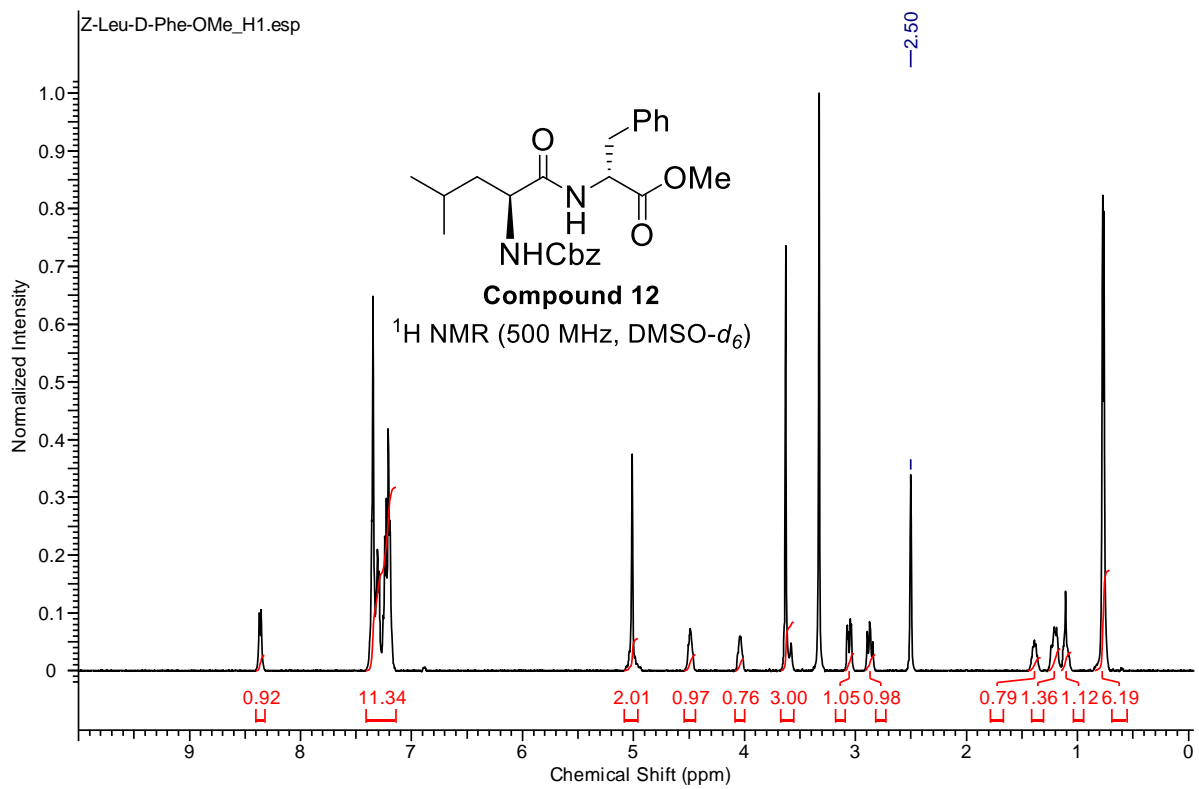


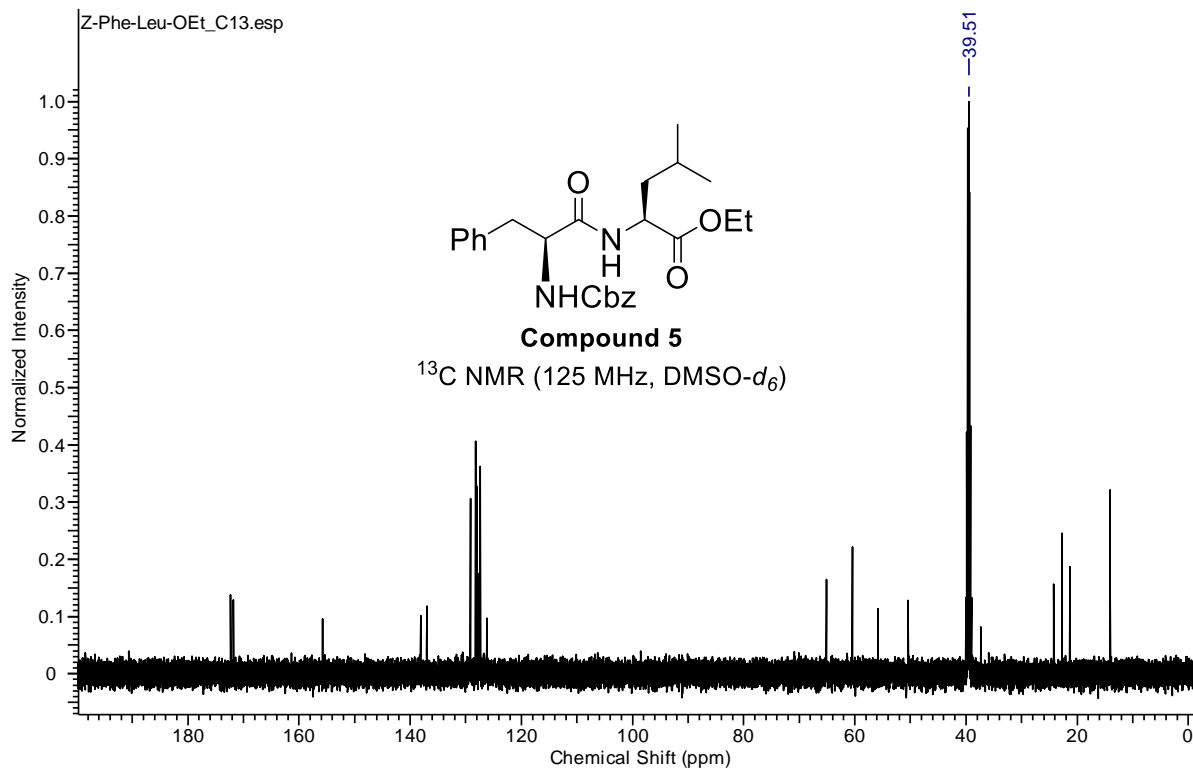
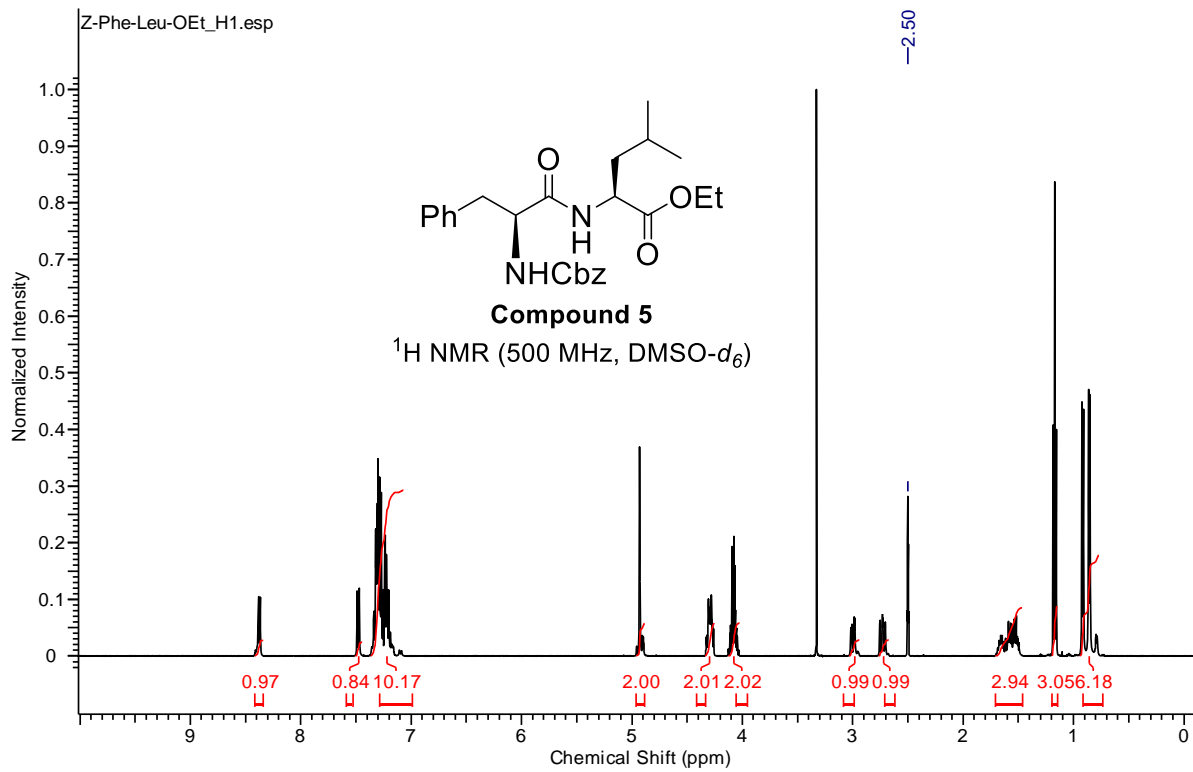


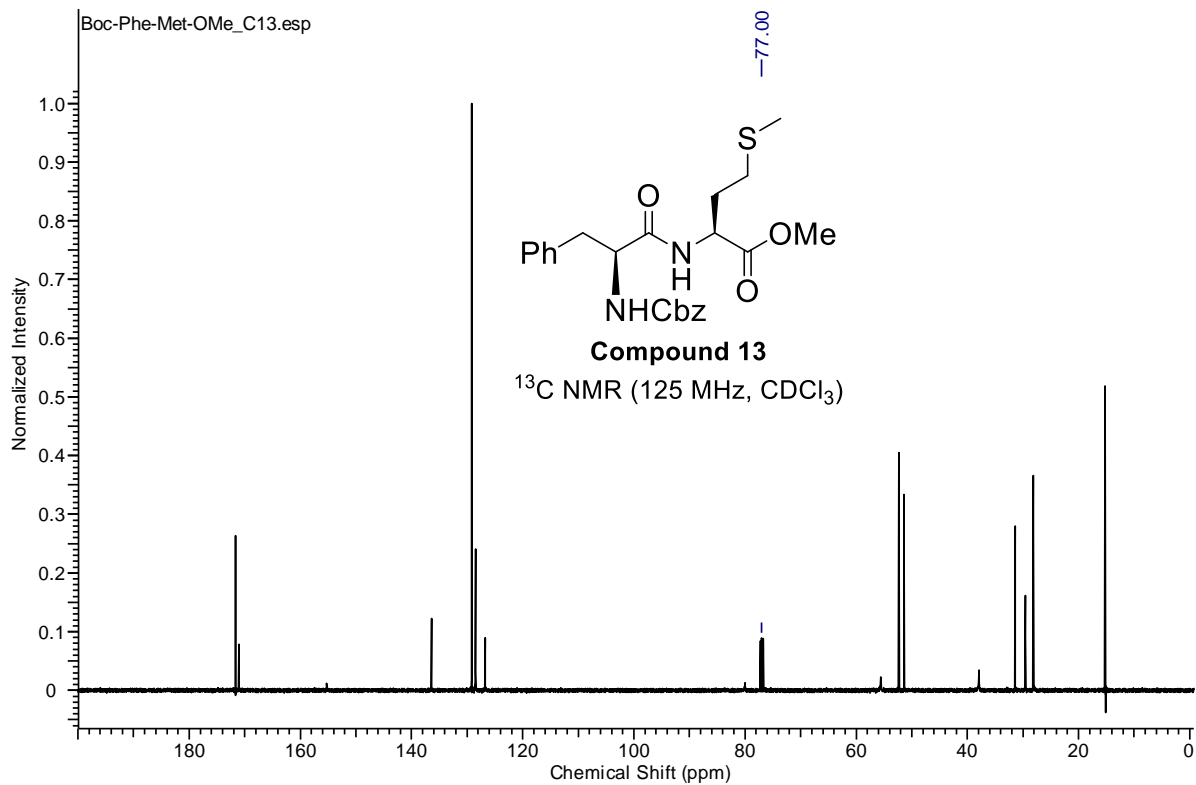
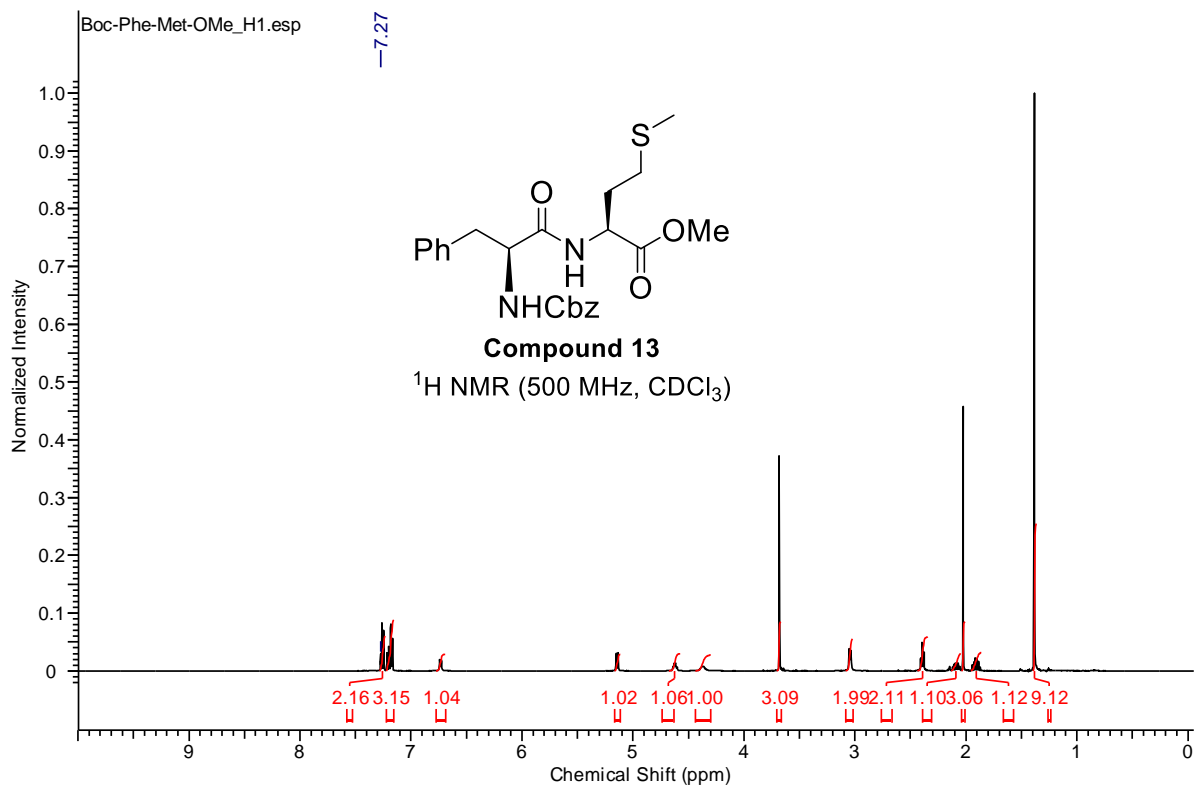


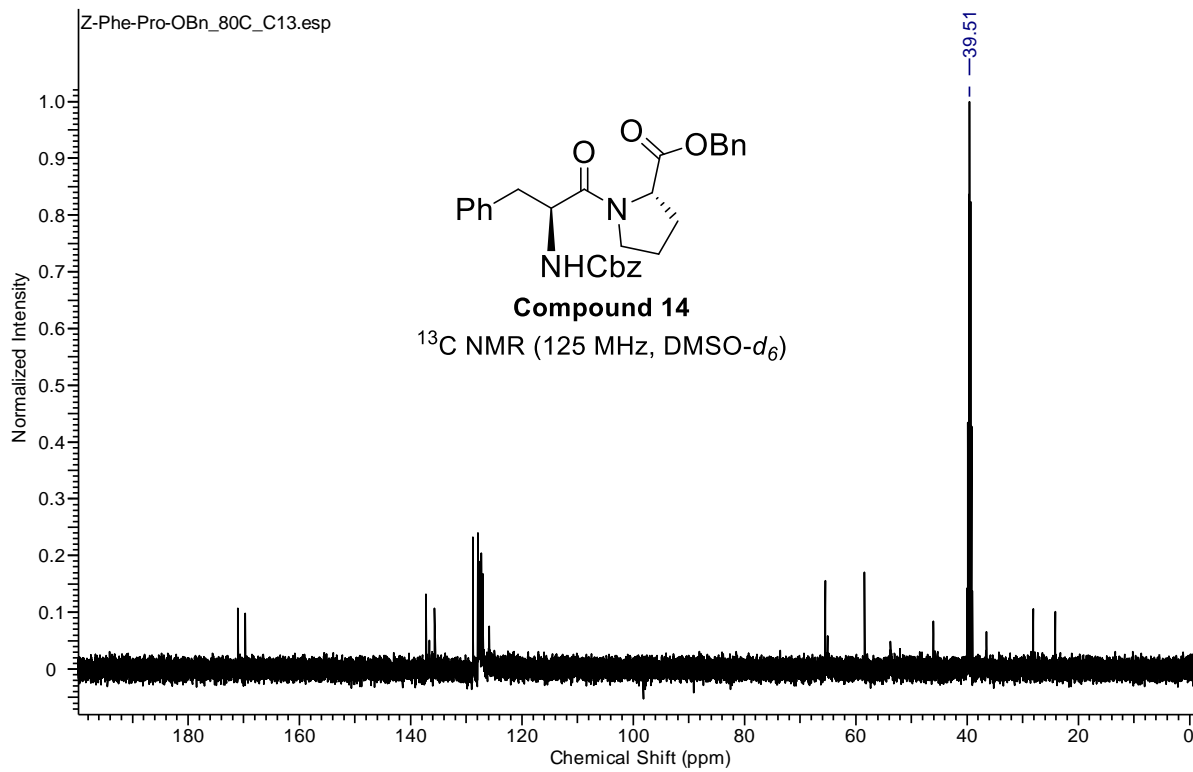
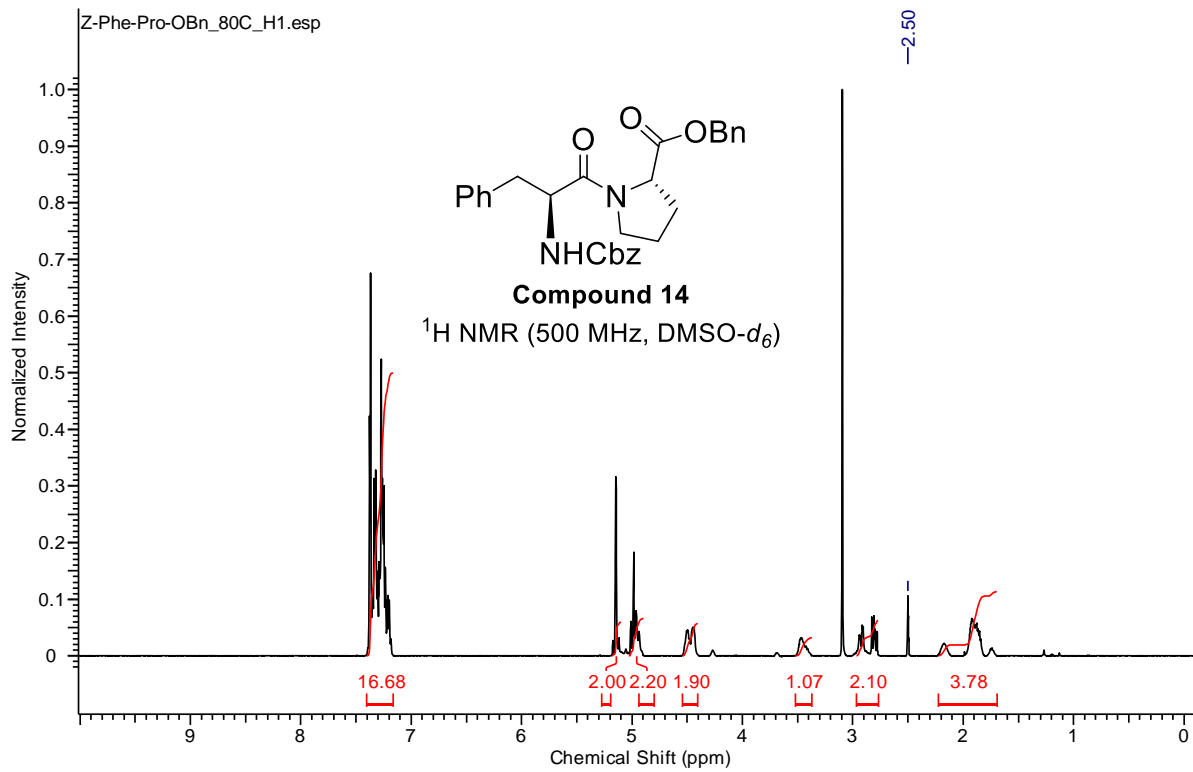


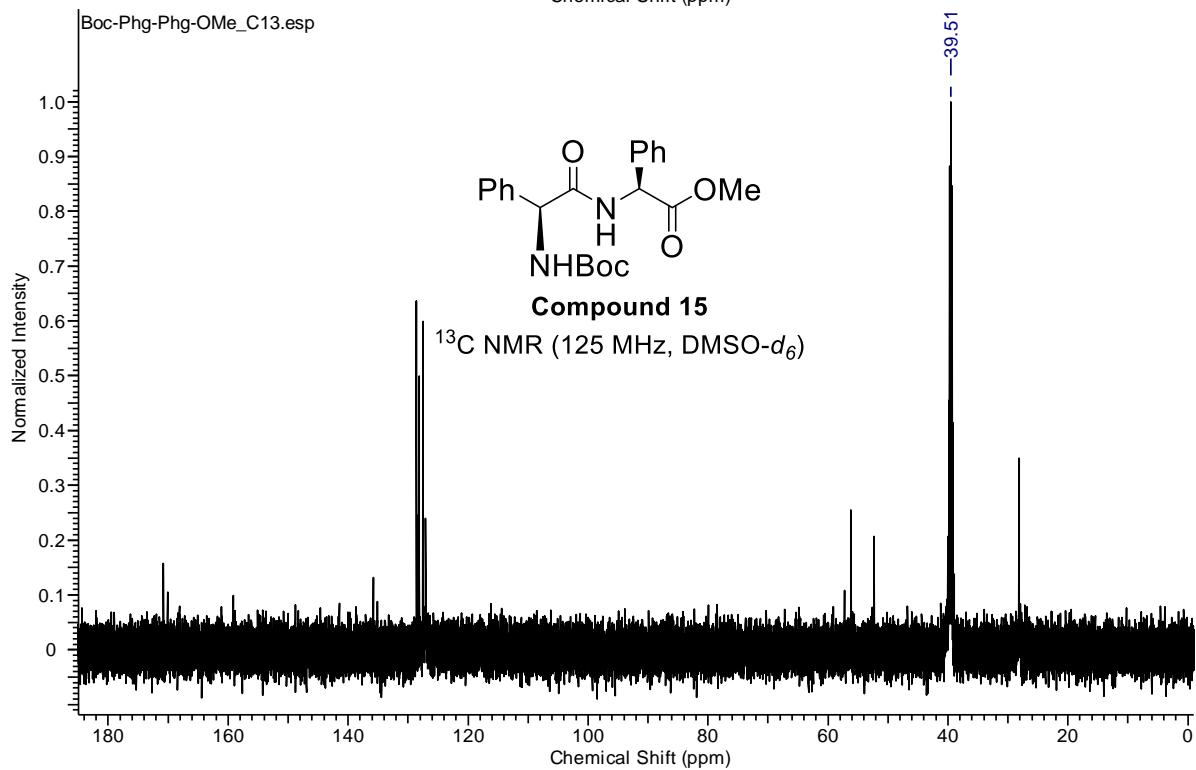
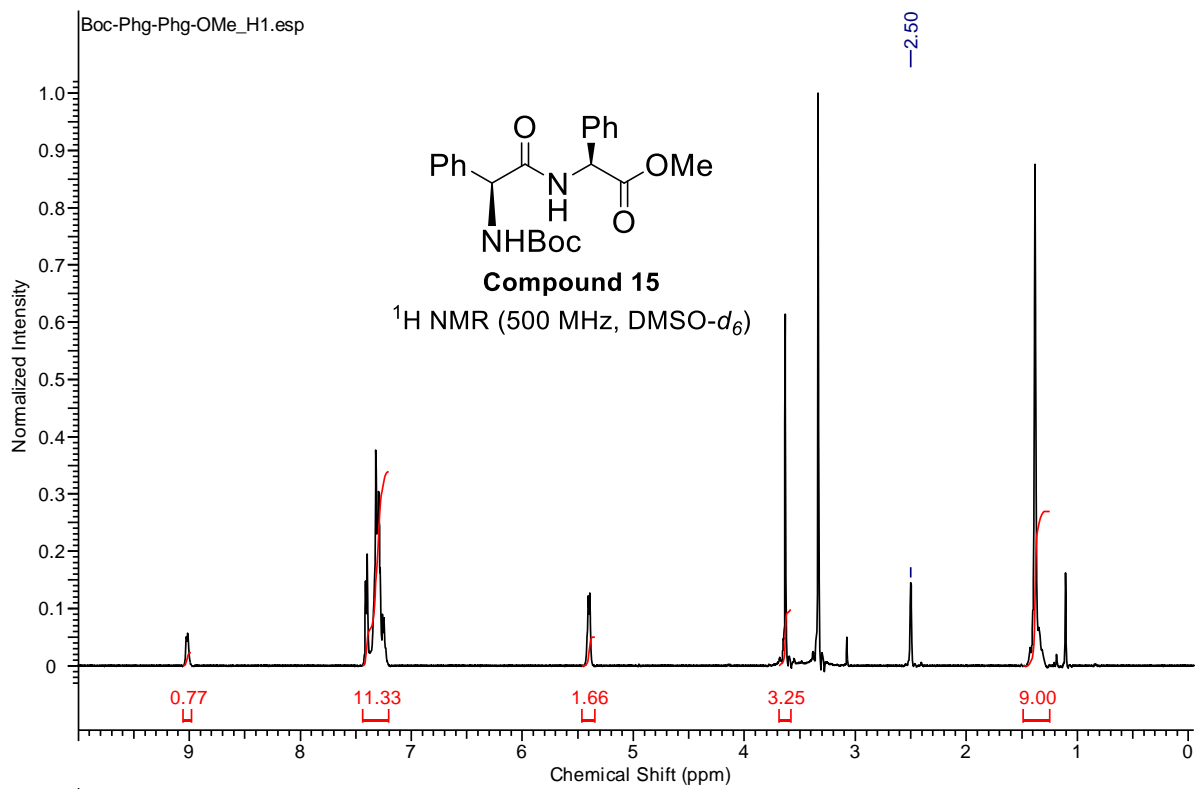


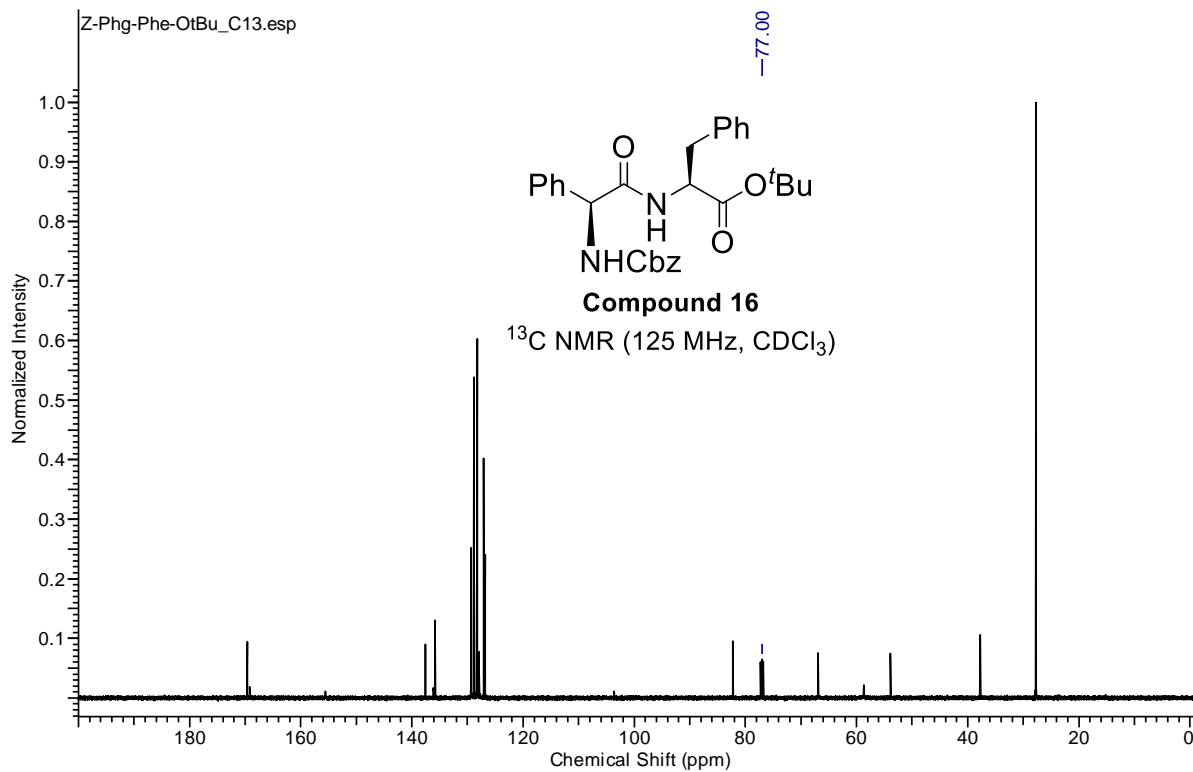
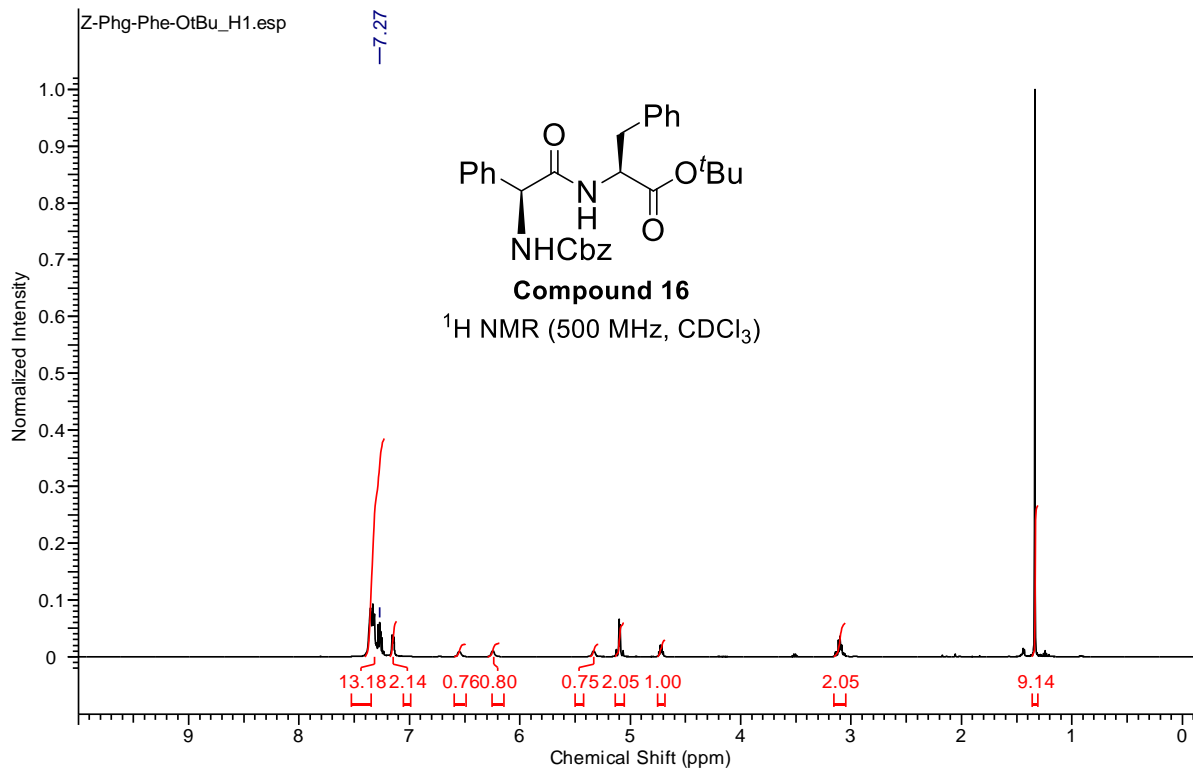


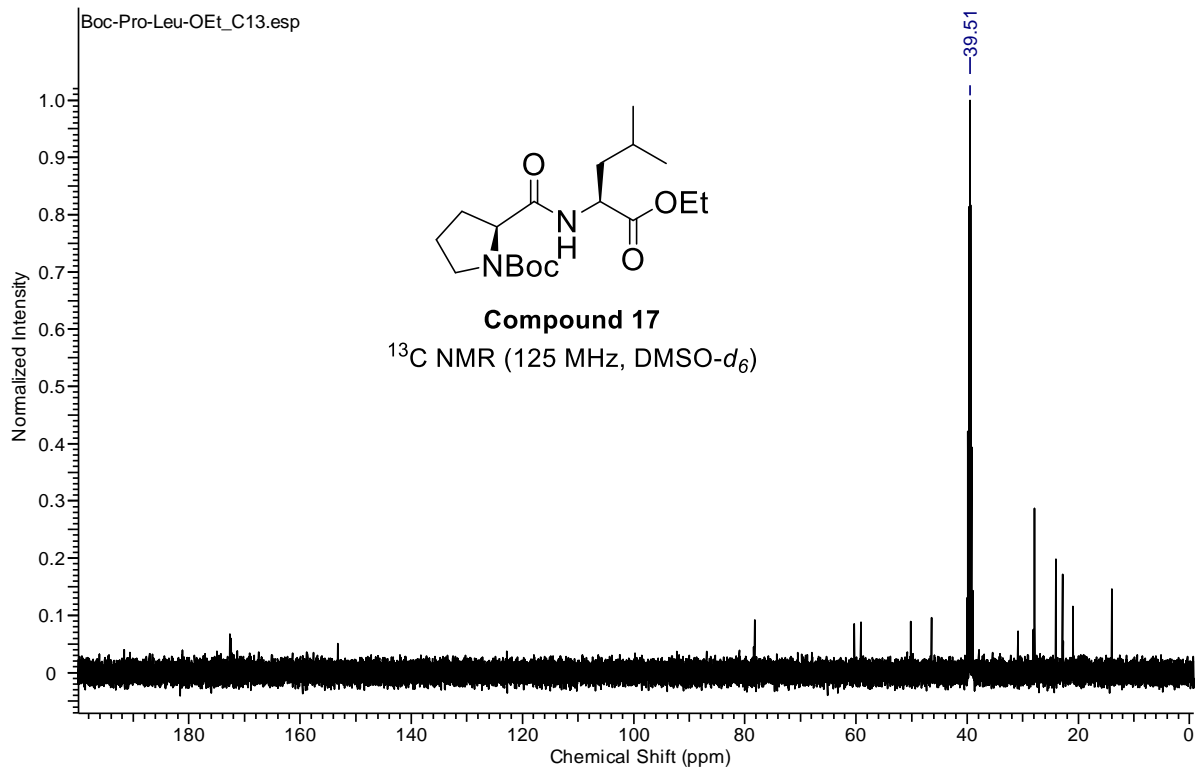
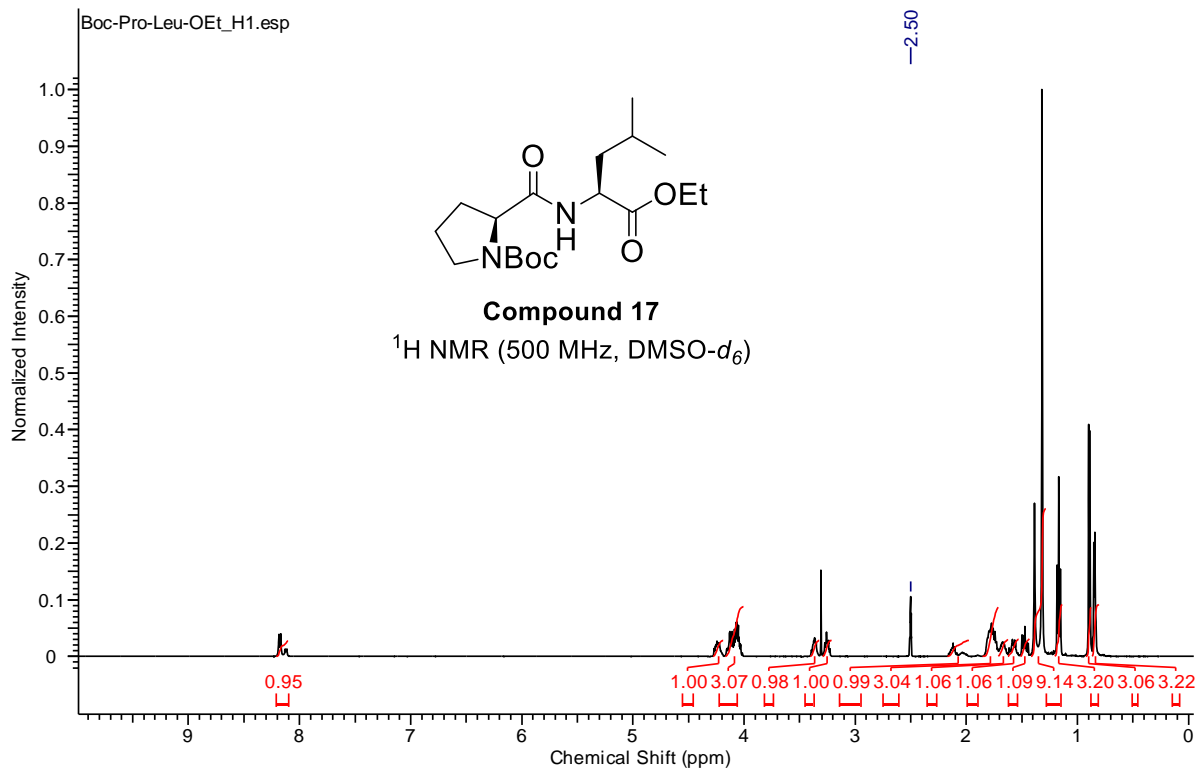


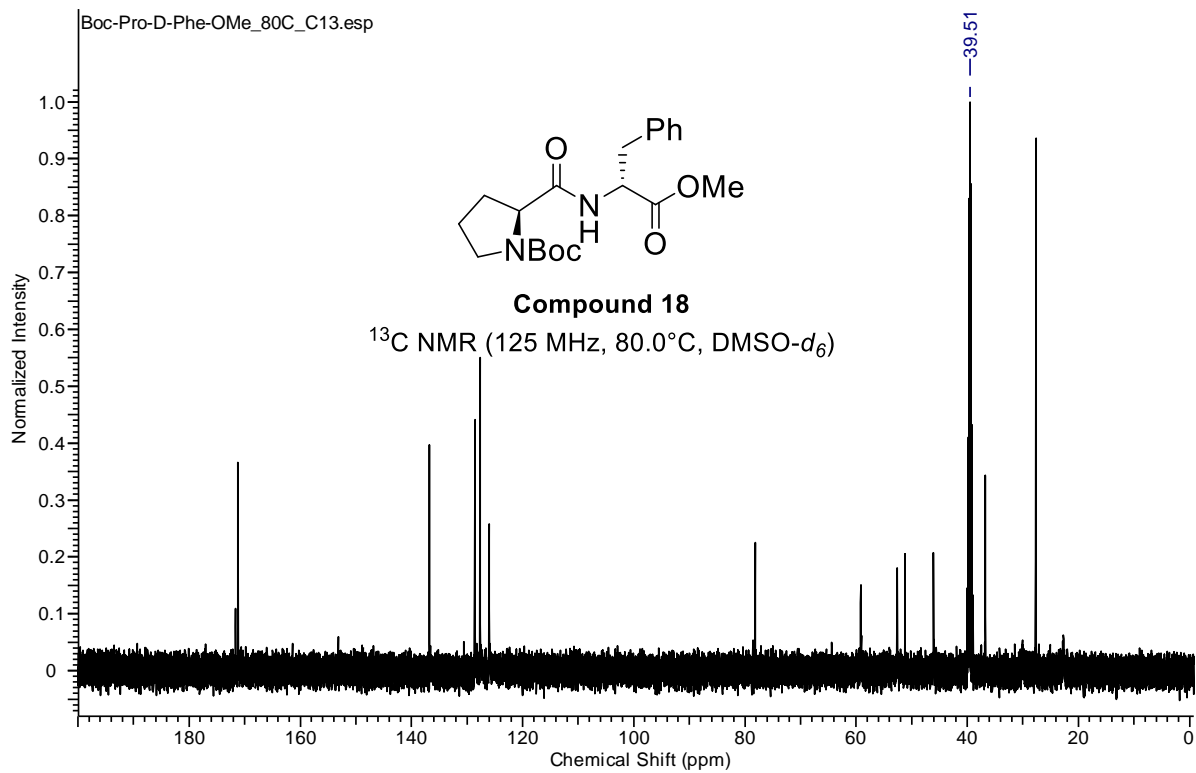
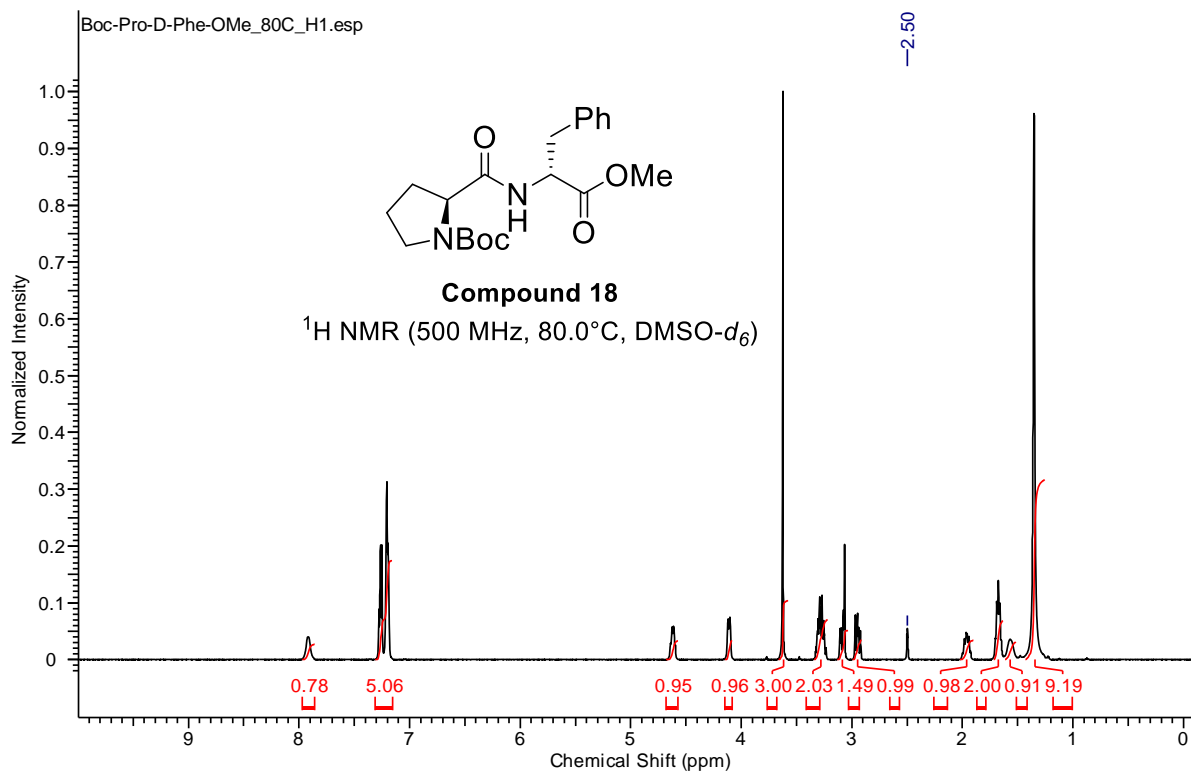


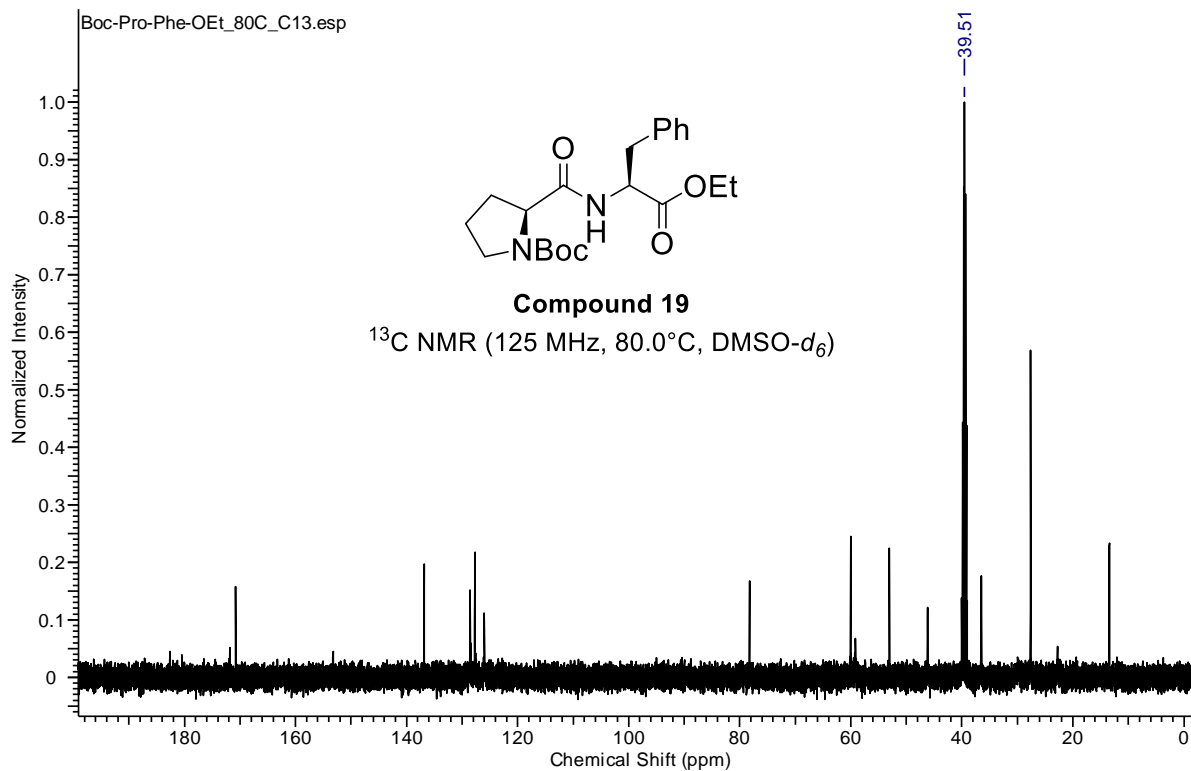
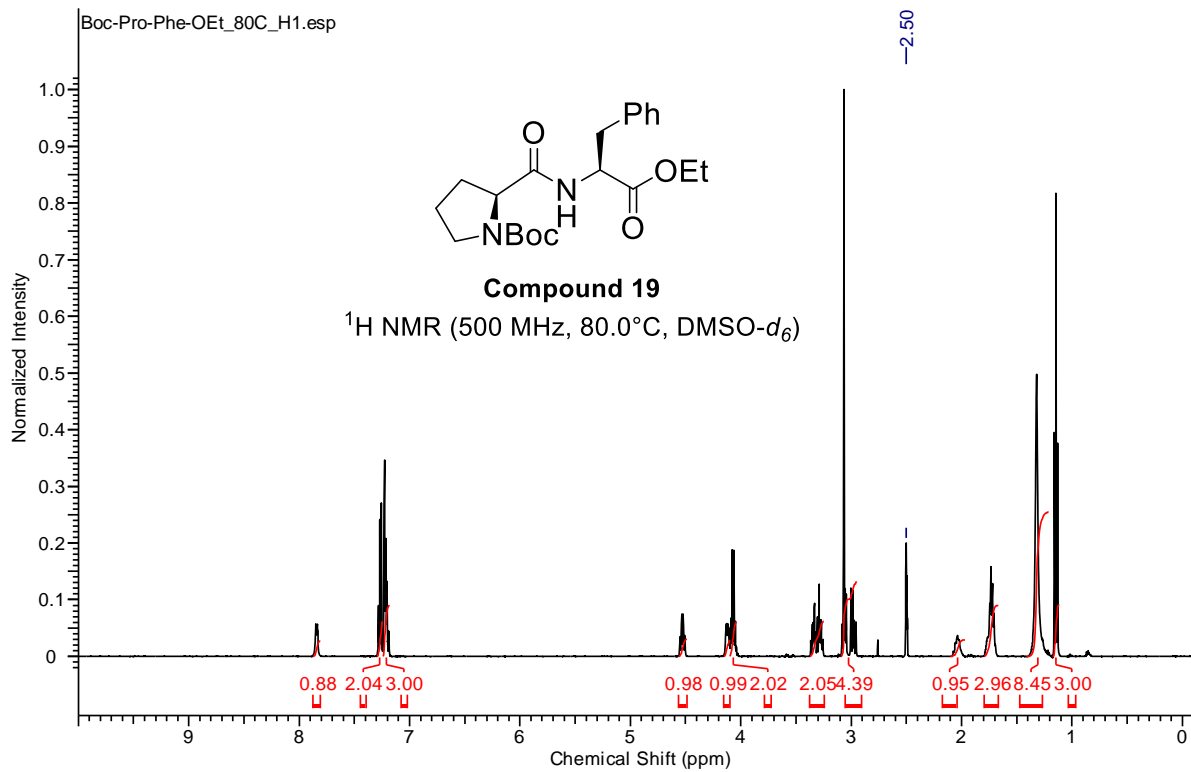


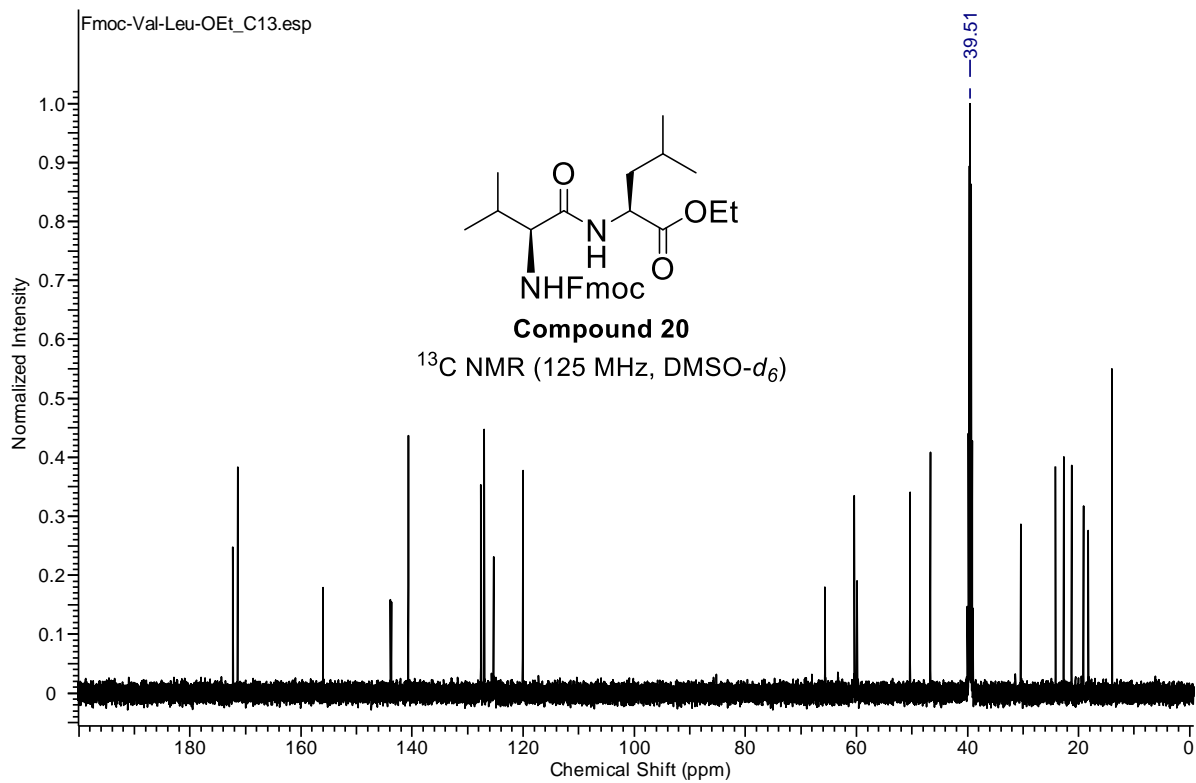
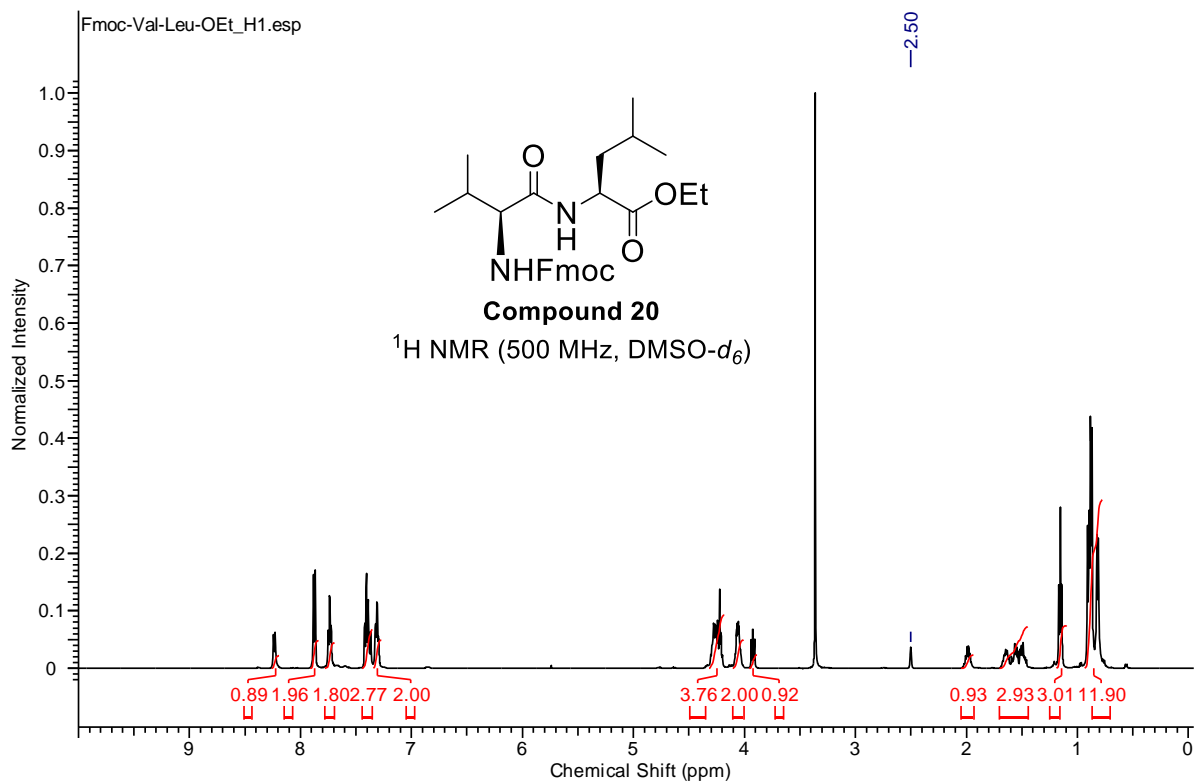


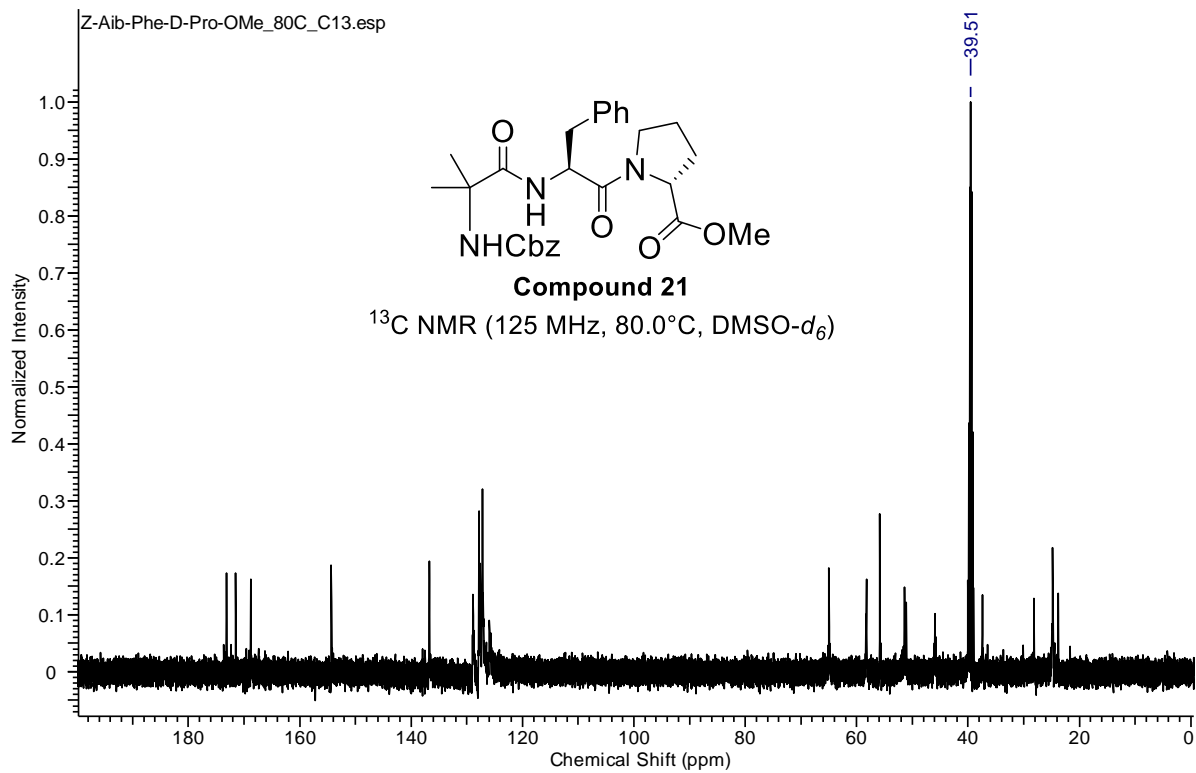
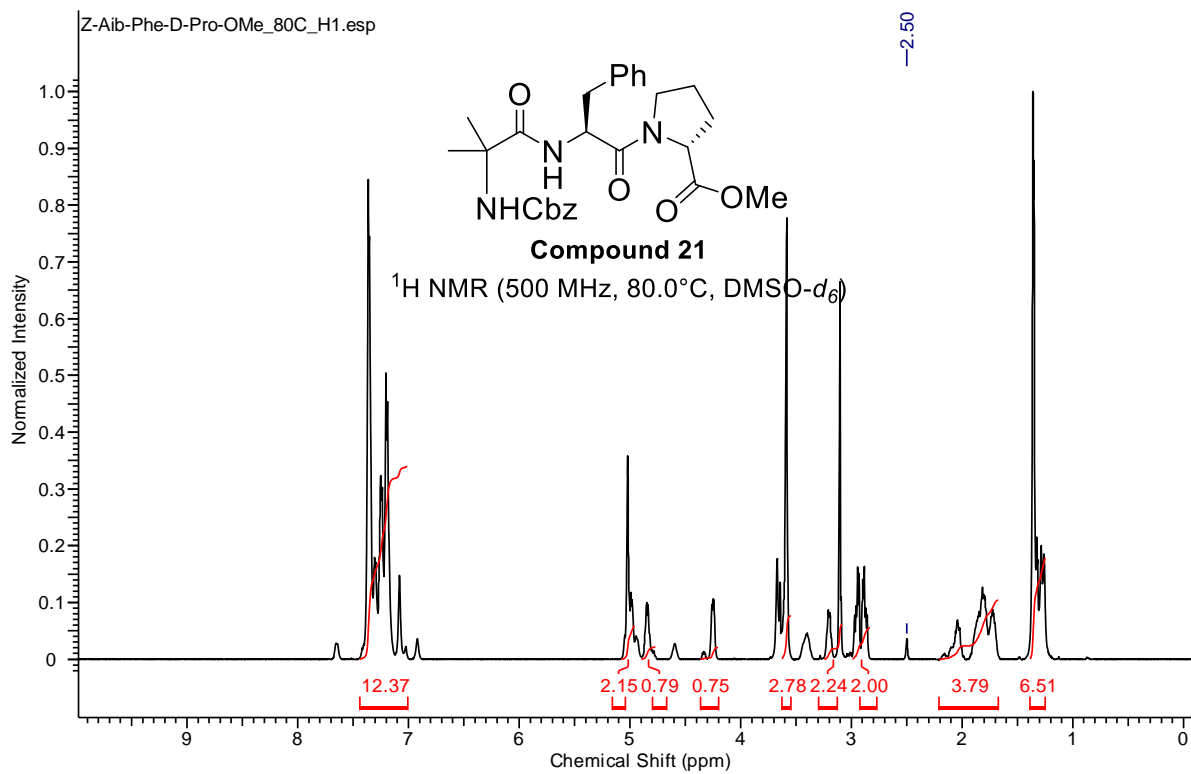


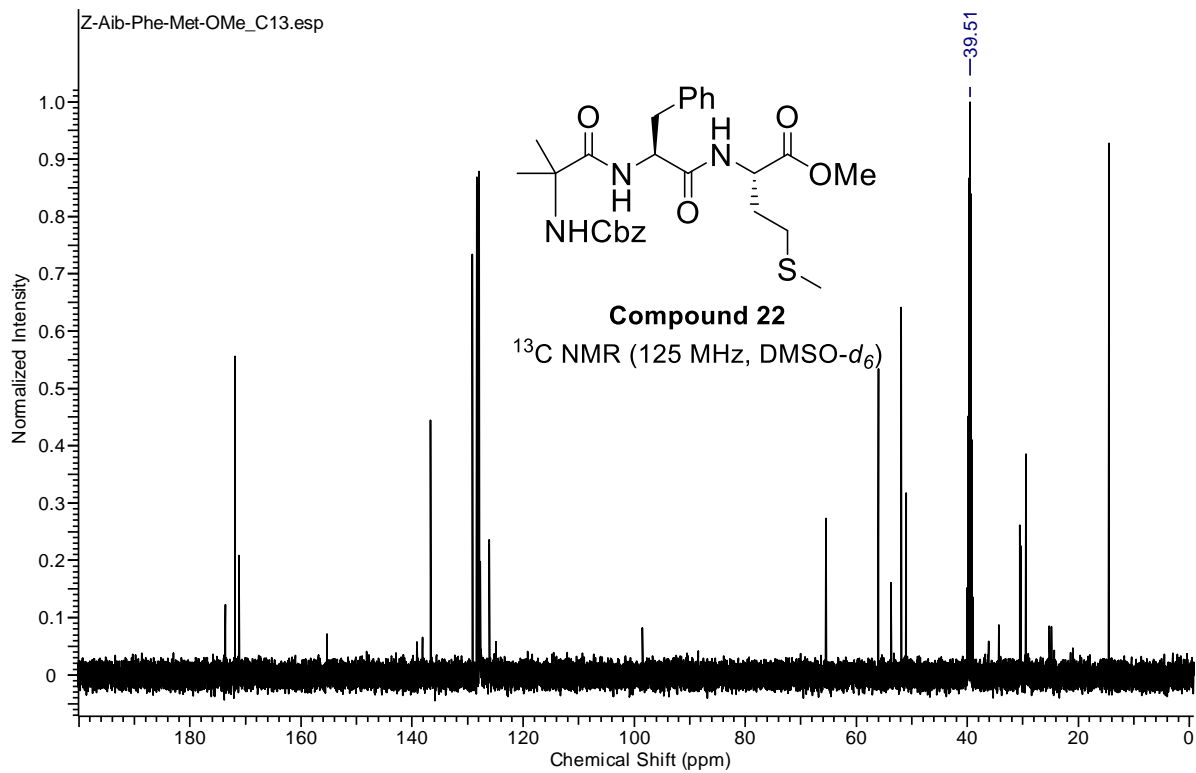
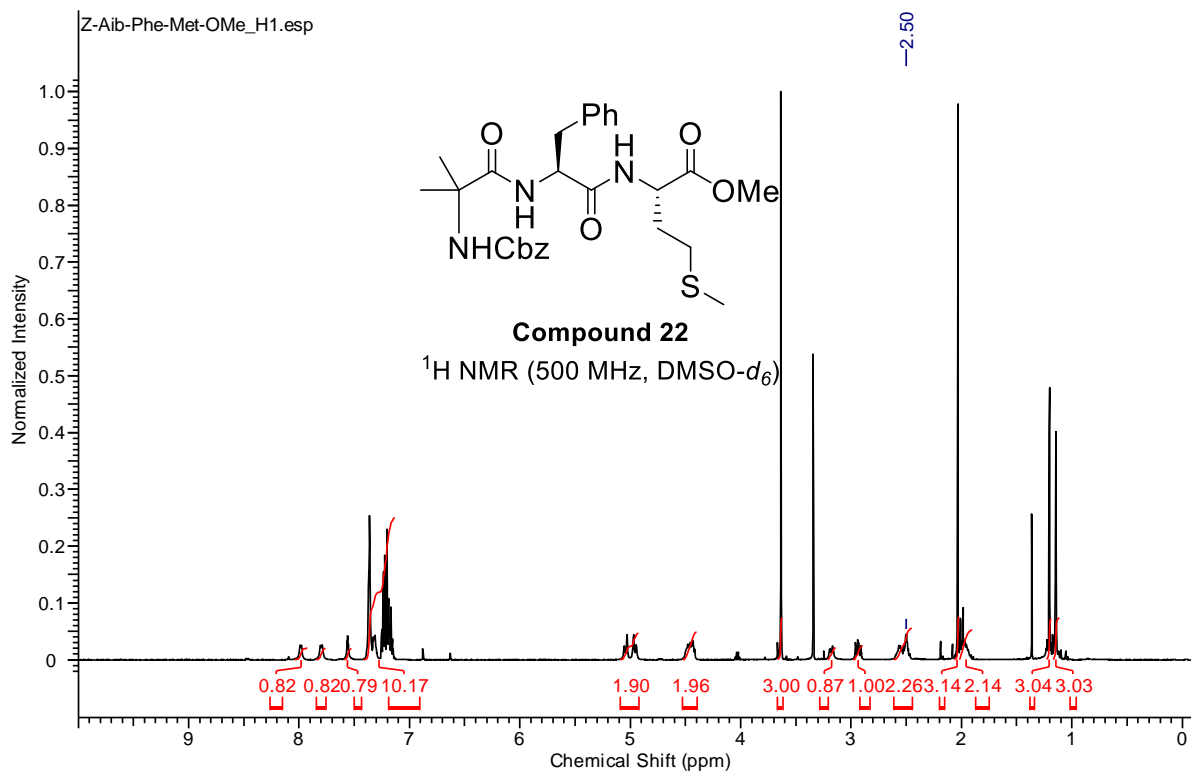


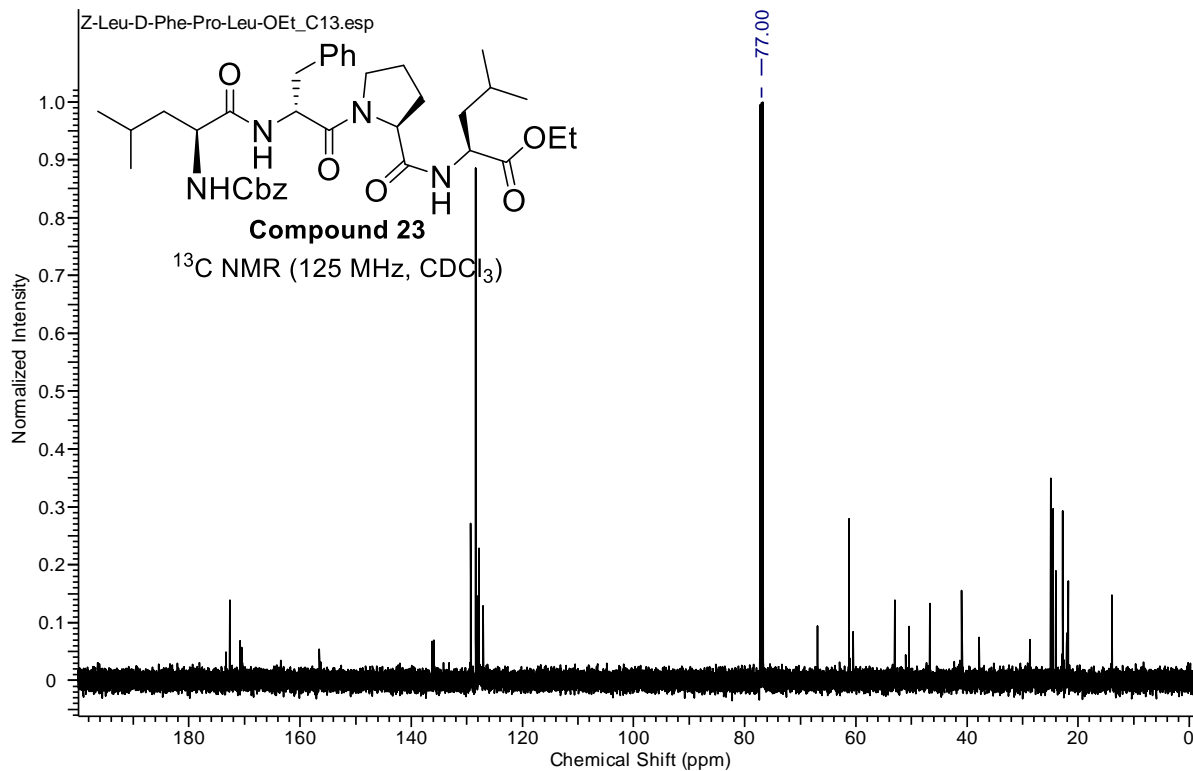
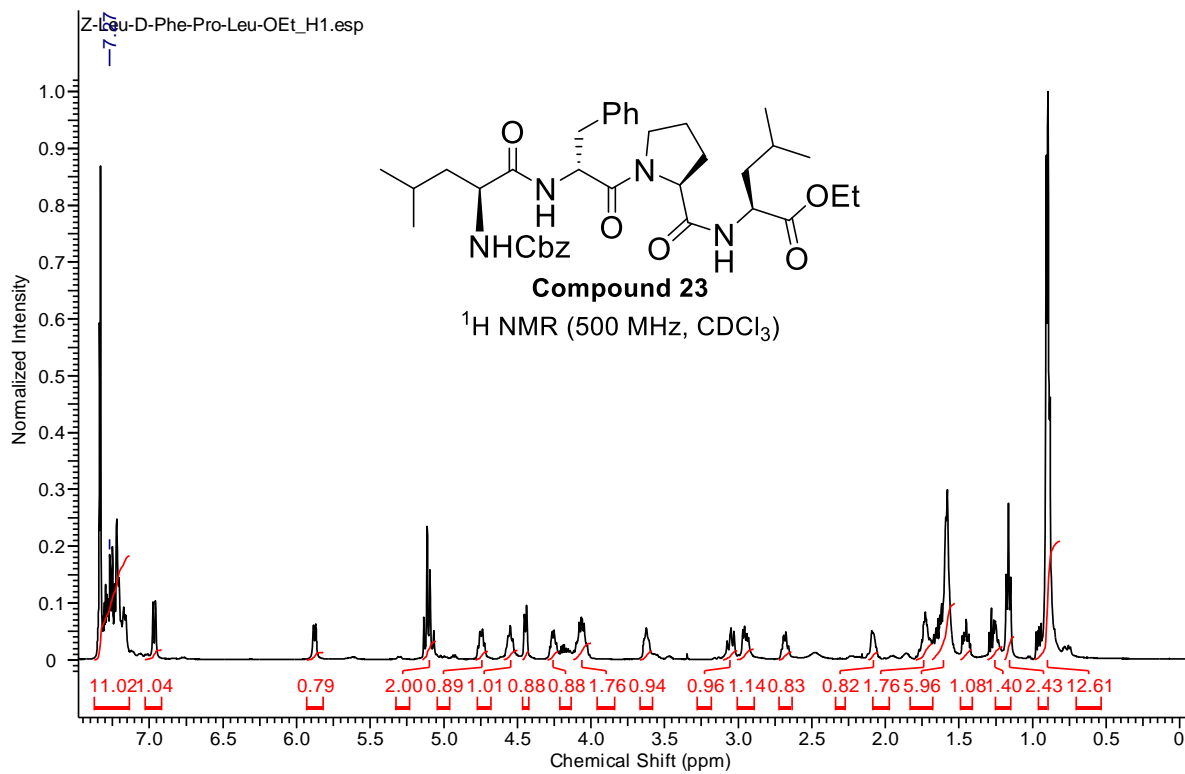


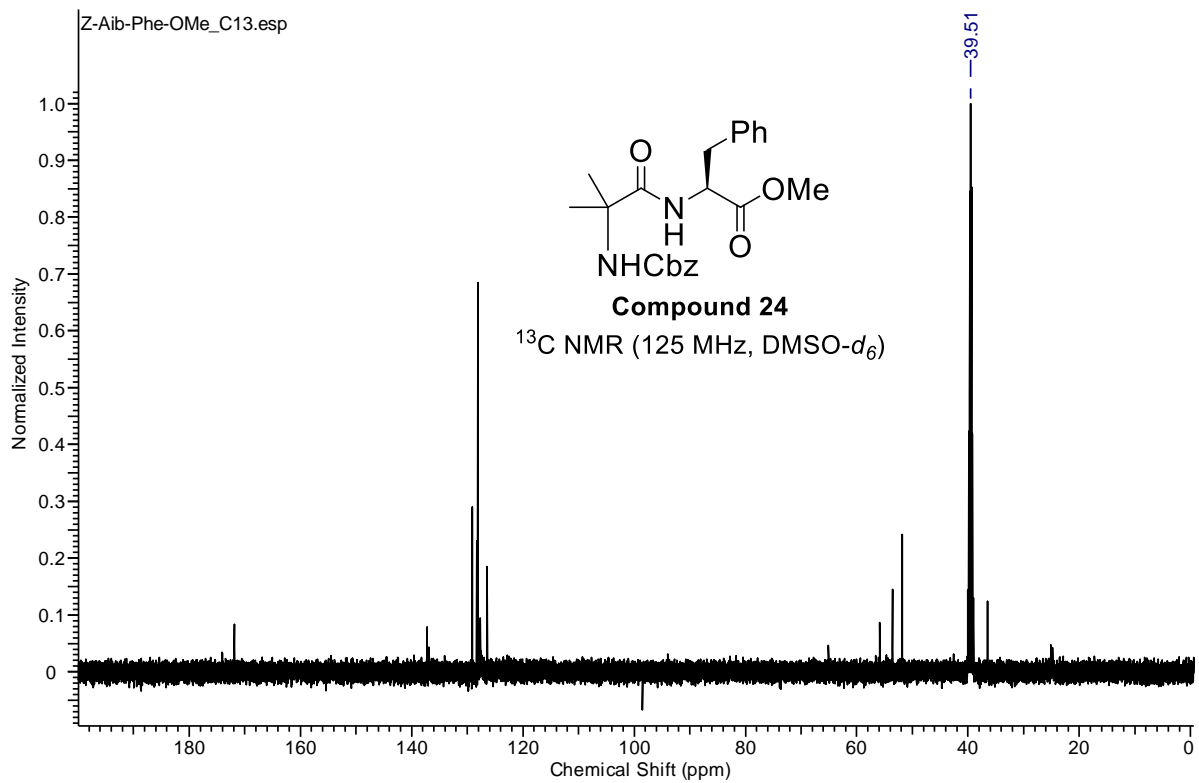
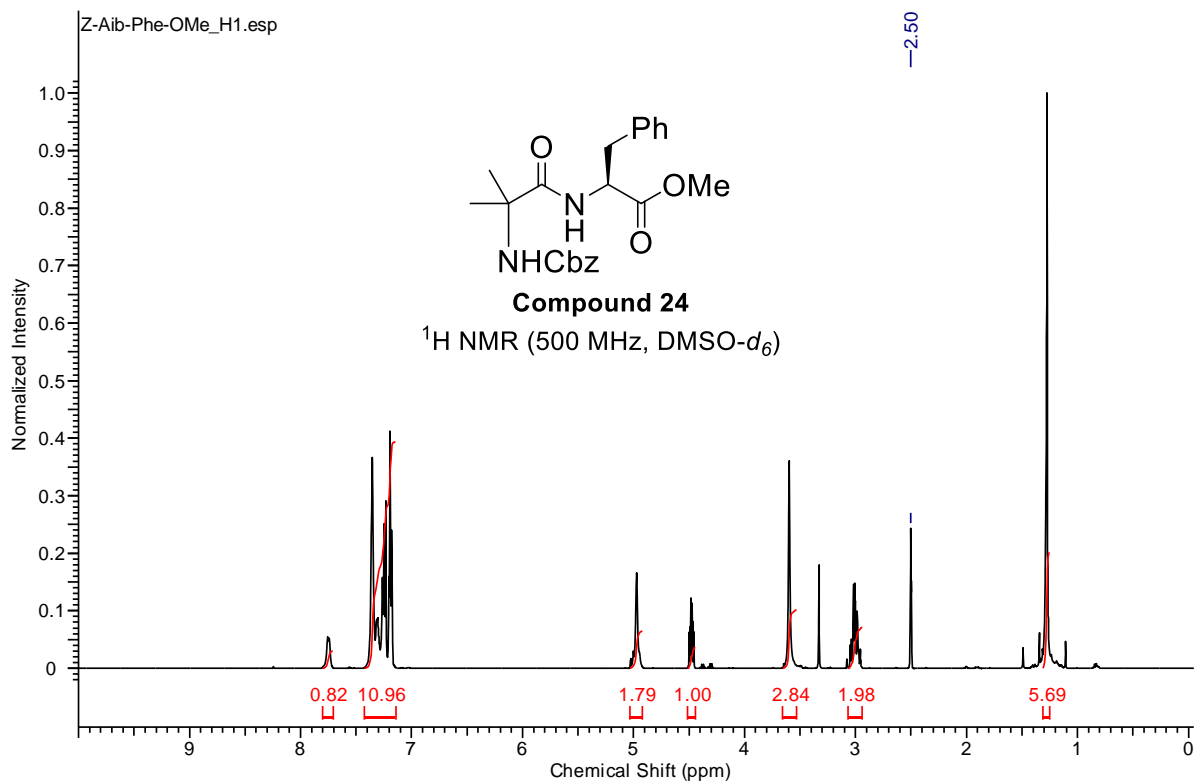


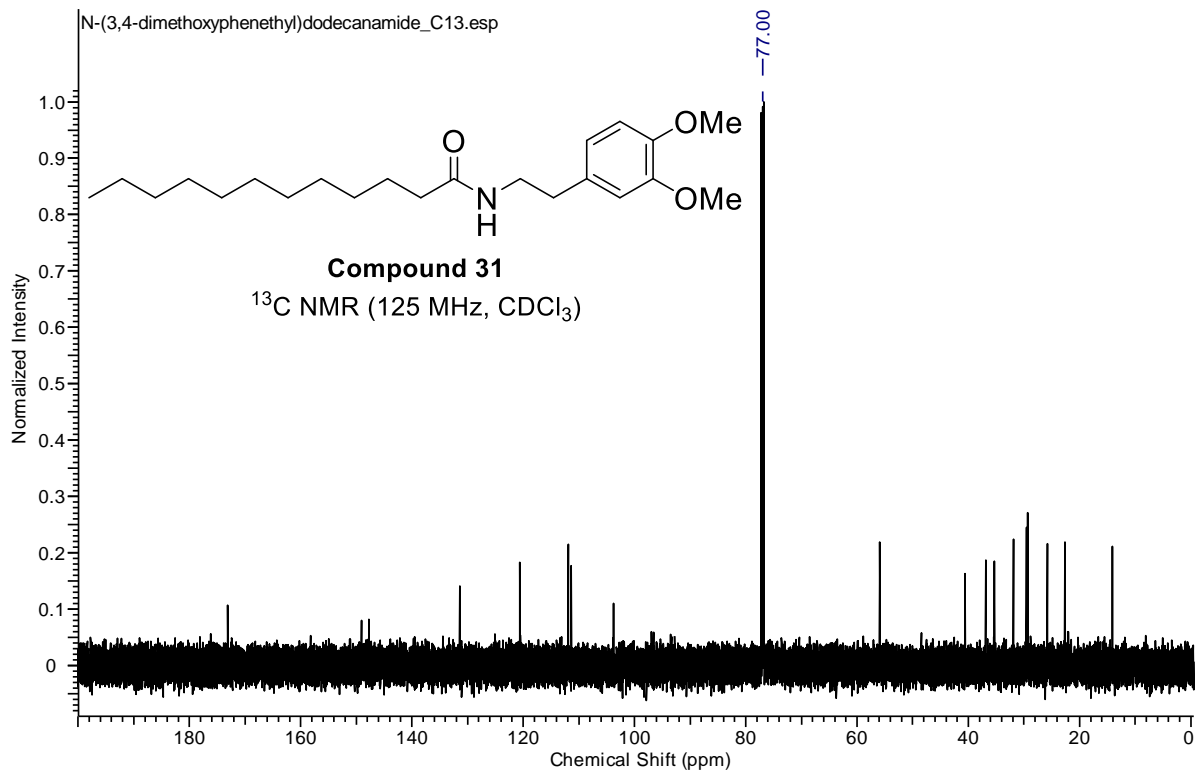
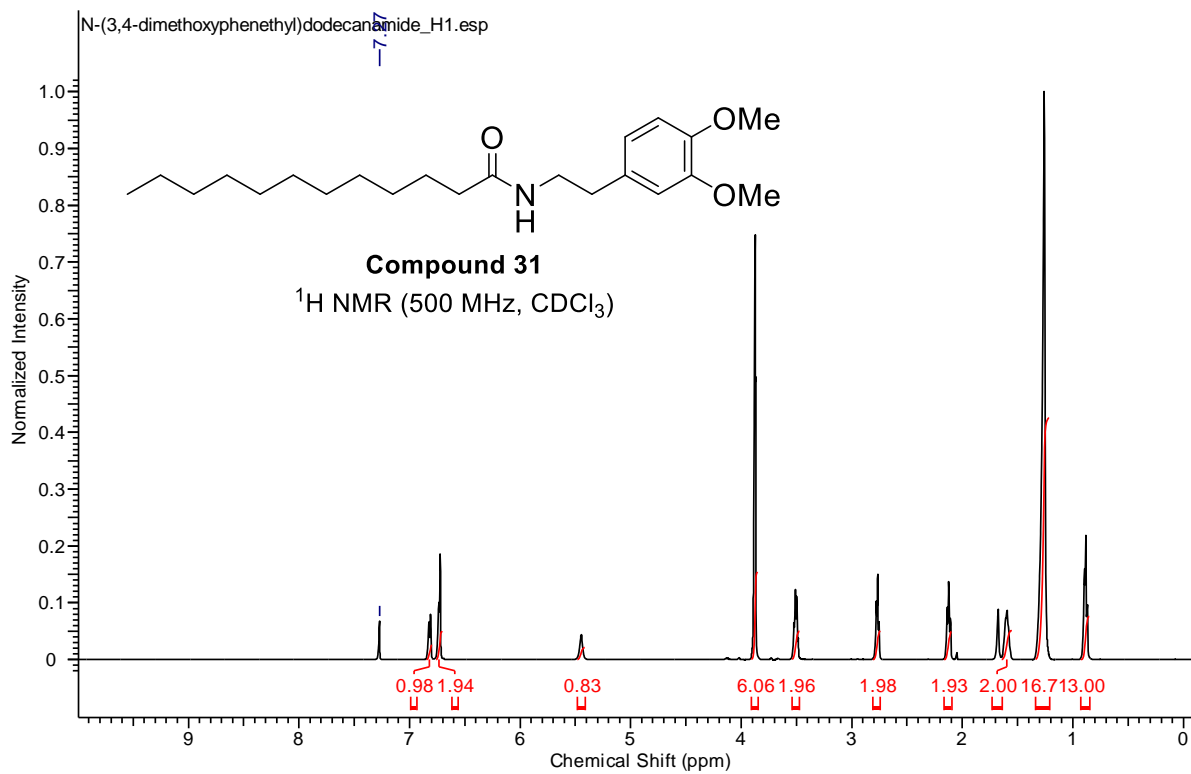


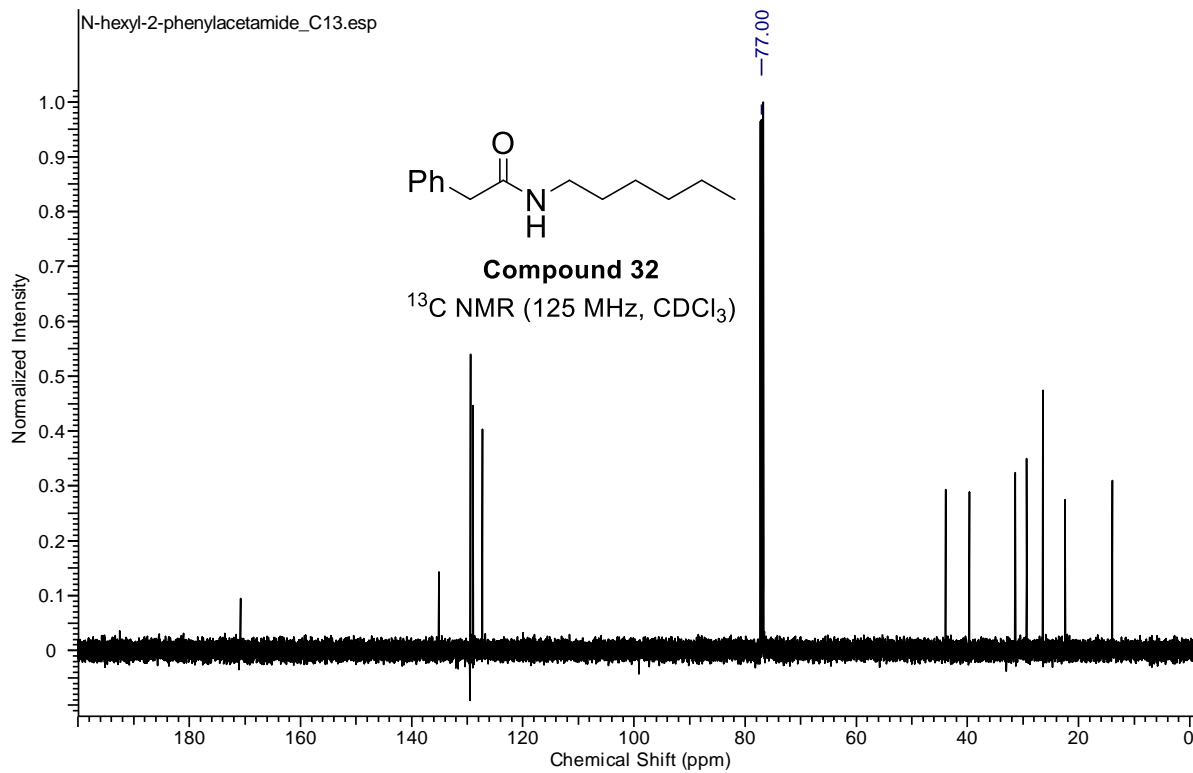
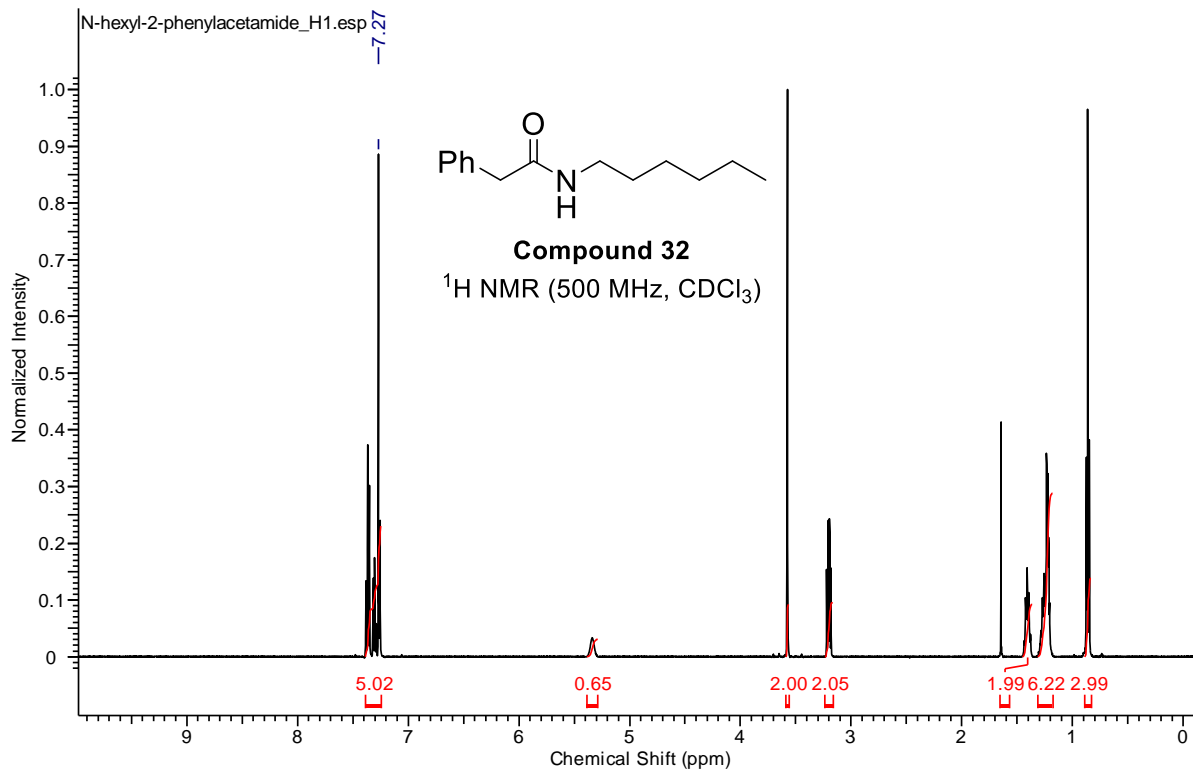


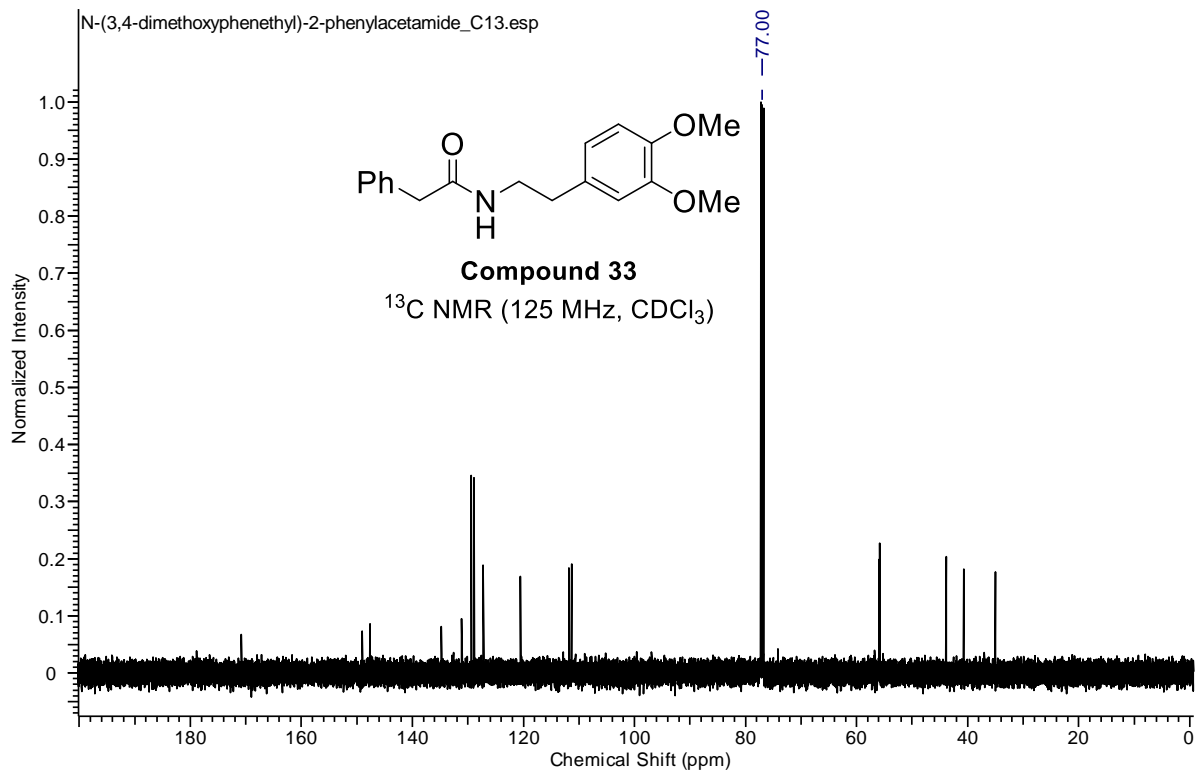
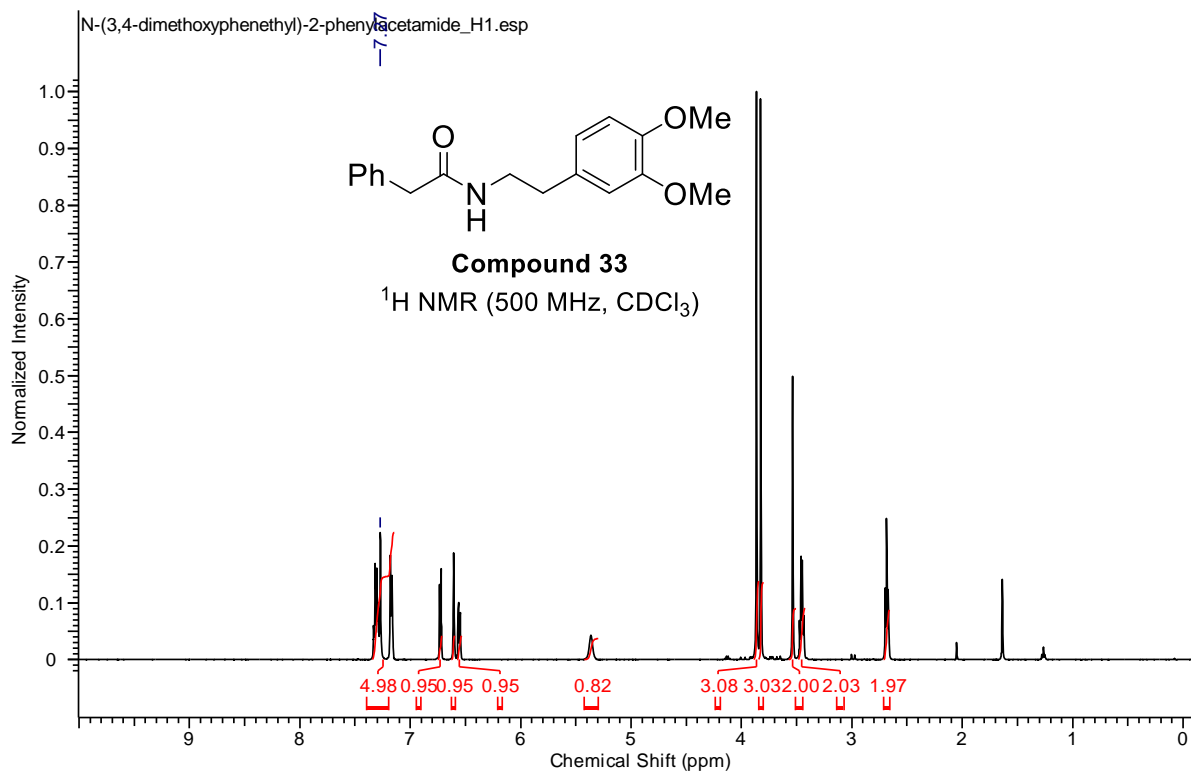


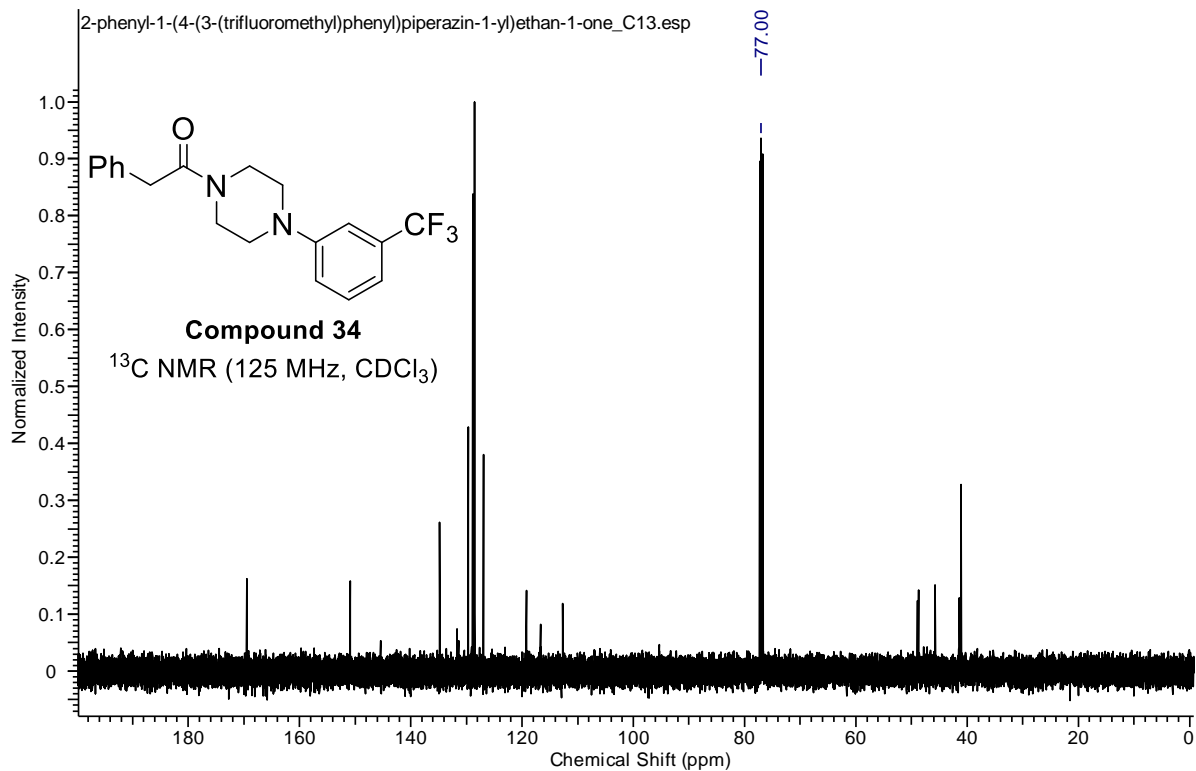
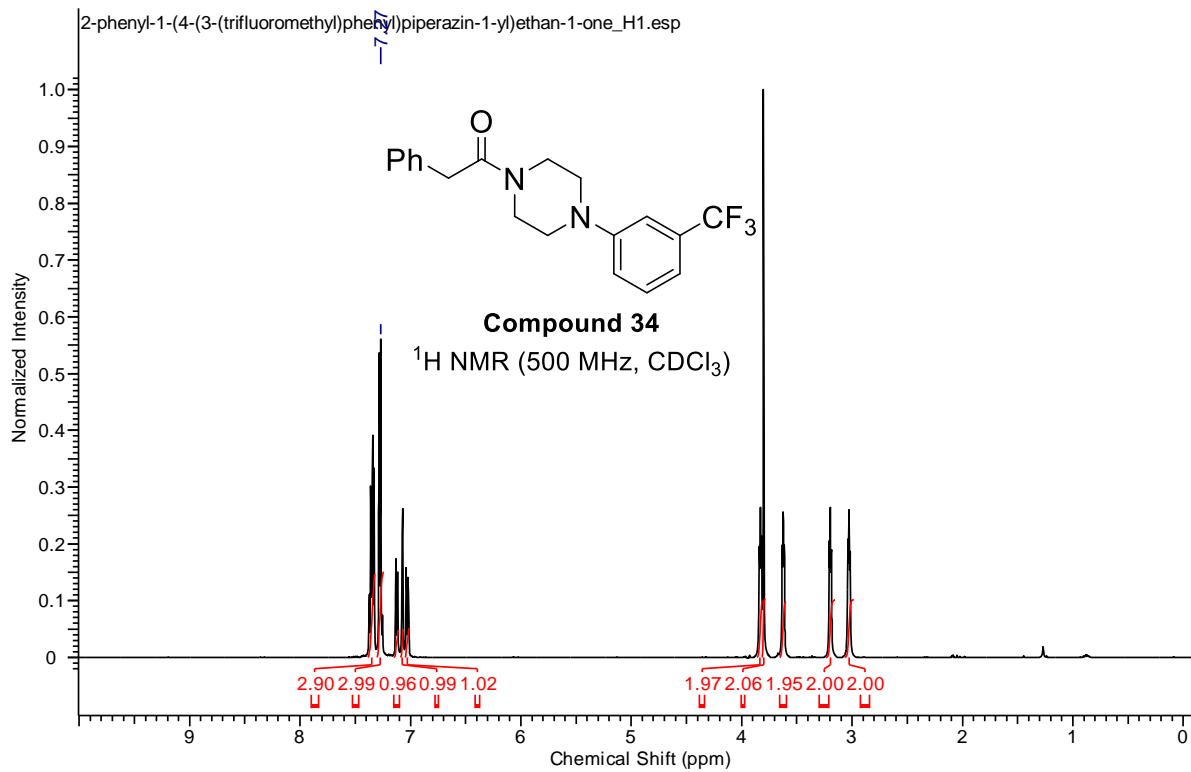


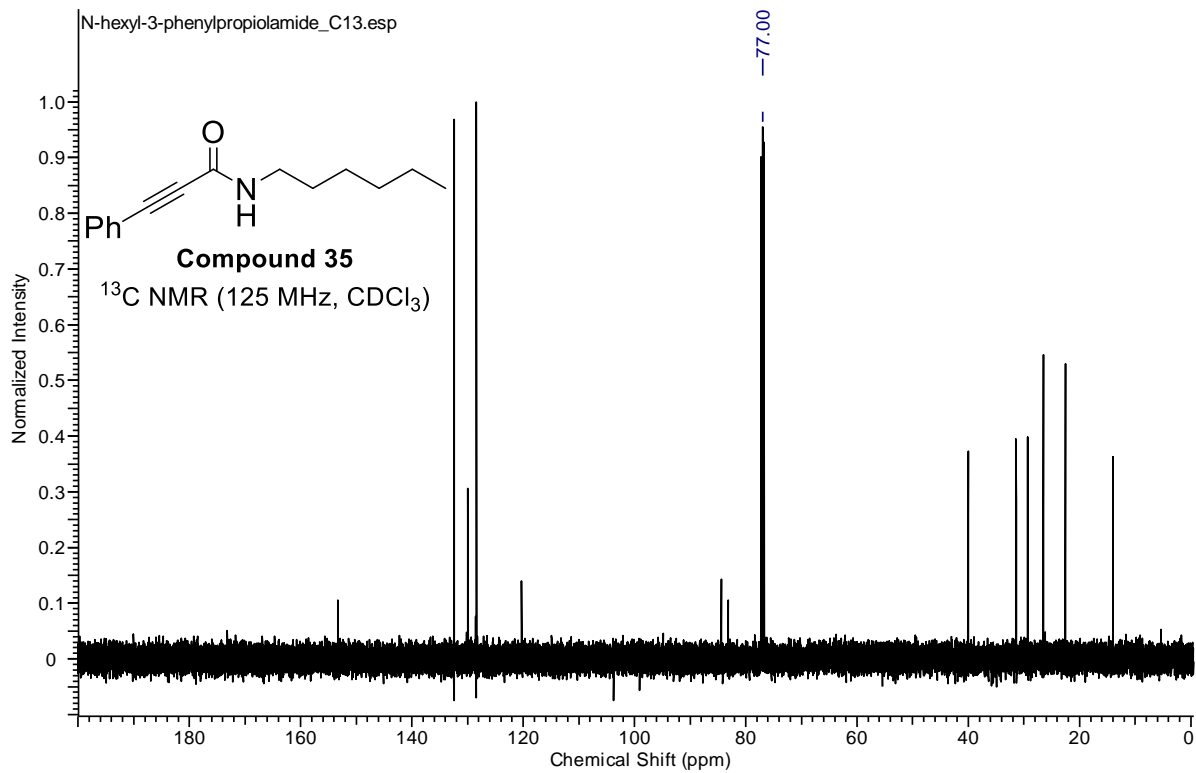
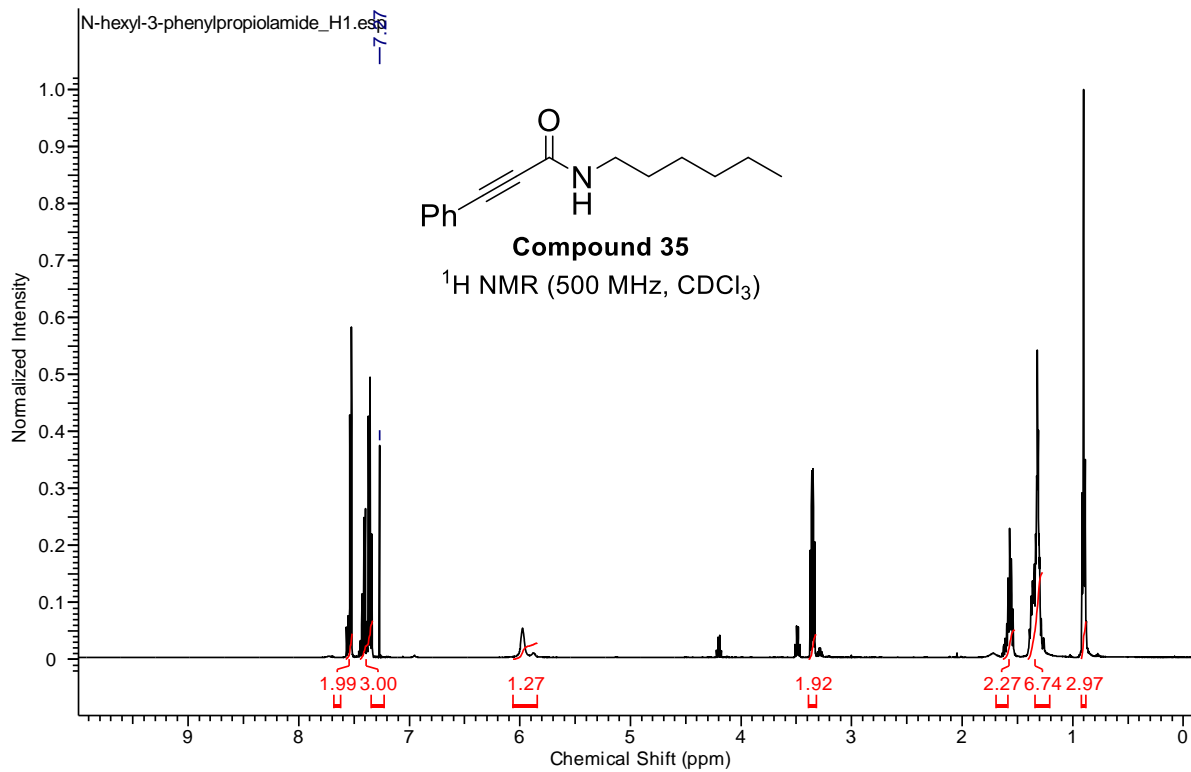


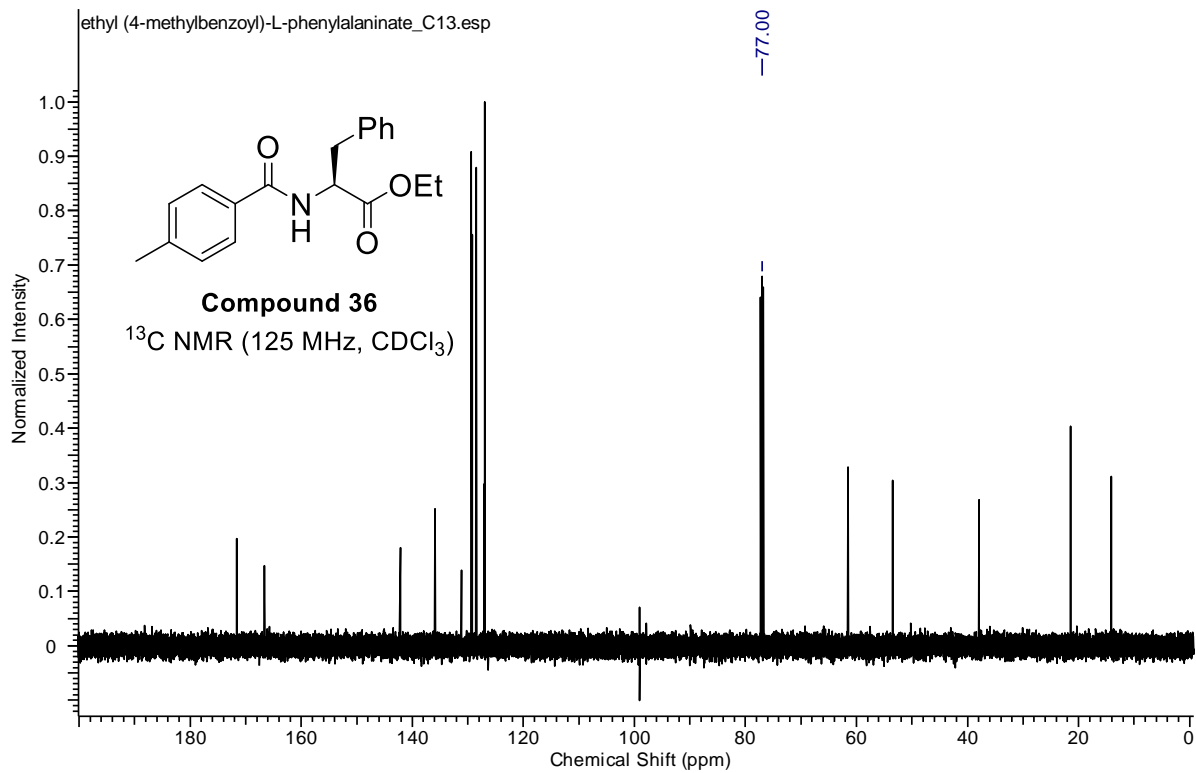
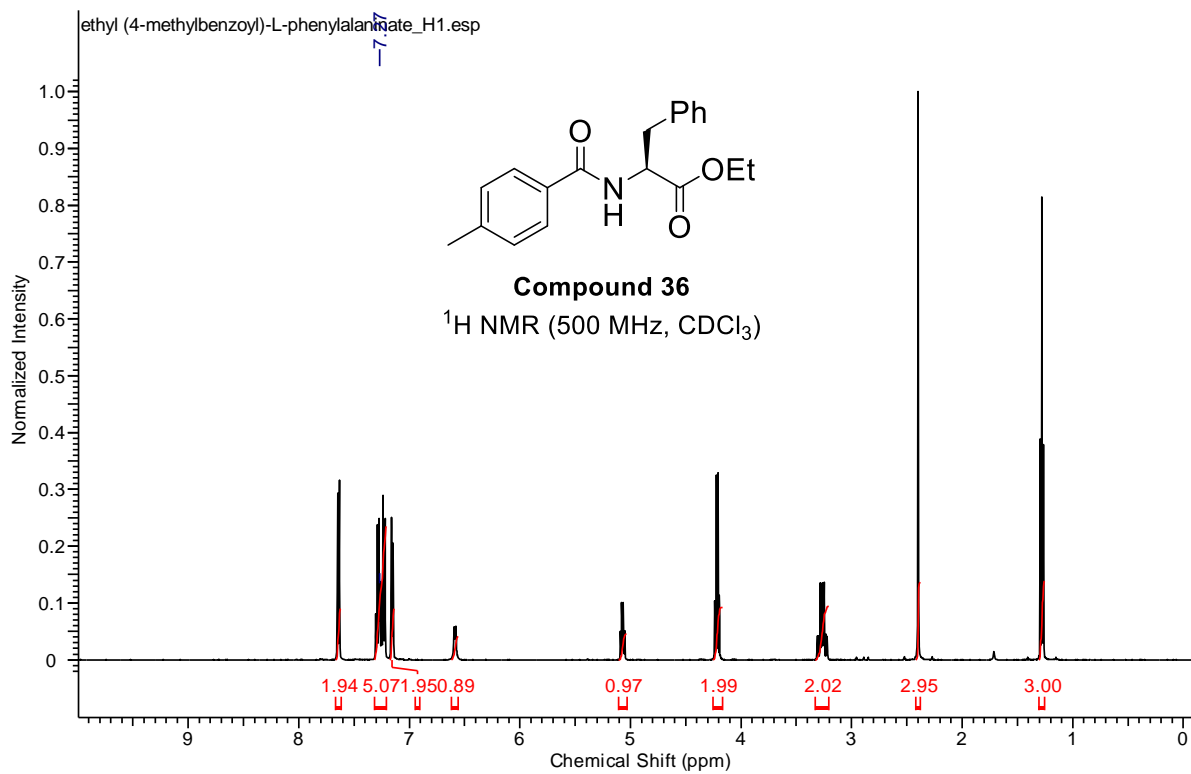


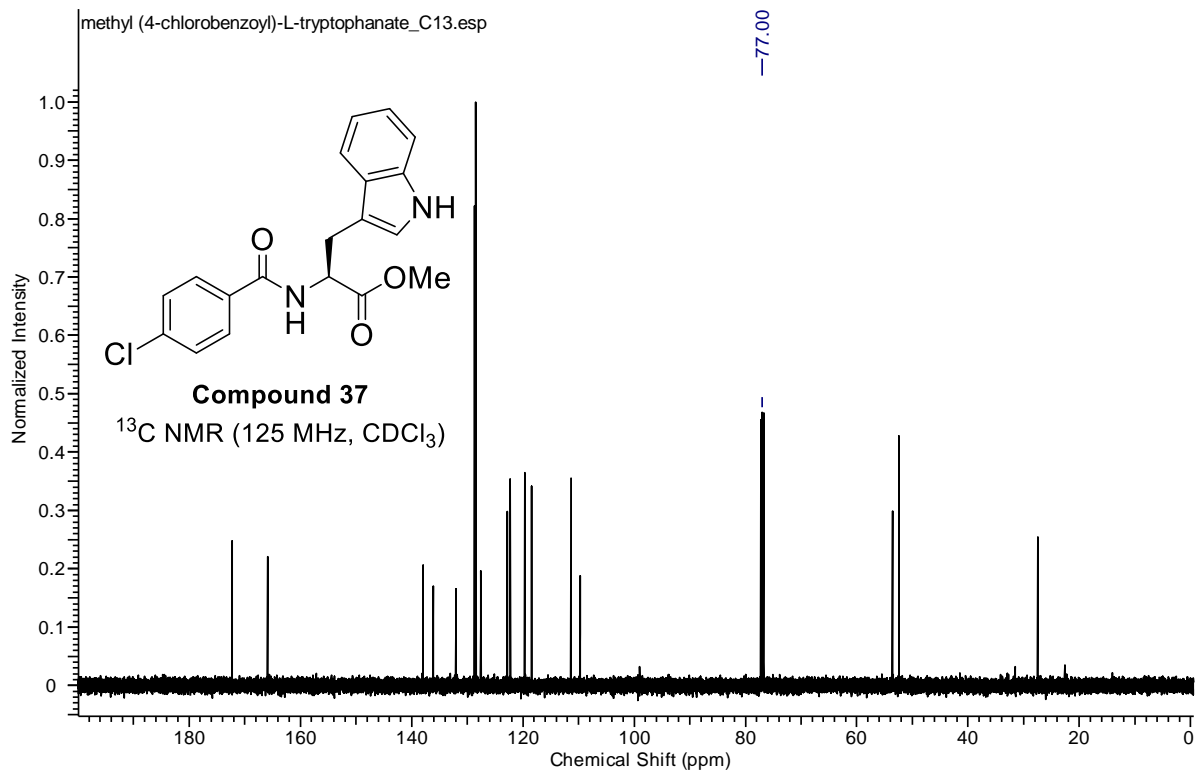
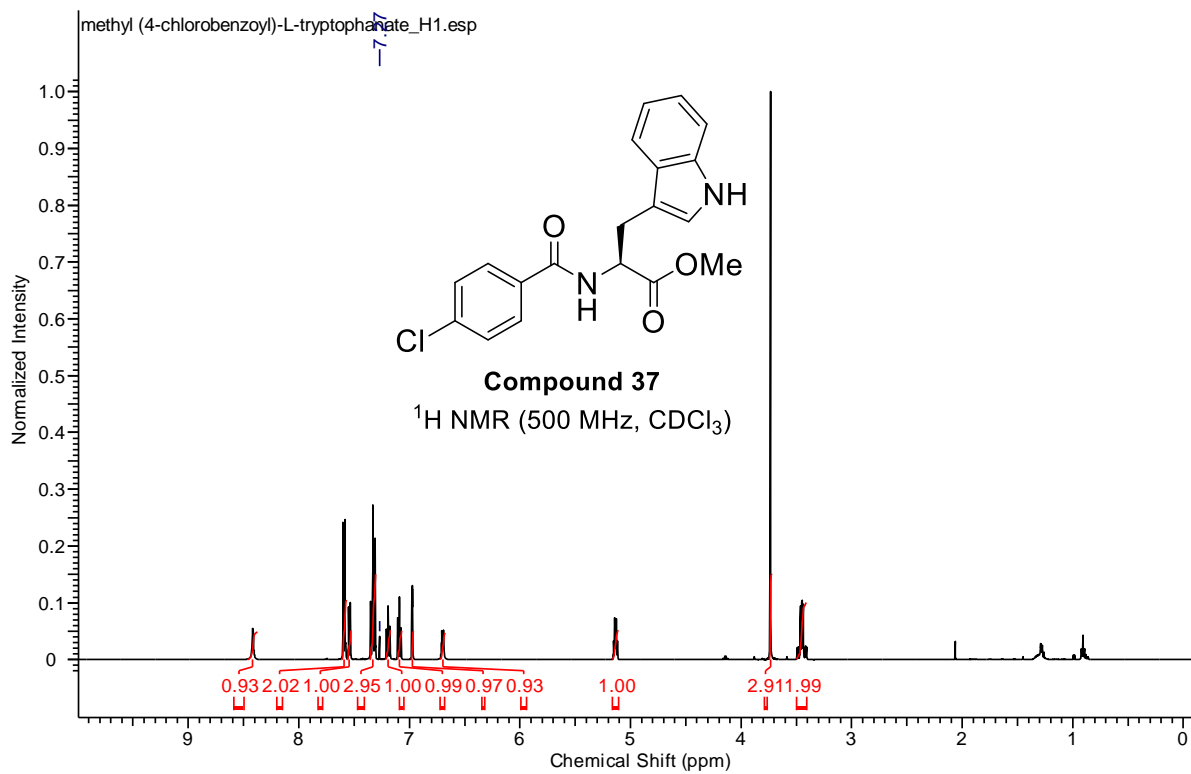


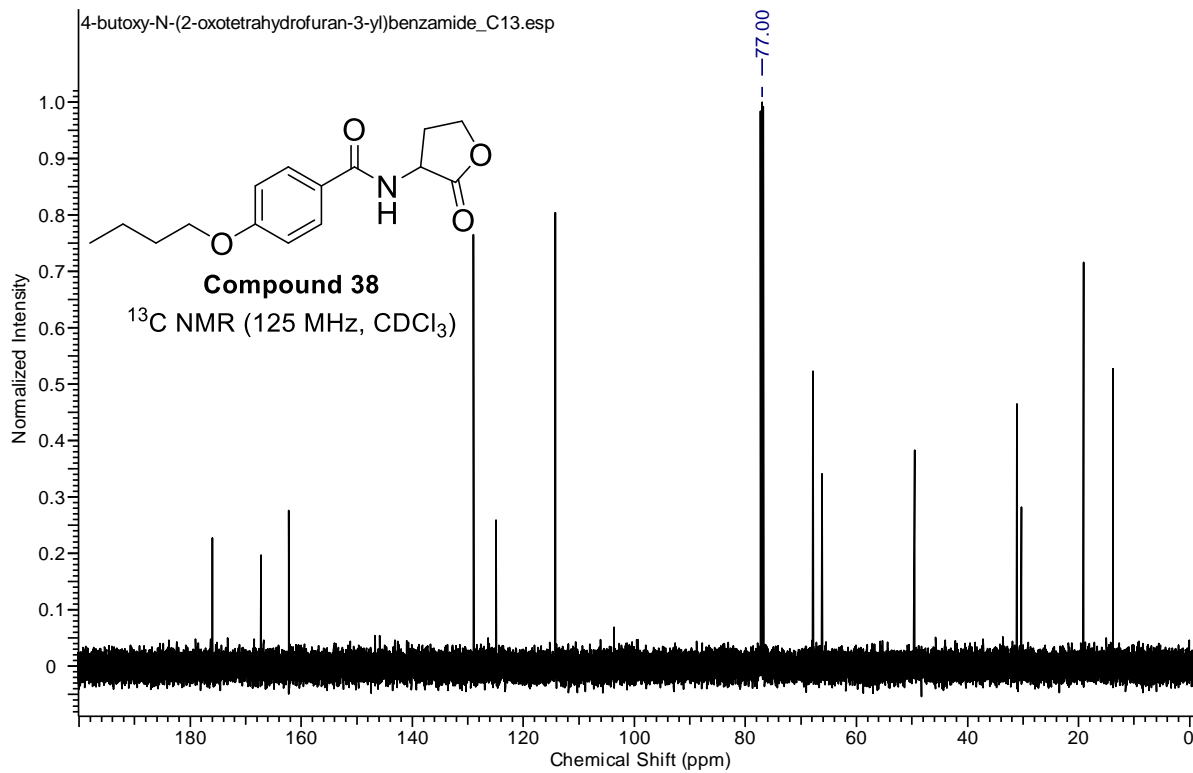
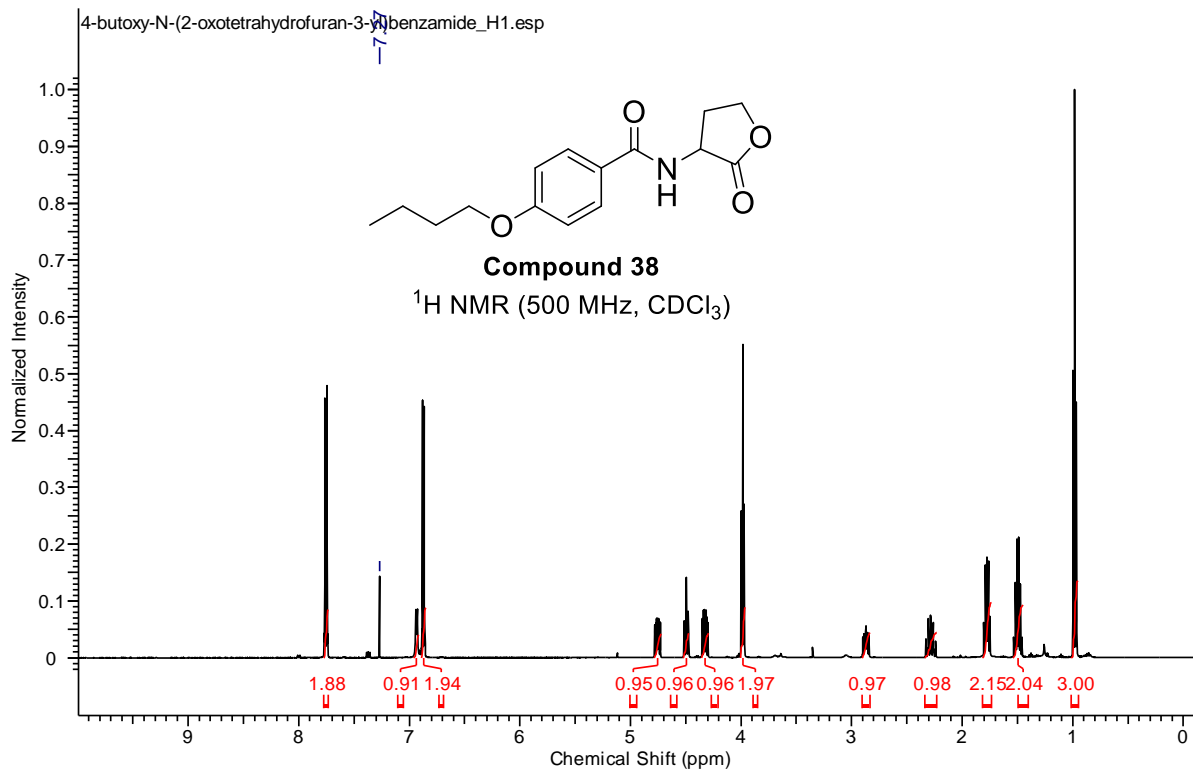


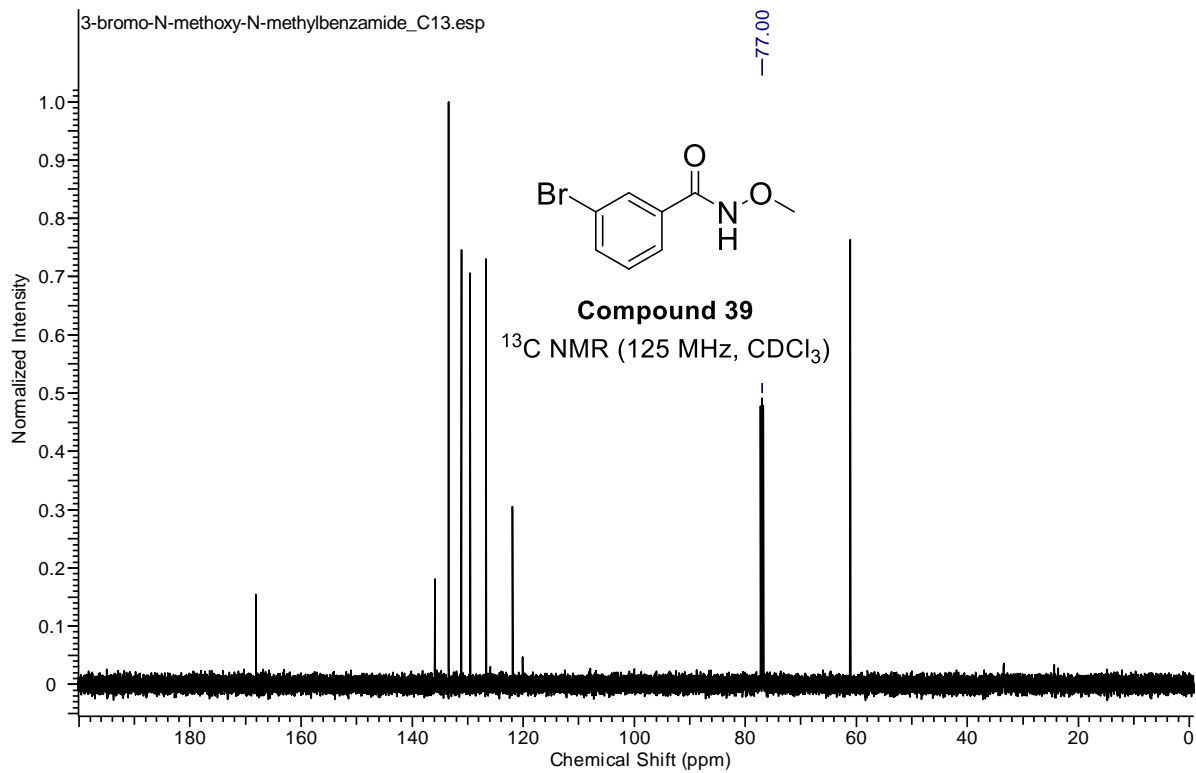
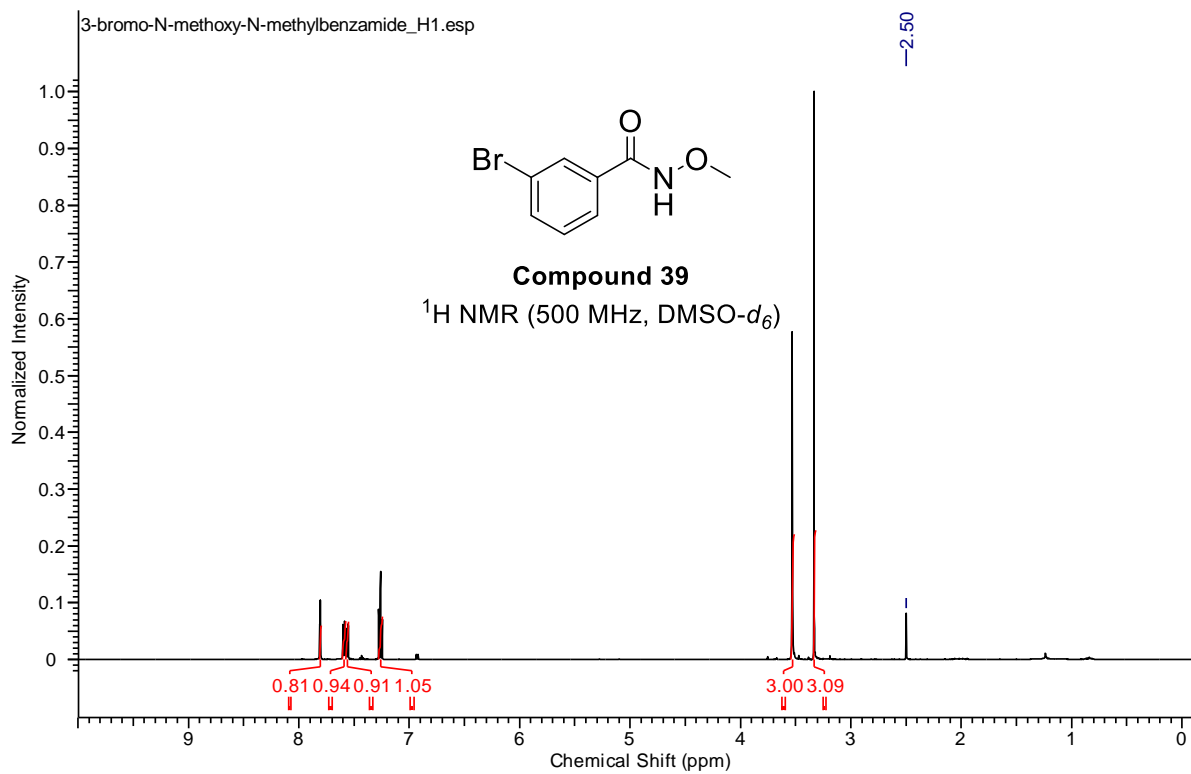


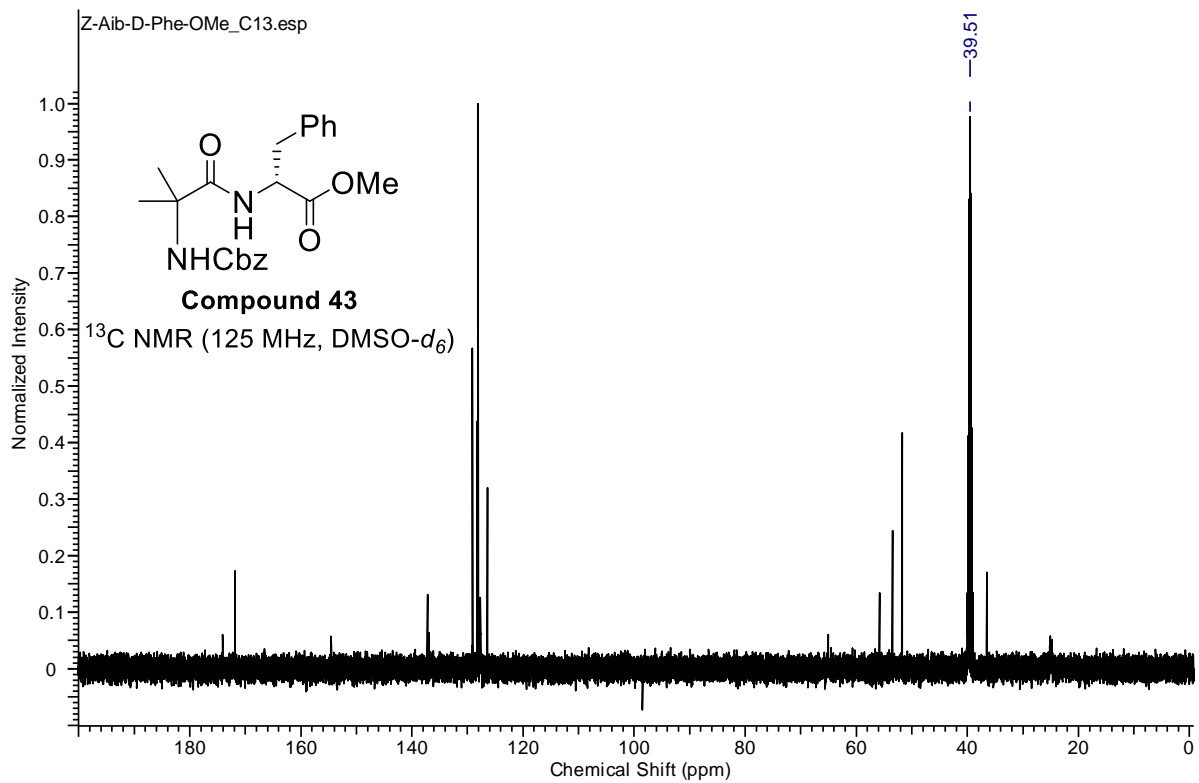
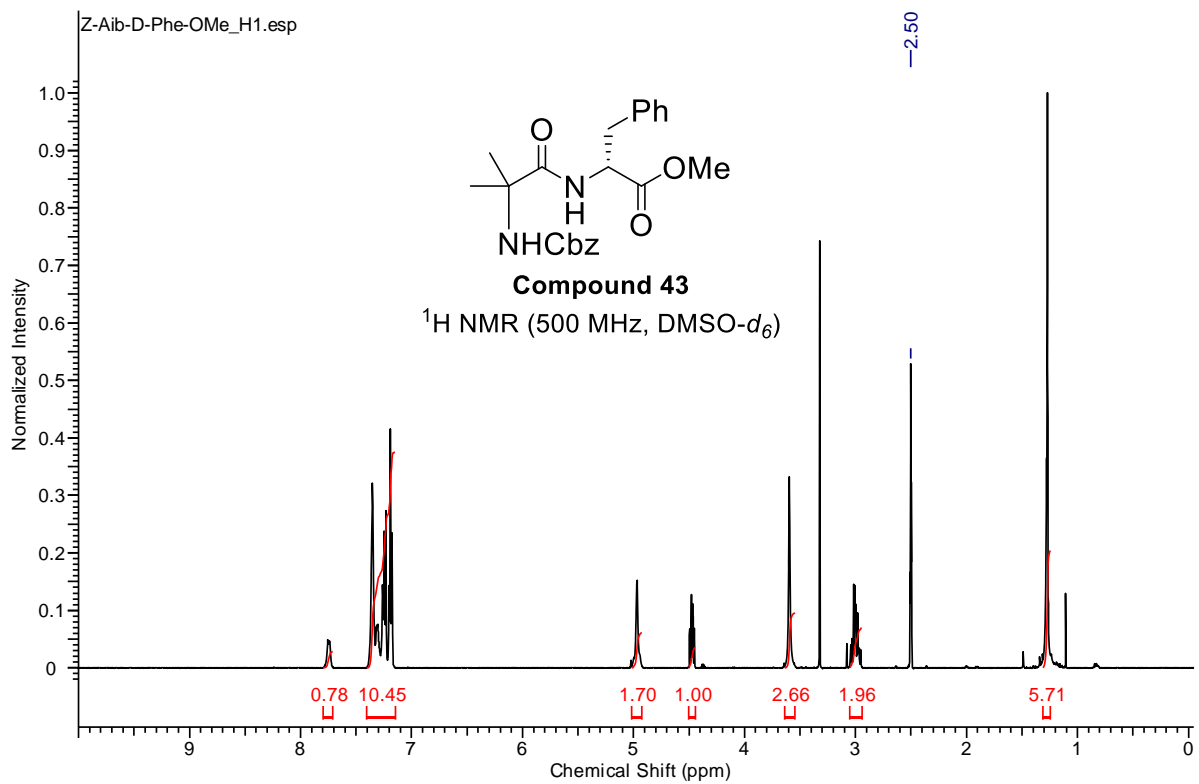


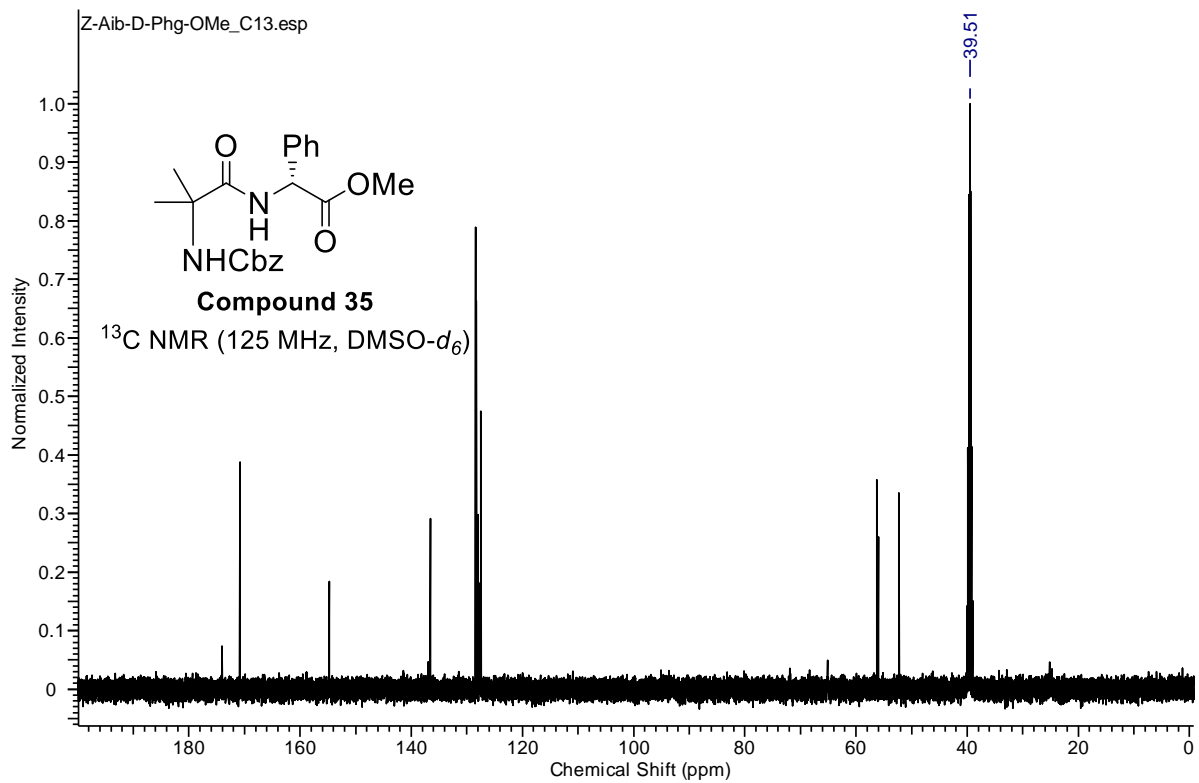
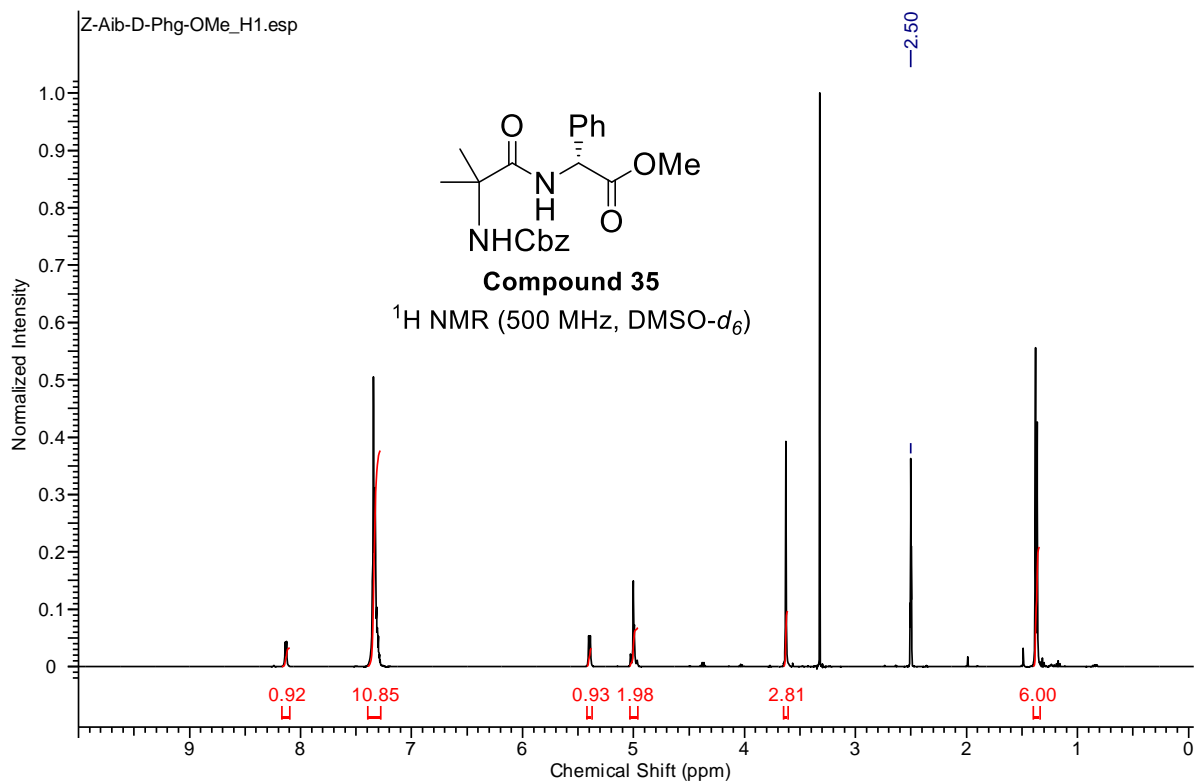






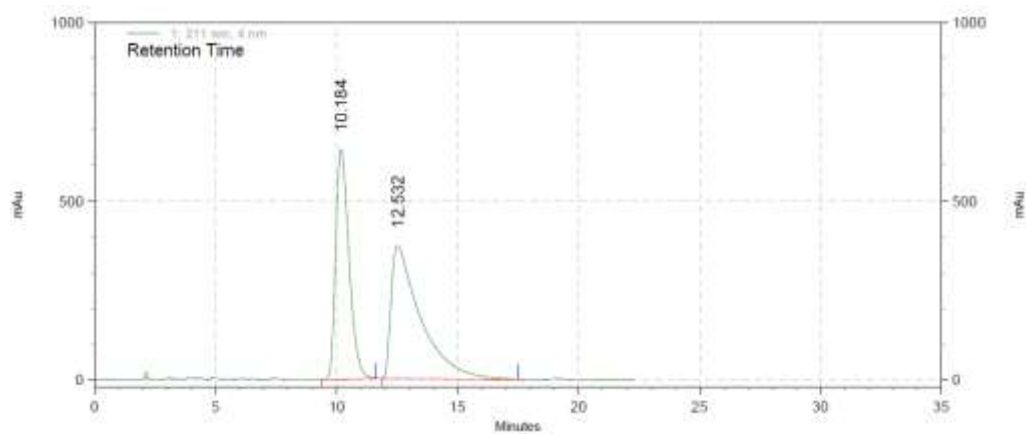






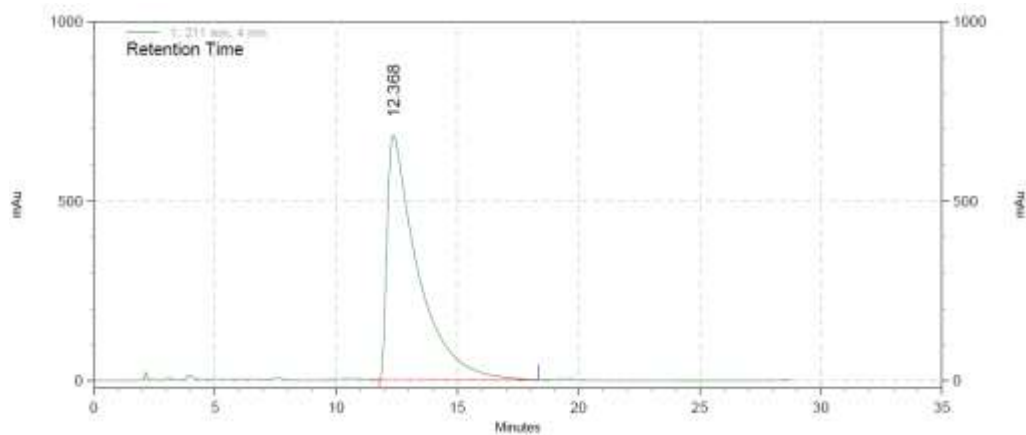
3.10 HPLC Chromatograms

Z-Aib-Phe-OMe Racemic Standard



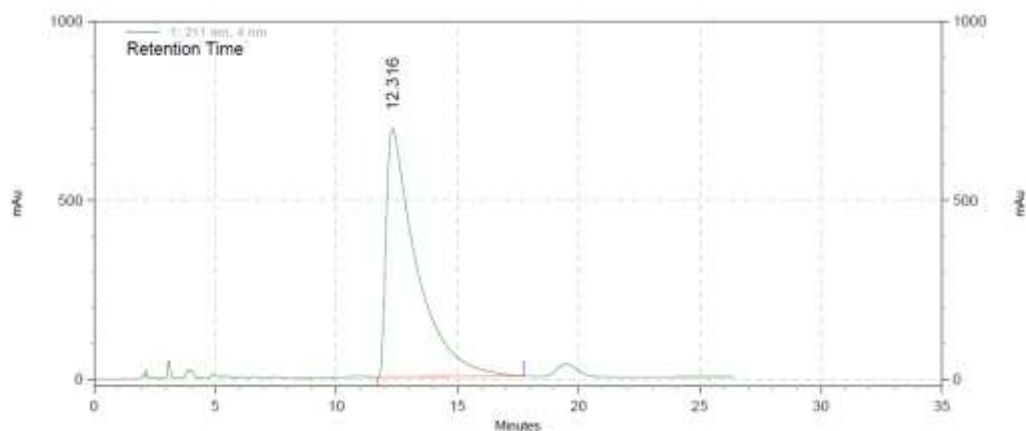
Peak	Product	Retention Time (min)	Area [%]
1	Z-Aib-D-Phe-OMe, 43	10.184	44.02
2	Z-Aib-Phe-OMe, 24	12.532	55.08

Z-Aib-L-Phe-OMe with 2,6-lutidine as base



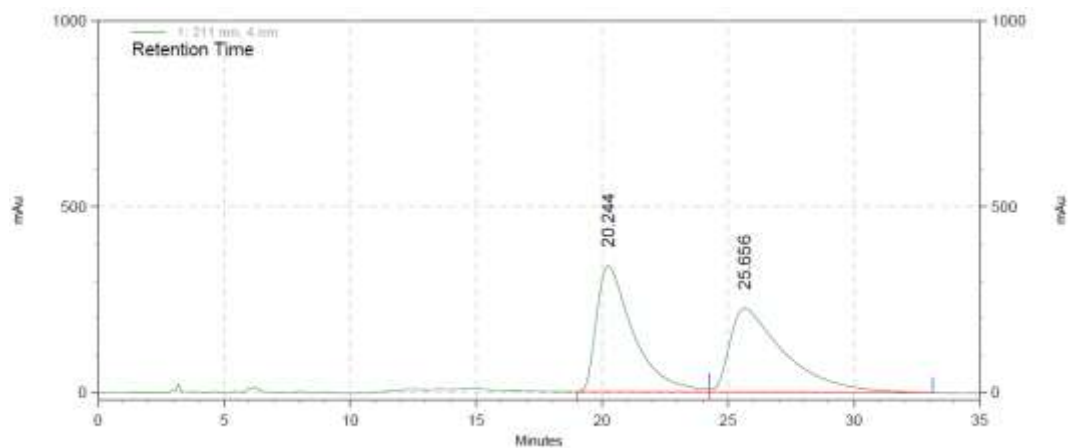
Peak	Product	Retention Time (min)	Area [%]
1	Z-Aib-Phe-OMe, 24	12.368	100.0

Z-Aib-L-Phe-OMe with pyridine as base



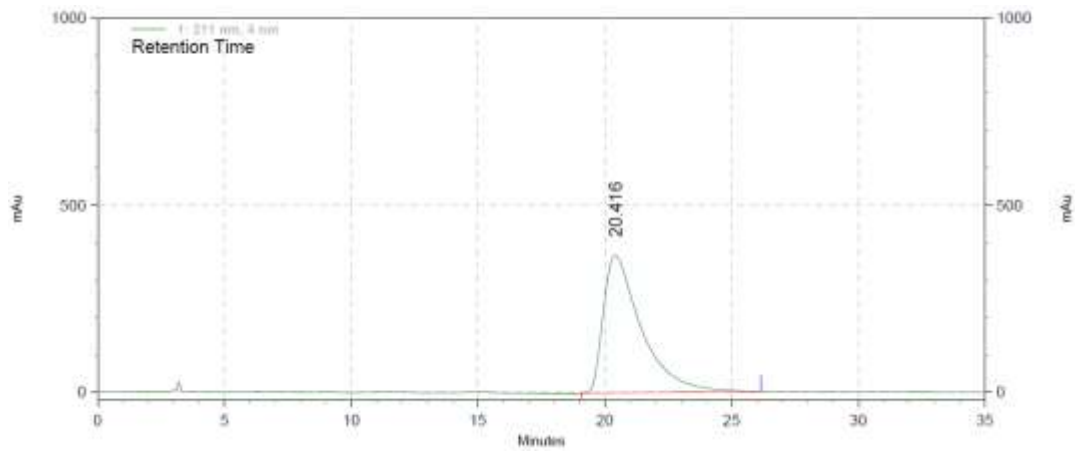
Peak	Product	Retention Time (min)	Area [%]
1	Z-Aib-Phe-OMe, 24	12.316	100.0

Z-Aib -Phg-OMe Racemic Standard



Peak	Product	Retention Time (min)	Area [%]
1	Z-Aib-Phg-OMe, 9	20.244	50.23
2	Z-Aib-D-Phg-OMe, 44	25.656	49.73

Z-Aib-L-Phe-OMe with 2,6-lutidine as base



Peak	Product	Retention Time (min)	Area [%]
1	Z-Aib-Phg-OMe, 9	20.416	100.0

3.11 References

1. Fosgerau, K.; Hoffmann, T. *Drug Discovery Today* **2015**, *20*, 122.
2. a) Linton, B. R.; Reutershan, M. H.; Aderman, C. M.; Richardson, E. A.; Brownell, K. R.; Ashley, C. W.; Evans, C. A.; Miller, S. J. *Tetrahedron Lett.* **2007**, *48*, 1993. b.) Miller, S. J.; Jarvo, E. R. *Tetrahedron* **2002**, *58*, 2481. b) Romney, D. K.; Miller, S. J. *Org Lett.* **2012**, *14*, 1138. c) Abascal, N. C.; Miller, S. J. *Org. Lett.* **2016**, *18*, 4646.
3. a) Hart, J. S.; Nichol, G. S.; Love, J. B. *Dalton Trans.* **2012**, *41*, 5785. b) Doyle, M. *Angew. Chem., Int. Ed. Engl.* **2009**, *48*, 850. c) Zhang, J.; Liu, Q.; Duan, C.; Shao, Y.; Ding, J.; Miao, Z.; You, X. Z.; Guo, Z. *J. Chem. Soc., Dalton Trans.* **2002**, *15*, 591. d) Trost, B. M.; Hung, M. H. *J. Am. Chem. Soc.* **1983**, *105*, 7757. e) Trost, B. M.; Tometzki, G. B.; Hung, M.H. *J. Am. Chem. Soc.* **1987**, *109*, 2176.
4. a) Zhu, R. -Y.; Farmer, M. E.; Chen, Y.-Q.; Yu, J. -Q. *Angew. Chem., Int. Ed.* **2016**, 10578. b) Zhou, Y.; Yuan, J.; Yang, Q.; Xiao, Q.; Peng, Y. *ChemCatChem* **2016**, *8*, 2178. c) Wencel-Delord, J.; Colobert, F. *Synlett* **2015**, *26*, 2644. d) Rit, R. K.; Yadav, M. R.; Ghosh, K.; Sahoo, A. K. *Tetrahedron*, **2015**, *71*, 4450.
5. Zahn, D. *Eur. J. Org. Chem.* **2004**, 4020. b) Larock, R. C. *Comprehensive Organic Transformations*, 2nd ed., Wiley: New York, NY, **1999**, pp. 1976-1977. c) Bagno, A.; Lovato, G.; Scorrano, G. *J. Chem. Perkin Trans.* **1993**, *2*, 1091.
6. a) Bordwell, F. G.; Bartmess, J. E.; Hautala, J. A. *J. Org. Chem.* **1978**, *43*, 3095. b) Bordwell, F. G.; Fried, H. E.; Hughes, D. L.; Lynch, T. Y.; Satish, A. V.; Whang, Y. E. *J. Org. Chem.* **1990**, *55*, 3330. c) Bordwell, F. G. *Acc. Chem. Res.* **1988**, *21*, 456. d) Bordwell, F. G.; Harrelson, J. A.; Lynch, T. Y. *J. Org. Chem.* **1990**, *55*, 3337.
7. a) Mowry, D. T. *Chem. Rev.* **1948**, *42*, 189. b) Krynitsky, J. A.; Carhart, H. W. *Org. Synth.* **1963**, *IV*, 436. c) Rickborn, B.; Jensen, F. R. *J. Org. Chem.* **1962**, *27*, 4608. d) Zhou, S.; Junge, K.; Addis, D.; Das, S.; Beller, M. *Org. Lett.* **2009**, *11*, 2461.
8. Bohme, H.; Viehe, H. G. *Advances in Organic Chemistry: Methods and results, Iminium Salts in Organic Chemistry*, Vol. 9, Wiley: New York, NY, **1977**.
9. Volkov, A.; Tinnis, F.; Adolfsson, H. *Org. Lett.* **2014**, *16*, 680.
10. a) Bichler, A.; Napieralski, B. *Ber. Dtsch. Chem. Ges.* **1893**, *26*, 1903. b) Fodor G.; Nagubandi, S. *Tetrahedron* **1980**, *36*, 1279.

11. a) Nahm, S.; Weinreb, S. M. *Tetrahedron Lett.* **1981**, 22, 3815. b) Gomtsyan, A.; Koenig, R. J.; Lee, C. –H. *J. Org. Chem.* **2001**, 66, 3619. c) Sun, Y. –G.; Jung, J. –K.; Seo, S. –Y.; Min, K. –H.; Shin, D. –Y.; Lee, Y. –S.; Kim, H. –J.; Park, H. –J. *J. Org. Chem.* **2002**, 67, 4127. d) Kurosu, M.; Kishi, Y. *Tetrahedron Lett.* **1998**, 39, 4793.
12. a) Cope, A. C.; Ciganek, E. *Org. Synth.* **1963**, IV, 339. b) Moffett, R. B. *Org. Synth.* **1963**, IV, 354.
13. a) Stevens, R. V.; Lai, J. T. *J. Org. Chem.* **1972**, 37, 2138. b) Trofimenko, S. *J. Org. Chem.* **1964**, 29, 3046.
14. a) Zhou, S.; Junge, K.; Addis, D.; Das, S.; Beller, M. *Angew. Chem., Int. Ed.* **2009**, 48, 9507. b) Sunada, Y.; Kawakami, H.; Imaoka, T.; Motoyama, Y.; Nagashima, H. *Angew. Chem., Int. Ed.* **2009**, 48, 9511. c) Das, S.; Addis, D.; Zhou, S.; Junge, K.; Beller, M. *J. Am. Chem. Soc.* **2010**, 132, 1770. d) Das, S.; Join, B.; Junge, K.; Beller, M. *Chem. Commun.* **2012**, 48, 2683. e) Cabrero-Antonino, J. R.; Alberico, E.; Junge, K.; Junge, H.; Beller, M. *Chem. Sci.* **2016**, 7, 3432. f) Nakatani, N.; Hasegawa, J.-Y.; Sunada, Y.; Nagashima, H. *Dalton Trans.* **2015**, 44, 19344. g) Tinnis, F.; Volkov, A.; Slagbrand, T.; Adolfsson, H. *Angew. Chem., Int. Ed.* **2016**, 55, 4562. h) Das, S.; Li, Y.; Bornschein, C.; Pisiewicz, S.; Kiersch, K.; Michalik, D.; Gallou, F.; Junge, K.; Beller, M. *Angew. Chem., Int. Ed.* **2015**, 54, 12389. i) Simmons, B. J.; Hoffman, M.; Hwang, J.; Jackl, M. K.; Garg, N. K. *Org. Lett.* In Press.
15. a) Hilborn, J. W.; Lu, Z. –H.; Jurgens, A. R.; Fang, Q. K.; Byers, P.; Wald, S. A.; Senanayaka, C. H. *Tetrahedron Lett.* **2001**, 42, 8919. b) Finger, G. C.; Starr, L. D.; Roe, A.; Link, W. J. *J. Org. Chem.* **1962**, 27, 3965. c) Shapiro, R.; DiCosimo, R.; Hennessey, S. M.; Stieglitz, B.; Campopiano, O.; Chiang, G. C. *Org. Process. Res. Dev.* **2001**, 5, 593. d) Poullennec, K. G.; Romo, D. *J. Am. Chem. Soc.* **2003**, 125, 6344.
16. Beckwith, A. L. J. *The Chemistry of Amides*; Zabicky, J., Ed.; Synthesis of Amides; Interscience, London, **1970**; pp. 105-109.
17. a) El-Faham, A.; Albericio, F. *Chem. Rev.* **2011**, 111, 6557. b) Montalbetti, C. A. G. N.; Falque, V. *Tetrahedron* **2005**, 61, 10827. c) Joullié, M. M.; Lassen, K. M. *Arkivoc*, **2010**, VIII, 189. d) Klausner, Y. S.; Bodansky, M. *Synthesis* **1972**, 453. E) Rich, D. H.; Singh, J., *The Peptides: Analysis, Synthesis, Biology*; Academic: New York, NY, **1979**.
18. Carpino, L. A.; Beyermann, M.; Wenschuh, H.; Bienert, M. *Acc. Chem. Res.* **1996**, 29, 268.

19. a) Darapsky A. *J. Prakt. Chem.* **1936**, *146*, 250. b) A. Darapsky; D. Hillers *J. Prakt. Chem.* **1915**, *92*, 297. c) Gagnon; P. E.; Boivin, P. A.; Craig, H. M. *Can. J. Chem.* **1951**, *29*, 70. d) Shioiri, T.; Ninomiya, K.; Yamada, S. *J. Am. Chem. Soc.* **1972**, *94*, 6203.
20. a) Paul, R.; Anderson, W. *J. Am. Chem. Soc.* **1960**, *82*, 4596. b) Staab, H. A. *Justus Liebigs Ann. Chem.* **1957**, *609*, 75. c) Staab, H.; Lueking, M.; Duerr, F. H. *Chem. Ber.* **1962**, *95*, 1275.
21. a) Wittenberger, S. J.; McLaughlin, M. A. *Tetrahedron Lett.* **1999**, *40*, 7175. b) Belleau, B.; Malek, G. *J. Am. Chem. Soc.* **1968**, *90*, 1651. c) Mikolajczyk, M.; Kielbasinski, P. *Tetrahedron* **1981**, *37*, 233.
22. a) Pizey J. S. (Ed.), *Synthetic Reagents*, Vol. 1, Wiley: New York, NY, **1974**, pp. 321–357. b) Pearson, A. J.; Roush W. R. (Eds.), *Handbook of Reagents for Organic Synthesis: Activating Agents and Protecting Groups*, Wiley: New York, NY, **1999**, pp. 370–373. c) Chu, W.; Tu, Z.; McElveen, E.; Xu, J.; Taylor, M.; Luedtke, R. R.; Mach, R. H. *Bioorg. Med. Chem.* **2005**, *13*, 77.
23. a) Adams, R.; Ulrich L. H. *J. Am. Chem. Soc.* **1920**, *42*, 599. b) Kuwajima, I.; Urabe, H. In *Organic Syntheses*; Wiley: New York, NY, Collect. Vol. VIII, **1993**, pp. 486–489. c) Knapp, S.; Gibson, F. S. In *Organic Syntheses*; Wiley: New York, **1998**, Collect. Vol. IX, pp. 516–521.
24. a) Pearson, A. J.; Roush W. R. (Eds.), *Handbook of Reagents for Organic Synthesis: Activating Agents and Protecting Groups*, Wiley: New York, NY, **1999**, pp. 333. b) Klosa, J. *J. Prakt. Chem.* **1963**, *19*, 45. c) Patai, S. (Ed.), *The Chemistry of Acyl Halides*, Interscience: London, **1972**, pp. 40–44. d) Pearson, A. J.; Roush W. R. (Eds.), *Handbook of Reagents for Organic Synthesis: Activating Agents and Protecting Groups*, Wiley: New York, NY, **1999**, pp. 335–338. e) Rayle, H. L.; Fellmeth L. *Org. Process Res. Dev.* **1999**, *3*, 172.
25. Wuts, P. G. M.; *Greene, T. W. Greene's Protective Groups in Organic Synthesis*; Wiley: Hoboken, NJ, **2014**.
26. Luknitskii, F. I.; Vovsi, B. A. *Usp. Khim.* **1969**, *38*, 1072.
27. a) Leuchs, H. *Ber. Dtsch. Chem. Ges.* **1906**, *39*, 857. b) Poduska, K.; Gross, H. *Chem. Ber.* **1961**, *49*, 527.
28. a) Stoye, P. In *The Chemistry of Amides (The Chemistry of Functional Groups)*; Zabicky, J., Ed.; Interscience: New York, **1970**, pp. 515. b) Shiori, T.; Ninomiya, K.; Yamada, S. *J. Am. Chem. Soc.* **1972**, *94*, 6203.

29. a) Todd, D., *Org. React.* **1948**, 4, 378. b) Szmant, H. H. *Angew. Chem., Int. Ed. Engl.* **1968**, 7, 120. c) Reusch, W. *Reduction*; Dekker: New York, NY, **1968**, pp. 171. d) Clark, C. *Hydrazine*; Mathieson Chemical Corp.: Baltimore, MD, **1953**. e) Bräse, S.; Gil, C.; Knepper, K.; Zimmermann, V. *Angew. Chem., Int. Ed.* **2005**, 44, 5188.
30. LeBel, N. A.; Cherluck, R. M.; Curtis, E. A. *Synthesis* **1973**, 678.
31. Staab, H. A.; Wendel, K. *Q. Rev., Chem. Soc.* **1968**, 48, 44.
32. Belleau, B.; Malek, G. *J. Am. Chem. Soc.* **1968**, 90, 1651.
33. a) Smith, G. G.; Sivakua, T. *J. Org. Chem.* **1983**, 48, 627. b) Stroud, E. D.; Fife, D. J.; Smith, G. G. *J. Org. Chem.* **1983**, 48, 5368.
34. a) Kurzer, F.; Douraghi-Zader, K. *Chem. Rev.* **1967**, 67, 107. b) Shchukina, L. A.; Kara-Murza, S. N.; Vdovina, R. G. *Zh. Obshch. Khim.* **1959**, 29, 340. c) Schmidt, E.; Striewsky, W. *Chem. Ber.* **1941**, 74, 1285.
35. Pickersgill, I. F.; Bishop, J.; Lo, Y.; Chiu, F. -T.; Kulkarni, V. R. *Synthesis of Bortezomib* EP Patent 2377868 A1, Oct 19, **2011**.
36. Dounay, A. B. *Telaprevir (Incivek) and Boceprevir (Victrelis): NS3/4A Inhibitors for Treatment for Hepatitis C Virus (HCV)*, in *Innovative Drug Synthesis*; Eds J. J. Li and D. S. Johnson, Wiley: Hoboken, NJ, **2015**.
37. Wehrstedt, K. D.; Wandrey, P. A.; Heitkamp, D. *J. Hazard. Mater.* **2005**, 126, 1.
38. a) Itoh, M. *Bull. Chem. Soc. Jpn.* **1973**, 46, 2219. b) Subirós-Funosas, R.; Prohens, R.; Barbas, R.; El-Faham, A.; Albericio, F. *Chem. Eur. J.* **2009**, 15, 9394.
39. a) El-Faham, A.; Subirós-Funosas, R.; Prohens, R.; Albericio, F. *Chem. Eur. J.* **2009**, 15, 9404. b) El-Faham, A.; Albericio, F. *J. Pept. Sci.* **2010**, 16, 6. c) Subirós-Funosas, R.; Nieto-Rodríguez, L.; Jensen, K. J.; Albericio, F. *J. Pept. Sci.* **2013**, 19, 408. d) Cherkupally, P.; Acosta, G. A.; Nieto-Rodríguez, L.; Spengler, J.; Rodríguez, H.; Khattab, S. N.; El-Faham, A.; Shamis, M.; Luxembourg, Y.; Prohens, R.; Subiros-Funosas, R.; Albericio, F. *Eur. J. Org. Chem.* **2013**, 19, 6372.
40. Gernigon, N.; Al-Zoubi, R. A.; Hall, D. G. *J. Org. Chem.* **2012**, 77, 8386. (b) Maki, T.; Ishihara, K.; Yamamoto, H. *Tetrahedron* **2007**, 63, 8645. (c) Ishihara, K.; Ohara, S.; Yamamoto, H. *J. Org. Chem.* **1996**, 61, 4196.

41. Hie, L.; Nathel, N. F. F.; Shah, T. K.; Baker, E. L.; Hong, X.; Yang, Y. -F.; Liu, P.; Houk, K. N.; Garg, N. K. *Nat. Commun.* **2015**, *524*, 79.
42. Krause, T.; Baader, S.; Erb, B.; Gooßen L. J. *Nat. Commun.* **2016**, *7*, 11732.
43. König, W.; Geiger, R. *Chem. Ber.* **1970**, *103*, 788.
44. MacMillan, D. S.; Murray, J.; Sneddon, H. F.; Jamieson, C.; Watson, A. J. B. *Green Chem.* **2013**, *15*, 596.
45. Gabriel, C. M.; Keener, M.; Gallou, F.; Lipshutz, B. H. *Org. Lett.* **2015**, *17*, 3968.
46. a) Hojo, K.; Ichikawa, H.; Onishi, M.; Fukumori, Y.; Kawasaki, K. *J. Pept. Sci.* **2011**, *17*, 487. b) Hojo, K.; Hara, A.; Kitai, H.; Onishi, M.; Ichikawa, H.; Fukumori, Y.; Kawasaki, K. *Chem. Cent. J.* **2011**, *5*, 49. c) Hojo, K.; Ichikawa, H.; Fukumori, Y.; Kawasaki, K. *Int. J. Pept. Res. Ther.* **2008**, *14*, 373. d) Hojo, K.; Ichikawa, H.; Maeda, M.; Kida, S.; Fukumori, Y.; Kawasaki, K. *J. Pept. Sci.* **2007**, *13*, 493.
47. Palomo, J. M. *RSC Adv.* **2014**, *4*, 32658.
48. De Marco, R.; Tolomelli, A.; Greco, A.; Gentilucci, L. *ACS Sustainable Chem. Eng.* **2013**, *1*, 566.
49. Eckert, H.; Forster, B. *Angew. Chem., Int. Ed. Engl.* **1987**, *26*, 894.
50. Wang, Q.; Wang, Y.; Kurosu, M. *Org. Lett.* **2012**, *14*, 3372.
51. Kunishima, M.; Imada, H.; Kikuchi, K.; Hioki, K.; Nishida, J.; Tani, S. *Angew. Chem., Int. Ed.* **2005**, *44*, 7254.
52. Kelly, S. M.; Lipshutz, B. H. *Org. Lett.* **2014**, *16*, 98.
53. Klumphu, P.; Lipshutz, B. H. *J. Org. Chem.* **2014**, *79*, 888.
54. Newkirk, T. L.; Bowers, A. A.; Williams, R. W. *Nat. Prod. Rep.* **2009**, *26*, 1293.
55. Gebhardt, K.; Pukall, R.; Fiedler, H.-P. *J. Antibiot.* **2001**, *54*, 428.
56. a) Kaminski, Z. J.; Kolesinska, B.; Kolesinska, J.; Sabatino, G.; Chelli, M.; Rovero, P.; Blaszczyk, M.; Glowka, M. L.; Papini, A. M. *J. Am. Chem. Soc.* **2005**, *127*, 16912. b) Quirin, C.; Kazmaier, U. *Eur. J. Org. Chem.* **2009**, *3*, 371.

57. a) Carpino, L. A.; El-Faham, A. *J. Org. Chem.* **1994**, *59*, 695. b) Brieke, C.; Cryle, M. *J. Org. Lett.* **2014**, *16*, 2454.
58. Hahne, W. F.; Jensen, R. T.; Lemp, G. F.; Gardner, J. D. *Proc. Natl. Acad. Sci. U. S. A.* **1981**, *78*, 6304.
59. a) Sheldon, R. A. *Chem. Ind.* **1992**, 903. b) Lipshutz, B. H.; Ghorai, S. *Green Chem.* **2014**, *16*, 3660. c) Lipshutz, B. H.; Isley, N. A.; Fennewald, J. C.; Slack, E. D. *Angew. Chem., Int. Ed.* **2013**, *52*, 10911.
60. Hoch, M.; van Gorsel, H.; van gerven, J.; Dingemanse, J. *J. Clin. Pharmacol.* **2014**, *54*, 97910.
61. Parmentier, M.; Wagner, M. K.; Magra, K.; Gallou, F. *Org. Process. Res. Dev.* **2016**, *20*, 1104.
62. a) Lipshutz, B. H.; Ghorai, S.; Abela, A. R.; Moser, R.; Nishikata, T.; Duplais, C.; Krasovskiy, A. *J. Org. Chem.* **2011**, *76*, 4379. b) Lipshutz, B. H.; Ghorai, S. *Aldrichimica Acta* **2008**, *41*, 59.
63. Suppo, J. –S.; Subra, G.; Berges, M.; Marcia De Figueiredo, R.; Campagne, J. –M. *Angew. Chem., Int. Ed.* **2014**, *53*, 538.
64. ISIS Inovation Limited; Gouverneur, V.; Sandford, G. Patent: WO2014/68341 A2, 2014.
65. Gudasheva, T. A.; Zaitseva, N. I., Bondarenko, N. A., Scherbakova, I. É.; Asmakova, L. S.; Rozantsev, G. G.; Ostrovskaya, R. U.; Voronina, T. A.; Seredenin, S. B. *Pharm. Chem. J.* **1997**, *31*, 574.
66. Baldwin, A.; Godfrey, P. *Tetrahedron*, **1993**, *49*, 7837.
67. Kaminski, Z. J.; Kolesinska, B.; Kolesinska, J.; Sabatino, G.; Chelli, M.; Rovero, P.; Blaszczyk, M.; Glowka, M. L.; Papini, A. M. *J. Am. Chem. Soc.* **2005**, *127*, 16912.
68. Saidov, A. S.; Levkovich, M. G.; Vinogradova, V. I. *Chem. Nat. Compd.* **2012**, *49*, 897.
69. Kim, K.; Kang, B.; Hong, S. H. *Tetrahedron*, **2015**, *71*, 4565.
70. Fong, H. K. H.; Copp, B. R. *Mar. Drugs* **2013**, *11*, 274.

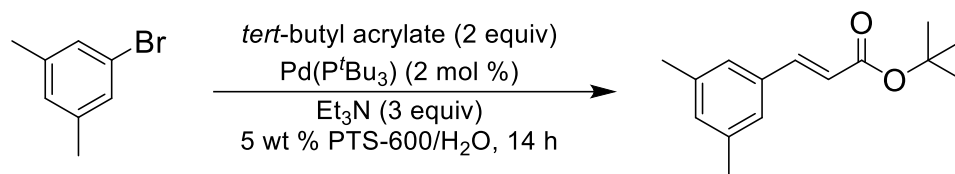
IV. Effects of Co-solvents on Reactions Run Under Micellar Catalysis

Conditions

4.1 Introduction

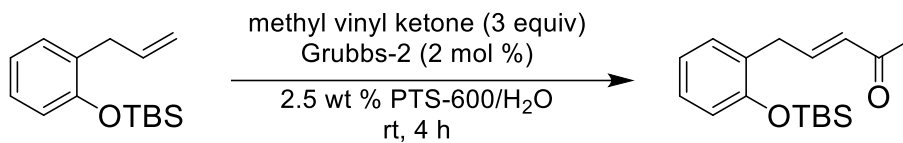
The expanding list of applications of designer surfactants such as TPGS-750-M and their *in situ* derived nanomicelles as an alternative reaction medium to organic solvents in which numerous synthetic transformations can be carried out is now quite extensive.¹ While several types of transition metal-catalyzed processes are especially well-suited to these conditions (e.g., Pd- and Ni-catalyzed cross-couplings,^{1b,2b} Au-catalyzed processes,³ etc.), many other reaction types not only are amenable but also offer unique opportunities to benefit from the presence of the surrounding water.

Salt additives, for example have shown a pronounced effect on reaction rates and yields for a variety of transformations. An extensive study was conducted by our group in 2011 which highlighted the effects of salt additives on Heck couplings, cross-metathesis, as well as ring closing metathesis.⁴ In this report, it was presented that Heck cross coupling products could be produced in high yields in the presence of NaCl under micellar catalysis conditions which would otherwise require heating to afford similar results (Figure 1). This same modification translated to a moderate increase in metathesis yields as well, however the presence of minimal KHSO₄ was found to greatly accelerate these reactions by effecting the pH of the system (Figure 2). Another example of the salt effect is presented in a communication from our group for the Pd-catalyzed reductions of aryl bromides in water where the extent of conversion was directly associated with NaCl concentration (Figure 3).⁵



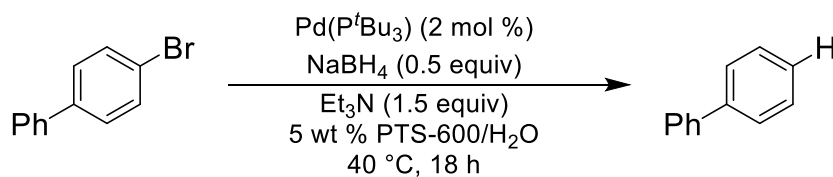
entry	surfactant	temp (°C)	isolated yield
1	PTS/H ₂ O	rt	43
2	PTS/H ₂ O	40	94
3	3 M NaCl, PTS/H ₂ O	rt	95

Figure 1. Effect of NaCl on the Heck Reaction in PTS/H₂O.



entry	surfactant	isolated yield
1	PTS/H ₂ O	64
2	3 M NaCl, PTS/H ₂ O	75
3	0.02 M KHSO ₄ , PTS/H ₂ O	95

Figure 2. Salt Effect on Olefin Cross-Metathesis in PTS/H₂O.



entry	NaCl (M)	conv. (%)
1	0	61
2	1	76
3	3	87
4	4	>99

Figure 3. Effect of NaCl on aryl bromide reductions in PTS/H₂O.

The initial report described these effects examined the effects of various salts on average micelle size as determined by dynamic light scattering (DLS). A general trend was observed where a “salting out effect” led to particle growth with NaCl and several other salts tested which was attributed to the success of this procedure (Figure 4). Interestingly, weakly hydrated salts such as iodides and thiocyanates led to a “salting in” effect causing particle contraction and these systems were found to lead to lower product yields for the Heck coupling described in Figure 1.

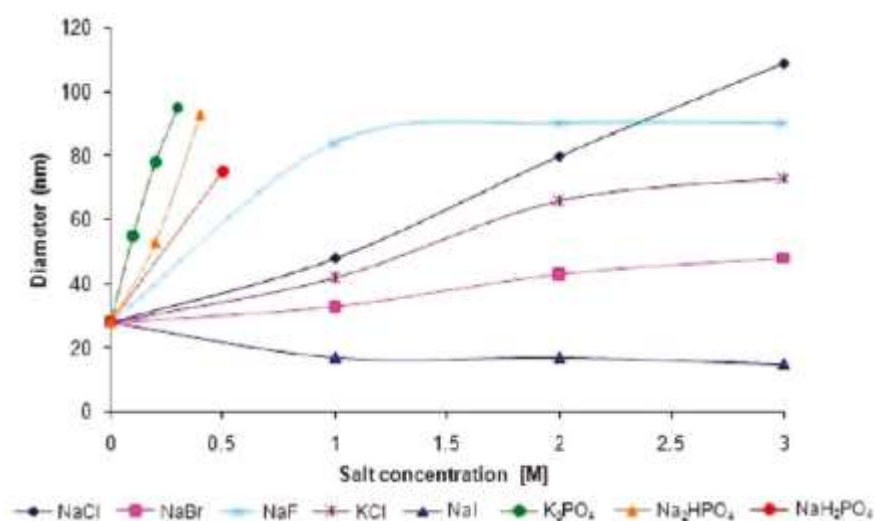
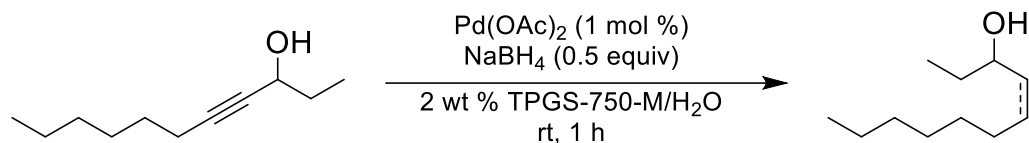


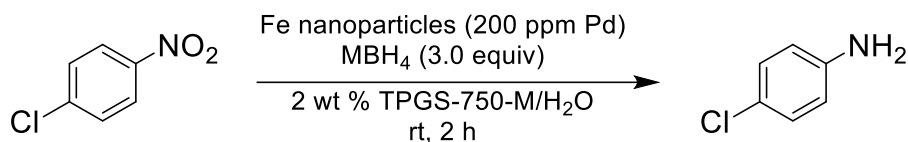
Figure 4. Effect of different salt concentrations on the diameter of PTS micelles.

In addition to effecting particle size and reaction rate, salt additives have been found to greatly influence selectivity for Pd-catalyzed semi-reductions in aqueous TPGS-750-M (Chapter II).⁶ Here, it was discovered that LiCl could be used to yield *Z*-alkenes with excellent selectivity from functionalized alkynes such as propargyl alcohols which otherwise showed poor selectivity (Figure 5). Nitro group reductions catalyzed by Fe/ppm-Pd nanoparticles are affected by the salt effect as well (Chapter V), where the rate enhancement observed by the use of KBH₄ can be mimicked by the use of NaBH₄ in with KCl (Figure 6).⁷



entry	additive	Z:E:alkane	conv. (%)
1	N/A	1:1:1	100
2	LiBr (2.0 equiv)	3:1:0	100
3	LiCl (2.0 equiv)	96:4:0	100

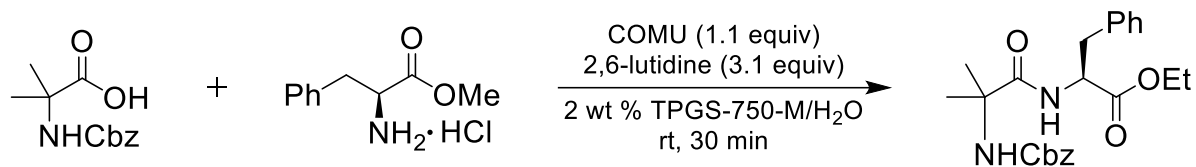
Figure 5. Salt effect on selectivity of alkyne semi-reductions.



entry	reductant	additive	conv. (%)
1	KBH ₄	N/A	>99
2	NaBH ₄	N/A	91
3	NaBH ₄	KCl (1 equiv)	>99

Figure 6. Effect of KCl on Fe/ppm-Pd catalyzed nitro group reductions.

Another parameter that can be effected under aqueous conditions is pH. A profound correlation between reaction yield and pH was observed for amide bond formation (Chapter II), where treating the system with aqueous NaOH or HCl affording lower conversions than for the optimized conditions at pH = 6-7 (Figure 7).⁸



entry	final pH	additive	isolated yield (%)
1	6	N/A	95
2	5	HCl	75
3	8	NaOH	73

Figure 7. Effect of pH on amide bond formation.

In addition to reaction tuning by leveraging the presence of water, aqueous micellar catalysis has been proven as a viable alternative to egregious dipolar aprotic and water-miscible organic solvents. The broad generality of this reaction medium allows for tandem processes to be developed, where sequences of reactions that no longer require differing reaction solvents can be run in a single pot, maximizing efficiency and minimizing waste.^{4,12-16}

While the notion of “getting organic solvents out of organic reactions” remains our goal, we have developed an appreciation for the vagaries associated with the solubility properties of starting materials, most notably highly crystalline solids that can be quite slow to gain entry into the hydrophobic micellar core, making use of this technology potentially impractical. Flocculent solids can be tough to fully consume, and in some cases, educts viewed as “brick dust” that are only soluble in highly polar media may be outside the scope of this green chemistry.

Initial solubility, however, is but one of the potential problems that may arise, especially with reactions run at scale.¹⁷ Starting materials, and/or the desired product(s), may present unpredictable practical issues during or post-reaction at the workup stage. For

example, materials at any stage may adhere to the stirrer and form an intractable gum, preventing continued stirring and/or full conversion. Extraction of the product from such intractable solids can be time-consuming and may require extensive handling, including solubilization in copious amounts of undesirable organic solvents.

4.2 Early Work

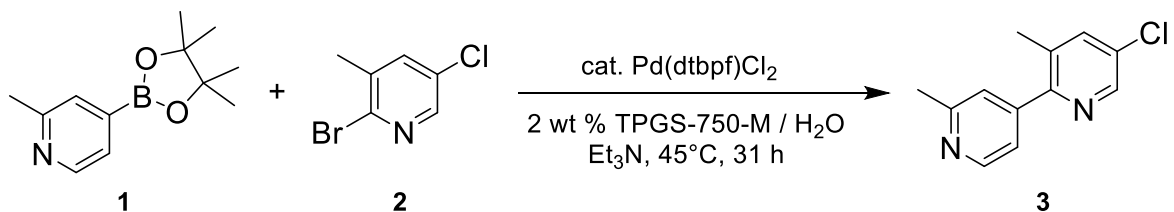
A straightforward modification to existing, otherwise optimized conditions that serves to further generalize this aqueous technology and overcome these limitations has been found; that is, the role that selected organic co-solvents can play in facilitating many types of reactions run in water, and under very mild conditions, can be influential.

This work was based on a few preliminary findings for the effect that co-solvents may have under micellar catalysis conditions. The first report of the use of co-solvents from our group was for the asymmetric Au-catalyzed lactonizations in water, where the concept of “lattice softening” was presented.^{3a} Many of the compounds used in the study were highly crystalline offering challenges for the formation of a microemulsion in aqueous surfactant which was overcome by the use of DMSO, benzene, or toluene, found to increase both product yields and enantioselectivity of the system. In another report, our group disclosed a new ligand, Handaphos, which was found to catalyze Suzuki-Miyaura cross couplings at exceptionally low catalyst loadings (500-1200 ppm).¹¹ The use of nearly negligible mass of the catalyst brought forth the use of toluene for catalyst complexation and as a vehicle for catalyst transfer leading to the use of <10% toluene as cosolvent in this reaction. The seminal publication for nitro group reductions catalyzed by Fe/ppm-Pd nanoparticles represents another case involving the use of THF as co-solvent.¹³ This modification was considered on the basis of the highly crystalline and poorly soluble nature of nitroarenes. The

effect of THF under these conditions is described later in this chapter. In 2015, Parmentier and co-workers at Novartis described a method for amide bond formation in water on scale.¹⁸ As the physical properties of the mixture is an important parameter for a pharmaceutical process both in terms of stirring and product isolation, the use of THF, acetone, and PEG-200 as co-solvent with TPGS-750-M in water were found as the solvents of choice by eliminating “oiling out” in the reaction mixture.

4.3 Results and Discussion

Suzuki-Miyaura (SM) Cross-Couplings.^{1a} Figure 8 shows the results of an SM reaction involving solids **1** and **2**, in 2 wt % TPGS-750-M/H₂O. For this case, it was found that while the use of a co-solvent had essentially no effect on the physical appearance of the reaction mixture run at 45 °C, the presence of 10% acetone (by volume) increased the isolated yield from 68% to 85%. Further increases in the acetone content (e.g., to 50%) led to a dramatic decrease in isolated product (25%).



entry	co-solvent	isolated yield (%)
A	none	68
B	10% THF	75
C	10% acetone	85
D	50% acetone	25

Figure 8. Effects of THF and acetone on SM cross coupling.

As mentioned previously, our group released a communication introducing HandaPhos, a highly active ligand for SM couplings enabled by only ppm levels of its 1:1 complex with palladium.¹¹ Examination of THF, acetone, and toluene as co-solvents at the 10% level identified both THF and acetone as effective additives, thereby enhancing the rate of the coupling between solid **4** and liquid **5**, shown in Figure 9. In comparison to the control system, higher isolated yields were produced using 10% co-solvent. And while the highest yield of **6** was achieved by utilizing THF (81%), 10% toluene showed a more uniform and stable suspension without precipitation.

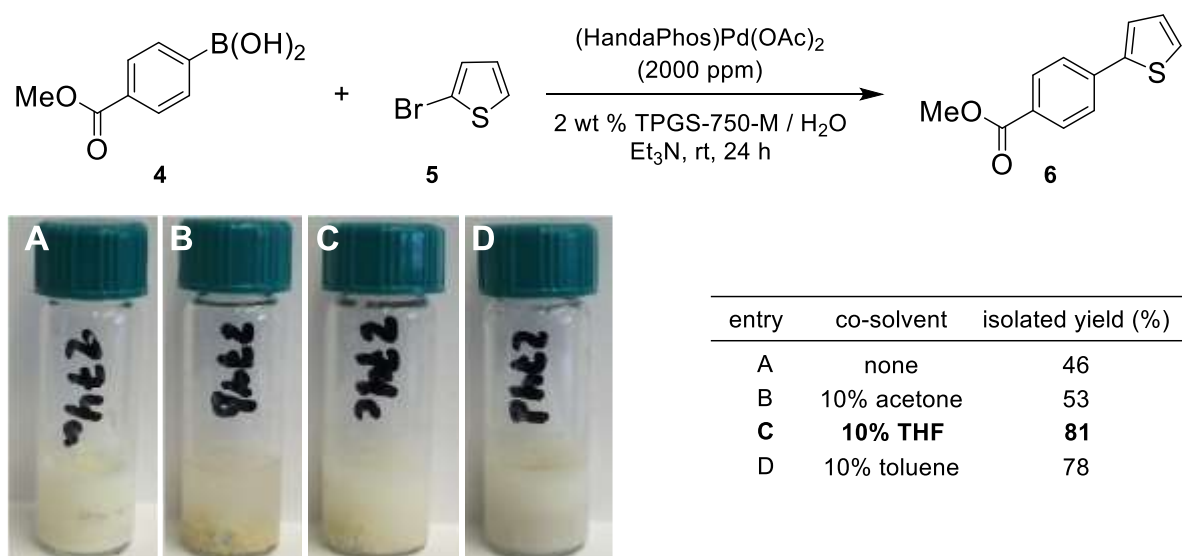


Figure 9. Impact of co-solvent on SM cross-coupling.

Miyaura Borylation.¹⁹ C-BPin bond-forming reactions may also benefit by the addition of a co-solvent, due mainly to the flocculent/crystalline nature of B₂Pin₂. This reagent has the tendency to float upon the surface of the aqueous reaction mixture, which may lead to increased reaction times and undesirable behavior at scale. Use of either 10% THF or

acetone, where the B_2Pin_2 could be added as a predissolved solution to solid educt **7**, completely eliminated this phenomenon affording product **8** (Figure 10).

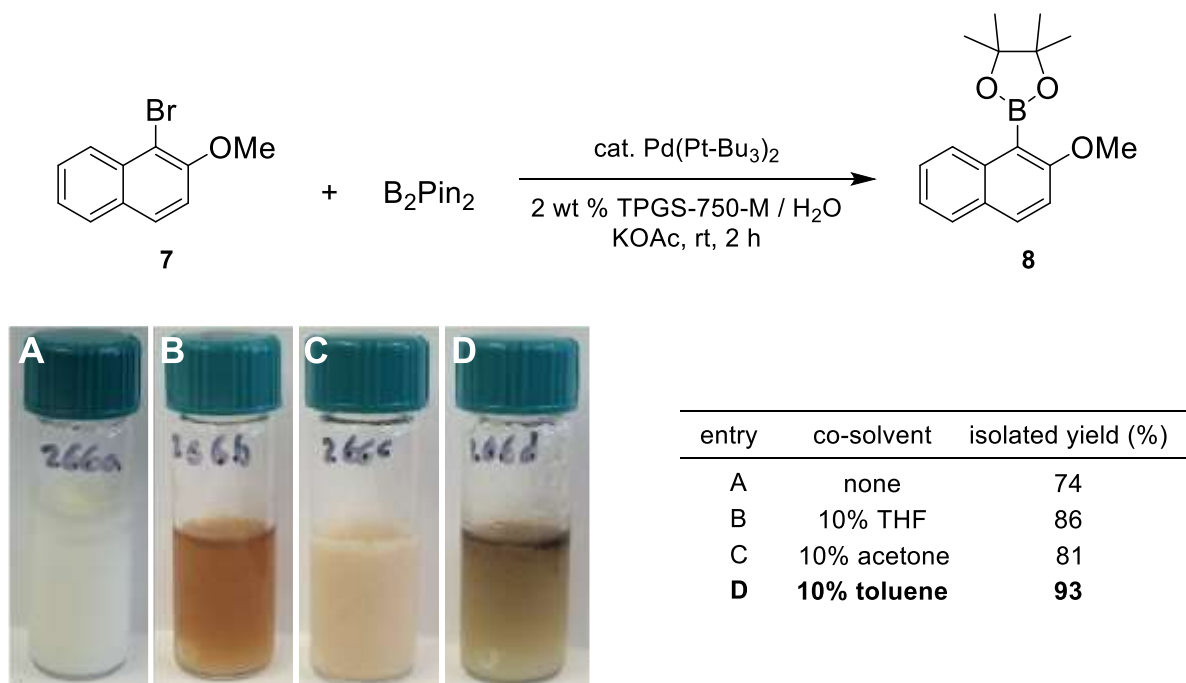
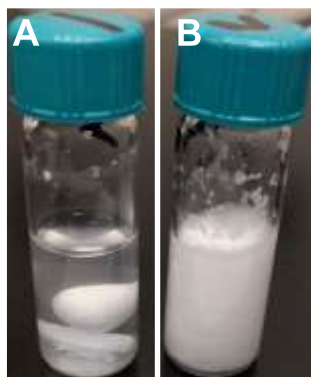
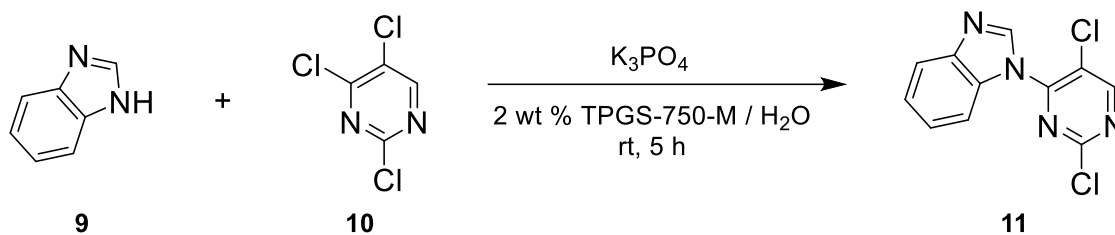


Figure 10. Miyaura borylation with co-solvents.

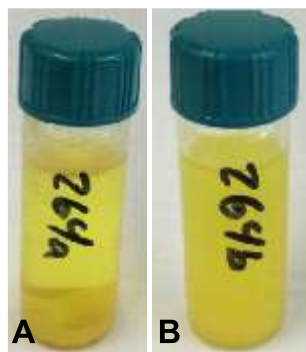
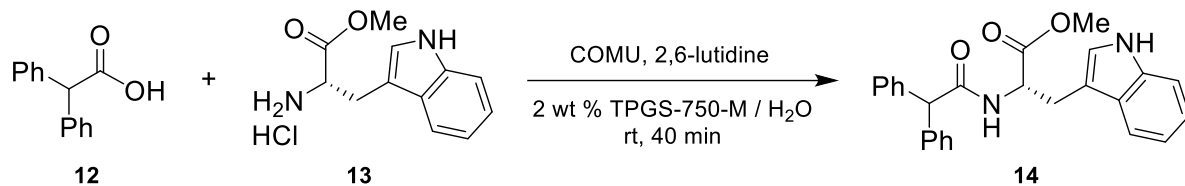
S_NAr Reactions.¹⁰ When performing these substitution reactions involving equimolar amounts of solid benzimidazole **9** and liquid 2,4,5-trichloropyrimidine, **10**, use of co-solvent led to a distinct difference in reaction appearance compared with that seen in water alone (Figure 11). Under standard S_NAr conditions, aggregation of the product was observed, and while only a modest improvement in reaction yield was achieved by the use of 15% THF, the mixture was transformed into a stable suspension, an important consideration when run at scale.



entry	co-solvent	isolated yield (%)
A	none	76
B	15% THF	80

Figure 11. Representative S_NAr reaction.

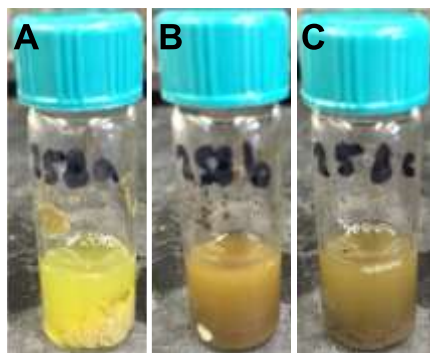
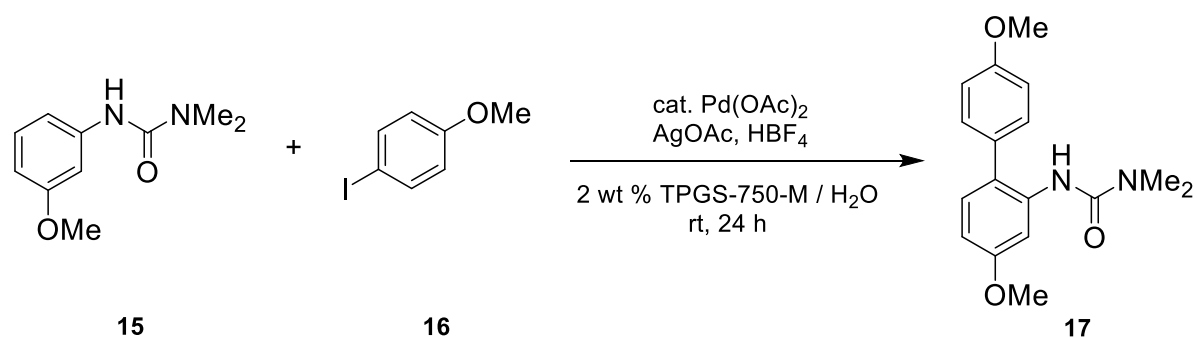
Amide Bond Formation.⁸ As a representative case, coupling of solid diphenylacetic acid, **12**, with solid *L*-tryptophan methyl ester, **13**, under standard (co-solvent-free) conditions led to conversion to amide **14**. However, precipitation of the accumulated product onto the stir bar halted stirring of the reaction mixture after only 30 min (Figure 12). This type of precipitation can grossly effect the extent of conversion, rendering these conditions unsuitable for scale-up. On the other hand, use of 10% THF leads to a stable suspension, thus allowing the reaction to stir freely and proceed to a higher degree of conversion.



entry	co-solvent	isolated yield (%)
A	none	76
B	15% THF	83

Figure 12. COMU-mediated amide bond formation.

C-H Activation.²⁰ Palladium-catalyzed C-H activation of aryl urea solid **15**, followed by coupling with solid 4-iodoanisole, **16**, afforded a higher yield in the absence of a co-solvent (Figure 13). Nonetheless, utilizing 10% THF or acetone led to freely flowing material in the reaction mixture, which also produced heavy precipitation of the product and silver salt.

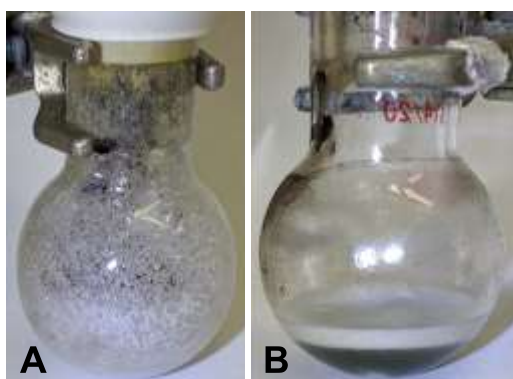
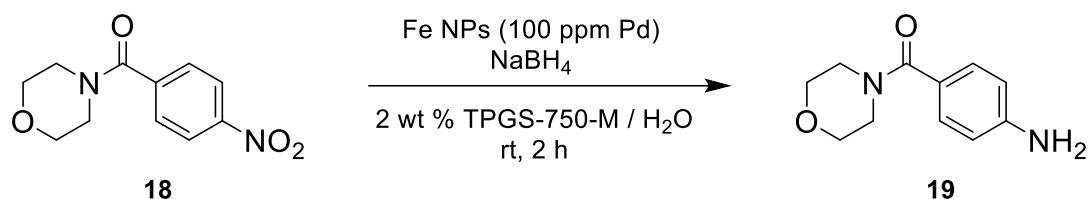


entry	co-solvent	isolated yield (%)
A	none	72
B	10% THF	59
C	10% acetone	65

Figure 13. Pd-catalyzed C-H activation.

Reductions of Nitroaromatics.¹³ Aromatic/heteroaromatic nitro compounds are often challenging substrates in general due to their limited solubility in aqueous nanomicelles, a result of their highly crystalline nature and relatively high melting points. Recently, we have disclosed a new method for efficient Fe/ppm Pd-catalyzed/ NaBH_4 nitro group reductions in water that utilizes a co-solvent to assist with highly crystalline, sparingly soluble substrates.¹³ For this system, the co-solvent not only enhances solubilization of the starting material and intermediates within the micellar core but also shows a pronounced effect on the amount of foaming resulting from the evolution of H_2 . An excellent example of this is the reduction of (solid) nitroaromatic **18** to amine **19**, where the absence of co-solvent increases nucleation sites for gas evolution leading to foaming, which can grow to occupy the entire volume of the flask (Figure 14A). When carried out with 20% THF, foaming is

negligible due to the decrease in surface tension of the solvent, leading to rapid reduction of any foam, along with greatly improved stirring (Figure 14B). Furthermore, solid precipitation is not observed throughout the course of the reaction, which in the composite affords a significant increase in yield from 84% to 95%.

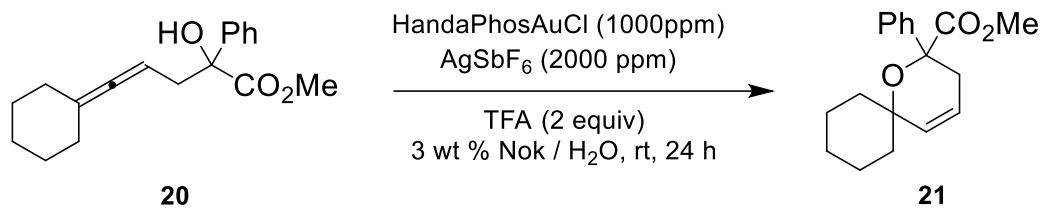


entry	co-solvent	isolated yield (%)
A	none	84
B	20% THF	95

Figure 14. Fe/ppm-Pd NP-catalyzed nitro group reduction.

Cyclizations of Allenic Alcohols. As part of a more general study on HandaPhos technology applied to ppm level Au-catalyzed reactions run under these micellar catalysis conditions, cyclization of liquid allenic alcohol **20** was effected using (HandaPhos)Au (1000 ppm, or 0.10 mol %) to produce cyclic ether **21** in good yield (Figure 15). In the same manner as ppm Pd-catalyzed SM couplings with HandaPhos, a low catalyst loading results from precomplexation in organic solvent, which is then used as a means of transferring the catalyst to the aqueous reaction mixture. For this transformation, a distinct relationship between co-solvent selection and yield was revealed. That is, the addition of 10% toluene

(but not acetone or THF) was found to increase the yield from 33% to 91%, further exemplifying the potential impact of co-solvent screening in these systems.



entry	co-solvent	isolated yield (%)
A	none	33
B	20% toluene	91

Figure 15. ppm (HandaPhos)Au(I)-catalyzed ether formation.

Notwithstanding the observed benefits associated with co-solvent usage, the question remains as to whether nanomicelles still exist in the presence of organic solvent. Insight was obtained using dynamic light scattering data acquired for samples containing TPGS-750-M in the presence of 5%, 10%, and 15% THF (Table 1). As the data illustrate, particles of initially 57 nm increase in size to ca. 100 nm, with populations becoming more diverse when compared to the control sample measured in water only. The expansion of micelles in the presence of organic solvent is expected, as solvent molecules can organize themselves within the micellar framework, causing particle growth until saturation, at which point no additional swelling is observed.²¹ These observations are in agreement with the DLS data collected (Figure 16). Likewise, particles of this surfactant also increased in size upon introduction of 15% acetone (Table 1, entry 5).

entry	co-solvent (% v/v)	ave particle size (nm)
1	none (control)	57.4
THF		
2	5.0	104.3
3	10.0	128.6
4	15.0	101.2
acetone		
5	15.0	112.7

Table 1. Average particle size of micelles + co-solvent.

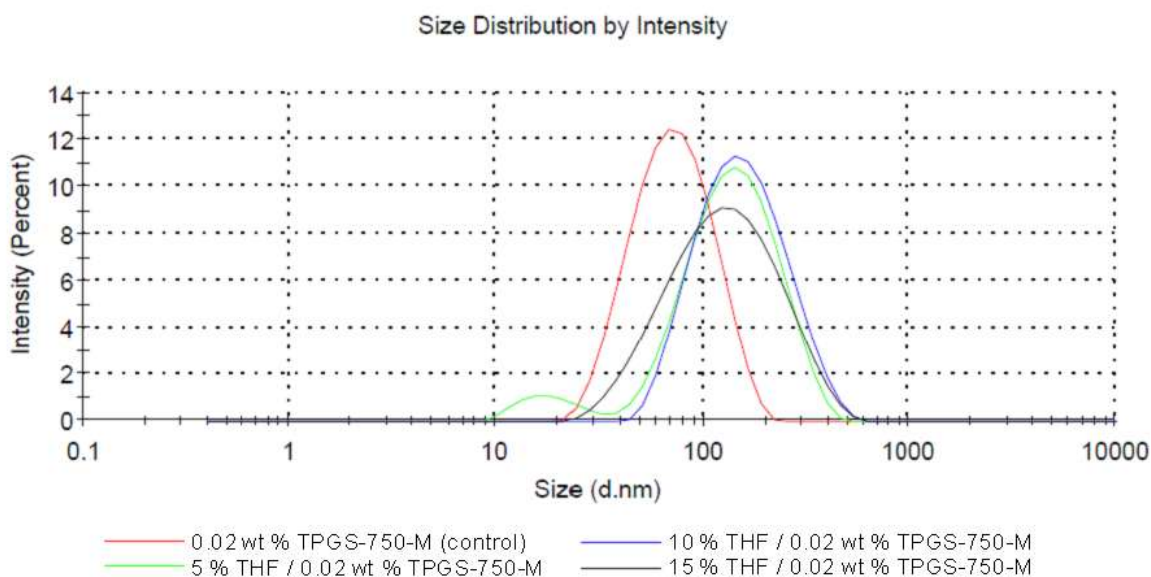
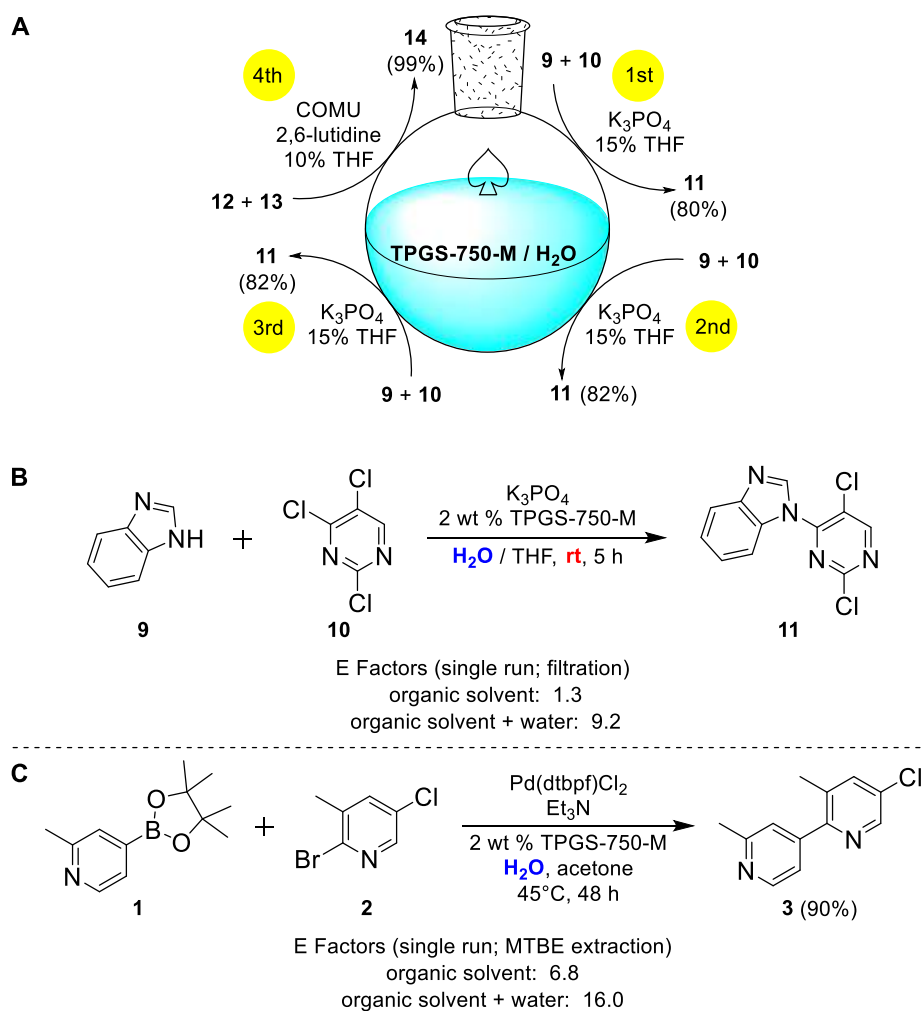


Figure 16. DLS data (particle size): TPGS-750-M/H₂O + THF.

As previously reported, the use of TPGS-750-M for micellar catalysis lends itself for the opportunity to recycle the reaction medium by simply removing organic components from the reaction via extraction with minimal EtOAc. As Scheme 1A highlights, the aqueous medium used for the S_NAr reaction to produce **11** can be recycled two additional times for the same reaction without effecting yield. Upon neutralization of the remaining aqueous

medium, a nearly quantitative yield of **14** from **12** and **13** under COMU-mediated peptide coupling conditions was obtained. And although this modification requires the addition of organic solvent to the reaction mixture, the amount of organic waste generated is still quite low when calculating Sheldon's E Factor.²² By means of a simple filtration, **11** was isolated in 80% yield resulting in an exceptionally low E Factor of 1.25. The low E Factor of 6.8 was achieved by extraction with minimal MTBE to afford **3**.



Scheme 1. Recycle and E Factor Studies.

4.4 Summary and Conclusions

In summary, use of a co-solvent as an additive to aqueous solutions containing nanomicelles derived from TPGS-750-M adds yet another dimension to micellar catalysis as an attractive alternative approach to traditional organic solvents alone as reaction media. The preferred co-solvents are THF, acetone, and PEG-200, although toluene is occasionally advantageous. These observations can help address those occasions where substrate and/or catalyst solubility may be an issue, and when various practical aspects, especially at scale,^{7,17,18,23} can otherwise be problematic. Such aqueous solutions are amenable to recycling, while DLS measurements have shown that added co-solvent enlarges the size of the nanoreactors in which the chemistry is taking place. Since the communication of the findings described above,²⁴ scale-up protocols for nitro group reductions⁷ and S_NAr reactions²³ have been published incorporating the use of co-solvent in combination with aqueous TPGS-750-M.

4.5 Experimental and Compound Data

General Information

A solution of 2 wt % TPGS-750-M/H₂O solution was prepared by dissolving TPGS-750-M in degassed HPLC grade water and was stored under argon. TPGS-750-M was made as previously described^{1a} and is available from Sigma-Aldrich (catalog #733857). All commercially available reagents were used without further purification. Thin layer chromatography (TLC) was done using Silica Gel 60 F254 plates (Merck, 0.25 mm thick). Flash chromatography was done in glass columns using Silica Gel 60 (EMD, 40-63 μm) or with pre-packed 25 gram KP-Sil Biotage[®] SNAP Cartridges on the Biotage[®] Isolera Prime autocolumn. ¹H and ¹³C NMR were recorded at 22 °C on a Varian UNITY INOVA at

600MHz and 500 MHz. Chemical shifts in ^1H NMR spectra are reported in parts per million (ppm) on the δ scale from an internal standard of residual CDCl_3 (7.27 ppm). Data are reported as follows: chemical shift, multiplicity (s = singlet, d = doublet, t = triplet, q = quartet, quin = quintet), and integration. Chemical shifts in ^{13}C chemical spectra are reported in ppm on the δ scale from the central peak of residual CDCl_3 (77.00 ppm). IR data were collected on a Perkin Elmer Spectrum Two UATR FT-IR Spectrometer and peaks were described according to relative intensity and resolution as follows: s = strong, m = medium, w = weak, br = broad. Dynamic Light Scattering (DLS) data were collected using a Malvern Zetasizer ZS equipped with 173° backscatter detection and a He-Ne, 4 mW, 633 nm red laser.

Suzuki-Miyaura Cross Coupling Procedures

A 1-dram vial with a Teflon coated magnetic stir bar under argon atmosphere was charged with $\text{PdCl}_2(\text{dtbpf})$ (6.5 mg, 0.01 mmol), 98% 2-bromo-5-chloro-3-methylpyridine, **2**, (105.3 mg, 0.5 mmol), 2-methyl-4-(4,4,5,5-tetramethyl-1,3,2-dioxaborolan-2-yl)pyridine, **1**, (169.4 mg, 0.75 mmol), and acetone (0.1 mL) and stirred for 5 min at rt. TPGS-750-M/ H_2O (2 wt %, 0.9 mL) and Et_3N (0.21 mL, 1.5 mmol) were then charged into the reaction and allowed to stir at 45°C for ca. 31 h. The reaction mixture was extracted with 3 x 2 mL EtOAc, dried over anhydrous Na_2SO_4 , filtered, condensed via rotary evaporation, and purified by column chromatography eluting with hexanes/EtOAc to afford 5-chloro-2',3-dimethyl-2,4'-bipyridine, **3**, as a white solid (186 mg, 85% yield).

A 1-dram vial with a Teflon coated magnetic stir bar under argon atmosphere was charged with $\text{Pd}(\text{OAc})_2$ (2.1 mg, 0.0094 mmol), HandaPhos (5.6 mg, 0.0103 mmol), and toluene (0.94 mL). The solution was allowed to stir for 15 min at 23°C . An aliquot (0.25 mL) of this mixture was transferred to a 1-dram vial, stripped of toluene under reduced

pressure, and then dissolved in the corresponding co-solvent (0.25 mL) when appropriate. For the control (no co-solvent), the reaction components were added directly to the vial containing 2000 ppm (0.20 mol %) concentrated Pd/HandaPhos complex in the order described below. A 1-dram vial with a Teflon coated magnetic stir bar under argon atmosphere was charged with 2-bromothiophene, **5**, (81.5 mg, 0.5 mmol), (4-(methoxycarbonyl)phenyl)boronic acid, **4**, (99.0 mg, 1.1 mmol), bis(pinacolato)diboron (380.9 mg, 1.5 mmol), and 2 wt % TPGS-750-M/H₂O (0.9 mL). The mixture was stirred for 10 min before introducing Et₃N (0.14 mL, 1.0 mmol). After stirring for an additional 5 min, Pd/HandaPhos solution in co-solvent (0.1 mL, 0.001 mmol) was added and the reaction stirred for 24 h at 23 °C. The reaction mixture was then extracted with 3 x 2 mL EtOAc, dried over anhydrous Na₂SO₄, filtered, condensed via rotary evaporation, and purified by column chromatography eluting with hexanes/Et₂O to afford methyl 4-(thiophen-2-yl)benzoate, **6**, as a white solid (177 mg, 81% yield).

Miyaura Borylation Procedure

A 1-dram vial with a Teflon coated magnetic stir bar under argon atmosphere was charged with Pd(P-*t*-Bu₃)₂ (7.7 mg, 0.015 mmol), KOAc (122.7 mg, 1.25 mmol), bis(pinacolato)diboron (380.9 mg, 1.5 mmol), and co-solvent (0.3 mL). After stirring for 2 min, 2 wt % TPGS-750-M/H₂O (1.7 mL) was charged into the mixture and allowed to stir for 10 min before adding 1-bromo-2-methoxynaphthalene, **7**, (118.6 mg, 0.5 mmol) in 3 portions over 1 h (~40 mg every 30 min). The reaction was then stirred for ca. 2 h after the final portion of **7** had been added. The reaction mixture was extracted with 3 x 2 mL EtOAc, dried over anhydrous Na₂SO₄, filtered, condensed via rotary evaporation, and purified by column chromatography eluting with hexanes/Et₂O to afford 2-(2-methoxynaphthalen-1-yl)-4,4,5,5-tetramethyl-1,3,2-dioxaborolane, **8**, as a white solid (133 mg, 93% yield).

SNAr Procedure

A 1-dram vial with a Teflon coated magnetic stir bar was charged with K_3PO_4 (254 mg, 1.2 mmol) and 98% benzimidazole, **9**, (120.4 mg, 1 mmol). The vial was flushed with argon and charged with 2 wt % TPGS-750-M/ H_2O [1.7 mL (with co-solvent); 2.0 mL (without co-solvent)], 97% 2,4,5-trichloropyrimidine, **10**, (118.2 μ L, 1.0 mmol), and THF (0.3 mL). The reaction stirred for ca. 5 h after which the reaction mixture was extracted with 3 x 2 mL EtOAc. The organic extracts were combined, dried over anhydrous Na_2SO_4 , filtered, condensed via rotary evaporation, and purified by flash chromatography eluting with hexanes/EtOAc to afford 1-(2,5-dichloropyrimidin-4-yl)-1H-benzo[d]imidazole, **11**, as a white solid (212 mg, 80% yield).

Amide Bond Formation Procedure

A 1-dram vial with a Teflon coated magnetic stir bar was charged with diphenylacetic acid, **12**, (116.7 mg, 0.55 mmol), 2 wt % TPGS-750-M/ H_2O (2.7 mL), 2,6-lutidine (0.18 mL, 1.55 mmol), and THF (0.3 mL). After stirring for 5 min, a solution was achieved and *L*-tryptophan methyl ester hydrochloride, **13**, (127.4 mg, 0.5 mmol) was added followed by the quick addition of COMU (321.2 mg, 0.75 mmol). The reaction was then stirred for ca. 40 min and then extracted with 3 x 2 mL EtOAc. The organic extracts were combined, washed with 2 M HCl (6 mL), saturated Na_2CO_3 solution (3 x 6 mL), dried over anhydrous Na_2SO_4 , filtered, condensed via rotary evaporation, and purified by flash chromatography eluting with hexanes/EtOAc to afford methyl (2,2-diphenylacetyl)-*L*-tryptophanate, **14**, as a white solid (172 mg, 83% yield).

C-H Activation Procedure

A 1-dram vial with a Teflon coated magnetic stir bar was charged with 3-(3-methoxyphenyl)-1,1-dimethylurea, **15**, (97.1 mg, 0.5 mmol), 1-iodo-4-methoxybenzene, **16**,

(234.0 mg, 1.0 mmol), Pd(OAc)₂ (11.2, 0.05 mmol) and co-solvent (0.2 mL). After stirring for 2 min, 2 wt % TPGS-750-M/H₂O (1.8 mL) was charged into the mixture and 48 wt % HBF₄ solution (1.25 mmol, 0.16 mL) was added by syringe and vigorously stirred for ca. 20 h. After completion, the contents of the flask were quenched with NaHCO₃ and extracted with EtOAc (3 x 2 mL). The solution obtained was filtered through a plug of silica gel and anhydrous MgSO₄, and concentrated by rotary evaporation. The residue was purified by flash chromatography eluting with hexanes/EtOAc to afford 3-(4,4'-dimethoxy-[1,1'-biphenyl]-2-yl)-1,1-dimethylurea, **17**, the product as an off-white solid (108 mg, 72% yield).

Nitro Group Reduction Procedure

A 10 mL round bottom flask with a Teflon coated magnetic stir bar was charged with Fe/ppm Pd nanoparticles (FeNPs; 10 mg, 0.071 μmol) and morpholino(4-nitrophenyl)methanone, **18**, (118 mg, 0.5 mmol). The flask was flushed with argon and charged with THF (0.2 mL), stirred, and then 2 wt % TPGS-750-M/H₂O (0.8 mL, with co-solvent trial) was added; or 1.0 mL 2 wt % TPGS-750-M/H₂O (without co-solvent trial). After briefly stirring, the flask was charged with NaBH₄ (113 mg, 3 mmol). The reaction was stirred for 2 h, then the reaction mixture was extracted with 3 x 1 mL EtOAc (in the co-solvent trials, compressed air was briefly blown across the surface of the reaction to remove some co-solvent prior to extraction). The organic extracts were combined, dried over anhydrous Na₂SO₄, filtered, concentrated by rotary evaporation, and purified by flash chromatography eluting with 100% EtOAc to afford (4-aminophenyl)(morpholino)methanone, **19**, as an off-white solid (99 mg, 96% yield).

Allenic Alcohol Cyclization

To a 1-dram vial equipped with Teflon-coated magnetic stir bar, 100 μL of gold pre-catalyst in DCM (1000 ppm or 0.1 mol %) was added and the DCM was removed under

reduced pressure. Hydroxyallene **20** (28 mg, 0.1 mmol) was added to the vial followed by toluene (200 μ L), 3 wt % Nok / H₂O (0.2 mL), and trifluoroacetic acid (23 mg, 0.2 mmol). The resulting mixture was stirred at rt for ca. 24 h. After completion, the product was extracted with EtOAc (3 x 0.1 mL), and concentrated by rotary evaporation. The residue was purified by flash chromatography eluting with hexanes/EtOAc to afford methyl 2-phenyl-1-oxaspiro[5.5]undec-4-ene-2-carboxylate, **21**, as a colorless liquid (26 mg, 91% yield).

Aqueous Surfactant Recycling Procedures

Reaction A (S_NAr). A microwave vial with a Teflon coated magnetic stir bar was charged with K₃PO₄ (254 mg, 1.2 mmol) and 98% benzimidazole, **9**, (120.4 mg, 1 mmol). The vial was flushed with argon and charged with 2 wt % TPGS-750-M/H₂O (1.7 mL), 97% 2,4,5-trichloropyrimidine, **10**, (118.2 μ L, 1.0 mmol), and THF (0.3 mL). The reaction stirred for ca. 5 h and the reaction mixture was then extracted with 3 x 2 mL EtOAc. The organic extracts were combined, dried over anhydrous Na₂SO₄, filtered, condensed via rotary evaporation, and purified by flash chromatography eluting with hexanes/EtOAc to afford 1-(2,5-dichloropyrimidin-4-yl)-1H-benzo[d]imidazole, **11**, as a white solid (212.1 mg, 80% yield).

Reaction B (1st Recycle, S_NAr). The microwave vial was briefly opened and charged with K₃PO₄ (254 mg, 1.2 mmol) and 98% benzimidazole, **9**, (120.4 mg, 1 mmol). The vial was flushed with argon and charged with 2 wt % TPGS-750-M/H₂O (1.7 mL), 97% 2,4,5-trichloropyrimidine, **10**, (118.2 μ L, 1.0 mmol), and THF (0.3 mL). The reaction stirred for ca. 8 h and the reaction mixture was extracted with 3 x 2 mL EtOAc. The organic extracts were combined, dried over anhydrous Na₂SO₄, filtered, condensed via rotary evaporation, and purified by flash chromatography eluting with hexanes/EtOAc to afford 1-(2,5-dichloropyrimidin-4-yl)-1H-benzo[d]imidazole, **11**, as a white solid (217.4 mg, 82% yield).

Reaction C (2nd Recycle, S_NAr). The microwave vial was briefly opened and charged with K₃PO₄ (254 mg, 1.2 mmol) and 98% benzimidazole, **9**, (120.4 mg, 1 mmol). The vial was flushed with argon and charged with 2 wt % TPGS-750-M/H₂O (1.7 mL), 97% 2,4,5-trichloropyrimidine, **10**, (118.2 μL, 1.0 mmol), and THF (0.3 mL). The reaction stirred for ca. 8 h and the reaction mixture was extracted with 3 x 2 mL EtOAc. The organic extracts were combined, dried over anhydrous Na₂SO₄, filtered, condensed via rotary evaporation, and purified by flash chromatography eluting with hexanes/EtOAc to afford 1-(2,5-dichloropyrimidin-4-yl)-1H-benzo[d]imidazole, **12**, as a white solid (216.7 mg, 82% yield).

Reaction D (3rd Recycle, amide bond formation). The microwave vial was briefly opened and charged with 0.16 mL 2 M HCl (final pH = 6-7), followed by diphenylacetic acid, **13**, (70.0 mg, 0.33 mmol), 2,6-lutidine (0.11 mL, 0.93 mmol), and THF (0.18 mL). After stirring for 5 min, a solution was achieved and *L*-tryptophan methyl ester hydrochloride (76.4 mg, 0.3 mmol) was added followed by the quick addition of COMU (192.7 mg, 0.45 mmol). The reaction stirred for ca. 1 h and the reaction mixture was extracted with 3 x 2 mL EtOAc. The organic extracts were combined, washed with 2 M HCl (6 mL), saturated Na₂CO₃ solution (3 x 6 mL), dried over anhydrous Na₂SO₄, filtered, condensed via rotary evaporation, and purified by flash chromatography eluting with hexanes/EtOAc to afford methyl (2,2-diphenylacetyl)-*L*-tryptophanate, **15**, as a white solid (123.7 mg, 99% yield).

E Factor Procedures and Calculations

A 1-dram vial with a Teflon coated magnetic stir bar under argon atmosphere was charged with PdCl₂(dtbpf) (6.5 mg, 0.01 mmol), 98% 2-bromo-5-chloro-3-methylpyridine, **2**, (105.3 mg, 0.5 mmol), 2-methyl-4-(4,4,5,5-tetramethyl-1,3,2-dioxaborolan-2-yl)pyridine, **1**, (169.4 mg, 0.75 mmol), and acetone (0.1 mL) and then stirred for 5 min at rt. TPGS-750-

M/H₂O (2 wt %; 0.9 mL) and Et₃N (0.21 mL, 1.5 mmol) were then charged into the reaction and the mixture allowed to stir at 45 °C for ca. 48 h. The reaction was then stirred for ca. 30 min under a stream of Ar at 45 °C to remove acetone, followed by extraction with 2 x 0.4 mL MTBE. The organic extracts were dried over anhydrous Na₂SO₄, filtered, condensed via rotary evaporation, and purified by column chromatography eluting with hexanes/EtOAc to afford 5-chloro-2',3-dimethyl-2,4'-bipyridine, **3**, as a white solid (98.2 mg, 90%).

E Factor Calculations (without water):

$$\text{E Factor} = (\text{Mass of Organic Waste}) / (\text{Mass of Product})$$

$$\text{Mass of Organic Waste} = (0.8 \text{ mL MTBE})(0.740 \text{ g/mL}) + (0.1 \text{ mL acetone})(0.791 \text{ g/mL}) = 671 \text{ mg}$$

$$\text{Mass of Product} = 98.2 \text{ mg}$$

$$\text{E Factor} = (671 \text{ mg}) / (98.2 \text{ mg}) = \mathbf{6.8}$$

E Factor Calculations (with water):

$$\text{E Factor} = (\text{Mass of Organic Waste} + \text{Aqueous Waste}) / (\text{Mass of Product})$$

$$\text{Mass of Water} = (0.9 \text{ mL}) (1.0 \text{ g/mL}) = 900 \text{ mg}$$

$$\text{E Factor} = (671 \text{ mg} + 900 \text{ mg}) / (98.2 \text{ mg}) = \mathbf{16.0}$$

A microwave vial with Teflon coated magnetic stir bar was charged with K₃PO₄ (254 mg, 1.2 mmol) and 98% benzimidazole, **9**, (120.4 mg, 1 mmol). The vial was flushed with argon and charged with 2 wt % TPGS-750-M/H₂O (1.7 mL), 97% 2,4,5-trichloropyrimidine, **10**, (118.2 μL, 1.0 mmol), and THF (0.3 mL). The reaction was stirred for ca. 5 h and then extracted with 3 x 2 mL EtOAc. The organic extracts were combined, dried over anhydrous Na₂SO₄, filtered, condensed via rotary evaporation, and purified by flash chromatography

eluting with hexanes/EtOAc to afford 1-(2,5-dichloropyrimidin-4-yl)-1H-benzo[d]imidazole, **11**, the product as a white solid (213.3 mg, 80% yield).

E Factor Calculations (without water):

$$\text{E Factor} = (\text{Mass of Organic Waste}) / (\text{Mass of Product})$$

$$\text{Mass of Organic Waste} = (0.30) \text{ mL THF } (0.889 \text{ g/mL}) = 266.7 \text{ mg}$$

$$\text{Mass of Product} = 213.3 \text{ mg}$$

$$\text{E Factor} = (266.7 \text{ mg}) / (213.3 \text{ mg}) = \mathbf{1.3}$$

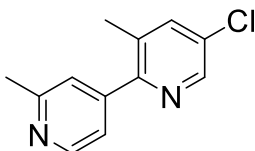
E Factor Calculations (with water):

$$\text{E Factor} = (\text{Mass of Organic Waste} + \text{Aqueous Waste}) / (\text{Mass of Product})$$

$$\text{Mass of Water} = (1.7 \text{ mL}) (1.0 \text{ g/mL}) = 1700 \text{ mg}$$

$$\text{E Factor} = (266.7 \text{ mg} + 1700 \text{ mg}) / (213.3 \text{ mg}) = \mathbf{9.2}$$

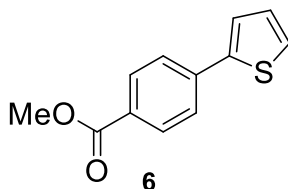
Characterization of Products



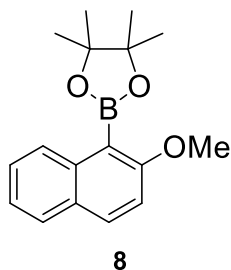
3

5-Chloro-2',3-dimethyl-2,4'-bipyridine (3). R_f 0.27 (1:1 EtOAc/hexanes); white solid, mp 63-64 °C, 186 mg (85%). ^1H NMR (500 MHz, CDCl_3) δ 8.52 (d, 1H), 8.43 (d, 1H), 7.55 (dd, 1H), 7.24 (s, 1H), 7.15 (d, 1H), 2.56 (s, 3H), 2.29 (s, 3H); ^{13}C NMR (101 MHz, CDCl_3) δ 158.54, 154.06, 148.90, 147.07, 145.84, 138.02, 132.23, 131.06, 122.91, 120.44, 24.37, 19.51. IR (neat): ν = 3392 (br), 3042 (m), 3011 (m), 2960 (m), 2923 (m), 2870 (w), 1604 (s),

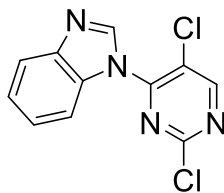
1575 (m), 1541 (s), 1451 (s), 1426 (s). HRMS (EI, [C₁₂H₁₁ClN₂ - H]) calcd. 217.0538, found *m/z* 217.0529.



Methyl 4-(thiophen-2-yl)benzoate (6). *R_f* 0.31 (1:9 EtOAc/hexanes); mp 132-133 °C, 177 mg, (81%). ¹H NMR (500 MHz, CDCl₃) δ 8.05 (dt, 2H), 7.68 (dt, 2H), 7.43 (dd, 1H), 7.37 (dd, 1H), 7.13 (dd, 1H), 3.94 (s, 3H); ¹³C NMR (101 MHz, CDCl₃) δ 166.73, 138.59, 130.24, 128.72, 128.29, 126.27, 125.49, 124.45, 123.58, 52.13. IR (neat) ν = 3099 (m), 3076 (m), 2991 (w), 2947 (m), 2848 (w), 1714 (s), 1605 (m), 1283 (s), 1114 (s). HRMS (EI, [C₁₂H₁₀O₂S]) calcd. 218.0402, found *m/z* 218.0397.

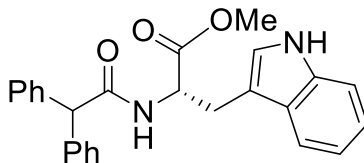


2-(2-Methoxynaphthalen-1-yl)-4,4,5,5-tetramethyl-1,3,2-dioxaborolane (8). *R_f* 0.20 (15:85 diethyl ether/hexanes); mp 93-94 °C, 133 mg (93%). ¹H NMR (500 MHz, CDCl₃) δ 7.94 (d, 1H), 7.86 (d, 1H), 7.77 (d, 1H), 7.45 (m, 1H), 7.32 (m, 1H), 7.23 (d, 1H), 3.93 (s, 3H), 1.50 (s, 12H); ¹³C NMR (101 MHz, CDCl₃) δ 161.41, 137.04, 131.60, 128.83, 128.09, 126.75, 126.50, 123.25, 112.81, 83.90, 56.56, 24.88. IR (neat) ν = 3055 (w), 2976 (m), 2932 (m), 2837 (w), 1620 (m), 1589 (m), 1576 (m), 1144 (s), 1132 (s). ¹H & ¹³C NMR was in agreement with previously reported data on this compound.²⁵



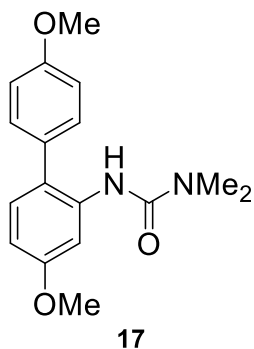
11

1-(2,5-Dichloropyrimidin-4-yl)-1H-benzo[d]imidazole (11). R_f 0.27 (4:6 EtOAc/hexanes); white solid, mp 150-152 °C, 212 mg (80%). ^1H NMR (500 MHz, CDCl_3) δ 8.178 (s, 1H), 8.76 (s, 1H), 8.01 (m, 1H), 7.87 (m, 1H), 7.44 (m, 2H); ^{13}C NMR (101 MHz, CDCl_3) δ 161.50, 158.78, 153.65, 143.41, 140.90, 131.83, 125.27, 124.77, 120.80, 119.74, 114.22. IR (neat) ν = 3145 (w), 3126 (w), 1528 (m), 1425 (m), 1365 (m), 1150 (s), 1133 (s), 748 (s). HRMS (EI, $[\text{C}_{11}\text{H}_6\text{Cl}_2\text{N}_4]$) calcd 263.997, found m/z 263.996.

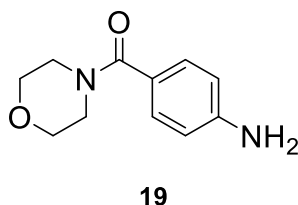


14

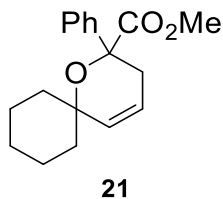
Methyl (2,2-diphenylacetyl)-L-tryptophanate (14). R_f 0.38 (1:1 EtOAc/hexanes); mp 62-64 °C, 172 mg (83%). ^1H NMR (500 MHz, CDCl_3) δ 8.35 (s, 1H), 7.43 (d, 1H), 7.34-7.22 (m, 2H), 7.65 (m, 9H), 7.20 (m, 1H), 7.16-7.12 (m, 2H), 7.08 (m, 1H), 6.57 (d, 1H), 6.23 (d, 1H), 5.02 (dt, 1H), 4.89 (s, 1H), 4.89 (s, 1H), 3.69 (s, 3H), 3.28 (d, 2H); ^{13}C NMR (101 MHz, CDCl_3) δ 172.12, 171.66, 138.96, 138.91, 135.98, 128.85, 128.70, 128.61, 128.56, 127.20, 127.16, 127.07, 122.79, 121.96, 119.49, 118.28, 111.24, 109.12, 58.78, 52.78, 52.28, 27.27. IR (neat) ν = 3409 (br), 3313 (br), 3060 (w), 3028 (w), 2951 (w), 2925 (w), 2851 (w), 1507 (s), 1656 (s). HRMS (EI, $[\text{C}_{26}\text{H}_{24}\text{N}_2\text{O}_3]$) calcd. 412.1787, found m/z 412.1780.



3-(4,4'-Dimethoxy-[1,1'-biphenyl]-2-yl)-1,1-dimethylurea (17). R_f 0.22 (1:1 EtOAc/hexanes); mp 131-133 °C, 108 mg (72%). ^1H NMR (500 MHz, CDCl_3) δ 7.94 (d, 1H), 7.27 (dt, 2H), 7.06 (d, 1H), 6.99 (dt, 2H), 6.64-6.59 (m, 2H), 3.85 (2 x s, 6H), 2.81 (s, 6H); ^{13}C NMR (125 MHz, CDCl_3) δ 159.45, 158.92, 155.29, 137.44, 130.58, 130.44, 130.30, 123.01, 114.38, 109.10, 104.21, 55.30, 55.25, 36.13. IR (neat) ν = 3439 (w), 3015 (w), 2938 (w), 2838 (w), 1666 (m). ^1H & ^{13}C NMR were in agreement with previously reported data on this compound.²⁰

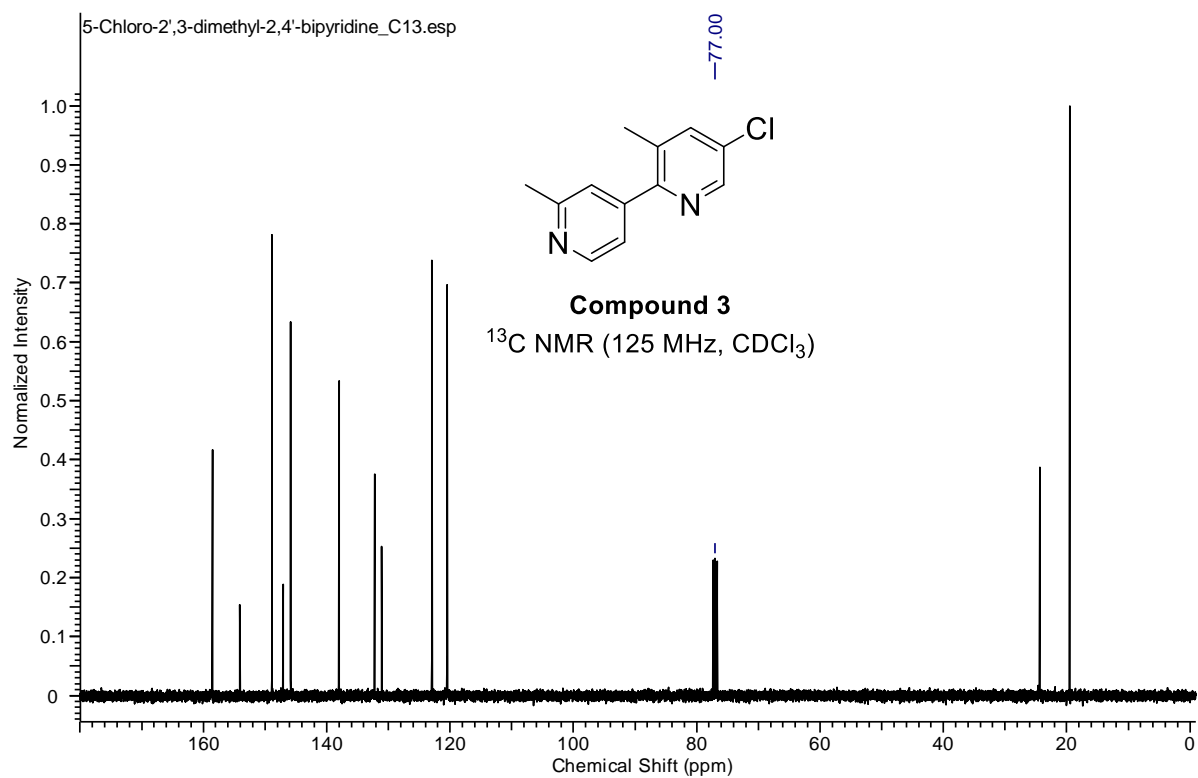
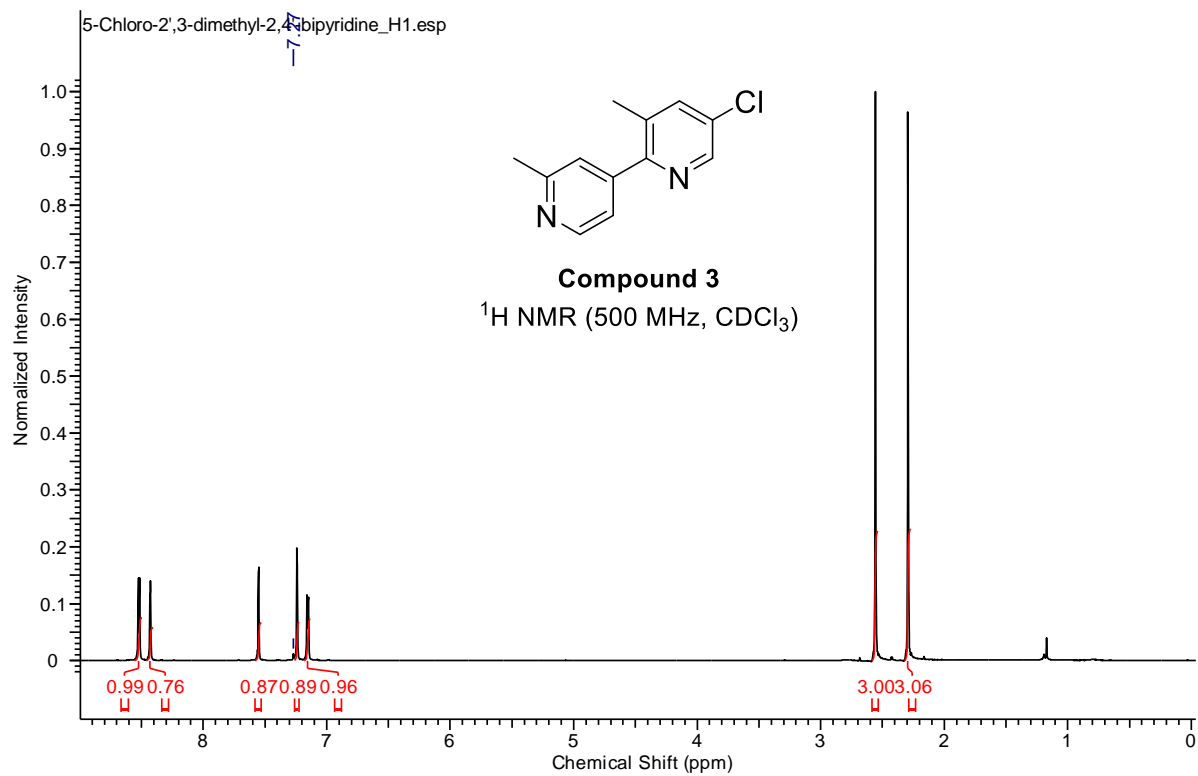


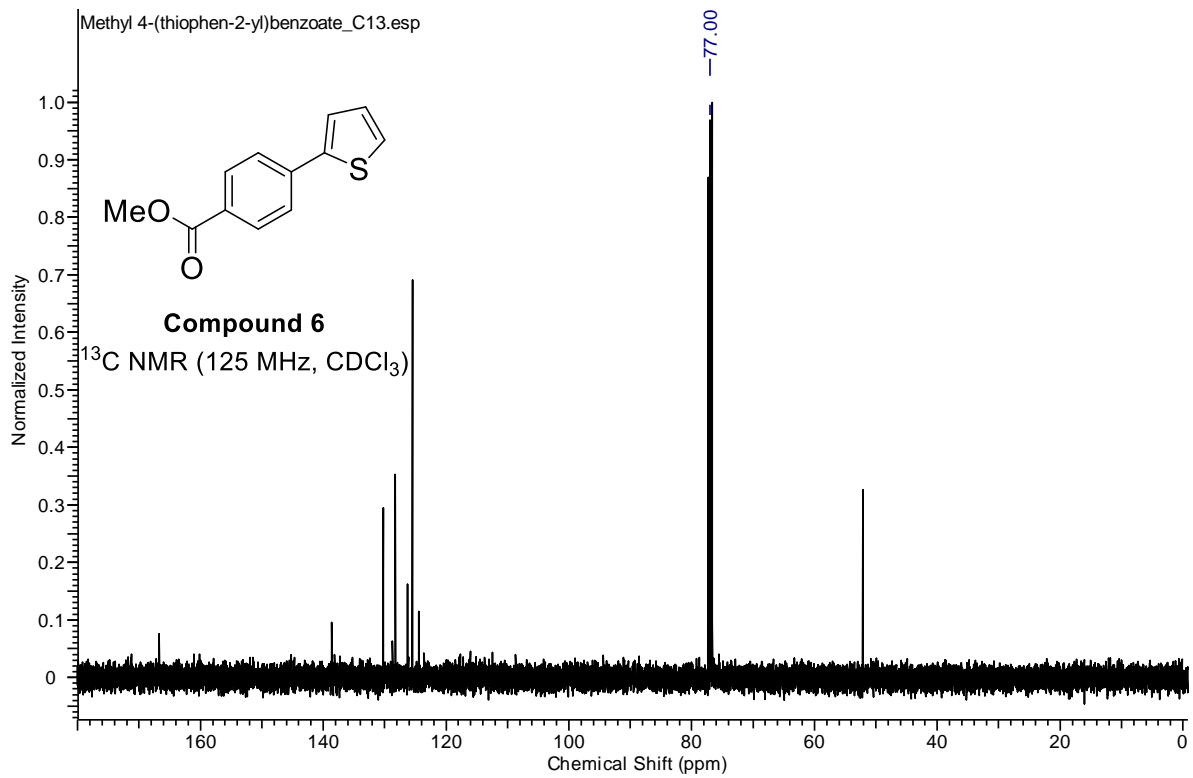
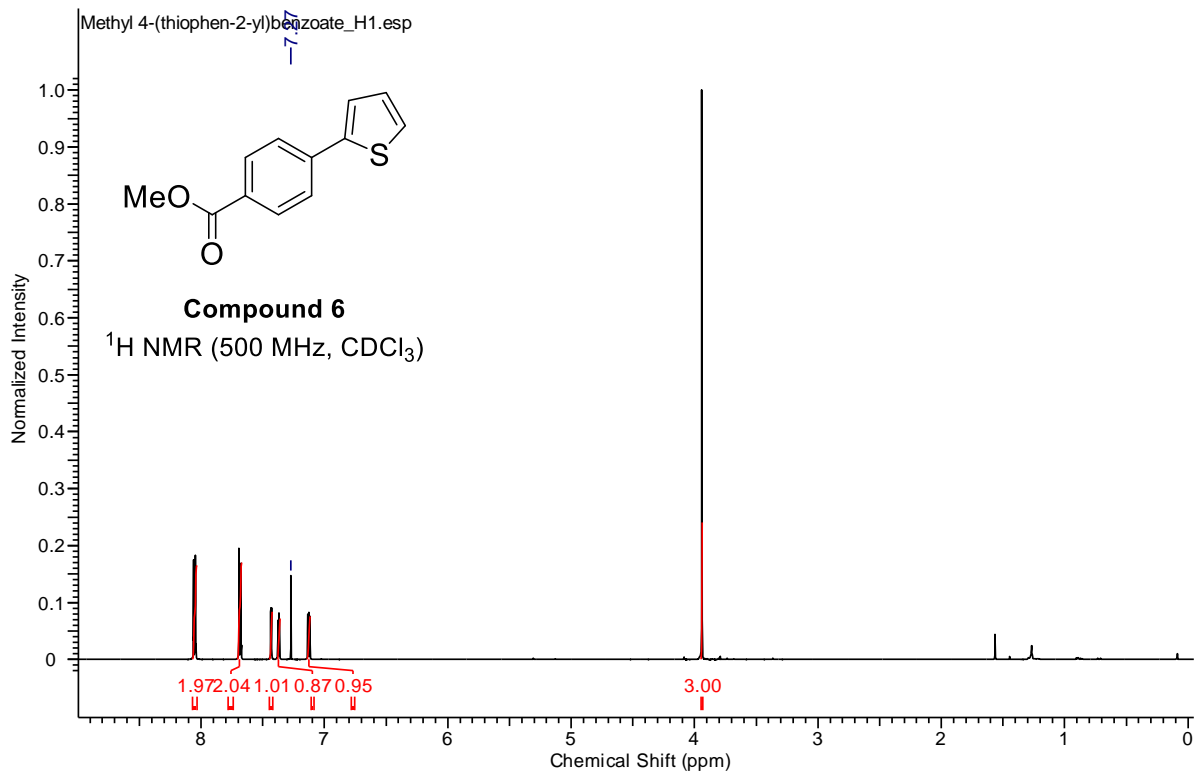
(4-Aminophenyl)(morpholino)methanone (19). R_f 0.3 (EtOAc); off-white solid, mp 129-131 °C, 99 mg (96%). ^1H NMR (600 MHz, CDCl_3) δ 7.23 (d, 2H), 6.61 (d, 2H), 3.90 (s, 2H), 3.66 (s, 4H), 3.61 (s, 4H). ^{13}C NMR (101 MHz, CDCl_3) δ 170.83, 148.28, 129.33, 124.39, 114.12, 66.90. IR (neat) ν = 3418 (m), 3330 (m), 3222 (m), 2980 (w), 2921 (m), 2866 (m), 1592 (s), 1428 (m), 1257 (m), 1103 (m). HRMS (EI, $[\text{C}_{11}\text{H}_{14}\text{N}_2\text{O}_2]$) calcd. 206.1055 found m/z 206.1050. ^1H and ^{13}C NMR were in agreement with previously reported data on this compound.²⁶

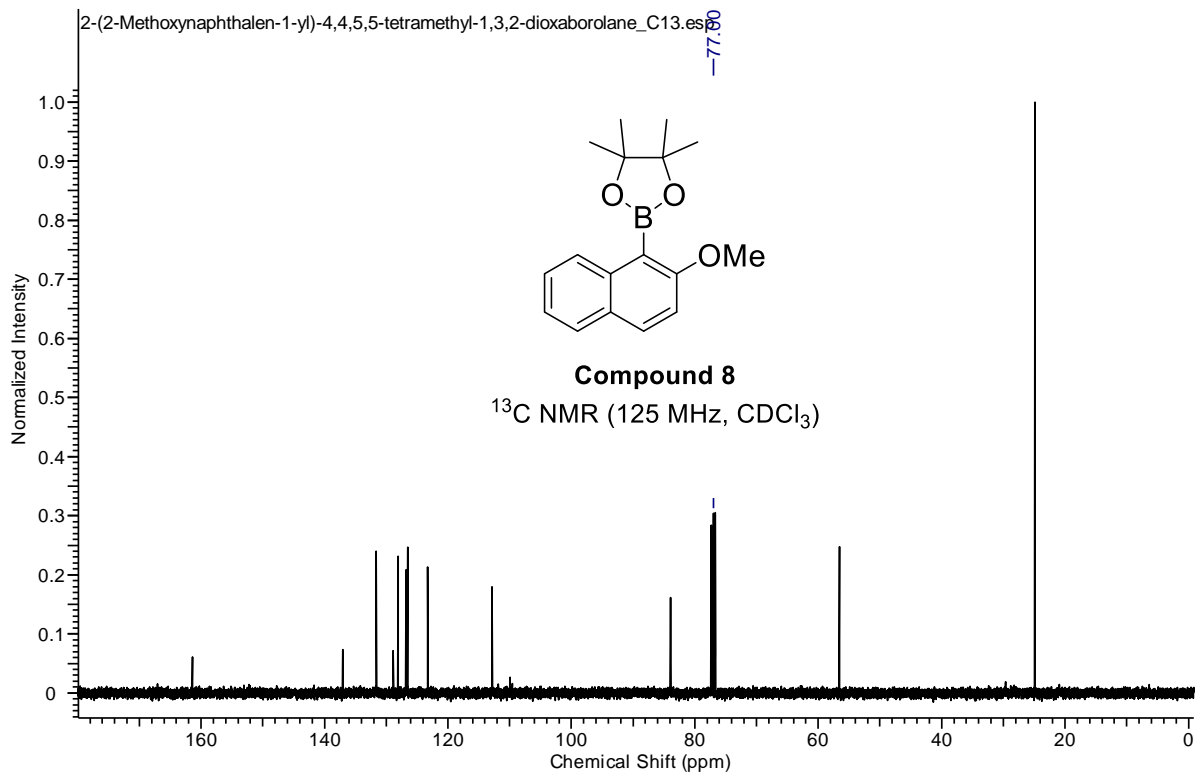
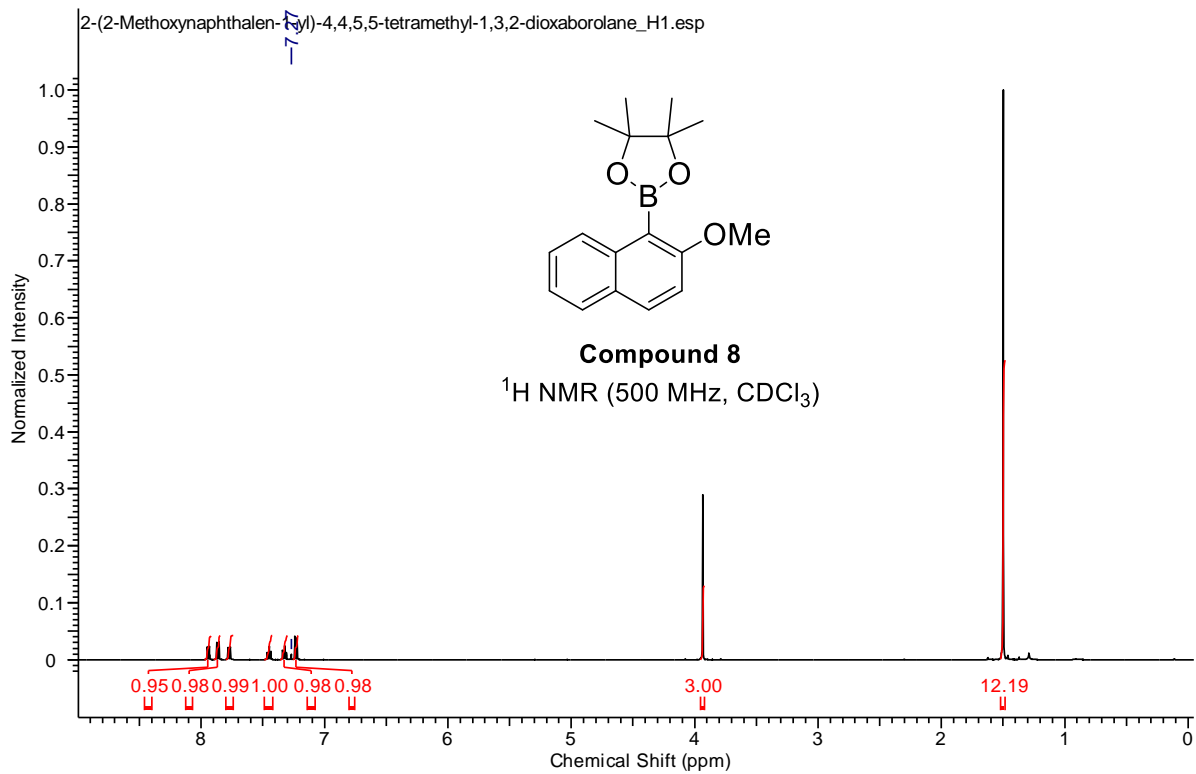


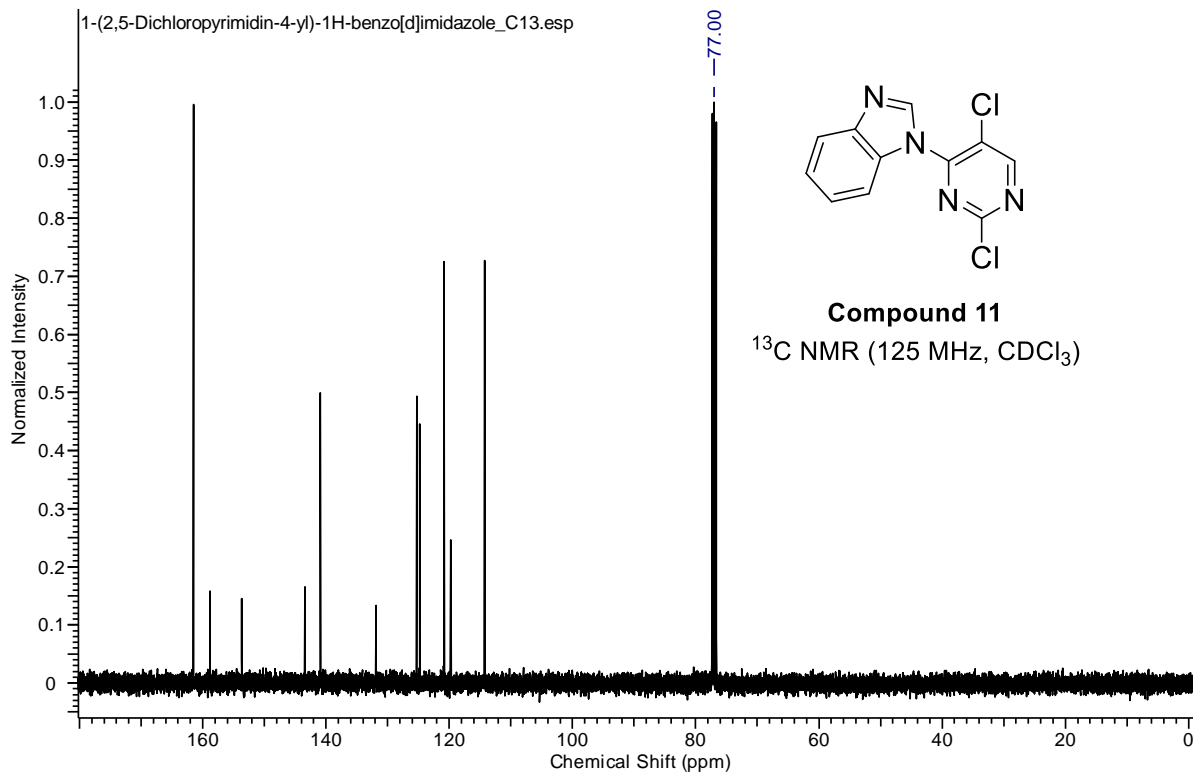
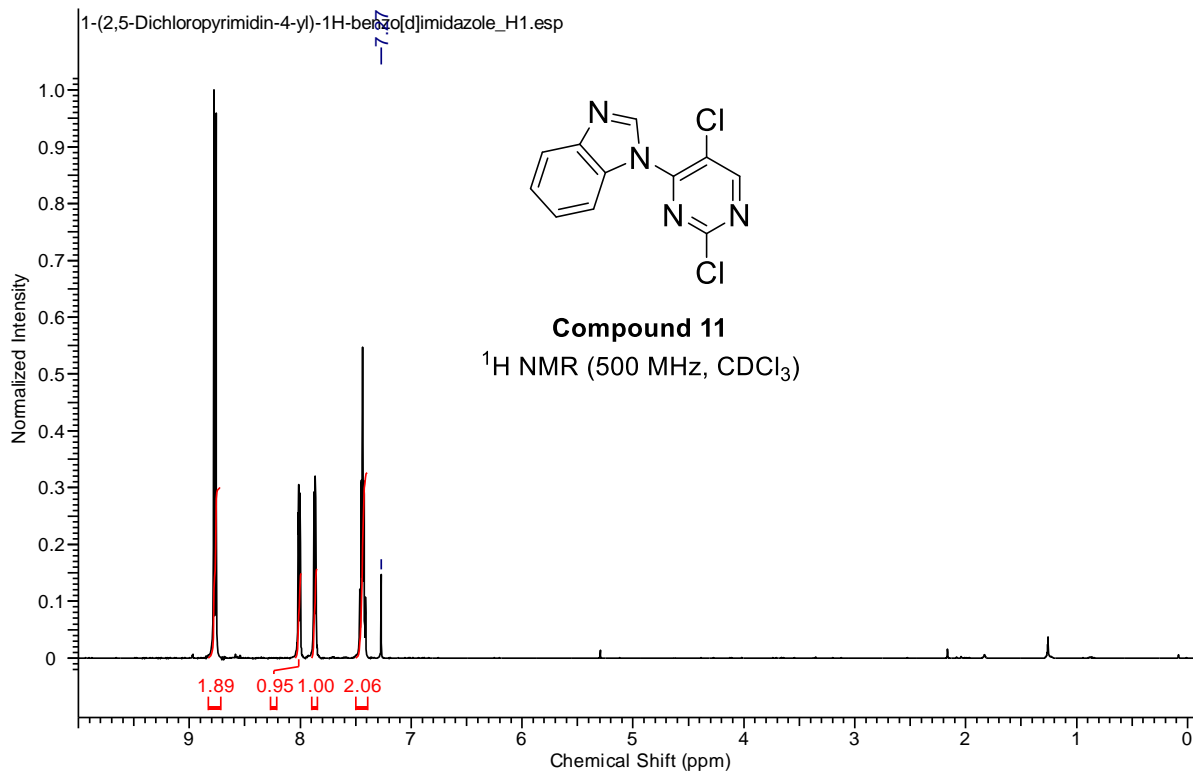
Methyl 2-phenyl-1-oxaspiro[5.5]undec-4-ene-2-carboxylate (21). R_f 0.44 (1:9 EtOAc/hexanes), 26 mg (91%). ^1H NMR (600 MHz, CDCl_3) δ 7.53 (d, 2H), 7.33 (t, 2H), 7.26 (t, 1H), 5.89 (dq, 1H), 5.77 (dd, 1H), 3.60 (s, 3H), 3.09 (dd, 1H), 2.18 (dt, 1H), 1.90 (m, 2H), 1.70 (m, 1H), 1.63 (m, 2H), 1.56-1.42 (m, 3H), 1.40-1.23 (m, 3H); ^{13}C NMR (125 MHz, CDCl_3) δ 174.36, 143.36, 133.75, 128.23, 127.41, 124.56, 121.69, 78.05, 74.83, 51.92, 39.25, 36.20, 33.09, 29.67, 25.47, 22.19, 21.54. IR (neat) ν = 3034 (w), 2931 (m), 2856 (m), 1732 (s), 1456 (w), 1448 (m), 1435 (m), 1057 (s). HRMS (EI, $[\text{C}_{18}\text{H}_{22}\text{O}_3]$) calcd. 286.1569, found m/z 286.1571.

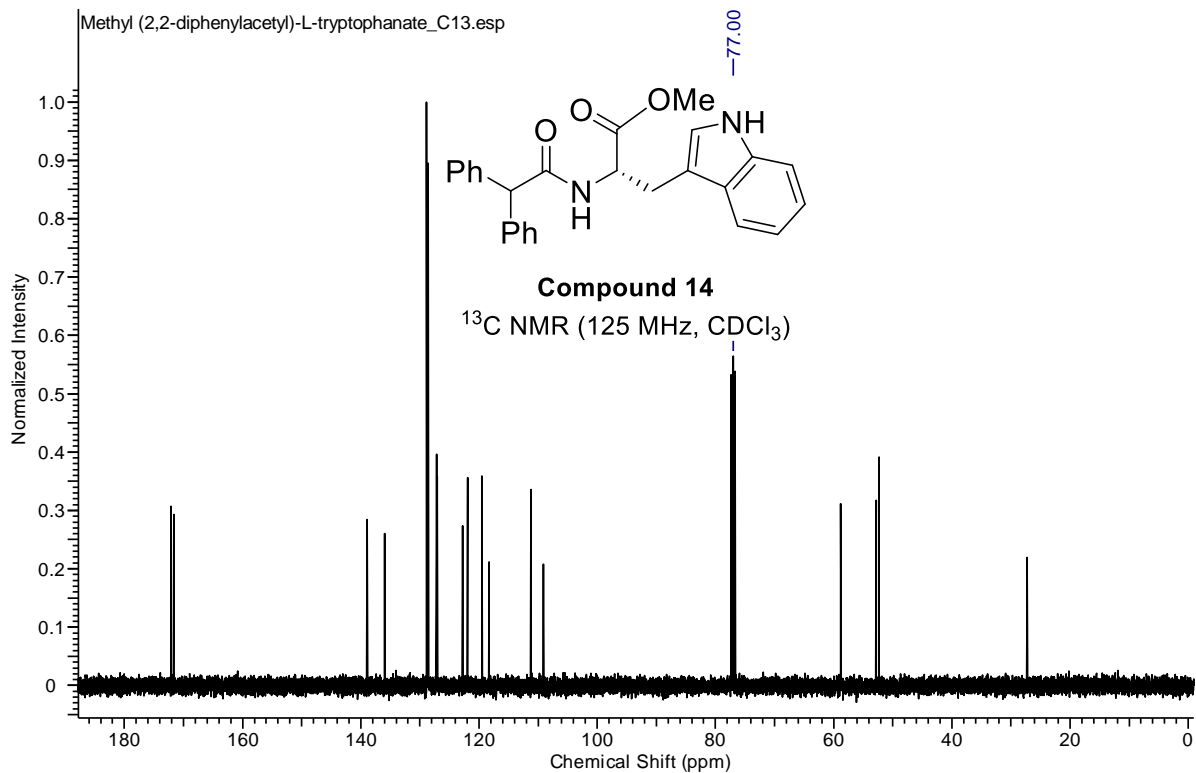
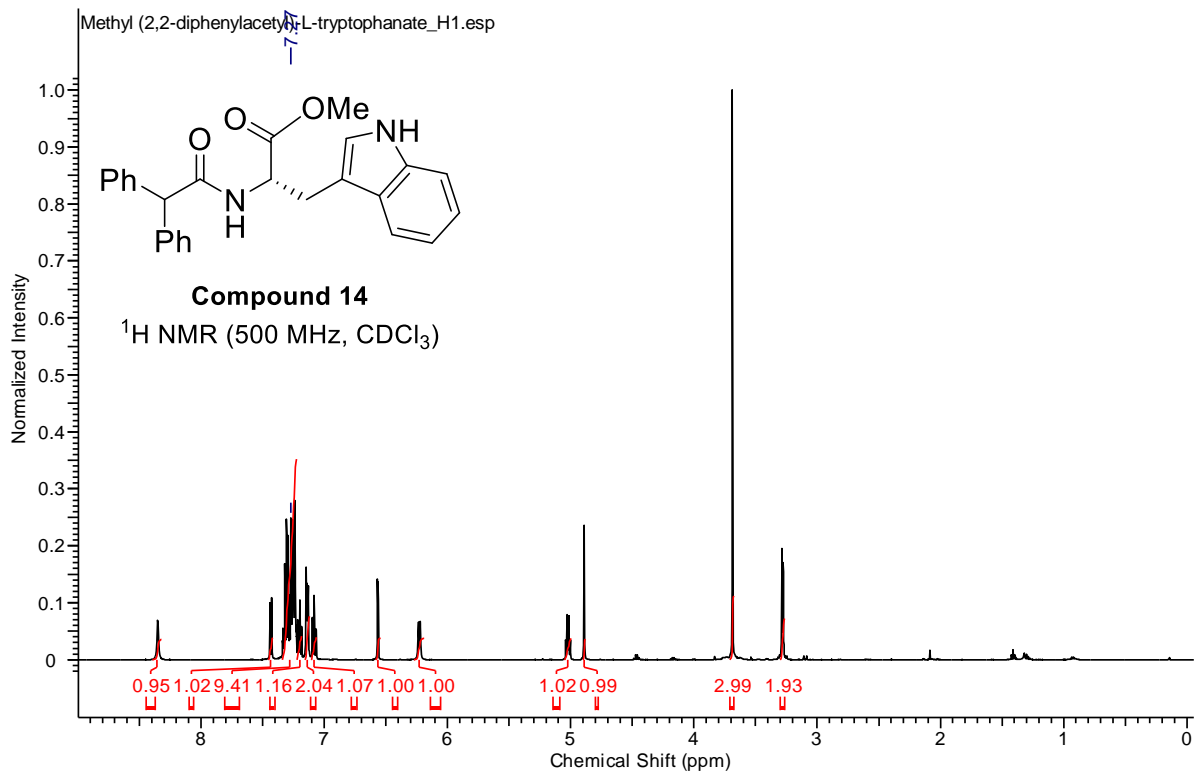
4.6 NMR Spectra

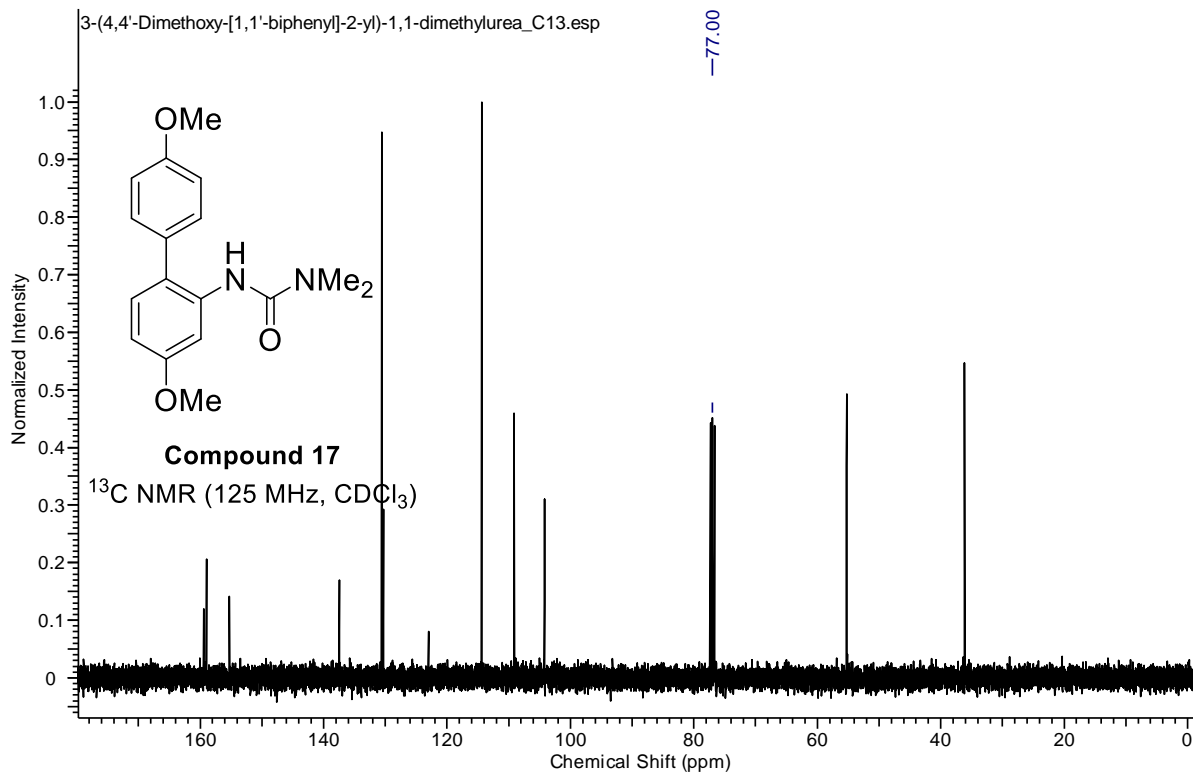
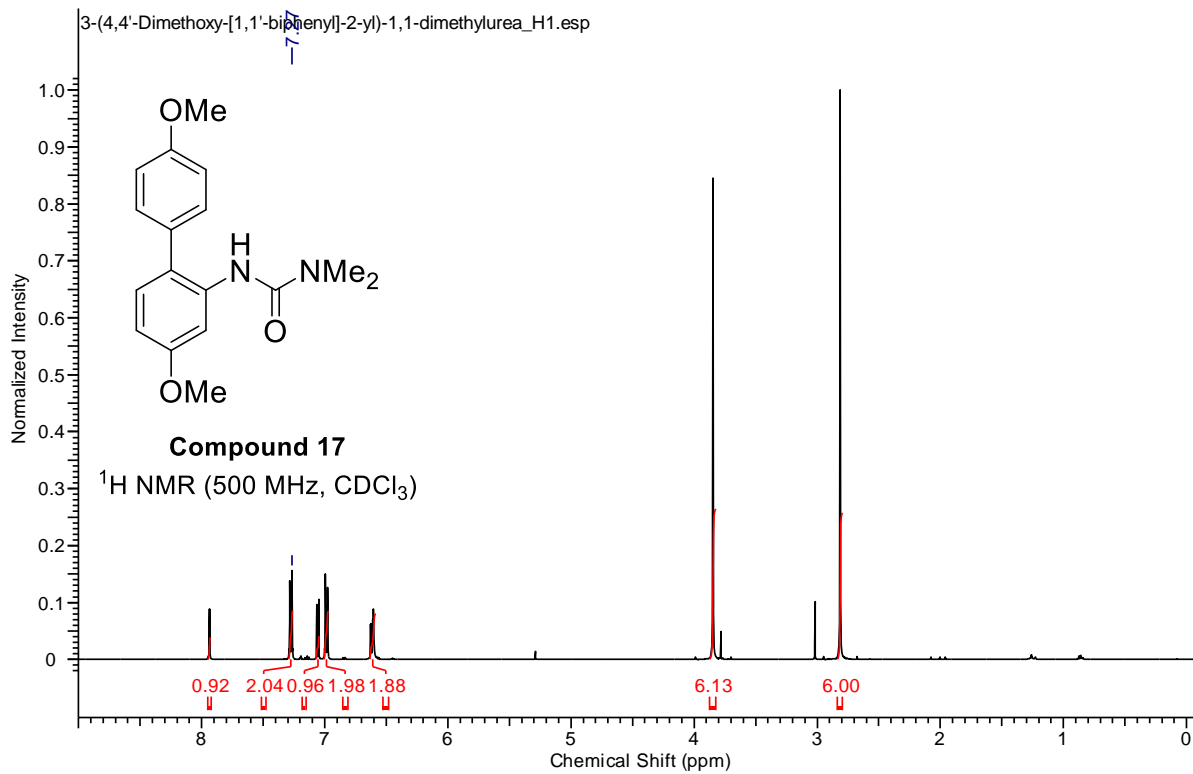


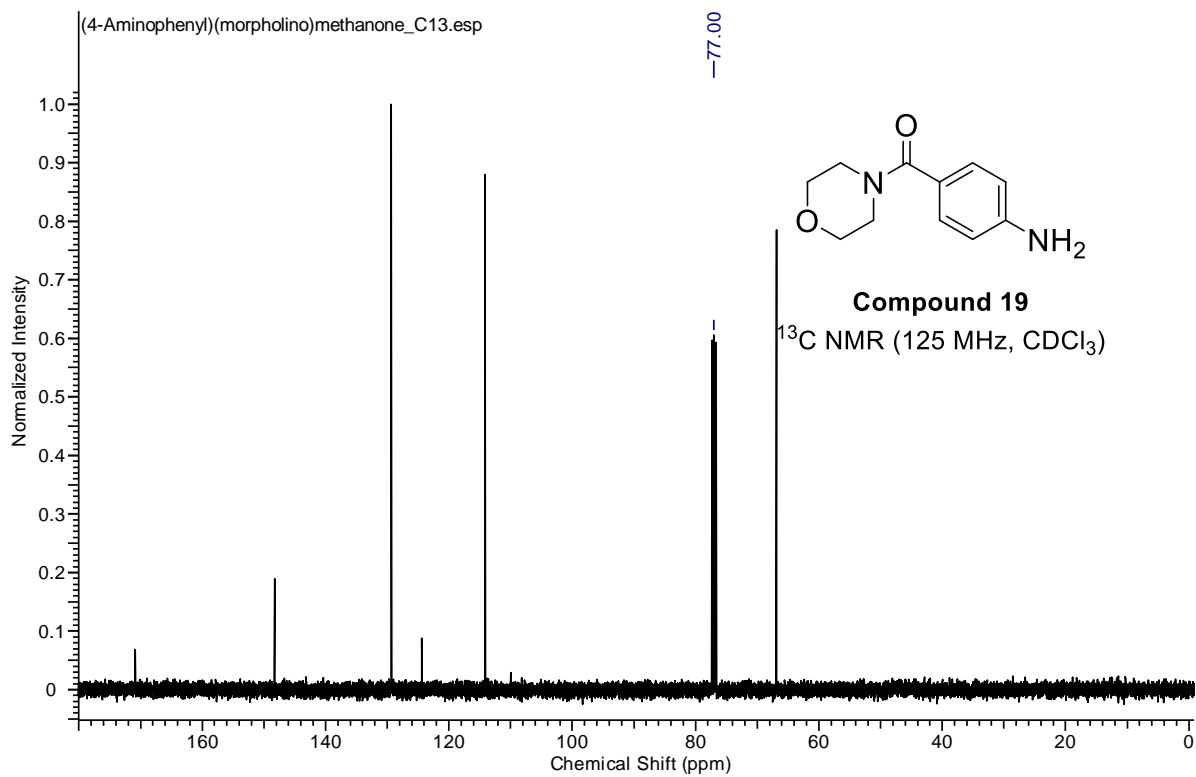
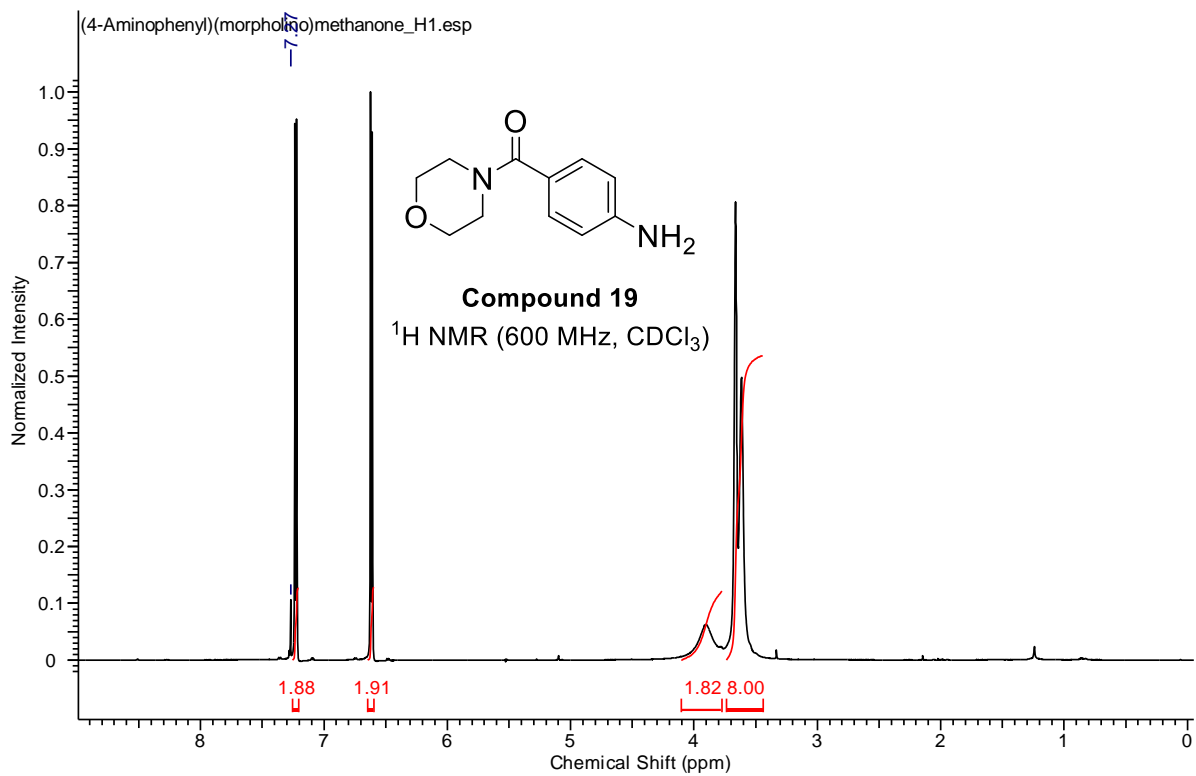


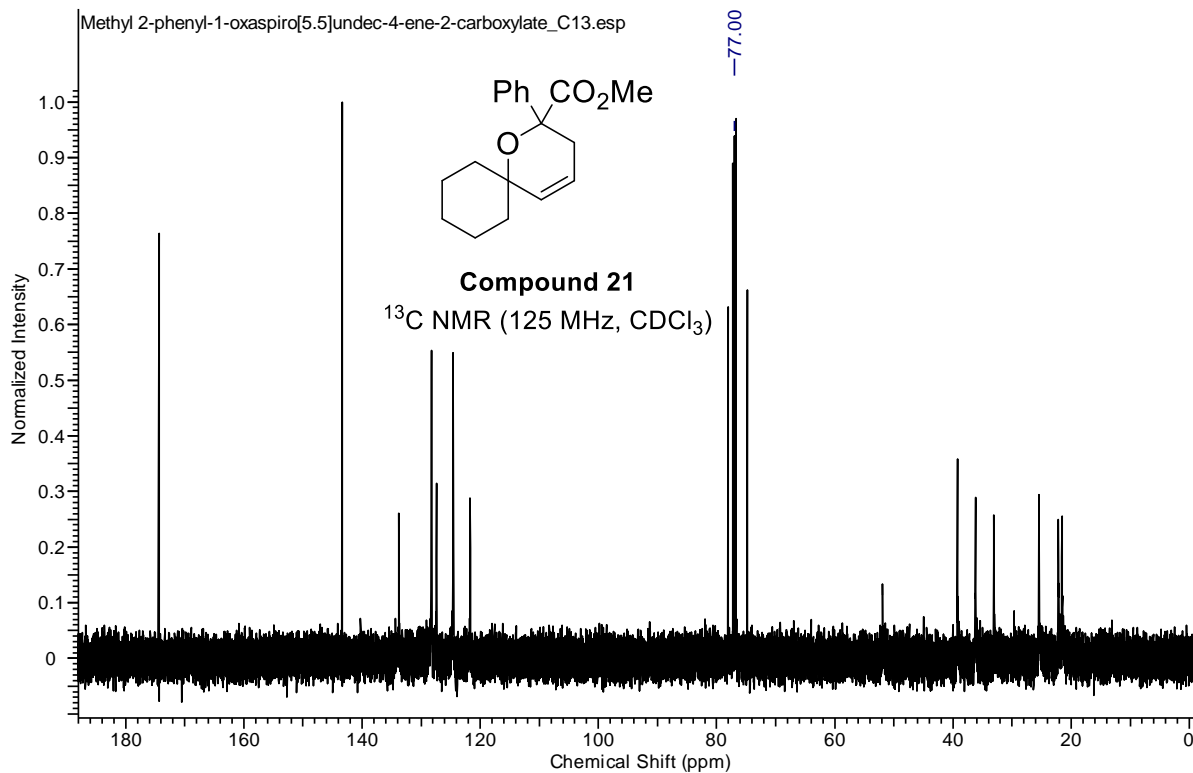
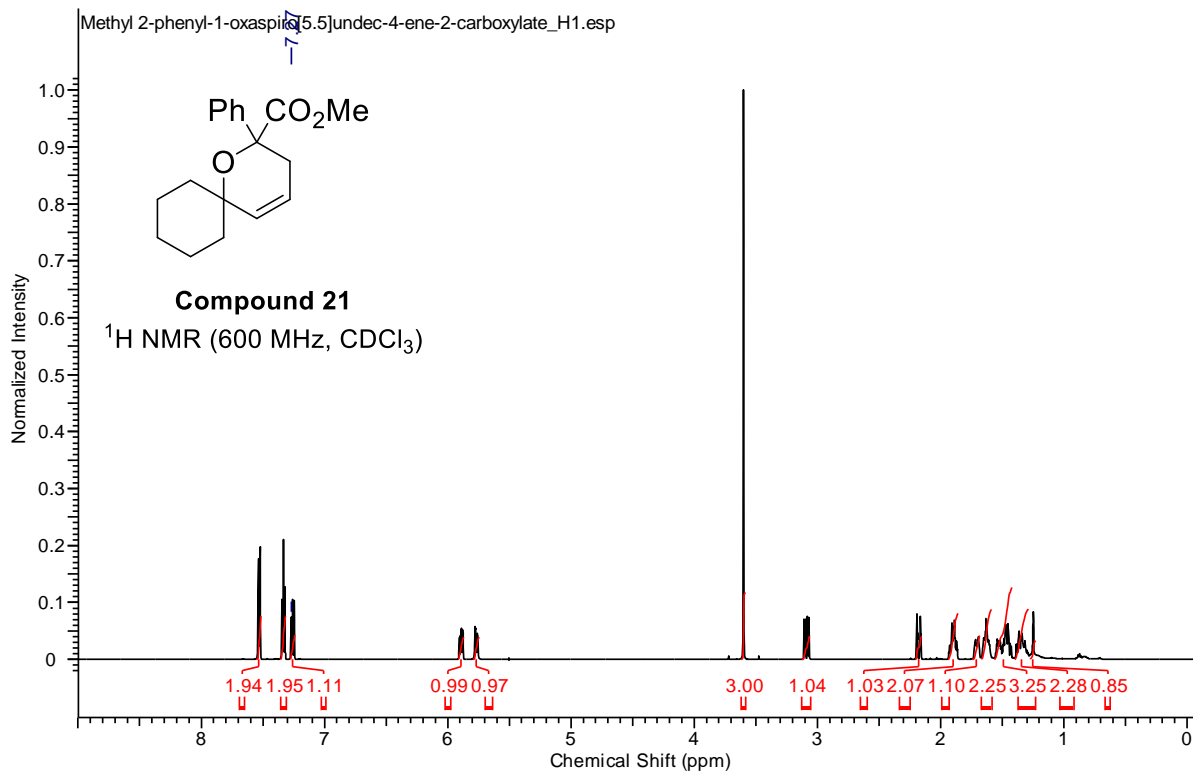












4.7 References

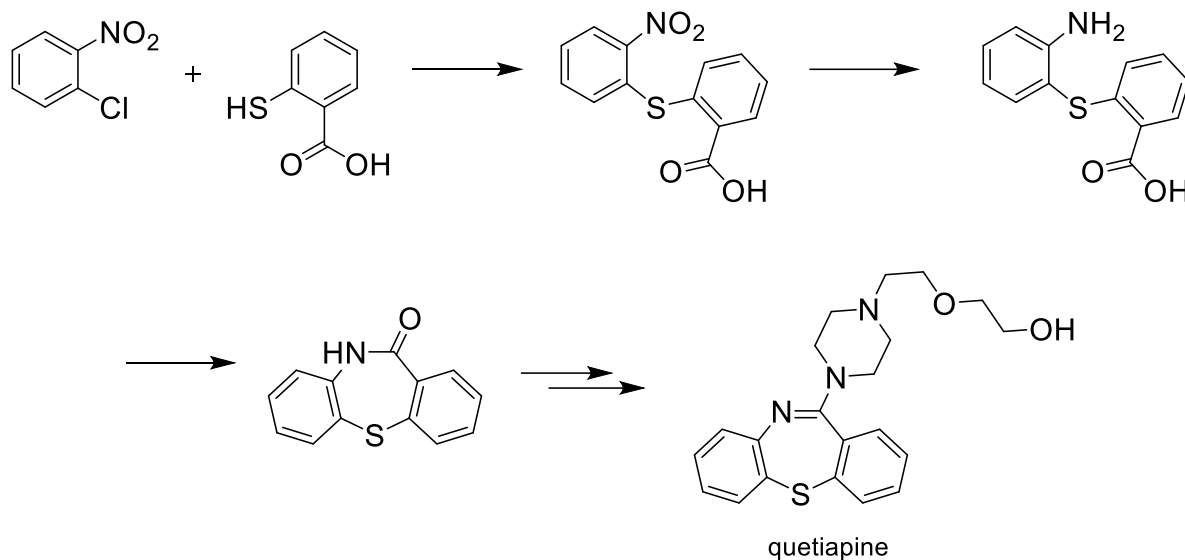
1. Lipshutz, B. H.; Ghorai, S.; Abela, A. R.; Moser, R.; Nishikata, T.; Duplais, C.; Krasovskiy A. *J. Org. Chem.* **2011**, *76*, 4379. b) Lipshutz, B. H.; Gallou, F.; Handa, S. *ACS Sustainable Chem. Eng.* **2016**, *4*, 5838. c) For a general overview on the use of surfactants in synthesis, see: La Sorella, G.; Strukul, G.; Scarso, A. *Green Chem.* **2015**, *17*, 644.
2. Lipshutz, B. H.; Ghorai, S. *Aldrichimica Acta*, **2012**, *45*, 3.
3. Handa, S.; Lippincott, D. J.; Aue, D. H.; Lipshutz, B. H. *Angew. Chem., Int. Ed.* **2014**, *53*, 10658. b) Minkler, S. R. K.; Isley, N. A.; Lippincott, D. J.; Krause, N.; Lipshutz, B. H. *Org. Lett.* **2014**, *16*, 724. c) Minkler, S. R. K.; Lipshutz, B. H.; Krause, N. *Angew. Chem., Int. Ed.* **2011**, *50*, 7820.
4. Lipshutz, B. H.; Ghorai, S.; Leong, W. W. Y.; Moser, R.; Taft, B. R. *J. Org. Chem.* **2011**, *76*, 5061.
5. Fennewald, J. C.; Landstrom, E. B.; Lipshutz, B. H. *Tetrahedron Lett.* **2015**, *56*, 3608.
6. Slack, E.; Gabriel, C. M.; Lipshutz, B. H. *Angew. Chem., Int. Ed.* **2014**, *53*, 14051.
7. Gabriel, C. M.; Parmentier, M.; Riegert, C.; Lanz, M.; Handa, S.; Lipshutz, B. H.; Gallou, F. *Org. Process Res. Dev.* **2017**, *21*, 247.
8. Gabriel, C. M.; Keener, M.; Gallou, F.; Lipshutz, B. H. *Org. Lett.* **2015**, *17*, 3968.
9. Voigtritter, K.; Ghorai, S.; Lipshutz, B. H. *J. Org. Chem.* **2011**, *76*, 4697.
10. Isley, N. A.; Linstadt, R. T. H.; Kelly, S. M.; Gallou, F.; Lipshutz, B. H. *Org. Lett.* **2016**, *17*, 4734.
11. Handa, S.; Andersson, M. P.; Gallou, F.; Reilly, J.; Lipshutz, B. H. *Angew. Chem., Int. Ed.* **2016**, *55*, 4914.
12. Isley, N. A.; Dobarco, S.; Lipshutz, B. H. *Green Chem.* **2014**, *16*, 1480.
13. Feng, J.; Handa, S.; Gallou, F.; Lipshutz, B. H. *Angew. Chem., Int. Ed.* **2016**, *55*, 8979.
14. Handa, S.; Wang, Ye; Gallou, F.; Lipshutz, B. H. *Science* **2015**, *349*, 1087.
15. Bhattacharjya, A.; Klumphu, P.; Lipshutz, B. H. *Org. Lett.* **2015**, *17*, 1122.

16. Handa, S.; Fennewald, J. C.; Lipshutz, B. H. *Angew. Chem., Int. Ed.* **2014**, *53*, 3432.
17. Gallou, F.; Guo, P.; Parmentier, M.; Zhou, J. *Org. Process Res. Dev.* **2016**, *20*, 1388.
18. Parmentier, M.; Wagner, M. K.; Magra, K.; Gallou, F. *Org. Process Res. Dev.* **2016**, *20*, 1104.
19. Lipshutz, B. H.; Moser, R.; Voigtritter, K. R. *Isr. J. Chem.* **2010**, *50*, 691.
20. Nishikata, T.; Abela, A. R.; Lipshutz, B. H. *Angew. Chem., Int. Ed.* **2010**, *49*, 781.
21. Hoffman, H.; Ebert, G. *Angew. Chem., Int. Ed.* **1988**, *527*, 902.
22. a) Lipshutz, B. H.; Ghorai, S. *Green Chem.* **2014**, *16*, 3660. b) Lipshutz, B. H. Isley, N. A.; Fennewald, J. C.; Slack E. D. *Angew. Chem., Int. Ed.* **2013**, *52*, 10911. c) Sheldon, R. A. *Green Chem.* **2007**, *9*, 1273.
23. Lee, N.; Gallou, F.; Lipshutz, B. H. *Org. Process Res. Dev.* **2017**, *21*, 218.
24. Gabriel, C. M.; Lee, N. R.; Bigorne, F.; Klumphu, P.; Parmentier, M.; Gallou, F.; Lipshutz, B. H. *Org. Lett.* **2017**, *19*, 194.
25. Ansuman Bej, A.; Srimania, D.; Sarkar, A. *Green Chem.* **2012**, *14*, 661.
26. Lu, H.; Geng, Z; Li, J.; Zou, D.; Wu, Y.; Wu, Y. *Org. Lett.* **2016**, *18*, 2774

V. Sustainable and Scalable Fe/ppm Pd Nanoparticle Nitro Group Reductions in Water at Room Temperature

5.1 Introduction

Nitro group reductions represent a transformation in the synthetic chemist's toolbox that is used extensively to access a broad range of products. The ubiquity of this transformation comes as the consequence of the ease and predictability at which nitro groups may be installed.¹ Typically, nitro groups are installed by nucleophilic aromatic substitution reactions utilizing cheap and readily available nitric and sulfuric acid. In addition, by utilizing nitro group reductions, the synthetic route benefits from the electronic differences between starting materials and products. For example, by utilizing the resonantly electron withdrawing characteristics of a nitro group, one can routinely perform S_NAr reactions on activated aryl chlorides^{1,3} and fluorides,^{4,5} or utilize the electron deficient nature to participate in facile oxidative addition in cross coupling events with aryl halides.⁶⁻⁷ The nitro group reduction can then be performed on the substituted aryl product thereby unmasking the nitro group as a free amine which can act as a nucleophile for subsequent chemistry, including amide bond formations⁷⁻⁹ and heterocyclic transformations. The sequence of exploiting the relatively inert and highly electron withdrawing nature of the nitro functionality followed by reduction and nucleophilic substitution is a prevalent route to a variety of pharmaceuticals. Scheme 1 shows one such example of this route, where quetiapine (Seroquel) is accessed from a sequential S_NAr /nitro-group reduction/lactamization.³ Other important cases include the synthesis of imiquimod,¹ linezolid,⁴ boscalid,⁷ imatinib,⁹ and levofloxacin.¹¹



Scheme 1. Preferred synthetic route to quetiapine from S_NAr /nitro-group reduction/lactamization sequence.

5.2 Background

The reduction of nitro groups has been a transformation of intense interest for nearly a century and a half,¹² where the Béchamp¹³ reduction of nitrobenzene was used as the method of choice for the large scale production of aniline. The development of catalytic hydrogenation methods redefined how chemists approach nitro group reductions and remains the most widely utilized method to date. Common catalysts for hydrogenation include Pd/C,¹³ Raney-Ni,¹⁴ and PtO₂¹⁵ which are generally employed under ambient to very high pressures of H₂. Hydrogenation from catalytic non-platanoids is also an intense field of research with many impressive developments being made from systems with Fe,¹⁷ Cu,¹⁸ Co,^{18c,19} Pt/Zn,²⁰ Ti,²¹ Ir,²¹ and Rh.²³ Similar to the Béchamp reduction, other methods rely on less expensive metals such as Fe,²³ Zn,²⁴ and Sn,²⁵ however these conditions generally require stoichiometric or even super stoichiometric amounts of metals and/or harsh reaction conditions which may be a concern in terms of safety, waste generation, and functional

group compatibility. Additionally, many of the described reduction conditions may stall at intermediate stages, and/or go through accumulation of highly energetic species such as nitroso- or hydroxylamine intermediates. The ubiquity of this transformation for the synthesis of pharmaceuticals, dyes, explosives, agrochemicals, functional materials, and bioactive natural products²⁷ certainly raises the questions: how safe/environmentally responsible are the state of the art technologies, and what can be done to address these concerns for nitro group reductions on scale?

For a given transformation in a process, safety and cost are important considerations when evaluating current technologies. For instance, if a given advanced intermediate can be functionalized in near quantitative conversion in high purity, safety may take a back seat due to the influence of cost and reproducibility of the method. An excellent example of this is the synthesis of varenicline where the Upjohn Dihydroxylation using toxic OsO₄ is preferred over other oxidants due improved yield, selectivity, and purity profile over other less harmful oxidants such as KMnO₄.²⁸ This is not unlike catalytic hydrogenation where the hazards and cost associated with the use of H₂ under high pressures are considered acceptable due to the success of these methods. If hydrogenation is considered state-of-the-art and developments focus predominately on the front of catalyst improvements,¹² the major hazard of the highly flammable gas is still not addressed because it is perceived as an acceptable reagent. In fact, much effort today in the field looks towards a less expensive catalysts, often in the form of Fe nanoparticles,²⁸ to address cost, and safety improvements focus on flow reaction development.²⁹ While there is tremendous merit to these advancements, there still remains the issue of high pressure reaction systems. It is well understood that a method is likely to be overlooked in systems requiring an atmosphere of

O₂,³¹ yet the hazards of this gas are no greater than those associated with H₂. So why are we still using it?

5.3 Early Work

Recently, a new catalyst has been developed for nitro group reductions which meets many of the safety and environmental concerns associated with expensive platanoid catalyzed hydrogenation of the nitro group functionality.⁴⁸ Developed from earlier finding from our group in the areas of Pd nanoparticle-catalyzed semi-reduction of alkynes³³ (Chapter 2) and the Fe nanoparticle supported ppm Pd-catalyzed Suzuki-Miyaura cross couplings,³⁴ the developed precatalyst nanoparticles (NPs) are synthesized from the treatment of Pd(OAc)₂-doped FeCl₃ with 1.1 equivalents of MeMgCl. Nitro compounds can be effectively reduced to their corresponding amines by the use of NaBH₄ as the source of hydrogen under aqueous micellar conditions alleviating the need for H₂ to be charged into the system. Taking place at room temperature, this method delivers exceptional yields (80-98%) with short reaction times (typically 2-4 hours) at ambient temperature. Key features of these conditions are the preferred use of aqueous TPGS-750-M over organic solvent as well as the functional group compatibility to a broad range of reducible structural motifs including aryl halides, alkenes, alkynes, esters, amides, nitriles, and ketones, as well as benzyl protected alcohols and amines which would otherwise be cleaved under Pd-catalyzed hydrogenation conditions (Figure 1).³⁵ In addition to the versatility of this method, the use of only trace amount of Pd for catalysis yields the purified product with residual Pd content of less than 1 ppm. These mild conditions were envisioned as an amenable alternative to standard hydrogenation conditions for nitro group reductions of active pharmaceutical ingredients (API's) where late stage Pd-catalyzed transformations would generally be

disregarded on the basis of residual metal content. This advancement would allow for more flexibility in process route development to fit within the maximum allowable limits of Pd in a final API under the FDA Guidelines⁴² and other processes, especially with those reductions catalyzed by $\geq 1\%$ Pd will generally fail to meet this criteria when performed in the final stages of a synthetic route.

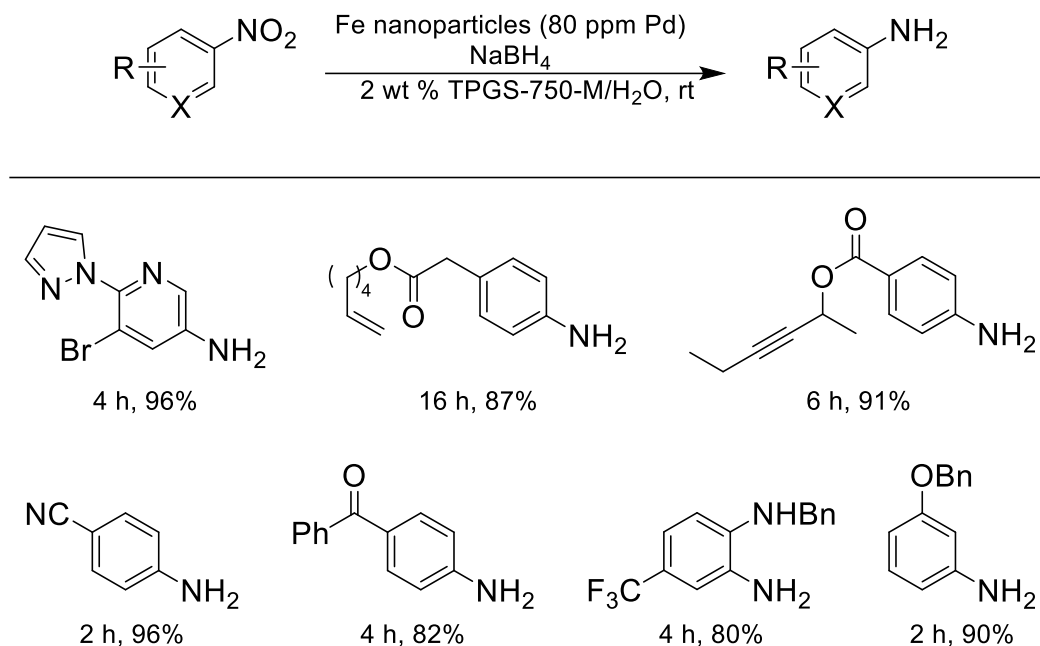


Figure 1. Representative examples of reduced nitroarenes catalyzed by Fe/ppm Pd nanoparticles with NaBH₄.

The standard procedure for Fe/ppm Pd-catalyzed reduction of nitro compounds calls for generating Fe nanoparticles (≥ 80 ppm Pd) in a 2 wt % TPGS-750-M solution in water by dissolving the precatalyst in the water and charging NaBH₄ (1.5-3.0 equiv) to the mixture arriving at the active nanomaterial catalyst (activation). It is during this activation step that the gross reductant for the system is present for the subsequent reduction as well. In a separate vessel, the nitro group-containing starting material is dispersed in 2 wt % TPGS-750-M/H₂O prior to its addition into the reaction mixture. The reaction typically proceeds in

a sealed dram vial and allowed to stir at room temperature until full conversion of starting material and productive intermediates is determined by TLC or GC/MS. Isolation and purification of the product amine is carried out via extraction of the crude product with ethyl acetate or *t*-butyl methyl ether (MTBE) from the reaction mixture, followed by column chromatography. Alternately, direct recrystallization of the amine as the corresponding HCl may be effected from the extraction solvent, thus providing another indication that this process is well suited for scale up.

Encouraged by the efficiency and ease of this method, in combination with reduced environmental impact and purity profile, development of a scale-up process was pursued at Novartis AG in Basel, Switzerland, as was a study of several other reaction parameters including calorimetry in the safety lab.

5.4 Results and Discussion

In order to successfully achieve this task, we broke down the method into a process flow diagram (Figure 2). Looking at concerns from the perspective of a process chemist, initial focus was on the physical aspects of the system, where quite frequently nitroarenes are generally highly crystalline in water leading to unstable emulsions or suspensions and in some cases starting material will appear like sand stirring in water. This could lead to issue in terms of transferring large amount of the reagent to a reactor and lead to poor homogeneity of the system. This was also a concern in terms of intermediates that precipitate and deposit above the solvent level of the reaction leading to inconsistent results. Furthermore, the role of NaBH₄ was unclear, and as the previous method was carried out in a sealed vial, we wanted to investigate if the pressure build up was a requirement of the system as in a classical hydrogenation, or if this process could be carried out in a standard reactor.

Foaming observed as a result of the effervescent hydrogen evolution from the aqueous surfactant solution was yet another obstacle which would require additional headspace in a reactor and may deposit catalyst and starting material/intermediates above the solvent level. Finally, the process would require the system to go to full completion such that purification could be carried out via recrystallization from the extraction solvent without the need for column chromatography to obtain pure product.

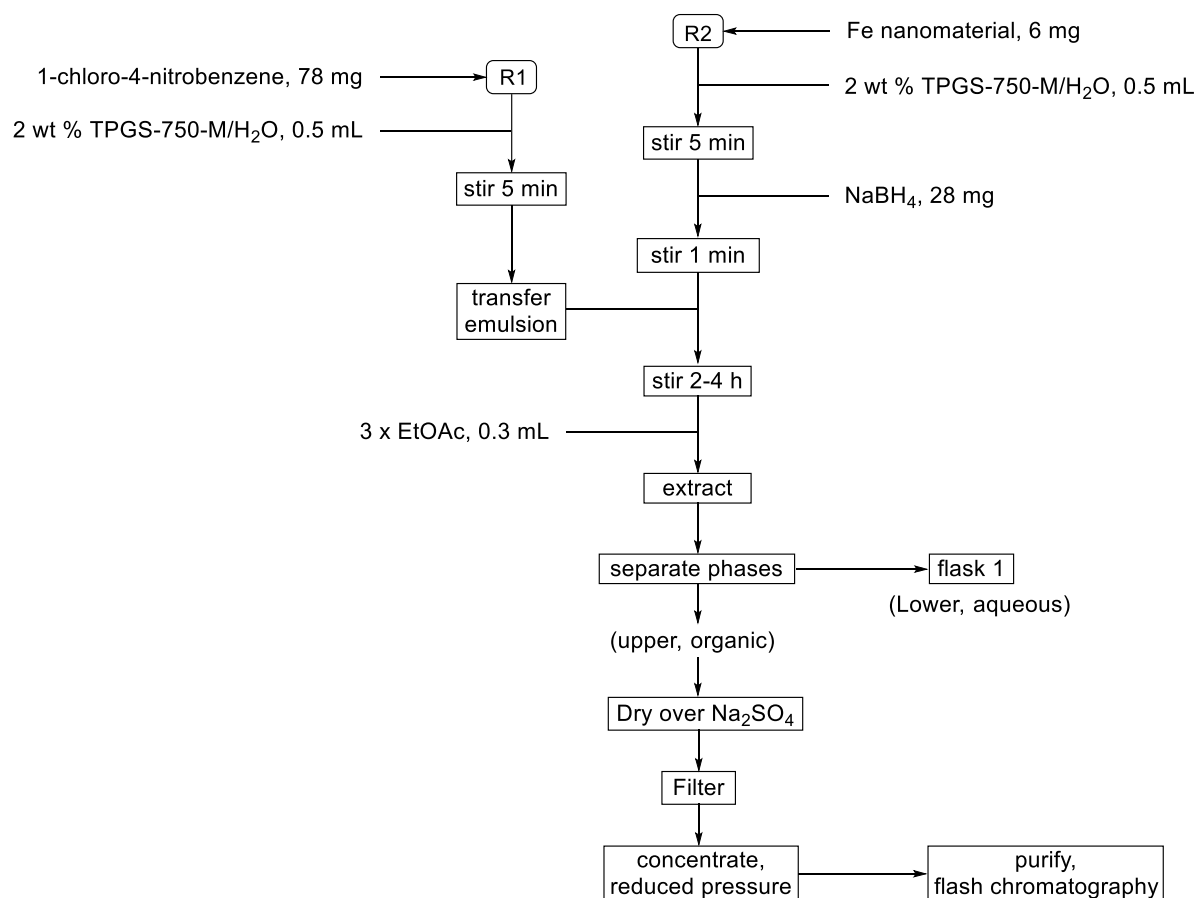


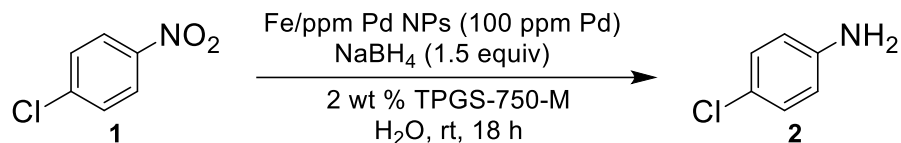
Figure 2. Process Flow Diagram of literature conditions for the reduction of 1-chloro-4-nitrobenzene catalyzed by Fe/ppm Pd nanoparticles with NaBH₄.

Due to the highly crystalline nature of as well as structural and physical similarities to, the Novartis intermediate of interest, we investigated 4-chloronitrobenzene as the model

substrate. Initially, considering the physical aspects of the system, an array of co-solvents were screened as previous findings found that the use of co-solvent could drastically affect the homogeneity and success of reactions under micellar catalysis conditions.^{48,37-40}

Solubility and the formation of a stable emulsion were important parameters to investigate, as nitro-group containing compounds are typically highly crystalline solids, oftentimes unfavorable for reactions in which water is used as the reaction medium. While the use of surfactants at or above their critical micellar concentrations (CMC) can be used to stabilize organic material as a microemulsion, liberating material from its energetically more favorable crystalline state may require “softening” of the lattice, especially at higher concentrations such as those used in this process (0.3-0.5 M). As a result, heterogeneous polyphasic mixtures with suspended solids can provide challenges on scale and was foreseen as a potential pitfall for this method. The results for reactions run at a 0.5 mmol scale (78 mg 4-chloronitrobenzene) are outlined in Table 1 where the co-solvents screened included: THF, 2-Me-THF, toluene, and PEG-200. Consistent with our previous efforts,^{48,40} THF was found to be the co-solvent of choice showing, for this specific transformation based on observations highlighted below, slightly better conversion than literature conditions. Additionally the presence of 2 vol THF (156 μ L co-solvent per 78 mg **1**) was sufficient to solubilize intermediates which would have otherwise precipitated and formed a solid ring of material above the solvent level in the absence of co-solvent. This explains the higher conversion to the product amine under co-solvent conditions: upon analysis of the precipitate (by NMR and UPLC/MS) for the control system (no co-solvent), the makeup of the solid was found to be predominately nitroso- intermediate **3**, hydroxylamine intermediate **4**, and the corresponding azoxy condensation byproduct **5**. The higher local concentration of the two intermediates not only entropically favors the condensation pathway but also removes

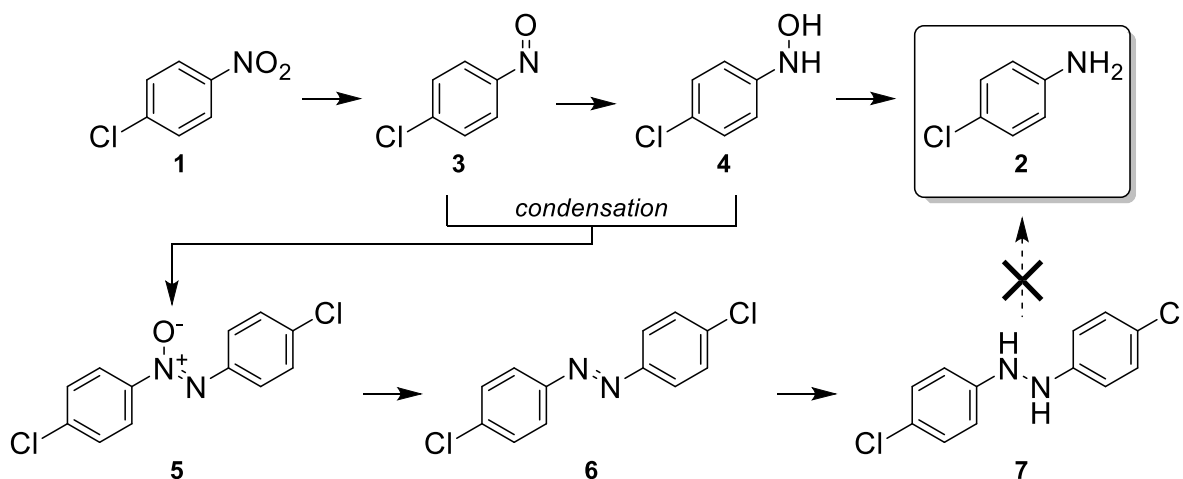
productive intermediates from the active catalyst mixture. The success of PEG-200 supports this hypothesis, where even though this cosolvent was ineffective in forming a stable emulsion or solubilizing precipitated intermediates, no caking was observed above the solvent level. This solvent was disregarded for further development towards our process due to the instability of the emulsion; however, these data provide a useful modification that may be implemented in later work. Interestingly, the addition of a solution of **1** in THF directly to the reaction mixture yielded surprisingly poor results in comparison to the formation of a microemulsion prior to transfer (Table 1, entry 6). Water-miscible alcohols such as methanol and isopropanol were not considered as co-solvents due to their inability to dissolve **1** prior to addition of the aqueous surfactant solution. Another improvement that was effected by the use of THF as co-solvent was the ability to collapse foaming resulting from activation of the catalyst. In fact, it was observed that addition of the starting material emulsion with THF to the reaction could collapse the foam, while the addition of THF or **1** alone did not result in the same physical change.



entry	cosolvent ^a	1 ^b	2
1	none	4%	88%
2	THF	0%	99%
3	2-Me-THF ^c	29%	31%
4	toluene ^c	26%	47%
5	PEG-200	0%	98%
6	THF ^d	41%	18%

^a156 μ L cosolvent per 78 mg **1**, 0.5 mL 2 wt % TPGS-750-M/H₂O, ^bUPLC/MS analysis at 210-450 nm, ^cSeveral by-products detected, ^dSM dissolved in 2 vol (156 μ L) THF and transferred directly followed by 0.5 mL 2 wt % TPGS-750-M/H₂O.

Table 1. Co-solvent screening for the reduction of **1**.



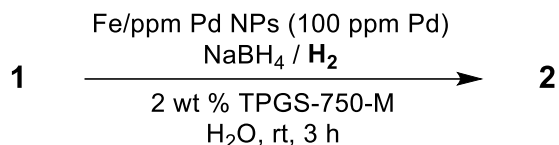
Scheme 2. Nitro group reduction and condensation pathways.

In forming an emulsion for a given starting material, it was found that dissolution in THF prior to addition to 2 wt % TPGS-750-M/H₂O achieves the desired ‘milky’ appearance much faster than other addition sequences. This should be done at high stirring rates (>800 rpm)

and can be achieved easily at the lab scale by high-speed vortexing of the mixture in a cylindrical vessel such as a dram vial.

As mentioned previously, when this reaction was run at lab scale, it was routinely carried out in a sealed vial, allowing the build-up of pressure over the course of the reaction. Upon completion of the reaction, it was evident that a large amount of pressure was generated due to the decomposition of NaBH_4 to give off H_2 , so we set out to investigate this system under hydrogenation conditions to better understand the role of NaBH_4 as the reductant.

This study was carried out to assess whether NaBH_4 acts as the direct hydride source or as an H_2 precursor. Using what was already known about this system, each reaction was treated in two stages: catalyst activation and substrate reduction. Upon addition of NaBH_4 to the homogeneous catalyst solution, the iron(III) salt is quickly reduced, as it precipitates as fine black particles while the reaction mixture foams due to gas evolution. The hypothesis was that NaBH_4 may directly reduce that catalyst and the subsequent reduction goes by means of a hydrogenation mechanism. This mechanism was eliminated when activation of the precatalyst with a catalytic amount of NaBH_4 (0.15 equiv) followed by the addition of substrate, and then placing the system under H_2 atmosphere even under high pressures of 11 bar, did not deliver the desired aniline product in sufficient quantities (Table 2, entries 1, 2) which was in agreement with the findings in the initial communication.⁴⁸ No catalyst activation was observed in the absence of NaBH_4 suggesting that the precatalyst requires hydride reduction to initiate activation. When the precatalyst is treated with H_2 prior to activation, poor conversion was observed yet again leading to the conclusion that this reduction does not go by means of a standard hydrogen pathway but rather by means of a palladium hydride.

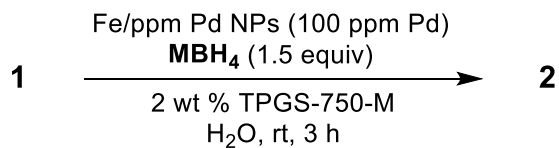


entry	catalyst activation	reductant	pressure	1 ^a	2
1	NaBH ₄ ^b	H ₂	1 bar	89%	2%
2	NaBH ₄ ^b	H ₂	11.0 bar	61%	2%
3	H ₂	H ₂	3.0 bar	91%	3%
4	H ₂ ^c	NaBH ₄ ^d	1.0-3.0 bar ^e	46%	5%

^aUPLC/MS analysis at 210-450 nm, ^b0.15 equivalents, ^cPressurized to 6 bar for 30 minutes prior to NaBH₄ addition, ^d1.5 equivalents, ^eData represent the pressure generated by gas evolution in a closed system over 3 h.

Table 2. Conversion data for activation/hydrogenation investigations.

At this stage, we proposed that by varying the nature of the counterion on the borohydride might impact the success of the reduction. This modification seemed likely as the Z-selective semihydrogenation of alkynes with Pd(OAc)₂ and NaBH₄ could be drastically influenced in terms of selectivity by the incorporation of LiCl.³³ Not surprisingly, replacing NaBH₄ by other metal borohydride salts, a pronounced effect is observed depending on the nature of the counterion (Table 3). KBH₄ was found to be more effective as a reductant as the reaction rate increased both for starting material conversion and for the rate determining step of reduction from hydroxylamine **4** to aniline **2** (Scheme 2). These findings not only benefit the process in terms of reaction time but also reduce the accumulation of highly energetic and toxic intermediates **3** and **4**. No catalyst activation was observed for the case using LiBH₄, which led to poor conversion of the starting material.



entry	reductant	1 ^a	2	3	4	5	6	7
1	LiBH ₄	94%	1%	0%	3%	5%	0%	0%
2	NaBH ₄	2%	37%	3%	52%	5%	1%	0%
3	KBH ₄	0%	64%	3%	23%	8%	3%	0%

^aUPLC/MS analysis at 210-450 nm

Table 3. Screening of various metal borohydride salts for the reduction of **1**.

When monitoring the amount of pressure accumulated for the metal borohydride screening it was observed that KBH₄ decomposes to form H₂ to a much greater extent than does NaBH₄ (1.0 bar for KBH₄ compared to 0.7 bar for NaBH₄ at 0.5 mmol scale). Quite interestingly, only a negligible amount of pressure was accumulated when LiBH₄ was used as the reductant.

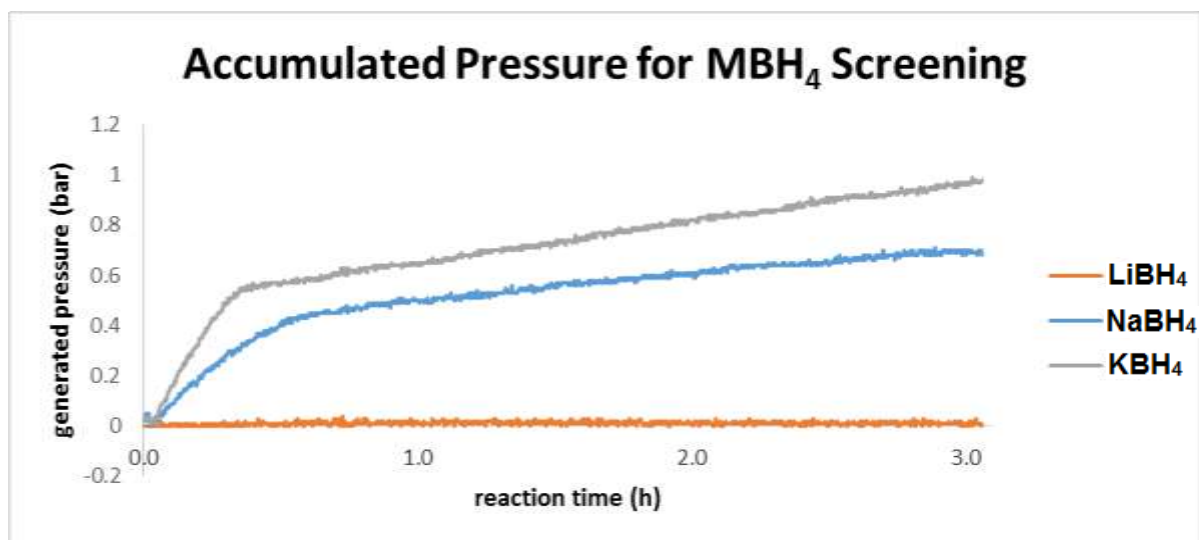


Figure 3. Measured pressure for the evolution of H₂ from the decomposition of various metal borohydride salts during the reduction of **1**.

Scheme 2 represents the two typical pathways by which nitroarenes may be reduced, both of which result from the concurrent reductions of the nitro and nitroso- intermediates. In order to understand the productive pathways of this methodology, isolated hydroxylamine **4**, azoxy **5**, and diazo compound **6** were submitted under standard reduction conditions (Table 4). Within one hour, 0.5 mmol **4** was cleanly converted to **2** while only trace amounts of azoxy **5** were reduced to **6**, and no conversion of **6** to **7** even after allowing the reaction to age for ca. 18 hours. This study confirmed that the condensation pathway as a dead end under our conditions. The condensation by-products **4**, **5**, and **6** are not only a concern in terms of overall conversion to product, but also in terms of safety, as this class of by-products has been found to be genotoxic and carcinogenic.⁴¹ Therefore, conditions were required for avoiding this pathway so as to ultimately arrive at a safer, more efficient process.

entry	intermediate/by-product	2	3	4	5	6	7
1	4	100%	0%	0%	0%	0%	0%
2	5	0%	0%	0%	98%	2%	0%
3	6	0%	0%	0%	0%	100%	0%

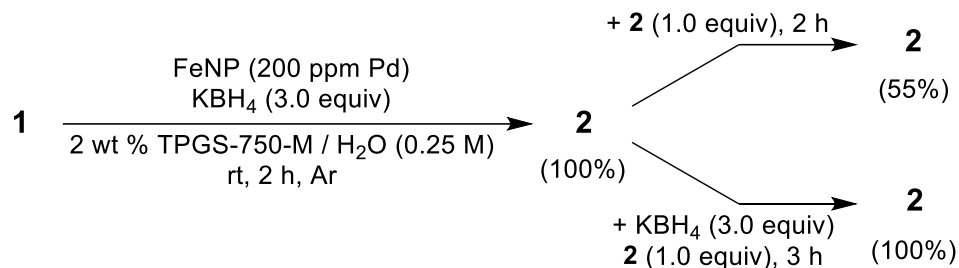
^a UPLC/MS analysis at 210-450 nm

Table 4. Conversion data for intermediates/condensation by-products under standard reduction conditions.

The studies described above provided the data necessary for the development of a robust process. Where increasing the reaction rate and diluting the system would lead to preference of the productive pathway, rate enhancement could be effected by simultaneously influencing catalyst loading, the nature of the reductant, and equivalents of the reductant. Catalyst loading was increased to 200 ppm Pd loading, while substituting NaBH₄ to the

more reactive KBH_4 , an increasing reductant loading from 1.5 to 3.0 equivalents. Dilution was considered on the basis of the entropic factor of condensation so the substrate concentration was decreased from 0.5 to 0.25 M. Finally, because H_2 had been shown previously to inhibit reactivity of the system (Table 3, entry 4), the reaction was performed under a balloon of Ar.

Within one hour, quantitative conversion of **1** was achieved and by two hours the reaction had gone to completion free of by-products (Scheme 3). An additional equivalent of **1** was then charged to the reaction mixture, achieving full conversion of the initial reduction, however a build-up of hydroxylamine **4** was observed as the remaining hydride in the system was not sufficient to bring the reaction to completion, ultimately converging to the condensation pathway. Reproducing the initial step of the modified system, quantitative conversion of **1** to **2** was observed once again within two hours and by charging the reaction with 3.0 additional equivalents KBH_4 prior to adding the second portion of starting material, quantitative conversion to product was achieved. In fact, a portion-wise addition of reagents in this manner can be continued up to at least ten additional times without effecting reaction conversion, however, precipitation of product leads to a decrease in homogeneity of the reaction mixture which may not be desirable for this process at a larger scale. When carried out on a 100 mmol scale, similar results were realized, yielding quantitative conversion to **2** after only 3 hours for the first portion and reaction completion 11 hours after addition of reagents for the second portion, affording **2** in 94% isolated yield as the HCl salt. The reaction profile for the 100 mmol reaction is shown in Figure 4, where the major peak corresponds to the product **2**.



Scheme 3. Effects of increase reductant and catalyst loading with portion-wise addition of reagents.

Incorporation of all modifications to the existing methodology on the 100 mmol scale is represented by the process flow diagram in Figure 5. Modifications including: co-solvent usage, swapping NaBH_4 for KBH_4 as well as the portion-wise addition of reagents are outlined, with the addition of each portion of KBH_4 with starting material being considered an individual process (i.e. Stage 1; Stage 2). It was envisioned that the portion wise addition at this scale could simulate the constant slow addition of materials over the course of the reaction, however this procedure has yet to be explored.

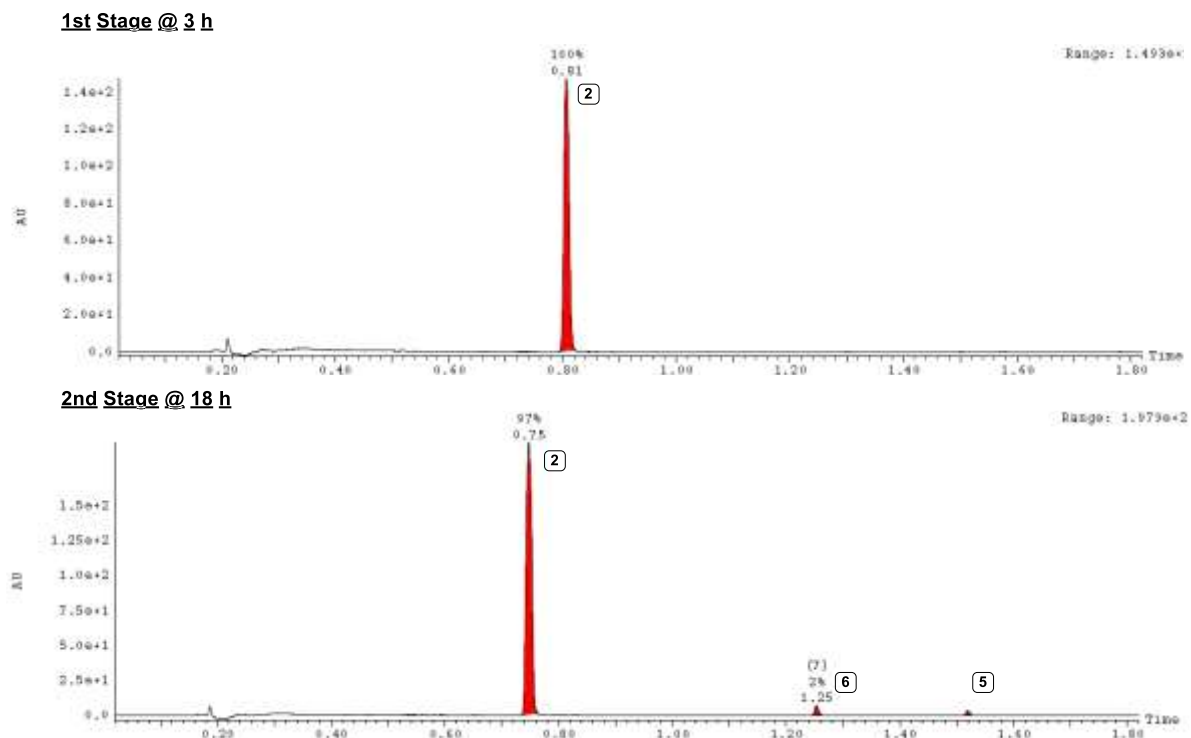


Figure 4. Reaction profiles for the reduction of **1** on a 100 mmol scale.

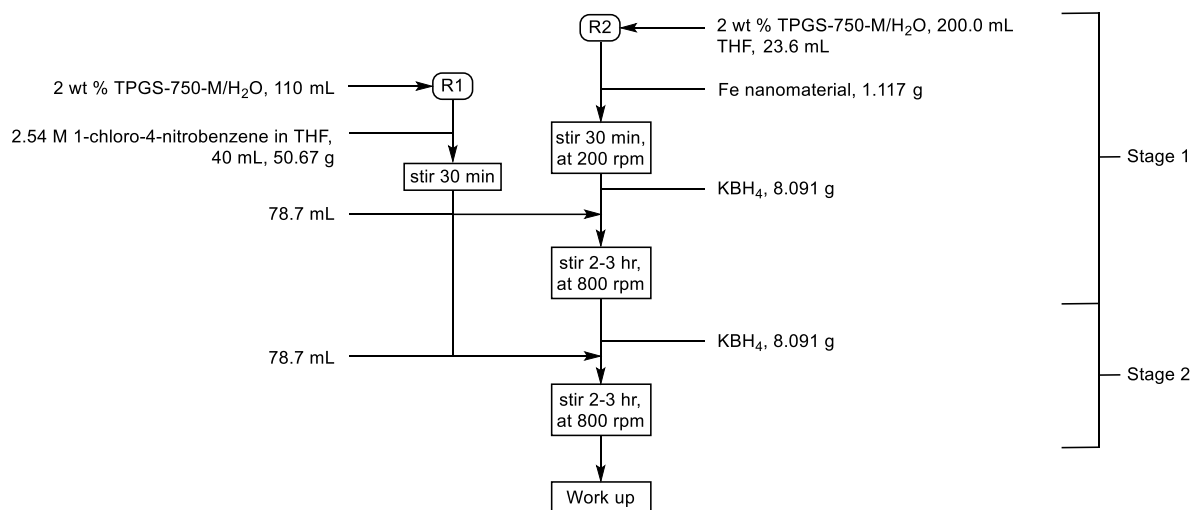


Figure 5. Process Flow Diagram for the developed process at 100 mmol scale.

Examining this process in terms of the physical aspects of the system, the process begins by adding a solution of **1** to a vessel containing the aqueous solution of 2 wt % TPGS-750-M under an atmosphere of Ar, (Figure 5, R1) which achieves the desired appearance of a milky emulsion upon stirring at ≥ 800 rpm for approximately 30 minutes (Figure 6). The emulsion requires constant stirring at high speed to maintain the ideal consistency (otherwise recrystallization of **1** proceeds) and is generally started before the parallel reactor (Figure 5, R2) is charged with material. The parallel reactor is charged with Fe nanomaterial to a solution of 2 wt % aqueous TPGS-750-M and THF under an Ar atmosphere which appears as a red/orange solution upon stirring for ca. 5 minutes (Figure 7).



Figure 6. Emulsion of **1**, in 2 wt % TPGS-750-M/H₂O/THF.



Figure 7. Dissolved precatalyst (FeNP) in 2 wt % TPGS-750-M/H₂O/THF.

Charging the system by the slow addition of KBH₄ spontaneously activates the catalyst as observed by the presence of finely dispersed black particles with the evolution of a large amount of foam (Figure 8). It is at this stage that the majority of gas is evolved from the system over the entire process. Due to the high surface tension of the surfactant solution and the gas generated in-situ, foaming can be expected to increase the volume of the reaction up to four times the original solvent level (for example, 200 mL of catalyst solution can generate ~600 mL of foam). It was found that the amount of foaming was approximately the same in the absence of THF, however low stirring speeds at 200 rpm have been effective in slowing this process. In addition the conical reactor was utilized to increase the surface area of the foam as it expands thereby slowing the evolution of foam as well. The purpose of the

THF in the initial solution was merely for calibration purposes for the initial calorimetry experiment.



Figure 7. Catalyst activation with KBH_4 at ca. 15 minutes.

In order to charge the system with the emulsion of **1** from R1, it was determined that adding a uniform mixture of **1** would require stirring during the course of the addition. In order to achieve this, an addition funnel was affixed to the reactor which was mixed at 800 rpm via overhead stirring in the funnel itself (Figures 8 & 9).



Figure 8. Starting material emulsion in an addition funnel with overhead stirring.

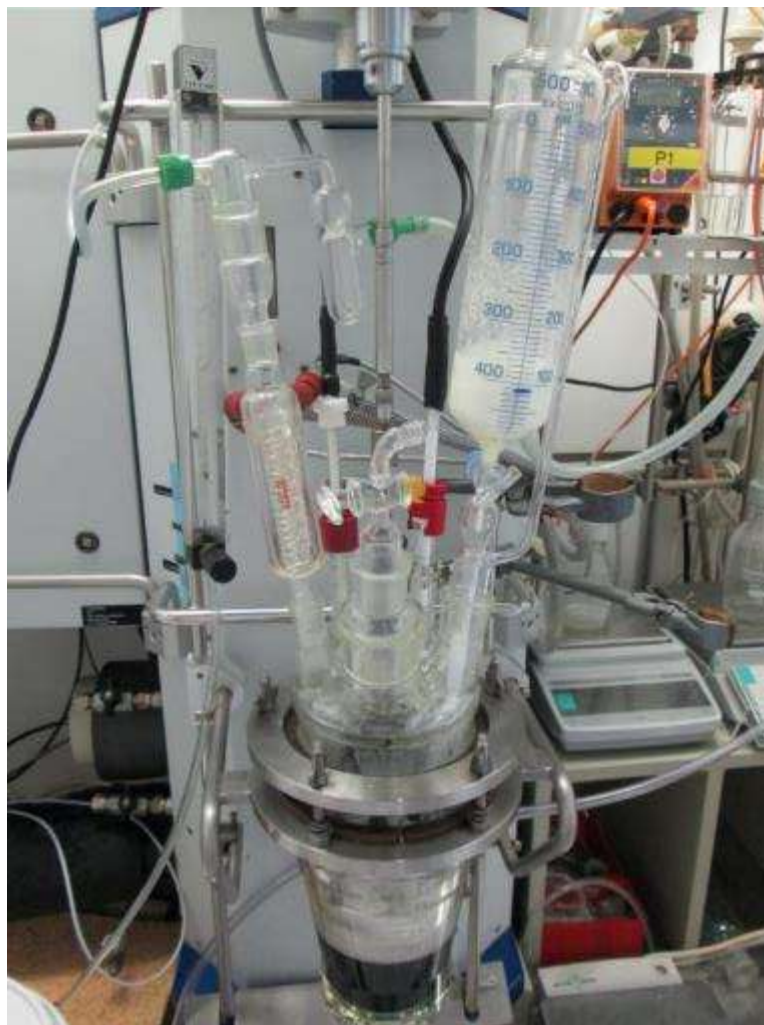


Figure 10. Addition of starting material to RC1 reactor via addition funnel with overhead stirring.

Upon charging the system with the emulsion of **1** to the center of the foam in R2, the foam collapses within ca. 15 minutes, leaving negligible material suspended on the walls of the reactor above the solvent level (Figure 11). A few important notes about this stage should be mentioned in that the foam dissipation is effected by the mixture including solute **1** and THF, not merely THF alone, and charging additional KBH_4 to the system at any later stage will not result in the generation of significant foaming.



Figure 11. Reaction aspect upon complete addition of starting material emulsion.

Reaction work-up proceeds via acidification under air with concentrated HCl that deactivates and solubilizes the catalyst, quenches the remaining KBH_4 (and reactive decomposition products thereof), and solubilizes the product amine in water. Complete KBH_4 decomposition can be determined by monitoring gas evolution upon reaction neutralization and this should be investigated prior to further work-up and purification procedures. However, all KBH_4 is assumed to be consumed at the working pH of 2-3. Also, catalyst deactivation goes by means of an oxidation pathway from O_2 present in the air, so an insoluble form of the catalyst will persist if the quench is carried out under Ar. As the condensation by-products are poorly basic and very nonpolar, extraction with a minimal amount of low polarity organic solvent such as heptanes or MTBE can be used to enrich the

aqueous mixture (Figure 12). As stated earlier, many of the modifications made during the course of developing this process focused on minimizing the occurrence of condensation by-products, and as such, the isolation of all by-products associated with this pathway represented less than 0.1% of the total crude mass at the 100 mmol scale further exemplifying the efficiency of this process.

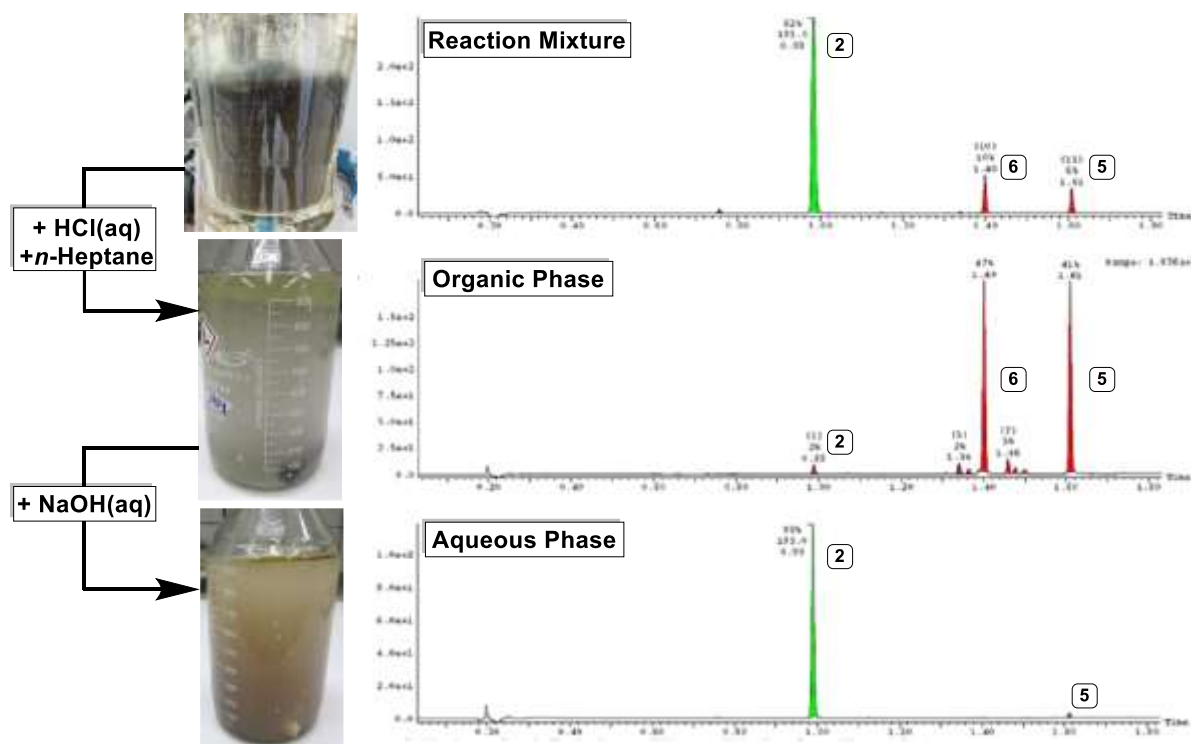


Figure 12. Enrichment of 2, by acidification/extraction/neutralization sequence.

Isolation of the product is carried out by neutralization of the enriched aqueous phase with aqueous NaOH solution, extraction with *i*-PrOAc (isopropyl acetate), and filtration of the combined organic extracts through a plug of filter aid such as Celite® (Figure 13). The volume of the filtrate is then concentrated to approximately 1/3 the original volume followed by recrystallization of the product by the dropwise addition of 1 M HCl solution in ethyl

acetate to yield the HCl salt of **2** as white crystals in >99.8% purity. Consistent with the initial report, ICP analysis revealed residual Pd content at < 1 ppm, demonstrating the applicability of this process as one that can be used at a late stage en route to an API.

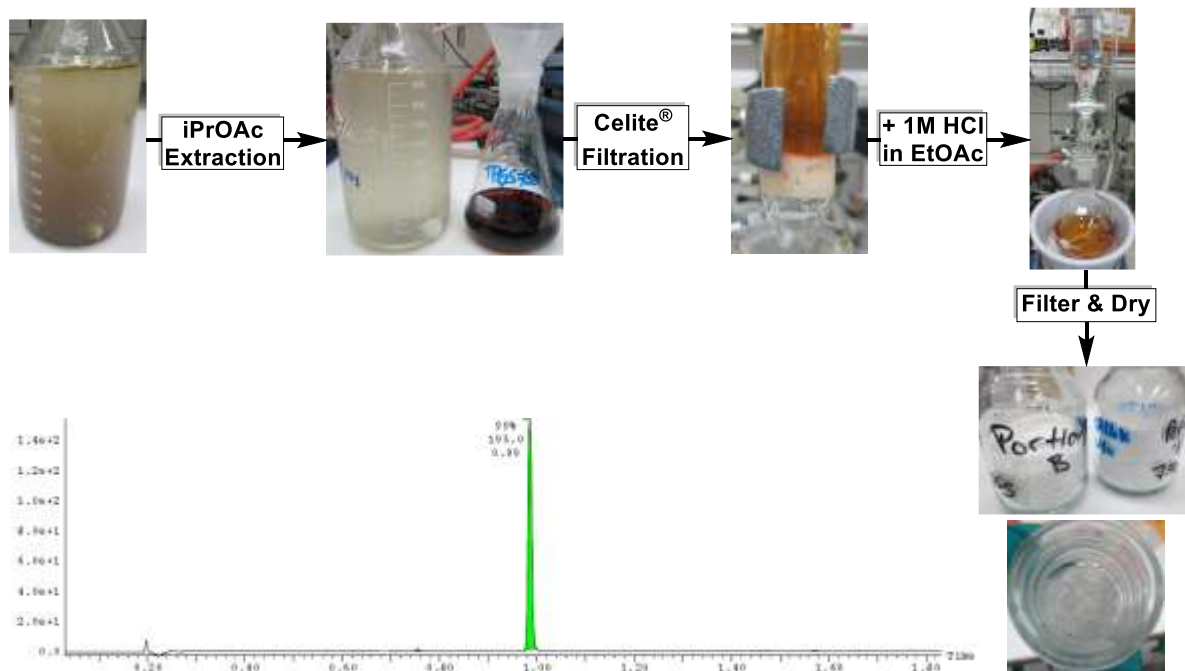
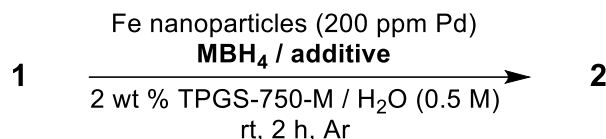


Figure 13. Product isolation/purification by recrystallization as the HCl salt of **2**.

To assure that all parameters of the system were considered on the basis of maximum efficiency, the limitations of the conditions were investigated, such as decreasing catalyst and reductant loading (Table 5, entries 2, 3 respectively). For both modifications, the undesired condensation by-products were observed once more as the result of the more sluggish reaction rate in comparison to the control system. Further examining the effect of counterion realized by the use of KBH_4 , experiments proceeded with less reactive reductants LiBH_4 and NaBH_4 in the presence of KCl . It was observed that NaBH_4 (3.0 equiv) in combination with 1.0 equivalent of KCl mirrored the optimized conditions (entry 6) while

decreasing KCl loading to 0.1 equivalent showed no significant effect on NaBH₄ (entry 5) and the LiBH₄/KCl system was found to remain as an inferior reductant for this system (entry 4). This modification to the existing protocol not only sheds light on the components which effect rate enhancement, but also may allow for of KCl with NaBH₄ as a replacement for KBH₄ which would serve as a more cost effective alternative on scale.⁴²



entry	reductant ^a	additive ^b	time (h)	1 ^c	2	3	4	5	6	7
1	KBH ₄	-	2	0%	100%	0%	0%	0%	0%	0%
2 ^d	KBH ₄	-	4	2%	37%	0%	47%	10%	2%	3%
3 ^e	KBH ₄	-	3	0%	91%	1%	0%	4%	4%	0%
4	LiBH ₄	KCl	2	88%	2%	3%	0%	8%	0%	0%
5 ^f	NaBH ₄	KCl	3	0%	91%	0%	0%	9%	0%	0%
6	NaBH ₄	KCl	2	0%	100%	0%	0%	0%	0%	0%
7	KBH ₄	KCl	2	0%	100%	0%	0%	0%	0%	0%

^a3.0 equiv unless otherwise noted, ^b1.0 equiv unless otherwise noted, ^cUPLC/MS analysis at 210-450 nm, ^d0.5% catalyst loading, ^e2.0 equiv KBH₄, ^f0.1 equiv KCl.

Table 5. Catalyst/reductant loading and the effect of KCl.

Further demonstrating the capabilities of the newly optimized conditions, additional nitroarene substrates bearing reducible functionalities including aryl bromide, a dihalocyclopropane, a protected acylhydrazine derivative, and an α,β -unsaturated ester were successfully reduced to the corresponding anilines in good isolated yields (Figure 14). This shows once more that mild conditions are compatible with a high range of substrate types which may be present in advanced intermediates.

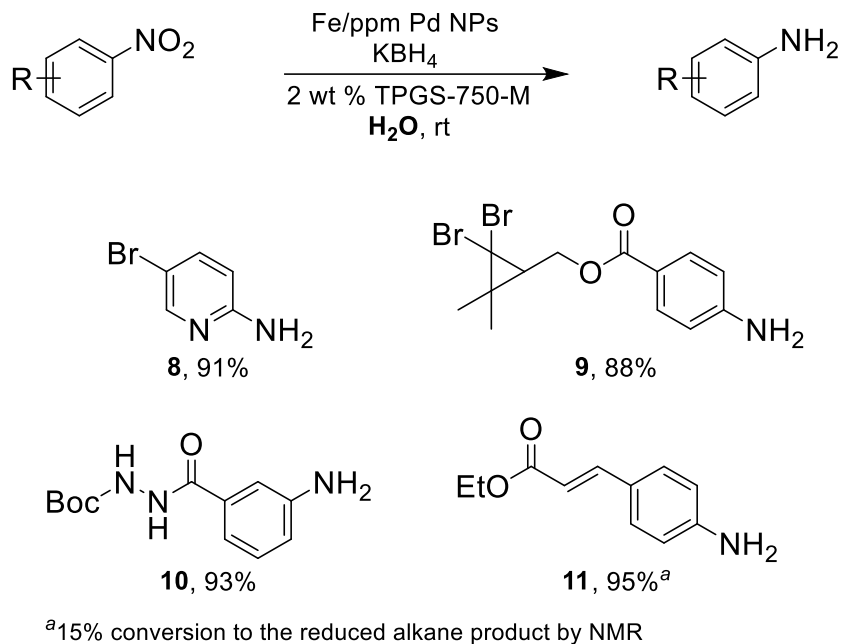


Figure 14. Advanced substrate scope under modified process conditions.

5.5 Calorimetry

To assess the safety of the Fe/ppm Pd-catalyzed nitro group reduction for eventual transfer to the pilot plant, the process was carried out in a 0.5 L RC1 reactor for a calorimetry study, following the process flow diagram (PFD) outlined in Figure 5 on a 40 mmol scale, sequentially charging KBH_4 and **1** stepwise and portion-wise the results of which are concisely summarized in Figure 15. Addition of each portion of KBH_4 and **1** was considered a separate process and continued upon conformation of full conversion to **2** by UPLC/MS analysis of an aliquot from the reaction mixture. Energy corresponding to the nitro group reduction and decomposition of KBH_4 was measured by calorimetric analysis. It was found that the heat of reaction (kJ/mol) was within the same order of magnitude for a standard nitro group reduction via hydrogenation, finding values in the range of approximately -896 to -850 kJ/mol after each addition. As anticipated, the heat of reaction is

directly correlated to the concentration of the unreduced species in the reaction mixture, where a strong exotherm occurs [ca. -153 kJ/kg FRM (final reaction mass), corresponding to a theoretical adiabatic temperature increase of about 37 °C] in the initial portion and ca. -115 kJ/kg FRM corresponding to theoretical adiabatic temperature increase of about 29 °C in the subsequent portion. Approximately 50% of the whole energy is accumulated at the end of the addition corresponding to a theoretical adiabatic temperature increase of about 18 °C to 15 °C. In the event of an undetected loss of cooling for this process, the maximum theoretical temperature that could be reached is approximately 62 °C ($IT + \Delta T_{ad} = 25 + 37^{\circ}\text{C} = 62^{\circ}\text{C}$), well below the boiling point of water thereby making the major concern in terms of safety the potential increase of H₂ evolved. Within 10 minutes of charging the system with the second portion of **1** at 20 °C, a sample was removed for analysis via dynamic SEDEX thermostability test resulting in no significant exothermal decomposition up to 160 °C (Figure 16). From a 3:1 stoichiometry of KBH₄ to **1**, it is calculated that the expected H₂ evolved would be 36.7 L / kg FRM⁴³ from which the majority of this gas is evolved at the stages of catalyst activation and reaction work-up. However, it is necessary to evaluate the accumulation of KBH₄ as this will result in higher gas release. Performing the reduction under continuous flow of Ar alleviates the need for additional safety measures for accumulated gas in the headspace of the reactor and may be required for optimal performance of the catalyst to obtain good conversion. In addition, without the need for maintaining pressurized H₂ gas within the headspace this process lends itself to being safer than hydrogenation alleviating the need for specialized high pressure reactors.

-approximate heat of reaction from -896 to - 850 kJ/mol.
-50% of the energy accumulated at the end of the addition.
-an undetected loss of cooling could result in an increase to only 62 °C
-no significant exothermic decomposition reaction up to 160°C.

Figure 15. Summary of results from calorimetry study at 40 mmol scale.

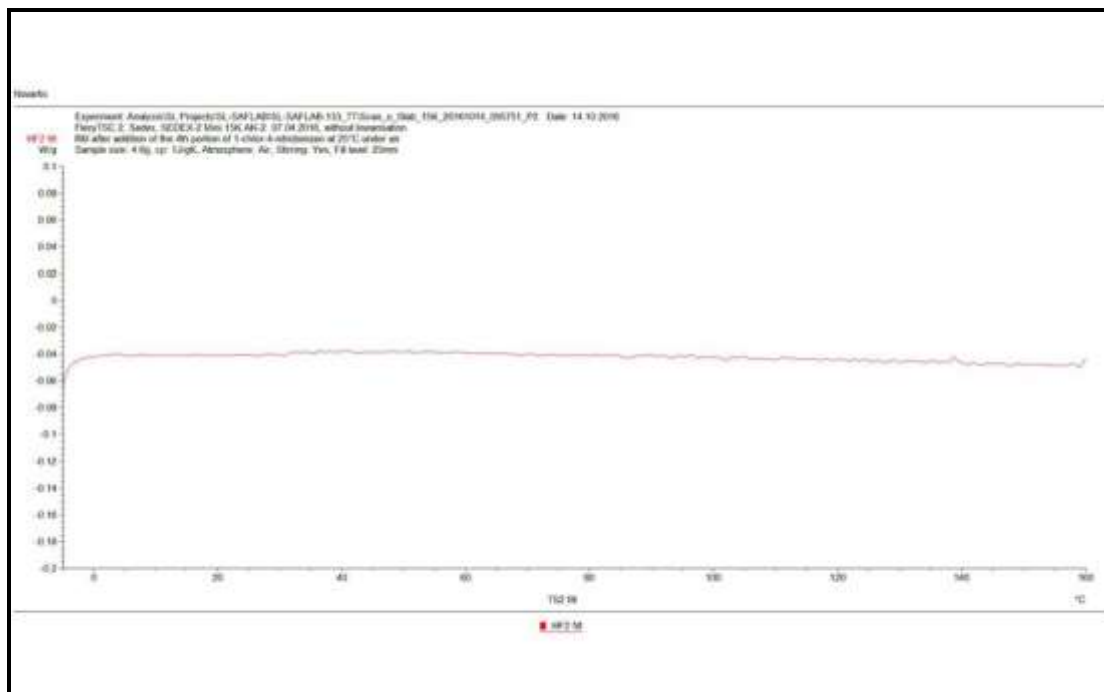


Figure 16. Dynamic SEDEX thermogram of the reaction mixture after second portion addition of 1-chloro-4-nitrobenzene emulsion within 10 minutes at 20°C.

5.6 Summary and Conclusions

In conclusion, a safe, mild, and environmentally responsible scale-up process for the Fe/ppm Pd-catalyzed reduction of nitro compounds in water at room temperature was developed. This process benefits from the use of minimal amounts of palladium (80-200 ppm) to catalyze the transformation, aqueous conditions leveraging micellar catalysis from a solution of TPGS-750-M, short reaction times to deliver highly pure product without

accumulation of highly energetic and toxic intermediates. Moreover, the developed process alleviates the necessity for highly pressurized hydrogenation equipment and can be run in any standard reactor showing no major safety concerns as determined through calorimetry experiments in comparison to classical hydrogenation. The work-up of this process is operationally simple, taking advantage of the aqueous nature of the process itself. This process is envisioned as offering promising conditions for late stage reductions of nitro-group containing compounds involving mild conditions that have little-to-no-effect on functionalized substrates while yielding products with exceptionally low levels of residual Pd content.

5.7 Experimental and Compound Data

General Information

Unless otherwise noted, all reactions were performed under an atmosphere of argon. A solution of 2 wt % TPGS-750-M/H₂O solution was prepared by dissolving TPGS-750-M in degassed Millipore purified water. All commercially available reagents and solvents were used without further purification including TPGS-750-M (CAS-No. 1309573-60-1). Thin layer chromatography (TLC) was done using Silica Gel 60 F₂₅₄ plates (Merck, 0.25 mm thick). The developed chromatogram was analyzed by UV lamp (254 nm). Flash chromatography was performed using a Biotage IsoleraTM Four using prepacked Biotage[®] SNAP Ultra cartridges. Hydrogenation experiments utilized Argonaut Technologies EndeavorTM Katalysator Screening system. ¹H and ¹³C NMR were recorded at 297.8 K on a Bruker[®] 400 MHz spectrometer. The FID was processed using ACD Labs NMR analysis software. Chemical shifts in ¹H NMR spectra are reported in parts per million (ppm) on the δ scale from an internal standard of residual CDCl₃ (7.27 ppm) or the central peak of DMSO-

d_6 (2.50 ppm). Data are reported as follows: chemical shift, multiplicity (s = singlet, d = doublet, t = triplet, q = quartet, quin = quintet), and integration. Chemical shifts in ^{13}C chemical spectra are reported in ppm on the δ scale from the central peak of residual CDCl_3 (77.0 ppm) or the central peak of $\text{DMSO}-d_6$ (39.51 ppm). ICP-OES measurements were conducted by Solvias AG. Reaction profile based on analysis of UPLC/MS data using Acquity HSS T3 1.8 μm 2.1 x 50 mm at 60°C with the following eluent system: (A: water + 0.05 % formic acid + 3.75 mM ammonium acetate; B: acetonitrile + 0.04% formic acid); gradient from 5 to 98 % B in 1.4 min; flow 1.0 mL/min.

Preparation of Fe NP Precatalyst

According to the procedure outlined in the literature,⁴⁸ 0.003 equiv of $\text{Pd}(\text{OAc})_2$ was used in relation to FeCl_3 . An Ar-purged, flame-dried 50 mL round bottom flask with Teflon coated stir bar was charged with $\text{Pd}(\text{OAc})_2$ (27.5 mg, 0.123 mmol) in a drybox, sealed with a septum, and then charged with 3.60 mL of dry THF. The mixture stirred under argon until a solution was achieved after ca. 15 min. A separate Ar-purged, flame-dried 150 mL round bottom flask with Teflon-coated stir bar was charged with anhydrous FeCl_3 (1871.3 mg, 11.54 mmol) in a drybox, sealed with a septum, and then charged with 30 mL of dry THF. The mixture was allowed to stir at rt for ca. 10 min before the addition of 1.13 mL $\text{Pd}(\text{OAc})_2$ solution in THF (0.034 M). The mixture was allowed to stir for ca. 15 minutes before the dropwise addition of freshly titrated 2.7 M MeMgCl (~1 drop/sec). The dark black/brown endpoint was observed after a total of 4.80 mL (12.96 mmol; 1.12 equiv) MeMgCl had been added. The mixture continued to stir for ca. 15 min before removal of the stir bar and the mixture was evaporated to dryness under reduced pressure. The material was then scraped from the sides of the flask with a spatula and pulverized in flask before treatment with 25 mL pentane. The solvent was stripped from the solid material and the pulverizing/stripping

procedure was continued twice more. The light grey, free flowing powder was transferred to an oven-dried 20-mL scintillation vial and set under high vac for ca. 2 days in a lyophilization chamber. The product catalyst was isolated as a light grey/brown free-flowing powder (5411.7 mg). The Pd content of the final product was calculated as follows:

Total Pd in batch:

$$0.0385 \text{ mmol Pd(OAc)}_2 = 0.0385 \text{ mmol Pd}$$

$$0.0385 \text{ mmol Pd} \times 106.4 \text{ mg/mmol Pd} = 4.1 \text{ mg Pd}$$

From the total batch yield:

$$5411.7 \text{ mg NP}$$

Pd content by mass (ppm):

$$(4.1 \text{ mg Pd} / 5411.7 \text{ mg NP}) \times 10^6 = \mathbf{757 \text{ ppm Pd by mass}}$$

“Molecular Weight” of Pd NP:

$$0.0385 \text{ mmol Pd} / 5411.7 \text{ mg NP} = 7.11 \times 10^{-6} \text{ mmol/mg}$$

Preparation of 4-chloroaniline hydrochloride (2)

In a three-neck RC1 reactor with overhead stirring at 200 rpm, 1.117 g Fe nanomaterial (11.4 $\mu\text{mol Pd}$) was dissolved in 200.0 mL 2 wt % TPGS-750-M/H₂O and 23.6 mL THF. KBH₄ (8.091 g, 150 mmol) was slowly charged to the catalyst solution resulting in catalyst precipitation as black solids, foaming, and gas evolution. In a separate 500 mL reactor with overhead stirring, 1-chloro-4-nitrobenzene **1** (15.76 g, 100 mmol), was dissolved in 40 mL THF followed by the slow addition of 110.0 mL 2 wt % TPGS-750-M/H₂O while stirring at 1000 rpm. A milky emulsion was achieved after stirring ca. 30 min. Chloro-4-nitrobenzene emulsion (78.7 mL) was then transferred dropwise (1 drop/sec) via addition funnel with overhead stirring to the center of the reaction mixture. Upon reaction completion (as determined by TLC and UPLC/MS), the reaction was charged with an additional KBH₄

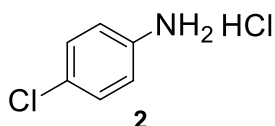
(8.091 g, 150 mmol) followed by the remaining 70 mL of the chloro-4-nitrobenzene emulsion as described above. Upon completion after ca. 11 h, the reaction was exposed to air and quenched with 37% HCl to pH = 3 and stirred for ca. 1 h. The quenched reaction mixture was then extracted with 50 mL *n*-heptane to remove condensation by-products. The aqueous phase was then separated, charged back into the reaction flask and neutralized with 11 M NaOH, precipitating 4-chloroaniline (**2**). The mixture was then extracted with 3 x 50 mL isopropyl acetate, the organic layers were combined, filtered through Celite into a 500 mL round bottom flask, concentrated under reduced pressure to ~75 mL and 75 mL *n*-heptane was charged into the flask. The flask was then charged with a Teflon coated stir bar and 1 M HCl solution in EtOAc (110 mL, 110 mmol) was transferred via addition funnel at a rate of 1 drop/sec while stirring at 200 rpm leading to the precipitation of 4-chloroaniline hydrochloride as white crystals. Stirring continued for an additional 1 h after complete addition of HCl solution, the solid was collected via vacuum filtration and dried at 45 °C and 0 torr for 18 h to afford 15.49 g (94%).

General Nitro Group Reduction Procedure

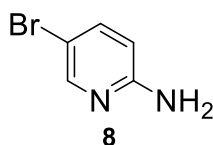
A 50 mL round bottom flask with Teflon-coated stir bar was charged with 16 mg Fe nanomaterial (0.11 μ mol Pd) and was dissolved in 1.5 mL 2 wt % TPGS-750-M/H₂O. KBH₄ (162 mg, 3.0 mmol) was slowly charged to the catalyst solution resulting in catalyst precipitation as black solids, foaming, and gas evolution. A separate 8 mL dram vial with a Teflon coated stir bar was charged with nitroarene (1.0 mmol), 0.4 mL THF, followed by the slow addition of 1.5 mL 2 wt % TPGS-750-M/H₂O. The mixture was mixed via vortex and stirred at high speed (>1000 rpm) and approximately half of the mixture was transferred to the catalyst reaction. After complete conversion was observed via analysis by TLC and GC/MS (usually about ca. 4 h), the reaction was charged with KBH₄ (162 mg, 3.0 mmol)

and the remaining portion of the starting material mixture. After ca. 16 h (reaction time not optimized), the crude product was extracted with 3 x 3 mL EtOAc, dried over anhydrous Na₂SO₄, and purified via flash chromatography.

Characterization of Products

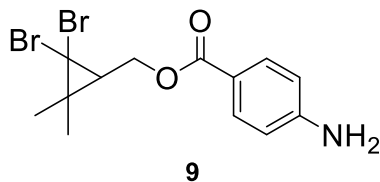


Preparation of 4-chloroaniline hydrochloride (2). ¹H NMR (500 MHz, DMSO-*d*₆) δ 10.12 (brs, 3H), 7.53 (dt, 2H), 7.39 (dt, 2H). ¹³C NMR (125 MHz, DMSO-*d*₆) δ 132.02, 131.66, 129.58, 124.68.



5-Bromopyridin-2-amine (8).

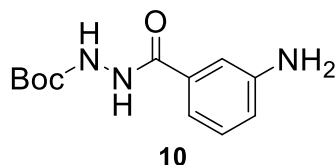
157.6 mg, 91%. ¹H NMR (500 MHz, CDCl₃) δ 7.85 (dd, 1H, *J* = 2.60, 0.52 Hz), 7.21 (dd, 1H, *J* = 8.56, 0.52 Hz), 6.88 (dd, 1H *J* = 8.56, 3.11 Hz). ¹³C NMR (125 MHz, CDCl₃) δ 142.06, 137.01, 129.48, 127.75, 124.68. ¹H & ¹³C NMR was in agreement with previously reported data on this compound.⁴⁴



(2,2-Dibromo-3,3-dimethylcyclopropyl)methyl 4-amino-benzoate (9).

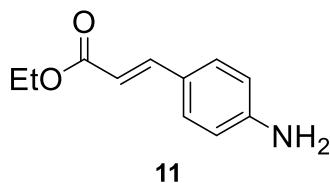
400.5 mg, 88%. ¹H NMR (500 MHz, CDCl₃) δ 7.88 (dt, 2H), 6.66 (m, 2H), 4.38 (m, 2H), 4.12 (s, 2H), 1.78 (t, 1.78), 1.45 (s, 3H), 1.33 (s, 3H). ¹³C NMR (125 MHz, CDCl₃) δ

166.37, 151.02, 131.69, 119.24, 113.74, 103.67, 99.03, 63.20, 43.73, 37.25, 28.96, 27.12, 19.67.



***t*-Butyl 2-(3-aminobenzoyl)hydrazine-1-carboxylate (10).**

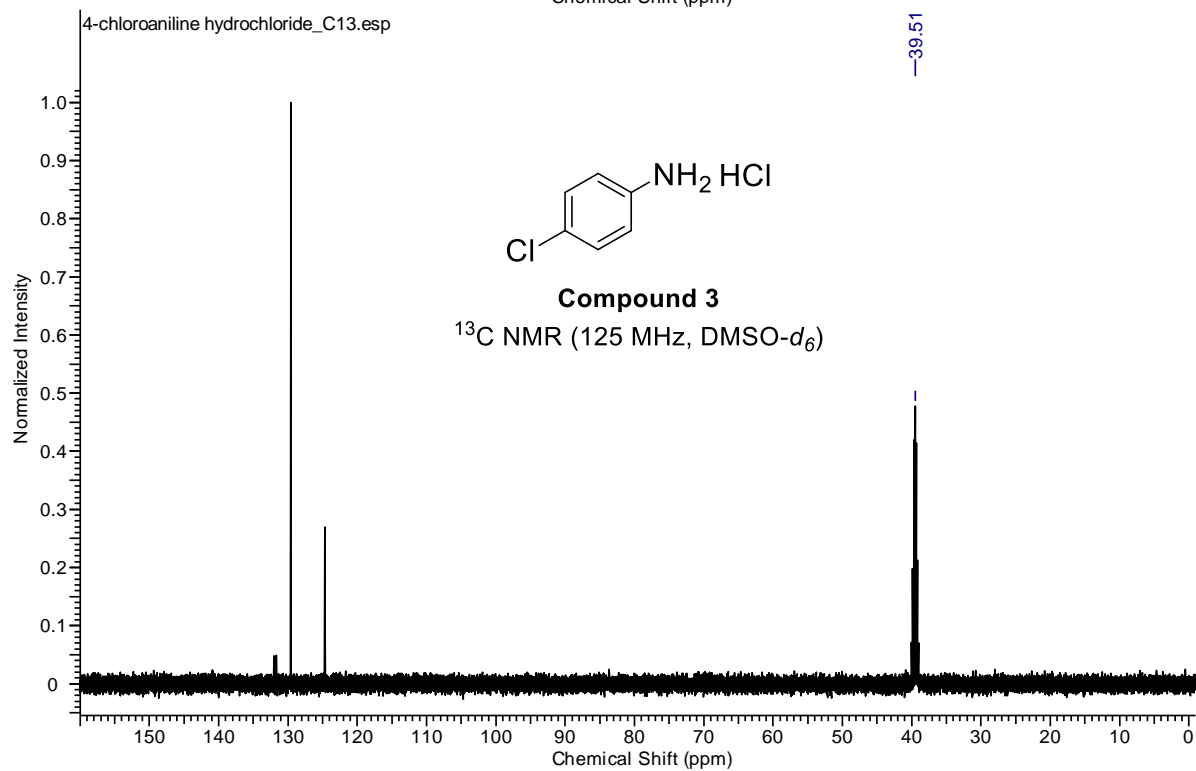
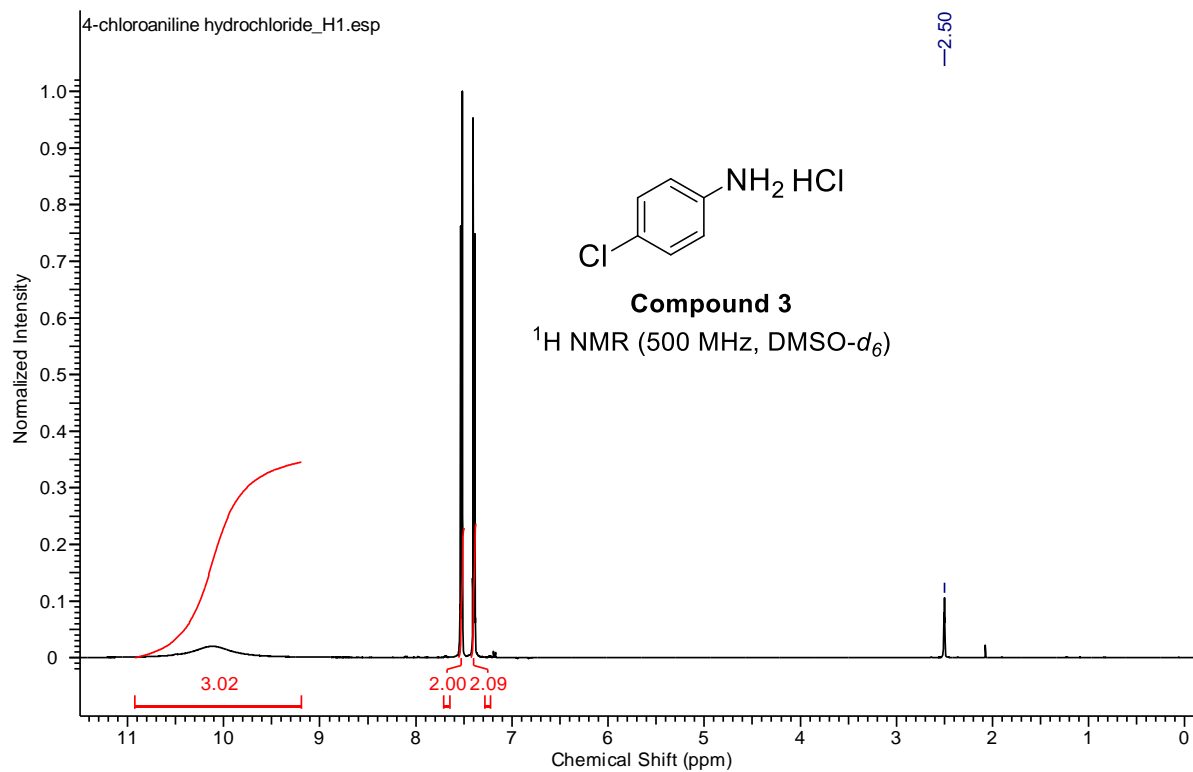
233.0 mg, 93%. ¹H NMR (500 MHz, DMSO-*d*₆) δ 9.91 (d, 1H, *J* = 1.30 Hz), 8.78 (s, 1H), 7.08 (t, 1H, *J* = 7.79 Hz), 7.03 (s, 1H), 6.95 (d, 1H, *J* = 7.53), 6.71 (ddd, 1H, *J* = 7.79, 2.34, 0.78 Hz), 5.29 (s, 2H), 1.42 (s, 9H). ¹³C NMR (125 MHz, DMSO-*d*₆) δ 166.73, 155.45, 148.49, 133.49, 128.72, 116.97, 114.46, 113.05, 79.01, 28.11.

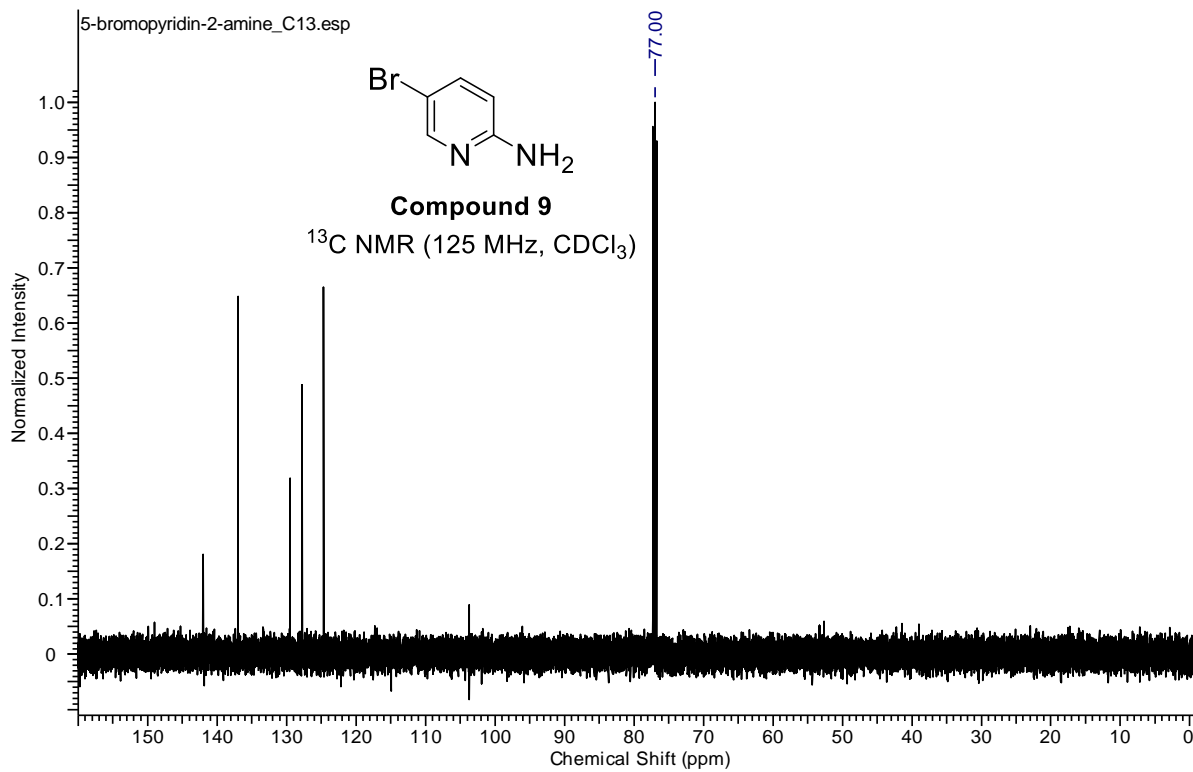
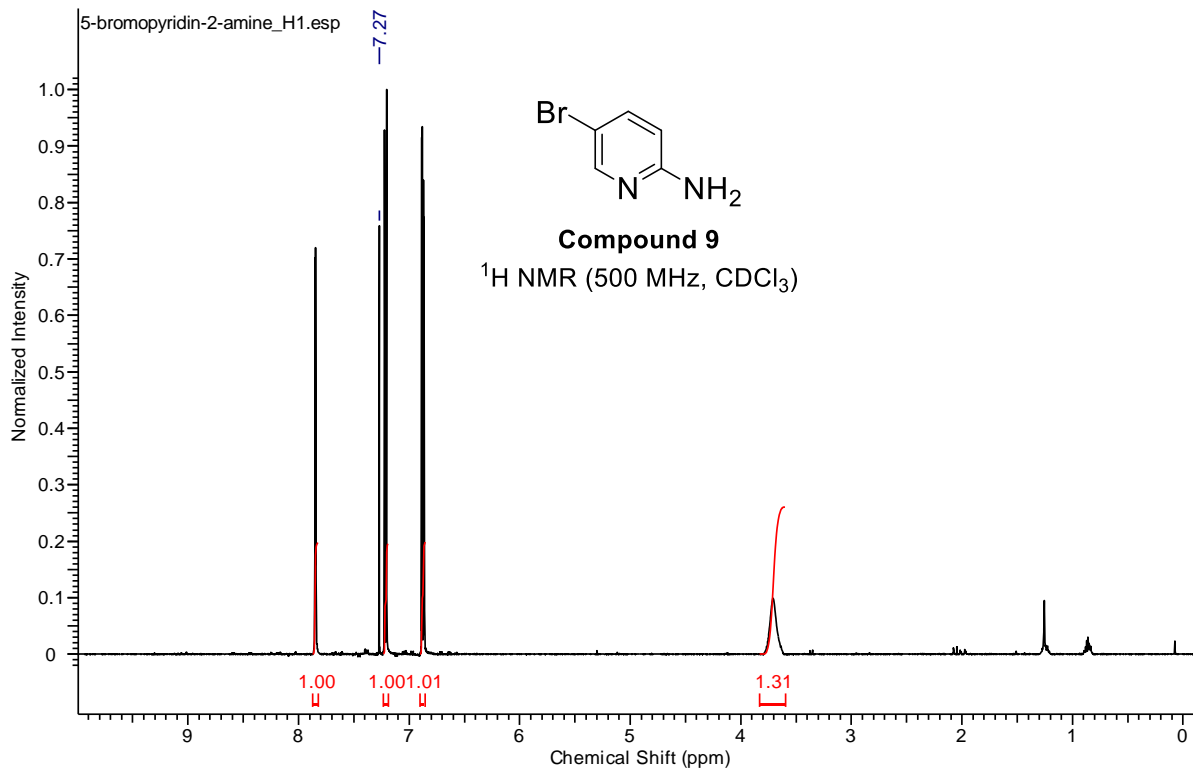


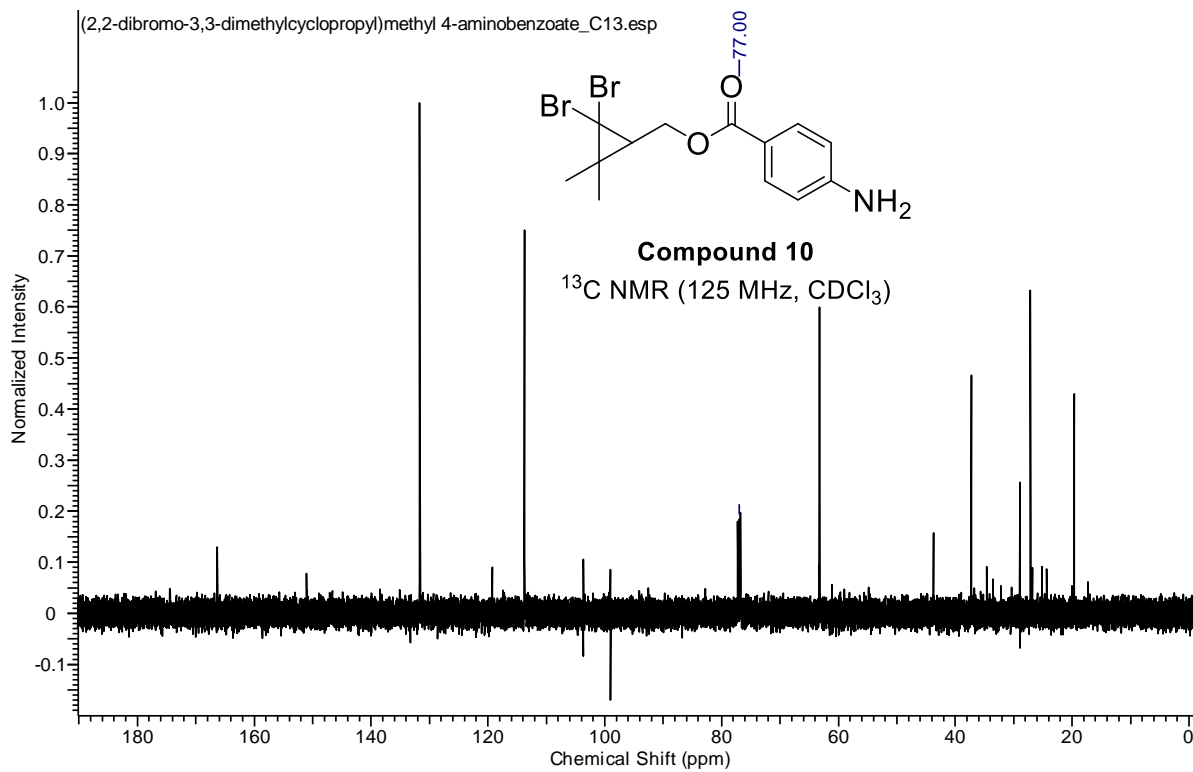
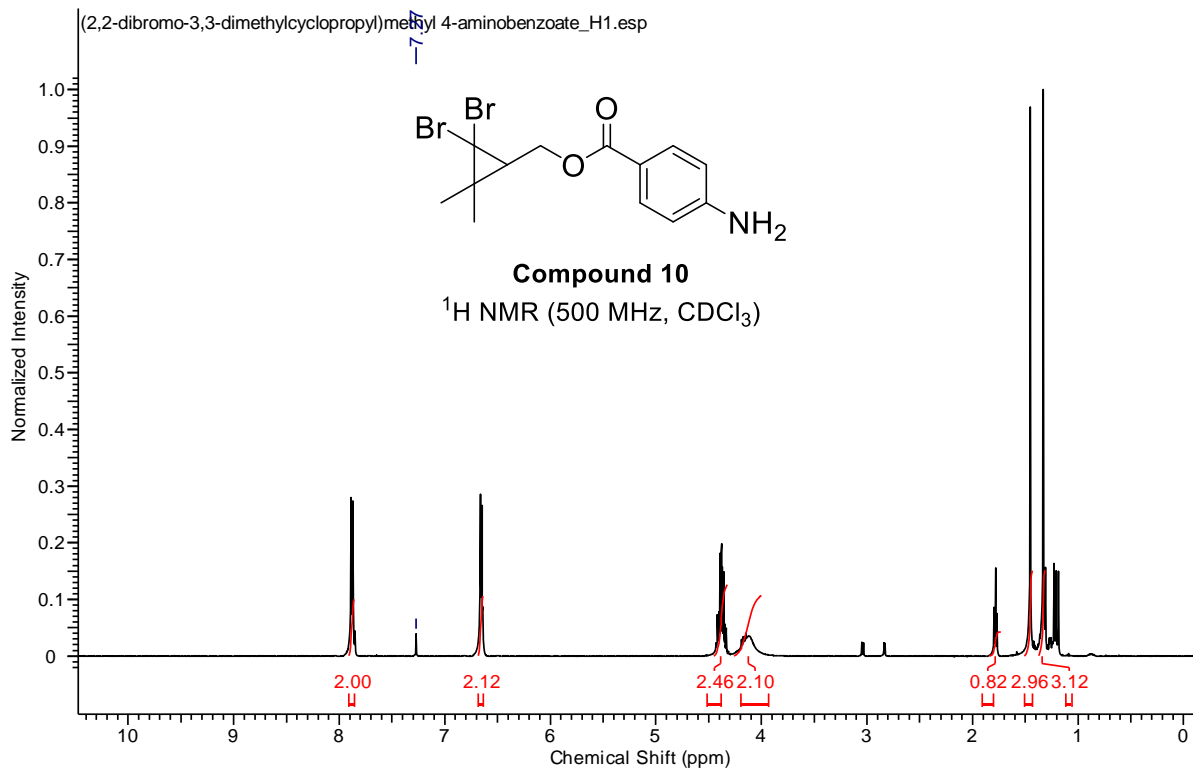
Ethyl (E)-3-(4-aminophenyl)acrylate (11).

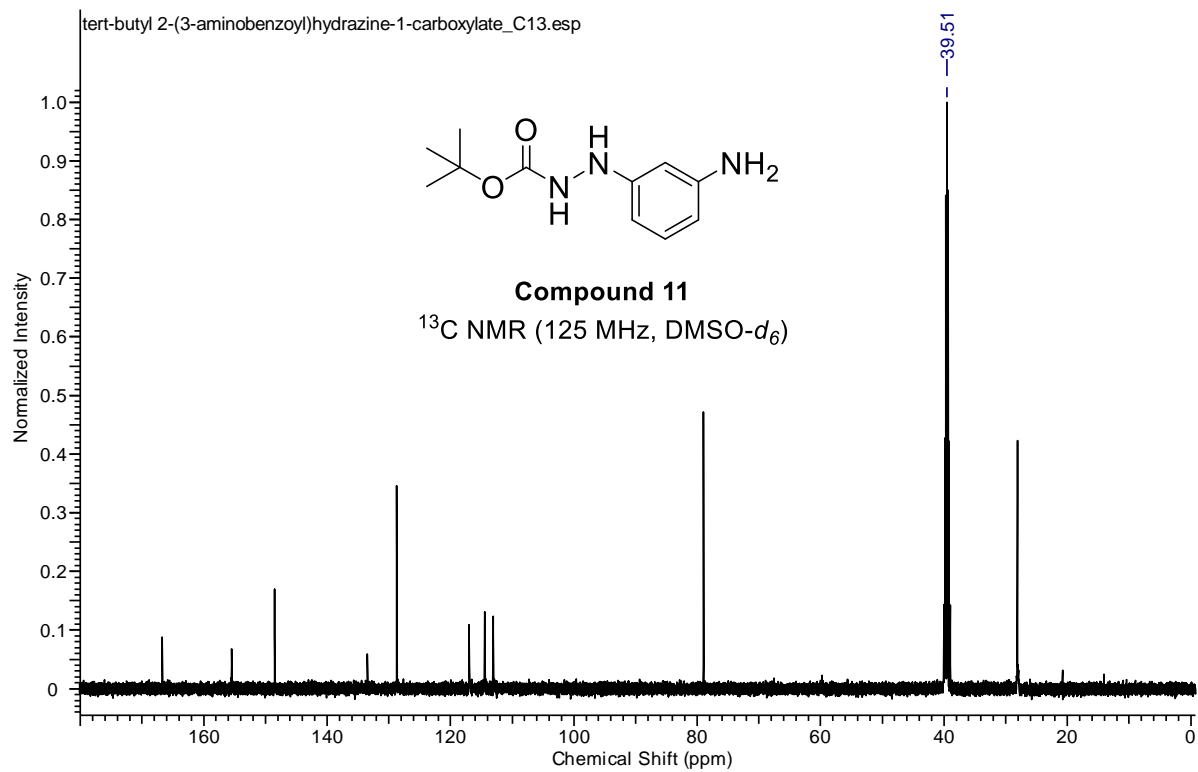
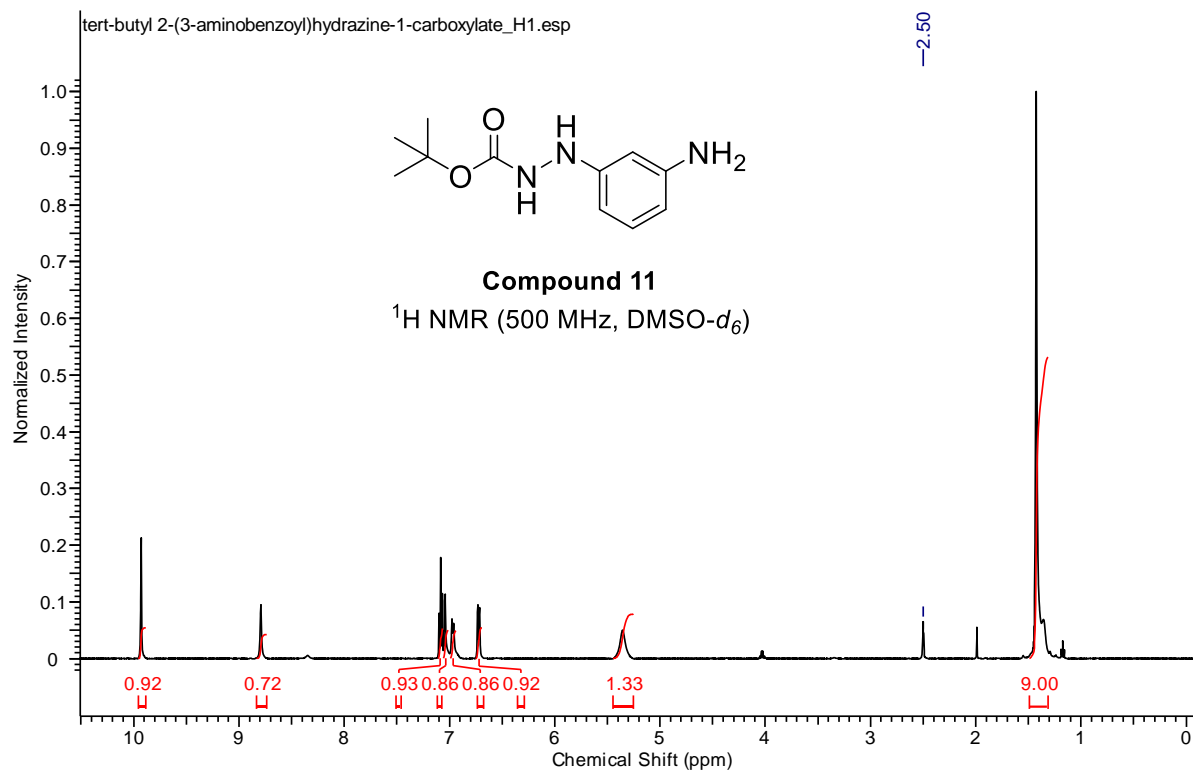
181.9 mg, 93%. ¹H NMR (500 MHz, CDCl₃) δ 7.60 (d, 1H, *J* = 16.09 Hz), 7.36 (m, 2H), 6.65 (m, 2H), 6.24 (d, 1H, *J* = 15.8 Hz), 4.25 (q, 2H), 1.33 (t, 3H). ¹³C NMR (125 MHz, CDCl₃) δ 167.65, 148.60, 144.79, 129.82, 124.76, 114.80, 113.75, 60.13, 14.37. ¹H & ¹³C NMR was in agreement with previously reported data on this compound.⁴⁵

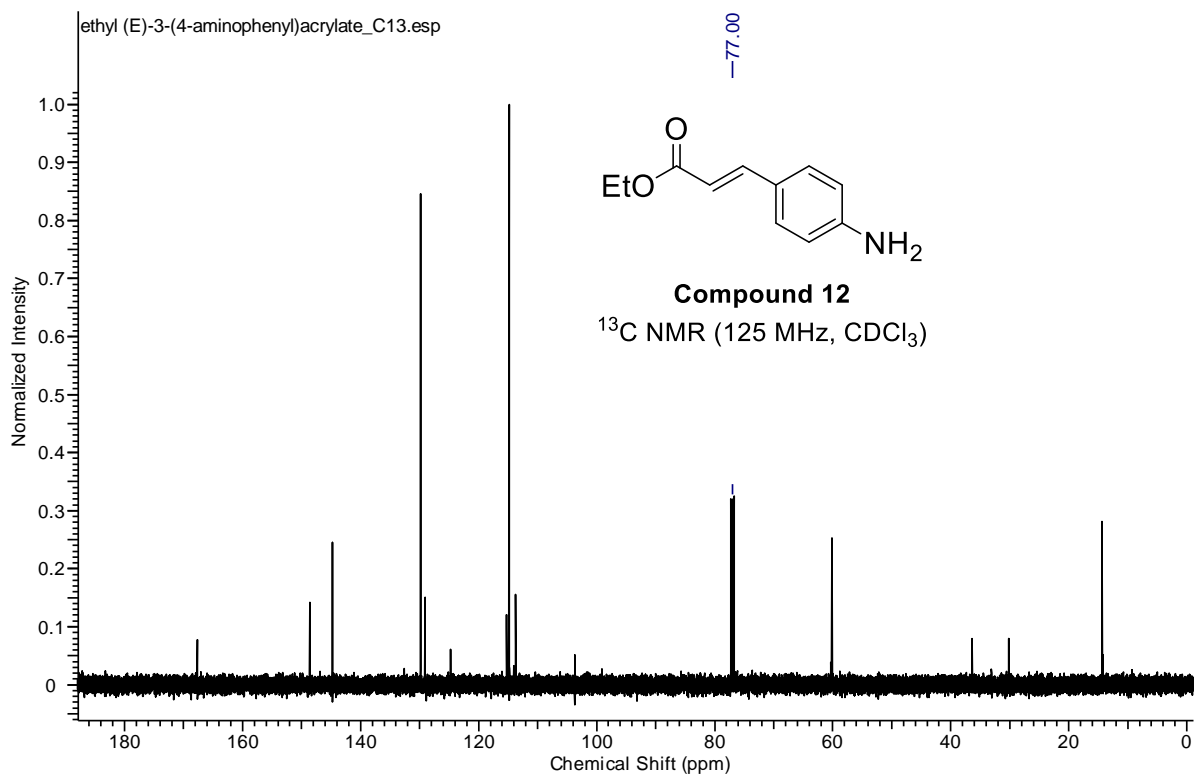
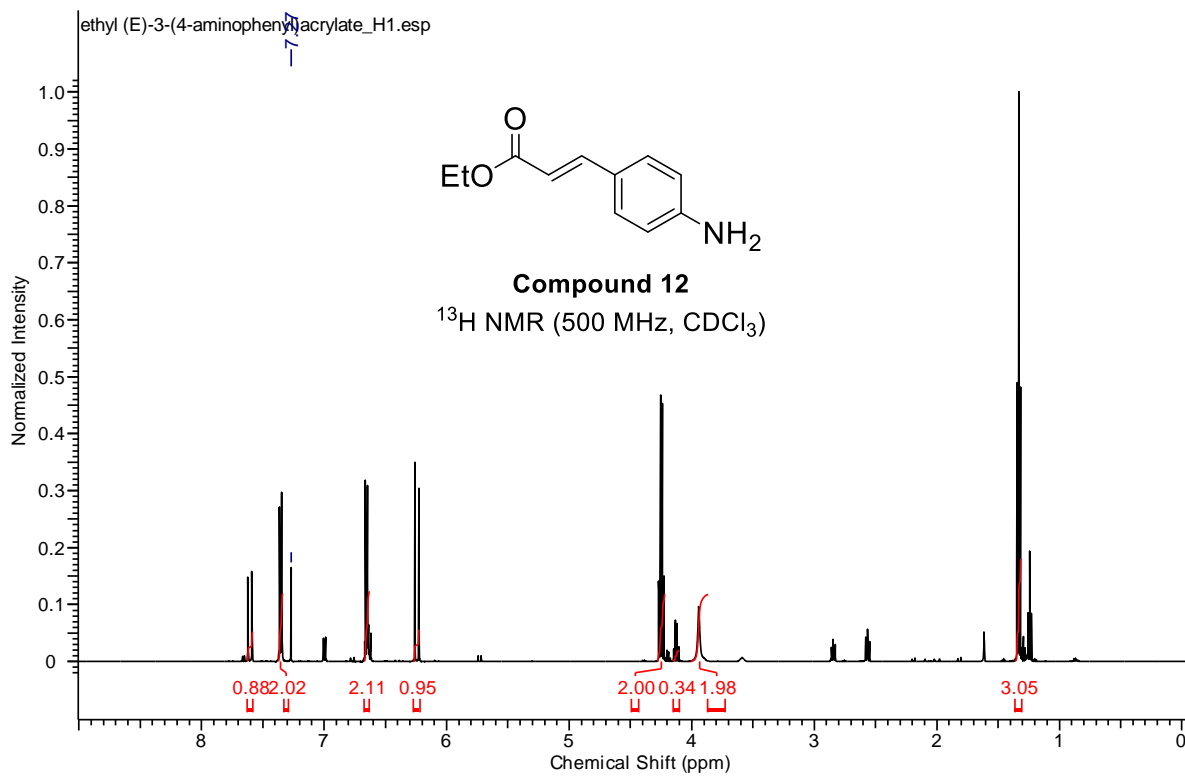
5.8 NMR Spectra











5.9 Calorimetry Plots

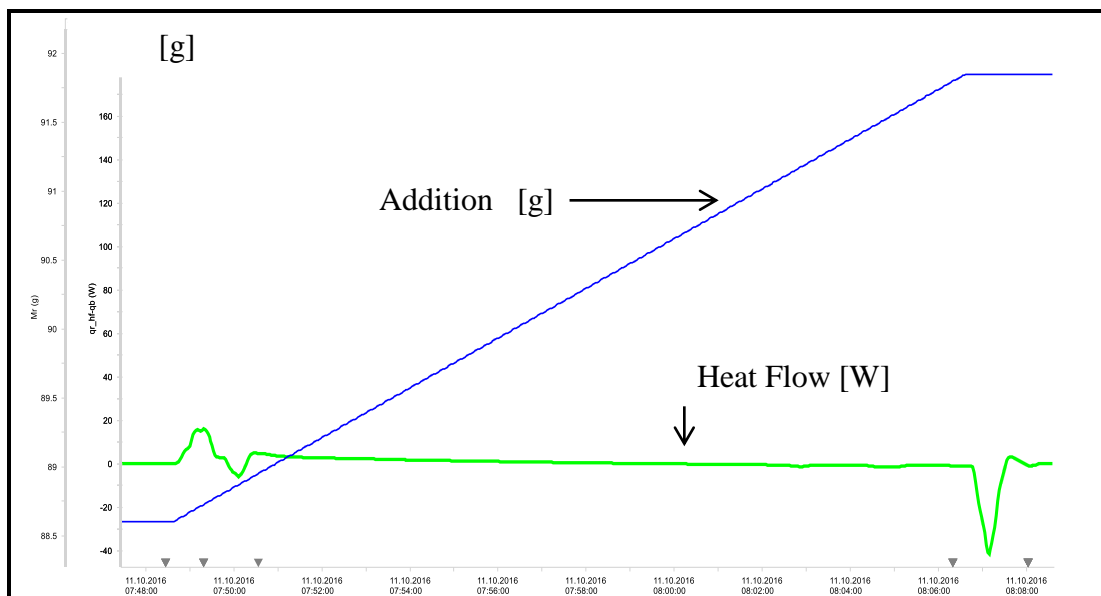


Figure 17. Reaction calorimetry of the initial KBH_4 addition (3.2 g) within 10 min at 20°C.

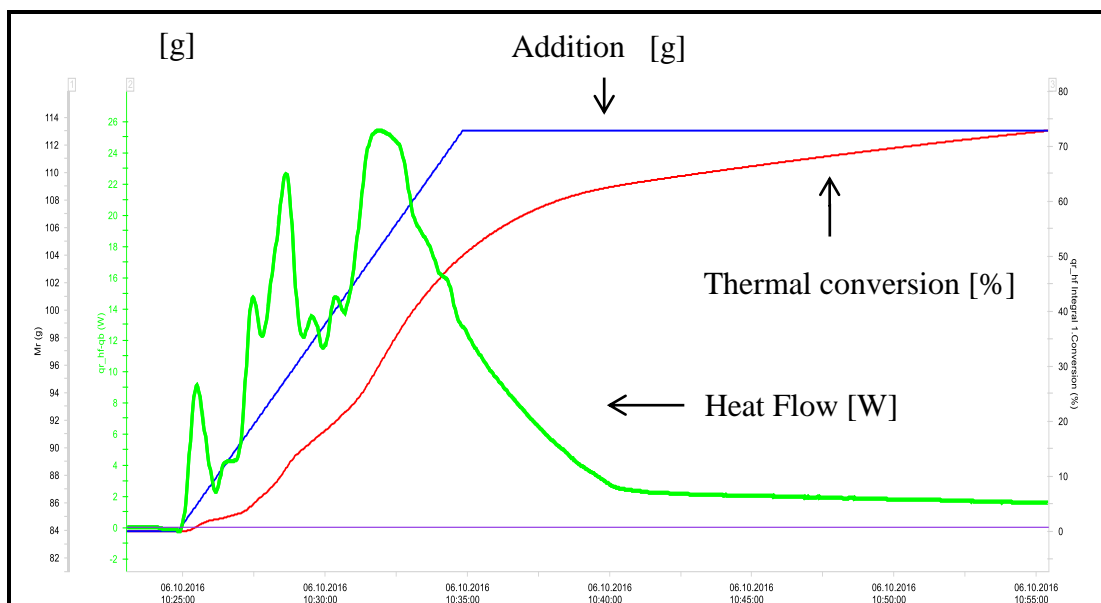


Figure 17. Reaction calorimetry of the initial 1-chloro-4-nitrobenzene emulsion addition within 10 minutes at 20 °C.

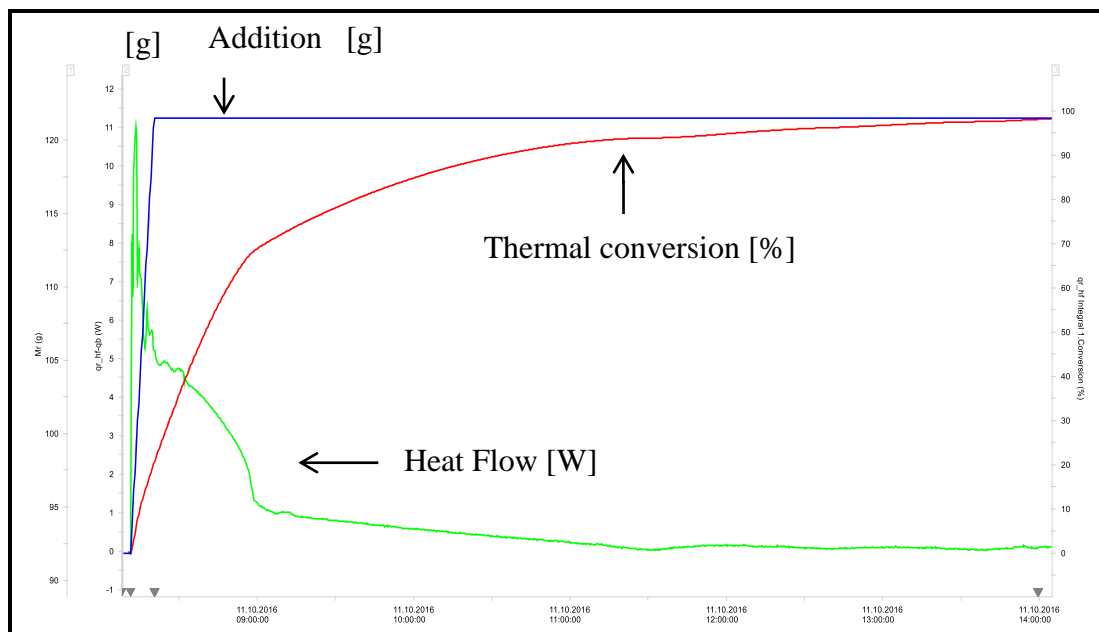


Figure 18. Reaction calorimetry of the second portion addition of 1-chloro-4-nitrobenzene emulsion addition within 10 minutes at 20 °C and 5 hours aging.

5.10 References

1. Ono, N. *The Nitro Group in Organic Synthesis*; Wiley-VCH: New York, **2001**.
2. Baxter, M. G.; Elphick, A. R.; Miller, A. A.; Sawyer, D. A. Substituted Aromatic Compounds. U.S. Patent 4,560,687, Dec 24, **1985**. b) Gerster, J. F.; Lindstrom, K. J. Process for Preparing Imidazoquinolinamines. WO Patent 01997048704, Dec 24, **1997**.
3. Harrington, P. J. *Pharmaceutical Process Chemistry for Synthesis: Rethinking the Routes to Scale-up*; Wiley: Hoboken, NJ, **2011**.
4. Raman, J. V.; Rathod, D.; Vohra, I.; Chavan, M.; Ahirrao, M.; Ponnaiah, R. US Patent 0,137,864, May 30, **2013**.
5. Kuroda, K.; Tsuyumine, S.; Kodama, T. *Org. Process Res. Dev.* **2016**, *20*, 1053.
6. Yu, J.; Wang, J. *Org. Process Res. Dev.* **2017**, *21*, 133.
7. Angelaud, R.; Reynolds, M.; Venkatramani, C.; Savage, S.; Trafelet, H.; Landmesser, T.; Demel, P.; Levis, M.; Ruha, O.; Rueckert, B.; Jaeggi, H. *Org. Process Res. Dev.* **2016**, *20*, 1509.
8. a) Mayer, W.; Ziegler, H.; Schneider, K.-H.; Kröhl, T.; Mayer, H.; Erk, P.; Cox, G.; Stierl, R. Neue Kristalline Modifikation des Anhydrates von Boscalid WO Patent 2004072039, Aug 26, **2004**. b) Jiao, D.; Jiang, R.; Zhang, P.; Zheng, Y. CN Patent 103980192, Aug 13, **2014**.
9. Szczepek, W.; Luniewski, W.; Kaczmarek, L.; Zagrodzki, B.; Samson-Lazinska, D.; Szelejewski, W.; Skarzynski, M. Process for Preparation of Imatinib Base U.S. Patent 7,674,901, Aug 28, **2012**.
10. Cantillo, D.; Wolf, B.; Goetz, R.; Kappe, C. O. *Org. Process Dev.* **2017**, *21*, 125.
11. Hayakawa, I. D. S.; Tanaka, Y. D. S. Tricyclic compounds, a Process for their Production and Pharmaceutical Compositions Containing said Compounds. EP Patent 101 829, Dec 30, **1986**.
12. For reviews on nitro group reductions, also see a) Orlandi, M.; Brenna, D.; Harms, R.; Jost, S.; Benaglia, M. *Org. Process. Res. Dev.* **2016** In Press. b) Hudlicky, M. *Reductions in Organic Chemistry*; American Chemical Society: Washington, D.C., 1996.
13. Béchamp, A. J. *Ann. Chim. Phys.* **1854**, *42*, 186.

14. a) Vanier G. S., *Synlett* **2007**, 131. b) Hoogenraad, M.; van der Linden, J. B.; Smith, A. A.; Hughes, B.; Derrick, A. M.; Harris, L. J.; Higginson, P. D.; Pettman, A. *J. Org. Process Res. Dev.* **2004**, *8*, 469. c) Dale, D. J.; Dunn, P. J.; Golightly, C.; Hughes, M. L.; Levett, P. C.; Pearce, A. K.; Searle, P. M.; Ward, G. W.; Wood, A. S. *Org. Process Res. Dev.* **2000**, *4*, 17. d) Bae, J. W.; Cho, Y. J.; Lee, S. H.; Yoon, C. M. *Tetrahedron Lett.* **2000**, *41*, 175. e) Ram, S.; Ehrenkauf, R. E. *Tetrahedron Lett.* **1984**, *25*, 3415. f) Mendenhall, G. D.; Smith, P. A. S. *Org. Synth.* **1966**, *46*, 85.
15. a) Pogorelić, I.; Filipan-Litvić, M.; Merkaš, S.; Ljubić, G.; Capanec, I.; Litvić, M. *J. Mol. Catal. A: Chem.* **2007**, *274*, 202. b) Gowda, D. C.; Gowda, A. S. P.; Baba, A. R. *Synth. Commun.* **2000**, *30*, 2889. c) Yuste, F.; Saldana, M.; Walls, F. *Tetrahedron Lett.* **1982**, *23*, 147. d) Dimroth, K.; Berndt, A.; Perst, H.; Reichardt, C. *Org. Synth.* **1969**, *49*, 116. e) Icke, R. N.; Redemann, C. E.; Wisegarver, B. B.; Alles, G. A. *Org. Synth.* **1949**, *29*, 6. f) Allen C. F. H.; Van Allan J. *Org. Synth.* **1942**, *22*, 9.
16. a) Adams, R.; Cohen, F. L. *Org. Synth.* **1928**, *8*, 66. b) Chandrasekhar S., Prakash S. Y., Rao C. L., *J. Org. Chem.*, **2006**, *71*, 2196.
17. a) Wienhöfer, G.; Sorribes, I.; Boddien, A.; Westerhaus, F.; Junge, K.; Junge, H.; Llusar, R.; Beller, M. *J. Am. Chem. Soc.* **2011**, *133*, 12875. b) Zhu, K.; Shaver, M. P.; Thomas, S. P. *Chem. Sci.* **2016**, *7*, 3031.
18. a) Saha, A.; Ranu, B. *J. Org. Chem.* **2008**, *73*, 6867. b) Duan, Z.; Ma, G.; Zhang, W. *Bull. Korean Chem. Soc.* **2012**, *33*, 4003. c) Sharma, U.; Kumar, P.; Kumar, N.; Kumar, V.; Singh, B. *Adv. Synth. Catal.* **2010**, *352*, 1834.
19. a) Yadav, S.; Kumar, S.; Gupta, R. *Inorg. Chem. Front.* **2017**, *4*, 324. b) Westerhaus, F. A.; Jagadeesh, R. V.; Wienhöfer, G.; Pohl, M.-M.; Radnik, J.; Surkus, A.-E.; Rabeah, J.; Junge, K.; Junge, H.; Nielsen, M.; Brückner, A.; Beller, M. *Nature Chem.* **2013**, *5*, 537.
20. Iihama, S.; Furukawa, S.; Komatsu T. *ACS Catal.* **2016**, *6*, 742.
21. Shiraishi, Y.; Togawa, Y.; Tsukamoto, D.; Tanaka, S.; Hirai, T. *ACS Catal.* **2012**, *2*, 2475.
22. a) Chen, S.; Lu, G.; Cai, C. *New J. Chem.* **2015**, *39*, 5360. b) Xu, D.; Diao, P.; Jin, T.; Wu, Q.; Liu, X.; Guo, X.; Gong, H.; Li, F.; Xiang, M.; Ronghai, Y. *ACS Appl. Mater. Interfaces* **2015**, *7*, 16738.
23. Cai, S.; Duan, H.; Rong, H.; Wang, D.; Li, L.; He, W.; Li, Y. *ACS Catal.* **2013**, *3*, 608.
24. a) Bauer, I., Knölker H.-J. *Chem. Rev.* **2015**, *115*, 3170. b) Wienhöfer G., Sorribes I., Boddien A., Westerhaus F., Junge K., Junge H., Llusar R., Beller M., *J. Am. Chem. Soc.* **2011**, *133*, 12875. c) Chandrappa S., Vinaya T., Ramakrishna T., Rangappa

- K. S., *Synlett* **2010**, 3019. d) Liu, Y.; Lu, Y.; Prashad, M.; Repič, O.; Blacklock, T. J. *Adv. Synth. Catal.* **2005**, *347*, 217. e) Deshpande R. M., Mahajan A. N., Diwakar M. M., Ozarde P. S., Chaudhari R. V. *J. Org. Chem.*, **2004**, *69*, 4835. f) Vass, A.; Dudar, J.; Varma, R.S. *Tetrahedron Lett.* **2001**, *42*, 5347. g) Meshram, H. M.; Ganesh, Y. S. S.; Sekhar, K. C.; Yadav, J. S. *Synlett* **2000**, 993. h) Sadavarte, V. S.; Swami, S. S.; Desai, D. G. *Synth. Commun.* **1998**, *28*, 1139. i) Kumbhar, P. S.; Valnte, J. S.; Figueras, F. *Tetrahedron Lett.* **1998**, *39*, 2573. j) Marlic, C. A.; Motamed, S.; Quinn, B. *J. Org. Chem.* **1995**, *60*, 3365. k) B. A. Fox B. A.; Threlfall T. L. *Org. Synth.* **1964**, *44*, 34. l) Hazlet, S. E.; Dornfeld, C.A. *J. Am. Chem. Soc.* **1944**, *66*, 1781. m) Mahood, S. A.; Schaffner, P. V. L. *Org. Synth.* **1931**, *11*, 32.
25. a) Kelly, S. M.; Lipshutz, B. H. *Org. Lett.* **2014**, *16*, 98. b) Mahdavi, H.; Tamami, B. *Synth. Commun.* **2005**, *35*, 1121. c) Gowda, S.; Gowda, B. K. K.; Gowda, D. C. *Synth. Commun.* **2003**, *33*, 281. d) Shundberg, R.; Pitts, W. *J. Org. Chem.* **1991**, *56*, 3048 e) Burawoy, A.; Critchley, J. P. *Tetrahedron* **1959**, *5*, 340. f) Coleman, G. H.; McClosky, S. M.; Suart, F. A., *Org. Synth.* **1945**, *25*, 80. g) Hartman, W. W.; Fierke S. S. *Org. Synth.* **1939**, *19*, 70. h) Kock, E. *Chem. Ber.* **1887**, *20*, 1567.
26. a) De, P. *Synlett* **2004**, 1835. b) Doxsee, K. M.; Figel, M.; Stewart, K. D.; Canary, J. W.; Knobler, C. B.; Cram, D. J. *J. Am. Chem. Soc.* **1987**, *109*, 3098. c) Bellamy, F. D.; Ou, K. *Tetrahedron Lett.* **1984**, *25*, 839. d) Hartman W. W., Dickey J. B., and Stampfli J. G. *Org. Synth.* **1935**, *15*, 8. e) Clarke H. T.; Hartman, W. W. *Org. Synth.* **1929**, *9*, 74.
27. Booth, G. Nitro Compounds, Aromatic. In *Ullman's Encyclopedia of Industrial Chemistry*; Wiley-VCH: Weinheim, Germany, **2000**.
28. Gadamasetti, K. G.; Braish, T. In *Process Chemistry in the Pharmaceutical Industry*; CRC: Boca Raton, **2008**; pp 29–32.
29. a) Cantillo, D.; Moghaddam, M. M.; Kappe, O. *J. Org. Chem.* **2013**, *78*, 4530. b) Day, R.; Mukherjee, N.; Ahammed, S.; Ranu, B. C. *Chem. Commun.* **2012**, *48*, 7982. c) Kim, S.; Kim, E.; Kim, B. M. *Chem. Asian J.* **2011**, *6*, 1921. d) Kotha, S. S.; Sharma, N.; Sekar, G. *Tetrahedron Lett.* **2016**, *57*, 1410. e) Parmekar, M. V.; Salker, A. V. *RSC Adv.* **2016**, *6*, 108458. f.) Aditya, T.; Pal, A.; Pal, T. *Chem. Commun.* **2015**, *51*, 9410. g) Pradhan, N., Pal, A.; Pal, T. *Colloids Surf. A* **2002**, *196*, 247. h) Cui, Q.; Yashchenok, A.; Li, L.; Mohwald, H.; Bargheer, M. *Colloids Surf. A* **2015**, *470*, 108.
30. a) Kobayashi, J.; Mori, Y.; Okamoto, K.; Akiyama, A.; Ueno, M.; Kitamori, T.; Kobayashi, S. *Science* **2004**, *304*, 1305. b) Tarleton, M.; McCluskey, A. *Tetrahedron Lett.* **2011**, *52*, 1583. c) Ekholm, F. S.; Mandity, I. M.; Fulop, F.; Leino, R. *Tetrahedron Lett.* **2011**, *52*, 1839. d) Jones, R. V.; Godorhazy, L.; Varga, N.; Szalay, D.; Urge, L.; Darvas, F. *J. Comb. Chem.* **2006**, *8*, 110. e) Spadoni, C.; Jones, R.; Urge L.; Darvas, F.; *Chim. Oggi* **2005**, *23*, 36. f) Saaby, S.; Knudsen, K. - R.; Ladlow, M.; Ley, S. V. *Chem. Commun.* **2005**, 2909. g) Oyamada, H.; Naito, T.; Kobayashi, S. *Beilstein J. Org. Chem.* **2011**, *7*, 735.

31. Gavriilidis, A.; Constantinou, A.; Hellgardt, K.; Hii, K. K.; Hutchings, G. J.; Brett, G. L.; Kuhn, S.; Marsden, S. P. *React. Chem. Eng.* **2016**, *1*, 595.
32. Feng, J.; Handa, S.; Gallou, F.; Lipshutz, B. H. *Angew. Chem., Int. Ed.* **2016**, *55*, 8979.
33. Slack, E.; Gabriel, C. M.; Lipshutz, B. H. *Angew. Chem., Int. Ed.* **2014**, *53*, 14051.
34. Handa, S.; Wang, Ye; Gallou, F.; Lipshutz, B. H. *Science* **2015**, *349*, 1087.
35. Wuts, P. G. M.; Greene, T. W. *Greene's Protective Groups in Organic Synthesis*; Wiley: Hoboken, NJ, **2014**.
36. US Food and Drug Administration: *Q3D Elemental Impurities Guidance for Industry*. www.fda.gov.
37. Handa, S.; Lippincott, D. J.; Aue, D. H.; Lipshutz, B. H. *Angew. Chem., Int. Ed.* **2014**, *53*, 10658.
38. Handa, S.; Andersson, M. P.; Gallou, F.; Reilly, J.; Lipshutz, B. H. *Angew. Chem., Int. Ed.* **2016**, *55*, 4914.
39. Parmentier, M.; Wagner, M. K.; Magra, K.; Gallou, F. *Org. Process Res. Dev.* **2016**, *20*, 1104.
40. Gabriel, C. M.; Lee, N. R.; Bigorne, F.; Klumphu, P.; Parmentier, M.; Gallou, F.; Lipshutz, B. H. *Org. Lett.* **2017** *19*, 194.
41. Galloway, S. M.; Reddy, M. V.; McGattigan, K.; Gealy, R.; Bercu, J. *Regul. Toxicol. Pharm.* **2013**, *66*, 326.
42. Price comparison for (ACROS Organics, 98+% pure powder): NaBH₄ \$597.70/2.5 kg (\$9.04/mol) ACD code MFCD00003518; KBH₄ \$751.00/2.5 kg (\$16.20/mol) ACD code MFCD00011396.
43. H₂ evolution determined from a 20 mmol portion of 60 mmol KBH₄ and 20 mmol nitro compound. 60 mmol 3KBH₄ = 240 mmol H⁻ and H⁻ consumed by the nitro compound = 20 mmol x 3 reductions = 60 mmol (scheme 1) leaves an excess of 240 mmol – 60 mmol = 180 mmol H⁻ for the conversion to H₂. From the ideal gas law (PV=nRT) at STP (P = 1 atm; T = 298 K), 4.40 L of gas evolved for a 0.120 kg reaction arrives at 36.7 L / kg.
44. Leboho, T. C.; Giri, S.; Popova, I.; Cock, I.; Michael, J. P.; de Koning C. B. *Bioorg. Med. Chem.* **2015**, *23*, 4943.
45. Hagiwara, H.; Sato, K.; Hoshi, T.; Suzuki, T. *Synlett* **2011**, 2905.

VI. Pd-Catalyzed Hydrazone Cross Coupling with Aryl Halides for One-Pot Access to Functionalized *N*-Heteroaromatic Scaffolds in Water

6.1 Introduction

One of the most significant structural components of pharmaceuticals is nitrogen containing heterocycles. In fact, in a 2014 survey of U.S. FDA approved drugs (1035 total) conducted by Njardarson and coworkers, they concluded that 59% of unique small molecule drugs contain a nitrogen heterocycle.¹ Of these heterocycles, the ninth most prevalent was found to be indole which accounts for seventeen approved drugs. In addition to the frequency of indoles in approved drugs, this scaffold is found in an incredible number of natural products² and is present in the essential amino acid tryptophan (Figure 1).

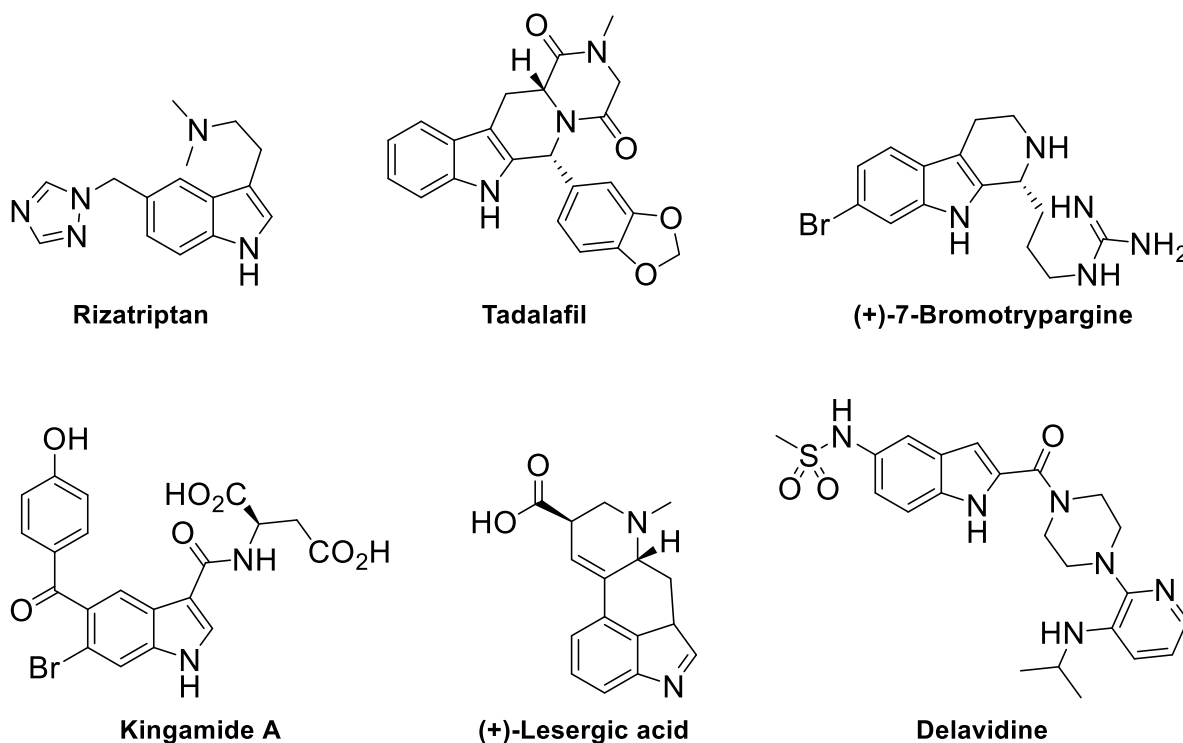
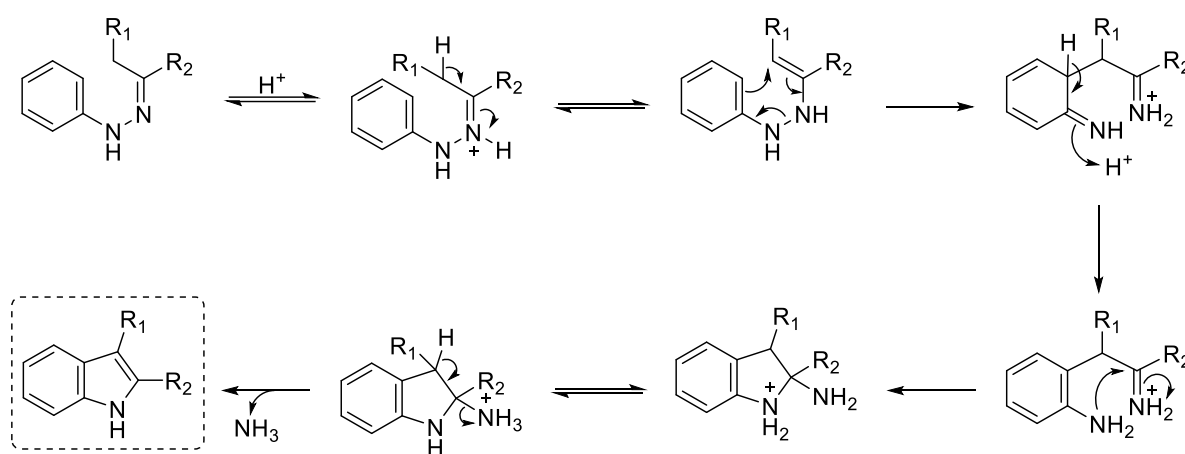


Figure 1. Drugs and natural products containing indoles.

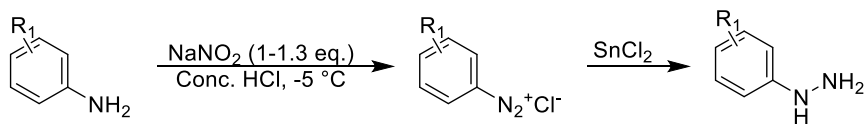
Discovered over a hundred years ago by Hermann Emil Fischer,³ indoles are classically prepared by condensation of an aryl hydrazine onto an enolizable ketone, catalyzed by a Lewis or Brønsted acid.⁴ This process is known as the Fisher indole synthesis, and goes by means of first, condensation of hydrazine with a ketone, followed by isomerization to the corresponding ene-hydrazine. A [3,3]-sigmatropic rearrangement affords the corresponding diamine intermediate that tautomerizes to restore aromaticity followed by condensation and extrusion of ammonia to afford the indole product (Scheme 1).⁵



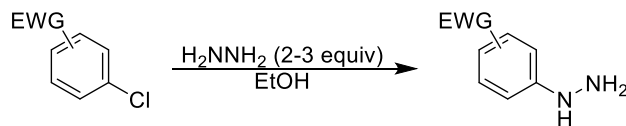
Scheme 1. Mechanism of the Fisher indole synthesis.

This classical method is still employed today in many pharmaceutical processes due to its predictability, simplicity, atom economy, and inexpensive components.⁶ Using this process, one can arrive at indoles with an array of substitution patterns depending on the nature of the aryl hydrazine and the enolizable ketone. What plagues this transformation, however is the limited structural diversity of available aryl hydrazines due to the methods by which they are generally prepared. Traditionally, aryl hydrazines are prepared using two classical methods, namely diazotization/reduction⁷ and nucleophilic aromatic substitution (S_NAr) (Scheme 2).⁸

Diazotization/Reduction (Sandmeyer Reaction):



Nucleophilic Aromatic Substitution (S_NAr):



Scheme 2. Classical methods for the preparation of aryl-hydrazines.

Due to the low cost and simplicity of diazotization, as well as the extent to which the transformation has been studied (this reaction first appeared in the literature over 130 years ago), this method remains as one of the most utilized procedure for the preparation of diazols and diazol derivatives such as hydrazines. While this inexpensive transformation can be pursued as an orthogonal approach to S_NAr or Pd-catalyzed cross-coupling in obtaining hydrazines, considering that aryl halides are stable under these conditions, the cost still outweighs the benefits, especially in terms of safety. The use of concentrated HCl not only requires special handling, reaction vessels, and waste disposal, but also limits appropriate substrates in terms of stability and solubility properties. The stability requirement of the starting material is also complicated by the subsequent reduction step of the thermally labile diazonium salt. Each stage of this transformation possesses its own safety concerns including: a) the toxic nature of anilines,⁹ b) the use of highly caustic concentrated HCl, c) the thermal instability of diazonium salts, d) the use of highly toxic stannous chloride,¹⁰ and e) the production of highly toxic aryl hydrazines (as opposed to hydrazine surrogates).¹¹ Needless to say, this method is far from being regarded as environmentally responsible.

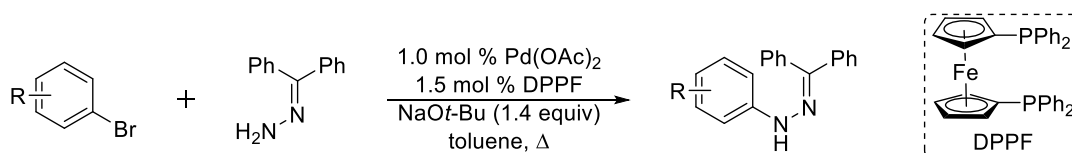
In comparison, S_NAr reactions are widely utilized, not only for the synthesis of aryl hydrazines, but also for the synthesis of phenyl ethers, anilines, benzonitriles, and thioethers from activated aryl chlorides and fluorides.⁸ The ability of the substrate to undergo this substitution reaction relies heavily upon the presence of an electron withdrawing group, most commonly a nitro group, which allows for resonance stabilized Meisenheimer complex.¹² While S_NAr has been proven as a highly effective and often environmentally responsible method for aromatic substitution, this method is limited by the structural characteristics of the aryl halide which must be activated toward the position being substituted (i.e. *ortho/para* nitro substitution). Based on these criteria, the resulting electron-deficient aryl hydrazine will require forcing conditions to effect the [3,3]-sigmatropic rearrangement in the Fisher indole synthesis mechanism.

The drawbacks of the described methods for preparing aryl hydrazines can be summed up simply by saying, these methods lack generality. Therefore it can be concluded that more ideal conditions are necessary for the synthesis of aryl hydrazines, where the desired transformation would not be constrained by the structural diversity of the aryl component both in terms of electronics as well as functional group compatibility. Also, the ideal system would not pose the same environmental concerns as the classical approach, addressing both safety (which is clearly present for the diazotization/reduction procedure), as well as sustainability. This method would not only expand the scope of available precursors to the Fisher indole synthesis, but also for other important *N*-heteroaromatics which are synthesized from aryl hydrazines such as carbazoles,¹³ pyrazoles,¹⁴ cinnolines,¹⁵ and many more which are found ubiquitously in pharmaceuticals and natural products.¹

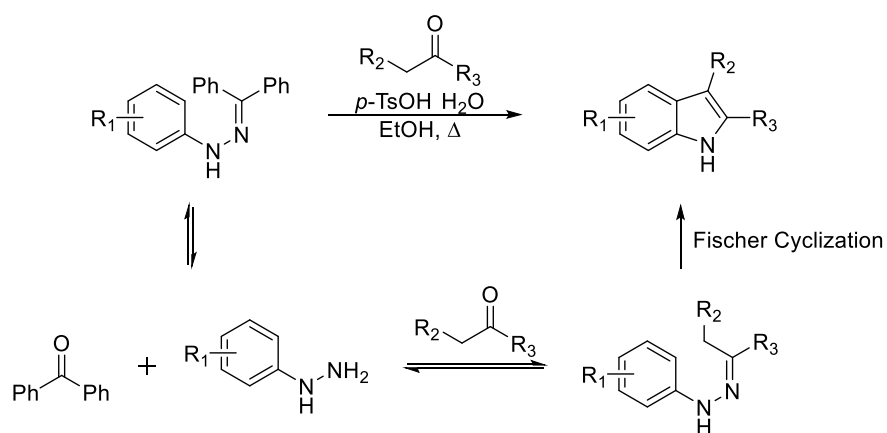
6.2 Background

Since the recent advances in the field of palladium-catalyzed cross-coupling reactions, C-N bond formation of aryl halides via the Buchwald-Hartwig amination reaction has become a predominant method for preparing anilines and their derivatives.¹⁶ Relevant to the synthesis of aryl hydrazines, *N*-arylated benzophenone hydrazones can be accessed from the corresponding aryl halide (Scheme 3a).¹⁷ The benzophenone moiety can serve as a handle for selective coupling, hydrazone protection, and purification/isolation. Most commonly, the benzophenone hydrazone is hydrolyzed in methanolic *p*-toluenesulfonic acid followed by subsequent cyclization to form indoles or condensation to the corresponding pyrazole (Scheme 3b).

a.) Pd-catalyzed *N*-arylation of Benzophenone Hydrazone:

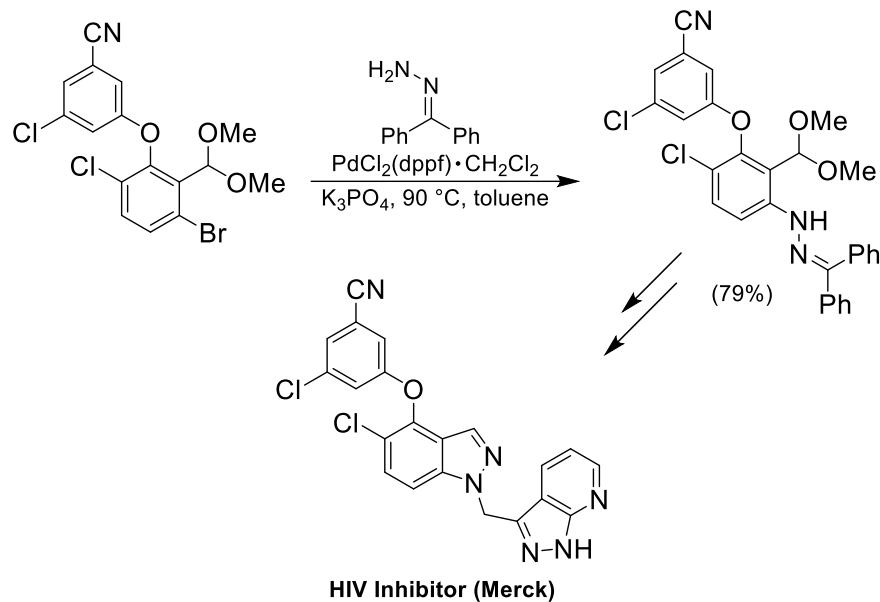


b.) Buchwald Modification to the Fischer Indole Synthesis:



Scheme 3. Buchwald Modification of the Fischer indole synthesis.

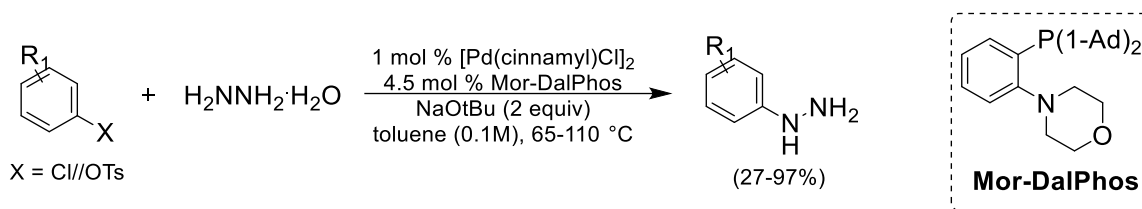
The coupling of aryl halides and benzophenone hydrazone has surfaced in the literature several times, and while reaction conditions are relatively general in regards to base selection, reaction temperature, and solvent (KO^tBu and refluxing toluene), notable improvements to the method were achieved by swapping the ligand, BINAP,^{17a} for dppf^{17b} or MePhos¹⁸ showing a very strong relationship between ligand selection and catalyst loading. The current conditions in the literature which may be regarded as the “greenest” method for performing this transformation requires a) low catalyst loading [0.1 mol % Pd(OAc)₂, 0.2 mol % MePhos], b) the use of inexpensive base NaOH, and c) the reaction to be run at ~100 °C in amyl alcohol.¹⁸ To date, the method of choice industrially utilizes either BINAP or dppf as ligand in refluxing toluene (Scheme 4).¹⁹ The reason for this is most likely the result of the generality of these methods. For example, conditions utilizing BINAP have proven to be suitable for heterocyclic and functionalized substrates,^{17a} while only simple, non-functionalized substrates such as 4-bromoanisole and 4-bromotoluene have been reported utilizing the MePhos/Pd(OAc)₂ catalyst system.¹⁸ Regardless of which method is used, the use of organic solvents and high temperatures are not ideal in terms of environmental impact. In fact, solvents with relatively high boiling points such as toluene and *tert*-amyl alcohol require additional energy for their removal. Therefore, a method that uses an alternate solvent system while retaining low catalyst loading and conserves energy would be ideal.



Scheme 4. Hydrazone cross coupling for access to an indazole scaffold.

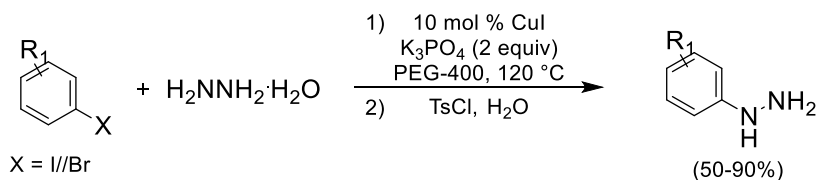
Another approach to the synthesis of aryl hydrazines is the cross coupling of hydrazine directly to an aryl halide. One such example of this was accomplished by Stradiotto and co-workers from aryl chlorides and tosylates (Scheme 5).²⁰ This procedure employs Mor-DalPhos as ligand which is coordinated *in situ* from the $[\text{Pd}(\text{cinnamyl})\text{Cl}]_2$. This method was found to effectively deliver a wide range of substrates including those bearing electron-withdrawing and donating groups, as well as heterocycles including pyridine, quinoline, pyrrole, affording product yields in the range of 27-97%. While the scope of this work is quite impressive, some drawbacks of this procedure should be noted. Presumably, the key to success of this method is the use of aryl electrophiles such as aryl chlorides and tosylates which undergo oxidative addition much less readily than their bromide or iodide counterparts in dilute concentration (0.1 M) which diminishes production of the diaryl hydrazine in the final product. Further limitations of this method are the use of high reaction temperatures (65-110 °C) under highly basic conditions which is not suitable for substrates

bearing more sensitive functionalities. Finally, the direct synthesis of aryl hydrazines is often undesirable due to their highly toxic nature and the difficulty by which they are purified.



Scheme 5. Pd-catalyzed cross coupling of aryl chlorides and tosylates with hydrazine.

Another interesting report for the direct synthesis of aryl hydrazines from aryl iodides describes copper-catalyzed cross coupling of aqueous hydrazine in PEG-400 (Scheme 6).²¹ This procedure further highlights limitations of direct aryl hydrazine synthesis as a one-pot procedure for subsequent *N*-tosylation, required for isolation of the product the efficiency of which is reflected in their yields (most are within the 50-90% range). In comparison to Stradiotto's report,²⁰ this method requires the use of more labile aryl iodides for decent yields as other aryl halides produced the products in lower yields, even at 120 °C. Where both of these methods suffer is from the use of aqueous hydrazine which is explosive and toxic.²² This is a major concern as both methods employ high reaction temperatures. In addition, the removal of residual hydrazine during the work-up stage is another safety concern, and the waste would require special disposal.

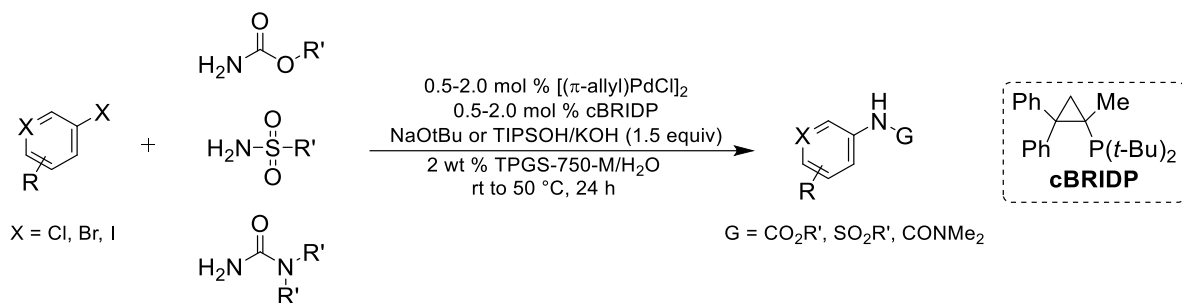


Scheme 6. Pd-catalyzed cross coupling of aryl bromides and iodides with hydrazine.

With the advances in the area of accessing aryl hydrazines and their protected analogues, even the best systems require the use of organic solvents at high reaction temperatures. The consequence of this is that not only are recycling capabilities essentially non-existent, but also that isolation of the product is generally required prior to the subsequent condensation reactions. This seems tedious, considering that condensations to the corresponding *N*-heterocycle simply requires a solvent switch (usually conducted in EtOH) and pH adjustment. We envisioned a process where the initial coupling would be conducted in aqueous surfactant at lower temperatures which would allow for either outcome where a protected hydrazine could be isolated or proceed to the formation of an *N*-heteroaromatic in one pot. Our hypothesis seemed reasonable for a system that produced aryl hydrazones via Pd-catalyzed cross coupling, as hydrolysis would be favorable under aqueous conditions, and the heterocyclic transformation would be pushed to completion by aromatization.

6.3 Previous Work

The capability of Pd-catalyzed cross coupling has been well established in our group, where we have shown numerous examples of these transformations over the past nine years, including: Suzuki-Miyaura,²³ Heck,²⁴ Kumada,²⁵ Stille,²⁶ Nigishi,²⁷ Sonogashira,²⁸ Buchwald-Hartwig amination,²⁹ and C-H activation.³⁰ In 2010, our group reported the synthesis of protected anilines via Buchwald-Hartwig cross-coupling of protected ammonia equivalents (carbamates, sulfonamides, ureas) with aryl and heteroaryl halides in water enabled by micellar catalysis (Scheme 7).^{29a} Notable features of this work include relatively low reaction temperatures, room temperature to 50 °C, in comparison to standard Pd-catalyzed amination chemistry. These mild conditions are facilitated by the use of Takasago ligand, cBRIDP,³¹ and [Pd(allyl)Cl]₂ in aqueous surfactant solution of 2 wt % TPGS-750-M.



Scheme 7. Installation of Protected Ammonia Equivalents onto Aromatic and Heteroaromatic Rings in Water Enabled by Micellar Catalysis.

Based on this report we believed that this system could be used for the cross coupling of aryl halides and benzophenone hydrazone. The initial attempts included the coupling of 1,4-dibromobenzene (**1**) as well as 4-bromoanisole (**4**) with benzophenone hydrazone, **2**, (Figure 2). From these initial results, it was determined not only was this transformation possible in aqueous surfactant, but also that only minor tuning would be necessary to develop a suitable method that with a broad substrate scope. In addition to the goals of developing a method for hydrazone coupling in water and one-pot access to *N*-heteroaromatics, it was envisioned that further optimization could potentially lead to a system under more mild conditions by replacing KOtBu with a weaker base in order to access scaffolds bearing labile functional groups which has yet to be addressed in prior reports of hydrazone coupling in the literature.^{17,18}

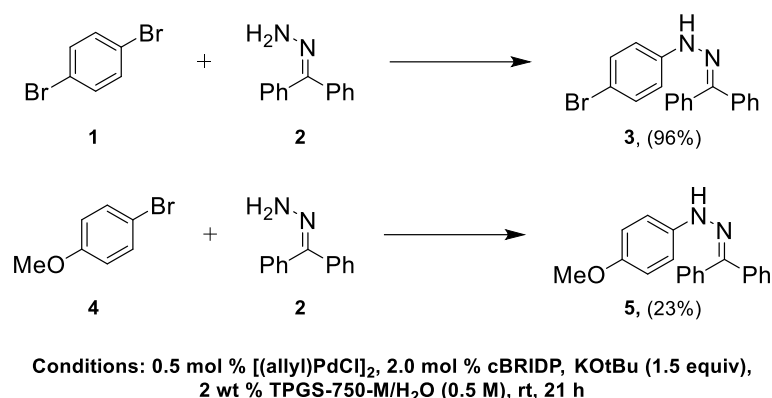
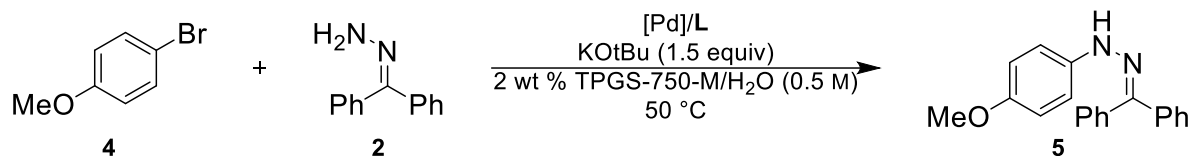


Figure 2. Initial reactions for Pd-catalyzed cross coupling with benzophenone hydrazone.

6.4 Results and Discussion

From the initial report for amination under these conditions for the installation of protected ammonia equivalents, heating the reaction to 50 °C resulted in the expected outcome of improving reaction rate and conversion. It was considered that the yield for the coupling product of **4** to the corresponding benzophenone hydrazone (**5**) could be improved by heating, which was found to be true, affording 92% conversion after only two hours (Figure 3, entry 1). In comparison, other catalyst systems were screened, showing decreased conversion when Pd(OAc)₂ was used in place of [Pd(allyl)Cl]₂. The lower conversion is likely due to the higher activation barrier for generating the active Pd(0) from Pd(OAc)₂ in comparison to [Pd(allyl)Cl]₂ which is reduced via a different mechanism.³² Pd(tBu₃)₂ led to 91% conversion, however, the reaction profile contained >5 unidentified impurities which were not present in any of the other systems (entry 3). In comparison to the catalysts typically used for this transformation in organic solvent, BINAP, dppf, and dtbpf yielded little-to-no-product (entries 4-6).

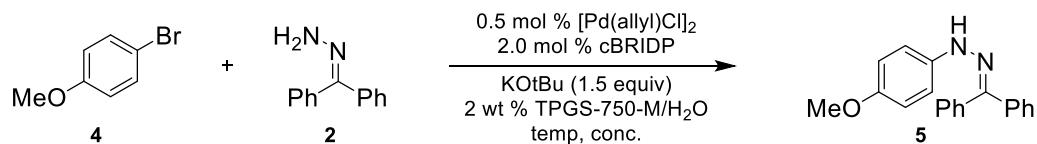


entry	[Pd]/L	time (hr)	% conversion
1	[Pd(allyl)Cl] ₂ (1.0 mol %)/cBRIDP (2.0 mol %)	2	92%
2	Pd(OAc) ₂ (2.0 mol %)/cBRIDP (2.0 mol %)	4	48%
3	Pd[P(tBu) ₃] ₂ (2.0 mol %)	15	91% ^a
4	Pd(OAc) ₂ (2.0 mol %)/BINAP (2.0 mol %)	4	0%
5	Pd(dppf)Cl ₂ ·CH ₂ Cl ₂ (2.0 mol %)	19	4%
6	Pd(dtbpf)Cl ₂ (2.0 mol %)	19	10%

^aSeveral by-products observed

Figure 3. Initial catalyst screening for the synthesis of **5**.

Once it was determined that **4** could be successfully coupled under these conditions, a temperature screening was carried out in order to determine the maximum heat requirement of the system. It was found that by increasing the global concentration to 1.0 M, essentially the same outcome could be achieved at 30 °C as compared to 50 °C (Figure 4, entries 1 and 4).



entry	T (°C)	conc. (M)	time (hr)	% conversion
1	50	0.5	2	92%
2	40	0.5	2	90%
3	40	1.0	2	94%
4	30	1.0	2	91%

Figure 4. Temperature and concentration screening for the synthesis of **5**.

Base screening for this system was carried out on the coupling of 3-bromobenzonitrile (**6**) examining conditions in the presence of various bases (Figure 5). Compound **6** was

chosen as the optimization substrate in this case for two reasons: (1) it is electronically deficient that facilitates oxidative addition readily. The idea was that if conditions were not suitable to turn over significant product for this “loaded case,” then the chances of coupling more difficult (electron rich) aryl halides would be unlikely; (2) one of the major by-products encountered *en route* to Merck’s HIV inhibitor (Scheme 4) was due to the condensation of the benzophenone hydrazone onto the nitrile present in the product. As the goal of this base screening was to find a milder alternative to KOtBu, screening with **6** which bears a nitrile serves to investigate functional group compatibility from the starting point of development. After screening only a few bases, it was realized that Et₃N outperformed KOtBu (Figure 5; entries 1 and 4). This outcome was quite surprising as very few methods in the literature utilize an amine base for Pd-catalyzed aminations.³³ In fact, it was investigated extensively by Norrby and co-workers at AstraZeneca for the coupling of bromobenzene with morpholine, for the requirements of the Buchwald-Hartwig amination in terms of base. In these reports, it was concluded that the oxo-palladium species arising from ligation of the base to the palladium center was a requirement of the mechanism as shown by the lack of coupling product observed under conditions employing DBU as base.³⁴

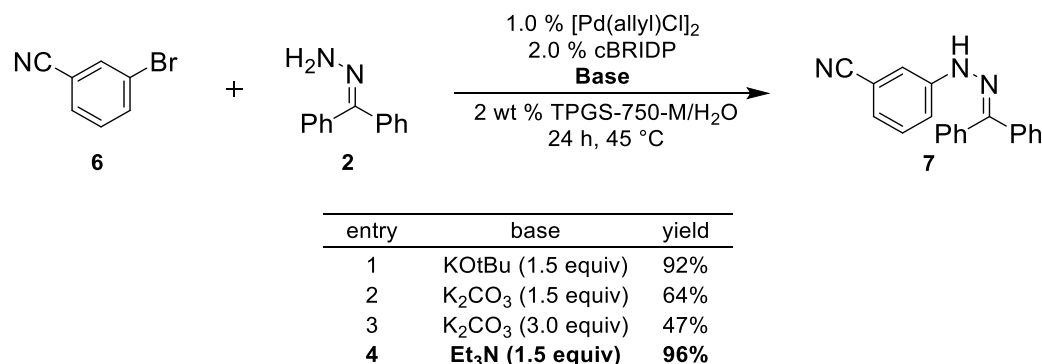
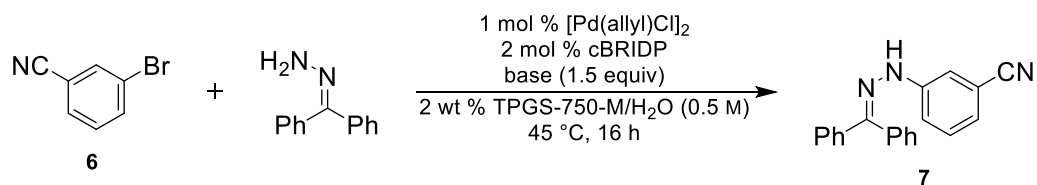


Figure 5. Base screening for the synthesis of **7**.

We can explain our findings by considering the aqueous nature of the system. Presumably, an equilibrium will exist where Et₃N will deprotonate water to form hydroxide. The protonated amine may then act as a phase transfer catalyst to shuttle hydroxide into the micellar core thus allowing this transformation to proceed via Hartwig's proposed mechanism.³⁵ This was investigated for our system by employing our conditions in anhydrous toluene. In support of our findings, poor conversion to the coupled product **7** was observed (Figure 6, entry 1). Next, a phase transfer system was used employing tetramethylammonium hydroxide pentahydrate (TMAOH) in anhydrous toluene which afforded the coupled product in 59% yield. Finally, when the phase transfer system was used under micellar conditions, high conversion was met yet again, achieving a yield of 77%.

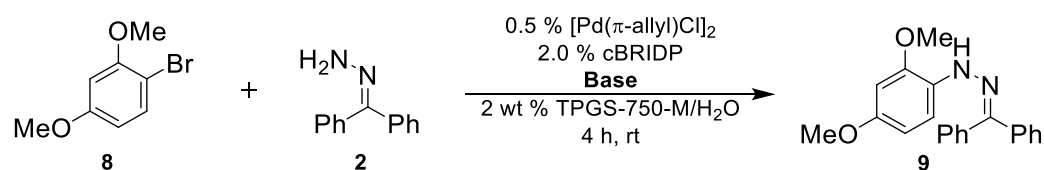


entry	solvent	base	% yield
1	toluene	Et ₃ N	22%
2	toluene	TMAOH	59%
3	TPGS/H ₂ O	TMAOH	77%
4	TPGS/H ₂ O	Et ₃ N	96%

Figure 6. Hydrazone cross coupling with a phase transfer catalyst.

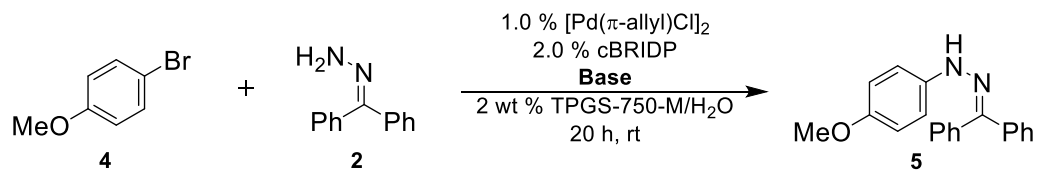
It should be noted that the base screening did expand past what is presented in Figure 6, as initial optimization was carried out on more difficult electron-rich aryl bromides **4** and **8** (Figures 7 and 8). The stark contrast in conversion achieved, as shown in these Tables led to a very important observation that the order of addition is especially important for this system. It was found that for the initial screening represented in Figures 7 and 8, that adding base prior to addition of the coupling partners (e. g. the aryl halide and **2**) caused a change

from pale yellow to red. By contrast, when base was added last for the screening represented in Figure 6 there was no change in appearance (the reaction remained yellow). Furthermore, those reactions which are represented in Figures 7 and 8 seemed to stall at very early reaction times. This is likely explained on the basis of work done by Colacot and co-workers where generation of the desired Pd(0) species from the corresponding allyl chloride complex is in competition with the comproportionation to the dinuclear Pd(I) species (Scheme 8).³⁶ While Pd(I) has been shown to catalyze a number of cross coupling reactions it may be inactive under these conditions. To this, we found that the diminished activity of the system under conditions where base was allowed to stir for an extended period of time prior to the addition of coupling components should be avoided, making the data acquired by this method somewhat irrelevant. Thus the screening represented in Figures 7 and 8 should be taken only under modest consideration in determining the correct base for the system. It was from this screening in fact that Et₃N was considered as a suitable base for our conditions.



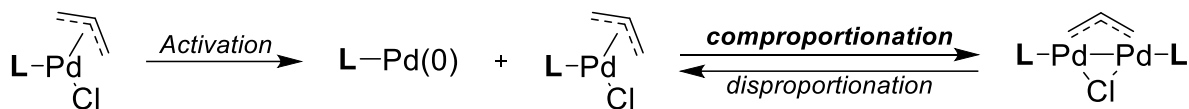
entry	base	time (h)	conv.
1	NaOtBu (1.5 equiv)	1	21%
2	NaOtBu (1.5 equiv)	4	27%
3	K ₃ PO ₄ (1.5 equiv)	1	7%
4	K ₃ PO ₄ (1.5 equiv)	4	11%
5	K ₂ CO ₃ (1.5 equiv)	1	14%
6	K ₂ CO ₃ (1.5 equiv)	4	17%
7	Cs ₂ CO ₃ (1.5 equiv)	1	10%
8	Cs ₂ CO ₃ (1.5 equiv)	4	10%
9	NaHCO ₃	4	17%

Figure 7. Base screening for the synthesis of **9**.



entry	base	time (h)	conv.
1	Et ₃ N	1	54%
2	Et ₃ N	4	59%
3	Et ₃ N	20	61%
4	DIPEA	1	28%
5	DIPEA	4	42%
6	DIPEA	20	55%
7	Cy ₂ NMe	1	23%
8	Cy ₂ NMe	4	26%
9	Cy ₂ NMe	20	48%
10	NMM	1	14%
11	NMM	4	15%
12	NMM	20	36%
13	TEA	1	15%
14	TEA	4	28%
15	TEA	20	41%
16	DBU	1	79%
17	DBU	4	82%
18	DBU	20	83%

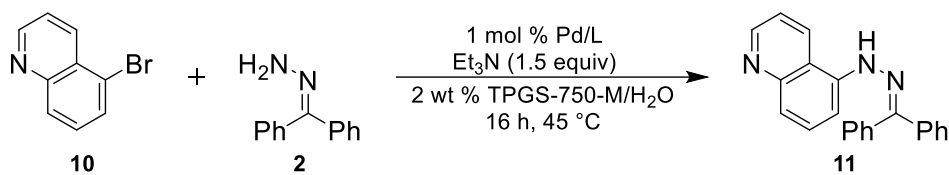
Figure 8. Base screening for the synthesis of **5**.



Scheme 8. Comproportionation pathway proposed by Colacot and co-workers.

Et₃N was considered the choice base for this system as a result of both its lower basicity in comparison to KO^tBu, which could have major implications in terms of functional group compatibility, as well as its ubiquity in most organic labs. Because the conditions had changed to incorporate Et₃N as base, an additional catalyst screening was conducted (Figure 9). The screening was based on the coupling of 5-bromoquinoline (**10**) with **2**. It is commonplace in methods development for all screening to optimize the transformation

based on a single substrate which may not translate well for other substrates even with structural and electronic similarity (see Chapter 3). For this reason, screening with **10** was chosen in order to consider important heterocycles such as quinolines. The previously established optimized conditions for the installation of ammonia equivalents^{29a} were found to outperform all other systems tested (entry 9) with the exception of the pre-complexed Pd(II) species, PdCl(allyl)(cBRIDP) which afforded the product in quantitative yield (entry 10). This screening probed some of the structural components required by the catalyst system for these conditions in that bulky, electron-rich ligands delivered products in highest yields (entries 4, 8, and 12). For these cases, it appears that the presence of the di-*tert*-butyl phosphine is a key feature of the ligand for highest conversion, likely due to their superior ability to facilitate reductive elimination. This hypothesis is supported by the comparison of cBRIDP to its dicyclohexylphosphine analogue Cy-cBRIDP which only yielded 19% product (entry 11). Pd(dtbpf)Cl₂ resulted in the lowest overall yield for the series, which is quite interesting considering its reputation for facilitating reductive elimination in many transformations (entry 3).³⁷ This suggests that the active 12 electron Pd(0) species is responsible for the facile conversion for this system, where the 14 electron Pd(0) species from the bi-dentate the bisphosphine in Pd(dtbpf)Cl₂ is not especially effective for this system.

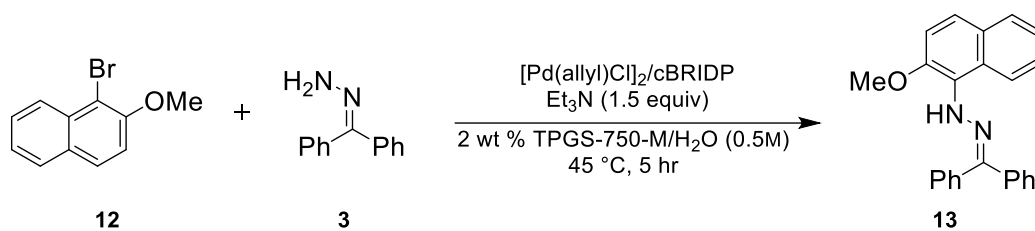


entry	catalyst	isolated yield
1	[Pd(allyl)Cl] ₂ /BINAP	10%
2	Pd(dppf)Cl ₂ CH ₂ Cl ₂	20%
3	Pd(dtbpf)Cl ₂	4%
4	[Pd(allyl)Cl] ₂ /JohnPhos	77%
5	[Pd(allyl)Cl] ₂ /MePhos	6%
6	[Pd(allyl)Cl] ₂ /tBuMePhos	70%
7	PdCl ₂ (Xantphos)	38%
8	Pd(PtBu ₃) ₂	68%
9	[Pd(allyl)Cl]₂/cBRIDP	98%
10	PdCl(allyl)(cBRIDP)	100%
11	[Pd(allyl)Cl] ₂ /Cy-cBRIDP	19%
12	[Pd(allyl)Cl] ₂ /vBRIDP	78%

Conditions: [Pd] 0.01 mmol, L (0.01 mmol), **10** (0.5 mmol), **2** (0.525 mmol), Et₃N (1.5 equiv), 2 wt % TPGS-750-M/H₂O (1.0 mL), 45 °C, Ar, 16 h.

Figure 9. Catalyst screening with Et₃N as base.

The pre-complexed form of PdCl(allyl)(cBRIDP) was then compared to the use of (Pd(allyl)Cl)₂ and cBRIDP individually (Figure 10). This screening was carried out for the coupling of 1-bromo-2-methoxynaphthalene (**12**) with **2**, investigating the lower threshold for catalyst loading. Naphthyl bromide **12** was chosen based on the electron rich nature of the aryl halide due to its electron rich *ortho*-methoxy group which makes oxidative addition more difficult in comparison to **10**. Best results were found at 2 mol % palladium loading in both cases with the individual catalyst components added individually affording a 92% isolated yield (entry 3) in comparison to the use of 2 mol % pre-coordinated complex which afforded an 86% yield (entry 1).



entry	PdCl(allyl)(cBRIDP)	[Pd(allyl)Cl] ₂	cBRIDP	yield (%)
1	2.0%	-	-	86%
2	0.5%	-	-	36%
3	-	1.0%	2.0%	92%
4	-	0.25%	0.5%	26%
5	-	0.5%	1.0%	34%

Figure 10. Comparison of PdCl(allyl)(cBRIDP) to [Pd(allyl)Cl]₂ + cBRIDP.

The optimized conditions examined for a representative scope of aryl halides are shown in Figure 11. In most cases, aryl hydrazone products were achieved in high yields within short reaction times. As expected, nitriles survive the conditions affording products in near quantitative yields, with 2-bromobenzonitrile coupling in only 30 minutes to afford **14**. Compound **15** was isolated in 94% yield, showing great improvement over Buchwald's method which required refluxing toluene over 16 hours to afford the same product in 72% yield.^{17a} Sterics provided by *ortho*-substituents showed no obvious limitations (compounds **13**, **14**, **16**, **17**, and **20**) with no substitution for chloride being observed for products **17** and **20**. The low yield obtained for **19** was simply a factor of oxidative decomposition on the bench following purification, and it is believed that a higher yield is certainly achievable. Similarly, product **20** was isolated in only 60% yield most likely due to the short reaction time. Limitations were observed for this system, however, in that many electron rich aryl halides do not undergo coupling to an appreciable extent (<10% yield). Examples are shown in Figure 12, and it is believed that under conditions employing a stronger base (e.g. KOtBu), higher yields are achievable. This will be the focus of future investigations.

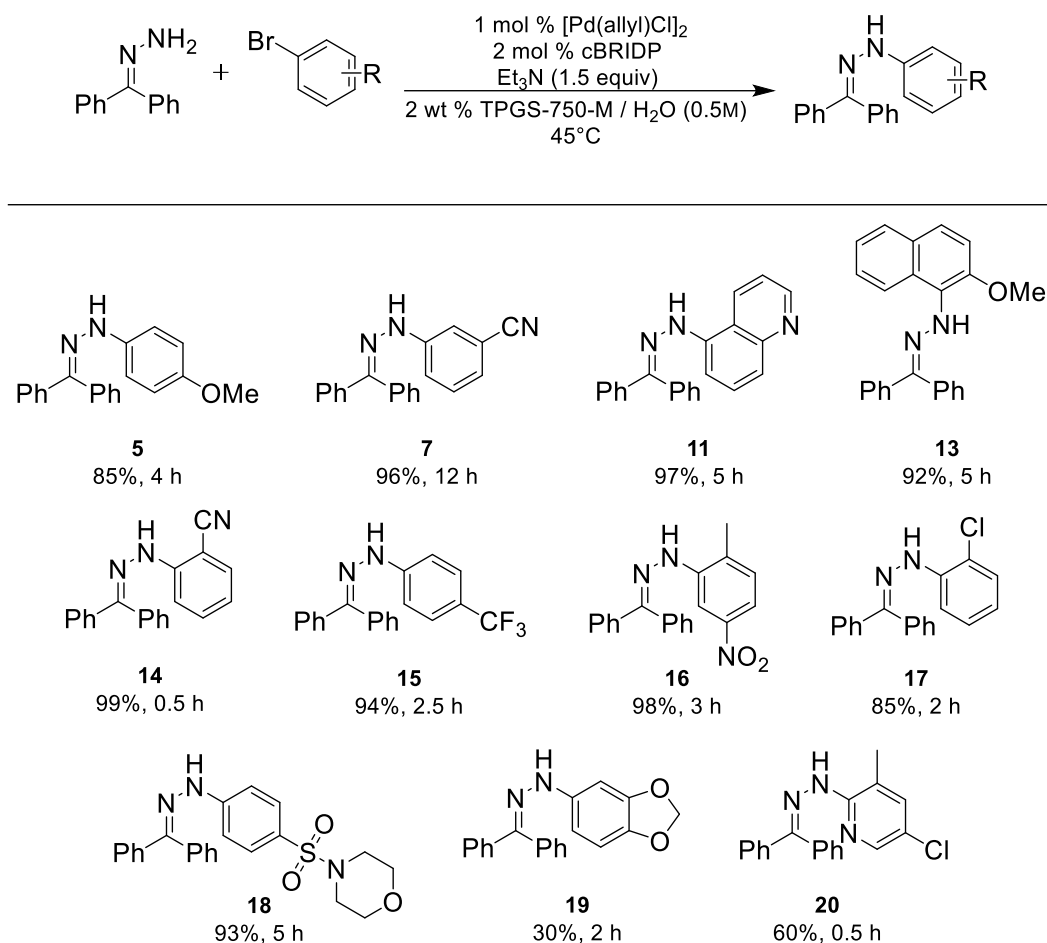


Figure 11. Representative examples of hydrazone coupling products under optimized conditions.

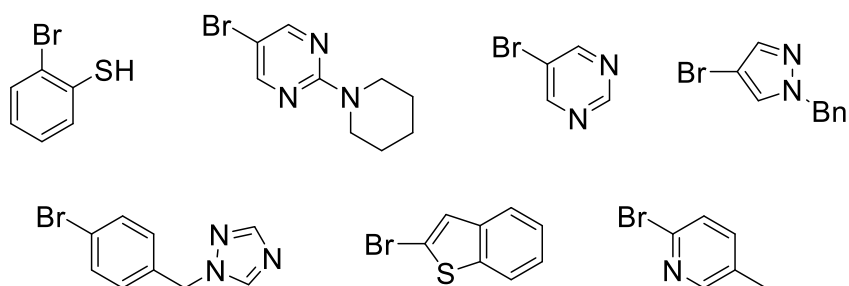
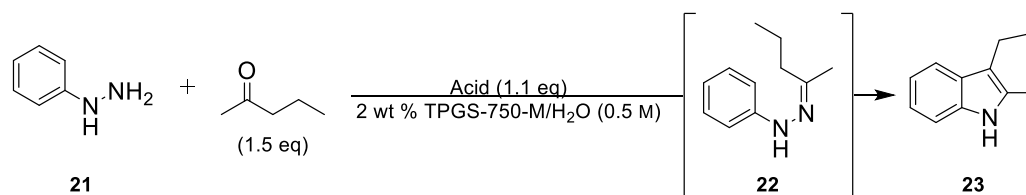


Figure 12. Aryl halides affording <10% yield under optimized conditions.

As mentioned previously, one of the ultimate objectives of this methodology was to allow for one-pot access to *N*-heteroaromatics. Initial focus in this area was examination of the

ability of phenylhydrazine (**21**) to undergo the Fisher indole synthesis with 2-propanone in aqueous TPGS-750-M (Figure 13). At the onset of these experiments, it was found that the cyclization will proceed at room temperature with 1.1 equivalent of *p*-toluenesulfonic acid (*p*-TsOH). However, the rate at which condensation/cyclization occurs is not sufficient for practical use, and when the temperature was increased to 70 °C complete conversion to the desired indole was achieved (entry 1). Examining this transformation at lower temperatures, it was found that 50 °C led to the product indole cleanly in only two hours which was found to be independent of the presence of surfactant (entries 5, 6). As the Fisher indole synthesis is acid catalyzed, acid loading was decreased to 0.5 and 0.05 equivalents resulting in much slower conversion (entries 7, 8). Interestingly, ZnCl₂ led only to the imine intermediate with cyclization only occurring in the presence of Brønsted acid (entries 9, 10).



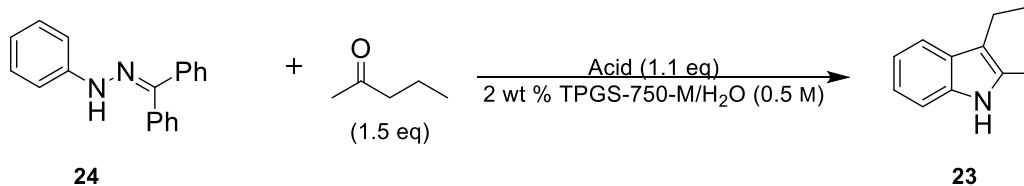
Entry	Acid	Eq.	T (°C)	time (hr)	21 ^a	22	23
1	<i>p</i> -TsOH · H ₂ O	1.1	23	16	22%	56%	22%
			70	+48	0%	0%	100%
2	<i>p</i> -TsOH · H ₂ O	1.1	70	16	0%	0%	100%
3	None	1.1	70	16	20%	80%	0%
4	<i>p</i> -TsOH · H ₂ O	1.1	60	6	0%	0%	100%
5	<i>p</i> -TsOH · H ₂ O	1.1	50	2	0%	0%	100%
6 ^b	<i>p</i> -TsOH · H ₂ O	1.1	50	2	0%	0%	100%
7	<i>p</i> -TsOH · H ₂ O	0.5	50	7	0%	75%	31%
8	<i>p</i> -TsOH · H ₂ O	0.05	50	2	16%	76%	8%
9	<i>p</i> -TsOH · H ₂ O, ZnCl ₂	1.1, 1.1	50	2	3%	40%	57%
10	ZnCl ₂	1.1	50	2	31%	69%	0%
11	<i>p</i> -TsOH · H ₂ O	1.1	40	7	0	74%	26%

^aConversion determined by GC-MS analysis; ^bRun in the absence of surfactant.

Figure 13. Condition screening for the Fisher indole synthesis from **21** and 2-pentanone.

Of course these preliminary experiments were only intended to understand the energy requirements for indole synthesis, and the actual desired transformation would require hydrolysis to liberate benzophenone from the aryl-hydrazone prior to indole synthesis. Focus then turned to examination of the same system from the corresponding hydrazone, **24**, (Figure 14). First, in order to get a comparative reference, the reaction was conducted under standard literature conditions by refluxing in ethanol overnight in the presence of 1.1 equivalents of *p*-TsOH affording an isolated yield of 82% (entry 1). Hydrolysis of the benzophenone was found to be quite difficult, affording no detectable product after 16 hours at 50 °C (entry 2). Increasing to 70 °C, indolization did occur, however these conditions required an extended reaction time of three days to afford only 73% conversion (entry 3). Similar to the findings in Figure 13, the use of Lewis acids offered no improvement with most systems being incapable of hydrolyzing the benzophenone hydrazone (entries 4-10).

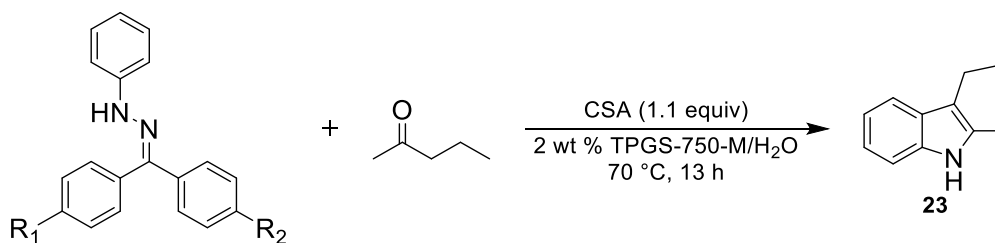
At this stage, it was considered that an alternate hydrazone could be used which would more readily undergo hydrolysis. In designing such a system, it was considered that substitution on the benzophenone scaffold would lead to hydrolysis at lower temperatures. Candidates were considered based on the IR C=O stretching frequencies, where a longer C-O bond (lower wavenumber) suggests a weaker, more hydrolyzable bond. This hypothesis was met with success when the model reaction was conducted from four phenyl hydrazone derivatives at 70 °C with camphorsulfonic acid (CSA) affording quantitative conversion from the substrate bearing Michler's Ketone hydrazone, **27** (Figure 15). The trend observed from the data in Figure 15 shows the direct correlation between resonantly donating groups and the extent of hydrolysis after ca. 13 hours.



Entry	Solvent	Acid ^a	T (C)	time (hr)	conv. ^b
1	EtOH	<i>p</i> -TsOH·H ₂ O	Reflux	16	82% ^c
2	2% TPGS	<i>p</i> -TsOH·H ₂ O	50	16	0%
3	2% TPGS	<i>p</i>-TsOH·H₂O	70	16	17%
				72	73%
4	2% TPGS	LiCl	70	48	0%
5	2% TPGS	FeCl ₃	70	48	0%
6	2% TPGS	<i>p</i> -TsOH·H ₂ O; FeCl ₃	70	48	0%
7	2% TPGS	<i>p</i> -TsOH·H ₂ O; Eu(NO ₃) ₃ ·6H ₂ O	70	16	4%
8	2% TPGS	Eu(NO ₃) ₃ ·6H ₂ O	70	16	0%
9	2% TPGS	PTSA·H ₂ O; Dy(NO ₃) ₃ ·5H ₂ O	70	16	2%
10	2% TPGS	Dy(NO ₃) ₃ ·5H ₂ O	70	16	0%

^a1.1 eq.; When a Lewis acid is used in combination, used 1.1 eq. of each. ^bconversion by GC-FID. ^cIsolated yield.

Figure 14. Condition screening for the Fischer indole synthesis from **24** and 2-pentanone.



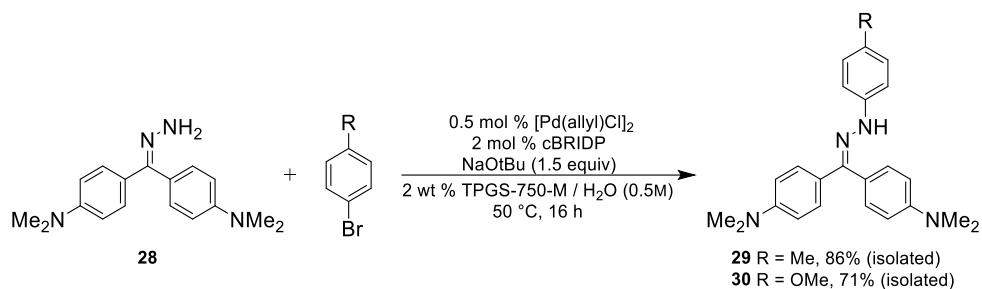
entry	compound	R ₁	R ₂	conv. ^a	¹³ C ppm (CDCl ₃)	ν (cm ⁻¹)
1	24	H	H	2%	196.7	1660
2	25	OMe	H	18%	195.5	1650
3	26	OMe	OMe	60%	194.4	1635
4	27	NMe₂	NMe₂	99%	193.9	1600

^aconversion by GC-FID.

Figure 15. Fischer indole synthesis in water from substituted *N*-phenylbenzophenone hydrazones.

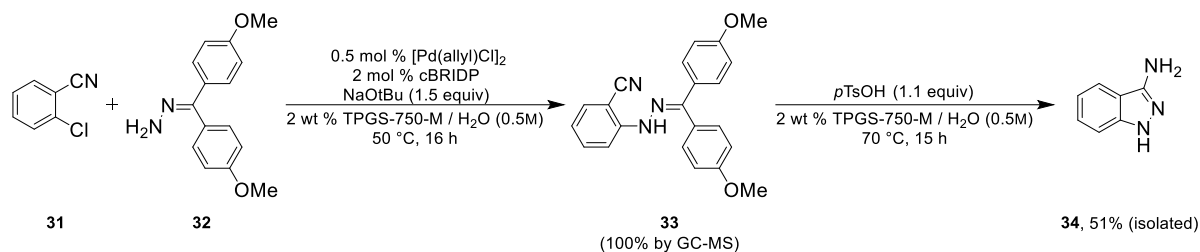
Showing that hydrolysis could be effected by the substitution of benzophenone hydrazone with Michler's ketone hydrazone, the cross coupling of the parent hydrazone (**28**)

was investigated to prove its suitability as a nucleophile for the developed methodology. Not surprisingly, **28** was effectively coupled to 4-bromotoluene and 4-bromoanisole to afford the corresponding aryl hydrazones in good isolated yields (Scheme 9). It should be noted that these reactions were carried out prior to complete system optimization described above (e.g. catalyst loading and base screening), and these couplings should be carried out under those conditions which we believe will result in higher product yields.



Scheme 9. Coupling procedure with Michler's ketone hydrazone (**28**) as the nucleophile.

In 2010, Fabis and co-workers described a method for the two step synthesis of substituted 3-aminoindazoles from 2-bromobenzonitriles via Pd-catalyzed arylation of benzophenone hydrazone followed by an acid catalyzed cyclization sequence.³⁸ As an initial attempt at accessing the 3-aminoindazole scaffold in one pot, 2-chlorobenzonitrile (**31**) was coupled with hydrazone **32**, affording the corresponding aryl hydrazone in quantitative conversion (Scheme 10). *p*-TsOH (1.1 equiv) was then charged to the system and the mixture was allowed to stir at 70 °C overnight to deliver 3-aminoindazole **34** in 51% isolated yield. Again, it should be noted that this reaction was carried out prior to system optimization (as many of the hydrolysis experiments were carried out in parallel), so this example simply shows the capabilities of the system and it is believed that this product could be isolated in higher yields from the procedures described below.



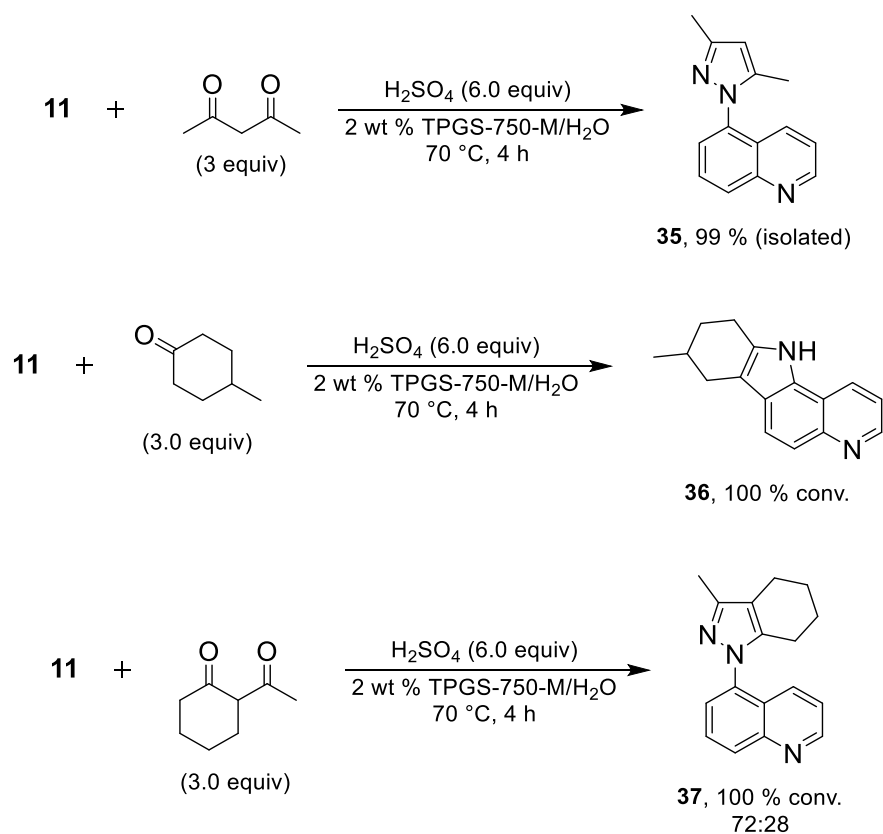
Scheme 10. One pot synthesis of 3-amino indazole **34**.

The concept of developing a more hydrolyzable aryl hydrazone was originally pursued such that hydrolysis could occur at lower temperatures facilitating the one-pot transformation where heating of the system is minimized. Here, we are met with a trade-off between atom economy and energy input. While these systems may be desirable for temperature or acid sensitive substrates, it should be considered that for the synthesis of a *N*-heteroaromatic scaffold, at most two nitrogens from the parent hydrazone are present in the final product (for pyrazoles and indazoles), or only one for the synthesis of indoles which simply translates to poor atom economy. Furthermore, the condensation/cyclization sequence may require additional energy input beyond what is required for hydrazone hydrolysis thus making this modification unnecessary.

Because heating the system to 70 °C was already required for effective hydrolysis of Michler's ketone, we had considered the use of higher loading of a stronger acid for the hydrolysis of benzophenone hydrazone. In addition to atom economy, this route was pursued on the basis of cost and availability. For example, the synthesis of **2** is simply achieved by refluxing hydrazine hydrate with benzophenone in EtOH from which the product is recrystallized in the reaction flask upon cooling. In comparison, synthesis of **28** is carried out in a bomb flask at 200 °C overnight requiring recrystallization in a separate step.³⁹ Also, **2** is commercially available, relatively inexpensive, and unlike Michler's ketone, benzophenone

is nontoxic.⁴⁰ Furthermore, the use of an acid such as H₂SO₄ is significantly more cost effective than *p*-TsOH even when used in excess.

Using **11** as a model substrate for the synthesis of *N*-heteroaromatic compounds, a few ketones were tested in the presence of 6.0 equivalents H₂SO₄ (Scheme 11). It was found that heating to 70 °C afforded products within short reaction times in quantitative conversion. It should be noted that this is the same temperature required for the most electron rich benzophenone hydrazone derivatives which required longer reaction times to reach completion. From these experiments, pyrazole **35** was produced in 99% isolated yield, where under the same conditions with 4-methylcyclohexanone afforded the corresponding indole (**36**) in quantitative conversion. Reaction of **11** with 2-acetylcyclohexanone under these conditions afforded pyrazoles **37** as a 72:28 mixture of regioisomers.



Scheme 11. Representative examples of *N*-heteroaromatic synthesis in H₂O.

The effect of reducing acid loading was investigated for the synthesis of **35**. Figure 16 shows the completion time for each loading, where 5.0 equivalents of H₂SO₄ afforded a parallel kinetic profile to the system with 6.0 equivalents. Full conversion was also achieved when acid loading was dropped to 3.0 equivalents, however, reaction completion required 5 h.

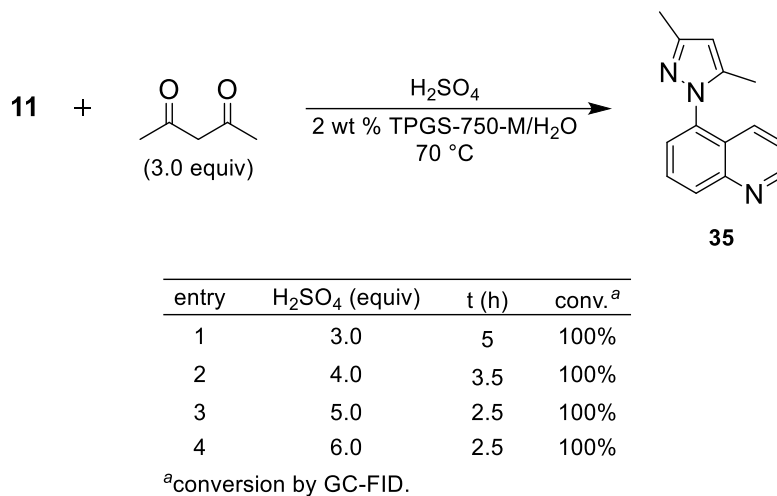
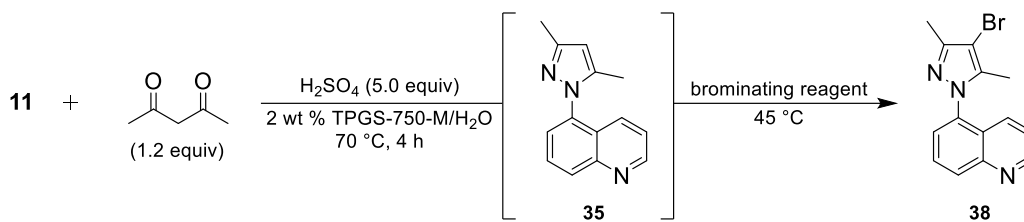


Figure 16. Kinetic profile of pyrazole **35** synthesis at different acid loadings.

In addition to investigating the one-pot route to heterocycles, we envisioned a tandem *N*-heteroaromatic synthesis followed by a sequential functionalization. As an example, **35** was synthesized from **11**, and then submitted to bromination conditions. An initial attempt at this procedure showed only moderate conversion under previous conditions. It was found that the brominating reagent was being consumed by the excess ketone in the pot, undergoing α -bromination. By reducing the ketone equivalents to 1.2 and increasing the bromination reagent equivalents to 1.5, it was found that high yields could be realized of the

corresponding brominated pyrazole (**38**) from *N*-bromosuccinimide (NBS), pyridinium tribromide, and BnNMe₃Br₃ (Figure 17).



entry	reagent	t (h)	conv. ^a	isolated yield
1	NBS	0.5	100%	91%
2	pyridinium tribromide	0.5	100%	87%
3	BnNMe ₃ Br ₃	0.5	100%	89%

^aconversion by GC-FID.

Figure 17. One-pot pyrazole cyclization/bromination from **11**.

6.5 Summary and Conclusions

In conclusion, a method has been developed for the synthesis of aryl hydrazones via Pd-catalyzed amination using benzophone hydrazones with aryl halides in water affording high yields within short reaction times. This system relies on Takasago's ligand, cBRIDP, with [Pd(allyl)Cl]₂, used under mild reaction conditions. Notable features of this method include the use of relatively low temperatures (rt to 45 °C) and Et₃N, which is unprecedented for amination chemistry. Furthermore, this method allows for the one-pot synthesis of *N*-heteroaromatics including pyrazoles, indoles, and indazoles. Further exploiting these conditions for tandem operations, high yields were obtained for the synthesis of a pyrazole with subsequent bromination. Future development is now under way to expand the substrate scope to more electron rich aryl halides and the scope of *N*-heteroaromatic cyclizations. Additionally, we wish to investigate the hypothesis of disproportionation as it relates to the mode of reagent addition by synthesizing analogues of the PdCl(cBRIDP) pre-catalyst.

6.6 Experimental Procedures

General Information

A solution of 2 wt % TPGS-750-M/H₂O solution was prepared by dissolving TPGS-750-M in degassed HPLC grade water and was stored under argon. TPGS-750-M was made as previously described⁴¹ and is available from Sigma-Aldrich (catalog #733857). All commercially available reagents were used without further purification. Thin layer chromatography (TLC) was done using Silica Gel 60 F₂₅₄ plates (Merck, 0.25 mm thick). Flash chromatography was done in glass columns using Silica Gel 60 (EMD, 40-63 μm). GC-MS data was recorded on a 5975C Mass Selective Detector coupled with a 7890A Gas Chromatograph (Agilent Technologies). A capillary column (HP-5MS cross-linked 5% phenylmethyl-polysiloxanediphenyl, 30 m x 0.250 mm, 0.25 micron, Agilent Technologies) was employed. Helium was used as the carrier gas at a constant flow of 1 mL/min. ¹H and ¹³C NMR were recorded at 22 °C on a Varian UNITY INOVA at 500 MHz. Chemical shifts in ¹H NMR spectra are reported in parts per million (ppm) on the δ scale from an internal standard of residual CDCl₃ (7.27 ppm) or the central peak of DMSO-*d*₆ (2.50 ppm). Data are reported as follows: chemical shift, multiplicity (s = singlet, d = doublet, t = triplet, q = quartet, quin = quintet), integration, and coupling constant in Hertz (Hz). Chemical shifts in ¹³C chemical spectra are reported in ppm on the δ scale from the central peak of residual CDCl₃ (77.00 ppm) or the central peak of DMSO-*d*₆ (39.51 ppm).

Catalyst Screening with KO^tBu as Base

[Pd] (0.02 mmol), ligand (0.02 mmol), and degassed 2 wt % TPGS-750-M/H₂O (1.0 mL) were sequentially charged to an argon purged microwave vial with Teflon-coated stir bar. The mixture was allowed to stir at 50 °C under argon for ca. 5 min. KO^tBu (84.2 mg, 0.75 mmol) was then charged to the reaction mixture followed by **4** (93.5 mg, 0.5 mmol) and **2**

(107.9 mg, 0.55 mmol). The reaction was allowed to stir vigorously at 50 °C and monitored by TLC and GC-MS.

Temperature and Concentration Screening

[Pd(allyl)Cl]₂ (0.9 mg, 0.0025 mmol), cBRIDP (3.5 mg, 0.01 mmol), and degassed 2 wt % TPGS-750-M/H₂O were sequentially charged to an argon purged flask with Teflon-coated stirbar. The mixture was allowed to stir under argon for ca. 5 min. KO^tBu (84.2 mg, 0.75 mmol) was then charged to the reaction mixture followed by **4** (93.5 mg, 0.5 mmol) and benzophenone hydrazone (107.9 mg, 0.55 mmol). The reaction was allowed to stir vigorously for 2 h before analysis via GC-MS.

Base Screening Procedures

[Pd(allyl)Cl]₂ (0.9 mg, 0.0025 mmol), cBRIDP (3.5 mg, 0.01 mmol), and degassed 2 wt % TPGS-750-M/H₂O (1.0 mL) were sequentially charged to an argon purged microwave vial with Teflon-coated stir bar. The mixture was allowed to stir at 45 °C under argon for ca. 5 min. Base was then charged to the reaction mixture followed by **6** (91.0 mg, 0.5 mmol) and **2** (107.9 mg, 0.55 mmol). The reaction was allowed to stir at 45 °C for ca. 24 h. The reaction was then extracted with 3 x 2 mL EtOAc, the organic extracts were combined, dried over anhydrous Na₂SO₄, filtered, concentrated, and purified by flash chromatography.

[Pd(allyl)Cl]₂ (0.9 mg, 0.0025 mmol), cBRIDP (3.5 mg, 0.01 mmol), and degassed 2 wt % TPGS-750-M/H₂O (1.0 mL) and base were sequentially charged to an argon purged microwave vial with Teflon-coated stir bar. The mixture was allowed to stir at 45 °C under argon for ca. 5 min. **4** (93.5 mg, 0.5 mmol) or **8** (108.5 mg, 0.5 mmol) and **2** (107.9 mg, 0.55 mmol) were then added. The reaction was allowed to stir at 45 °C and monitored by UPLC/MS.

Catalyst Screening Procedure with Et₃N as Base

[Pd] (0.01 mmol), ligand (0.01 mmol), and degassed 2 wt % TPGS-750-M/H₂O (2.0 mL) were sequentially charged to an argon purged microwave vial with Teflon-coated stir bar. The mixture was allowed to stir at 45 °C under argon for ca. 5 min. Et₃N (75.9 mg, 1.5 mmol) was then charged to the reaction mixture followed by **10** (208.1 mg, 1.0 mmol) and **2** (215.6 mg, 1.1 mmol). The reaction was allowed to stir at 45 °C for ca. 16 h. The reaction was then extracted with 3 x 2 mL EtOAc, the organic extracts were combined, dried over anhydrous Na₂SO₄, filtered, concentrated, and purified by flash chromatography.

[Pd(allyl)Cl]₂ and cBRIDP or PdCl(allyl)cBRIDP and degassed 2 wt % TPGS-750-M/H₂O (2.0 mL) were sequentially charged to an argon purged microwave vial with Teflon-coated stir bar. The mixture was allowed to stir at 45 °C under argon for ca. 5 min. Et₃N (75.9 mg, 1.5 mmol) was then charged to the reaction mixture followed by **12** (237.1 mg, 1.0 mmol) and **2** (215.6 mg, 1.1 mmol). The reaction was allowed to stir at 45 °C for ca. 5 h. The reaction was then extracted with 3 x 2 mL EtOAc, the organic extracts were combined, dried over anhydrous Na₂SO₄, filtered, concentrated, and purified by flash chromatography.

General Procedure

[Pd(allyl)Cl]₂ (3.7 mg, 0.01 mmol), cBRIDP (7.0 mg, 0.02 mmol), and degassed 2 wt % TPGS-750-M/H₂O (2.0 mL) were sequentially charged to an argon purged flask with Teflon-coated stir bar. The mixture was allowed to stir at 45 °C under argon for ca. 5 min. Et₃N (75.9 mg, 1.5 mmol) was then charged to the reaction mixture followed immediately by the aryl halide (1.0 mmol) and benzophenone hydrazone (215.6 mg, 1.1 mmol). The reaction was allowed to stir at 45 °C until reaction completion by TLC. The reaction was then extracted with 3 x 2 mL EtOAc, the organic extracts were combined, dried over anhydrous Na₂SO₄, filtered, concentrated, and purified by flash chromatography.

Condition Screening for Fisher Indole Synthesis from Phenylhydrazine (21)

21 (54.1 mg, 0.5 mmol), 2-pentanone (129.2 mg, 1.5 mmol), 2 wt % TPGS-750-M/H₂O (1.0 mL), and acid were sequentially charged into a microwave vial Teflon-coated stir bar. The reaction was allowed to stir at a given temperature and analyzed by GC-MS.

Condition Screening for Fisher Indole Synthesis from N-Phenyl Benzophenone Hydrazone (24)

24 (136.2 mg, 0.5 mmol), 2-pentanone (129.2 mg, 1.5 mmol), 2 wt % TPGS-750-M/H₂O (1.0 mL), and acid were sequentially charged into a microwave vial Teflon-coated stir bar. The reaction was allowed to stir at a given temperature and analyzed by GC-MS.

Fisher Indole Synthesis Procedure from Substituted N-Phenyl Benzophenone Hydrazones

Substituted *N*-Phenyl-benzophenone hydrazone (0.5 mmol), 2-pentanone (129.2 mg, 1.5 mmol), 2 wt % TPGS-750-M/H₂O (1.0 mL), and CSA (255.5 mg, 0.55 mmol) were sequentially charged into a microwave vial Teflon-coated stir bar. The reaction was allowed to stir at 70 °C for ca. 13 h and analyzed by GC-MS.

One Pot Synthesis of 1H-indazol-3-amine (34)

[Pd(allyl)Cl]₂ (3.7 mg, 0.01 mmol), cBRIDP (7.0 mg, 0.02 mmol), and degassed 2 wt % TPGS-750-M/H₂O (2.0 mL) were sequentially charged to an argon purged flask with Teflon-coated stir bar. The mixture was allowed to stir at 45 °C under argon for ca. 5 min. Et₃N (75.9 mg, 1.5 mmol) was then charged to the reaction mixture followed by the aryl halide (1.0 mmol) and benzophenone hydrazone (215.6 mg, 1.1 mmol). The reaction was allowed to stir at 45°C until reaction completion by TLC. The reaction was then extracted with 3 x 2 mL EtOAc, the organic extracts were combined, dried over anhydrous Na₂SO₄, filtered, concentrated, and purified by flash chromatography.

[Pd(allyl)Cl]₂ (0.9 mg, 0.0025 mmol), cBRIDP (3.5 mg, 0.01 mmol), and degassed 2 wt % TPGS-750-M/H₂O (1.0 mL) were sequentially charged to an argon purged flask with Teflon-coated stir bar. The mixture was allowed to stir under argon for ca. 5 min. KO^tBu (84.2 mg, 0.75 mmol) was then charged to the reaction mixture followed by **31** (68.8 mg, 0.5 mmol) and benzophenone hydrazone (107.9 mg, 0.55 mmol). The reaction was allowed to stir at 50 °C for ca. 16 h. The reaction was determined complete by GC/MS analysis and the mixture was neutralized with 1 M HCl. pTsOH (94.7 mg, 0.55 mmol) was transferred to the reaction and the temperature was increased to 70 °C. After ca. 15 h, saturated aqueous NaHCO₃ was transferred to the reaction mixture and the crude product was extracted with 3 x 2 mL EtOAc. Organic extracts were combined, dried over anhydrous Na₂SO₄, filtered, condensed, and purified by flash chromatography to afford 40.6 mg **34** (51% yield).

Heterocycle Synthesis from 5-(2-(diphenylmethylene)hydrazinyl)quinolone (11)

11 (80.85 mg, 0.25 mmol), ketone (1.5 mmol), 2 wt % TPGS-750-M/H₂O (1.0 mL), and 6 M H₂SO₄ (0.25 mL, 1.5 mmol) were sequentially charged a microwave vial Teflon-coated stir bar. The reaction was allowed to stir at 70 °C and analyzed by TLC and GC-MS.

Acid Screening Procedure for the Synthesis of Pyrazole 35

11 (80.85 mg, 0.25 mmol), acetylacetone (75.0 mg, 0.75 mmol), 2 wt % TPGS-750-M/H₂O (1.0 mL), and aqueous H₂SO₄ (0.25 mL, 1.5 mmol) were sequentially charged a microwave vial Teflon-coated stir bar. The reaction was allowed to stir at 70 °C until reaction completion as determined by TLC and GC-MS analysis.

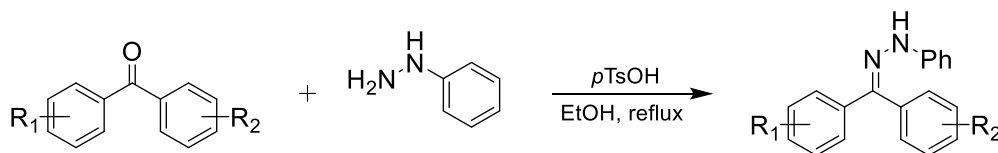
One Pot Pyrazole Synthesis/Bromination Procedure

11 (80.85 mg, 0.25 mmol), acetylacetone (30 mg, 0.3 mmol), 2 wt % TPGS-750-M/H₂O (1.0 mL), and 5 M H₂SO₄ (0.25 mL, 1.25 mmol) were sequentially charged a microwave vial Teflon-coated stir bar. The reaction was allowed to stir at 70 °C until

reaction completion at ca. 4 h as determined by TLC and GC-MS analysis. The reaction was allowed to cool to 45 °C for ca. 30 min followed by the addition of the brominating reagent (0.75 mmol). Upon reaction completion at ca. 30 minutes, saturated aqueous NaHCO₃ was transferred to the reaction mixture and the crude product was extracted with 3 x 2 mL EtOAc. Organic extracts were combined, dried over anhydrous Na₂SO₄, filtered, condensed, and purified by flash chromatography.

Synthesis of PdCl(allyl)(cBRIDP)

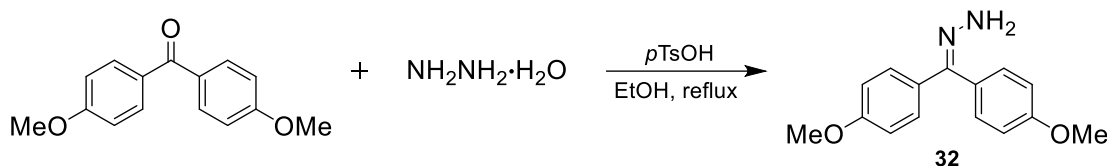
Following the literature procedure,^{31a} a flame-dried, argon-purged, 5 mL round bottom flask with a Teflon-coated stir bar, was charged [Pd(allyl)Cl]₂ (109.8 mg, 3.0 mmol) and dry THF (1.5 mL) to give a clear yellow solution. cBRIDP (4, 15.0 g, 42.6 mmol, 2.1 equiv) was then added causing immediate precipitation of a pale yellow solid. The suspension was stirred for 2 h at 30 °C and *n*-heptane (5.5 mL) was added at the same temperature. The mixture was stirred for 2 h at 30 °C and filtered, triturated with *n*-heptane and dried under vacuum overnight to afford 300.0 mg PdCl(allyl)(cBRIDP) as a pale yellow solid (93%).



Scheme 12. Preparation of substituted *N*-phenyl benzophenones.

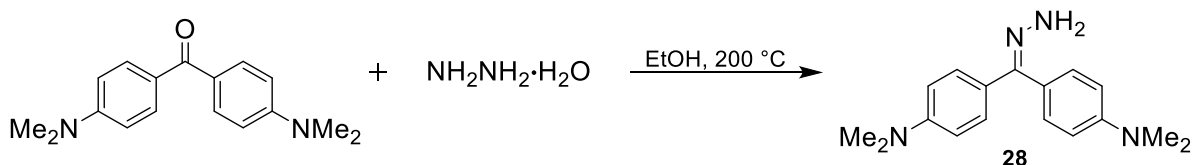
General Procedure for the Preparation of Substituted *N*-Phenyl Benzophenone Hydrazones.⁴² To an oven-dried 250 mL round bottom flask with Teflon coated stir bar and reflux condenser, argon was purged and benzophenone (3478.6 mg, 19.1 mmol), *p*-TsOH monohydrate (181.6 mg, 1.0 mmol), and EtOH (52 ml) were then added. Phenylhydrazine (1.9 mL, 19.1 mmol) was then transferred via syringe and the system was brought to reflux.

After ca. 4 h, the reaction mixture was removed from heating source and allowed to cool to rt and allowed to stand for ca. 16 h. The crystalline white solid was filtered and triturated with cold EtOH to afford pure benzophenone hydrazone **24** (4783.6 mg, 92%).



Scheme 13. Preparation of hydrazone **32**.

(Bis(4-methoxyphenyl)methylene)hydrazine (32). Prepared following the literature procedure:⁴³ To an oven-dried 50 mL round bottom flask with Teflon coated stir bar and reflux condenser, bis(4-methoxyphenyl)methanone (5009.4 mg, 20.7 mmol), *n*-Bu (2.1 mL), and 86 % hydrazine hydrate (1.51 mL, 1.5 mmol) were transferred and the reaction was heated to 140 °C overnight. 20 mL MeOH was then transferred as the reaction cooled to rt. The mixture was set in the freezer overnight causing a large amount of precipitation. The solid was filtered, rinsed with cold EtOH and transferred to a 250 mL flask. The crude was then recrystallized from methanol to afford **32** as white crystals (4023.4 mg, 69%).



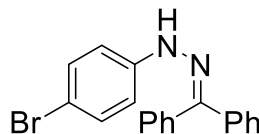
Scheme 14. Preparation of Michler's Ketone Hydrazone.

Michler's Ketone Hydrazone (28). Prepared following the literature procedure:³⁹ Michler's ketone (2.5 g, 9.3 mmol), 64% aqueous hydrazine (3.3 g, 66.1 mmol), and EtOH (1.7 mL) were heated to 200 °C in an autoclave (glass, applicable to 10 bar) for ca. 24 h. On

slow cooling and stirring, crystals deposited were separated by vacuum filtration and triturated with cold ethanol to afford pure **28** (2258.1 mg, 86%).

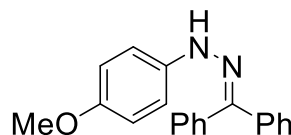
6.7 Compound Data

Characterization of Products



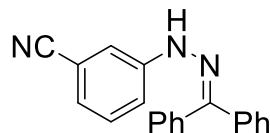
3

1-(4-Bromophenyl)-2-(diphenylmethylene)hydrazine (3). 72.2 mg (96%). ^1H NMR (500 MHz, CDCl_3) δ 7.62-7.56 (m, 4H), 7.52 (t, 1H), 7.42-7.24 (m, 7H), 7.06-6.99 (m, 2H). ^1H in agreement with previous reports of this compound.²⁹



5

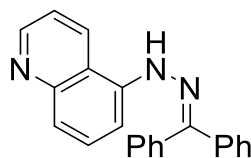
1-(Diphenylmethylene)-2-(4-methoxyphenyl)hydrazine (5). 256.8 mg (85%). ^1H NMR (500 MHz, CDCl_3) δ 7.63-7.58 (m, 4H), 7.56-7.48 (m, 2H), 7.37-7.28 (m, 5H), 7.14 (t, 1H), 6.80 (t, 1H), 6.58 (m, 1H), 6.43 (m, 1H), 3.83 (s, 3H). ^1H in agreement with previous reports of this compound.⁴⁴



7

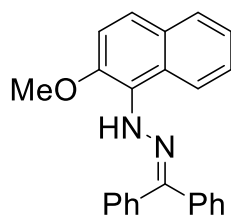
3-(2-(Diphenylmethylene)hydrazinyl)benzonitrile (7). 285.2 mg (96%). ^1H NMR (500 MHz, CDCl_3) δ 7.67-7.56 (m, 6H), 7.44 (t, 1H), 7.41-7.29 (m, 6H), 7.22 (m, 1H), 7.11 (dt, J = 7.53, 1.30 Hz, 1H); ^{13}C NMR (125 MHz, CDCl_3) δ 146.33, 144.96, 137.63, 132.12,

129.75, 129.70, 129.50, 128.79, 128.54, 128.19, 126.64, 123.12, 119.05, 117.04, 115.78, 112.88.



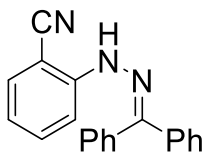
11

5-(2-(Diphenylmethylene)hydrazinyl)quinolone (11). 314.3 mg (97%). ¹H NMR (500 MHz, CDCl₃) δ 8.83 (dd, *J*=4.15, 1.30 Hz, 1H), 8.13 (s, 1H), 7.78 (dd, *J* = 7.27, 1.04 Hz, 1H), 7.73-7.57 (m, 8H), 7.47-7.42 (m, 2H), 7.41-7.32 (m, 3H), 7.19 (dd, *J* = 8.56, 4.15 Hz, 1H); ¹³C NMR (125 MHz, CDCl₃) δ 149.81, 148.71, 147.01, 139.26, 137.75, 132.39, 130.16, 129.75, 129.51, 128.83, 128.45, 128.17, 127.76, 126.66, 121.02, 119.42, 116.94, 108.50.



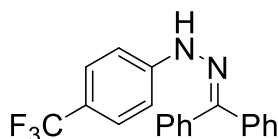
13

1-(Diphenylmethylene)-2-(2-methoxynaphthalen-1-yl)hydrazine (13). 325.8 mg (92%). ¹H NMR (500 MHz, CDCl₃) δ 9.18 (dd, 1H), 8.26 (s, 1H), 7.81 (dd, 1H), 7.69-7.64 (m, 4H), 7.61-7.55 (m, 2H), 7.54-7.50 (m, 3H), 7.43 (m, 1H), 7.39-7.30 (m, 3H), 7.20 (d, 1H), 3.81 (s, 3H); ¹³C NMR (125 MHz, CDCl₃) δ 146.62, 144.61, 138.42, 133.24, 130.22, 129.48, 129.09, 129.03, 128.14, 127.88, 127.87, 126.61, 126.35, 125.18, 125.07, 123.84, 122.61, 112.96, 56.88.



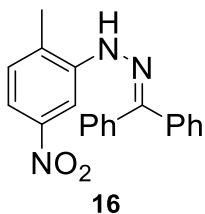
14

2-(2-(Diphenylmethylene)hydrazinyl)benzonitrile (14). 296.1 mg (99%). ^1H NMR (500 MHz, CDCl_3) δ 8.21 (s, 1H), 7.76 (dd, $J=8.56, 0.52$, 1H), 7.70-7.62 (m, 4H), 7.59 (m, 1H), 7.53 (m, 1H), 7.42-7.36 (m, 6H), 6.85 (td, $J=7.27, 1.04$ Hz, 1H; ^{13}C NMR (125 MHz, CDCl_3) δ 148.23, 146.71, 137.49, 134.16, 132.10, 131.61, 129.90, 129.88, 128.86, 128.51, 128.51, 128.26, 126.98, 119.32, 116.46, 113.52, 94.71. ^1H and ^{13}C NMR in agreement with previous reports of this compound.³⁸

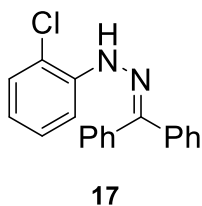


15

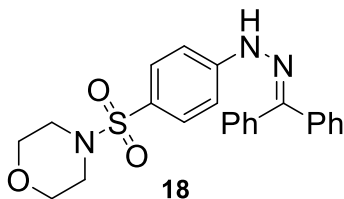
1-(Diphenylmethylene)-2-(4-(trifluoromethyl)phenyl)hydrazine (15). 339.3 mg (94%). ^1H NMR (500 MHz, CDCl_3) δ 7.27 (s, 1H), 7.70-7.64 (m, 4H), 7.61 (tt, 1H), 7.56 (d, $J=8.56$ Hz, 2H), 7.44-7.36 (m, 5H), 7.18 (d, $J=8.56$ Hz, 2H; ^{13}C NMR (125 MHz, CDCl_3) δ 147.06, 146.20, 137.87, 132.28, 129.74, 129.50, 128.93, 128.53, 128.24, 126.72, 126.54, 126.51, 126.48, 126.45, 112.42. ^1H and ^{13}C NMR in agreement with previous reports of this compound.^{17a}



1-(Diphenylmethylene)-2-(2-methyl-5-nitrophenyl)hydrazine (16). 323.5 mg (98%). ¹H NMR (500 MHz, CDCl₃) δ 8.47 (d, *J*=2.34 Hz, 1H), 7.71-7.56 (m, 6H), 7.54 (s, 1H), 7.41-7.35 (m, 5H), 7.11 (d, *J*=8.04 Hz, 1H), 1.91 (s, 3H); ¹³C NMR (125 MHz, CDCl₃) δ 147.74, 147.67, 142.98, 137.35, 132.30, 130.42, 129.79, 129.59, 128.71, 128.50, 128.25, 127.20, 126.77, 113.90, 106.79, 16.57.

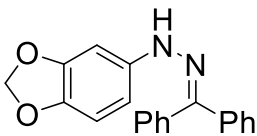


1-(2-Chlorophenyl)-2-(diphenylmethylene)hydrazine (17). 264.0 mg (85%). ¹H NMR (500 MHz, CDCl₃) δ 8.16 (s, 1H), 7.84 (m, 1H), 7.72 (m, 2H), 7.65 (m, 2H), 7.58 (m, 1H), 7.47-7.35 (m, 5H), 7.32 (m, 1H), 7.26 (m, 1H), 6.82 (m, 1H); ¹³C NMR (125 MHz, CDCl₃) δ 146.51, 140.49, 137.97, 132.54, 129.66, 129.35, 128.91, 128.71, 128.34, 128.17, 127.83, 126.69, 119.83, 117.32, 113.98. ¹H and ¹³C NMR in agreement with previous reports of this compound.⁴²



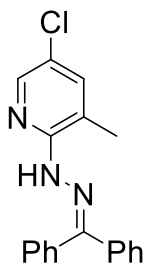
4-((4-(2-(Diphenylmethylene)hydrazinyl)phenyl)sulfonyl)morpholine (18). 391.6 mg (93%). ¹H NMR (500 MHz, CDCl₃) δ 7.80 (s, 1H), 7.66-7.54 (m, 7H), 7.39-7.32 (m, 5H),

7.18 (d, 2H), 3.72 (t, 4H), 2.97 (t, 4H); ^{13}C NMR (125 MHz, CDCl_3) δ 148.08, 147.37, 137.49, 131.92, 129.73, 129.60, 128.76, 128.19, 126.76, 124.53, 112.42, 65.96, 45.92.



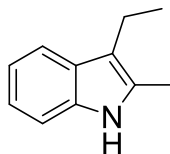
19

1-(Benzo[d][1,3]dioxol-5-yl)-2-(diphenylmethylene)hydrazine (19). 117.2 mg (37%). ^1H NMR (500 MHz, CDCl_3) δ 7.62-7.55 (m, 4H), 7.55-7.49 (m, 1H), 7.42-7.25 (m, 6H), 6.87 (d, 1H), 6.69 (d, 1H), 6.37 (dd, 1H), 5.91 (s, 2H); ^{13}C NMR (125 MHz, CDCl_3) δ 148.43, 143.61, 141.27, 140.35, 138.34, 132.81, 129.65, 129.17, 129.12, 128.14, 127.86, 126.35, 108.38, 104.74, 100.79, 95.80.



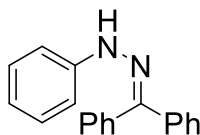
20

5-Chloro-2-(2-(diphenylmethylene)hydrazinyl)-3-methylpyridine (20). 96.7 mg (60%). ^1H NMR (500 MHz, CDCl_3) δ 8.06 (d, 1H), 7.93 (s, 1H), 7.65-7.57 (m, 4H), 7.54 (tt, 1H), 7.40-7.28 (m, 6H), 2.21 (s, 3H); ^{13}C NMR (125 MHz, CDCl_3) δ 151.81, 148.08, 143.73, 138.78, 137.64, 132.44, 129.77, 129.49, 119.30, 18.07.



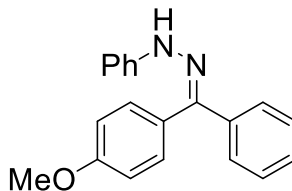
23

3-Ethyl-2-methyl-1H-indole (23). 131.0 mg (82%). ^1H NMR (500 MHz, CDCl_3) δ 7.63 (s, 1H), 7.57 (d, 1H), 7.29-7.26 (m, 1H), 7.17-7.10 (m, 2H), 2.76 (q, 2H), 2.39 (s, 3H), 1.27 (t, 3H); ^{13}C NMR (125 MHz, CDCl_3) δ 135.23 130.06 128.46 120.76 118.92 118.03 113.90 110.11 17.34 15.38 11.44. ^1H and ^{13}C NMR in agreement with previous reports of this compound.⁴⁵



24

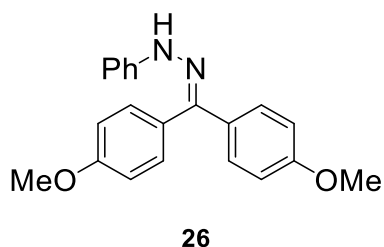
1-(Diphenylmethylene)-2-phenylhydrazine (24). 4783.6 mg (92%). ^1H NMR (500 MHz, CDCl_3) δ 7.63-7.58 (m, 4H), 7.54 (tt, 1H), 7.37-7.24 (m, 8H), 7.11-7.08 (m, 2H), 6.86 (tt, 1H); ^{13}C NMR (125 MHz, CDCl_3) δ 144.60, 144.18, 138.37, 132.77, 129.66, 129.22, 129.20, 129.15, 128.16, 127.98, 126.46, 120.04, 112.92. ^1H and ^{13}C NMR in agreement with previous reports of this compound.⁴²



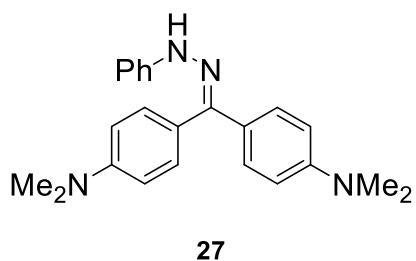
25

1-((4-Methoxyphenyl)(phenyl)methylene)-2-phenylhydrazine (25). 2553.9 mg (88%). ^1H NMR (500 MHz, CDCl_3) δ 7.63-7.50 (m, 3H), 7.36-7.22 (m, 7H), 7.13-7.05 (m, 4H), 6.89-6.83 (m, 3H), 3.91+3.83 (2xs 13:87); ^{13}C NMR (125 MHz, CDCl_3) δ 164.48, 160.05,

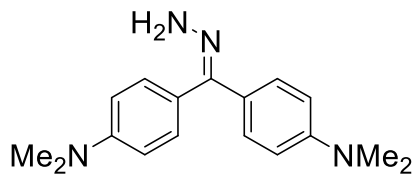
144.65, 144.10, 138.69, 130.53, 129.58, 129.18, 1290.8, 128.11, 127.90, 127.82, 126.53, 124.59, 119.91, 115.01, 113.59, 112.88, 112.77, 103.71, 103.70, 60.36, 55.34.



1-(Bis(4-methoxyphenyl)methylene)-2-phenylhydrazine (26). 6552.0 mg (94%). ¹H NMR (500 MHz, CDCl₃) δ 7.55 (dt, 2H), 7.30-7.22 (m, 5H), 7.11-7.05 (m, 4H), 7.68 (dt, 2H), 6.83 (tt, 1H), 3.91 (s, 3H), 3.83 (s, 3H).

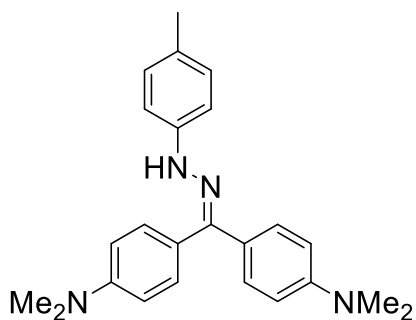


4,4'-((2-Phenylhydrazono)methylene)bis(*N,N*-dimethylaniline) (27). 1005.5 mg (74%). ¹H NMR (500 MHz, CDCl₃) δ 7.57-7.50 (m, 3H), 7.25-7.19 (m, 4H), 7.10-7.05 (m, 2H), 6.86 (d, 2H), 6.79 (dt, 2H), 6.70 (d, 2H), 3.07 (s, 6H), 2.98 (s, 6H); ¹³C NMR (125 MHz, CDCl₃) δ 150.42, 150.26, 145.90, 145.37, 130.11, 129.04, 127.85, 120.23, 118.91, 112.57, 112.49, 111.86, 40.45, 40.28.



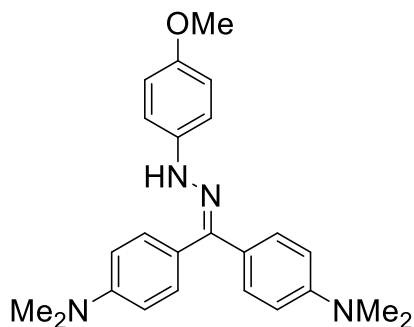
28

4,4'-(Hydrazonomethylene)bis(*N,N*-dimethylaniline) (28). 2258.1 mg (86%). ¹H NMR (500 MHz, CDCl₃) δ 7.41 (dt, 2H), 7.21 (dt, 2H), 6.82 (dt, 2H), 6.65 (dt, 2H), 3.03 (s, 6H), 2.97 (s, 6H). ¹H in agreement with previous reports of this compound.³⁹



29

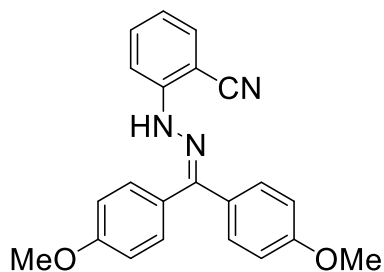
4,4'-((2-(*p*-Tolyl)hydrazono)methylene)bis(*N,N*-dimethylaniline) (29). 175.4 mg (86%). ¹H NMR (500 MHz, CDCl₃) δ 7.57 (d, 2H), 7.54 (s, 1H), 7.26 (dt, 2H), 7.09 (d, 2H), 7.03 (d, 2H), 6.90 (dt, 2H), 6.74 (d, 2H), 3.09 (s, 6H), 3.02 (s, 6H), 2.33 (s, 3H); ¹³C NMR (125 MHz, CDCl₃) δ 150.30, 150.13, 145.28, 143.16, 132.06, 130.04, 129.46, 127.94, 127.75, 127.69, 120.24, 112.51, 112.41, 111.77, 110.42, 40.36, 40.18, 39.96, 20.48.



30

4,4'-((2-(4-Methoxyphenyl)hydrazono)methylene)bis(*N,N*-dimethylaniline) (30).

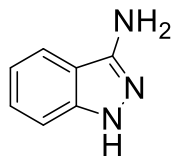
135.5 mg (70%). ¹H NMR (500 MHz, CDCl₃) δ 7.52 (dt, 2H), 7.41 (s, 1H), 7.22 (dt, 2H), 7.03 (d, 2H), 6.90-6.79 (m, 4H), 6.74-6.66 (m, 2H), 3.78 (s, 3H), 3.06 (s, 6H), 2.98 (s, 6H); ¹³C NMR (125 MHz, CDCl₃) δ 193.90, 152.60, 150.33, 132.10, 130.08, 129.35, 127.67, 126.20, 120.55, 120.35, 114.60, 113.79, 113.60, 112.46, 111.83, 110.46, 55.68, 55.04, 40.02.



33

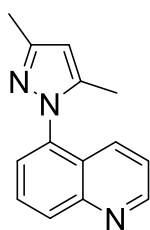
2-(2-(Bis(4-methoxyphenyl)methylene)hydrazinyl)benzonitrile (33). 182.9 mg (99%).

¹H NMR (500 MHz, CDCl₃) δ 8.21 (s, 1H), 7.71 (d, 1H), 7.58 (dt, 2H), 7.50 (m, 1H), 7.38 (dd, 1H), 7.30 (td, 2H), 7.12 (td, 2H), 6.89 (td, 2H), 6.81 (td, 1H), 3.90 (s, 3H), 3.84 (s, 3H); ¹³C NMR (125 MHz, CDCl₃) δ 160.41, 160.27, 148.08, 146.98, 134.13, 132.18, 130.78, 130.06, 128.53, 123.60, 118.88, 116.76, 115.14, 113.63, 113.45, 94.34, 55.31, 55.30, 55.29.



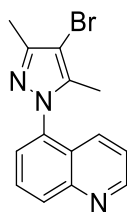
34

1H-Indazol-3-amine (34). 40.6 mg (51%). ¹H NMR (500 MHz, CDCl₃) δ 11.36 (s, 1H), 7.67 (d, 1H), 7.27-7.16 (m, 2H), 6.89 (m, 1H), 5.30 (s, 2H). ¹H in agreement with previous reports of this compound.³⁸



35

5-(3,5-Dimethyl-1H-pyrazol-1-yl)quinoline (35). 220.9 mg (99%). ¹H NMR (500 MHz, CDCl₃) δ 8.92 (dd, 1H), 8.19 (dt, 1H), 7.18-7.73 (m, 2H), 7.51 (dd, 1H), 7.38 (dd, 1H), 6.06 (s, 1H), 2.32 (s, 3H), 2.06 (s, 3H); ¹³C NMR (125 MHz, CDCl₃) δ 150.83, 149.28, 149.27, 148.52, 141.33, 135.86, 131.98, 130.48, 128.37, 126.10, 125.38, 122.00, 105.77, 13.49, 11.37.

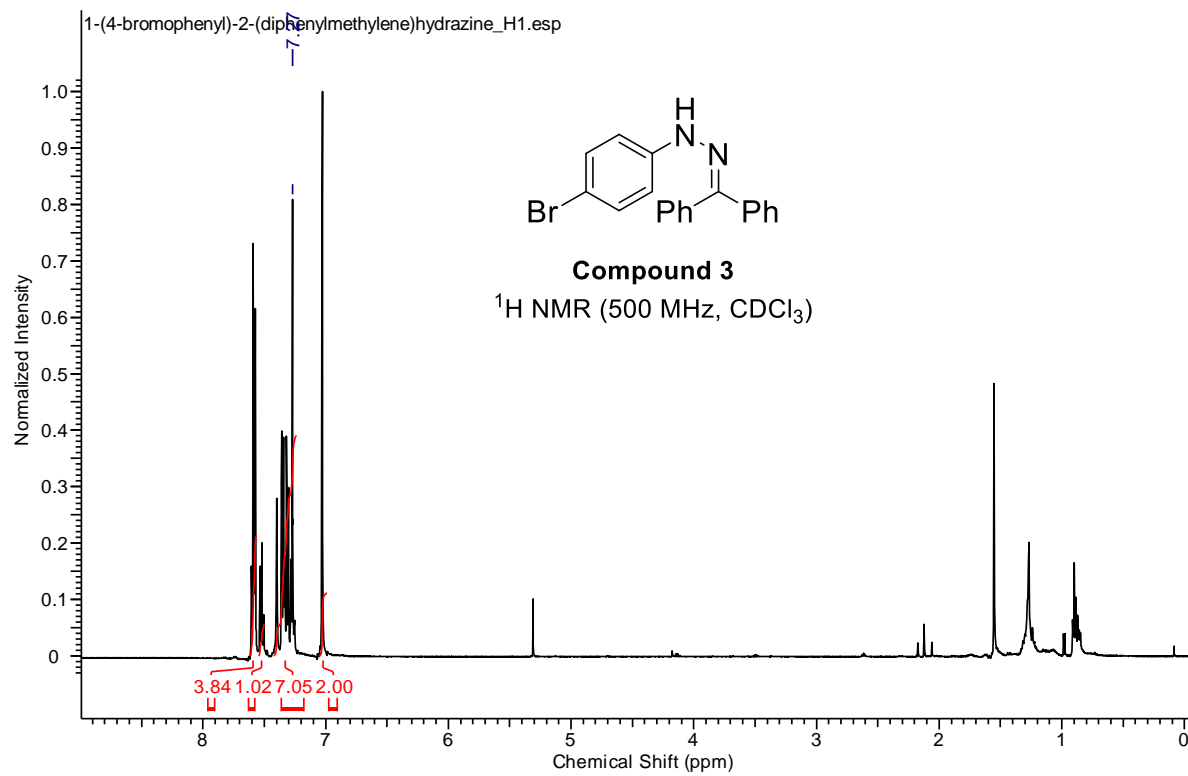


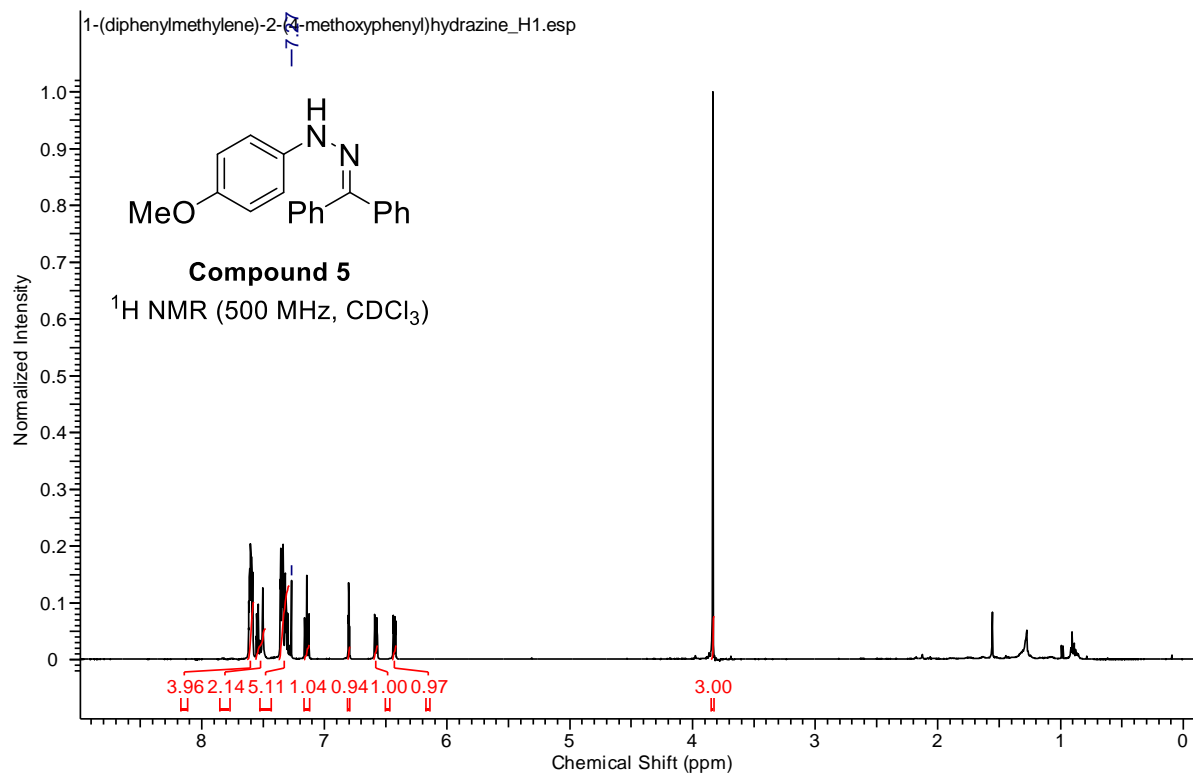
38

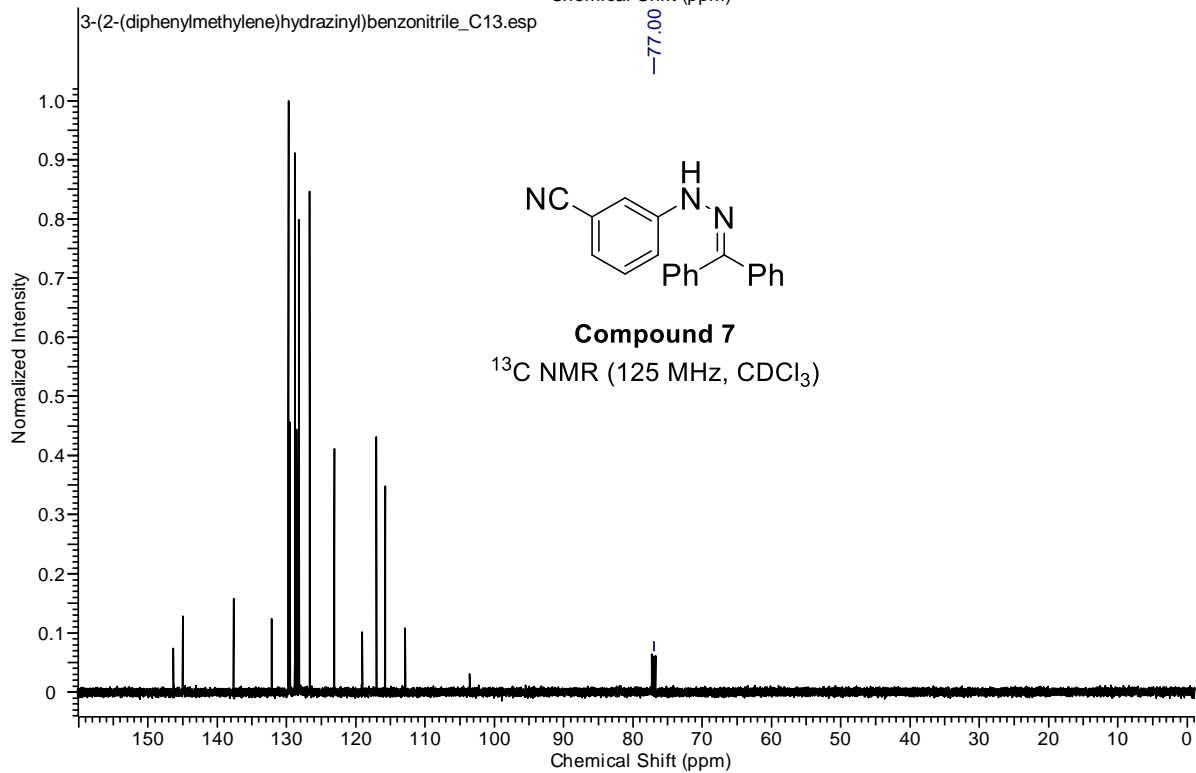
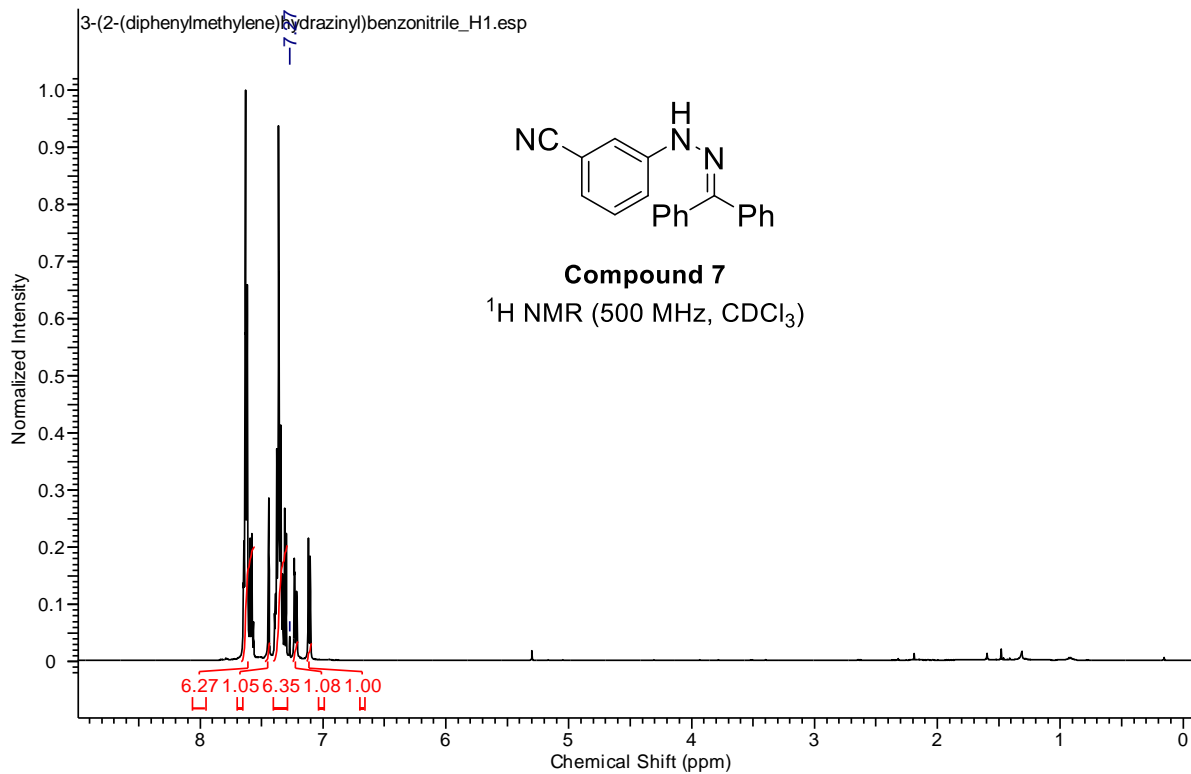
5-(4-Bromo-3,5-dimethyl-1H-pyrazol-1-yl)quinoline (39). 137.8 mg (91%). ¹H NMR (500 MHz, CDCl₃) δ 8.96 (dd, 1H), 8.23 (dt, 1H), 7.80-7.76 (m, 2H), 7.51 (dd, 1H), 7.42 (dd,

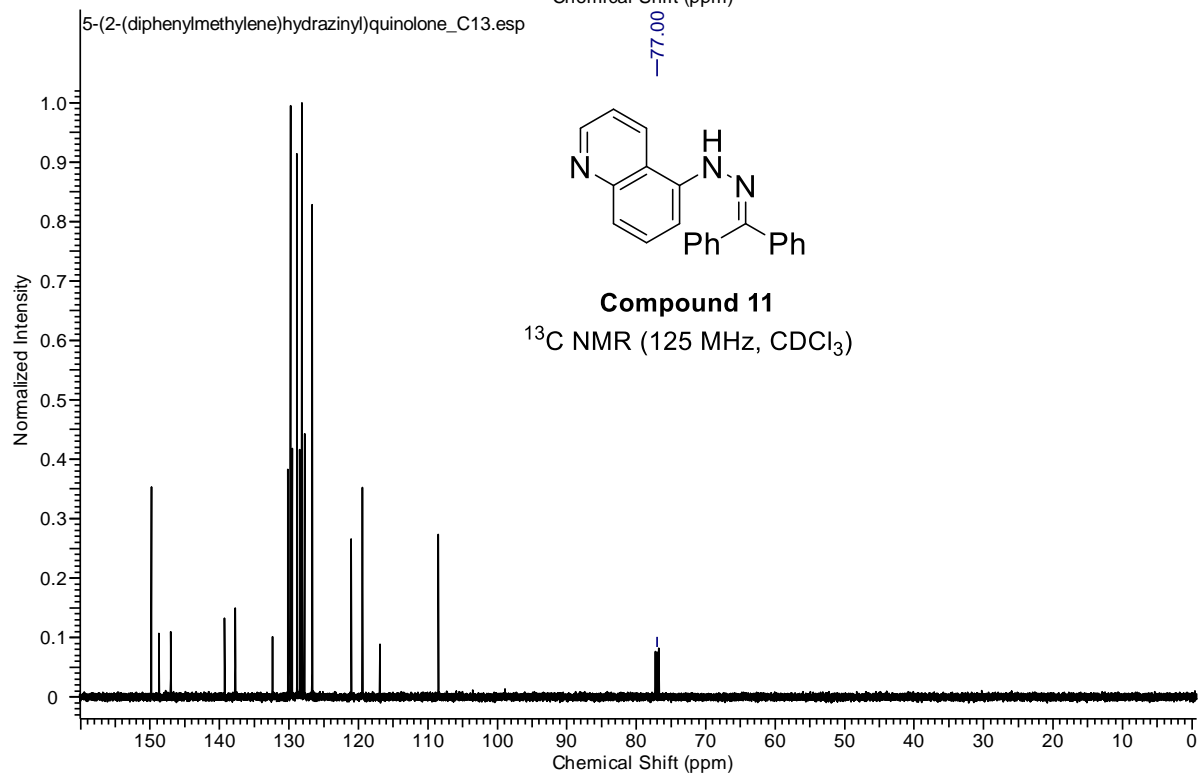
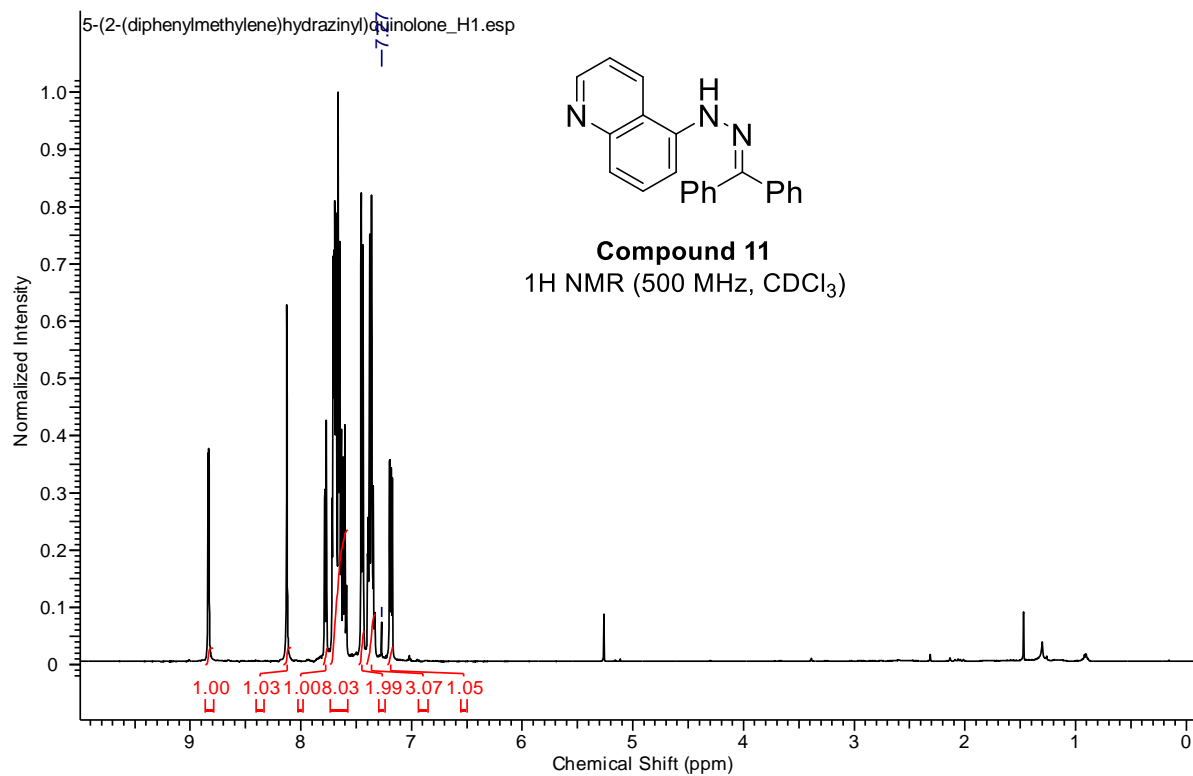
1H), 2.34 (s, 1H), 2.09 (s, 1H); ¹³C NMR (125 MHz, CDCl₃) δ 151.09, 148.57, 148.02, 139.54, 135.66, 131.67, 131.07, 128.43, 125.77, 125.48, 122.25, 95.55, 12.40, 10.91.

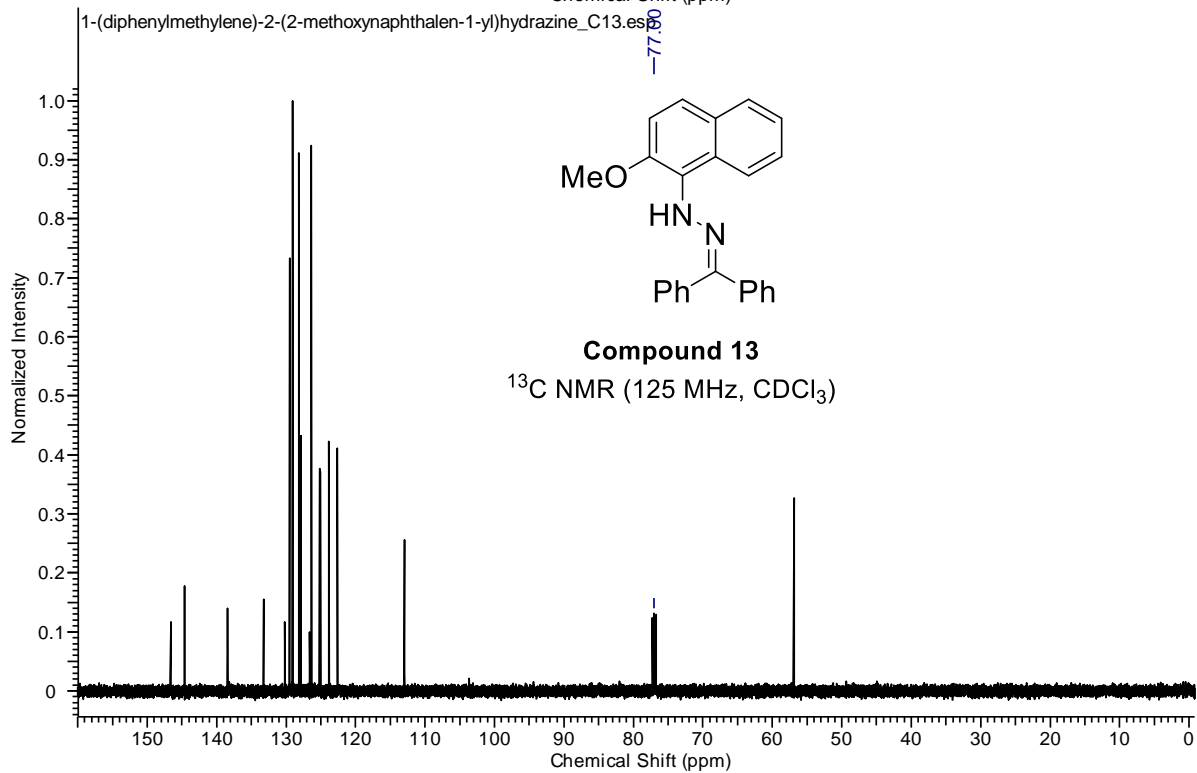
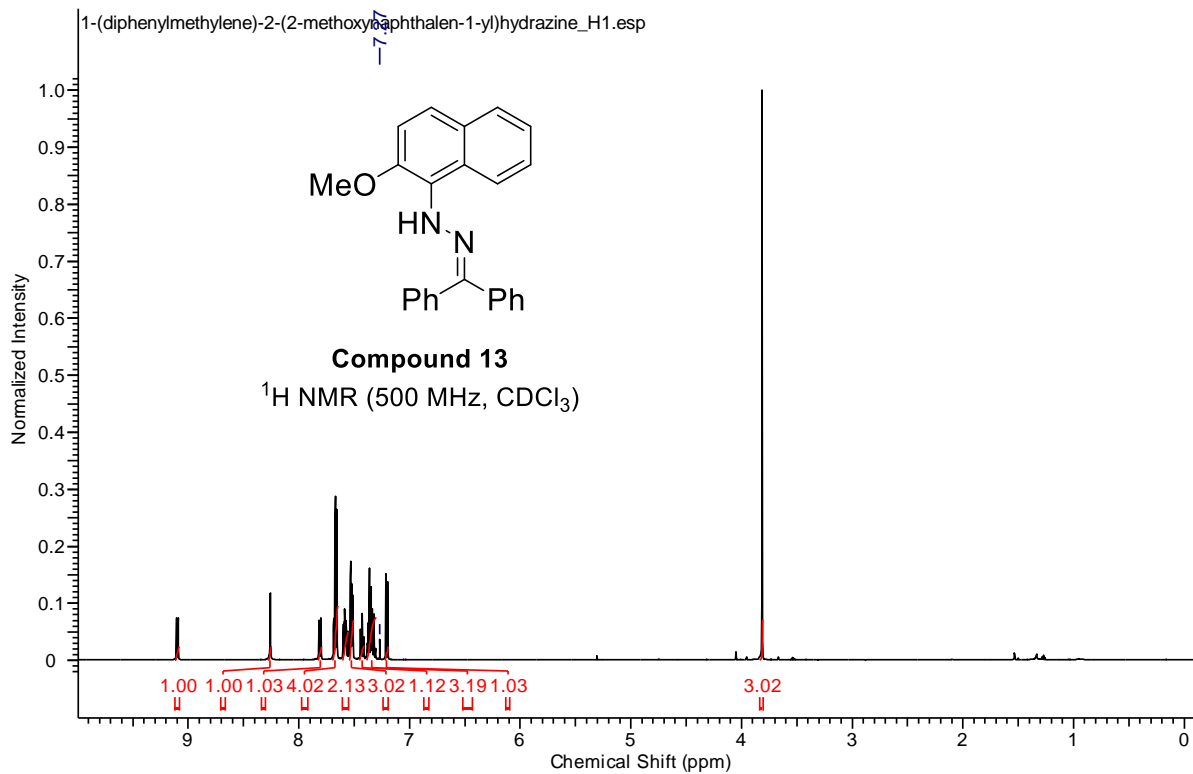
6.8 NMR Spectra

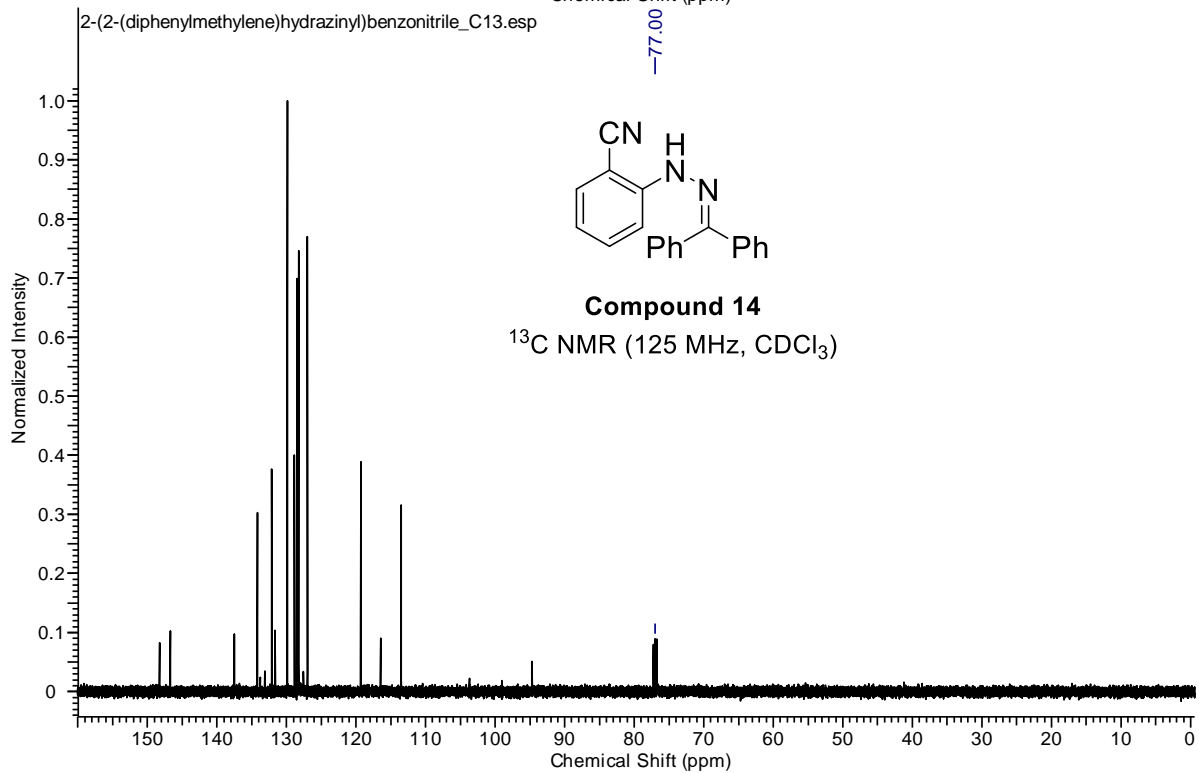
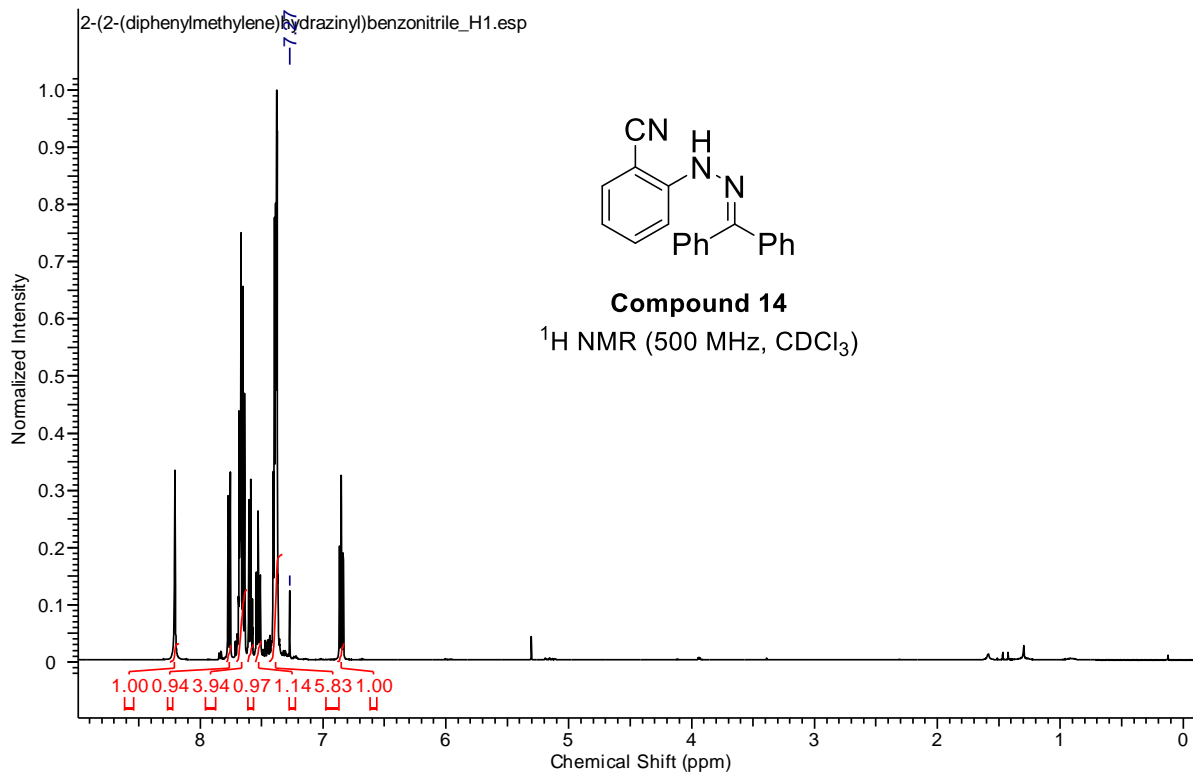


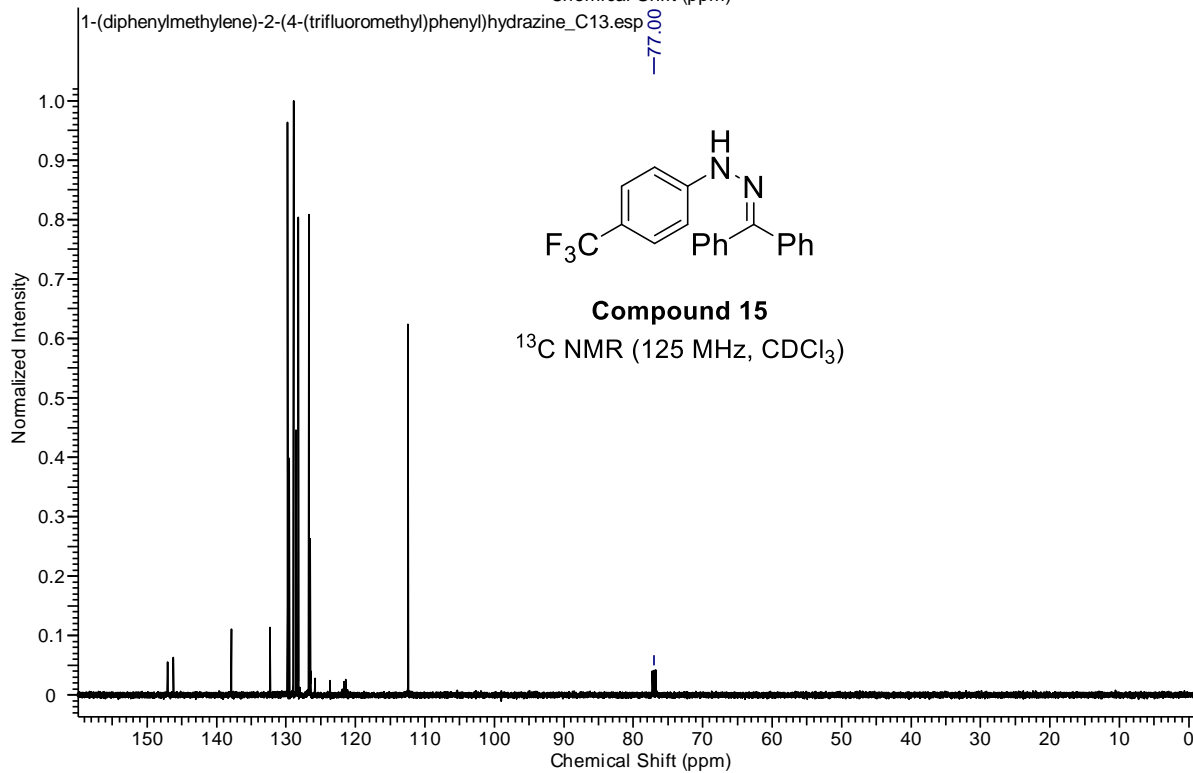
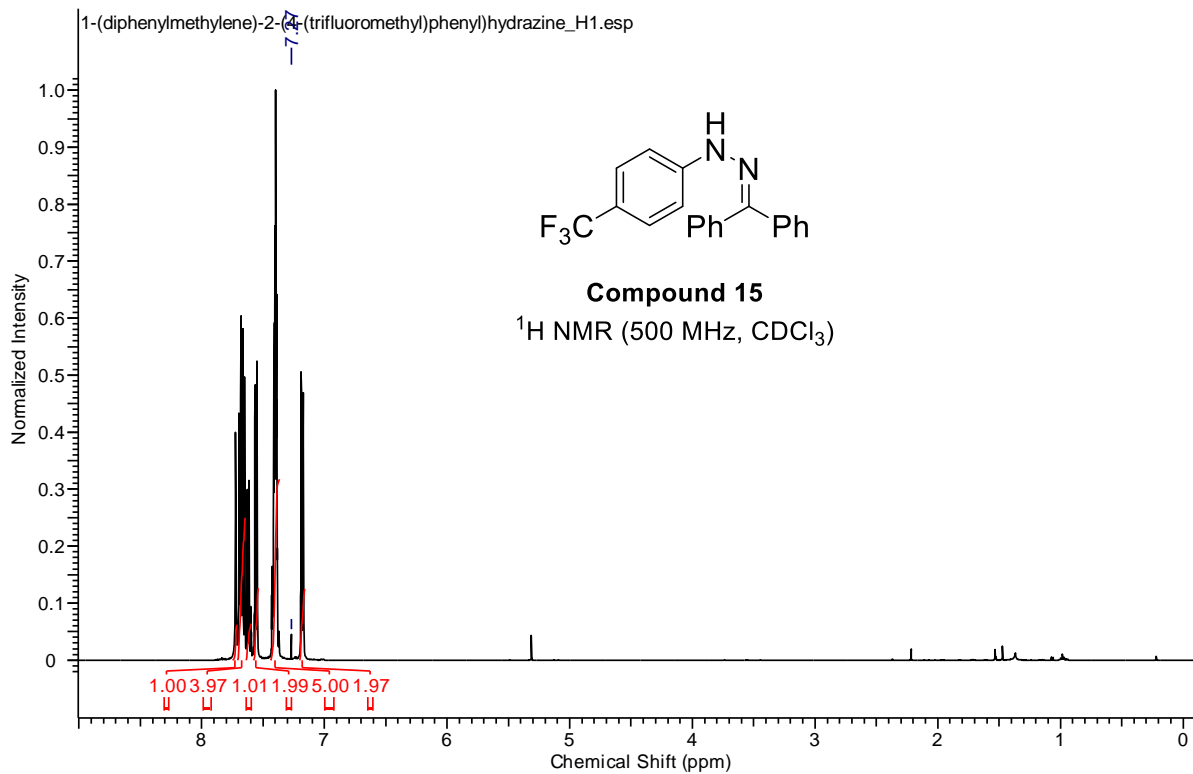


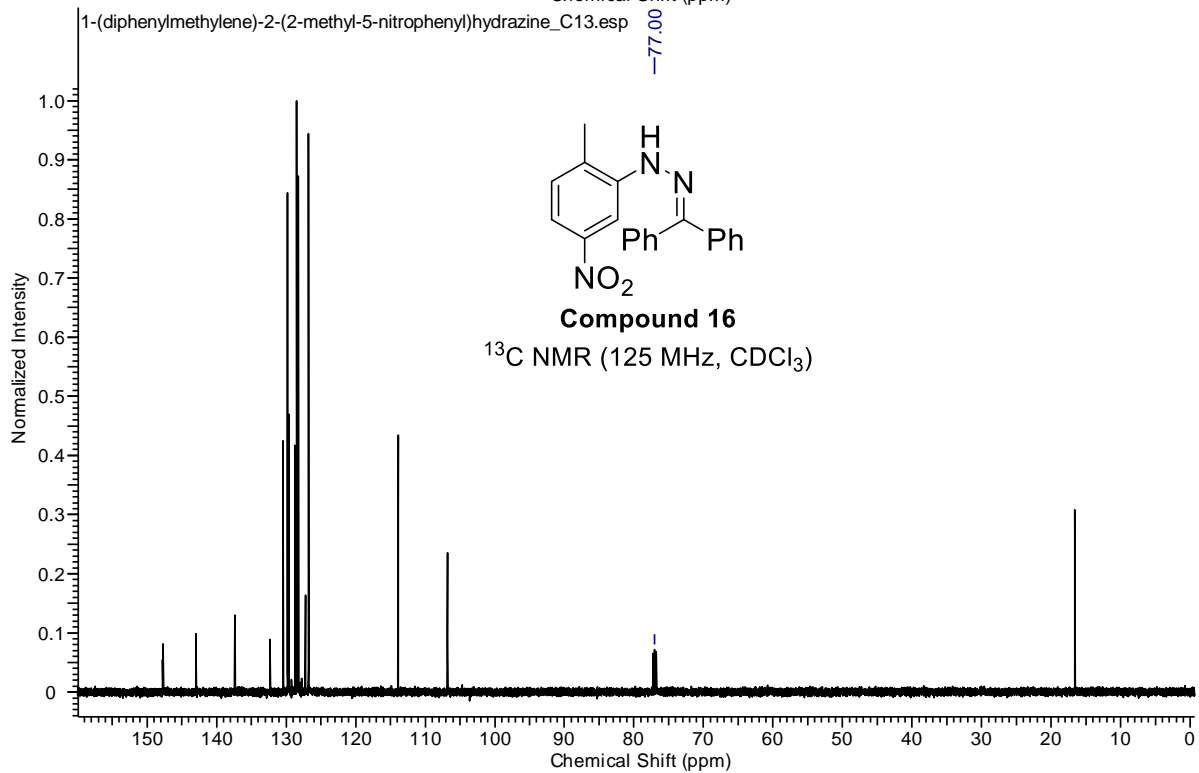
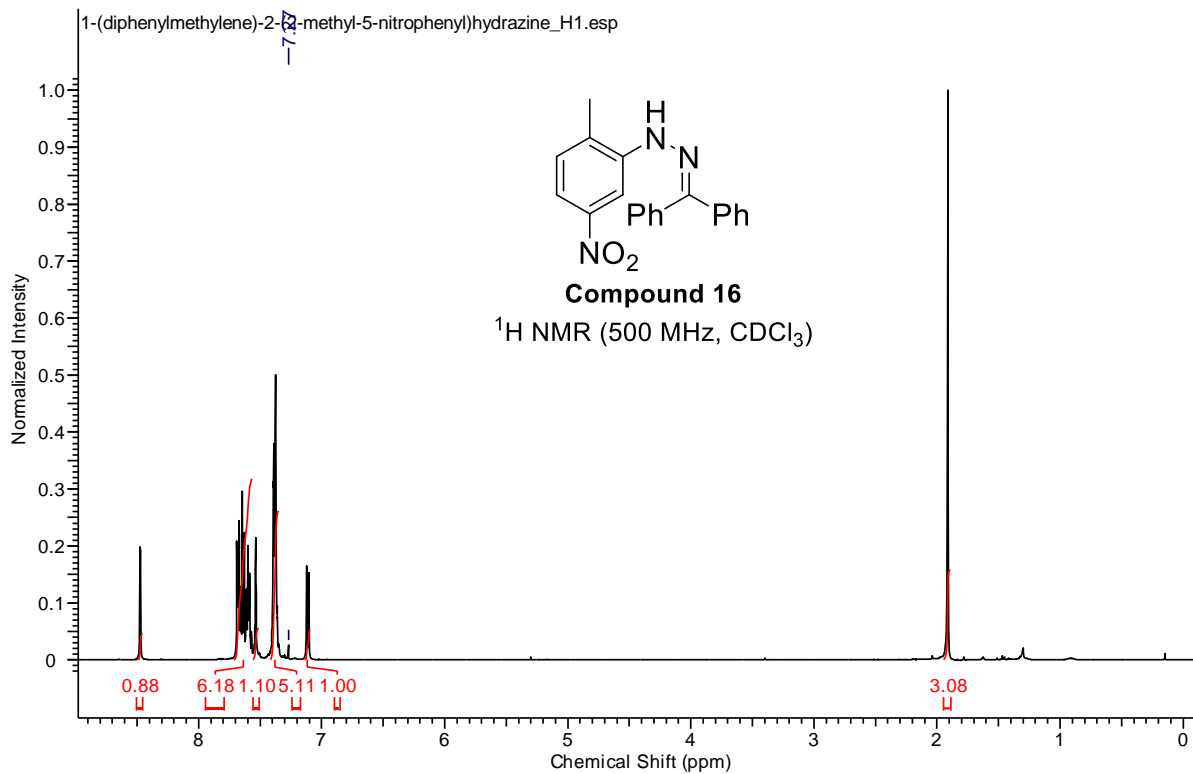


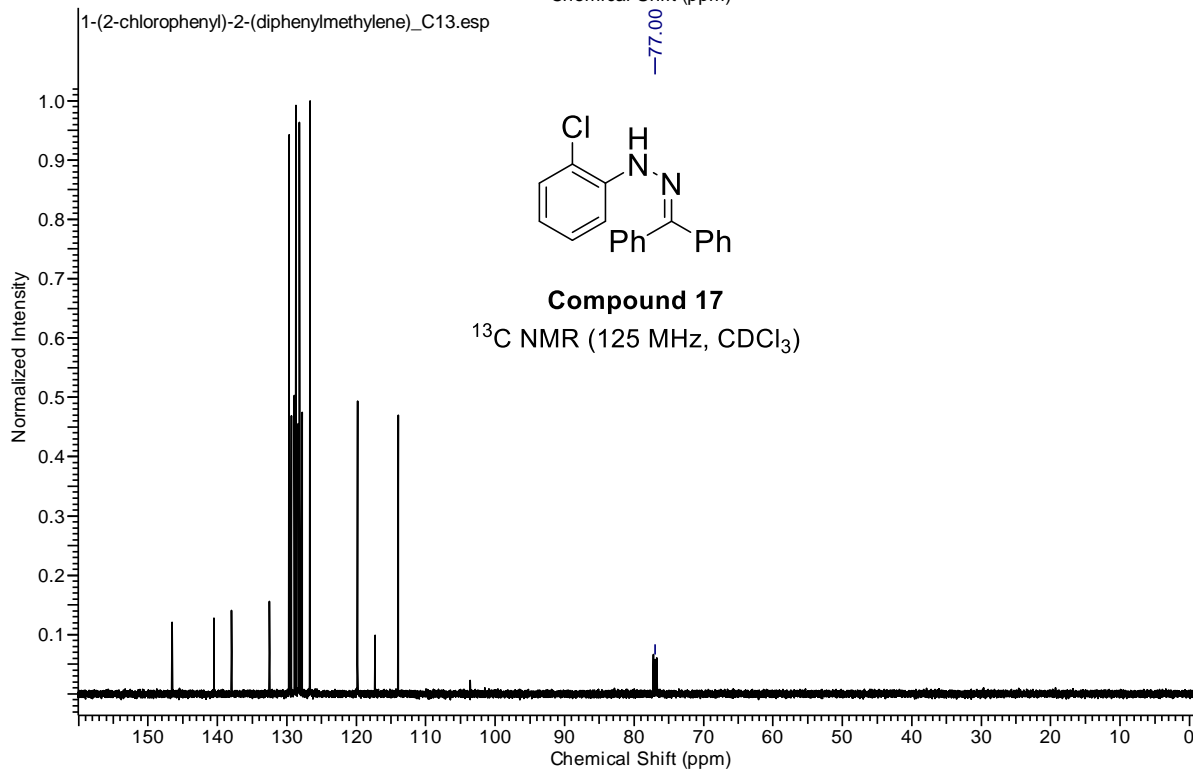
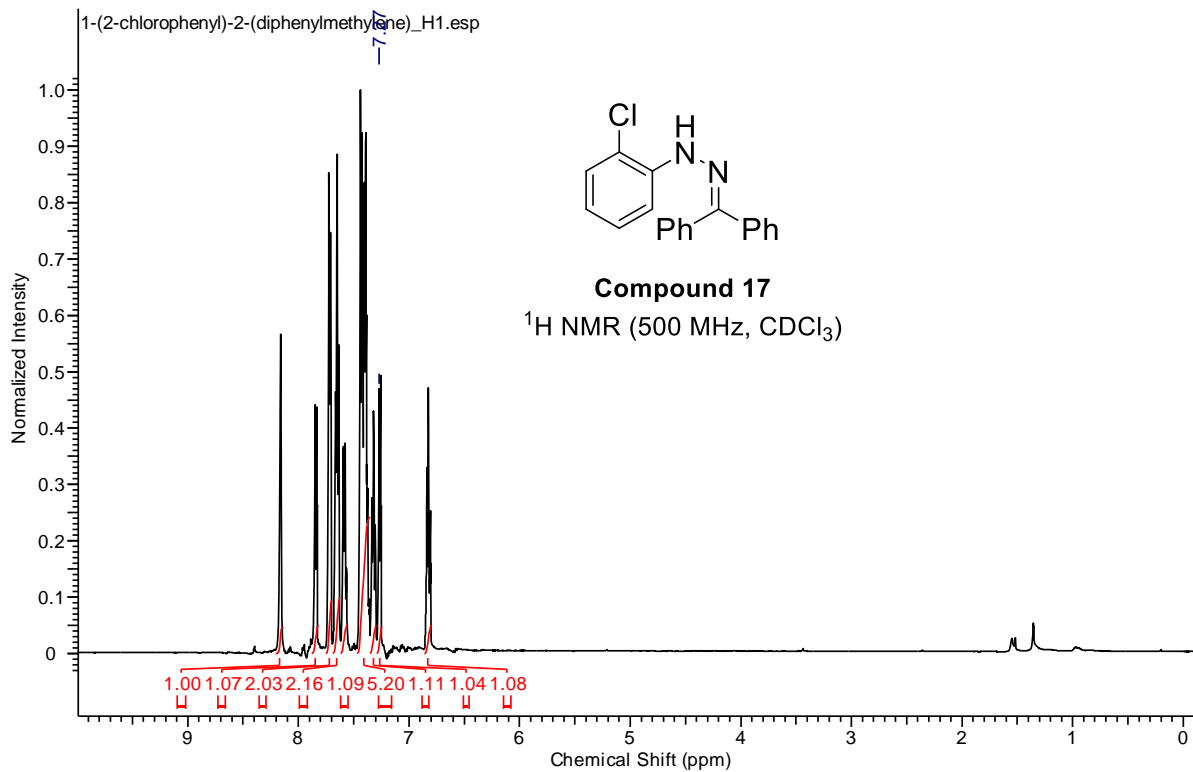


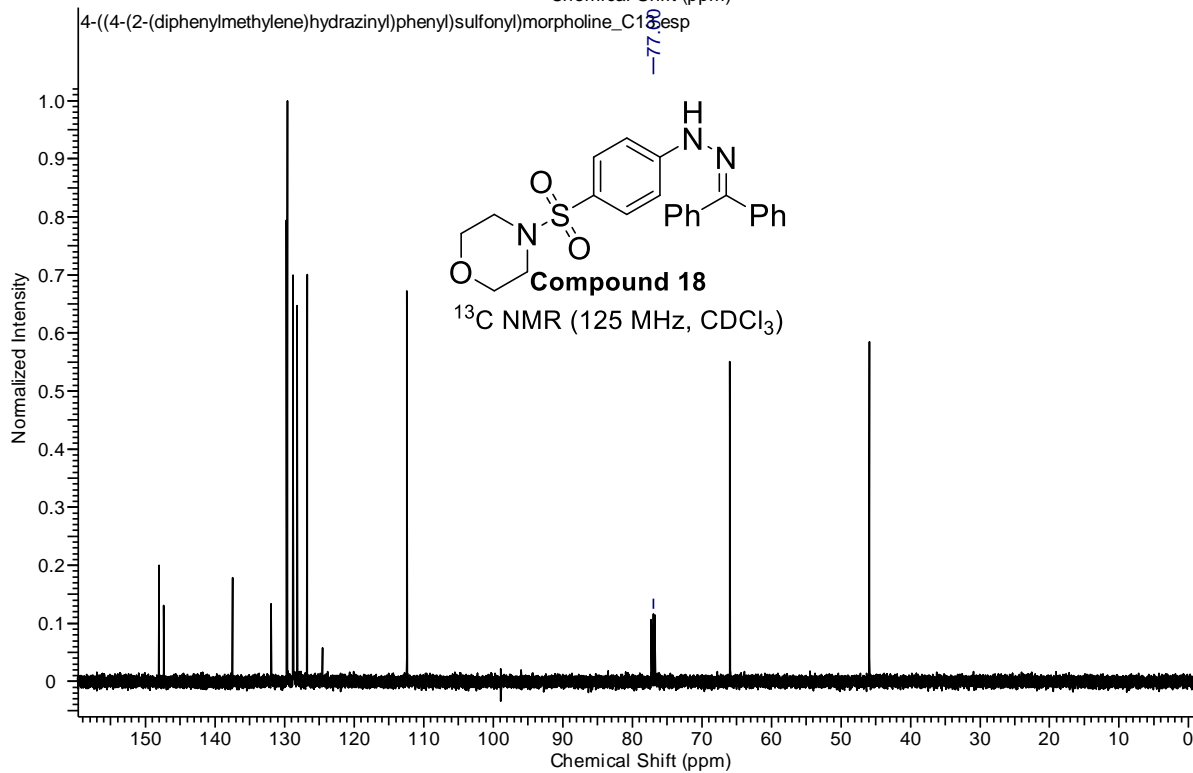
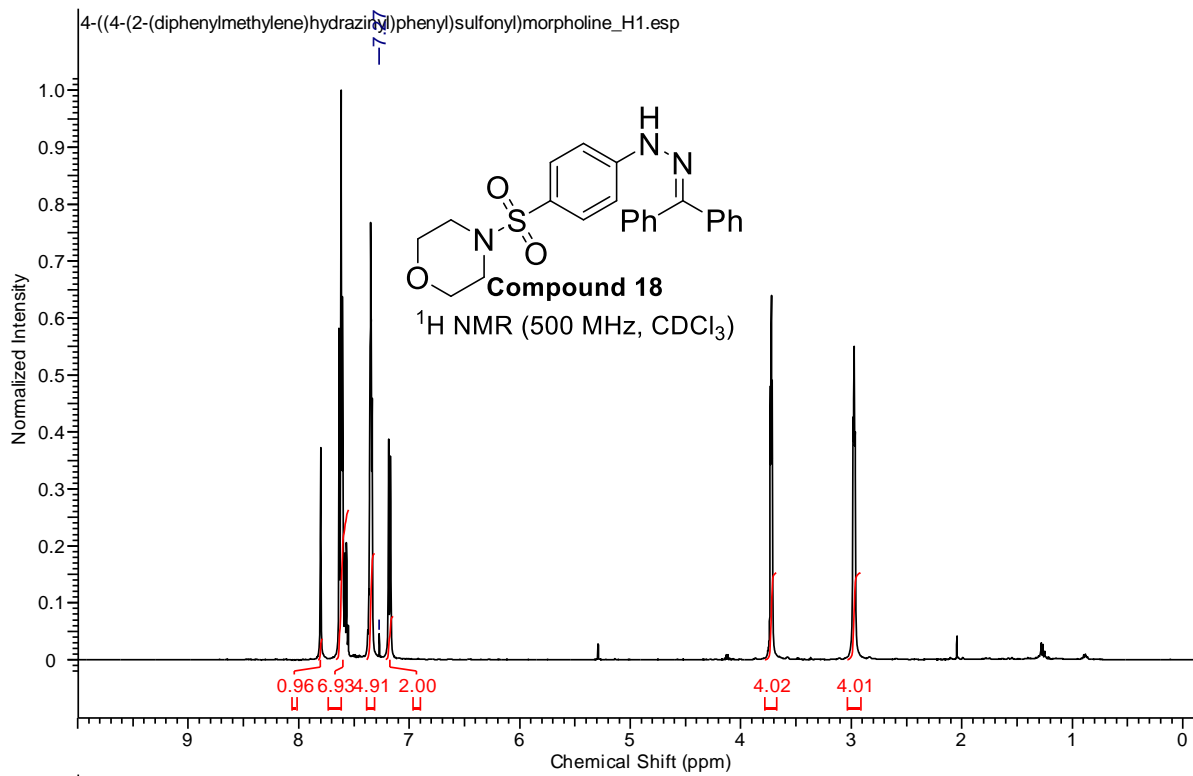


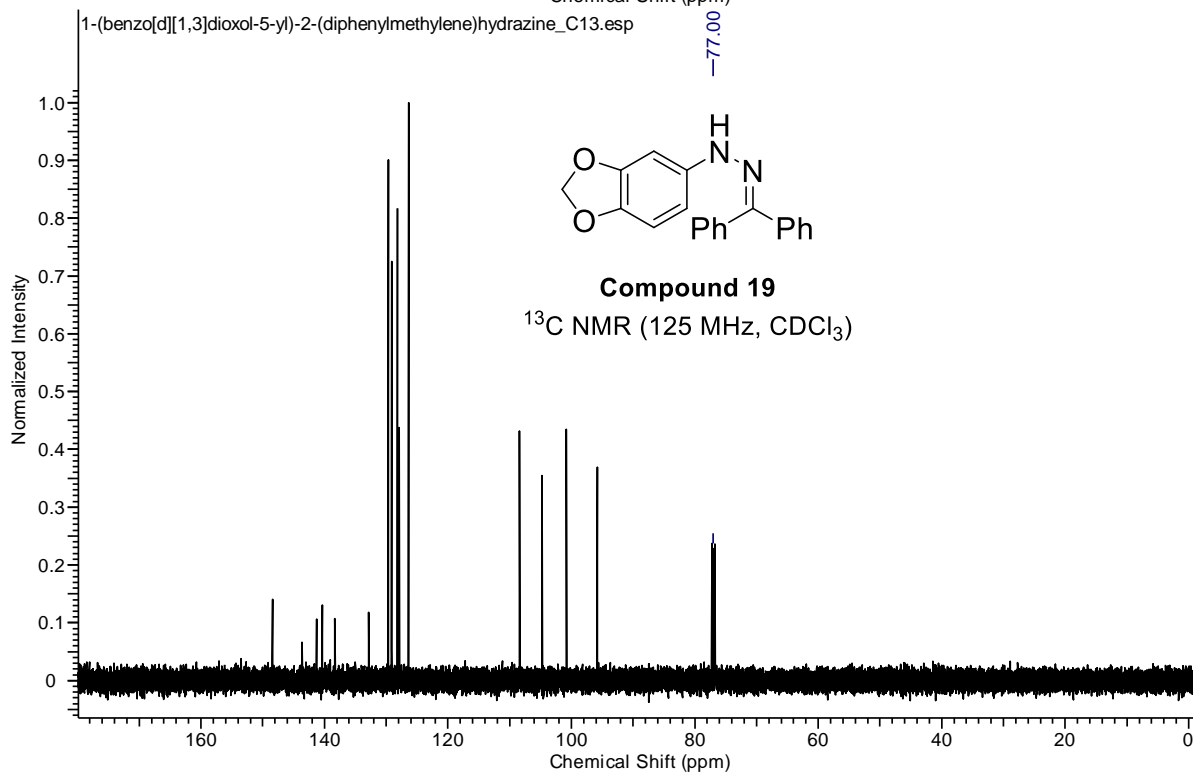
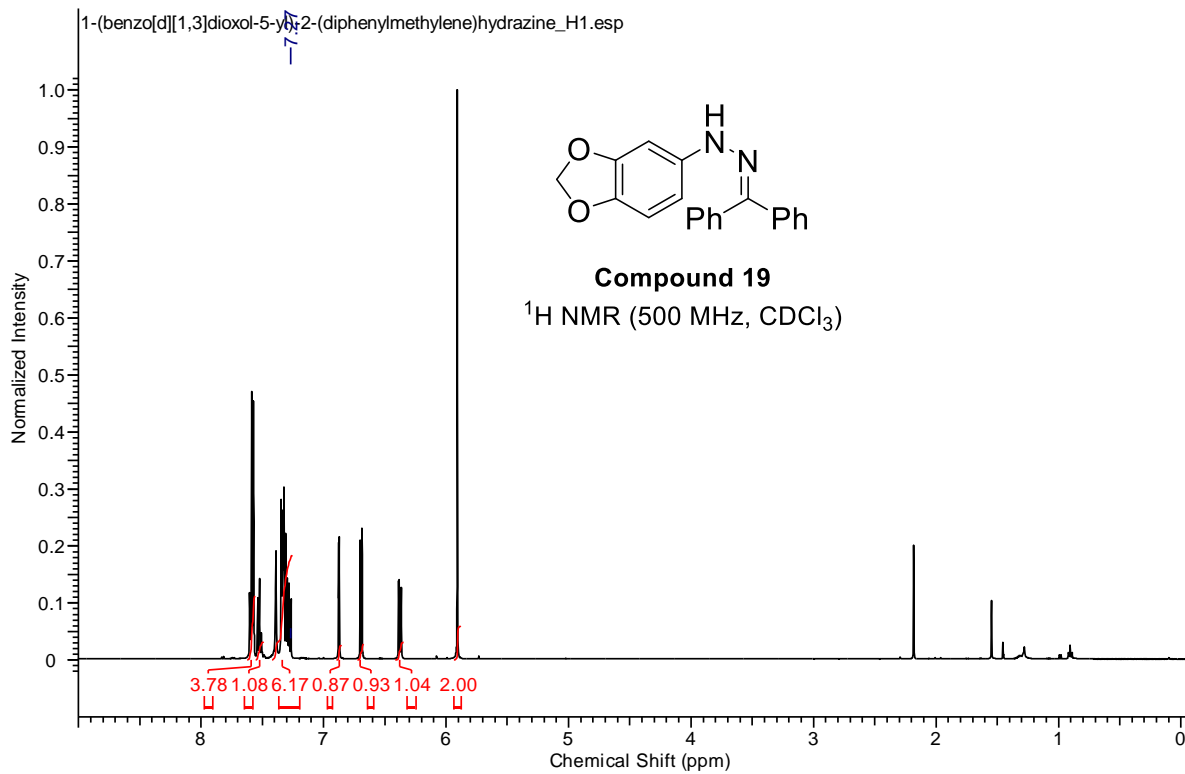


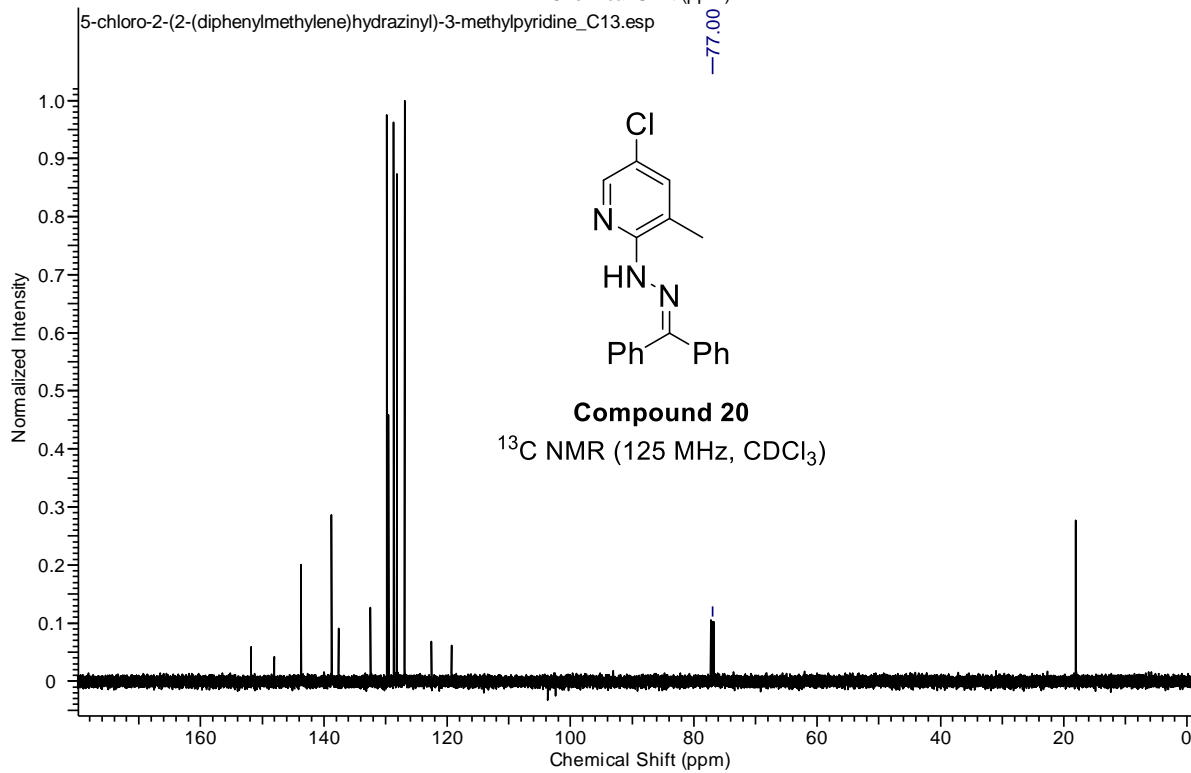
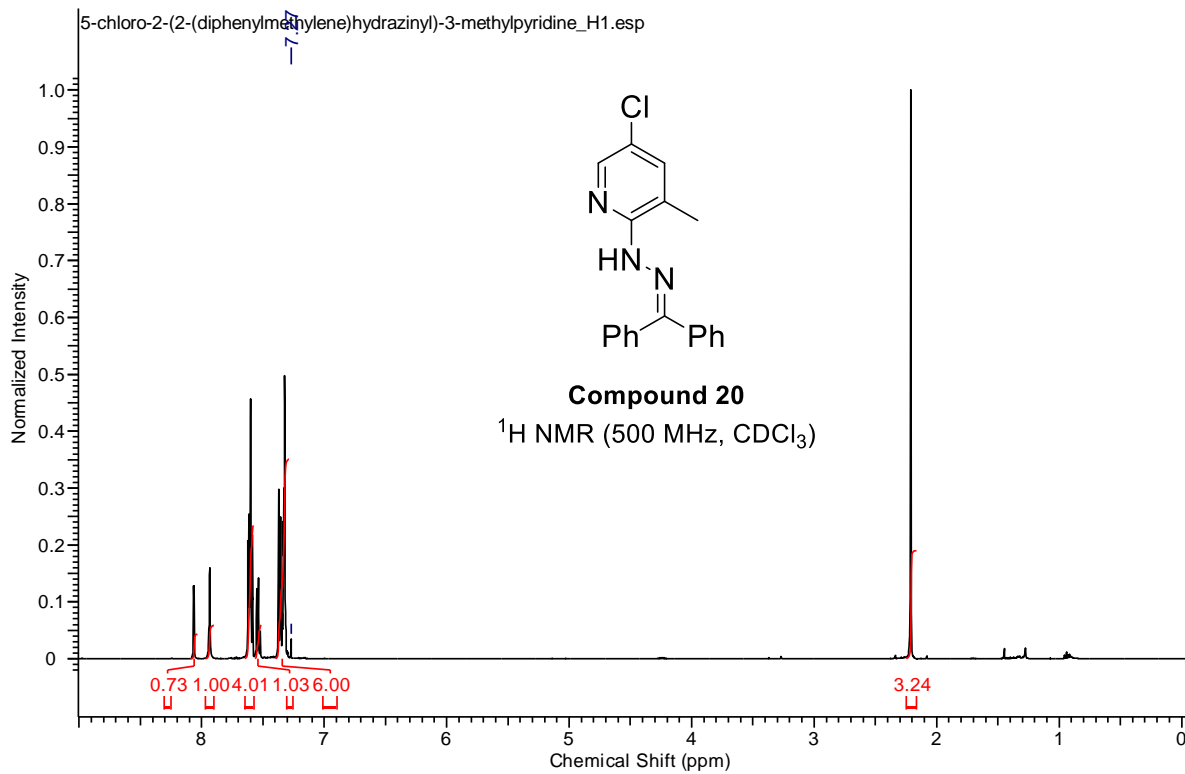


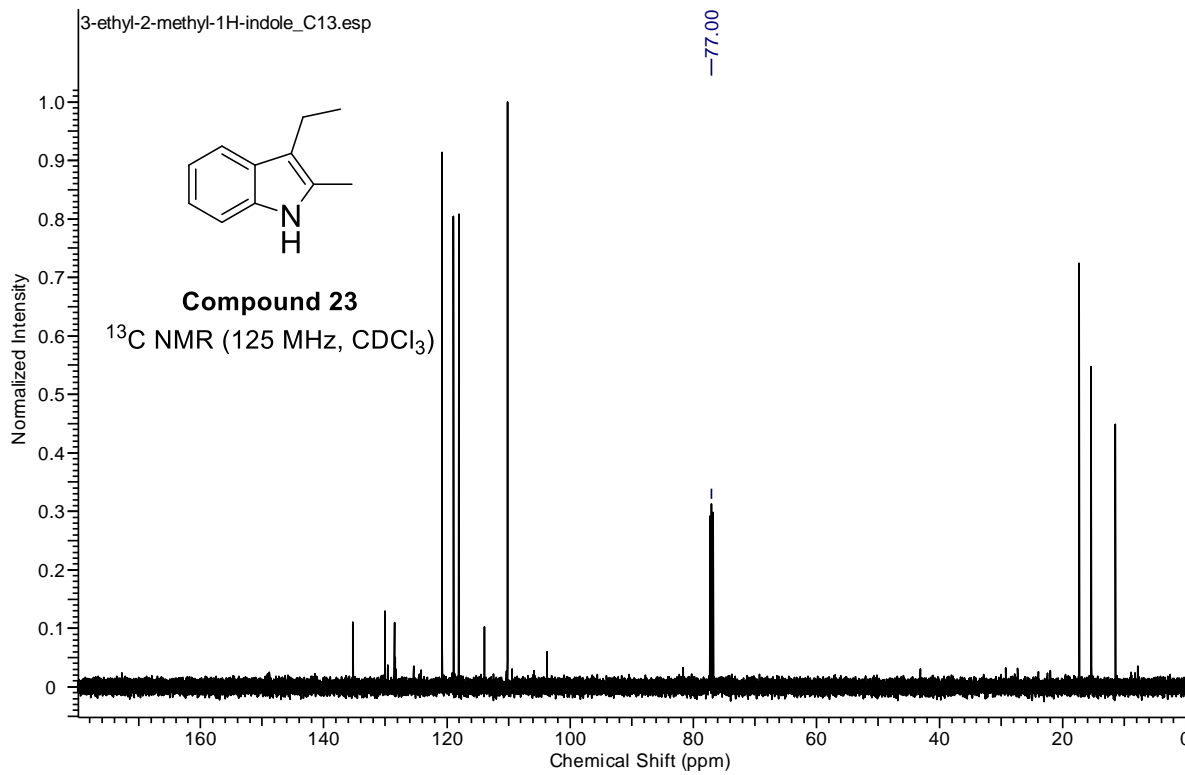
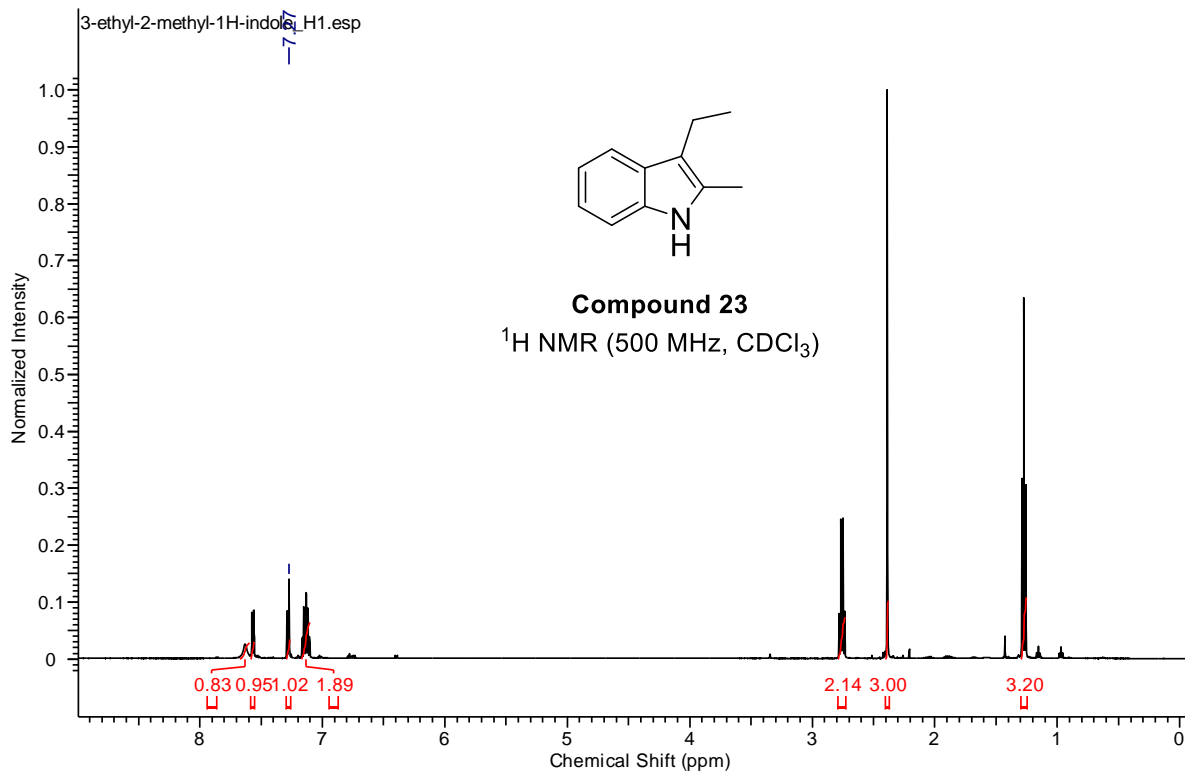


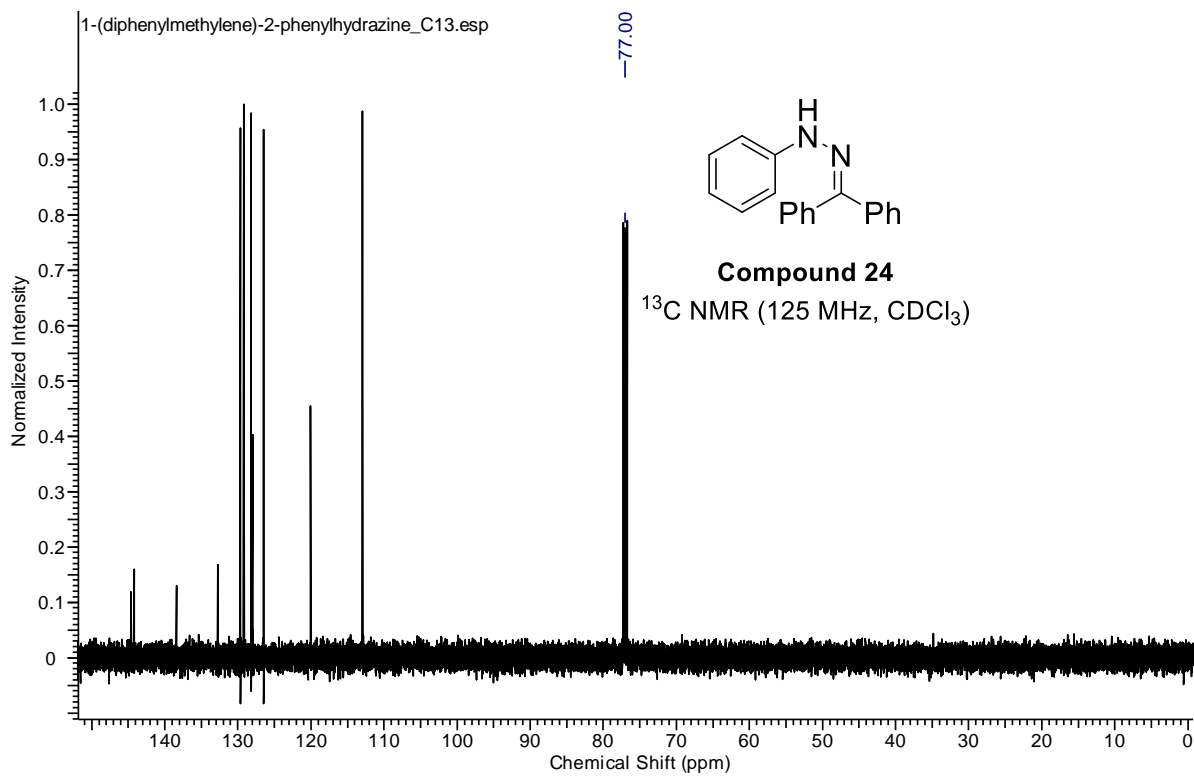
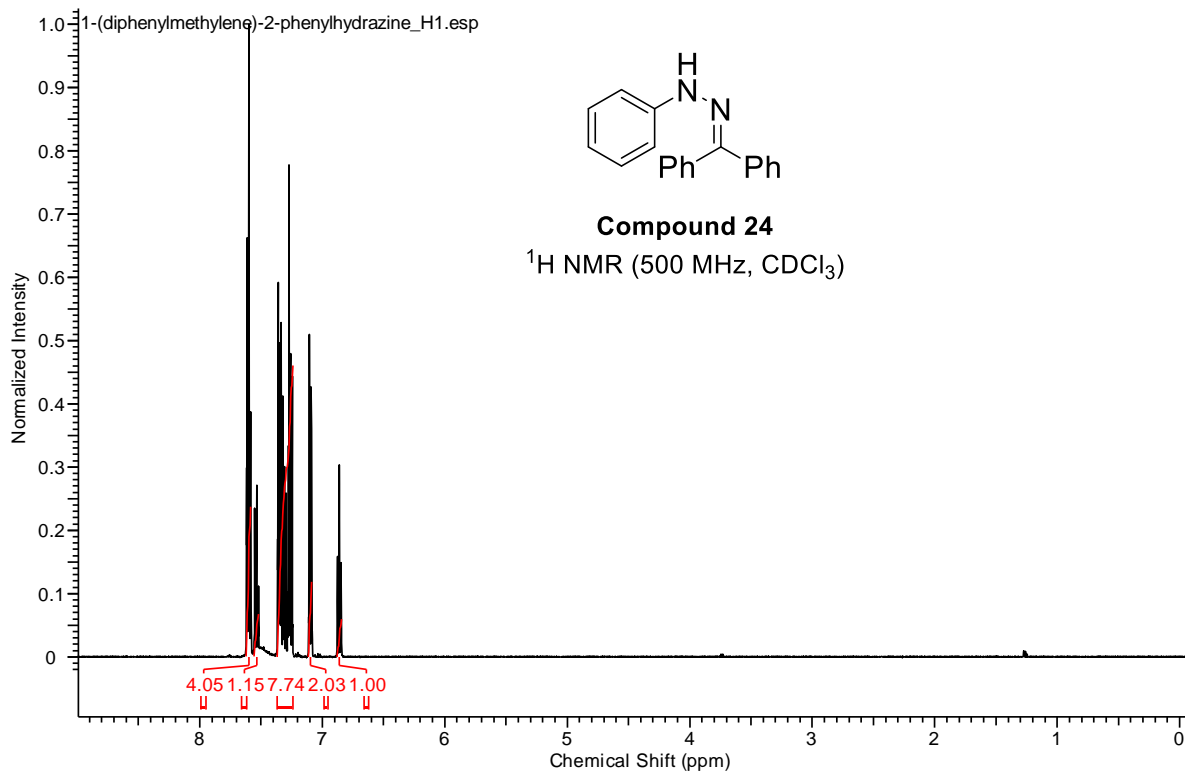


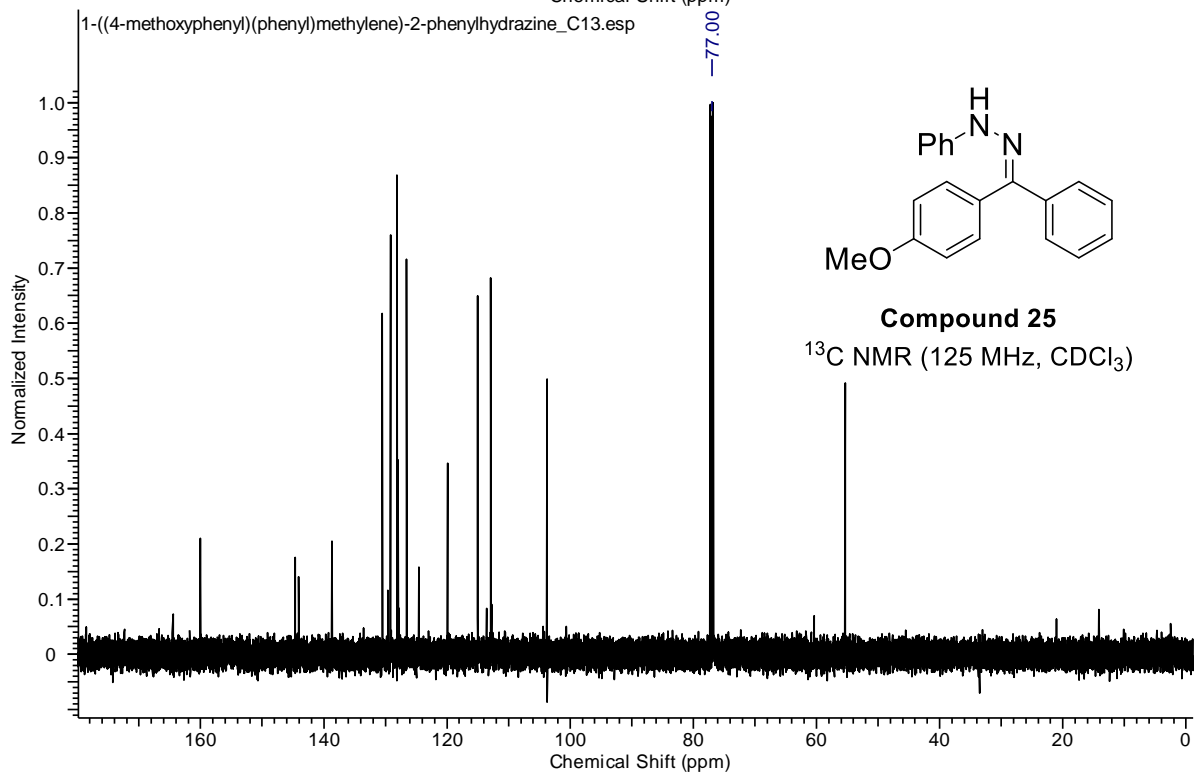
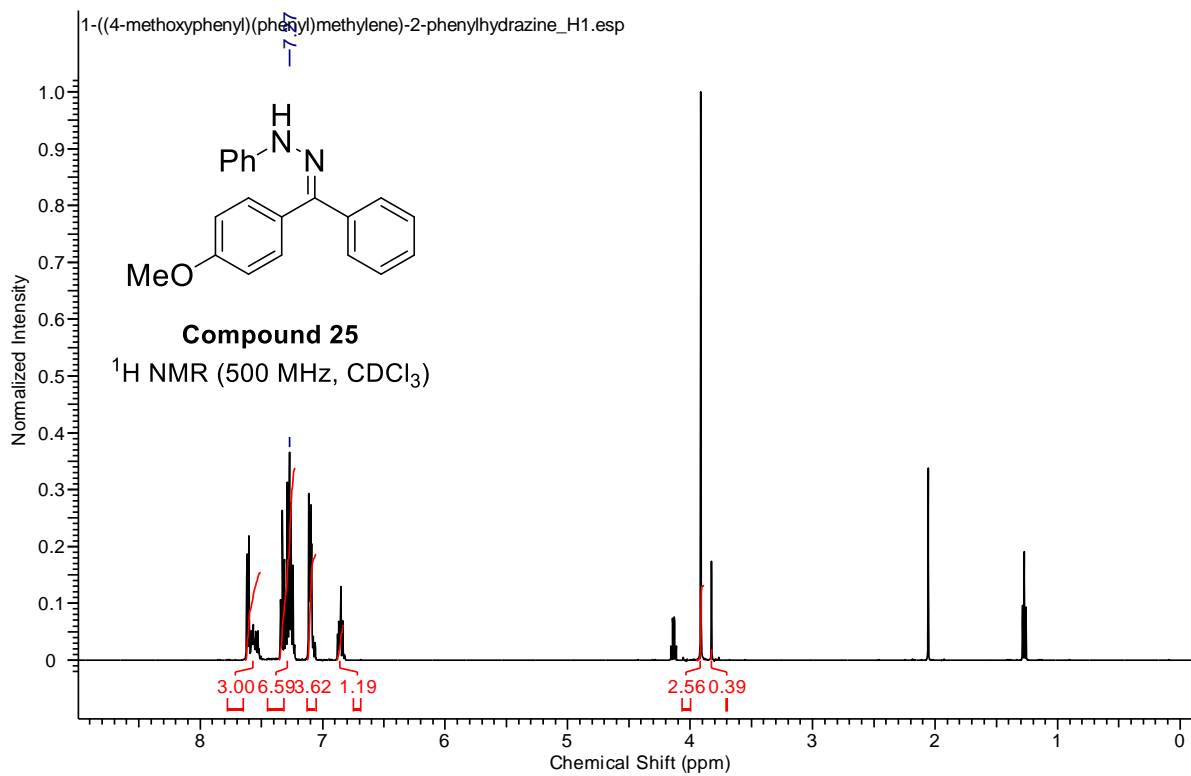


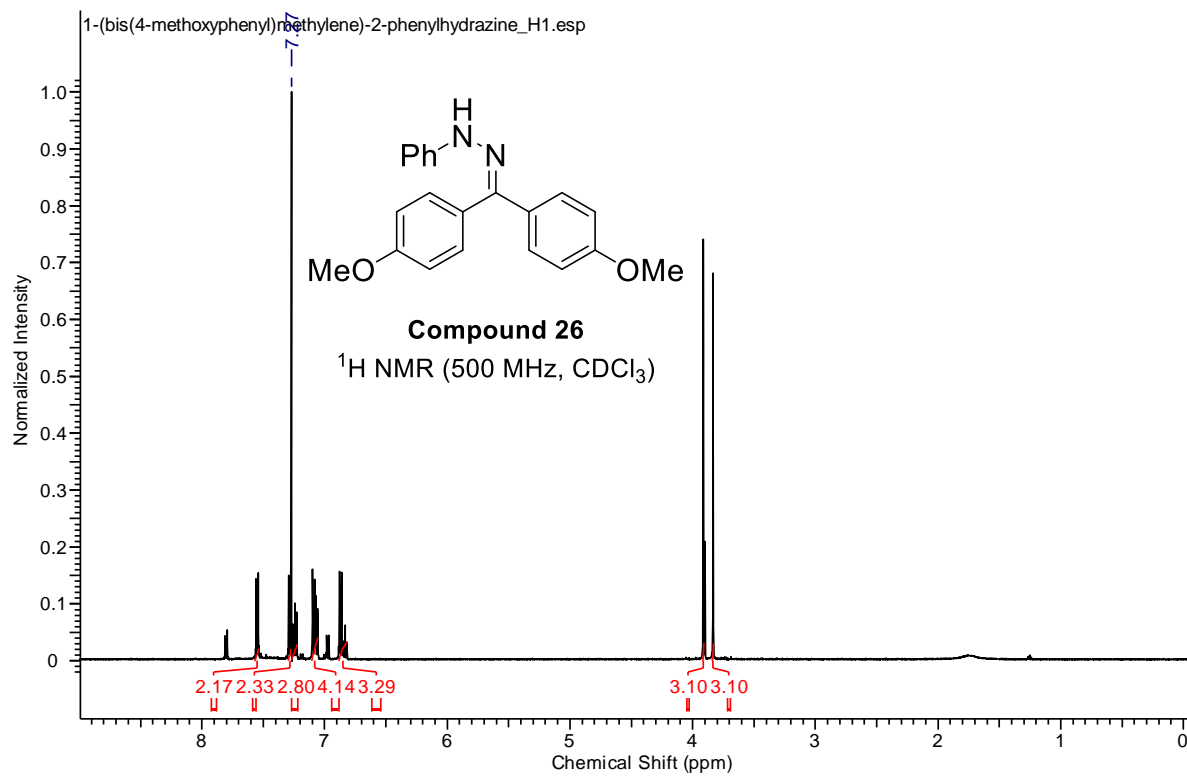


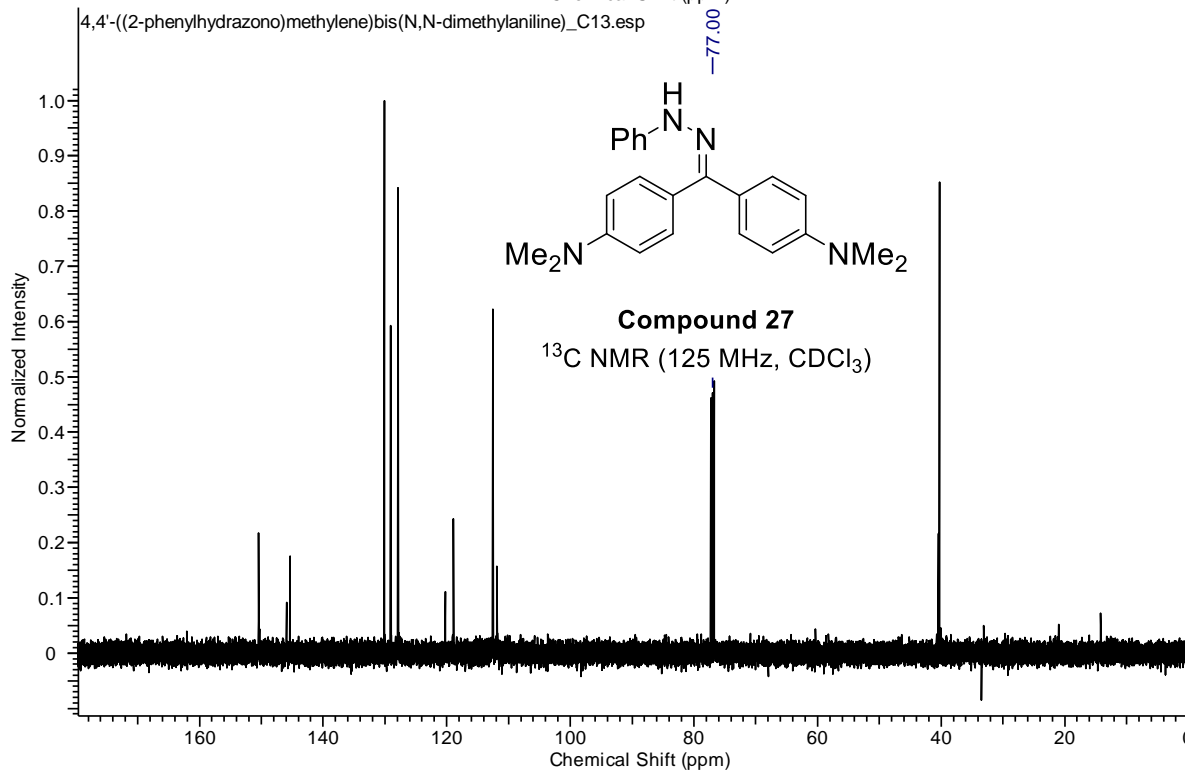
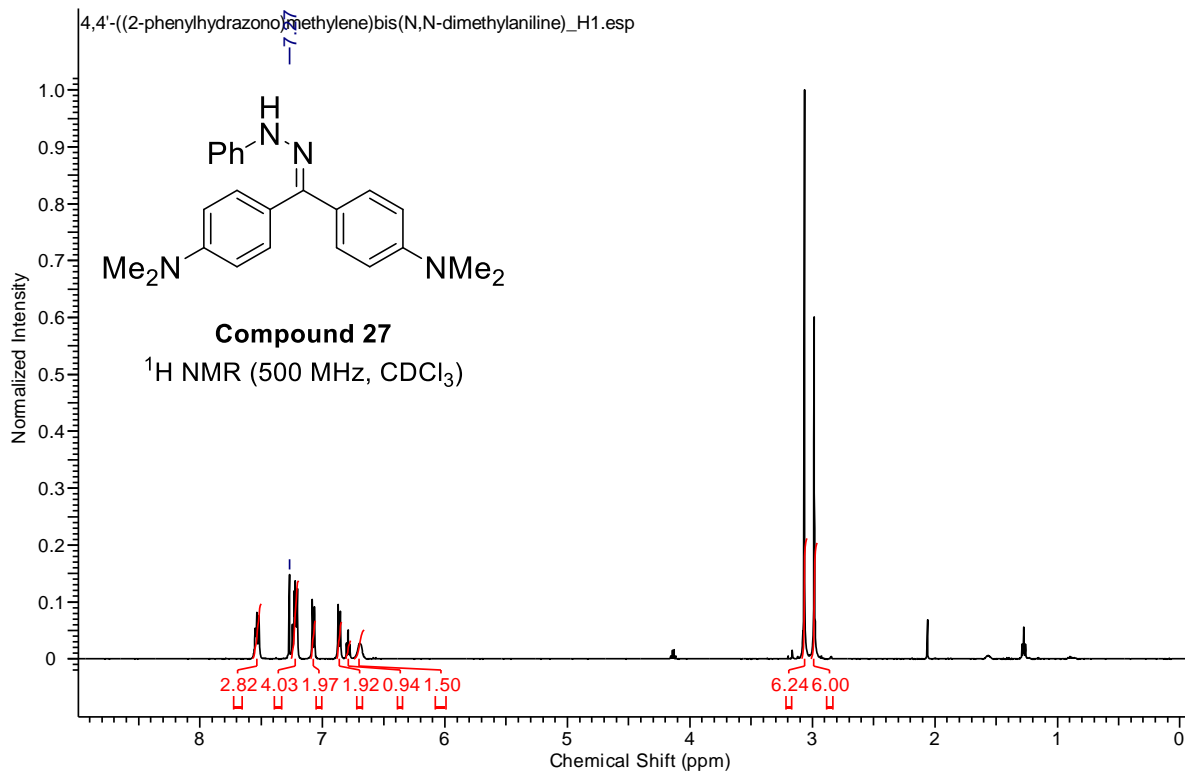


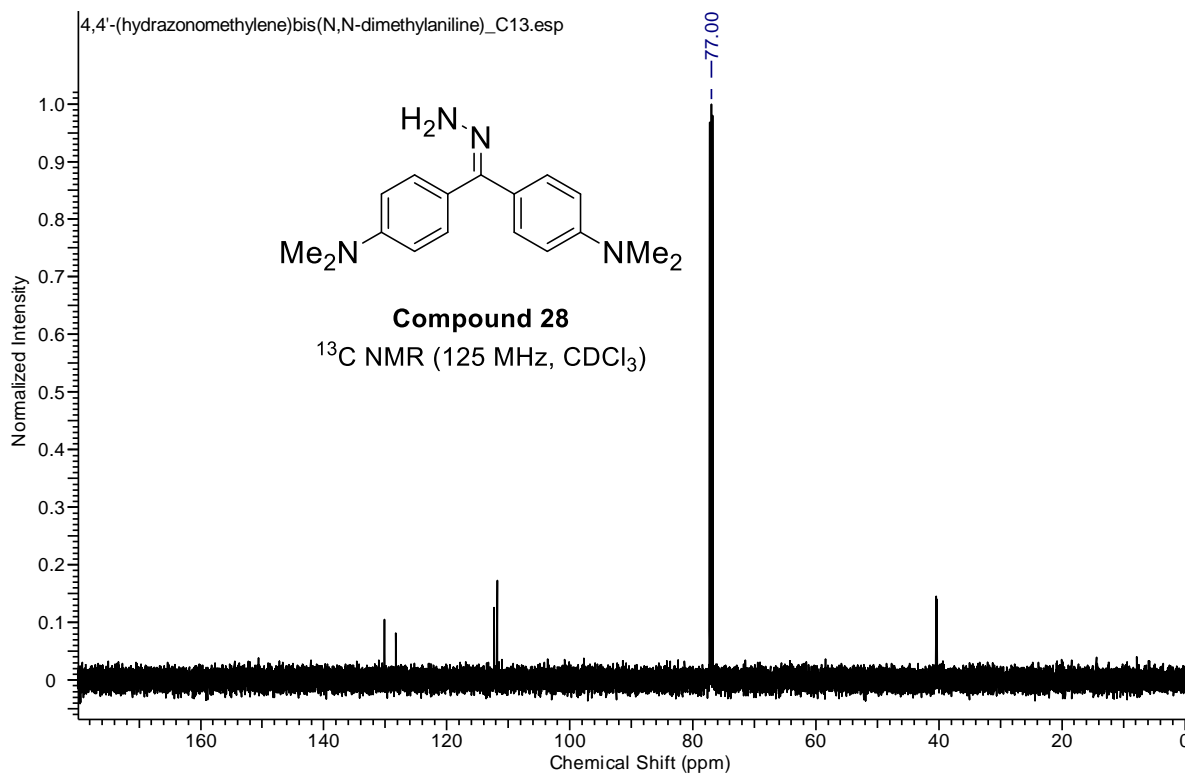
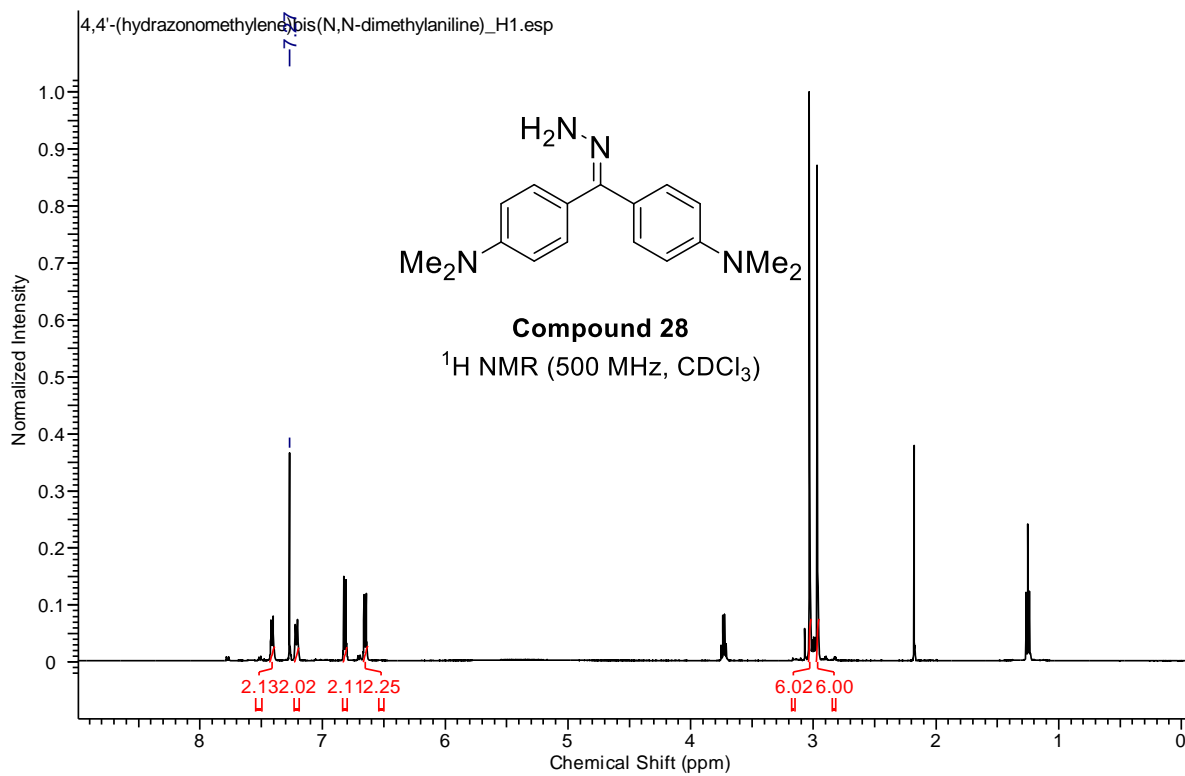


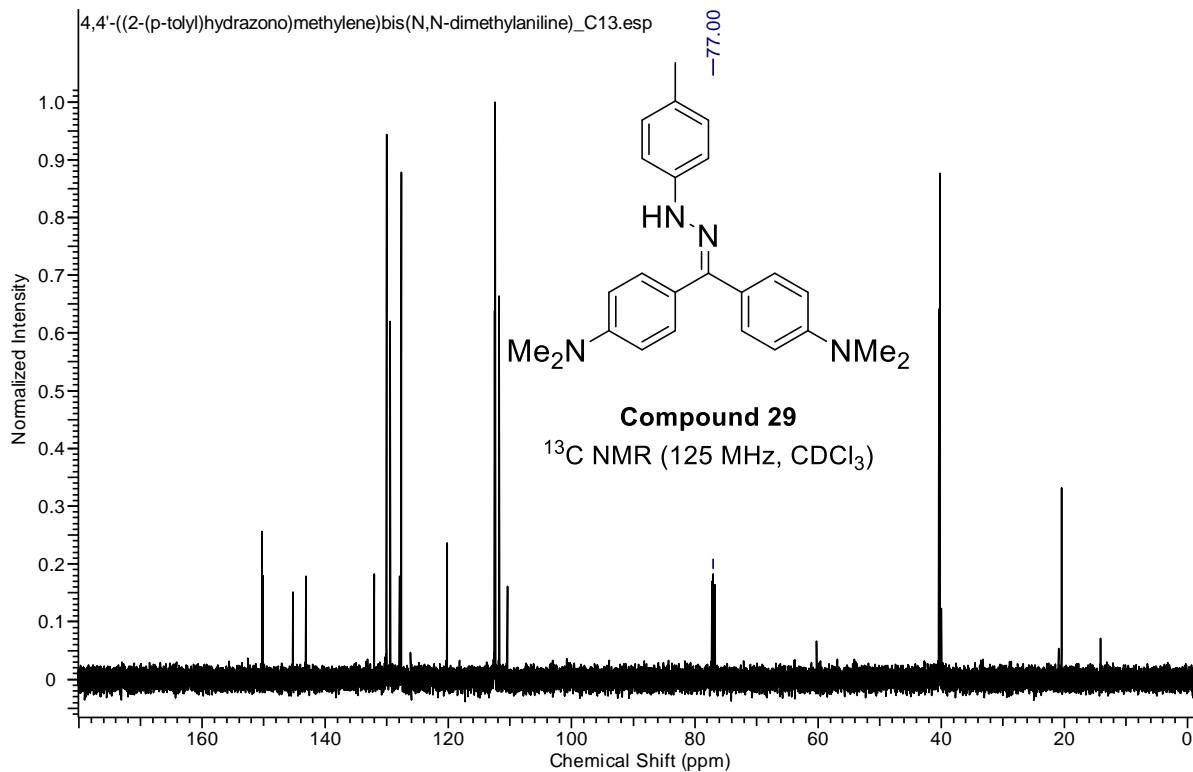
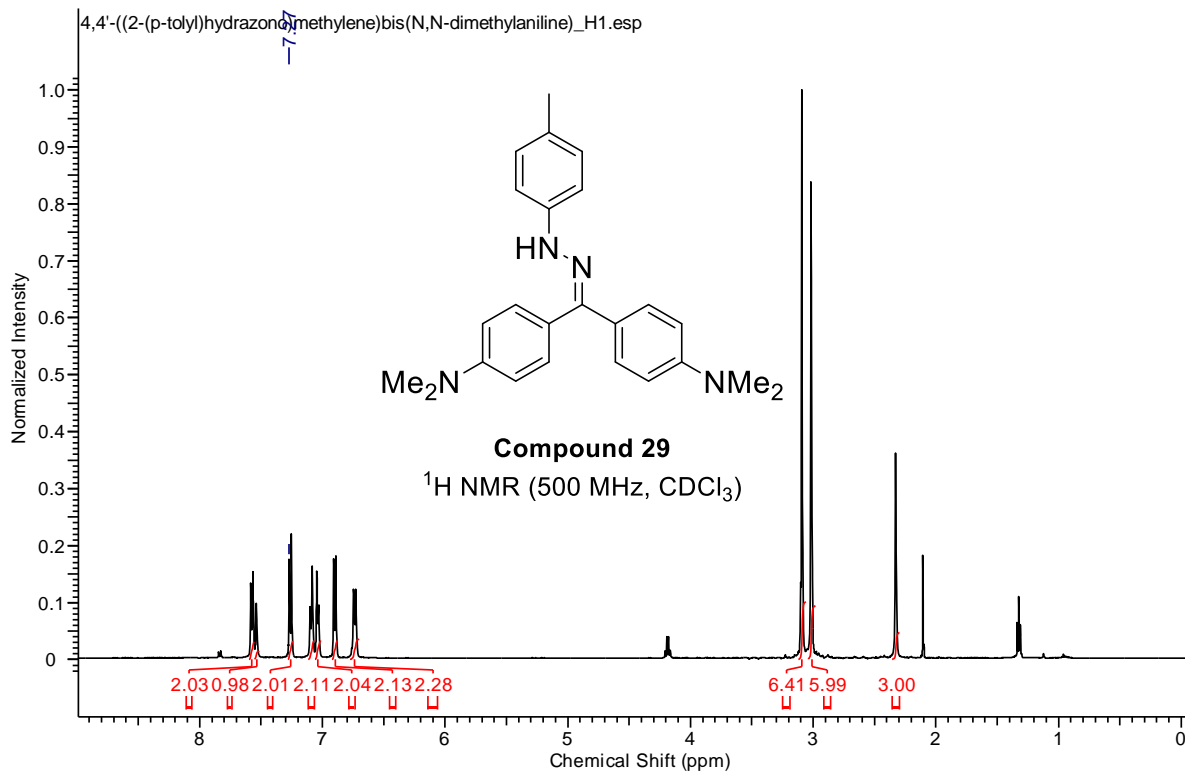


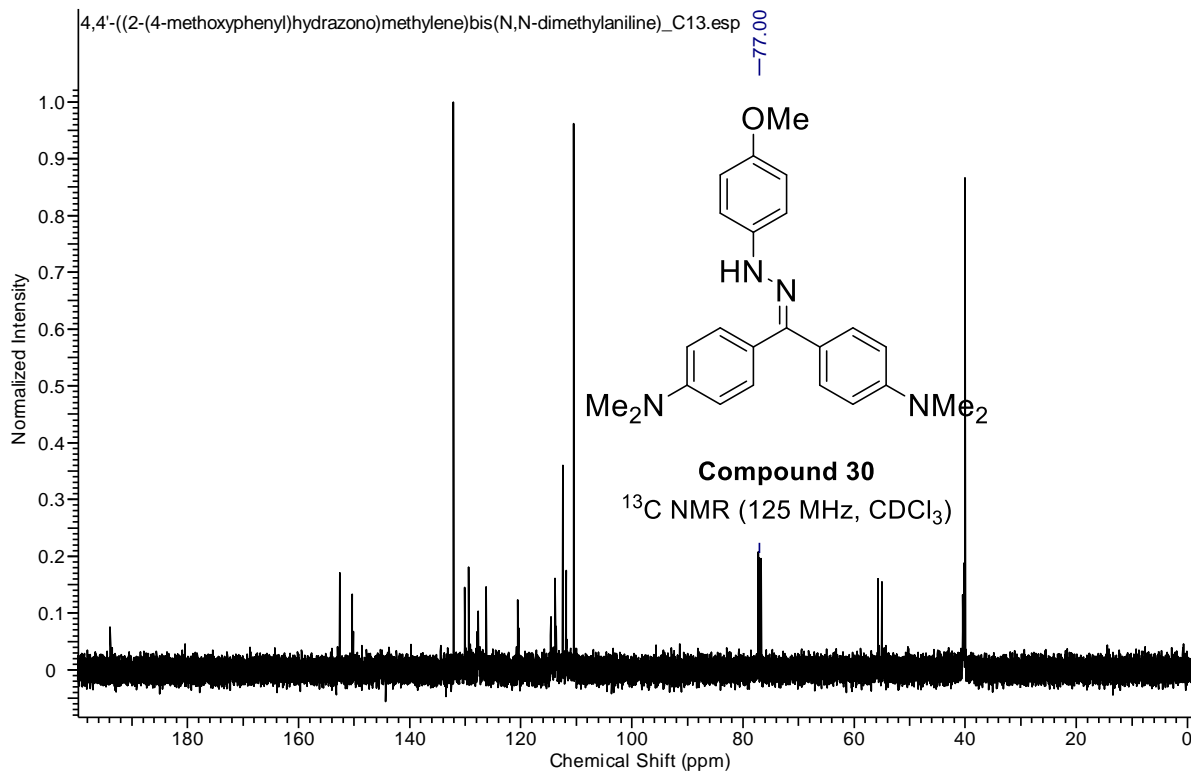
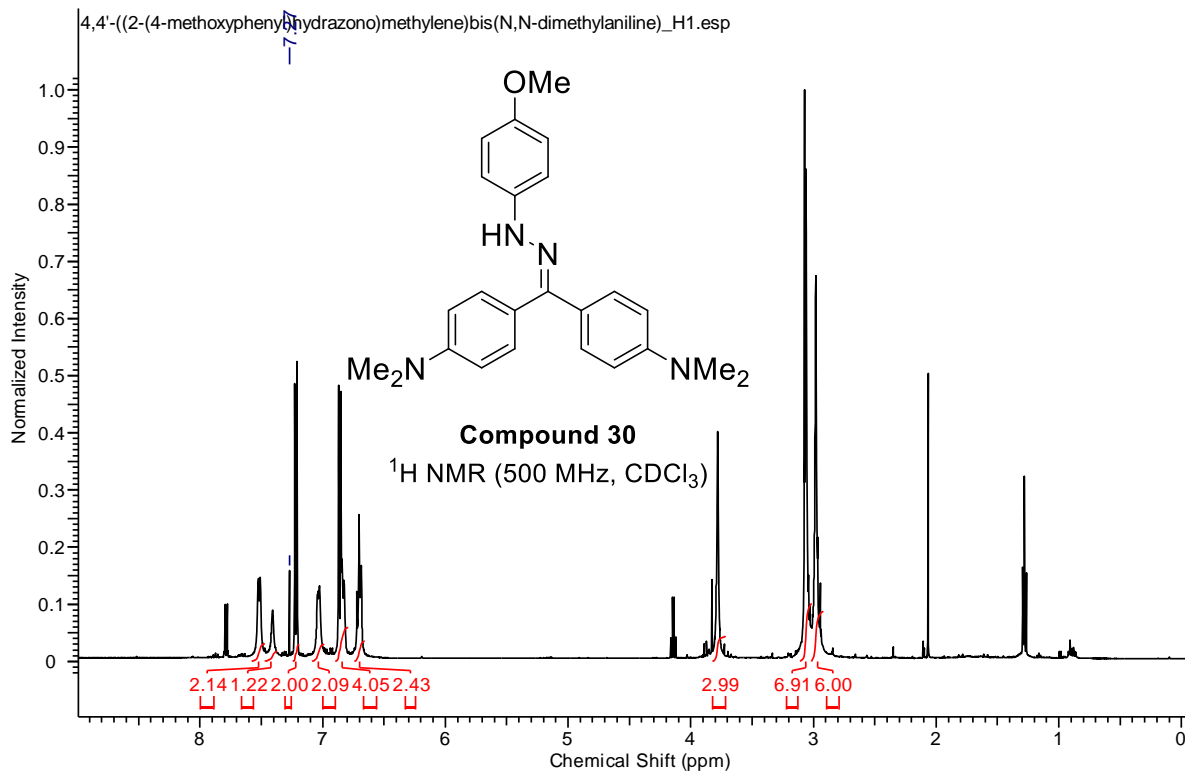


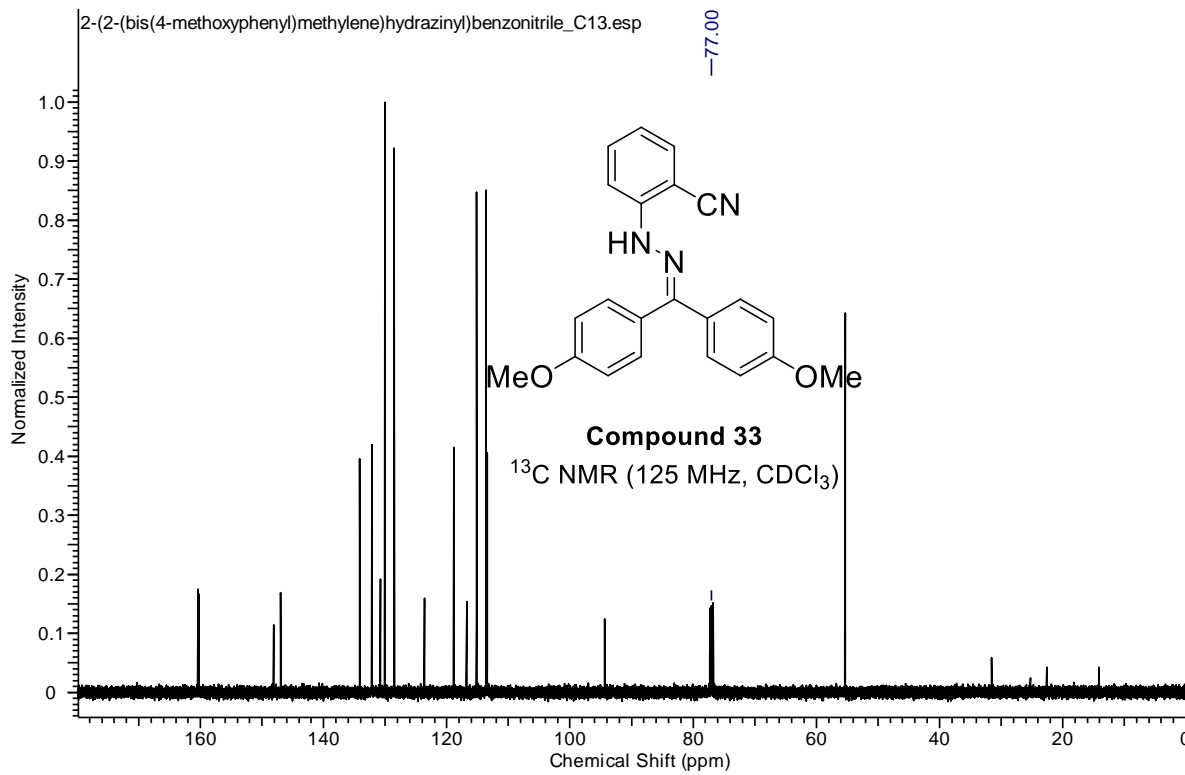
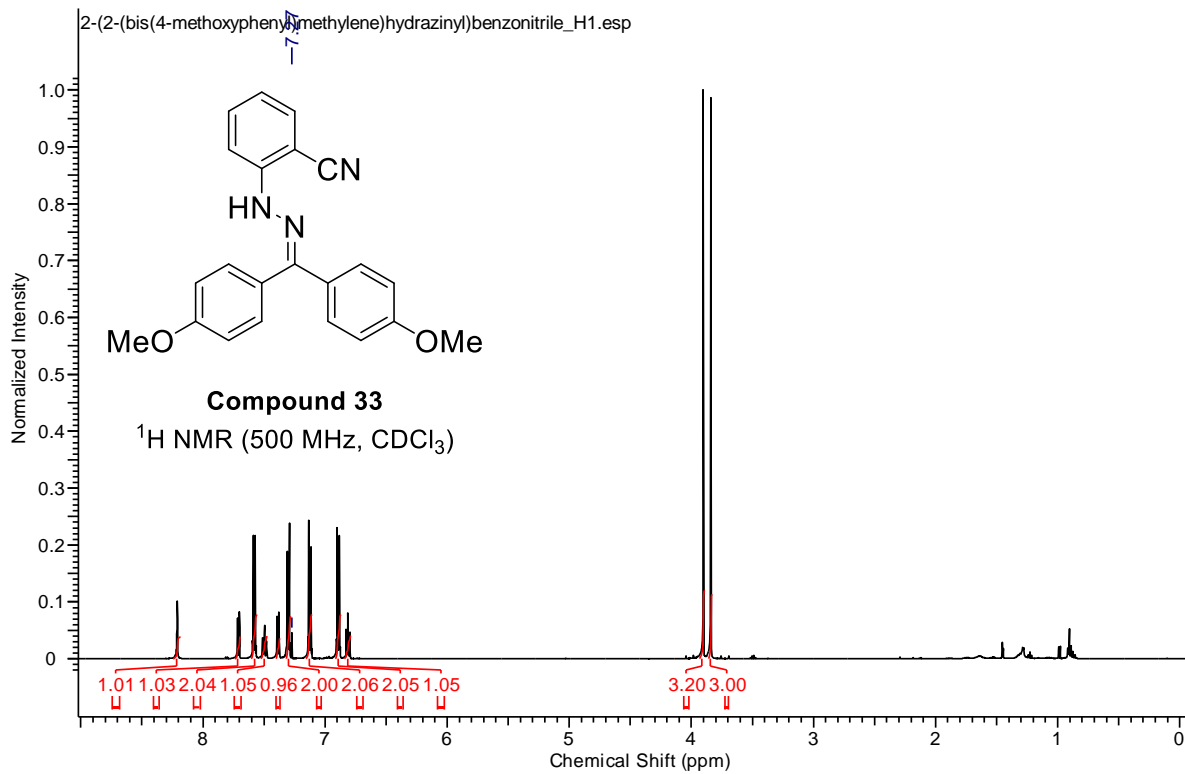


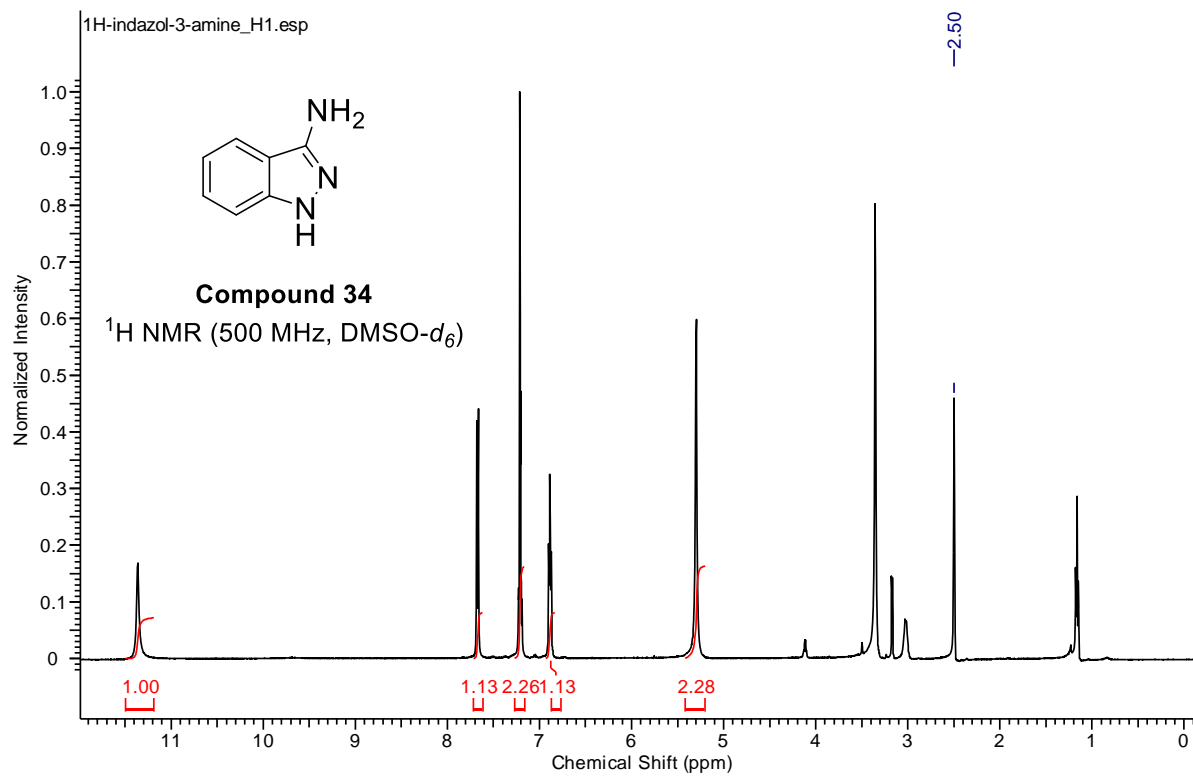


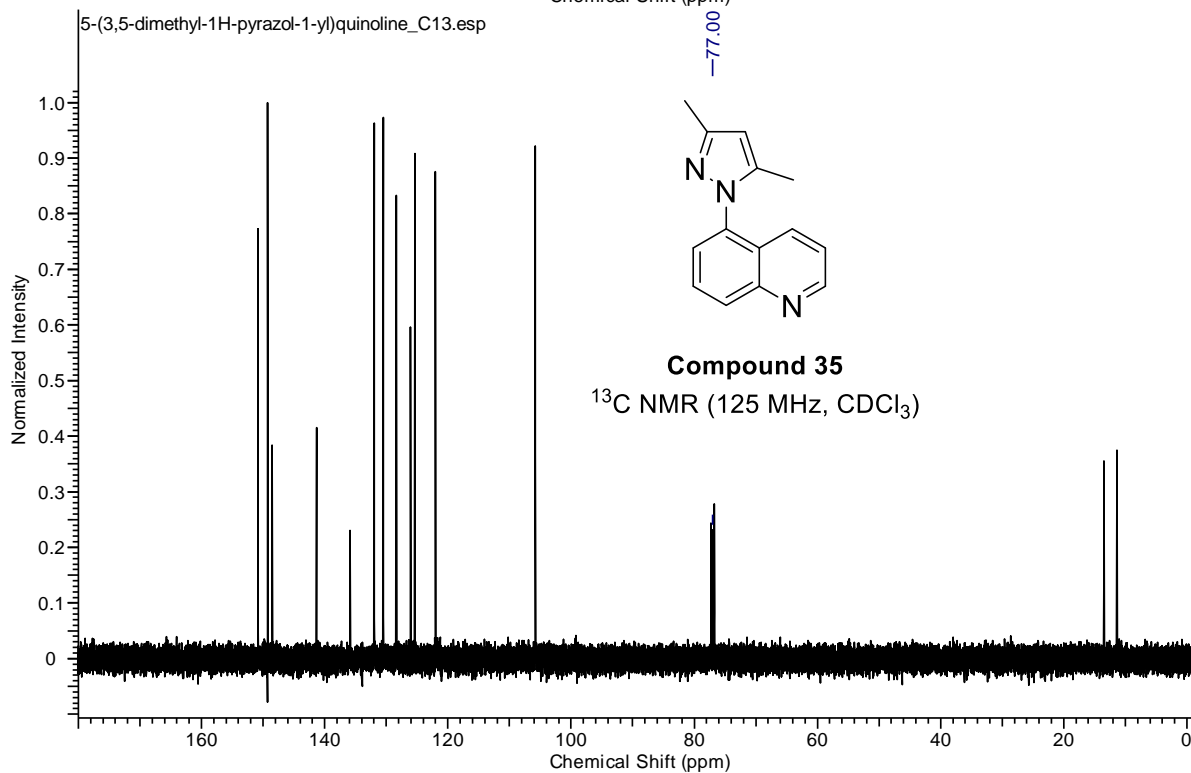
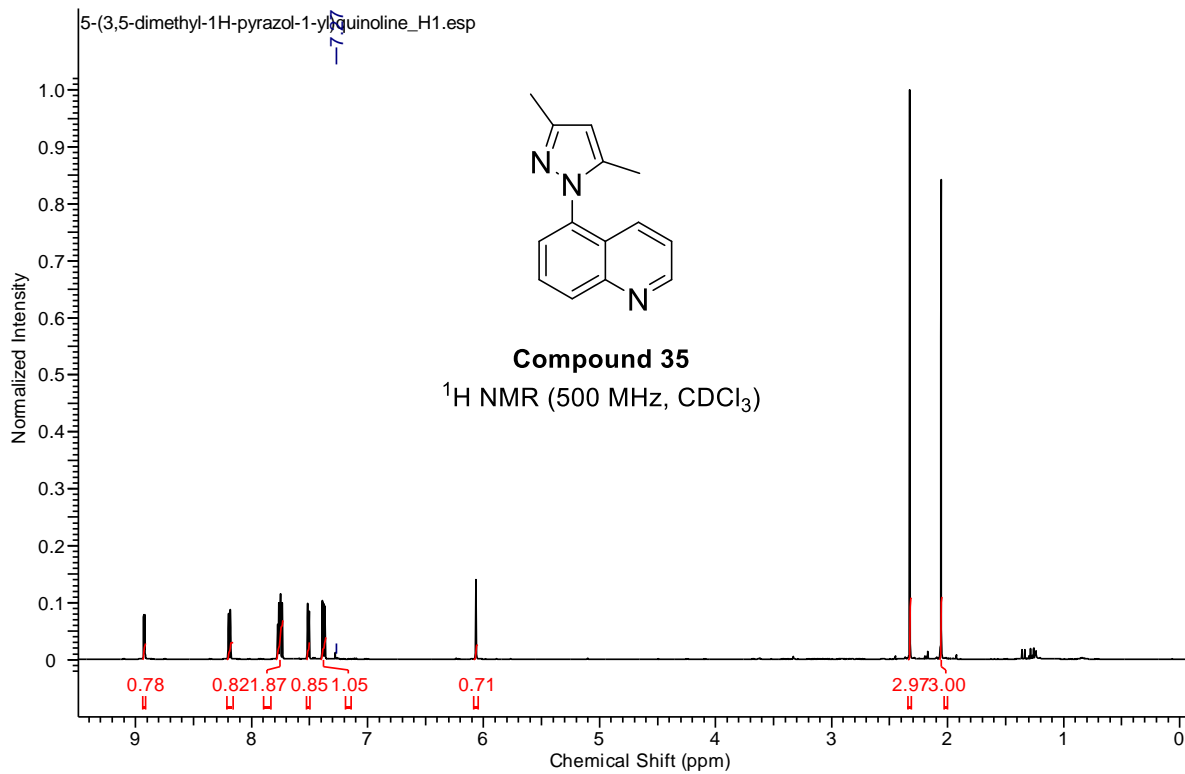


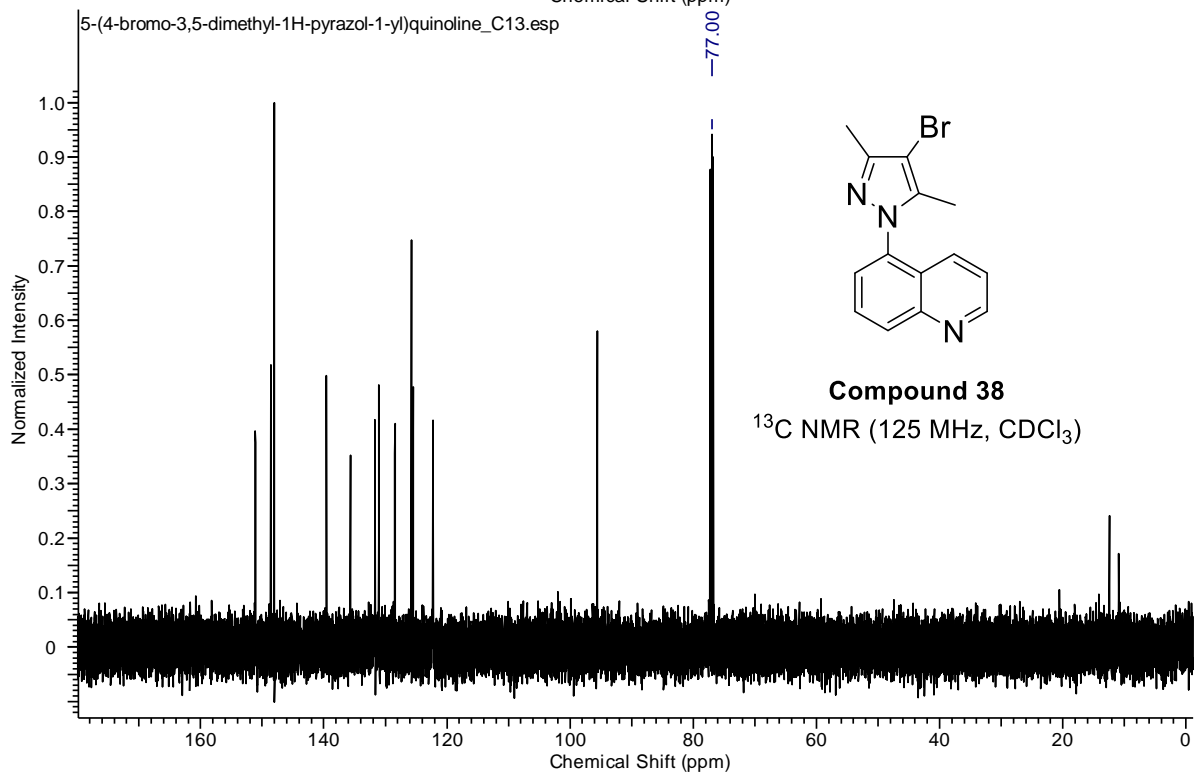
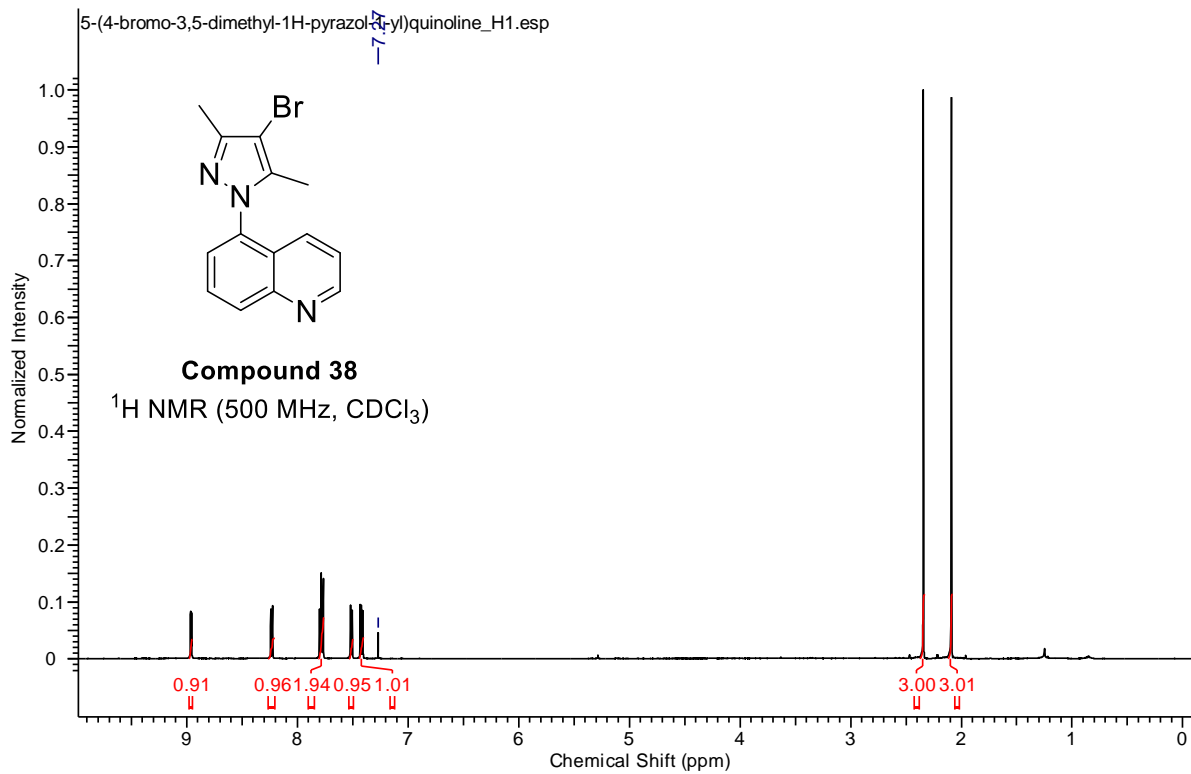












6.9 References

1. Vitaku, E.; Smith, D. T.; Njardarson, J. T. *J. Med. Chem.* **2014**, *57*, 10257.
2. Ishikura, M.; Abe, T.; Choshih, T.; Hibino, S. *Nat. Prod. Rep.* **2013**, *30*, 694.
3. a) Fischer, E.; Jourdan, F. *Chem. Ber.* **1883**, *16*, 2241. b) Fischer, E.; Hess, O. *Chem. Ber.* **1884**, *17*, 559.
4. a) Porcheddu, A.; Mura, M. G.; De Luca, L.; Pizzetti, M.; Taddei, M. *Org. Lett.*, **2012**, *14*, 6112. b) Park, I. -K.; Suh, S. -E.; Lim, B. -Y.; Cho, C. -G. *Org. Lett.*, **2009**, *11*, 5454. c) Hughes, D. L. *Org. Prep. Proced. Int.* **1993**, *25*, 607.
5. Elgersma, R. H. C.; Havinga, E. *Tetrahedron Lett.* **1969**, 1735.
6. a) Hobson, L. A.; Nugent, W. A.; Anderson, S. R.; Deshmukh, S. S.; Haley III, J. J.; Liu, P.; Magnus, N. A.; Sheeran, P.; Sherbine, J. P.; Stone, B. R. P.; Zhu, J. *Org. Process Res. Dev.* **2007**, *11*, 985. b) Prühs, S.; Dinter, C.; Blume, T.; Schütz, A.; Harre, M.; Neh, H. *Org. Process Res. Dev.* **2006**, *10*, 441.
7. Hunsberger, I. M.; Shaw, E. R.; Fugger, J.; Ketcham, R.; Lednicer, D. *J. Org. Chem.* **1956**, *21*, 394.
8. Zima, V.; Pytela, O.; Vecera, M. *Collect. Czech. Chem. Commun.* **1988**, *53*, 814.
9. Bus, J. S.; Popp, J. A. *Food Chem. Toxicol.* **1987**, *25*, 619.
10. El-Makawy, A. I.; Girgis, S. M.; Khalil, W. K. *Mutat. Res.* **2008**, *657*, 105.
11. Clark, C. *Hydrazine*; Mathieson Chemical Corp.: Baltimore, MD, **1953**.
12. Terrier, F. *Chem. Rev.* **1982**, *82*, 77.
13. Xiao, F.; Liao, Y.; Wua, M.; Deng, G. -J. *Green Chem.* **2012**, *14*, 3277.
14. Haddad, N.; Baron, J. *Tetrahedron Lett.* **2002**, *43*, 2171.
15. Castle, R. N. *Condensed pyridazines including cinnolines and phthalazines*; Wiley: New York, **1973**.
16. Ruiz-Castillo, P.; Buchwald, S. L. *Chem. Rev.* **2016**, *116*, 12564.

17. a) Wagaw, S.; Yang, B. H.; Buchwald, S. L. *J. Am. Chem. Soc.* **1998**, *120*, 6621. b) Wagaw, S.; Yang, B. H.; Buchwald, S. L. *J. Am. Chem. Soc.* **1999**, *121*, 10251.
18. Mauger, C.; Mignani, G. *Adv. Synth. Catal.* **2005**, *347*, 773.
19. Goodyear, A.; Linghu, X.; Bishop, B.; Chen, C.; Cleator, E.; McLaughlin, M.; Sheen, F. J.; Stewart, G. W.; Xu, Y.; Yin J. *Org. Process Res. Dev.* **2012**, *16*, 605.
20. Lundgren, R.L.; Stradiotto, M. *Angew. Chem. Int. Ed.* **2010**, *49*, 8686.
21. Chen, J.; Zhang, Y.; Hao, W.; Zhang, R.; Yi, F. *Tetrahedron* **2013**, *69*, 613.
22. Clark, C. *Hydrazine*; Mathieson Chemical Corp.: Baltimore, MD, **1953**.
23. a) Handa, S.; Andersson, M. P.; Gallou, F.; Reilly, J.; Lipshutz, B. H. *Angew. Chem., Int. Ed.* **2016**, *55*, 4914. b) Handa, S.; Wang, Ye; Gallou, F.; Lipshutz, B. H. *Science* **2015**, *349*, 1087. c) Handa, S.; Slack, E. D.; Lipshutz, B. H. *Angew. Chem., Int. Ed.* **2015**, *54*, 11994. d) Isley, N. A.; Gallou, F.; Lipshutz, B. H. *J. Am. Chem. Soc.* **2013**, *135*, 17707. e) Lu, G. -P.; Voigtritter, K. R.; Cai, C.; Lipshutz, B. H. *J. Org. Chem.* **2012**, *77*, 3700. f) Nishikata, T.; Lipshutz, B. H. *J. Am. Chem. Soc.* **2009**, *131*, 12103. g) Lipshutz, B. H.; Abela, A. R. *Org. Lett.* **2008**, *10*, 5329. h) Lipshutz, B. H.; Petersen, T. B.; Abela, A. *Org. Lett.* **2008**, *10*, 1333.
24. Lipshutz, B. H.; Taft, B. R. *Org. Lett.* **2008**, *10*, 1329.
25. a) Bhattacharjya, A.; Klumphu, P.; Lipshutz B. H. *Nat. Comm.* **2015**, *6*, 7401. b) Krasovskiy, A.; Haley, S.; Voidtritter, K.; Lipshutz, B. H. *Org. Lett.* **2014**, *16*, 4066.
26. a) Lu, G. -P.; Cai, C.; Lipshutz, B. H. *Green Chem.* **2013**, *15*, 105. b) Lu, G. -P.; Voigtritter, K. R.; Cai, C.; Lipshutz B. H. *Chem. Comm.* **2012**, *48*, 8661.
27. a) Duplais, C.; Krasovskiy, A.; Lipshutz, B. H. *Organometallics* **2011**, *30*, 6090. b) Krasovskiy, A.; Lipshutz, B. H. *Org. Lett.* **2011**, *13*, 3822. c) Krasovskiy, A.; Duplais, C.; Lipshutz, B. H. *Org. Lett.* **2011**, *13*, 3818. d) Krasovskiy, A.; Thome, I.; Graff, J.; Krasovskaya, V.; Konopelski, P.; Duplais, C.; Lipshutz, B. H. *Tetrahedron Lett.* **2011**, *52*, 2203. e) Krasovskiy, A.; Duplais, C.; Lipshutz, B. H. *Org. Lett.* **2010**, *12*, 4742. f) Duplais, C.; Krasovskiy, A.; Wattenberg, A.; Lipshutz, B. H. *Chem. Comm.* **2010**, *46*, 562. g) Krasovskiy, A.; Duplais, C.; Lipshutz, B. H. *J. Am. Chem. Soc.* **2009**, *131*, 15592.
28. Lipshutz, B. H.; Chung, D. W.; Rich, B. *Org. Lett.* **2008**, *10*, 3793.
29. a) Isley, N. A.; Dobarco, S.; Lipshutz, B. H. *Green Chem.* **2014**, *16*, 1480. b) Lipshutz, B. H.; Chung, D. W.; Rich, B. *Adv. Syn. Catal.* **2009**, *351*, 1717.

30. a) Nishikata, T.; Lipshutz, B. H. *Org. Lett.* **2012**, *12*, 1972. b) Nishikata, T.; Abela, A. R.; Lipshutz, B. H. *Angew. Chem., Int. Ed.* **2010**, *49*, 781.
31. a) Yokoyama, N.; Nakayama, Y.; Nara, H.; Sayo, N. *Adv. Synth. Catal.* **2013**, *355*, 2083. b) Suzuki, K.; Hori, Y.; Kobayashi, T. *Adv. Synth. Catal.* **2008**, *350*, 652.
32. Carole, W. A.; Bradley, J.; Sarwar, M.; Colacot, T. J. *Org. Lett.* **2015**, *17*, 5472.
33. R. E. Tundel, K. W. Anderson, S. L. Buchwald, *J. Org. Chem.* **2006**, *71*, 430.
34. Sunesson, Y.; Limé, E.; Lill, S. O. N.; Meadows, R. E.; Norrby, P. –O. *J. Org. Chem.* **2014**, *79*, 11961.
35. Hartwig, H. F. *Angew. Chem., Int. Ed.* **1998**, *37*, 2090.
36. DeAngelis, A. J.; Gildner, P. G.; Chow, R.; Colacot, T. J. *J. Org. Chem.* **2015**, *80*, 6794.
37. *New Trends in Cross-Coupling: Theory and Applications*, Colacot, T., Ed.; RSC: Cambridge, UK, **2015**.
38. Lefebvre, V.; Cailly, T.; Fabis, F.; Rault, S. *J. Org. Chem.* **2010**, *75*, 2730.
39. Hünig, S.; Aldenkortt, S.; Bäuerle, P.; Briehn, C. A.; Schäferling, M.; Perepichka, I. F.; Stalke, D.; Walfort, B. *Eur. J. Org. Chem.* **2002**, 1603.
40. Mirsalis, J. C.; Tyson, C. K.; Steinmetz, K.; Loh, E. K.; Hamilton, C. M.; Bakke, J. P.; Spalding, J. W. *Environ. Molec. Mut.* **1989**, *14*, 155.
41. Lipshutz, B. H.; Ghorai, S.; Abela, A. R.; Moser, R.; Nishikata, T.; Duplais, C.; Krasovskiy A. *J. Org. Chem.* **2011**, *76*, 4379.
42. Köhling, P.; Schmidt, A. M.; Eilbracht, P. *Org. Lett.* **2003**, *5*, 3213.
43. Kahraman, A.; Yasser, M. S. A.; Yaszynski, M.; Singh, G. S. *Arch. Pharm. Res.* **2012**, *35*, 1009.
44. Li, X.; He, L.; Chen, H.; Wu, W.; Jiang, H. *J. Org. Chem.* **2013**, *78*, 3636.
45. Lopez-Iglesias, M.; Busto, E.; Gotor, V.; Gotor-Fernandez, V. *J. Org. Chem.* **2012**, *77*, 8049.